Investigations into the Reactivity of an Anionic Gallium(I) *N*-Heterocyclic Carbene Analogue

by

David P. Mills

Thesis presented to the School of Chemistry, Cardiff University, for the degree of

Doctor of Philosophy, November 2007

ProQuest LLC
789 East Eisenhower Parkway
P.O. Box 1346
Ann Arbor, MI 48106-1346

Declaration

This work has not previously been accepted in substance for any degree and is not concurrently submitted in candidature for any degree.

Signed ....D Mill..... (candidate) Date 29/1/08.....

Statement 1

This thesis is being submitted in partial fulfilment of the requirements for the degree of PhD.

Signed ....D Mill..... (candidate) Date 29/1/08.....

Statement 2

This thesis is the result of my own independent work/investigation, except where otherwise stated. Other sources are acknowledged by explicit references.

Signed ....D Mill..... (candidate) Date 29/1/08.....

Statement 3

I hereby give consent for my thesis, if accepted, to be available for photocopying and for inter-library loan, and for the title and summary to be made available to outside organisations.

Signed ..D Mill..... (candidate) Date 29/1/08.....

Summary

This thesis is mainly concerned with investigations into the reactivity of the gallium(I) *N*-heterocyclic carbene (NHC) analogue, [K(tmeda)][:Ga{[N(Ar)C(H)]$_2$}] (Ar = $C_6H_3Pr^i_2$-2,6). Reactions of germanium, tin and lead alkyls, aryls, halides and heterocycles with [K(tmeda)][:Ga{[N(Ar)C(H)]$_2$}] afforded complexes such as [K(tmeda)][Sn{CH(SiMe$_3$)$_2$}$_2${Ga{[N(Ar)C(H)]$_2$}}], which exhibits the first structurally characterised Ga—Sn bond in a molecular complex. Group 6, 9 and 11 metal halide complexes were treated with [K(tmeda)][:Ga{[N(Ar)C(H)]$_2$}], yielding complexes such as [(IPr)Cu{Ga{[N(Ar)C(H)]$_2$}}] and [(IPr)Ag{Ga{[N(Ar)C(H)]$_2$}}]. These complexes exhibit the first structurally characterised Ga—Cu and Ga—Ag bonds in molecular complexes. A study of the reactivity of [(IPr)Cu{Ga{[N(Ar)C(H)]$_2$}}] with unsaturated organic substrates suggested that the Ga—Cu bond is quite inert. Salt metathesis reactions of group 10 metal halide complexes with [K(tmeda)] [:Ga{[N(Ar)C(H)]$_2$}] afforded complexes such as [(dppe)Pt{Ga{[N(Ar)C(H)]$_2$}}$_2$]. An investigation into the further reactivity of this complex towards *tert*-butylphosphaalkyne yielded a platinum(II) complex, [(dppe)Pt{Ga{[N(Ar)C(H)]$_2$}}{Ga{[PC(Bu^t)C(H)-(NAr)C(H)N(Ar)]}}], which exhibits a formally anionic P,N-heterocyclic gallium(I) ligand. The kinetics of the formation of this complex were studied. A novel gallium(III) complex, [GaI$_2${C(Bu^t)P(H)C(Bu^t)=P}]$_2$, was formed by the disproportionation reaction of [:Sn(η^4-$P_2C_2Bu^t_2$)] with "GaI". The oxidative insertion reaction of [K(tmeda)] [:Ga{[N(Ar)C(H)]$_2$}] with FisoH yielded the gallium(III) hydride, [{N(Ar)C(H)N(Ar)-K}(H)Ga{[N(Ar)C(H)]$_2$}]. Reaction of the digallane(4), [Ga{[N(Ar)C(H)]$_2$}]$_2$, with N_3-SiMe$_3$ afforded the paramagnetic complex, [{μ-N(SiMe$_3$)}Ga{[N(Ar)C(H)]$_2$$^{\cdot}$}]$_2$, which was studied by EPR spectroscopy. A synthetic route to the novel gallium(I) NHC analogue, [K(tmeda)][:Ga{[N(Ar)C(Me)]$_2$}], is also described. Work performed in Monash University, involving bulky amidinate and guanidinate ligands, is also discussed. A novel cationic boron heterocycle, [BrB(Giso)]$^+$ (Giso$^-$ = [{N(Ar)}$_2$CNCy$_2$]$^-$), was synthesised from BBr_3 and the gallium(I) guanidinate, [:Ga(Giso)]. The use of [Sm(Giso)$_2$] as a one-electron reducing agent is exploited in the coupling of two molecules of CS_2 by formation of a C—S bond to yield [{Sm(Giso)$_2$}$_2$(μ-η^2:η^2-SCSCS$_2$)]. The synthesis of novel η^6-arene rhodium(I) complexes such as [(η^4-COD)Rh(η^6-Giso)], and their thermal conversion into thermodynamically more stable η^2-chelating forms, are also reported.

Acknowledgements

Thanks go to Cameron for his excellent supervision and getting the most out of me by providing an interesting and rewarding project. I am sure that I wouldn't have been as productive if it were not for his David Brent-esque man-management skills.

I would also like to thank Andreas for performing X-ray crystallography, Shaun for DFT studies, Damien for EPR spectroscopy and Rob for kinetic experiments using NMR spectroscopy. I must acknowledge all of the helpful and friendly technical and support staff in Cardiff and Monash.

Thanks go to everyone in team HOMO (Bob, Andreas, Richard, Christian H., Glesni, Ben, Dan, Arnim, Timo, Christian S., Shaun, Kai, Graeme, Jade, Jamella and Dennis) for great times during the last three years. I would especially like to thank Bob for teaching me Schlenk techniques.

I must thank all of my friends and family for being there whenever I need them. Finally, I would like to thank Caroline for always being supportive and making me happy. I couldn't have done this without her.

Dedicated to the memory of Harry Bramwell Fowler.

Table of Contents

Glossary v

Chapter 1

General Introduction

1.1 The Physical and Chemical Properties of the Group 13 Elements 1

1.2 Subvalent Group 13 Chemistry 5

1.3 Preparation and Chemistry of the Metal Diyls 7

1.4 The Importance of the *N*-Heterocyclic Carbene Class of Ligand 11

1.5 Theoretical Studies on Group 13 NHC Analogues 15

1.6 The Synthesis and Coordination Chemistry of NHC Analogues 23

1.6.1 Four-Membered Group 13 Metal(I) Guanidinate Complexes 23

1.6.2 Five-Membered Analogues of 2,3-Dihydro-imidazol-2-ylidenes 27

1.6.3 Six-Membered Group 13 β-Diketiminate Complexes 34

1.7 References 43

Chapter 2

Complexes of an Anionic Gallium(I) *N*-Heterocyclic Carbene Analogue with Group 14 Element(II) Fragments

2.1 Introduction 53

2.2 Research Proposal 59

2.3 Results and Discussion 59

2.3.1 Preparation of Ionic Complexes 59

2.3.2 Preparation of Covalent Complexes 76

2.4 Conclusion 80

2.5 Experimental 81

2.6 References 89

Chapter 3

The Synthesis and Reactivity of Transition Metal Gallyl Complexes Stabilised by *N*-Heterocyclic Carbene Coordination

3.1 Introduction 93

3.1.1 Transition Metal Gallyl Complexes Incorporating the Heterocycle, $[:Ga\{[N(Ar)C(H)]_2\}]^-$ 93

3.1.2 Transition Metal Boryl Complexes 101

3.2 Research Proposal 103

3.3 Results and Discussion 103

3.3.1 The Preparation of a Group 6 Metal Gallyl Complex 103

3.3.2 The Preparation of a Group 9 Metal Gallyl Complex 107

3.3.3 The Preparation of Group 11 Metal Gallyl Complexes 109

3.3.4 The Reactivity of Group 11 Metal(I) Gallyls with Unsaturated Substrates 121

3.4 Conclusion 130

3.5 Experimental 130

3.6 References 141

Chapter 4

The Preparation of Novel Group 10 Metal Gallyl Complexes

4.1	Introduction	146
4.2	Research Proposal	148
4.3	Results and Discussion	148
4.3.1	The Preparation of Metal Gallyl Complexes with Monodentate Phosphines	148
4.3.2	The Preparation of Metal Gallyl Complexes with Chelating Ligands	161
4.3.3	The Reactivity of Chelated Metal Gallyl Complexes with Unsaturated Substrates	172
4.4	Conclusion	183
4.5	Experimental	184
4.6	References	194

Chapter 5

The Preparation of Novel Gallium(I), (II) and (III) Heterocycles

5.1	Introduction	198
5.1.1	The Reactivity of "GaI"	198
5.1.2	The Oxidation Chemistry of the Heterocycle, $[:Ga\{[N(Ar)C(H)]_2\}]^-$	199
5.1.3	Reactivity of the Digallane(4), $[Ga\{[N(Ar)C(H)]_2\}]_2$	200
5.2	Research Proposal	200
5.3	Results and Discussion	201
5.3.1	The Reactivity of "GaI"	201

5.3.2 Investigations into the Oxidation of the Heterocycle, $[:Ga\{[N(Ar)C(H)]_2\}]^-$ 204

5.3.3 The Reactivity of the Digallane(4), $[Ga\{[N(Ar)C(H)]_2\}]_2$ 209

5.3.4 Investigations into the Preparation of Novel Gallium(I) Heterocyclic Compounds 216

5.4 Conclusion 225

5.5 Experimental 226

5.6 References 232

Chapter 6

The Preparation and Reactivity of Novel Amidinate and Guanidinate Complexes

6.1 Introduction 235

6.2 Research Proposal 242

6.3 Results and Discussion 243

6.3.1 The Reactivity of the Heterocycle, $[:Ga\{[N(Ar)]_2CNCy_2\}]$ 243

6.3.2 The Reactivity of the Samarium(II) Complex, $[Sm(Giso)_2]$ 246

6.3.3 Preparation of Rhodium(I) Amidinate and Guanidinate Complexes 250

6.4 Conclusion 266

6.5 Experimental 266

6.6 References 273

Appendix 1 General Experimental Procedures 276

Appendix 2 Publications in Support of this Thesis 277

Glossary

18-crown-6	1,4,7,10,13,16-hexaoxacyclooctadecane
Å	Angstrom, 1 x 10^{-10} m
a_o	Hyperfine coupling value
ab initio	A quantum chemistry method
Ar, Ar', Ar'', Ar*, $Ar^{\#}$	A general aryl substituent
Ar^F, $Ar^{F'}$, $Ar^{F''}$, $Ar^{F'''}$	A general fluorinated aryl substituent
Ar-DAB	*N*,*N*'-Bis(diisopropylphenyl)diazabutadiene
br.	Broad
Bu^t	Tertiary butyl
Bu^t-DAB	*N*,*N*'-Bis(ditertiarybutyl)diazabutadiene
Bu^n	Normal butyl
ca.	*Circa*
cat	Catchecolato
CDA	Charge Decomposition Analysis
CDT	1,5,9-Cyclododecatriene
CHD	1,3-Cyclohexadiene
cm^{-1}	Wavenumber, unit of frequency (ν/c)
COD	1,5-Cyclooctadiene
COE	Cyclooctene
Cp	Cyclopentadienyl
Cp'	A general cyclopentadienyl
Cp*	Pentamethylcyclopentadienyl
Cy	Cyclohexyl
δ	Chemical shift in NMR spectroscopy (ppm)

DAB	Diazabutadiene
d	Doublet
dba	Dibenzylideneacetone
dcpe	1,2-Bis(dicyclohexylphosphino)ethane
dd	Doubled doublet
dec.	Decomposition
DFT	Density Functional Theory
DME	1,2-Dimethoxyethane
dppe	1,2-Bis(diphenylphosphino)ethane
dppm	1,2-Bis(diphenylphosphino)methane
dvds	1,1,3,3-Tetramethyl-1,3-divinyldisiloxane
E	A general element
ENC	Effective Nuclear Charge
EPR	Electron Paramagnetic Resonance
Et_2O	Diethyl ether
$Fiso^-$	*N*,*N*′-Bis(2,6-diisopropylphenyl)formamidine
FT-IR	Fourier transform infrared spectroscopy
η	Hapta
g_{iso}	Isotropic g value
G	Gauss
$Giso^-$	*N*,*N*′-Bis(2,6-diisopropylphenyl)dicyclohexylguanidinate
θ	Fold angle
HOMO	Highest Occupied Molecular Orbital
Hz	Hertz, s^{-1}
ICy	1,3-Bis(cyclohexyl)imidazol-2-ylidene
IMes	1,3-Bis(2,4,6-trimethylphenyl)imidazol-2-ylidene

IPr	1,3-Bis(2,6-diisopropylphenyl)imidazol-2-ylidene
ipso	*Ipso*-substituent
IR	Infrared
$^{n}J_{xy}$	Coupling constant between nuclei X and Y, over n bonds
K	Kelvin
k	A rate constant
kcal	Kilocalorie (1 kcal = 4.184 J)
kJ	Kilojoule
L	A general ligand
LUMO	Lowest Unoccupied Molecular Orpital
μ	Bridging
μB	Bohr Magneton, JT^{-1}
μ_{eff}	Effective magnetic susceptibility
m	*Meta*-substituent
m	Multiplet, medium
M	A general metal or molar (mol dm^{-3})
M^{+}	A molecular ion
Me	Methyl
Mes	Mesityl (2,4,6-trimethylphenyl)
Mes*	Supermesityl (2,4,6-tritertiarybutylphenyl)
mol	Mole
Mp	Melting point
MS(APCI)	Atmospheric Pressure Chemical Ionisation Mass Spectrometry
MS(EI)	Electron Ionisation Mass Spectrometry
m/z	Mass/charge ratio

nbd	Norbornadiene
NBO	Natural Bond Orbital
NHC	*N*-Heterocyclic carbene
NMR	Nuclear Magnetic Resonance
nor	Norbornene
o	*Ortho*-substituent
p	*Para*-substituent
Ph	Phenyl
pin	Pinacolato
$Piso^-$	*N,N'*-Bis(2,6-diisopropylphenyl)tertiarybutylamidinate
Pn	Pnictogen
Pr^i	Isopropyl
$Priso^-$	*N,N'*-Bis(2,6-diisopropylphenyl)diisopropylguanidinate
ppm	Parts per million
pw	Peak width
q	Quartet
R	General organic substituent
s	Singlet or strong
sept	Septet
t	Triplet
THF	Tetrahydrofuran
tmeda	*N,N,N',N'*-Tetramethylethylene-1,2-diamine
TMS	Trimethylsilyl or tetramethylsilane
UV	Ultraviolet
X	A general halide
xylyl	2,6-Dimethylphenyl

Chapter 1

General Introduction

1.1 The Physical and Chemical Properties of the Group 13 Elements

The group 13 elements are boron, aluminium, gallium, indium and thallium. They exhibit a ground state valence electron configuration of ns^2np^1, with the core electronic configurations varying on descent of the group.[1] The elements all possess fewer valence electrons than valence orbitals and as such are commonly referred to as "electron-deficient." In the case of boron this phenomenon, coupled with its high electronegativity and small atomic size, dominates its chemistry by encouraging extensive multi-centre covalent bonding in its compounds. Boron is non-metallic and high-melting and its physical and chemical properties are unlike those of the heavier congeners. These differences commonly lead to boron being discussed separately to the other group 13 elements, having more in common with its horizontal and diagonal neighbours carbon and silicon than its vertical neighbour aluminium.[2]

Some physical properties of the elements have been compiled below (Table 1). The metallic elements (Al-Tl) are good conductors of electricity and are typically low melting and soft. On descent of the group, the changes in physical properties of the metals are non-uniform, and all display unique characteristics.[1-3] Gallium is of particular relevance to this study and so its physical properties will be briefly summarised here. It is a low-melting solid that expands on freezing, displays the longest liquid range of any element and is remarkably non-toxic. Perhaps the most remarkable property of gallium is that it appears to form dimeric entities in the solid state, with one neighbouring atom being at least 26 pm closer than the other six

neighbouring atoms.[1] This finding has led to the proposal that in the solid state, gallium is comparable to iodine, which displays discrete I_2 units.

	B	Al	Ga	In	Tl
Atomic Number	5	13	31	49	81
Electronic Configuration	$[He]2s^22p^1$	$[Ne]3s^23p^1$	$[Ar]3d^{10}4s^24p^1$	$[Kr]4d^{10}5s^25p^1$	$[Xe]4f^{14}5d^{10}6s^26p^1$
Melting Point/°C	2300	660.1	29.8	156.2	302.4
Metallic Radius/pm	(80-90)	143	135	167	170
Ionisation Energy ($\Sigma 1^{st}$ 3 IE)/kJmol^{-1}	6887	5044	5521	5084	5439
Electronegativity, χ (Pauling)	2.04	1.61	1.81	1.78	2.04
Electronegativity, χ (Allred-Rochow)	2.01	1.47	1.82	1.49	1.44

Table 1 – Selected properties of the group 13 elements

Basic periodicity suggests that on descent of a group, both electronegativity and ionisation energies should decrease and the radius of the elements should increase.[1] This is because the small increase in effective nuclear charge (ENC) on descent of a group is superseded by the addition of an extra shell of electrons. However, gallium is roughly the same size as aluminium and has a greater electronegativity by both Pauling and Allred-Rochow classifications.[1-3] As well as this, the ionisation energies do not decrease as basic periodicity predicts. These observations can be explained by the effect of *d*-block contraction, or "scandide contraction" as it is rarely known.[1] This contraction occurs because *d*-orbitals are large and diffuse, and as such electrons in these orbitals do not shield the valence electrons from the nucleus as effectively as electrons in *s*- and *p*-orbitals. The result is that valence *s*- and *p*-electrons above a filled *d*-shell experience a greater ENC than would be expected as they are influenced more

strongly by the nucleus. As gallium immediately follows the first series of the *d*-block, the valence orbitals are contracted, leading to the observed electronegativity and radius of the element. A "lanthanide contraction" occurs for analogous reasons. This term is most commonly used to describe the observation of second and third row transition metals displaying similar properties, but can also be invoked in this argument to explain the small differences in the radii and electronegativity (Allred-Rochow) of indium and thallium.[1] The heavier homologue has a filled *f*-shell below the valence shell and electrons in this orbital are even poorer than *d*-electrons at shielding the valence electrons from the influence of the larger, more positively charged nucleus. Hence these factors help to explain seemingly anomalous periodic trends.

The "inert-pair" effect dominates the chemistry of the heavier group 13 elements.[4] This term describes the observed reluctance of the *ns* electrons to participate in bonding so that the heavier elements tend to exist in compounds in a subvalent state. Thallium, at the bottom of the group, exists mainly in the +1 oxidation state in its compounds, whereas aluminium, near the top of the group, tends to prefer the +3 oxidation state in most compounds. Gallium, in the middle of the group, is more intermediate in its preference of oxidation states, though is almost exclusively in the +3 oxidation state under aqueous conditions.[1] The tendency of an element to display an oxidation state two lower than expected is not due to any greater difficulty in removing the *ns* electrons on descent of the group, as the sum of the first three ionisation potentials for gallium, indium and thallium are quite similar.

The "inert-pair" effect is best illustrated by example, with the metal halides MX and MX_3 taken into consideration. On descent of group 13, the $s \rightarrow p$ promotion energy tends to increase. Hence, if additional M—X bonds are to be formed to the metal centre

in MX then a greater amount of energy is required to induce hybridisation of the metal orbitals to form sp^2 hybrids. In addition, the enthalpy of formation of an M—X bond decreases on descent of the group, due to larger and more diffuse metal orbitals resulting in poorer orbital overlap with ligands. The preference for an element to exist in the higher oxidation state depends on whether the energy required to promote the *s*-electrons for purposes of hybridisation is compensated for by the energy gained on formation of two additional M—X bonds. In the case of thallium, with a relatively large amount of energy required for $s \rightarrow p$ promotion, the tendency to prefer the lower oxidation state is particularly marked.

There is a third contributor to the observation of the "inert-pair" effect that only becomes a significant factor in the case of heavier elements, such as thallium. Relativistic effects are instigated by the large, highly positively charged nucleus of thallium causing the electrons in the 1*s* orbital to be an appreciable fraction of the speed of light, 0.6 *c*. Electrons orbiting at near the speed of light will tend to contract towards the nucleus, causing the 1*s* orbital to contract. As there is an overlap of the probability function of the 1*s* orbital into all subsequent *s*-orbitals, they are all made to contract. The result is that the valence 6*s* orbital in thallium is closer to the nucleus than expected, hence there is a larger $s \rightarrow p$ separation and the *s*-electrons are even more reluctant to take place in bonding. The intermediary position of gallium in this series makes studies of low valent gallium compounds particularly interesting.

1.2 Subvalent Group 13 Chemistry

Accessing the lower oxidation states of aluminium and gallium has in the past proved difficult, in comparison to their heavier homologues, indium and thallium. The last twenty years of research reveals that the two most common routes to accessing subvalent aluminium and gallium compounds are through substitution of the halide in subhalides, EX (E = Al, Ga, X = Cl, Br, I), with RM (M = Li, Na, K), or more simply by dehalogenation of $[R_2EX]$ or $[REX_2]$, most often by reduction with alkali metals, M (Scheme 1).[5] In both cases bulky R-groups are employed to kinetically protect the group 13 element in the product from thermodynamically favourable disproportionation processes. The method of reduction is most commonly employed in the synthesis of aluminium and gallium diyls, :E—R.[5] The importance of group 13 diyls is described in the next section (*vide infra*).

$$EX + RM \longrightarrow :ER + MX \quad (E = Al, Ga;\ X = Cl, Br, I;\ M = Li, Na, K)$$

$$2\,[R_2EX] + 2\,M \longrightarrow 2\,MX + [R_2E{-}ER_2]$$

$$n\,[REX_2] + 2n\,M \longrightarrow 2n\,MX + [(ER)_n] \quad (n = 1 - 4)$$

Scheme 1 – General synthesis of subvalent aluminium and gallium compounds

Organometallic aluminium and gallium compounds of oxidation states up to and including +3 can be accessed from their halides, the preparations of which are now described. Trihalides of all the group 13 elements are well established and easily prepared. Heating gallium metal, for example, in a stream of chlorine or bromine carried by an inert gas yields low melting hygroscopic solids that consist of Ga_2X_6 dimeric units.[2] Halides of intermediate valency are well known for gallium and indium, but not to any real extent for aluminium or thallium. The gallium dihalides, GaX_2, are

typically mixed valence compounds which can be formulated as $[Ga^{I}]^{+}[Ga^{III}X_4]^{-}$. True gallium(II) halides containing a metal-metal bond have been prepared, such as the dianions, $[Ga_2X_6]^{2-}$ (X = Cl, Br, I),[6] and the donor-solvent stabilised compounds, $[Ga_2X_4L_2]$ (X = Cl, Br, I; L = dioxane, pyridine, phosphine).[7] It is noteworthy that metal-metal bonded species stabilised in a similar manner have also been reported for indium(II) halides, such as $[In_2I_4(PPr^n)_2]$.[8] Complexes of the formulation $[Al_2X_4(donor)_2]$, formed from the disproportionation of AlX in solution, are known but have not been widely studied.[9]

Whilst the preparation of subvalent indium and thallium halides is relatively simple, routes to aluminium(I) and gallium(I) halides have in the past proved problematic. The preparation of "metastable" solutions of these halides was only made possible through the construction of specialised apparatus. Introduction of $HX_{(g)}$ into a vacuum chamber containing liquid aluminium or gallium at high temperature leads to the resultant $MX_{(g)}$ vapour condensing on the walls of the liquid nitrogen cooled vessel. In the presence of an appropriate donor solvent, the oligomeric aluminium(I) or gallium(I) species, $[\{EX(L)\}_n]$ (E = Al, Ga; X = Cl, Br, I, L = donor solvent n = integer), are stabilised.[10] These oligomers are unstable with respect to temperature, and only several examples have been characterised by X-ray crystallography, e.g. the octameric species, $[Ga_8I_8(PEt_3)_6]$,[11] and cyclic tetramers, $[Al_4Br_4(donor)_4]$.[12] Metal(I) halides proved to be suitable precursors to a range of alkyl-, silyl-, amido- and phosphido-complexes and have allowed the preparation of clusters such as $[Ga_{84}\{N(SiMe_3)_2\}_{20}]^{4-}$[13] and $[Al_{77}\{N(SiMe_3)_2\}_{20}]^{2-}$.[14] These clusters are of tremendous interest as they challenge existing theories on metal-metal bonding and give insight into the formation of metals; as such this work has been reviewed several times.[5]

The publication of a facile route to subvalent gallium iodide has revolutionised the investigation of subvalent gallium chemistry. This simple procedure involves ultrasonic activation of half an equivalent of gallium metal in a toluene solution of diiodine under an inert atmosphere, yielding a flocculent green solid that has been formulated as "GaI".[15] This highly reactive reagent may only be prepared in non-coordinating solvents and its molecular structure remains unknown. However, Raman studies have suggested the compound to be a mixture of subhalides, with the ionic species, $[Ga]^{+}_{2}[Ga_2I_6]^{2-}$, predominating.[16] The reagent is a useful source of gallium(I) and is an effective reducing agent in mediating C—C bond forming reactions.[17] The paucity of research in this area is surprising, considering that it is more reducing than the more extensively investigated compound, indium(I) iodide, which has proved useful in C—C bond forming procedures such as Reformatsky reactions and Barbier allylations.[18] The well-established merits of "GaI" as a versatile synthetic reagent have been recently reviewed.[19] It is also of note that "GaI" has been shown to have parallels with the aforementioned metastable gallium(I) halides in that many clusters have been prepared from it, generally from its treatment with bulky silyl or germyl anions. Complexes such as $[Ga_{22}\{Si(SiMe_3)_3\}_8]$[20] have arisen from this research, which had previously been prepared from "metastable" GaBr.[21] Of most relevance to this study, "GaI" is a frequently used reagent in the preparation of gallium diyls, a rapidly expanding area of research.

1.3 Preparation and Chemistry of the Metal Diyls

The coordination chemistry of the group 13 metal diyls, :E—R (E = Al, Ga, In, Tl), has been extensively studied and has recently been the subject of several reviews.[5b-c,22] In their monomeric states they can be viewed as having a singlet lone pair of

electrons in the valence *sp*-hybridised orbital, with two vacant *p*-orbitals orthogonal to the E—C bond (Figure 1), though they commonly aggregate into oligomeric forms in the solid state. They are isolobal with carbon monoxide, CO, and as such may donate their lone pair of electrons to a Lewis acid to form a σ-bond, and potentially accept electron density from coordinated transition metals into vacant *p*-orbitals to form π-bonds. The involvement of π-bonding in transition metal complexes of the metal diyls has been the subject of much debate (*vide infra*). It is apparent that the nature of the R-substituent has a great influence on the π-acceptor capabilities of metal diyls, as extensive theoretical studies have shown.[23] Some recent highlights in group 13 metal diyl chemistry will now be discussed.

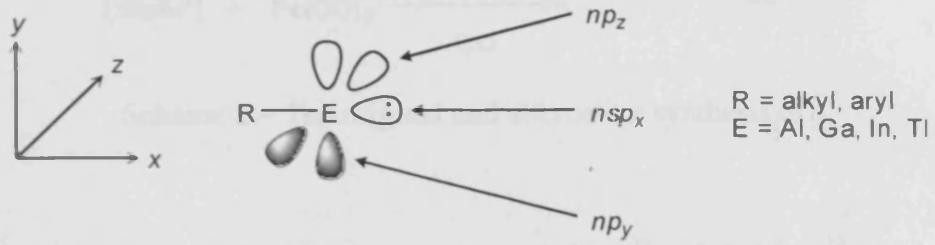

Figure 1 – A representation of the valence orbitals in group 13 metal diyls

A bulky terphenyl ligand was employed to facilitate the synthesis of the novel complex, **1**, by a salt metathesis reaction of the gallium(III) precursor, [Ar*$GaCl_2$] (Ar* = $C_6H_3(C_6H_2Pr^i_3$-2,4,6)$_2$-2,6) with $Na_2[Fe(CO)_4]$ (Scheme 2).[24] This complex was latterly synthesised directly by reaction of the isolated diyl, [:GaAr*], with $Fe(CO)_5$.[25] It was claimed in the original report that the unusually short Ga—Fe bond length of 2.2248 Å is indicative of a triple bond, and the complex as such was dubbed a "ferrogallyne".[24] However, this claim was widely disputed and a report published subsequently in the same journal showed, through an analysis of the CO stretches in the IR spectrum and the use of density functional theory (DFT) calculations, that this description of the bonding is inaccurate.[26] Several sets of calculations have followed

these articles in an attempt to bring an end to this dispute.[23,27] The current consensus is that although there may be some Ga←Fe π-back-donation in this complex, the bonding is mainly ionic and the bond order from an natural bond order (NBO) analysis is only 0.53, so **1** does not contain a Ga≡Fe triple bond. Group 13 metal diyls bearing a terphenyl group have not been studied to the same extent as those bearing alkyl, silyl and cyclopentadienyl substituents. Some of the more interesting findings in this area will now be discussed.

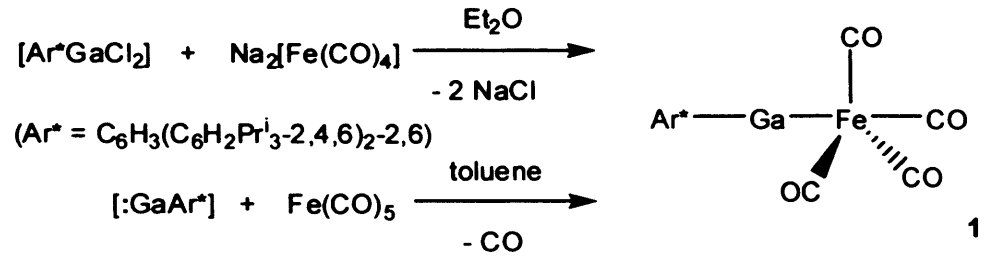

Scheme 2 – The original and alternative synthesis of **1**

Whilst the synthesis of cyclopentadienyl indium[28] and thallium[29] metal diyls had been known for some time, the preparation of the lighter homologues remained unknown. The advent of "metastable" solutions of aluminium(I) and gallium(I) halides, however, allowed the preparation of [:Al(η^5-Cp*)][30] **2a** and [:Ga(η^5-Cp*)][31] **2b** in low yields by the treatment of the subhalides with [Mg(η^5-Cp*)$_2$] (Cp* = C_5Me_5). The gallium homologue, **2b**, has been shown to form hexameric aggregates in the solid state.[32] Alternative, higher yielding synthetic procedures have since been developed for **2a**[33] and **2b**[34] that involve reductive dehalogenation through employment of an alkali metal. Both methods of preparation of the gallium homologue, **2b**, are summarised below (Scheme 3). The π-backbonding capability of **2a-b** differ from CO as partial π-donation of electron density from the Cp* ligand into the empty valence *p*-orbitals of the group 13 element reduces the ability of the metal to accept π-electron density from a transition metal that it ligates to.[22a-b]

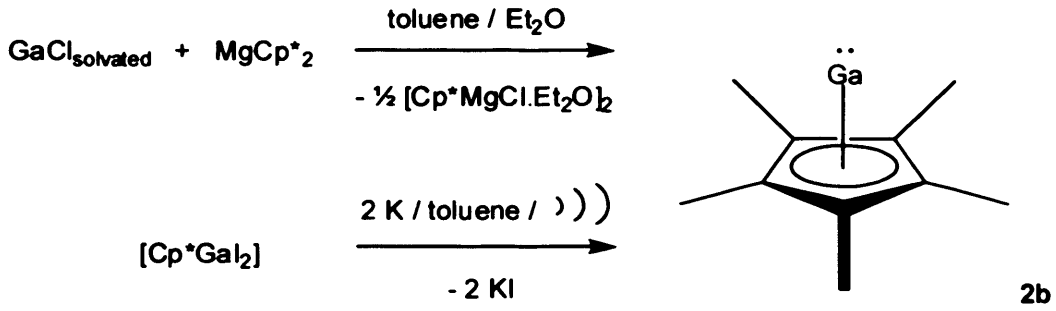

Scheme 3 – Methods of preparation of [:Ga(η^5-Cp*)], **2b**

The coordination chemistry of **2b** has been investigated thoroughly and has been the subject of several reviews.[5b-c,22a-b] It is noteworthy that homoleptic transition metal complexes of **2b** possessing four gallyl ligands have been synthesised; [M{Ga(η^5-Cp*)}$_4$] (M = Ni **3a**,[35] Pd **3b**,[36] Pt **3c**[36]) (Figure 2). The diyl, **2b**, displays analogies to CO in that it commonly exhibits bridging and terminal bonding modes in its complexes. As well as this, the hapticity of the Cp* ligand can change upon complexation in sterically crowded environments from the usual η^5-mode. Both of these characteristics are exemplified by the group 6 complexes, **4a-b**.[37] It is also noteworthy that **2b** has shown a tendency to insert into metal-halide bonds, a feature that has allowed an extension of its coordination chemistry.[38] The chemistry of **2b** continues to produce interesting results; a recent highlight being the synthesis of the [Ga$_2$(η^5-Cp*)]$^+$ cation, **5**.[39]

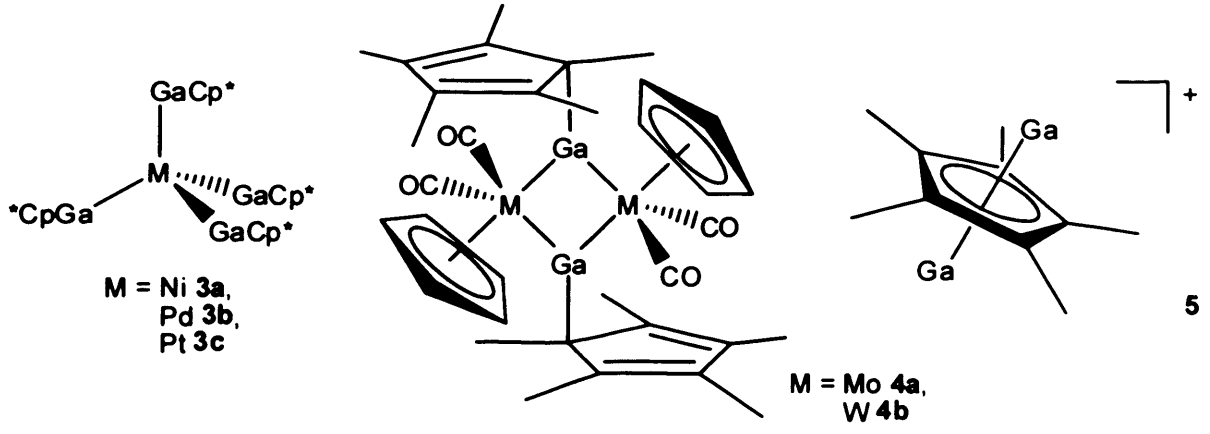

Figure 2 – Complexes **3a-c**, **4a-b** and **5**

Group 13 metal diyls bearing alkyl and silyl substituents are well explored.[5b-c, 22c] A series of tetrahedral, tetrameric aggregates, [{EC(SiMe$_3$)$_3$}$_4$] (E = Al **6a**,[40] Ga **6b**,[41] In **6c**,[42] Tl **6d**[43]), have been reported to be stabilised by the employment of the bulky and electronically stabilising tris(trimethylsilyl)methyl group (Figure 3).[44] A lack of investigation into the gallium analogue is easily explained by the low-yielding synthesis initially reported (< 15 %); an improved synthetic route with yields of over 70 % is now allowing this paucity to be addressed.[45] Studies suggest that complexes **6a-d** may insert into metal-halide bonds[37a,46] and act as bridging ligands[47] in a manner similar to **2b**. The preparation of the homoleptic complexes, [Ni{EC(SiMe$_3$)$_3$}$_4$] (E = Ga **7a**,[48] In **7b**[49]), has allowed a direct comparison of the π-backbonding capability of this ligand class with **2b**. The Ga—Ni bond length of 2.1700 Å observed in **7a**, the shortest ever reported, warranted a charge decomposition analysis (CDA) and NBO analysis to be carried out. The studies found that the π-component of the metal-ligand interaction was significant, with the π-contribution to the bonding being even greater than in the analogous complex, [Ni(CO)$_4$].[48]

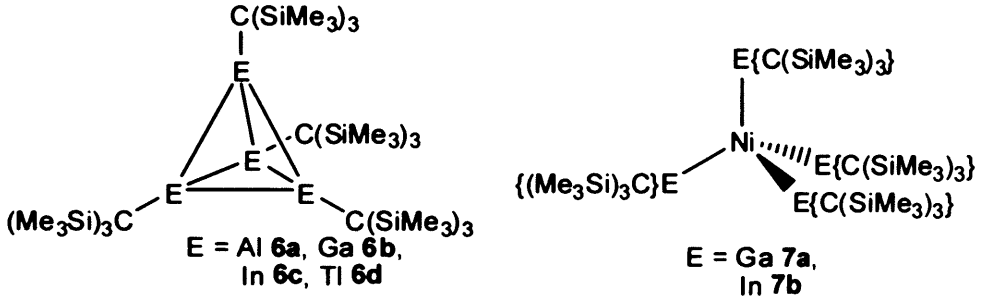

Figure 3 – Complexes **6a-d** and **7a-b**

1.4 The Importance of the *N*-Heterocyclic Carbene Class of Ligand

A carbene is defined as a neutral complex possessing an electron deficient divalent carbon atom.[50a,b] The carbon atom features six electrons in the valence shell, two of which are not involved in bonding. The geometry of carbenes is dependent on

the degree of hybridisation at the carbene centre. In the extreme case of a linear carbene, *sp*-hybridisation would produce two degenerate orbitals, p_x and p_y, though most carbenes display a bent geometry as they are sp^2-type hybridised, making the frontier orbitals a *p*-orbital (p_π) and an sp^2-type orbital (σ). The deviation from linearity, by inducing *s*-character into the p_x-orbital, dictates the energy gap between σ and p_π and therefore the ground-state multiplicity of the carbene and its reactivity. The two electrons not involved in bonding can either be spin-paired and both reside in the σ-orbital (singlet state), or unpaired with one electron in the σ-orbital and one in the p_π-orbital (triplet state) (Figure 4). A large $\sigma \rightarrow p_\pi$ energy gap (> 2 eV) favours the singlet ground state, which is generally more stable and should be ambiphilic in nature.[50a,b] Triplet ground state carbenes are generally short-lived and difficult to stabilise and as such will not be further discussed here.

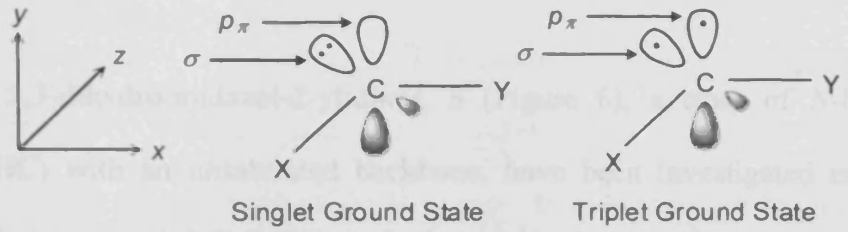

Figure 4 – Singlet and triplet ground states for carbenes

The substituents on the carbon atom may stabilise carbenes by electronic and steric effects.[50a] Of relevance to this discussion, diaminocarbenes are particulary stable as the N-substituents are π-donor and σ-attractors of electron density with respect to the carbon atom (Figure 5). This type of carbene stabilisation is known as a push, push mesomeric – pull, pull inductive substitution pattern. Symmetric combinations of the nitrogen lone pairs with the p_π-orbital raises the energy of this orbital relative to the σ-orbital, therefore favouring the singlet state. The formal four-electron, three-centre π-system that results stabilises the carbene mesomerically by creating some multiple bond character. It is this highly stabilising mesomeric effect, however, that causes the

diaminocarbenes to be very poor π- acceptor ligands, due to the partial occupancy of the p_π-orbital. The high electronegativity of the N-substituents creates a stabilising inductive effect by increasing the *s*-character of the non-bonding σ-orbital. The σ-orbital is therefore decreased in energy relative to the p_π-orbital, also favouring and stabilising the singlet state. Whilst bulky substituents are known to kinetically stabilise all carbenes, steric bulk tends to favour a triplet ground state and is not a major factor in the stabilisation of diaminocarbenes.

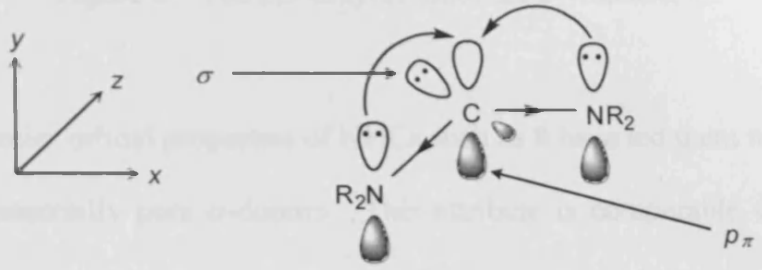

Figure 5 – The inductive and mesomeric stabilisation of diaminocarbenes

The 2,3-dihydroimidazol-2-ylidines, **8** (Figure 6), a class of *N*-heterocyclic carbene (NHC) with an unsaturated backbone, have been investigated extensively[50] since the first successful isolation and characterisation of this type of ligand by Arduengo *et al.*[51] Despite the fact that metal complexes of these ligands had been known for over twenty years previously, from the pioneering work of Wanzlick[52] and Öfele,[53] the study of these heterocycles and their complexes has only blossomed since they were found to be stable isolable compounds. This is perhaps mostly due to the catalytic properties that complexes of these ligands commonly display.[50c] The frontier orbitals of carbenes of type **8** make them strong nucleophiles and bases, and poor π-acceptors of electron density from metal centres. The M—C bond in NHC transition metal complexes is commonly described as inert, although there is substantial evidence that this is not always the case due to the possibility of reductive elimination, displacement and C—H/C—C activation of the NHC.[50d] In addition to studies of

transition metal complexes of NHCs, investigations have shown NHCs to react with a range of organic compounds and main group precursors.[50b,e-f]

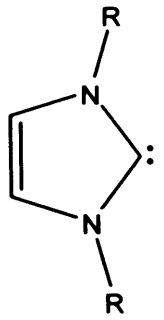

Figure 6 – The 2,3-dihydroimidazol-2-ylidenes, **8**

The frontier orbital properties of NHCs such as **8** have led them to be commonly described as essentially pure σ-donors. This attribute is comparable with the much-investigated electron-rich organophosphines, $:PR_3$, many transition metal complexes of which have been shown to display catalytic activity, such as Grubbs' "first generation" olefin metathesis catalyst, **9** (Figure 7).[54] The replacement of one phosphine ligand with an NHC gave the "second generation" catalyst, **10**, which displays increased reactivity.[55] Many other examples of such replacements were investigated[50c,56] and, coupled with the ability of NHCs to stabilise unusual oxidation states and incorporate bulky R-substituents,[50] this has lead to NHCs commonly being referred to as "phosphine mimics."[50c] This term is not strictly true, as in many cases phosphines may have substantial π-contributions in their bonding to metal complexes, and NHCs have largely superseded their phosphine congeners. Metal complexes of NHCs have generally been shown to have a greater activity and stability compared to their organophosphine analogues.[50]

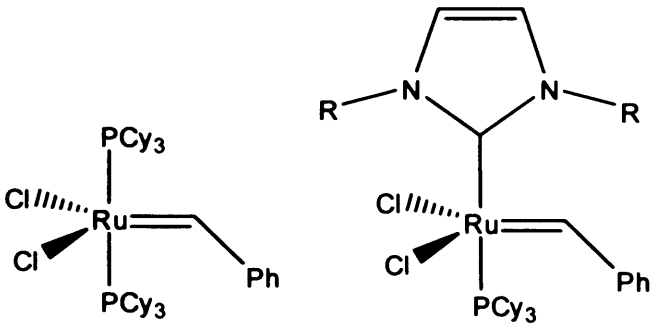

9 **10**

Figure 7 – The ruthenium catalysts, **9** and **10**

1.5 Theoretical Studies on Group 13 NHC Analogues

The high catalytic activity of transition metal complexes of NHCs prompted research into the synthesis of valence isoelectronic analogues of **8**. Following the successful synthesis of silylenes, **11c**,[57] germylenes, **11d**,[58] nitrenium cations, **11f**,[59] phosphenium cations, **11g**,[60] and arsenium cations, **11h**,[61] analogous to **8** (Figure 8), theoretical studies were performed to determine if anionic group 13 analogues, such as **11a-b**, would be stable, isolable compounds worthy of synthetic investigation.[62] As in the case of NHCs, a large $\sigma \rightarrow p_{\pi}$ energy gap in the frontier orbitals is required for the stable singlet state to be preferred over the reactive diradical triplet state. In addition to this, a high electron affinity of the group 13 element, E, is required for these anions to be stable. A DFT analysis on the model complexes, **12a-d** (Figure 9), showed that their N—E—N angles vary from 97.8° (E = B) to 77° (E = In), suggesting that the geometry of these complexes would be largely determined by the size of the group 13 element.[62a] Although the electron affinity for E = B was found to be small, the singlet-triplet energy separations were found to be large for all analogues, suggesting that all compounds would be thermodynamically stable. The heavier analogues are additionally stabilised by their high electron affinities.

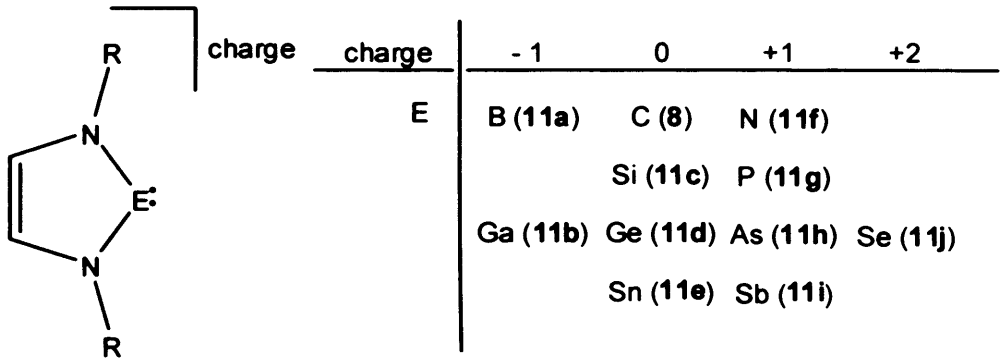

Figure 8 – Structurally characterised valence isoelectronic analogues of **8**

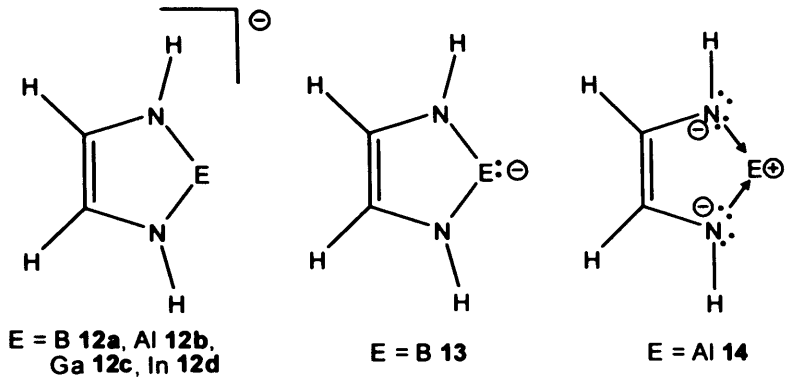

Figure 9 – The model complexes, **12a-d**, and the bonding depictions, **13** and **14**

An NBO analysis of the bonding in **12a-b** revealed very different electron distributions for the two analogues.[62a] Whilst the canonical structure, **13**, describes mostly covalent bonding for E = B, the donor-acceptor formulation, **14**, with the group 13 metal formally in the +1 oxidation state, best illustrates the bonding for E = Al (Figure 9). Formulation **14** becomes increasingly dominant for more electropositive atoms in the order E = Al < Ga < In. The E—N bond strength calculated for E = Al suggests an electron density approximating to almost half a bond; in the case of E = B it is almost a single bond. For E = Al, considerable electron density is released to the more electronegative N atoms, strengthening the E—N bond in this way. The *s*/*p* ratio for the lone pair of electrons for E = Al (1.660/0.536) is also much higher than E = B (1.378/0.918). The heavier anionic group 13 NHC analogues (E = Al, Ga, In) were predicted to not undergo a cyclic delocalisation of electrons, as is proposed to be the case for compounds of class **8**.[50a,c,f]

An *ab initio* study on model complexes similar to **12a-d** was published the same year as the DFT study.[62b] This study suggested that in model complexes such as **12a-d**, there is appreciable aromatic stabilisation for E = B and E = Al. However, an analysis of the HOMO – 4 of both models suggested that only in the case of the boron analogue is the "empty" p_x-orbital involved in the delocalised π-system, so the cyclic stabilisation of the Al analogue is much lower. The *ab initio* study concurred with the DFT study on the greater stabilisation of the lone pair in heavier analogues compared with E = B, and that this is located in the HOMO, which is high in energy and makes **12b-d** nucleophilic. The conclusion from both reports is that five-membered anionic group 13 NHC analogues are feasible synthetic targets.

Following the successful synthesis of the anionic gallium(I) NHC analogue, $[:Ga\{[N(Ar)C(H)]_2\}]^-$ **15** (Ar = $C_6H_3Pr^i_2$-2,6),[63] DFT studies were performed on the model complex, $[:Ga\{[N(Me)C(H)]_2\}]^-$ **16**, by Dr. J. A. Platts (Cardiff University) to determine the frontier orbitals of this species, employing the BP86/6-31G(d) basis set (Figure 10).[64] A large HOMO – LUMO gap (198.68 kJ mol^{-1}) was observed for this model complex. The main contribution to the LUMO is the large and diffuse *p*-orbital at gallium, which is high in energy, and is indicative of weak π-acceptor properties for this ligand. In contrast to the previous study,[62b] the HOMO was found to be mainly ligand-based, involving intra-heterocyclic π-interactions. The *sp*-type lone pair at gallium is the main contributor to the HOMO – 1, indicating that this species should act as a strong nucleophile with a directional lone pair.

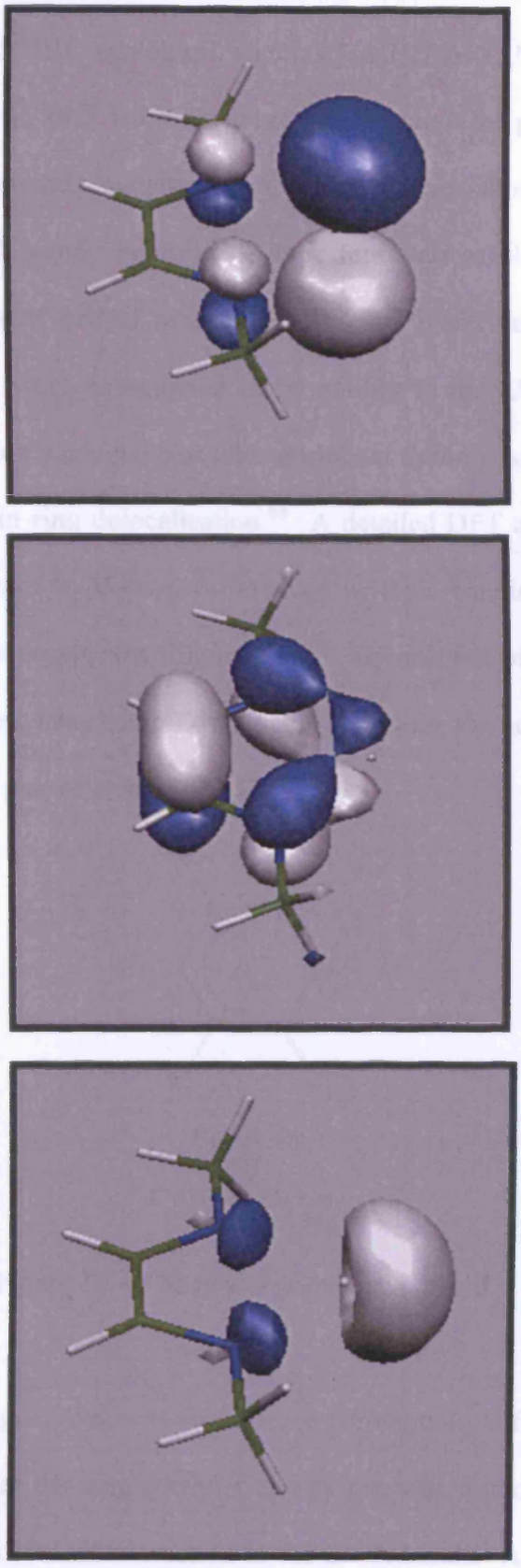

Figure 10 – DFT calculated frontier orbitals of the model complex, **16**

The employment of bulky β-diketiminate ligands to stabilise neutral monovalent group 13 six-membered NHC analogues, such as [:Al{[N(Ar)C(Me)]$_2$CH}] **17a**[65] and [:Ga{[N(Ar)C(Me)]$_2$CH}] **18**,[66] led to theoretical studies into the properties of this new ligand class.[67] Initial studies suggested that the complexes should behave as Lewis bases, with the HOMO mainly being an *sp*-type lone pair of electrons at E and the LUMO mainly being a π*-orbital associated with the ligand backbone, and not the empty p_x-orbital at E, which is assigned to be mainly in the LUMO + 1.[65,67a] The stability of the aluminium analogue was later attributed to the possibility of the *sp*-type lone pair participating in ring delocalisation.[68] A detailed DFT analysis of the model complexes, **19a-d**, sought to deduce differences in their bonding and therefore the relative stabilities of the complexes (Figure 11).[67b] By analysis of theoretical reactions between the heterocycles, **19a-d**, and Lewis acids and bases, the authors hoped to probe the possibility of a lone pair of electrons at E.

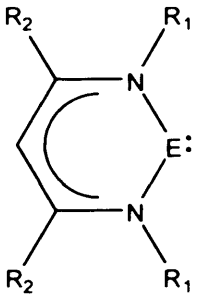

R_1 = H, Me
R_2 = H
E = B **19a**, Al **19b**,
Ga **19c**, In **19d**

Figure 11 – The model complexes, **19a-d**

The boron analogue, **19a**, was found to be substantially different to the heavier analogues, **19b–d**, in that the singlet-triplet energy gap was found to be minimal and that there is significant covalent interaction in the B—N bonds. Although the electron localisation function (ELF) and a theoretical reaction with BF_3 suggests that a lone pair of electrons exists at the boron centre, the small singlet-triplet energy gap suggests that

the boron analogue would not be thermodynamically stable and therefore is not a valid synthetic target. The boron atom in this species has been assigned a formal oxidation state of +2, and is best described by two diradical Lewis structures. The other analogues, **19b–d**, were found to have large singlet-triplet energy gaps and E was defined by the formal oxidation state of +1. As is the case for the model compounds, **12a-d**, the bonding in **19b–d** is best viewed as an anionic bidentate ligand chelating a formally positive metal cation E^+, the Lewis structures of which, **20a-c**, are depicted below (Figure 12).[67b]

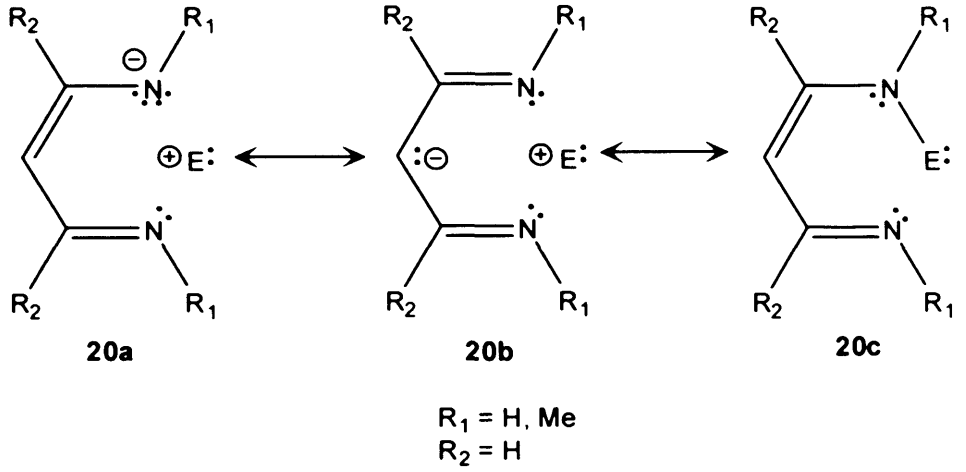

Figure 12 – The proposed Lewis structures, **20a-c**

Following these insightful theoretical investigations, the successful synthesis of the β-diketiminato complexes, [:E{[N(Ar)C(Me)]$_2$CH}], E = In **21a**,[69] E = Tl **22a**,[70] provoked further study into this ligand class.[71] By performing DFT calculations on complete molecules using coordinates taken directly from the X-ray crystal structures of **17**, **18**, **21a** and **22a**, the considerable steric bulk of the ligand was taken into account in calculations for the first time.[70b] The kinetic stabilisation induced by the ligand was cited as the major stabilisation factor, rather than the electronic factors originally proposed.[68] Most other conclusions drawn from the theoretical studies were in agreement with those already published. However, the thallium analogue, **22a**, analysed for the first time, displayed a significantly different ordering of its molecular

orbitals (MOs) compared to the lighter analogues, **17**, **18** and **21a**. Interpreted as a manifestation of the "inert-pair" effect, the p_π-orbital at thallium becomes the LUMO and the HOMO is ligand-based, with the lone pair of electrons more tightly held in the HOMO – 2, making this analogue more stable and less reactive. A recent DFT study correlates all previous calculations on the subject of neutral group 13 β-diketiminate complexes, with an in-depth view of their reactivities.[71] In addition, this study suggests that, despite the instability of the boron analogue, kinetically and thermodynamically stable B=B bonded dimers of the β-diketiminate ligand could be experimentally accessible, though not necessarily *via* the monomer.

The successful synthesis of the four-membered NHC analogues, [:Ga(Giso)] **23** and [:In(Giso)] **24** ($Giso^-$ = $[\{N(Ar)\}_2CNCy_2\}]^-$), prompted a DFT investigation of the model complexes, [:E{$[N(Ph)]_2CNMe_2$}] **25a–c** (Figure 13).[72] This report followed previous synthetic attempts to synthesise related amidinato group 13 NHC analogues, the most successful of which yielded η^2-*N*,arene-chelated amidinato complexes of indium(I) and thallium(I).[73] A parallel study yielded the gallium(II) dimer, [{Gal(η^2-*N*,*N*′-Piso)}$_2$] ($Piso^-$ = $[\{N(Ar)\}_2CBu^t]^-$), by disproportionation.[74] Models of the indium and thallium complexes were investigated by DFT against their *N*,*N*′-chelated analogues.[73] The study concluded that the *N*,*N*′-chelated model of the indium complex was 37.9 kJ mol^{-1} more stable than the *N*,arene-chelated complex. Isomerisation did not take place between the two forms because of a high barrier to conversion (85.0 kJ mol^{-1}), so it was deduced that the employment of a more *N*-electron rich ligand with a bulkier backbone substituent would be required to synthesise the η^2-*N*,*N*′-chelated complexes. This proved to be the case.

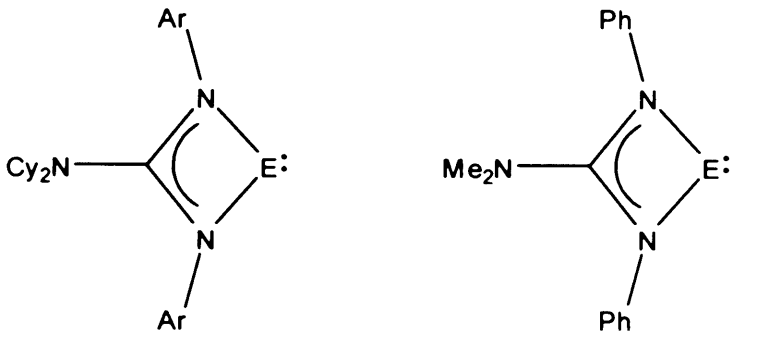

E = Ga **23**, In **24**
Ar = $C_6H_3Pr^i_2$-2,6

E = Al **25a**, Ga **25b**, In **25c**

Figure 13 – Complexes **23** and **24** and the model complexes, **25a-c**

In the model complexes, **25a-c**, the optimised geometries were similar and the HOMO and LUMO corresponded to the *sp*-type lone pair of electrons and the p_π-orbital at the metal centre respectively. The lone pair of electrons were found to be very high in *s*-character (*s*/*p* ratio Al = 1.85/0.41, Ga = 1.90/0.37, In = 1.90/0.36) and minimal interaction of the lone pairs in the N *p*-orbitals with the p_π-orbital at the metal were observed, with **25b** displaying a Ga—N bond order of 0.23. The Ga—N bonds are highly ionic, indicative of a formally monoanionic ligand binding a formally cationic group 13 element centre, similar to the five- and six-membered heterocycles discussed previously. The large HOMO – LUMO gaps (*ca.* 60 kcal mol^{-1}) for all model complexes are testament to the observed stabilities of **23** and **24**, although these gaps are smaller than in the six-membered heterocycles discussed previously (*ca.* 100 kcal mol^{-1}). The report suggests that the aluminium analogue of **23** and **24** should be synthetically viable, due to the model complex, **25a**, displaying a similar HOMO – LUMO gap to **25b** and **25c**.

1.6 The Synthesis and Coordination Chemistry of NHC Analogues

1.6.1 Four-Membered Group 13 Metal(I) Guanidinate Complexes

Synthesis of the four-membered η^2-*N*,*N*'-guanidinato gallium(I) and indium(I) NHC analogues, **23** and **24**, was achieved by treatment of the appropriate metal(I) halide with a toluene solution of the lithium guanidinate, [Li(Giso)] (Scheme 4).[74] Treatment of TlBr with [Li(Giso)] yielded the η^2-*N*,arene-guanidinato thallium(I) complex, **26**, most likely due to the increasing ionic radii in the series Ga(I)→Tl(I) not favouring *N*,*N*'-chelation in the heavier ion. The successful synthesis of these heterocycles is timely, taking into account that the first stable four-membered NHC was only recently reported.[75] Both **23** and **24** are remarkably thermally stable, considering that the element(I) centres are less sterically protected and have more acute N—M—N bite angles than in the corresponding five- and six-membered heterocycles. The bond lengths in the crystal structures obtained are indicative of extensive π-electron delocalisation over the CN_3 guanidinate backbones.

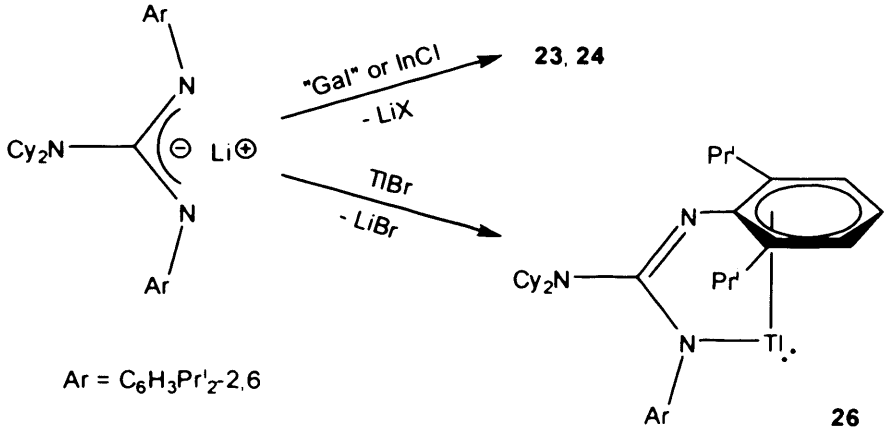

Scheme 4 – The synthesis of **23**, **24** and **26**

The coordination chemistry of **23** and **24** is currently being explored.[76-78] An initial report describes the treatment of group 10 metal(0) fragments with the

heterocycles.[76] Complexes **23** and **24** were reacted with $[Ni(\eta^4\text{-}COD)_2]$ (COD = 1,5-cyclooctadiene) and $[(dppe)Pt(\eta^2\text{-}C_2H_4)]$ under any stoichiometry to yield the disubstituted products, **27** – **29**, with the loss of one labile olefin ligand (Scheme 5). The attempted synthesis of the indium analogue of **27** led to deposition of metallic nickel at -10 °C; experimental evidence of the predicted poorer σ-donor capability of **24** over **23**. These results are in contrast with the reactions of group 13 metal(I) diyls with $[Ni(\eta^4\text{-}COD)_2]$, which yield kinetically inert homoleptic gallium and indium complexes (*vide supra*).[35,48] The reaction of **23** and **24** with $[Pd_2(dba)_3]$ (dba = dibenzylideneacetone) resulted in the deposition of palladium metal below 0 °C, but a homoleptic complex, **30**, was successfully synthesised from the treatment of three or four equivalents of **23** with $[Pt(\eta^2\text{-norbornene})_3]$.[76] The attempted synthesis of the analogous homoleptic indium complex led only to the cluster, **31**, in low yield, further proof of the differing σ-donor abilities of the two four-membered heterocycles.[77]

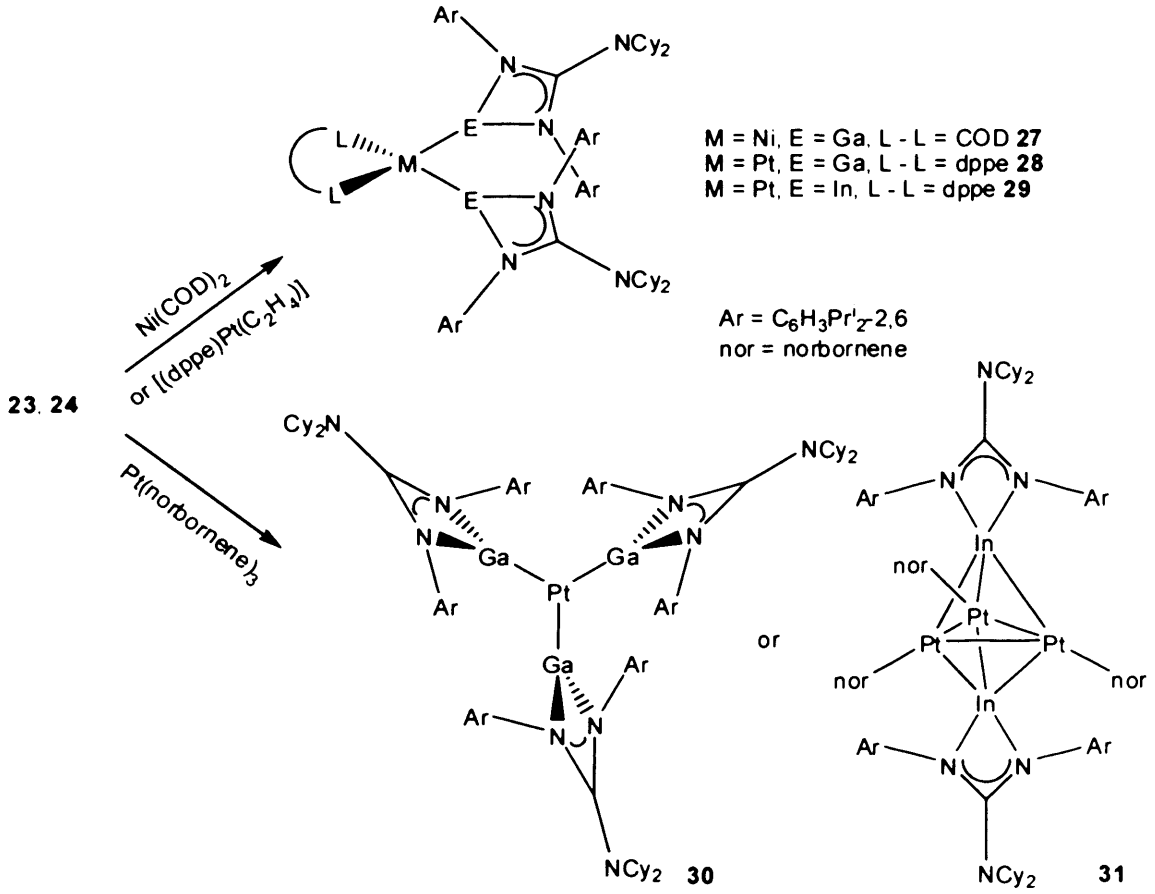

Scheme 5 – The synthesis of **27** – **31**

The steric bulk of the heterocycle, **23**, is cited as the reason why a trigonal planar three-coordinate platinum complex, **30**, is formed over a tetrahedral four-coordinate complex.[76] Despite the considerable steric crowding in **30**, the average Ga—Pt bond length of 2.309 Å is the shortest reported. This finding warranted a DFT study, utilising the model complex, $[Pt\{Ga[N(C_6H_3Me_2\text{–}2,6)]_2CNMe_2\}_3]$. A charge decomposition analysis (CDA) suggested a mean π-contribution of 39.8 % to the Ga—Pt bonds. However, this fraction only relates to the covalent component of the bonding, and given the considerable electrostatic component that must exist due to the polarisation of the Ga—Pt bonds, this π-bonding was not deemed substantial. An orbital population analysis suggested that the HOMO and HOMO – 1 of the model complex were derived from the back-donation of electron density from the filled platinum *d*-orbitals into empty *p*-orbitals at the gallium centres. These frontier orbitals represent the majority of the π-contribution to the Ga—Pt bonds.

Recent highlights of the investigation into the coordination chemistry of **23** and **24** include the synthesis of a range of platinum(II) alkyls. Treatment of the olefin precursors, $[(\eta^4\text{-CHD})Pt(Ar^F)_2]$ (CHD = 1,3-cyclohexadiene, $Ar^F = C_6F_4H$-4), $[(\eta^4\text{-CHD})Pt(Ar^{F'})_2]$ ($Ar^{F'} = C_6F_4OMe$-4), or $[(\eta^4\text{-CHD})Pt(Ar^{F''})_2]$ ($Ar^{F''} = C_6H_2F_3$-2,4,6), with two equivalents of **23** or **24** yielded the distorted square planar complexes, *cis*-$[\{Ga(Giso)\}_2Pt(Ar^F)_2]$ **32**, *cis*-$[\{Ga(Giso)\}_2Pt(Ar^{F'})_2]$ **33**, *trans*-$[\{Ga(Giso)\}_2\text{-}Pt(Ar^{F''})_2]$ **34**, *trans*-$[\{In(Giso)\}_2Pt(Ar^F)_2]$ **35**, and *trans*-$[\{In(Giso)\}_2Pt(Ar^{F'})_2]$ **36**. The five-coordinate complexes, $[\{In(Giso)\}_3Pt(Ar^F)_2]$ **37**, and $[\{In(Giso)\}_3Pt(Ar^{F'})_2]$ **38**, resulted from the addition of three equivalents of **24** to the olefin precursors.[77] The occurrence of *cis*- or *trans*-isomers in the four-coordinate complexes is thought to arise from the greater σ-donor ability of **23** over **24**, and the relative donor strengths of the differing alkyl ligands arising from their *para*-substitution patterns. The five-coordinate

compounds, **37** and **38**, are particularly noteworthy as two of the heterocycles in each exhibits In·····F interactions in the solid state. Compound **37** is depicted below as an example (Figure 14). All the platinum(II) complexes were found to be highly unstable in solution in the absence of an excess of the ligands, **23** and **24**, being present, suggesting that the heterocycles are labile in these complexes. Some success has also been achieved in the reactions of the metal(I) heterocycles with transition metal(0) carbonyl complexes.[77,78] The ruthenium complex, $[(PPh_3)_3Ru(CO)_2]$, reacts with **24** under any stoichiometry to yield the monosubstituted complex, $[(PPh_3)_2Ru\{In(Giso)\}(CO)_2]$ **39**, with the loss of one labile phosphine ligand.[77] The heterocycle occupies an equatorial position in the pseudo-trigonal bipyramidal arrangement of ligands. Unusually, the analogous gallium(I) coordination complex could not be structurally characterised. Other investigations show that **23** does not react with $[Fe(CO)_5]$, but successfully cleaves the dimer, $[Fe_2(CO)_9]$, to yield $[Fe(CO)_4\{Ga(Giso)\}]$ **40**.[78] The reaction of $[Co_2(CO)_8]$ with two equivalents of **23** gives the novel complex, **41**, in which the gallium(I) heterocycle has adopted an η^2-bridging mode. This exciting development has shown that **23** can behave like metal diyls in its coordination chemistry.

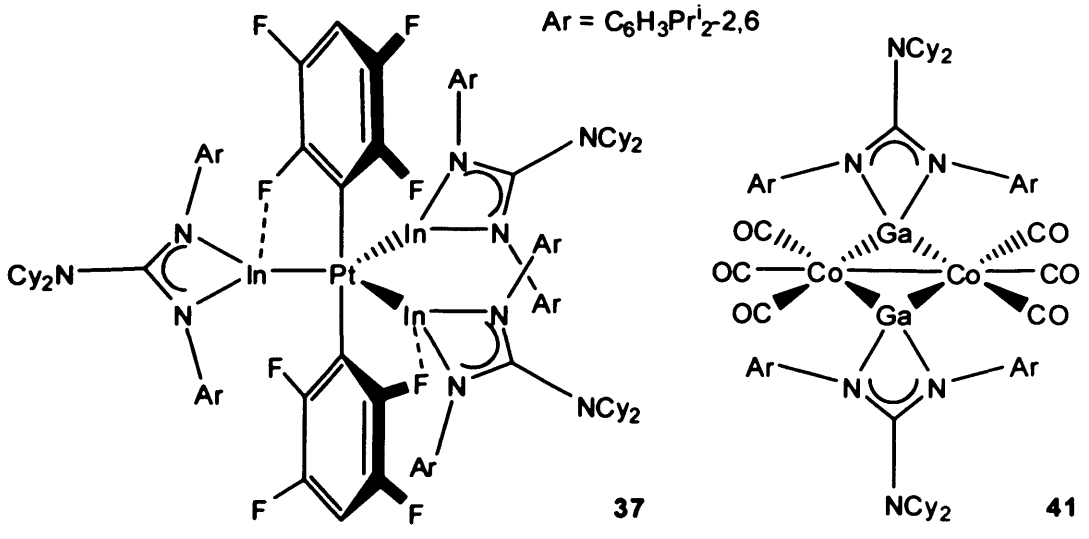

Figure 14 – Complexes **37** and **41**

1.6.2 Five-Membered Analogues of 2,3-Dihydro-imidazol-2-ylidenes

The first reported anionic group 13 five-membered NHC analogue, $[:Ga\{[N(Bu^t)C(H)]_2\}]^-$ **42**, was prepared in a multi-step synthetic route starting from $GaCl_3$.[79] Reduction of the initially formed gallium(III) complex over a potassium mirror for just over three days, through an isolable gallium(II) dimer, yielded only 4 % of the desired heterocycle as an ion-separated salt with a $[K(18\text{-crown-}6)((THF)_2]^+$ cation. A later modification of this synthetic route employed the bidentate amine tmeda (*N*,*N*,*N'*,*N'*-tetramethylethylenediamine) in the final reduction step to give an improved yield of 18 %.[80] The increased yield was obtained by increasing the reduction time to a total of fourteen days in the three step synthesis (Scheme 6). In contradiction to earlier work,[81] a (chloro)galla-imidazole was formed in good yield (80 %) from the treatment of $[\{LiN(Bu^t)C(H)\}_2]$ (Li_2Bu^t-DAB) with $GaCl_3$.[79,80] Reduction of this gallium(III) complex with two equivalents of potassium in THF yielded a gallium(II) dimer after ten days. Addition of tmeda and a further two equivalents of potassium furnished the desired gallium(I) compound after four days. The $[K(tmeda)]^+$ salt of **42** was found to aggregate into centrosymmetric dimers in the solid state, with Ga·····K contacts of 3.438 Å and 3.4681 Å.[80] Both synthetic procedures suffer from lengthy reduction times and poor yields, so the coordination chemistry of **42** was not investigated further.

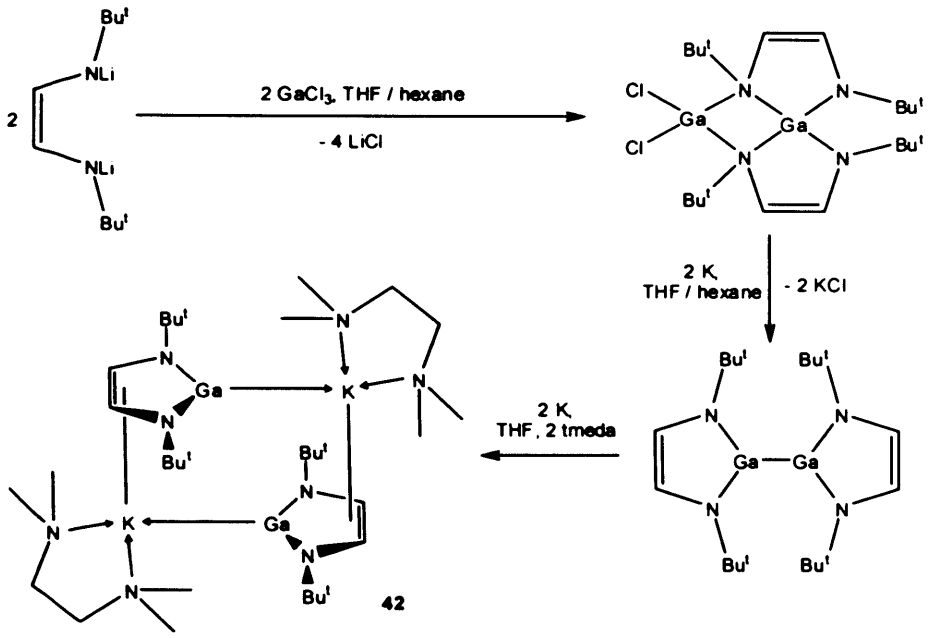

Scheme 6 – The synthesis of a potassium salt of **42**

A report on the discovery of a simple high-yielding synthetic route to an anionic five-membered gallium(I) NHC analogue, $[:Ga\{[N(Ar)C(H)]_2\}]^-$ **15** (Ar = $C_6H_3Pr^i_2$-2,6), starting from "GaI" followed several years later (Scheme 7).[63] The one-electron reduction of Ar-DAB ($\{N(Ar)C(H)\}_2$) with "GaI" gave, with the loss of one equivalent of gallium metal, a high yield (> 90 %) of the paramagnetic gallium(III) compound, $[I_2Ga\{[N(Ar)C(H)]_2^{\cdot}\}]$, which was independently synthesised by another group.[82] Reduction of this heterocycle over a potassium mirror in THF for eight hours, followed by treatment with a tmeda/Et_2O mixture, gave the salt, [K(tmeda)][**15**], in 68 % yield, presumably via the known gallium(II) dimer, $[Ga\{[N(Ar)C(H)]_2\}]_2$.[83] This salt has a similar structure to the previously reported compound, [K(tmeda)][**42**],[80] except that the Ga·····Ga distance in this compound is 4.21 Å, whereas in [K(tmeda)][**15**] this distance is only 2.88 Å, that is only 13 % longer than a typical Ga—Ga single bond. This remarkable difference is thought to arise, in addition to the electrostatic attraction between Ga^- and K^+, from a partial donation of electron density from the lone pair of electrons on each gallium centre into the empty *p*-orbital on the other. No Ga·····Ga interaction, however, was observed in the ion-separated salt, [{K(18-crown-6)}$_2$(μ–18-

crown-6)]$^{2+}$[**15**]$_2$. The high yield and ease of synthesis of **15** by this route has allowed extensive investigations into its chemistry, which has been recently reviewed.[84] A complete summary of all investigations performed into the reactivity of **15** with *s*- and *p*-block precursors is discussed in Chapter 2. The corresponding investigations into the reactivity of **15** with *d*- and *f*-block precursors are summarised in Chapter 3.

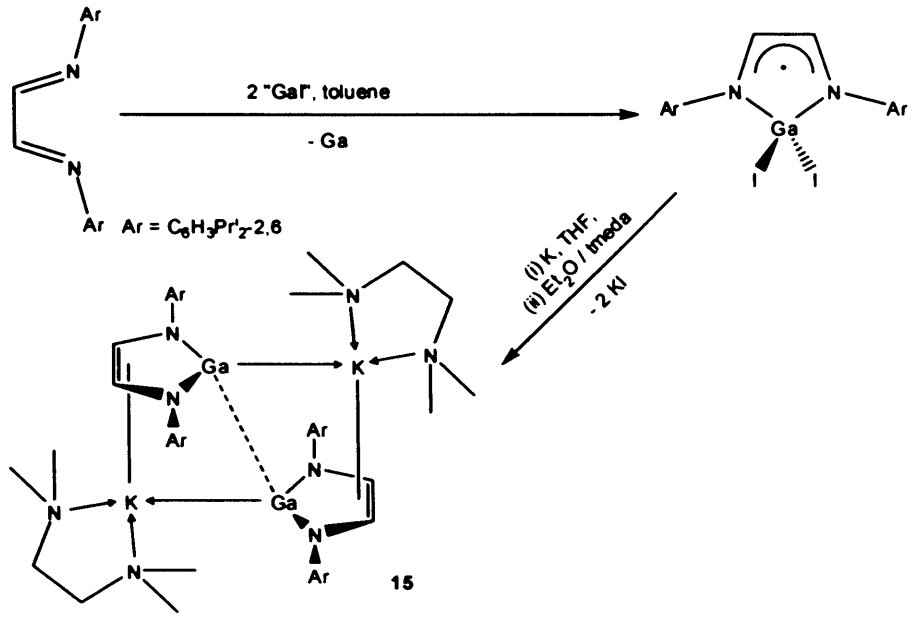

Scheme 7 – The synthesis of a potassium salt of **15**

A recent report detailing the synthesis of the boryllithium complex, [LiB{[N(Ar)C(H)]$_2$}] **43** (Ar = $C_6H_3Pr^i_2$-2,6), marks an exciting development in the investigation of anionic five-membered group 13 NHC analogues.[85a] The B—Li bond in **43** was described as lying between an ionic and covalent bond, as the bond length of 2.291 Å, derived from a structural characterisation, is 8.5 % longer than the sum of the covalent radii for boron and lithium atoms. The synthetic route to **43** involves the synthesis of a heterocyclic boron(III) precursor from di-reduced Ar-DAB and BBr_3 in 56 % yield (Scheme 8). Reduction of this precursor with lithium powder and naphthalene in THF at -45 °C affords the boryllithium, **43**, quantitatively. Spectroscopic and structural data indicate that the boron centre is sp^2-hybridised and exists in the theoretically predicted singlet state. The reactions of **43** with a selection of

organic electrophiles such as benzaldehyde confirmed the nucleophilic character of this heterocycle.[85a] Reaction of the boryllithium, **43**, with $MgBr_2$ in different stoichiometries afforded several borylmagnesium complexes, the most notable being the magnesium analogue of **43**, $[Mg(THF)_2\{B\{[N(Ar)C(H)]_2\}\}_2]$.[85b] The boryllithium, **43**, has recently been utilised in the synthesis of novel group 11 transition metal complexes, $[(IMes)MB\{[N(Ar)C(H)]_2\}]$ (M = Cu **44**, Ag **45**, Au **46**), by salt metathesis (Scheme 9).[86] Complexes **45** and **46** are the first examples of structurally characterised boryl silver and boryl gold molecular complexes, and these complexes will be discussed further in Chapter 3. At present, five-membered anionic aluminium, indium and thallium NHC analogues remain elusive.

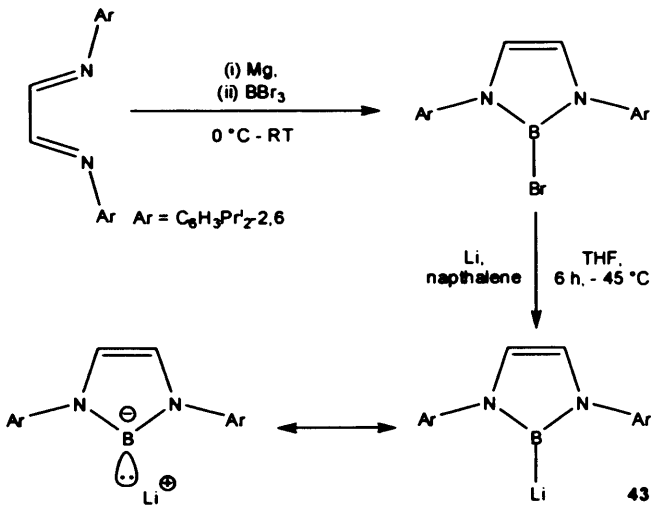

Scheme 8 – The synthesis of **43**

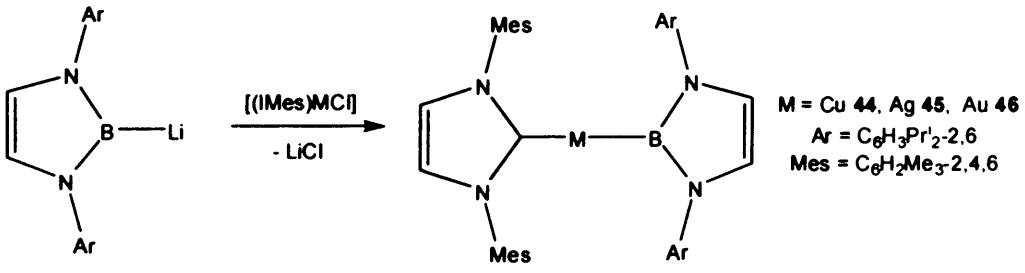

Scheme 9 – The synthesis of **44 – 46**

The first successful synthesis of a five-membered silicon(II) NHC homologue, $[:Si\{[N(Bu^t)C(H)]_2\}]$ **47**, was achieved by the reduction of a silicon(IV) precursor with

alkali metal in refluxing THF for five days (Scheme 10).[57] The chemistry of **47** and related silicon(II) NHC analogues has been, and continues to be investigated extensively; more so than any other *p*-block analogue of the NHC class of ligand.[87] In common with their lighter homologues, **8**, they have been shown to be nucleophilic (though to a lesser extent), but they display a unique chemistry due to the strong tendency of these heterocycles to oxidatively add to a wide range of complexes by bond insertion reactions.[87] The first germanium homologue of **47**, [:Ge{[N(Bu^t)C(H)]$_2$}] **48**, was prepared by salt elimination from Li_2Bu^t-DAB and [$GeCl_2$(dioxane)] (Scheme 10).[58] Investigations into the chemistry of **48** and related heterocycles are not as mature as those of the silicon analogues, but many similarities have been observed.[88] The stability of the silylene and germylene unsaturated NHC analogues is often attributed to a delocalisation of π-electron density throughout the five-membered ring.[87,88] This "aromatic" nature is less of a stabilising factor for the germylenes than the silylenes, and in both cases this delocalisation is less than that proposed for the dihydro-imidazol-2-ylidenes.

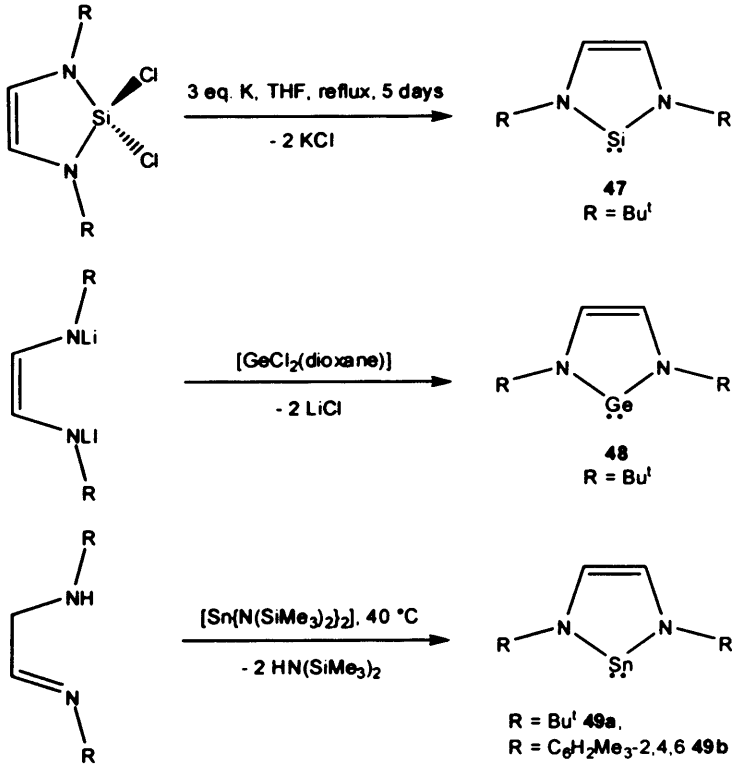

Scheme 10 – The synthesis of **47**, **48** and **49a-b**

The tin homologues of **47**, [:Sn{[N(R)C(H)]$_2$}] (**49a** R = Bu^t, **49b** R = Mes), have been synthesised by trans-amination of the α-amino aldimines with the tin(II) amide, [Sn{N(SiMe$_3$)$_2$}$_2$].[89] Their attempted synthesis from dilithiated DABs and tin dichloride in an analogous manner to the preparation of **47** proved unsuccessful. The heterocycles, **49a-b**, proved to be thermally unstable, decomposing to metallic tin and DAB at only 60 °C. The reason for this is that the tin homologues do not have extensive π-delocalisation in the five-membered ring. As such, these species are commonly depicted as a resonance form with tin(0) chelated by a DAB ligand. This resonance form explains the propensity for **49a-b** to react with other DAB ligands, not by nucleophilic attack but by formal transfer of the tin atom to the new DAB ligand to form a new tin heterocycle.[89] This unusual reactivity dominates the chemistry of these stannylenes, as the reaction of DABs with **49a-b** are the only reactions reported for these heterocycles.[89,90]

Nitrenium [**50**]$^+$,[59] phosphenium [**51**]$^+$,[60] arsenium [**52**]$^+$,[61] and stibenium [**53**]$^+$ [91] cationic group 15 analogues of **8** were first prepared by the methods depicted below (Scheme 11). Whilst the nitrenium cation, [**50**]$^+$, was synthesised by the treatment of a 1,2,3-triazole with methyl iodide,[59] [**51**]$^+$ and [**52**]$^+$ were synthesised initially by the treatment of the heterocycles, [Cl$_2$Si{[N(Bu^t)C(H)]$_2$}] and [Cl$_2$Ge{[N(Bu^t)C(H)]$_2$}], with ECl$_3$ (E = P, As) at ambient temperature, and latterly from dilithiated DAB at low temperature.[60,61] The precursor to the antimony analogues, [**53a-b**]$^+$, was synthesised from an α-amino aldimine, which was then treated with a chloride acceptor to yield the free heterocycle.[91] Subsequent investigations into the chemistry of the phosphenium cation, [**51**]$^+$Cl$^-$, have been carried out to see if the long P·····Cl distance (2.759 Å) is enough to warrant a description of this species as being a separate cation-anion pair.[92-94] The π-electrons on the *N*-substituents are thought to donate not only into the empty *p*-

orbital at P, but also into the low-lying σ* (P—Cl) orbital, weakening this bond. Treatment of $[\mathbf{51}]^+Cl^-$ with $AgPF_6$ yields the uncontested ion-separated salt, $[\mathbf{51}]^+PF_6^-$, by salt metathesis. All group 15 complexes, $[\mathbf{50}]^+$ – $[\mathbf{53a\text{-}b}]^+$, are stabilised by substantial π-electron delocalisation within the five-membered ring.[59-61,91-94] The series of valence isoelectronic analogues of **8** has recently been extended with the synthesis of a dicationic selenium analogue, $[\mathbf{54}]^{2+}$, from selenium tetrachloride and Ar-DAB (Ar = $C_6H_3Pr^i_2$-2,6) at ambient temperature, with tin dichloride as the reducing agent (Scheme 11).[95] This heterocycle is thought to have little π-delocalisation, and is viewed formally as a Se^{2+} cation chelated by a diimine fragment.

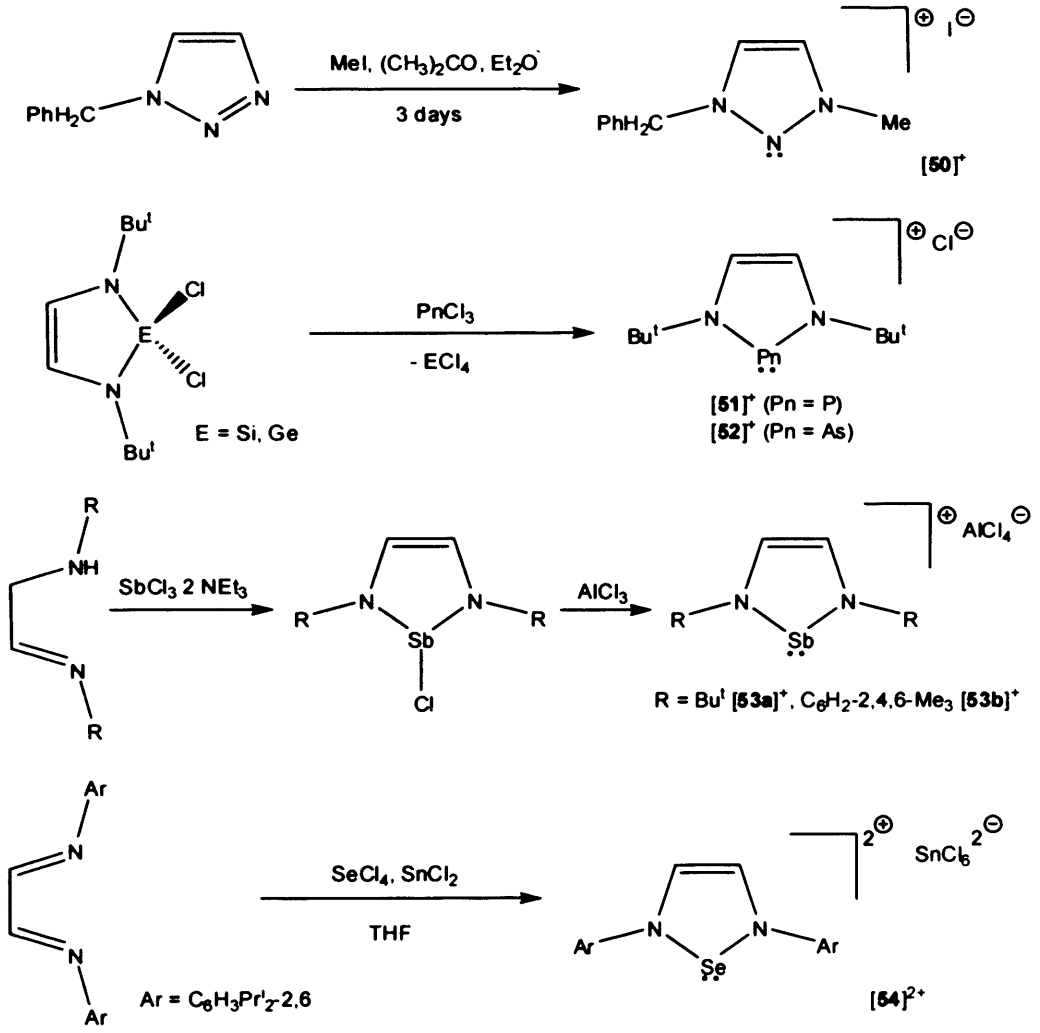

Scheme 11 – The synthesis of **50 – 54**

1.6.3 Six-Membered Group 13 β-Diketiminate Complexes

The synthetic routes to aluminium(I) **17a-b**,[65] gallium(I) **18**,[66] indium(I) **21a-b**[69,70] and thallium(I) **22a-c**[70] β-diketiminate complexes are summarised below (Scheme 12). The aluminium(I) compound, **17a**, is prepared in low yield by the reduction of the aluminium(III) precursor, **55a**,[65] whilst a salt metathesis reaction from a lithiated β-diimine and "GaI" was the favoured method for the synthesis of the gallium(I) heterocycle, **18**, also in a low yield (39 %).[66] A salt metathesis reaction has been shown to be a successful route for the preparation of the thallium(I) analogues, **22a-b**, in good yield (82 % and 80 % respectively).[70a] An alternative "one pot" preparation starting from the β-diimine was shown to be effective in the preparations of the indium(I) heterocycles, **21a** (36 % yield),[69] and **21b** (58 % yield).[70b] This procedure also proved successful in the preparation of the novel thallium analogue, **22c**, in *ca.* 40 % yield.[70b] Recently, the synthesis of a novel aluminium(I) β-diketiminate, **17b**, has been reported in poor yield by an analogous procedure to that employed for **17a**, in 20 % yield.[96] Only the thallium(I) analogues, **22a-c**, do not display planarity in the 6-membered ring, because of the large size of the metal.

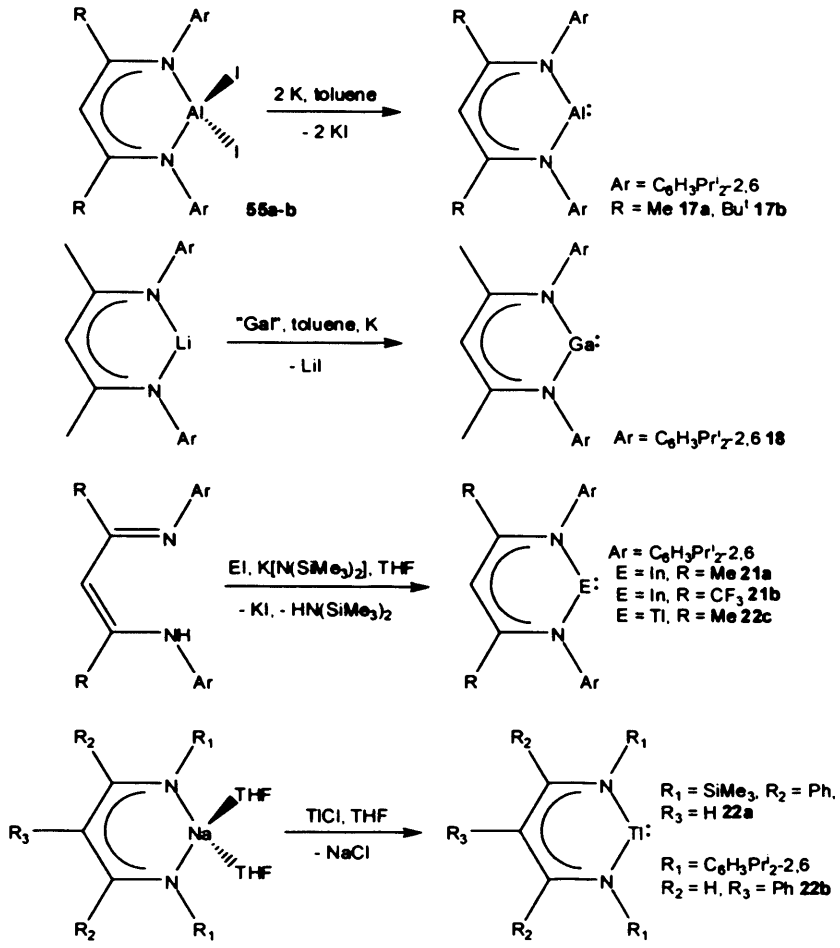

Scheme 12 – The synthesis of **17a-b**, **18**, **21a-b** and **22a-c**

The reactivity of the heterocycles, **17a-b**, **18**, **21a-b** and **22a-c** is currently being investigated, and will be summarised here. Most investigations to date have centred around the heterocycles, **17a** and **18**. Their reactions with group 13 precursors are summarised below (Scheme 13). Treatment of **18** with the Lewis base, $B(C_6F_5)_3$, gave the expected donor-acceptor complex, **56**.[97] In contrast, the reaction of **17a** with the same substrate led to the formation of **57**, which displays a relatively close Al·····F contact (2.156 Å).[97] The aluminium centre is formally acting as a Lewis base towards the electron deficient boron atom and as a Lewis acid to an *ortho*-fluorine atom. The authors have coined the term "Janus-faced" to describe the unique behaviour of the aluminium atom in this complex. Complexes **56** and **57** both display relatively long E—B bonds, and the boron centres exhibit a distorted tetrahedral geometry. An investigation into the redox reaction of **17a** with two equivalents of $PhB(OH)_2$ yielded

the aluminium(III) compound, **58**, proposed to be driven by the exothermic formation of two Al—O bonds.[99] The same product was obtained by reacting $PhB(OH)_2$ with an aluminium(III) hydride precursor.[99]

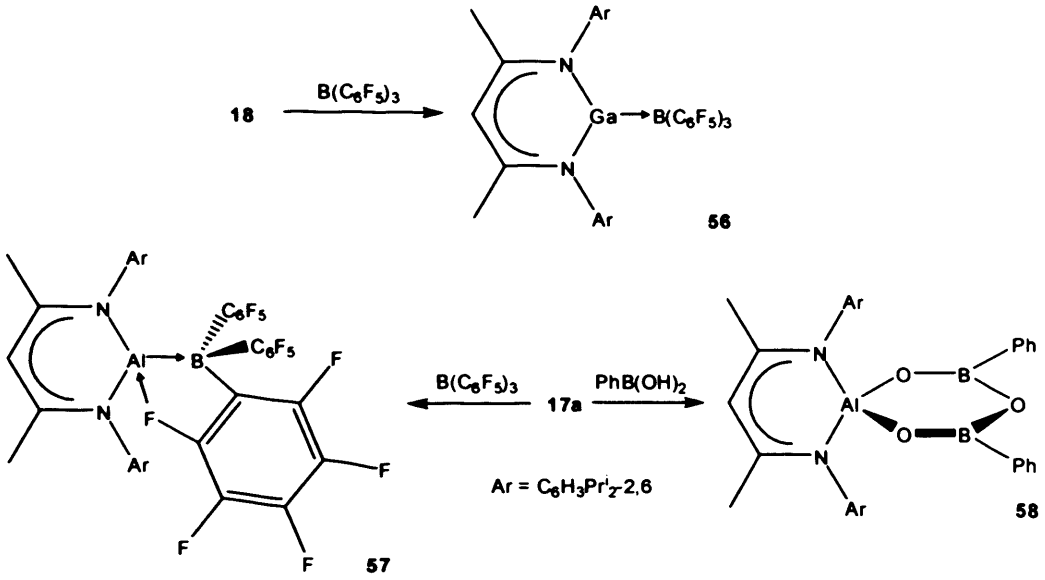

Scheme 13 – The reactions of **17a** and **18** with group 13 precursors

Investigations into the reactivity of the aluminium(I) heterocycle, **17a**, with organic substrates have proved fruitful. Alkynes react with equimolar quantities of **17a** to form the aluminacyclopropenes, **59a-d**, by an oxidative cycloaddition in excellent yields (Scheme 14).[100] This methodology provides a useful synthetic route to the aluminacyclopropenes, which were previously synthesised by the reduction of the aluminium(III) diiodide, **55a**, in the presence of alkynes.[101] Compounds **59a-b** could not be prepared by the reduction pathway due to the metallation of the acetylenic proton, hence the new synthetic route has proved useful. The further reactivity of these novel three-membered rings towards unsaturated precursors such as carbon monoxide, isocyanides, dioxygen, carbon disulphide, carbon dioxide, ketones, nitriles and azides has been extensively investigated.[101,102] A recent report into the reactivity of an aluminacyclopropene with pyridine and water has further illustrated the importance of these compounds.[103] The addition of an excess of terminal alkynes to **17a** yielded the

alkenylalkynyl aluminium complexes, **60** and **61**, by the migration of an acetylenic proton, whereas the addition of an excess of the internal alkynes gave only **59c-d**.[100]

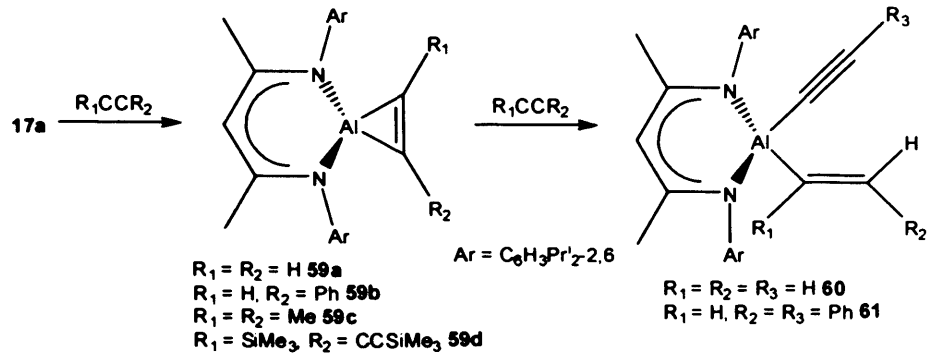

Scheme 14 – The reactivity of **17a** towards alkynes

The group 13 β-diketiminate complexes have proved reactive towards other organic substrates; a summary is given here (Figure 15). Heating **17a** and 2,3-dihydro-imidazol-2-ylidenes in the solid state gave the aluminium monohydride adducts, **62a-b**, by the migration of a proton from a methyl group on the β-diketiminato backbone.[104] The reaction of two equivalents of a bulky isocyanide with **55**, in contrast, gave the novel spirocycles, **63** and **64**, depending on the reaction conditions employed.[96] These heterocycles are formed via the oxidative coupling of two isocyanide units mediated by the aluminium centre. Treatment of **18** with an excess of the less bulky isocyanide, Bu^tNC, gave the simple oxidative insertion product, $[(Bu^t)(NC)Ga\{[N(Ar)C(Me)]_2CH\}]$ **65**.[105] The treatment of **17a** with two equivalents of diphenyldiazomethane gave the diiminylaluminium compound, **66**, with the loss of dinitrogen.[104] Experimental evidence points towards the initial formation of $Ph_2C{=}N{-}N{=}CPh_2$ and the subsequent oxidative addition of **17a** into the N—N bond. Azobenzene reacts with **17a** at elevated temperatures to give the spirocycle, **67**.[106] The reaction mechanism was proposed to involve initial η^2-coordination of the azo group followed by rearrangement of azobenzene by cleavage of the N—N bond and transfer of an *ortho*-phenyl proton to form the tertiary amine. Treatment of the indium(I) analogue, **21a**, with a variety of

alkyl halides gave the oxidative insertion products, **68a–e**.[107] The authors noted that the bromides, **68d** and **68e**, are easily converted to the iodides by addition of KI, and proposed a radical mechanism for the observed bond insertion.

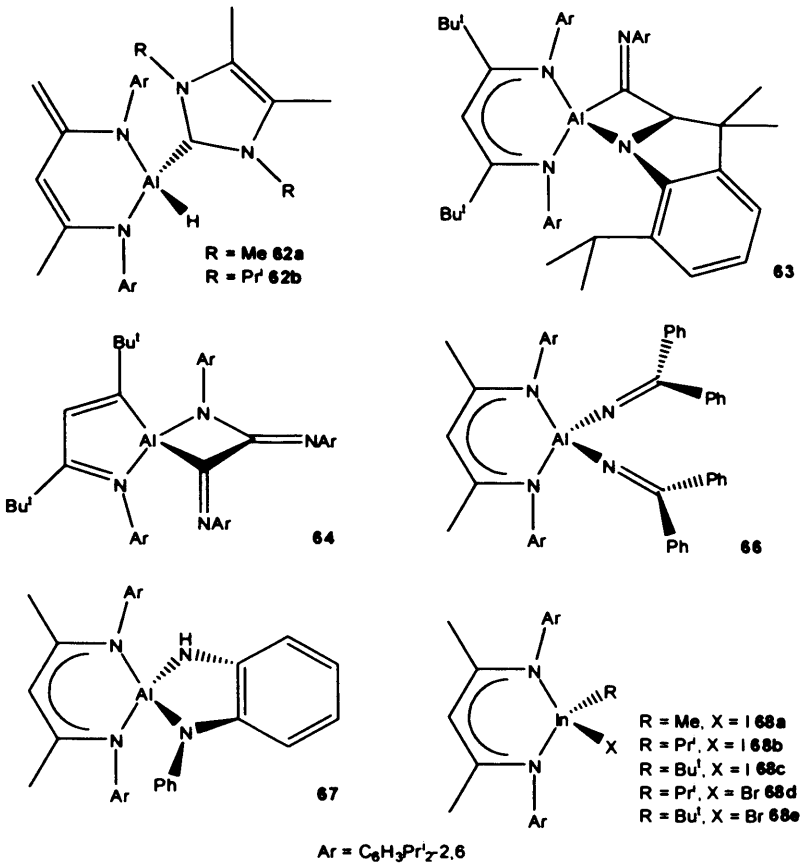

Figure 15 – Complexes **62 – 64** and **66 – 68**

The reactivity of group 13 β-diketiminate complexes towards a variety of azides continues to be examined thoroughly (Figure 16).[96,108] The employment of a sufficiently bulky terphenyl azide, N_3-Ar* (Ar* = $C_6H_3(C_6H_2Pr^i_3$-2,4,6)$_2$-2,6), allowed the synthesis of the stable monomeric imides, **69** and **70**, from **17a** and **18** respectively.[108a] A structural characterisation of the gallium analogue, **70**, revealed a short Ga=N imide bond, which was determined to have little π-bond character by DFT analysis. The reaction of **17a** with the less bulky terphenyl azide, N_3-Ar# (Ar# = $C_6H_3(C_6H_3Pr^i_2$-2,6)$_2$-2,6), gave the rearranged products, **71** and **72a**.[108b] Both compounds are thought to arise from a short-lived imide intermediate which undergoes either a [2 + 2] cycloaddition, to form **71**, or an intramolecular C—H activated addition,

to form **72a**. It is noteworthy that heating a toluene/hexane solution of **71** facilitated the thermal conversion of this strained compound into the more thermodynamically favourable product, **72a**. Treatment of the more bulky aluminium(I) heterocycle, **17b**, with N_3-Ar$^{\#}$ gave exclusively the thermodynamic product, **72b**.[96] The less bulky azide, $(N_3)_3$-SiBu^t, reacts with one equivalent of **17a** to yield the unprecedented dimeric compound, **73**.[108c] This mixed amide/azide compound is thought to arise from the migration of the azide group to aluminium in a short lived imide intermediate. An N=Si bond is formed, which may undergo a [2 + 2] cycloaddition to generate the observed product. Other azides, such as adamantyl azide (N_3-$C_{10}H_{15}$), N_3-$SiPh_3$ and N_3-$SiMe_3$ react with **17a** to yield the tetrazoles, **74a**, **74b** and **74c** respectively.[108c-d] Interestingly, the gallium(I) β-diketiminate complex, **18**, reacts with N_3-$SiMe_3$ to give a 1 : 3 mixture of the tetrazole, **75**, and the amide/azide isomer, **76**.[108d]

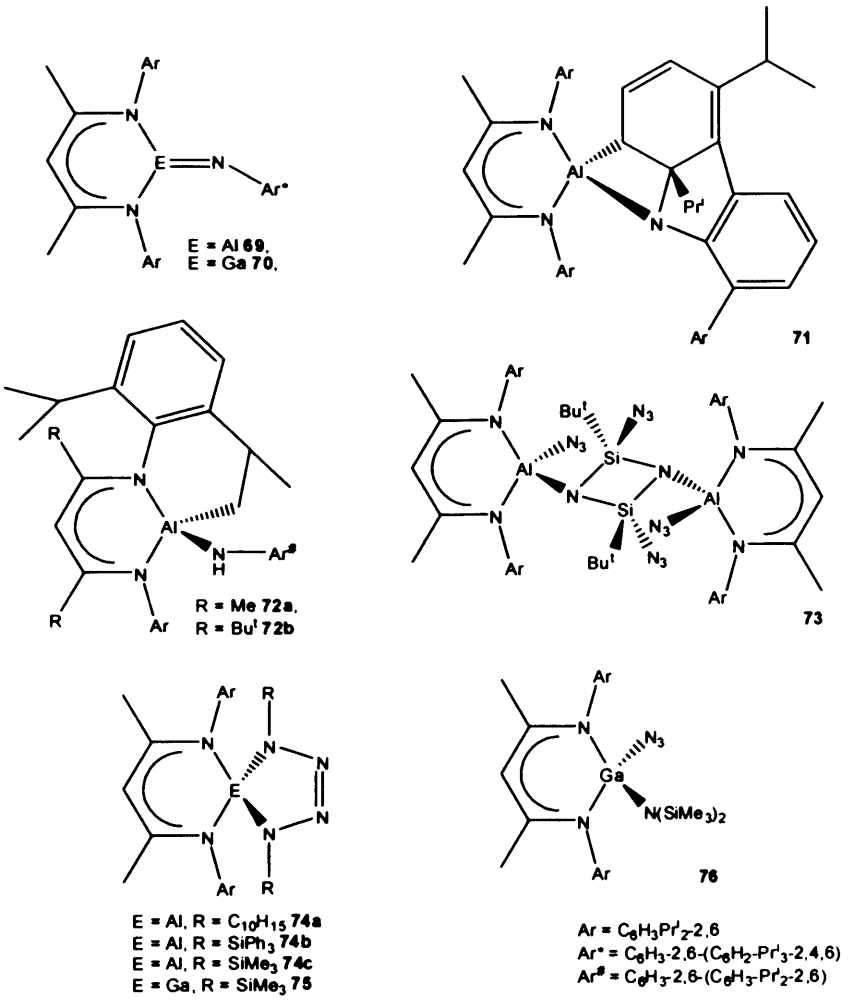

Figure 16 – Complexes **69 – 76**

The reactivity of group 13 β-diketiminate complexes towards group 15 and 16 precursors has been investigated (Figure 17).[96,109-112,114] Addition of **18** to the phosphenium-phosponium salt, $[Ph_3P—PPh_2][SO_3CF_3]$, yielded complex **77**, with the loss of triphenylphosphine.[109] This complex contains a rare example of a group 13 centre acting as a Lewis base towards the Lewis acceptor, phosphorus. The aluminium(I) heterocycle, **17a**, reacts with white phosphorus, P_4, in a 2 : 1 stoichiometry to yield **78**.[110] DFT studies of the bonding in this complex point toward highly ionic Al—P bonding and a formal $[P_4]^{4-}$ core in this complex. The controlled oxidation of **17b** with stoichiometric quantities of water have led to the isolable hydroxyaluminium hydride, **79**,[96] and **17a** and **18** react with an excess of $N_2O_{(g)}$ to yield the bridged dimers, **80a** and **81a**, which display short E·····E contacts (E = Al, Ga).[111,112] The reaction of **80a** with a stoichiometric amount of water gave the alumoxane, **82**, which had been previously synthesised by a different route.[113] Treatment of **18** with an excess of elemental sulphur, S_8, gave the bridged dimer, **81b**, which is isostructural to the oxygen analogue.[112] The aluminium(I) complex **17a**, in contrast, reacts with S_8 in a 2 : 6 stoichiometry to give the polysulphide, **83**, in low yield.[114] This complex exhibits two μ-S_3 chains connecting two aluminium atoms to give an Al_2S_6 bimetallic analogue of the S_8 ring. The bridged dimer, **80b**, analogous to the gallium complex, **81b**, can be prepared by changing the reaction conditions and had previously been synthesised by another method.[115]

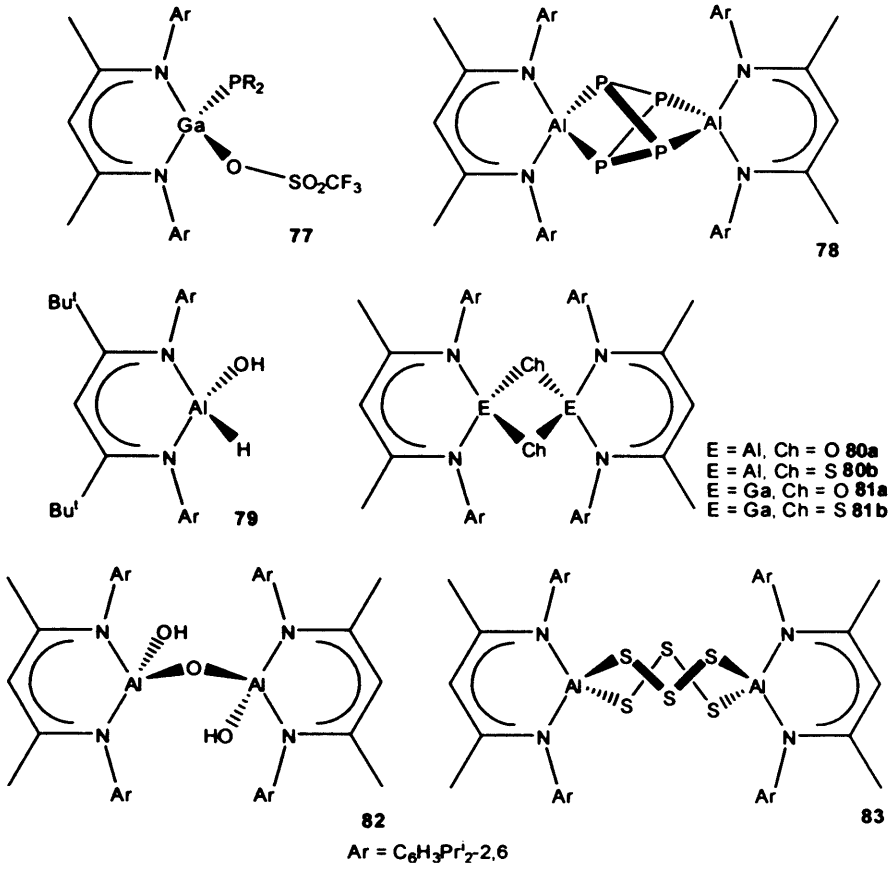

Figure 17 – Complexes **77 – 83**

The transition metal coordination chemistry of the group 13 β-diketiminate complexes is remarkably under-developed in comparison to the number of investigations concerned with *p*-block precursors. The reactions of **17a** and **18** with non-olefinic transition metal complexes are summarised below (Figure 18).[25,116,117] In an analogous manner to the metal(I) diyls previously discussed, **18** reacts with iron pentacarbonyl to give the monosubstituted product, **84**, by displacement of CO under any stoichiometry.[25] Recent reports show that **18** displays a tendency to insert into transition metal-halide bonds.[116,117] Addition of **18** to [(PPh_3)AuCl] gives the complexes, **85a** and **85b**, depending on the stoichiometry of the reaction.[116] Treatment of **85b** with $Na[BAr^{F'''}_4]$ ($Ar^{F'''}$ = $C_6H_3(CF_3)_2$-3,5) gave the linear homoleptic cation, **86**, by salt metathesis, with $BAr^{F'''}_4$ as the counter-ion.[117] Unusually, the reaction of **43** with

$[(PPh_3)_3RhCl]$ gave the chloride-bridged product, **87**.[117] This compound can be regarded as a "frozen intermediate" of the insertion of **18** into a Rh—Cl bond.

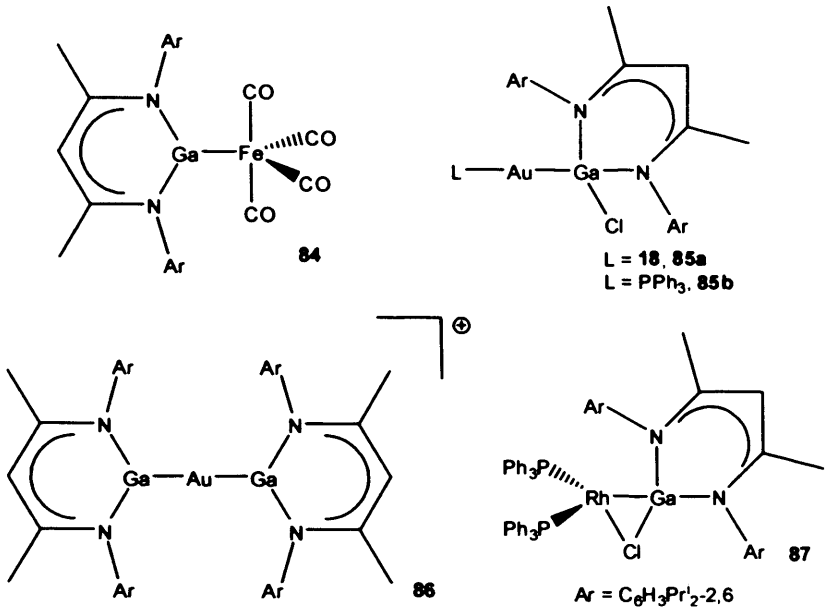

Figure 18 – Complexes **84** – **87**

The reactions of **17a** and **18** with olefinic transition metal precursors are summarised below (Figure 19).[105,117-119] The insertion of **17a** into the dimer, $[(\eta^2\text{-}COE)_2RhCl]_2$ (COE = cyclooctene), in benzene gives the "piano stool" complex, **88**.[117] No isolable products were obtained in the absence of benzene. A range of nickel(0) olefin complexes, **89a-d**, have been synthesised starting from $[Ni(\eta^6\text{-CDT})]$ (CDT = 1,5,9-cyclododectatriene), $[Ni(\eta^2\text{-}C_2H_4)_3]$ and **18**.[118] Careful manipulation of the reaction conditions yielded a number of Ga_xNi_y clusters (x = 1-2, y = 2-3), the most remarkable of which is the hydride, **90**. A number of platinum(0) and palladium(0) complexes have been prepared by the treatment of **17a** and **18** with $[Pd_2(dvds)_3]$ (dvds = 1,1,3,3-tetramethyl-1,3-divinyldisiloxane) and $[Pt(\eta^4\text{-COD})_2]$, such as **91** and **92**.[105,119] Such compounds have been shown to undergo further loss of olefins by reaction with $[:Ga(\eta^5\text{-Cp}^*)]$ to give clusters,[119] and with CO or Bu^tNC to give **93a-d**.[105] Treatment of $[Pt(\eta^4\text{-COD})_x(\mathbf{18})_y]$ (x = 1-2, y = 1-2) with hydrogen gas and triethylsilane gave a

variety of hydrides, such as **94**.[105] The reactivity of aluminium(I) and gallium(I) β–diketiminate complexes has been summarised in several reviews.[22a,85,120]

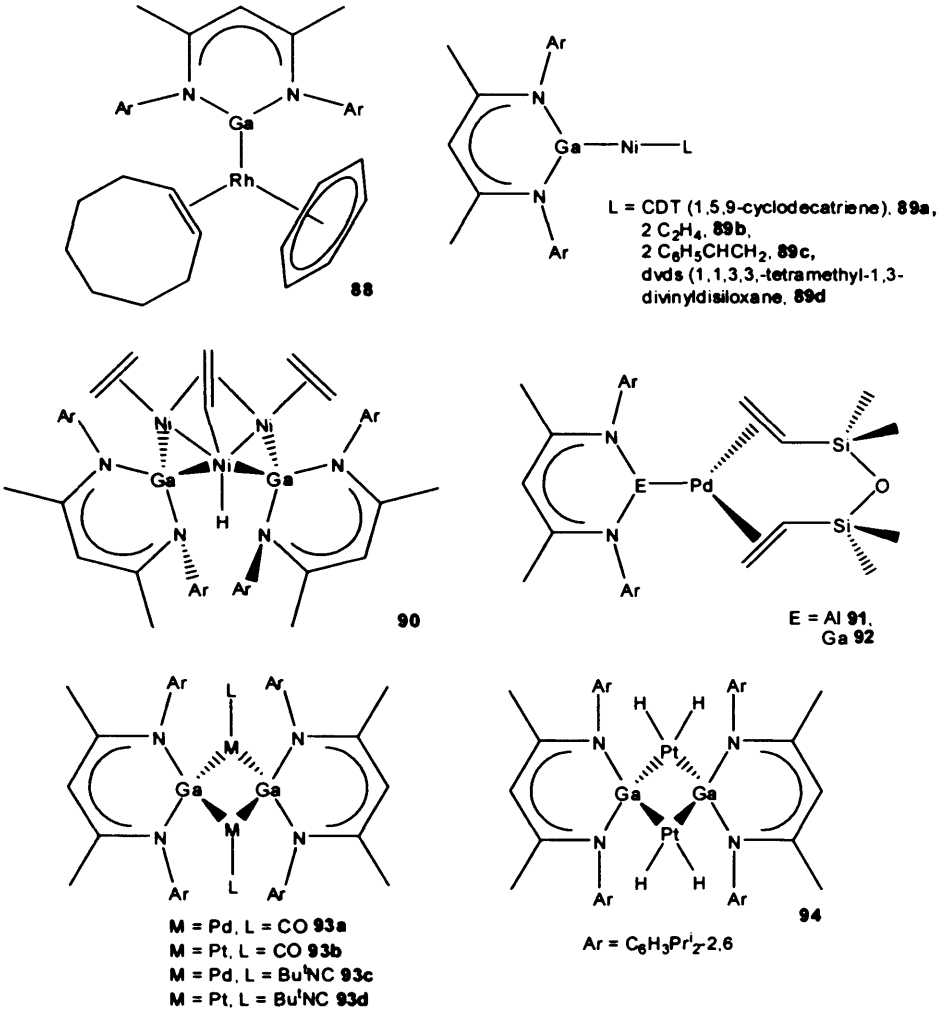

Figure 19 – Complexes **88 – 94**

In comparison to the large number of investigations into the reactivity of NHCs and group 13 metal diyls, studies of the chemistry of **15** are remarkably under-developed. It is the main objective of this thesis to describe further investigations into the reactivity of **15**.

1.7 References

1. N. N. Greenwood and A. Earnshaw, *The Chemistry of the Elements*, 2nd Edition, Oxford, Butterworth-Heinemann, 1997.

2. Ed. A. J. Downs, *Chemistry of Aluminium, Gallium, Indium and Thallium*, Glasgow, Blackie Academic and Professional, 1993.

3. J. Emsley, *The Elements*, 3rd Edition, New York, Oxford University Press, 1998.

4. J. E. Huheey, *Inorganic Chemistry: Principles of Structure and Reactivity*, 4th Edition, New York, Harper Collins College Publishers, 1993.

5. (a) A. Schnepf, H. Schnöckel, *Angew. Chem. Int. Ed.*, 2002, **41**, 3533; (b) H. Schnöckel, A. Schnepf, *Adv. Organomet. Chem.*, 2001, **47**, 235; (c) G. Linti, H. Schnöckel, *Coord. Chem. Rev.*, 2000, **206-207**, 285, and references therein.

6. (a) W. Hönle, G. Miller, A. Simon, *J. Solid State Chem.*, 1988, **75**, 147; (b) W. Hönle, A. Simon, *Z. Naturforsch.*, 1986, **41b**, 1391.

7. (a) J. C. Beamish, R. W. H. Small, I. J. Worral, *Inorg. Chem.*, 1979, **18**, 220; (b) P. Wei, X. –W. Li, G. H. Robinson, *Chem. Commun.*, 1999, 1287; (c) K. L. Brown, D. Hall, *Dalton Trans.*, 1973, 1843; (d) G. Gerlach, W. Hönle, A. Simon, *Z. Anorg. Allg. Chem.*, 1982, **486**, 7.

8. S. M. Godfrey, K. J. Kelly, P. Kramkowski, C. A. McAuliffe, R. G. Pritchard, *Chem. Commun.*, 1997, 1001.

9. (a) M. Mocker, C. Robl, H. Schnöckel, *Angew. Chem. Int. Ed. Engl.*, 1994, **33**, 862; (b) A. Ecker, E. Baum, M. A. Freisen, R. Koppe, M. A. Junker, C. Üffing, H. Schnöckel, *Z. Anorg. Allg. Chem.*, 1998, **624**, 513.

10. C. Dohmeier, D. Loos, H. Schnöckel, *Angew. Chem. Int. Ed. Engl.*, 1996, **35**, 129, and references therein.

11. C. U. Doriat, E. Baum, A. Ecker, H. Schnöckel, *Angew. Chem. Int. Ed. Engl.*, 1997, **36**, 1969.

12. (a) M. Mocker, C. Robl, H. Schnöckel, *Angew. Chem. Int. Ed. Engl.*, 1994, **33**, 1754; (b) A. Ecker, H. Schnöckel, *Z. Anorg. Allg. Chem.*, 1996, **622**, 149; (c) A.

Ecker, H. Schnöckel, *Z. Anorg. Allg. Chem.*, 1998, **624**, 813, and references therein.

13. A. Schnepf, H. Schnöckel, *Angew. Chem. Int. Ed.*, 2001, **40**, 711.

14. A. Ecker, H. Schnöckel, *Nature*, 1997, **387**, 379.

15. M. L. Green, P. Mountford, G. J. Smout, S. R. Speel, *Polyhedron*, 1990, **9**, 2763.

16. S. Coban, Diplomarbeit, Universität Karlsruhe, 1999.

17. (a) S. Green, C. Jones, A. Stasch, R. P. Rose, *New J. Chem.*, 2007, **31**, 127; (b) R. J. Baker, C. Jones, M. Kloth, D. P. Mills, *New J. Chem.*, 2004, **28**, 207; (c) R. J. Baker, C. Jones, *Chem. Commun.*, 2003, 390.

18. V. Nair, S. Ros, C. N. Jayan, B. S. Pillai, *Tetrahedron*, 2004, **60**, 1959, and references therein.

19. R. J. Baker, C. Jones, *Dalton Trans.*, 2005, 1341.

20. G. Linti, S. Coban, A. Rodig, N. Sandholzer, *Z. Anorg. Allg. Chem.*, 2003, **629**, 1329.

21. A. Schnepf, E. Weckert, G. Linti, H. Schnöckel, *Angew. Chem. Int. Ed.*, 1999, **38**, 3381.

22. (a) C. Gemel, T. Steinke, M. Cokoja, A. Kempter, R. A. Fischer, *Eur. J. Inorg. Chem.*, 2004, 4161; (b) R. A. Fischer, J. Weiss, *Angew. Chem. Int. Ed.*, 1999, **38**, 2830; (c) W. Uhl, *Coord. Chem. Rev.*, 1997, **163**, 1, and references therein.

23. C. Boehme, J. Uddin, G. Frenking, *Coord. Chem. Rev.*, 2000, **197**, 249, and references therein.

24. J. Su, X. -W. Li, R. C. Crittendon, C. F. Campana, G. H. Robinson, *Organometallics*, 1997, **16**, 4511.

25. N. J. Hardman, R. J. Wright, A. D. Phillips, P. P. Power, *J. Am. Chem. Soc.*, 2003, **125**, 2667.

26. F. A. Cotton, X. Feng, *Organometallics*, 1998, **17**, 128.

27. (a) J. Udding, G. Frenking, *J. Am. Chem. Soc.*, 2001, **123**, 1683; (b) C. Boehme, G. Frenking, *Chem. Eur. J.*, 1999, **5**, 2184; (c) D. L. Reger, D. G. Garza, A. L. Rheingold, G. P. A. Yap, *Organometallics*, 1998, **17**, 3624; (d) P. Jutzi, B. Neumann, G. Neumann, H. –G. Stammler, *Organometallics*, 1998, **17**, 1305.

28. E. O. Fischer, H. P. Hofmann, *Angew. Chem.*, 1957, **69**, 639.

29. E. O. Fischer, *Angew. Chem.*, 1957, **69**, 207.

30. C. Dohmeier, C. Robl, M. Tacke, H. Schnöckel, *Angew. Chem. Int. Ed. Engl.*, 1991, **30**, 564.

31. D. Loos, H. Schnöckel, *J. Organomet. Chem.*, 1993, **463**, 37.

32. D. Loos, E. Baum, A. Ecker, H. Schnöckel, A. J. Downs, *Angew. Chem. Int. Ed. Engl.*, 1997, **36**, 860.

33. (a) M. Schormann, K. S. Klimek, H. Hatop, S. P. Varkey, H. W. Roesky, C. Lehmann, C. Röpken, R. Herbst-Ermer, M. Noltemeyer, *J. Solid State Chem.*, 2001, **162**, 225; (b) S. Schulz, H. W. Roesky, H. J. Koch, G. M. Scheldrick, D. Stalke, A. Kuhn, *Angew. Chem. Int. Ed. Engl.*, 1993, **32**, 1729.

34. (a) P. Jutzi, L. O. Schebaum, *J. Organomet. Chem.*, 2002, **654**, 176; (b) P. Jutzi, B. Neumann, G. Reumann, H. –G. Stammler, *Organometallics*, 1998, **17**, 1305.

35. P. Jutzi, B. Neumann, L. O. Schebaum, A. Stammler, H. –G. Stammler, *Organometallics*, 1999, **18**, 4462.

36. C. Gemel, T. Steinke, D. Weiss, M. Cokoja, M. Winter, R. A. Fischer, *Organometallics*, 2003, **22**, 2705.

37. M. Cokoja, C. Gemel, T. Steinke, T. Welzl, M. Winter, R. A. Fischer, *J. Organomet. Chem.*, 2003, **684**, 277.

38. (a) M. Cokoja, C. Gemel, T. Steinke, F. Schröder, R. A. Fischer, *Dalton Trans.*, 2005, 44; (b) T. Steinke, C. Gemel, M. Cokoja, M. Winter, R. A. Fischer, *Dalton Trans.*, 2005, 55.

39. B. Buchin, C. Gemel, T. Cadenbach, R. Schmid, R. A. Fischer, *Angew. Chem. Int. Ed.*, 2006, **45**, 1074.

40. C. Schnitter, H. W. Roesky, C. Ropken, R. Herbst-Irmer, H. –G. Schmidt, M. Noltemeyer, *Angew. Chem. Int. Ed.*, 1998, **37**, 1952.

41. W. Uhl, W. Hiller, M. Layh, W. Schwarz, *Angew. Chem. Int. Ed. Engl.*, 1992, **31**, 1364.

42. (a) R. D. Schluter, A. H. Cowley, D. A. Atwood, R. A. Jones, J. L. Atwood, *J. Coord. Chem.*, 1993, **30**, 25; (b) W. Uhl, R. Graupner, M. Layh, U. Schütz, *J. Organomet. Chem.*, 1995, **493**, C1.

43. W. Uhl, S. U. Keimling, K. W. Klinkhammer, W. Schwarz, *Angew. Chem. Int. Ed. Engl.*, 1997, **36**, 64.

44. M. A. Cook, C. Eaborn, A. E. Jukes, D. R. M. Walton, *J. Organomet. Chem.*, 1970, **24**, 529.

45. W. Uhl, A. Jantschak, *J. Organomet. Chem.*, 1998, **555**, 263.

46. T. Steinke, C. Gemel, M. Cokoja, M. Winter, R. A. Fischer, *Chem. Commun.*, 2003, 1066.

47. W. Uhl, S. U. Keimling, M. Pohlmann, S. Pohl, W. Saak, W. Hiller, M. Neumayer, *Inorg. Chem.*, 1997, **36**, 5478.

48. W. Uhl, M. Benter, S. Melle, W. Saak, G. Frenking, J. Uddin, *Organometallics*, 1999, **18**, 3778.

49. W. Uhl, M. Pohlmann, R. Wartchow, *Angew. Chem. Int. Ed.*, 1998, **37**, 961.

50. (a) D. Bourissou, O. Guerret, F. P. Gabbai, G. Bertrand, *Chem. Rev.*, 2000, **100**, 39; (b) W. Kirmse, *Eur. J. Org. Chem.*, 2005, 237; (c) W. A. Herrmann, *Angew. Chem. Int. Ed.*, 2002, **41**, 1290; (d) C. M. Crudden, D. P. Allen, *Coord. Chem. Rev.*, 2004, **248**, 2247; (e) N. Kuhn, A. Al-Sheikh, *Coord. Chem. Rev.*, 2005,

249, 829; (f) C. J. Carmalt, A. H. Cowley, *Adv. Inorg. Chem.*, 2000, **50**, 1, and references therein.

51. A. J. Arduengo III, R. L. Harlow, M. Kline, *J. Am. Chem. Soc.*, 1991, **113**, 361.

52. H. –W. Wanzlick, H. –J. Schönherr, *Angew. Chem. Int. Ed. Engl.*, 1968, **7**, 141.

53. K. Öfele, *J. Organomet. Chem.*, 1968, **12**, P42.

54. (a) P. Schwabb, M. B. France, J. W. Ziller, R. H. Grubbs., *Angew. Chem. Int. Ed. Engl.*, 1995, **34**, 2039; (b) P. Schwabb, R. H. Grubbs, J. W. Ziller, *J. Am. Chem. Soc.*, 1996, **118**, 100.

55. M. Scholl, T. M. Trnka, J. P. Morgan, R. H. Grubbs, *Tetrahedron Let.*, 1999, **40**, 2247.

56. (a) M. –T. Lee, C. –H. Hu, *Organometallics*, 2004, **23**, 976; (b) W. A. Herrmann, T. Weskamp, V. P. W. Böhm, *Adv. Organomet. Chem.*, 2001, **48**, 1, and references therein.

57. M. K. Denk, R. Lennon, R. Hayashi, R. West, A. V. Belyakov, H. P. Verne, A. Haaland, M. Wagner, N. Metzler, *J. Am. Chem. Soc.*, 1994, **116**, 2691.

58. W. A. Herrmann, M. K. Denk, J. Behm, W. Scherer, F. –R. Klingan, H. Bock, B. Solouki, M. Wagner, *Angew. Chem. Int. Ed. Engl.*, 1992, **31**, 1485.

59. G. Boche, P. Andrews, K. Harms, M. Marsch, K. S. Rangappa, M. Schimeczek, C. Willeke, *J. Am. Chem. Soc.*, 1996, **118**, 4925.

60. M. K. Denk, S. Gupta, R. Ramachandran, *Tetrahedron Lett.*, 1996, **37**, 9025.

61. C. J. Carmalt, V. Lomeli, B. G. McBurnett, A. H. Cowley, *Chem. Commun.*, 1997, 2095.

62. (a) A. Sundermann, M. Reiher, W. W. Schoeller, *Eur. J. Inorg. Chem.*, 1998, 305; (b) N. Metzler-Nolte, *New J. Chem.*, 1998, 793.

63. R. J. Baker, R. D. Farley, C. Jones, M. Kloth, D. M. Murphy, *Dalton Trans.*, 2002, 3844.

64. Results presented in an invited lecture at the 36th International Conference on Coordination Chemistry, Merida, Mexico, July, 2004.

65. C. Cui, H. W. Roesky, H. –G. Schmidt, M. Noltemeyer, H. Hao, F. Cimpoesu, *Angew. Chem. Int. Ed.*, 2000, **39**, 4274.

66. N. J. Hardman, B. E. Eichler, P. P. Power, *Chem. Commun.*, 2000, 1991.

67. (a) N. J. Hardman, A. D. Phillips, P. P. Power, *ACS Symp. Ser.*, 2002, **822**, 2; (b) M. Reiher, A. Sundermann, *Eur. J. Inorg. Chem.*, 2002, 1854.

68. M. N. Sudheendra, H. W. Roesky, G. Anantharaman, *J. Organomet. Chem.*, 2002, **646**, 4.

69. M. S. Hill, P. B. Hitchcock, *Chem. Commun.*, 2004, 1818.

70. (a) Y. Cheung, P. B. Hitchcock, M. F. Lappert, M. Zhou, *Chem. Commun.*, 2005, 752; (b) M. S. Hill, P. B. Hitchcock, R. Pongtavornpinyo, *Dalton Trans.*, 2005, 273.

71. C. –H. Chen, M. –L. Tsai, M. –D. Su, *Organometallics*, 2006, **25**, 2766.

72. C. Jones, P. C. Junk, J. A. Platts, A. Stasch, *J. Am. Chem. Soc.*, 2006, **128**, 2206.

73. C. Jones, P. C. Junk, J. A. Platts, D. Rathmann, A. Stasch, *Dalton Trans.*, 2005, 2497.

74. C. Jones, P. C. Junk, M. Kloth, K. M. Proctor, A. Stasch, *Polyhedron*, 2006, **25**, 1592.

75. E. Despagnet-Ayoub, R. H. Grubbs, *J. Am. Chem. Soc.*, 2004, **126**, 10198.

76. S. P. Green, C. Jones, A. Stasch, *Inorg. Chem.*, 2007, **46**, 11.

77. C. Jones, A. Stasch, *unpublished results.*

78. G. B. Deacon, C. Jones, P. C. Junk, G. J. Moxey, A. Stasch, *unpublished results.*

79. E. S. Schmidt, A. Jockisch, H. Schmidbaur, *J. Am. Chem. Soc.*, 1999, **121**, 9758.

80. E. S. Schmidt, A. Schier, H. Schmidbaur, *Dalton Trans.*, 2001, 505.

81. D. S. Brown, A. Decken, A. H. Cowley, *J. Am. Chem. Soc.*, 1995, **117**, 5421.

82. T. Pott, P. Jutzi, W. Kaim, W. W. Schoeller, B. Neumann, A. Stammler, H. –G. Stammler, M. Wanner, *Organometallics*, 2002, **21**, 3169.

83. T. Pott, P. Jutzi, W. W. Schoeller, A. Stammler, H. –G. Stammler, *Organometallics*, 2001, **20**, 5492.

84. R. J. Baker, C. Jones, *Coord. Chem. Rev.*, 2005, **249**, 1857.

85. (a) Y. Segawa, M. Yamashita, K. Nozaki, *Science*, 2006, **314**, 113; (b) M. Yamashita, Y. Suzuki, Y. Segawa, K. Nozaki, *J. Am. Chem. Soc.*, 2007, **129**, 9570.

86. Y. Segawa, M. Yamashita, K. Nozaki, *Angew. Chem. Int. Ed.*, 2007, **46**, 6710.

87. (a) N. J. Hill, R. West, *J. Organomet. Chem.*, 2004, **689**, 4165; (b) M. Haaf, T. A. Schmedake, R. West, *Acc. Chem. Res.*, 2000, **33**, 704; (c) B. Gehrhus, M. F. Lappert, *J. Organomet. Chem.*, 2001, **617-618**, 209, and references therein.

88. O. Kühl, *Coord. Chem. Rev.*, 2004, **248**, 411.

89. T. Gans-Eichler, D. Gudat, M. Neiger, *Angew. Chem. Int. Ed.*, 2002, **41**, 1888.

90. T. Gans-Eichler, D. Gudat, K. Nättinen, M. Neiger, *Chem. Eur. J.*, 2006, **12**, 1162.

91. D. Gudat, T. Gans-Eichler, M. Neiger, *Chem. Commun.*, 2004, 2434.

92. M. K. Denk, S. Gupta, A. L. Lough, *Eur. J. Inorg. Chem.*, 1999, 41.

93. D. Gudat, A. Haghverdi, H. Hupfer, M. Neiger, *Chem. Eur. J.*, 2000, **6**, 3414.

94. T. Gans-Eichler, D. Gudat, M. Neiger, *Heteroatom Chem.*, 2005, **16**, 327.

95. J. L. Dutton, H. M. Tuonenen, M. C. Jennings, P. J. Ragogna, *J. Am. Chem. Soc.*, 2006, **128**, 12624.

96. X. Li, X. Cheng, H. Song, C. Cui, *Organometallics*, 2007, **26**, 1039.

97. N. J. Hardman, P. P. Power, J. D. Gorden, C. L. B. MacDonald, A. H. Cowley, *Chem. Commun.*, 2001, 1866.

98. Z. Yang, X. Ma, R. B. Oswald, H. W. Roesky, H. Zhu, C. Schulzke, K. Starke, M. Baldus, H. –G. Schmidt, M. Noltemeyer, *Angew. Chem. Int. Ed.*, 2005, **44**, 7072.

99. Z. Yang, X. Ma, R. B. Oswald, H. W. Roesky, M. Noltemeyer, *J. Am. Chem. Soc.*, 2006, **128**, 12406.

100. (a) H. Zhu, R. B. Oswald, H. Fan, H. W. Roesky, Q. Ma, Z. Yang, H. –G. Schmidt, M. Noltemeyer, K. Starke, N. S. Hosmane, *J. Am. Chem. Soc.*, 2006, **128**, 5100; (b) H. Zhu, J. Chai, H. Fan, H. W. Roesky, C. He, V. Jancik, H. –G. Schmidt, M. Noltemeyer, W. A. Merrill, P. P. Power, *Angew. Chem. Int. Ed.*, 2005, **44**, 5090.

101. C. Cui, S. Köpke, R. Herbst-Irmer, H. W. Roesky, M. Noltemeyer, H. –G. Schmidt, B. Wrackmeyer, *J. Am. Chem. Soc.*, 2001, **123**, 9091.

102. (a) Y. Gao, X. Cheng, H. Song, J. Zhang, C. Cui, *Organometallics*, 2007, **26**, 1308; (b) X. Li, C. Ni, H. Song, C. Cui, *Chem. Commun.*, 2006, 1763; (c) X. Li, H. Song, L. Duan, C. Cui, H. W. Roesky, *Inorg. Chem.*, 2006, **45**, 1912; (d) H. Zhu, J. Chai, Q. Ma, V. Jancik, H. W. Roesky, H. Fan, R. Herbst–Irmer, *J. Am. Chem. Soc.*, 2004, **126**, 10194.

103. X. Li, H. Song, C. Ni, C. Cui, *Organometallics*, 2006, **25**, 5665.

104. H. Zhu, J. Chai, A. Stasch, H. W. Roesky, T. Blunck, D. Vidovic, J. Magull, H. –G. Schmidt, M. Noltemeyer, *Eur. J. Inorg. Chem.*, 2004, 4046.

105. A. Kempter, C. Gemel, R. A. Fischer, *Chem. Eur. J.*, 2007, **13**, 2990.

106. H. Zhu, J. Chai, H. Fan, H. W. Roesky, U. N. Nehete, H. –G. Schmidt, M. Noltemeyer, *Eur. J. Inorg. Chem.*, 2005, 2147.

107. M. S. Hill, P. B. Hitchcock, R. Pongtavornpinyo, *Inorg. Chem.*, 2007, **46**, 3783.

108. (a) N. J. Hardman, C. Cui, H. W. Roesky, W. H. Fink, P. P. Power, *Angew. Chem. Int. Ed.*, 2001, **40**, 2172; (b) H. Zhu, J. Chai, V. Chandrasekhar, H. W.

Roesky, J. Magull, D. Vidovic, H. –G. Schmidt, M. Noltemeyer, P. P. Power, W. A. Merrill, *J. Am. Chem. Soc.*, 2004, **126**, 9472; (c) H. Zhu, Z. Yang, J. Magull, H. W. Roesky, H. –G. Schmidt, M. Noltemeyer, *Organometallics*, 2005, **24**, 6420; (d) C. Cui, H. W. Roesky, H. –G. Schmidt, M. Noltemeyer, *Angew. Chem. Int. Ed.*, 2000, **39**, 4531; (e) N. J. Hardman, P. P. Power, *Chem. Commun.*, 2001, 1184.

109. N. Burford, P. J. Ragogna, K. N. Robertson, T. S. Cameron, N. J. Hardman, P. P. Power, *J. Am. Chem. Soc.*, 2002, **124**, 382.

110. Y. Peng, H. Fan, H. Zhu, H. W. Roesky, J. Magull, C. E. Hughes, *Angew. Chem. Int. Ed.*, 2004, **43**, 3443.

111. H. Zhu, J. Chai, V. Jancik, H. W. Roesky, W. A. Merrill, P. P. Power, *J. Am. Chem. Soc.*, 2005, **127**, 10170.

112. N. J. Hardman, P. P. Power, *Inorg. Chem.*, 2001, **40**, 2474.

113. G. Bai, H. W. Roesky, J. Li, M. Noltemeyer, H. –G. Schmidt, *Angew. Chem. Int. Ed.*, 2003, **42**, 5502.

114. Y. Peng, H. Fan, V. Jancik, H. W. Roesky, R. Herbst-Irmer, *Angew. Chem. Int. Ed.*, 2004, **43**, 6190.

115. V. Jancik, M. M. M. Cabrera, H. W. Roesky, R. Herbst–Irmer, D. Neculai, A. M. Neculai, M. Noltemeyer, H. –G. Schmidt, *Eur. J. Inorg. Chem.*, 2004, 3508.

116. A. Kempter, C. Gemel, R. A. Fischer, *Inorg. Chem.*, 2005, **44**, 163.

117. A. Kempter, C. Gemel, N. J. Hardman, R. A. Fischer, *Inorg. Chem.*, 2006, **45**, 3133.

118. A. Kempter, C. Gemel, T. Cadenbach, R. A. Fischer, *Organometallics*, 2007, **26**, 4257.

119. A. Kempter, C. Gemel, R. A. Fischer, *Chem. Commun.*, 2006, 1551.

120. H. W. Roesky, *Inorg. Chem.*, 2004, **43**, 7284.

Chapter 2

Complexes of an Anionic Gallium(I) *N*-Heterocyclic Carbene Analogue with Group 14 Element(II) Fragments

2.1 Introduction

Investigations into the *s*- and *p*-block coordination chemistry of the anionic gallium(I) *N*-heterocyclic carbene (NHC) analogue, $[:Ga\{[N(Ar)C(H)]_2\}]^-$ **1** (Ar = $C_6H_3Pr^i_2$-2,6), have been frequent since the synthesis of potassium salts of this compound were first reported.[1] The only *s*-block complexes of **1** reported to date, apart from the dimeric potassium salts in the original report, are the bis(gallyl) magnesium, $[Mg(THF)_3\{Ga\{[N(Ar)C(H)]_2\}\}_2]$ **2**, and calcium, $[Ca(THF)_4\{Ga\{[N(Ar)C(H)]_2\}\}_2]$ **3**, compounds depicted below (Scheme 1).[2] The reduction of the previously reported gallium(III) heterocycle, $[I_2Ga\{[N(Ar)C(H)]_2^{\cdot}\}]$,[3] with the appropriate alkaline earth metal in the presence of mercury in THF gave **2** and **3** in low to good yields (Scheme 1), in a similar manner to the preparation of [K(tmeda)][**1**] by reduction of $[I_2Ga\{[N(Ar)C(H)]_2\}]$ with potassium metal.[1] The stepwise reduction was proposed to go through the previously reported paramagnetic gallium(II) dimer, $[IGa\{[N(Ar)C(H)]_2^{\cdot}\}]_2$,[4] and diamagnetic digallane(4), $[Ga\{[N(Ar)C(H)]_2\}]_2$,[5] with the group 2 metal oxidatively inserting into the Ga—Ga bond of the latter. Unlike the salt [K(tmeda)][**1**], **2** and **3** are molecular compounds and as such exhibit the first structurally characterised examples of Ga—Mg (2.7222 Å mean) and Ga—Ca (3.1587 Å mean) bonds. These bond lengths are outside the sum of the covalent radii of these element pairs (Ga—Mg 2.61 Å; Ga—Ca 2.91 Å).[6] A density functional theory (DFT) analysis was performed on model complexes to probe the nature of the Ga—M bonds, concluding that the bonds have significant ionic character. The attempted synthesis of

strontium and barium analogues proved unsuccessful, which is unusual because the heavier elements are more electropositive than the lighter metals.

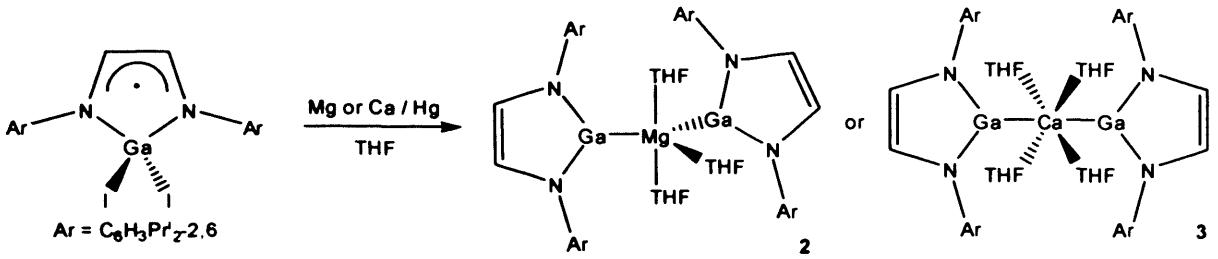

Scheme 1 – The synthesis of **2** and **3**

The heterocycle, **1**, has been shown to form complexes with group 13, 14, 15, 16 and 17 centres. The reaction of two equivalents of [K(tmeda)][**1**] with the group 13 hydrides, $[InH_3(NMe_3)]$ and $[GaH_3(quinuclidine)]$, in diethyl ether gave the trimetallic hydrides, **4** and **5**, in high yields (Scheme 2).[7] The reaction is proposed to proceed via elimination of KH to give neutral monosubstituted intermediates that are subsequently coordinated by a second equivalent of [K(tmeda)][**1**] to give **4** and **5**. Crystallographic characterisations of **4** and **5** highlighted the first structurally authenticated Ga—In bonds, with the presence of Li^+ in **4** explained by the *in situ* preparation of $[InH_3(NMe_3)]$, which generates lithium bromide as a by-product. A DFT analysis on model complexes revealed a significant amount of negative charge on the MH_2 fragments, explaining the contact ion pair in **5**. The attempted synthesis of an aluminium analogue of **4** and **5** proved unsuccessful. Complexes **4** and **5** are remarkably stable, with the decomposition temperature of **4** (116 °C) being comparable to that of the related InH_3-NHC complex $[InH_3(IMes)]$ (IMes = $[:C\{[N(Mes)C(H)]_2\}]$, Mes = $C_6H_2Me_3$-2,4,6) (115 °C).[8] Thus **1** displays close parallels with NHCs in its ability to stabilise thermally labile fragments.

The group 13 cyclopentadienyl complexes, InCp and TlCp, in contrast, caused the oxidative coupling of **1** with deposition of the group 13 metal and complexation of generated KCp to give the π-cyclopentadienyl-bridged digallane(4), **6**.[9] This complex, which exhibits the first structurally characterised example of a π-interaction with a gallium(II) centre, could also be directly prepared from KCp, tmeda (tmeda = tetramethylethylenediamine) and the digallane(4), $[Ga\{[N(Ar)C(H)]_2\}]_2$. Theoretical and experimental studies indicated that there is probably a fluxional complexation/decomplexation of the $K(tmeda)_2Cp$ unit from the gallium(II) dimer in solution.

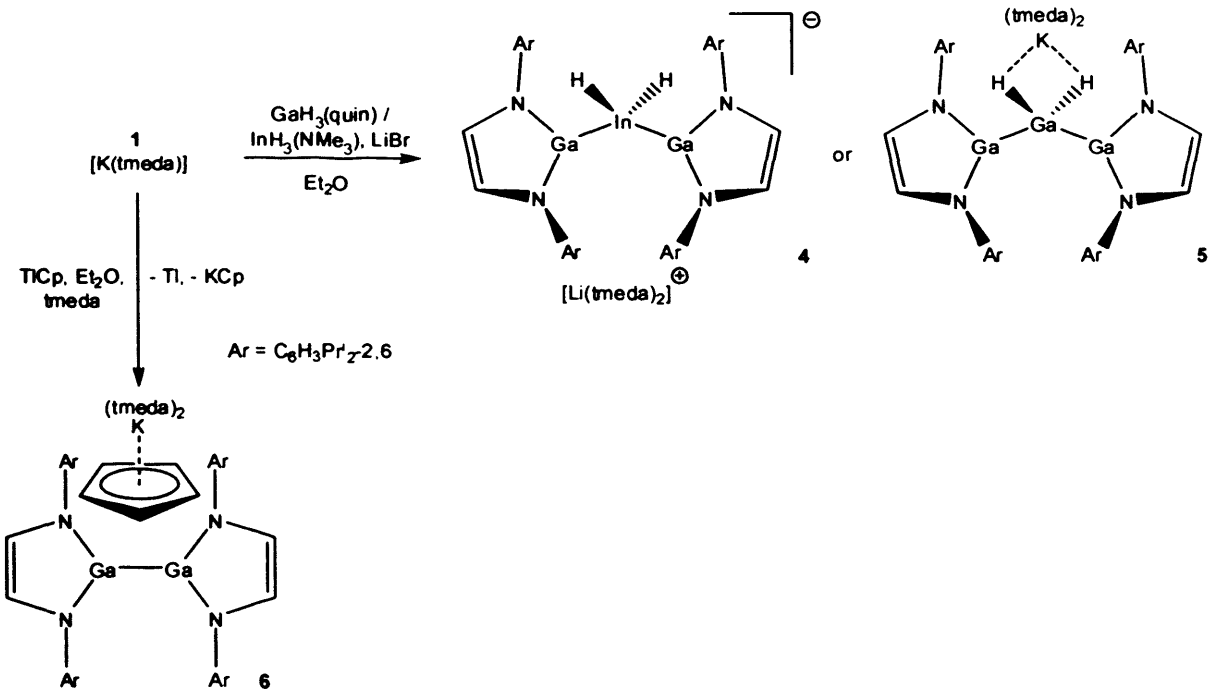

Scheme 2 – The reactions of [K(tmeda)][**1**] with group 13 complexes

Prior to the study discussed in this chapter (*vide infra*), attempts to form complexes of **1** with group 14 element(II) fragments were not as successful as those with group 13 precursors. Even very strong nucleophiles such as NHCs were found not to coordinate to the Ga centre of [K(tmeda)][**1**]. However, it should be noted that the reaction of [K(tmeda)][**1**] with the imidazolium salt, IMes.HCl, resulted in the oxidative insertion of its gallium centre into a C—H bond of the cation and the formation of the

NHC-gallium hydride heterocycle complex, **7** (Scheme 3).[10] In the presence of trace amounts of water the hydroxide-bridged gallium hydride salt, **8**, forms by partial hydrolysis of **7**. Since the publication of the work described in this chapter, [K(tmeda)][**1**] has been shown to react with other group 14 precursors.[11] This work will be discussed later in the chapter.

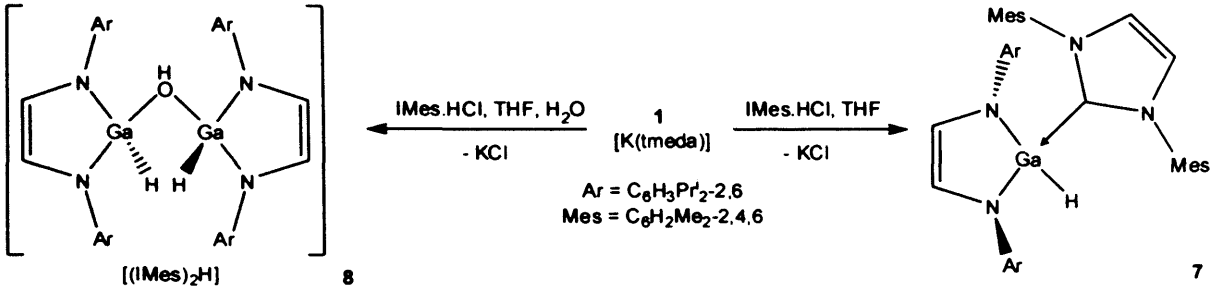

Scheme 3 – The reactions of [K(tmeda)][**1**] with group 14 complexes

The gallium(I) complex, [K(tmeda)][**1**], reacts with the triphosphabenzene, 1,3,5-$P_3C_3Bu^t_3$, to yield the known diphospholyl anion, 1,3-$P_2C_3Bu^t_3$, which forms *via* phosphorus abstraction from the heterobenzene (Scheme 4).[12] The only species detected by $^{31}P\{^1H\}$ NMR spectroscopy was 1,3-$P_2C_3Bu^t_3$, with the phosphorus-containing by-product presumably being an insoluble gallium phosphide complex. The same result is obtained in the reaction of 1,3,5-$P_3C_3Bu^t_3$ with elemental potassium,[13] which highlights the strongly reducing nature of **1**. The oxidative insertion of **1** into a P—P bond of *cyclo*-$(PPh)_5$ gave the spirocyclic complex, **9**, under any reaction stoichiometry, with the loss of a PPh fragment, most likely in the form of cyclic oligomers (Scheme 4).[14] This reactivity is in marked contrast to that of NHCs, which have been shown to form NHC-pnictinidene adducts on treatment with cyclic pnictanes,[15] and instead displays more similarities to the reactivity of related group 13 metal diyls.[16] Although the desired terminal gallium-imide complex was not formed in the reaction of [K(tmeda)][**1**] with azobenzene, this gave the novel ionic spirocyclic product, **10**.[14] The most likely mechanism for this reaction was deemed to involve the

[4 + 1] cycloaddition of the gallium centre with azobenzene, with a 1,3-migration of the *ortho*-phenyl proton to the nitrogen bearing the metallated phenyl group. It is noteworthy that no reaction occurred between [K(tmeda)][**1**] and MesN=NMes, Mes*P=PMes* (Mes* = $C_6H_2Bu^t_3$-2,4,6) or Ar*E=EAr* (E = As, Sb, Ar* = $C_6H_3(C_6H_2Pr^i_3$-2,4,6)-2,6), presumably due to the steric bulk of these precursors and their absence of *ortho*-aryl protons.

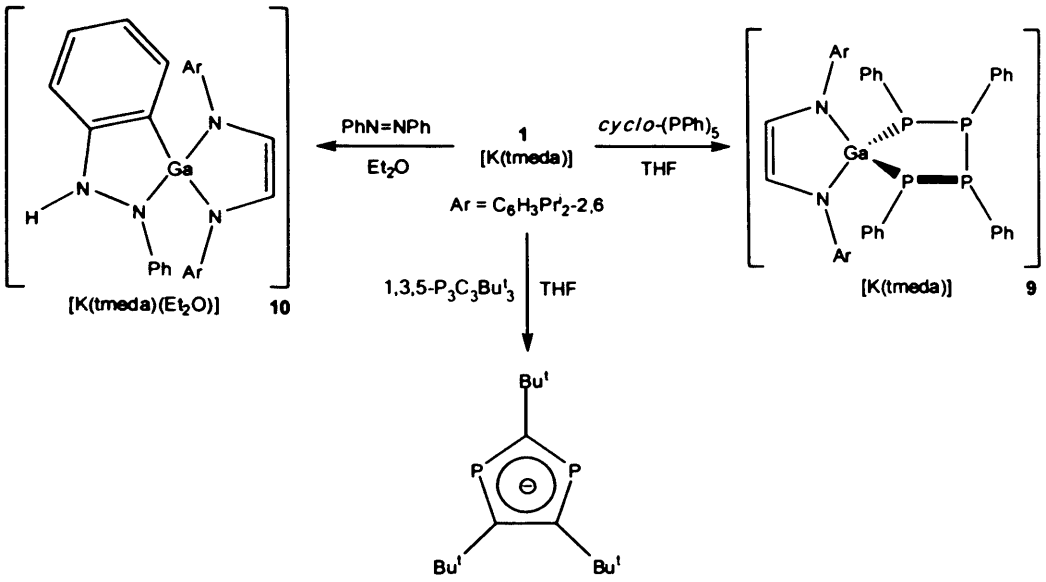

Scheme 4 – The reactions of [K(tmeda)][**1**] with group 15 complexes

A study into the reactions of [K(tmeda)][**1**] with group 16 precursors yielded some interesting results (Scheme 5).[17] Leading on from the observation that [K(tmeda)][**1**] showed no reaction towards elemental sulphur, selenium and tellurium, and decomposed in the presence of oxygen, it was decided to perform the controlled oxidation of [K(tmeda)][**1**] with a stoichiometric amount of $N_2O_{(g)}$ to give the dimeric dianionic complex, **11**. The reaction of $(Te)PEt_3$, a soluble source of tellurium, with [K(tmeda)][**1**] gave a similar dimeric species, **12**. The analogous reactions of [K(tmeda)][**1**] with soluble sources of sulphur gave only intractable mixtures of products. Structural characterisation of **11** and **12** showed that their solid state structures are markedly different, with the small electronegative oxygen centres in **11**

encouraging a short Ga·····Ga distance of 2.608 Å compared to the long Ga·····Ga separation of 3.408 Å in **12**. The small separation in **11** could be indicative of a small degree of Ga—O π-bonding. In other work the heterocycle, **1**, was shown to oxidatively insert into the E—E bond of the dichalcogenides, PhEEPh (E = Se, Te), to yield **13** and **14**.[17] No isolable products were liberated from the reactions of related oxygen and sulphur dichalcogenides with [K(tmeda)][**1**]. The selenium analogue, **13**, is polymeric in the solid state and the tellurium analogue, **14**, monomeric. In addition, they have different degrees of solvation around the potassium counter-ions.

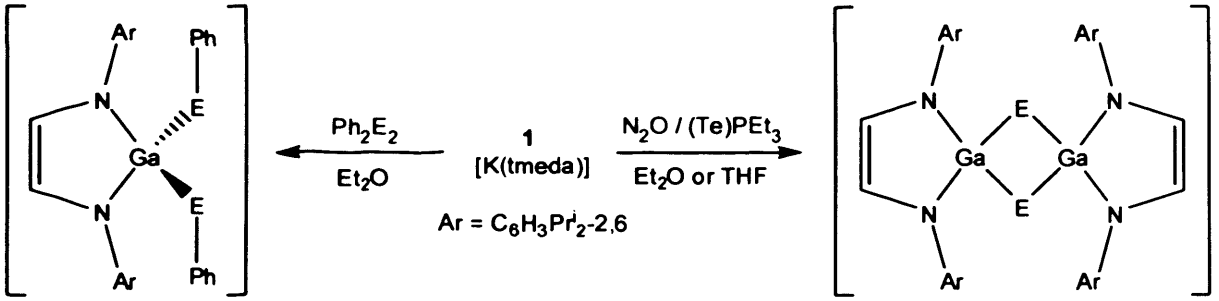

Scheme 5 – The reactions of [K(tmeda)][**1**] with group 16 precursors

It was envisaged that a study of the analogous behaviour of **1** and NHCs towards heavier group 14 precursors would be made possible with the correct choice of reagents. Previous studies by Weidenbruch *et al.* describe the reactivity of an NHC, [:C{[N(Pr^i)C(Me)]$_2$}], with Ar'$_2$E=EAr'$_2$, Ar' = C$_6$H$_2$Pr$^i_3$-2,4,6, E = Sn[18] or Pb.[19] These investigations show that in solution the distannene and diplumbene reaction precursors exist in equilibrium with their monomeric stannylene and plumbylene forms, :EAr'$_2$. These fragments form the weakly coordinated complexes, **15** and **16**, with the NHC (Figure 1). Evidence of the weakness of these interactions is supplied by the complexes exhibiting no E—C$_{(carbene)}$ double bond character, having very long E—C$_{(carbene)}$ interactions and possessing relatively obtuse fold angles (θ) between the donor and acceptor fragments. NHC complexes of GeI$_2$[20] and SnCl$_2$,[21] and benzannulated NHC

complexes of benzannulated *N*-heterocyclic silylenes, germylenes, stannylenes and plumbylenes[22] have been shown to display comparable structural features.

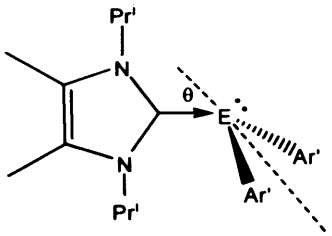

Ar' = $C_6H_2Pr^i_3$-2,4,6
E = Sn **15** (θ = 68.6°, Sn-$C_{(carbene)}$ = 2.379(5) Å)
E = Pb **16** (θ = 70.5°, Pb-$C_{(carbene)}$ = 2.540(5) Å)

Figure 1 – The complexes **15** and **16**

2.2 Research Proposal

NHC adducts of group 14 fragments are well known.[18-22] The chemistry of the anionic gallium(I) NHC analogue, **1**, with group 14 precursors is not as developed.[10,11] An investigation into the reactivity of [K(tmeda)][**1**] towards the heavier alkene analogues, $R_2E{=}ER_2$, E = Ge, Sn or Pb, was proposed in order to compare the chemistry of this heterocyle with NHCs. The preparation of gallyl complexes isostructural to **15** and **16** would yield a number of complexes with interesting bonding properties and also provide the first examples of structurally characterised Ga—Sn and Ga—Pb bonds. The previous work of Weidenbruch would then be comparable with the results of the reactions between [K(tmeda)][**1**] and the heavy alkene analogues, $R_2E{=}ER_2$.

2.3 Results and Discussion

2.3.1 Preparation of Ionic Complexes

Lappert's heavy alkene analogues, $R_2E{=}ER_2$, E = Ge or Sn; R = $CH(SiMe_3)_2$, were reacted in a 1 : 2 stoichiometry and the plumbylene, $:PbR_2$, in a 1 : 1 stoichiometry

with [K(tmeda)][**1**] in diethyl ether at -78 °C and slowly warmed to room temperature. When E = Ge or Sn, the anionic complexes, **17** and **18**, were formed in moderate to good yields (Scheme 6). These "adducts" display similarities to **15** and **16**, and likely result from coordination of the gallium heterocycle to $:ER_2$ fragments, which are known to be in equilibrium with $R_2E{=}ER_2$ in solution.[23] The reaction with the plumbylene, however, led to the deposition of lead metal and formation of the known digallane(4), $[Ga\{[N(Ar)C(H)]_2\}]_2$.[5] It is likely that the relatively strongly reducing nature of the Ga(I) centre of [K(tmeda)][**1**] causes this redox process. This reducing nature was previously observed when [K(tmeda)][**1**] was added to $SnCl_2$ in a 2 : 1 stoichiometry, which resulted in the deposition of elemental tin and the formation of the gallium(II) dimers, $[ClGa\{[N(Ar)C(H)]_2^{\cdot}\}]_2$ and $[Ga\{[N(Ar)C(H)]_2\}]_2$. The corresponding 2 : 1 reaction of [K(tmeda)][**1**] with $[GeCl_2(dioxane)]$ gave an intractable mixture of products, as did the reaction of two equivalents of [K(tmeda)][**1**] with $PbCl_2$ in the presence of IMes. Tin deposition was observed in the 1 : 1 reaction of [K(tmeda)][**1**] with the tin diphosphacyclobutadienyl complex, $[:Sn(\eta^4\text{-}P_2C_2Bu^t_2)]$. Similarly, the 1 : 1 reaction of [K(tmeda)][**1**] with the bulky amide $[Pb\{N(SiMe_3)_2\}_2]$ results in lead deposition and the formation of $[Ga\{[N(Ar)C(H)]_2\}]_2$. It is noteworthy that [K(tmeda)][**1**] does not react with the tin(II) amide, $[Sn\{N(SiMe_3)_2\}_2]$, most likely a result of the tin(II) centre being less redox-active than the metal centre of the lead(II) analogue.[6]

The preparation of 2 : 1 complexes of the gallium heterocycle with $:ER_2$ fragments was attempted by treating **17** and **18** with a further equivalent of [K(tmeda)][**1**]. No reaction occurred with **17** but, surprisingly, that with **18** afforded the digallyl stannate complex, **19**, in low isolated yield. No other products could be identified in the reaction mixture. We proposed that the reaction that yields **19** proceeds

via a dianionic intermediate, **20**, which subsequently eliminates "K[CH(SiMe$_3$)$_2$]." This mechanism seems plausible taking into account that we have previously observed the elimination of potassium alkyls in 2 : 1 reactions of [K(tmeda)][**1**] with other metal dialkyls.[24] It would appear that the lower reactivity of **17** towards [K(tmeda)][**1**] is due to the smaller radius and lower Lewis acidity of its Ge centre relative to the Sn centre of **18**. The attempted methylation of **18** with MeI gave an intractable mixture of products.

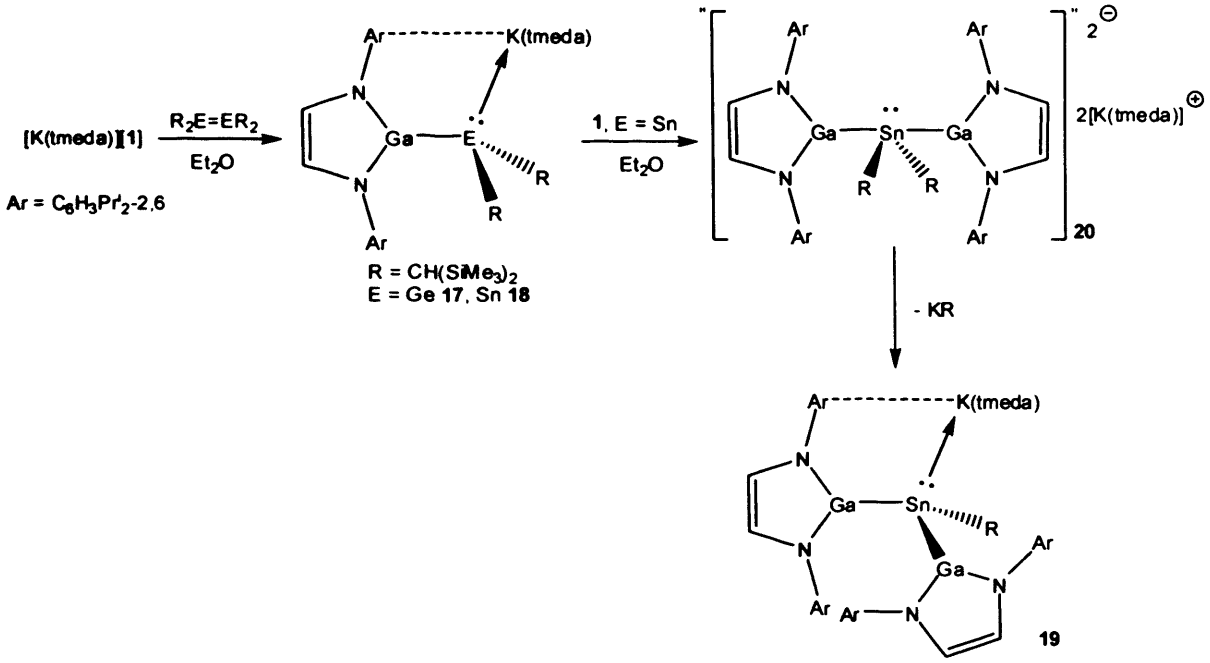

Scheme 6 – The synthesis of **17 – 19**

In order to draw closer comparisons with Weidenbruch's work and to test the generality of these reactions, [K(tmeda)][**1**] was reacted with Ar'$_2$E=EAr'$_2$, E = Ge, Sn (generated *in situ*) or Pb (Scheme 7). In contrast to the formation of **17**, no reaction was observed with Ar'$_2$Ge=GeAr'$_2$. This is easily rationalised by the Ge=Ge bond in Ar'$_2$Ge=GeAr'$_2$ being significantly shorter and stronger than that in [{(Me$_3$Si)$_2$C(H)}$_2$Ge=Ge-{(H)C(SiMe$_3$)$_2$}$_2$]. This difference in Ge=Ge bond lengths explains why the latter mostly dissociates into monomeric germylene fragments in solution,[23] whereas the former predominates as the dimeric digermene in solution,[25] although partial dissociation into germylene fragments is also likely for this compound.

Analogous to the formation of **18**, the reaction of [K(tmeda)][**1**] with an *in situ* generated solution of $Ar'_2Sn=SnAr'_2$ (which is known to be in equilibrium with the corresponding stannylene in solution) afforded the anionic complex, **21**, in almost quantitative yield (Scheme 2). In contrast to the formation of **19**, when **21** was treated with a second equivalent of [K(tmeda)][**1**], no reaction occurred. This can be explained by taking into account the reduced steric accessibility of the Ga heterocycle to the Sn centre of **21** relative to that in **18**.

As in the reaction of [K(tmeda)][**1**] with $[Pb\{CH(SiMe_3)_2\}_2]$, lead metal deposition was observed when [K(tmeda)][**1**] was reacted with $Ar'_2Pb=PbAr'_2$. In this instance, however, the gallium heterocycle, **22**, was isolated. This galladiazole is probably formed *via* the lead analogue of **21** which is most likely unstable at room temperature. It is noteworthy that the neutral NHC adduct, **16** (E = Pb), is unstable in solution above -70 °C and decomposes to form 1,3,5-triisopropylbenzene.[19] A closely related gallium heterocycle, $[(Me_3Si)_3CGa\{N(Pr^i)C(H)\}_2]$, has been recently reported to arise from the reaction of the diazabutadiene, $\{N(Pr^i)C(H)\}_2$, with the tetrameric gallium diyl, $[\{GaC(SiMe_3)_3\}_4]$.[26] This synthetic route to the galladiazole, **22**, is important because attempts to intentionally prepare it *via* the reaction of [K(tmeda)][**1**] with Ar'Br were unsuccessful and led to the formation of the known paramagnetic gallium(II) dimer, $[BrGa\{[N(Ar)C(H)]_2^{\cdot}\}]_2$.[4] A final attempt to prepare a first structurally characterised example of a Ga—Pb bonded complex was undertaken by adding a toluene solution of the benzannulated lead(II) NHC analogue, $[:Pb\{C_6H_4(Bu^tCH_2N)_2\text{-}1,2\}]$ **23**,[22a] to [K(tmeda)][**1**] at low temperature. A previous study revealed that **23** reacted with a benzannulated NHC to form a room temperature-stable adduct,[22a] so it was hoped that the corresponding complex of **1** with **23** would display similar stability. Unfortunately, no product could be isolated from this reaction,

but a trace amount of the starting material, **23**, crystallised from the reaction mixture. Hence the first structural characterisation of a lead(II) NHC analogue was undertaken (*vide infra*).

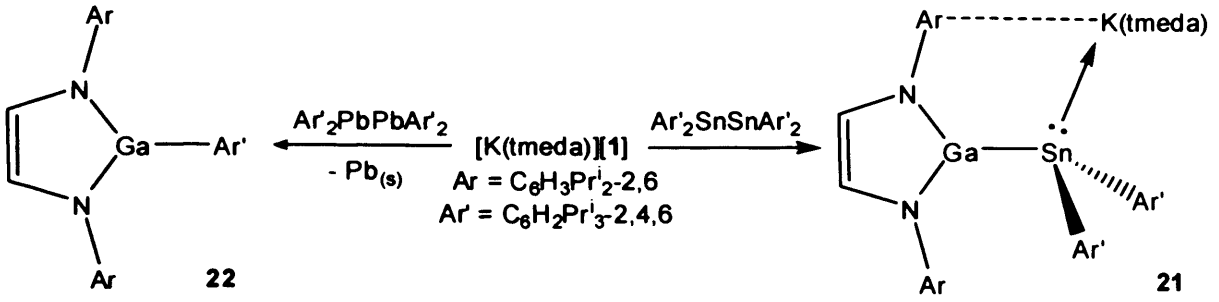

Scheme 7 – The synthesis of **21** and **22**

The spectroscopic data for the anionic 1 : 1 and 2 : 1 complexes, **17** – **19** and **21**, suggest that the gallium heterocycle(s) remain(s) coordinated to the germylene or stannylene fragments in solution. The ^{1}H and $^{13}C\{^{1}H\}$ NMR spectra are, however, more symmetrical than would be expected if the solid state structures of the complexes were retained in solution. It is likely that the aryl coordinated [K(tmeda)] cation of each complex either migrates rapidly (on the NMR timescale) between the aryl groups of the anions, or the complexes are in equilibrium between contact ion pairs and ion separate salts. Such equilibria may be facilitated by the arene solvent (C_6D_6) used for the NMR experiments. Variable temperature NMR studies were attempted to investigate the possible fluxional processes occurring in solution (D_8-toluene), but were thwarted by the poor solubility of the complexes at low temperatures. An examination of the ^{1}H, $^{13}C\{^{1}H\}$ and $^{29}Si\{^{1}H\}$ NMR spectra of **17** and **18** revealed these complexes to possess two sets of chemically inequivalent $SiMe_3$ groups in solution, as might be expected. The $^{119}Sn\{^{1}H\}$ NMR spectra of **18** and **21** displayed broad singlet resonances at considerably higher fields (δ -97.9 and -306.7 ppm respectively) than has been reported for the related neutral complex, **15** (E = Sn, δ 710 ppm).[18] This is not surprising considering the anionic nature of these complexes which can be compared to trialkyl

stannate anions, e.g. $LiSnMe_3$, $^{119}Sn\{^1H\}$ NMR δ-189.2 ppm.[27] No signal was observed in the $^{119}Sn\{^1H\}$ NMR spectrum of **19**, presumably due to the quadrupolar broadening of the resonance by the two gallium centres coordinated to the tin centre. Finally, the NMR spectra of the gallium heterocycle, **22**, are consistent with its solid state structure and warrant no further discussion.

X-ray crystallographic analyses of complexes **17** – **19** and **21** – **23** were carried out. The molecular structures of these compounds are depicted in Figures 2 – 7. The crystal structure of **21** is of poor quality due to weak diffraction data but indicates that the complex is structurally similar to **17** and **18**. Compounds **17** and **18** are not isomorphous but are isostructural. The complexes are monomeric contact ion pairs in which the germanium or tin centres are coordinated by two alkyl ligands and one gallium heterocycle. As in previously reported complexes of the gallium heterocycle, **1**,[2,7,9-12,14,17,28] its Ga—N distances and N—Ga—N angle are shorter and less actute respectively relative to those in the free heterocycle. A molecule of tmeda chelates the potassium centres of **17** and **18**, which have an η^6-interaction with one of the aryl substituents of the gallium heterocycle, and are coordinated by the lone pair of the group 14 element centre. The Ga—Ge bond in **17** (2.5396(8) Å) is very long and outside the known range (2.407 – 2.494 Å).[29] Although there have been no structurally characterised Ga—Sn bonds in molecular compounds reported previously, those observed in **18** (2.7186(6) Å), **19** (2.6361(5) Å, 2.6610(6) Å) and **21** (2.6660(18) Å) lie around the sum of the covalent radii for the two elements (2.65 Å)[6] and therefore can be considered weak. These weak Ga—E interactions are comparable to the weak NHC—E interactions in **15** and **16**.

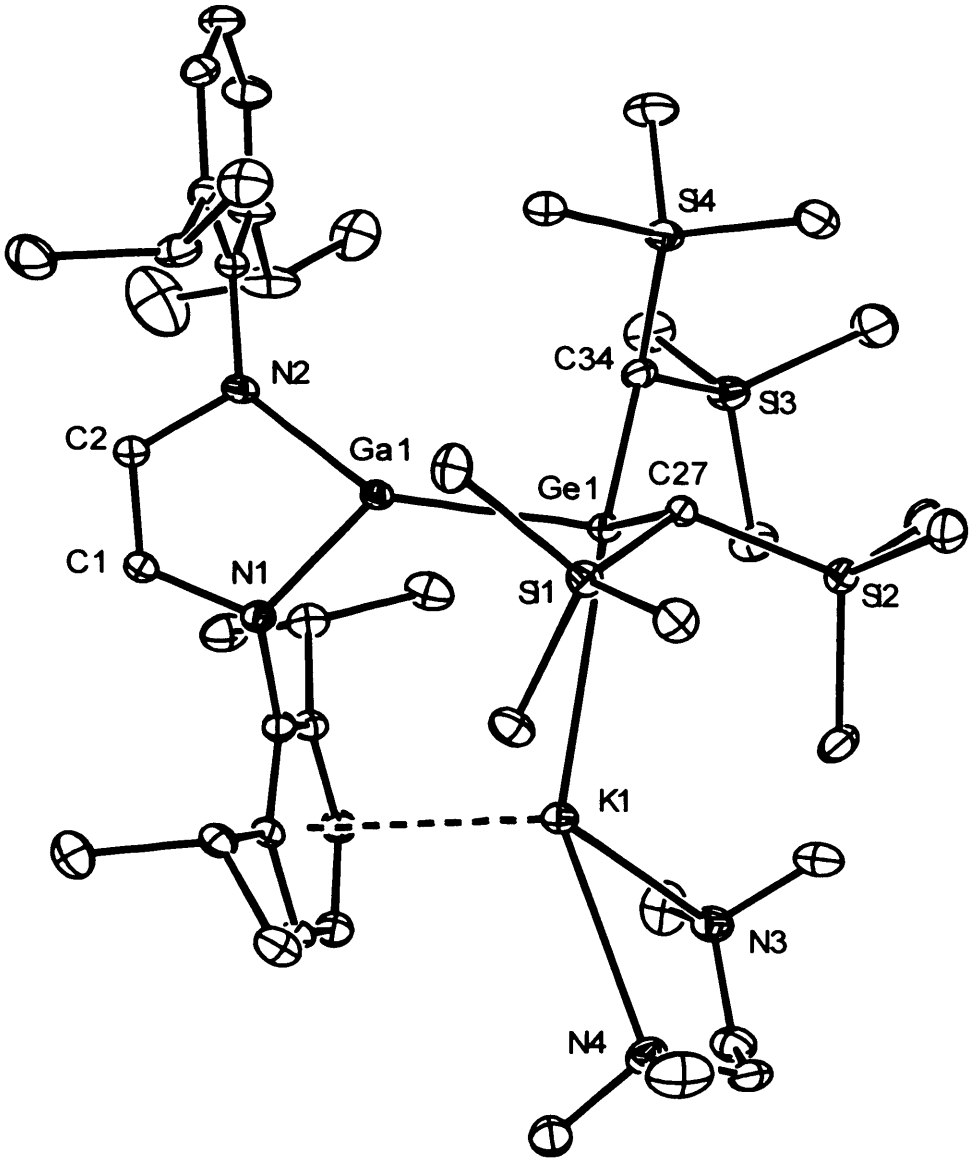

Figure 2 – Thermal ellipsoid plot (25 % probability surface) of the molecular structure of [K(tmeda)][Ge{CH(SiMe$_3$)$_2$}$_2${Ga{[N(Ar)C(H)]$_2$}}] **17**; hydrogen atoms omitted for clarity. Selected bond lengths (Å) and angles (°): Ge(1)—C(27) 2.085(4), Ge(1)—C(34) 2.091(4), Ge(1)—Ga(1) 2.5396(8), Ge(1)—K(1) 3.4418(12), Ga(1)—N(2) 1.911(4), Ga(1)—N(1) 1.925(4), K(1)—N(3) 2.783(4), K(1)—N(4) 2.959(4), N(1)—C(1) 1.398(6), N(2)—C(2) 1.404(6), C(1)—C(2) 1.324(6), K(1)—centroid (C(3)—C(8)) 2.931(3), C(27)—Ge(1)—C(34) 105.81(18), C(27)—Ge(1)—Ga(1) 106.13(12), C(34)—Ge(1)—Ga(1) 97.15(14), C(27)—Ge(1)—K(1) 106.21(12), C(34)—Ge(1)—K(1) 143.45(14), Ga(1)—Ge(1)—K(1) 90.47(2), N(2)—Ga(1)—N(1) 85.59(15), N(2)—Ga(1)—Ge(1) 148.55(11), N(1)—Ga(1)—Ge(1) 123.60(11).

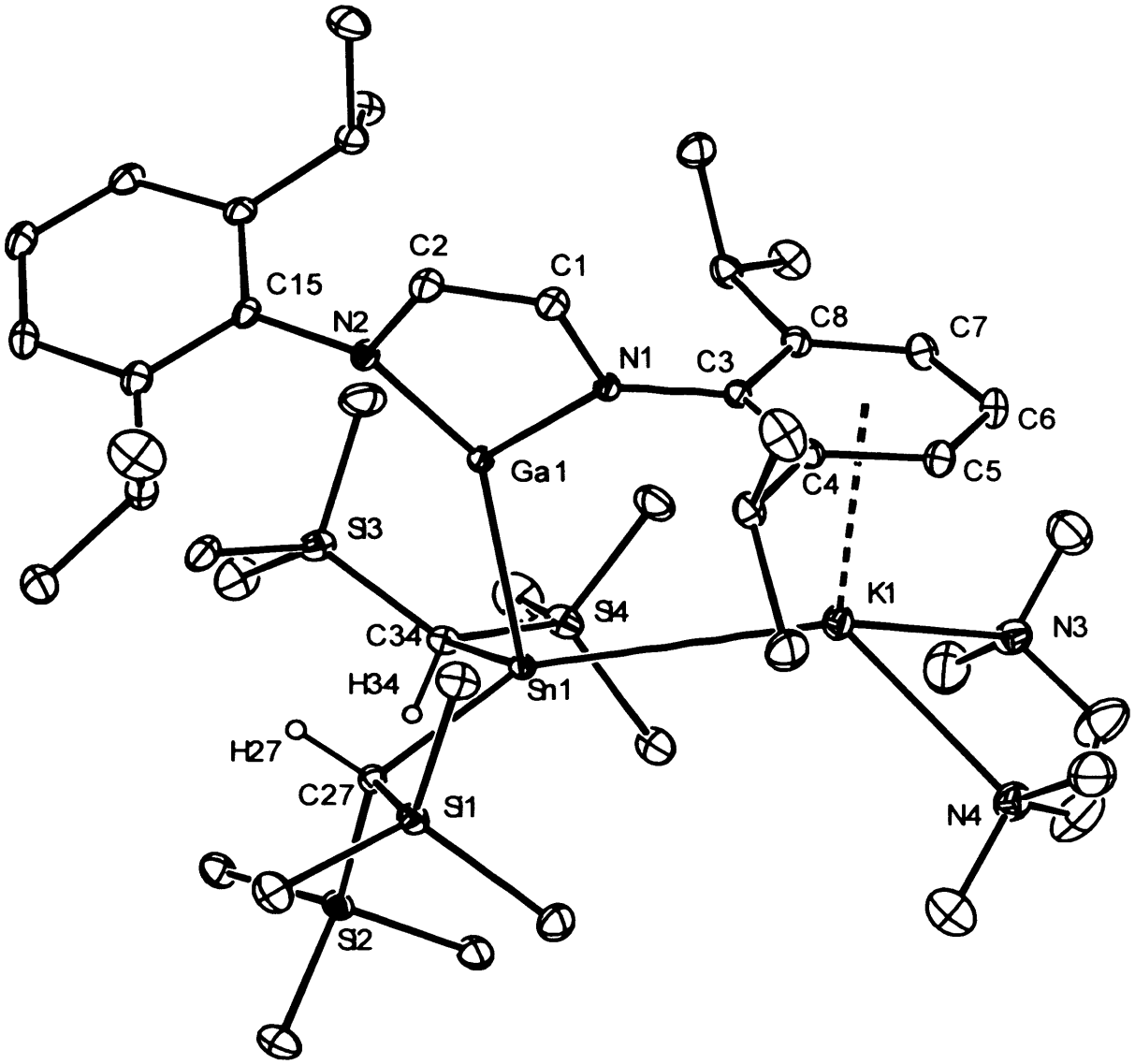

Figure 3 – Thermal ellipsoid plot (25 % probability surface) of the molecular structure of [K(tmeda)][Sn{CH(SiMe$_3$)$_2$}$_2${Ga{[N(Ar)C(H)]$_2$}}] **18**; hydrogen atoms (except H(27) and H(34)) omitted for clarity. Selected bond lengths (Å) and angles (°): Sn(1)—C(34) 2.268(2), Sn(1)—C(27) 2.280(2), Sn(1)—Ga(1) 2.7186(6), Sn(1)—K(1) 3.6407(9), Ga(1)—N(2) 1.909(2), Ga(1)—N(1) 1.9294(19), K(1)—N(4) 2.820(3), K(1)—N(3) 2.833(3), N(1)—C(1) 1.397(3), N(2)—C(2) 1.397(3), C(1)—C(2) 1.343(3), K(1)—centroid (C(3)—C(8)) 2.939(3), C(34)—Sn(1)—C(27) 99.81(9), C(34)—Sn(1)—Ga(1) 104.23(7), C(27)—Sn(1)—Ga(1) 100.10(6), C(34)—Sn(1)—K(1) 123.34(7), C(27)—Sn(1)—K(1) 133.40(6), Ga(1)—Sn(1)—K(1) 86.571(13), N(2)—Ga(1)—N(1) 85.79(8), N(2)—Ga(1)—Sn(1) 147.95(6), N(1)—Ga(1)—Sn(1) 120.10(6).

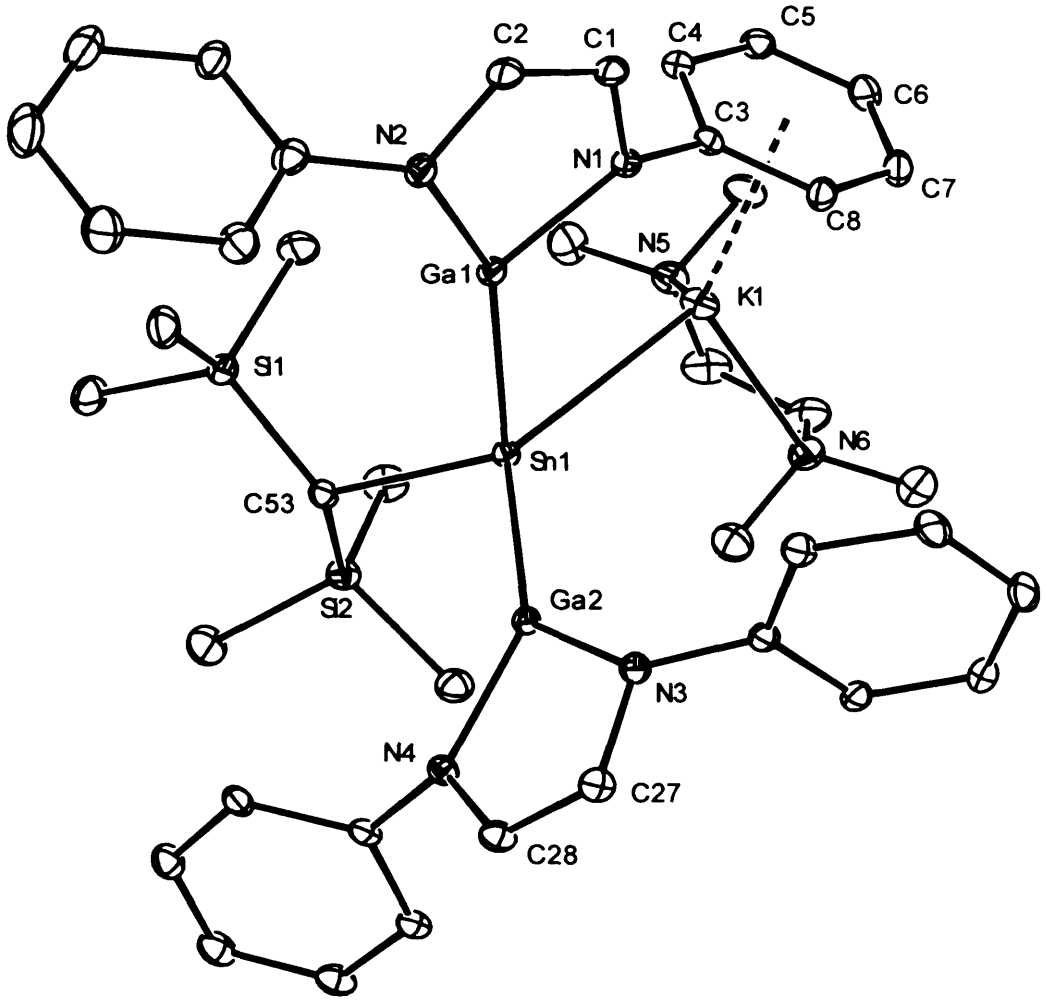

Figure 4 – Thermal ellipsoid plot (25 % probability surface) of the molecular structure of $[K(tmeda)][Sn\{CH(SiMe_3)_2\}\{Ga\{[N(Ar)C(H)]_2\}\}_2]$ **19**; isopropyl groups and hydrogen atoms omitted for clarity. Selected bond lengths (Å) and angles (°): Sn(1)—C(53) 2.259(3), Sn(1)—Ga(2) 2.6361(5), Sn(1)—Ga(1) 2.6610(6), Sn(1)—K(1) 3.5082(10), Ga(1)—N(2) 1.895(3), Ga(1)—N(1) 1.916(3), Ga(2)—N(3) 1.901(3), Ga(2)—N(4) 1.902(3), K(1)—N(5) 2.769(3), K(1)—N(6) 2.784(3), N(1)—C(1) 1.399(4), N(2)—C(2) 1.402(4), N(3)—C(27) 1.401(4), N(4)—C(28) 1.400(4), C(1)—C(2) 1.332(5), C(27)—C(28) 1.336(5), K(1)—centroid (C(3)—C(8)) 2.866(3), C(53)—Sn(1)—Ga(2) 98.11(8), C(53)—Sn(1)—Ga(1) 108.57(9), Ga(2)—Sn(1)—Ga(1) 96.009(16), C(53)—Sn(1)-K(1) 123.22(8), Ga(2)—Sn(1)—K(1) 134.39(2), Ga(1)—Sn(1)—K(1) 88.767(19), N(2)—Ga(1)—N(1) 86.73(12), N(2)—Ga(1)—Sn(1) 155.80(9), N(1)—Ga(1)—Sn(1) 117.35(8), N(3)—Ga(2)—N(4) 87.51(11), N(3)—Ga(2)—Sn(1) 138.80(8), N(4)—Ga(2)—Sn(1) 133.38(8).

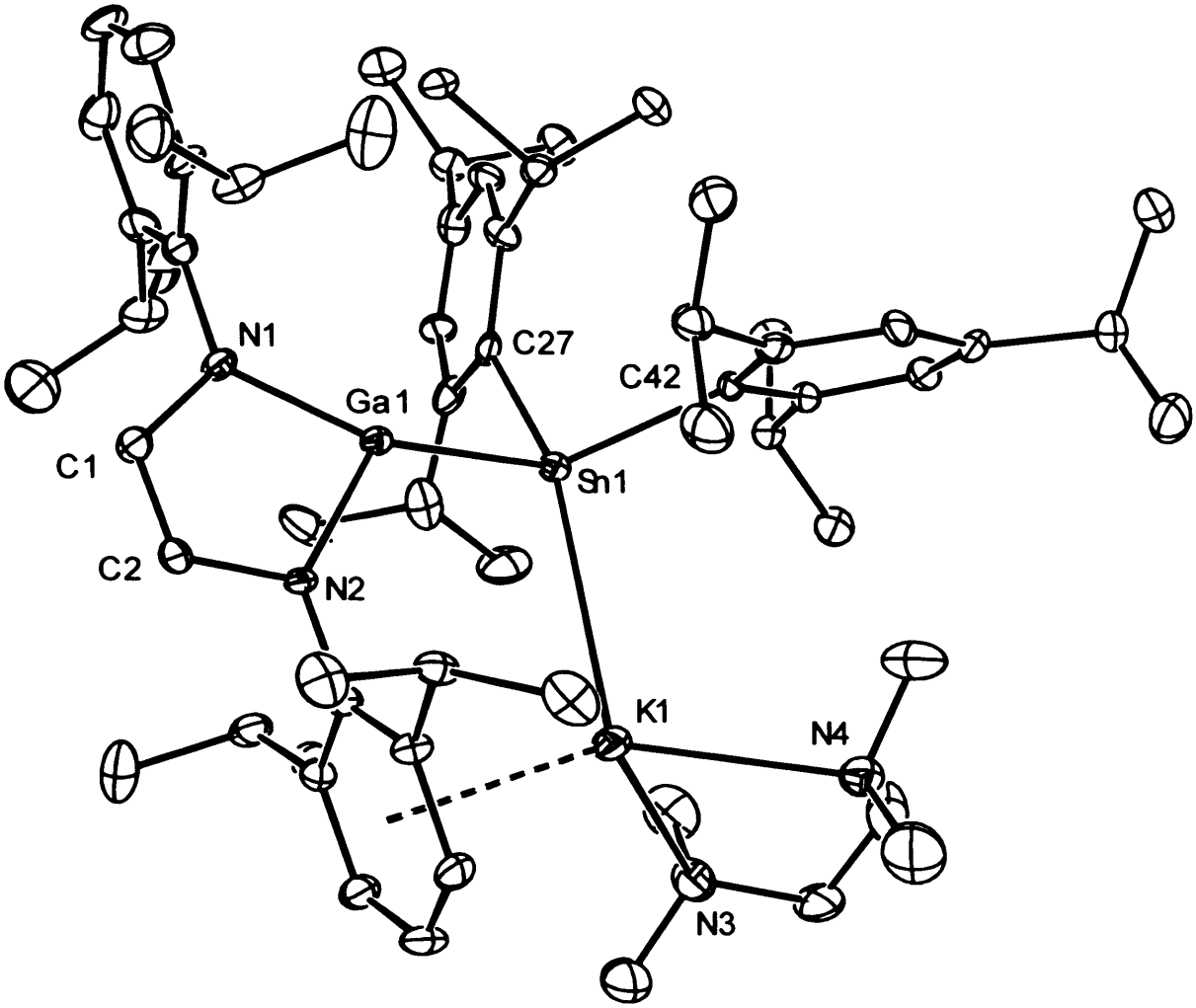

Figure 5 – Thermal ellipsoid plot (25 % probability surface) of the molecular structure of [K(tmeda)][Sn(Ar')$_2${Ga{[N(Ar)C(H)]$_2$}}] **21**; hydrogen atoms omitted for clarity. Selected bond lengths (Å) and angles (°): Sn1—C27 2.216(14), Sn1—C42 2.262(12), Sn1—Ga1 2.6660(18), Sn1—K1 3.495(4), Ga1—N1 1.914(11), Ga1—N2 1.923(11), K1—N3 2.768(17), K1—N4 2.816(16), N1—C1 1.395(17), N2—C2 1.388(17), C1—C2 1.328(19), C27—Sn1—C42 99.7(5), C27—Sn1—Ga1 98.0(3), C42—Sn1—Ga1 117.8(4), C27—Sn1—K1 154.9(4), C42—Sn1—K1 98.8(3), Ga1—Sn1—K1 88.22(7), N1—Ga1—N2 85.9(5), N3—K1—N4 66.1(5), C1—N1—Ga1 109.3(8), C2—N2—Ga1 109.8(8), C2—C1—N1 118.0(12), C1—C2—N2 117.0(12).

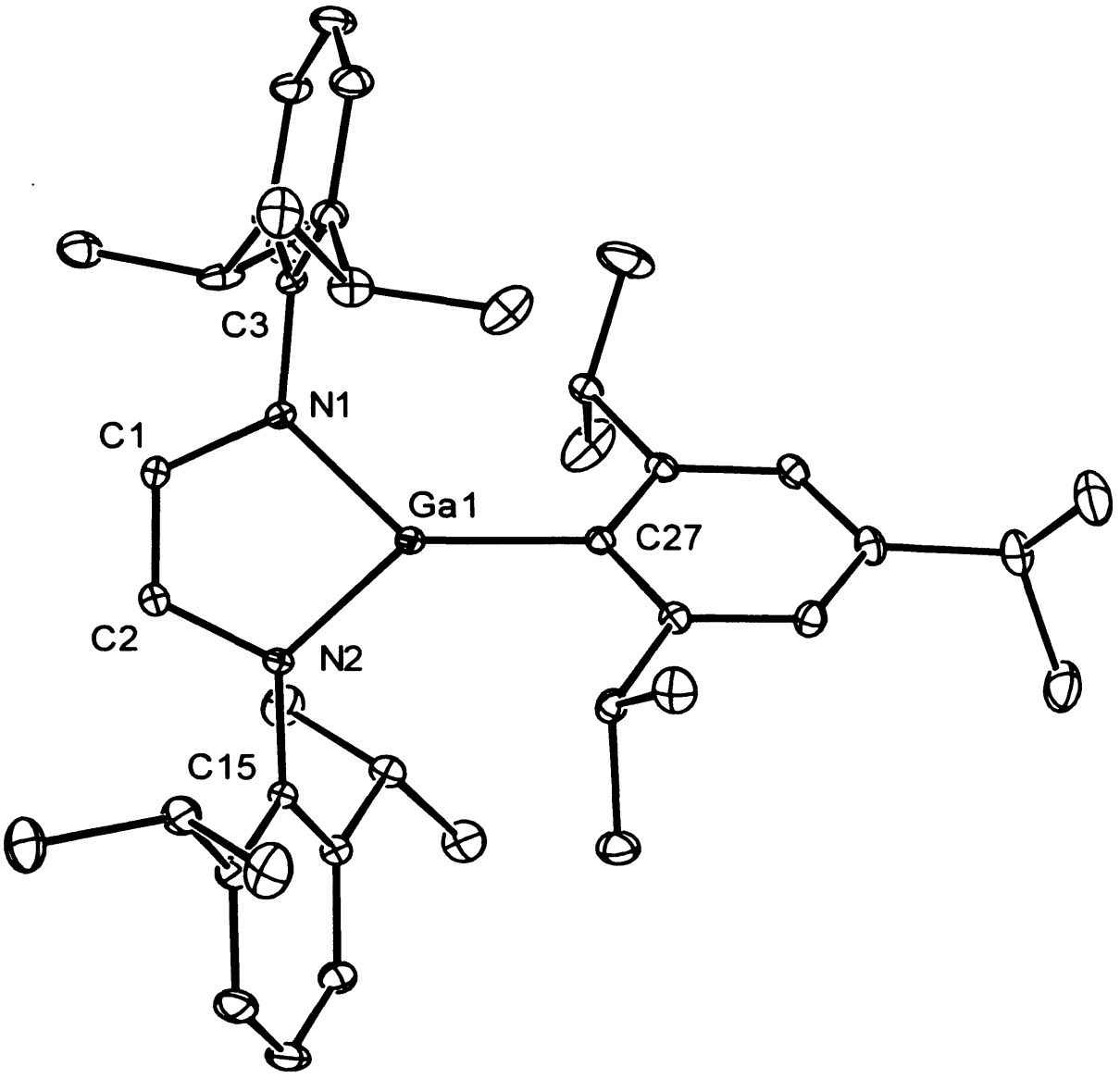

Figure 6 – Thermal ellipsoid plot (25 % probability surface) of the molecular structure of [Ar'Ga{[N(Ar)C(H)]$_2$}] **22**; hydrogen atoms omitted for clarity. Selected bond lengths (Å) and angles (°): Ga(1)—N(1) 1.846(2), Ga(1)—N(2) 1.848(2), Ga(1)—C(27) 1.936(3), N(1)—C(1) 1.400(3), N(2)—C(2) 1.406(3), C(1)—C(2) 1.343(4), N(1)—Ga(1)—N(2) 89.65(10), N(1)—Ga(1)—C(27) 134.58(10), N(2)—Ga(1)—C(27) 135.77(10), C(1)—N(1)—Ga(1) 108.76(17), C(2)—N(2)—Ga(1) 108.15(17).

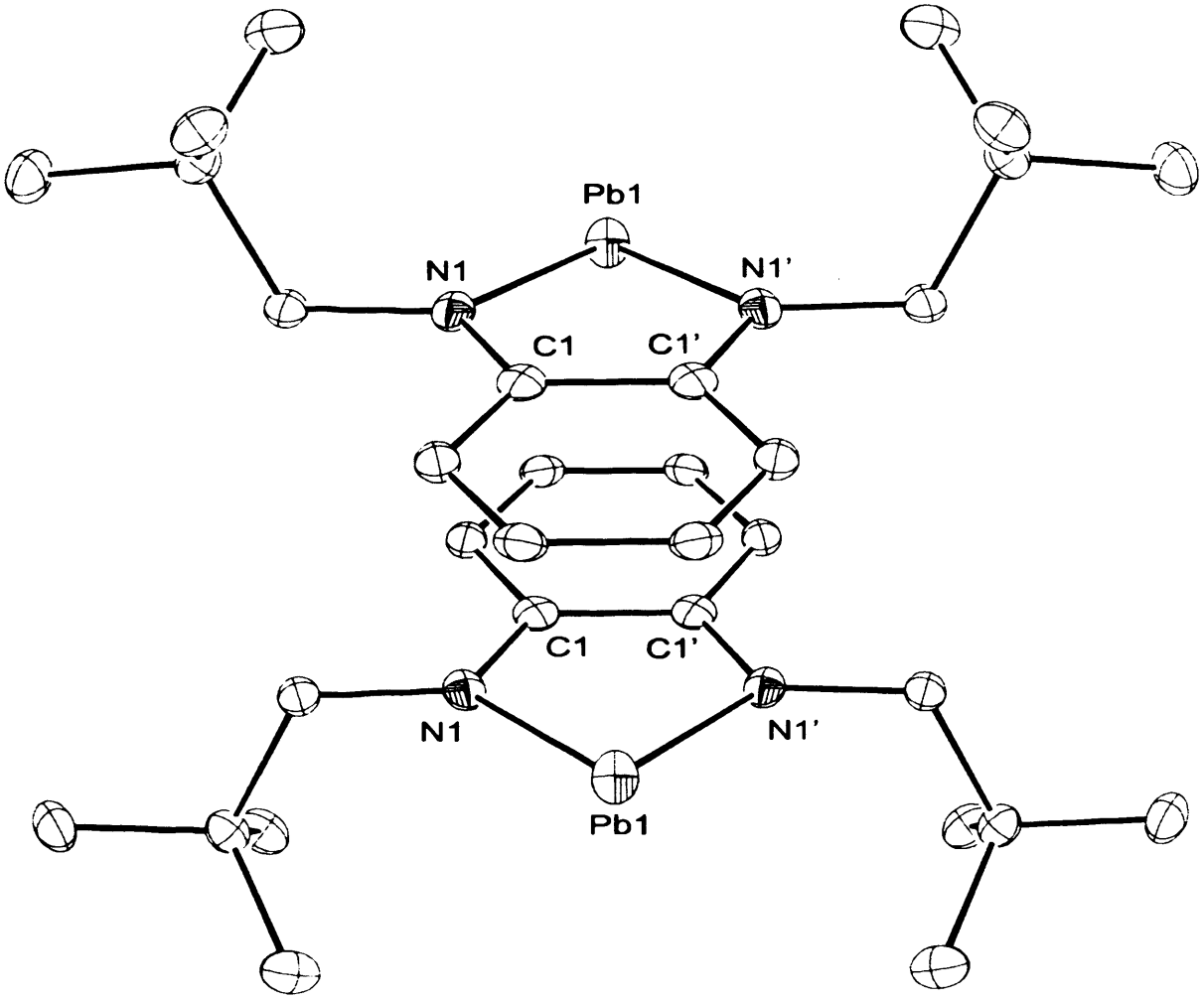

Figure 7 – Thermal ellipsoid plot (25 % probability surface) of the molecular structure of [:Pb{$C_6H_4(Bu^tCH_2N)_2$-1,2}] **23**; hydrogen atoms omitted for clarity. Selected bond lengths (Å) and angles (°): Pb(1)—N(1) 2.178(5), Pb(2)—N(2) 2.184(5), N(1)—C(1) 1.371(8), N(2)—C(9) 1.375(8), C(1)—C(1') 1.449(14), C(9)—C(9') 1.443(14), Pb(1)—centroid(C(1)—C(1')) 3.163, Pb(1)—centroid(C(9)—C(9')) 3.979, Pb(2)—centroid (C(1)—C(1')) 3.976, Pb(2)—centroid(C(9)—C(9')) 3.172, N(1)—Pb(1)—N(1') 74.8(3), N(2)—Pb(2)—N(2') 74.2(3), C(1)—N(1)—Pb(1) 116.2(4), C(9)—N(2)—Pb(2) 115.4(4), N(1)—C(1)—C(1') 115.9(4), N(2)—C(9)—C(9') 116.4(4), symmetry operation ': $x, y, -z$.

As in the NHC adducts, **15** and **16**, the fold angles, θ, between the Ga—E vector and the C—E—C least squares planes of **17** and **18** are acute at 70.5° and 70.9° respectively. Interestingly, this angle is considerably more acute in **21** (62.3°) but closer to the value for **15**, which incorporates the same stannylene fragment as **21**. The length of the Ga—E bonds and the magnitude of the fold angles, θ, for **17** and **18** suggest that the lone pair of the gallium heterocycle donates into the empty *p*-orbital of the germylene or stannylene fragments and that there is little "rehybridisation" of the germanium or tin centres upon coordination. Further evidence for this comes from the KEC_2 fragment which is not distorted far from planar as judged by the angle between the E—K vector and the EC_2 least squares plane (**17** = 26.1 °, **18** = 16.2 °). It is interesting that this angle is significantly more acute in **18**, which means that the coordination environment of the tin centre directly opposite the gallium heterocycle is exposed. This could allow a second gallium heterocycle to attack the metal, as proposed for the mechanism of formation of the digallyl stannate, **19**.

The molecular structure of **19** is depicted in Figure 5. It is a monomeric contact ion pair with a tin centre that possesses a distorted tetrahedral geometry. As in the previously described complexes, the potassium centre is chelated by a molecule of tmeda, has an η^6-arene interaction, and is coordinated by the tin lone pair. Both the Sn—K and Ga—Sn distances are significantly shorter than those in **18** and the intra-heterocyclic geometries are similar to those in previously reported complexes. The crystal structure of the monomeric, neutral gallium heterocycle, **22**, (Figure 6) contains two crystallographically independent molecules in the asymmetric unit that show no significant geometrical differences. As a result, geometric parameters for only one molecule are included in the caption of Figure 6. The gallium heterocycle is effectively planar and forms an angle of 52.3° with the Ar' plane. The Ga—N bond lengths and

N—Ga—N angle are similar to those observed in $[(Me_3Si)_3CGa\{[N(Pr^i)C(H)]_2\}]$,[26] but shorter and more obtuse respectively than is normal for metal complexes of the gallium heterocycle.[2,7,9-12,14,17,28]

The crystal structure of **23** (Figure 7) also contains two crystallographically independent molecules in the asymmetric unit with similar geometrical parameters. There is evidence for two types of Pb·····arene intermolecular interactions. Reciprocal (η^6-C_6H_4)—Pb interactions (Pb·····C_6(centroid) = 3.168 Å mean) exist for the π-stacked crystallographically identical molecules. In addition, the perpendicular approach of two crystallographically independent molecules results in a weak σ-interaction of the lone pair of electrons on lead with the arene ring (Pb·····C_6(centroid) = 3.978 Å mean). The lead compound, **23**, is isostructural but not isomorphous with the tin homologue, $[:Sn\{C_6H_4(Bu^tCH_2N)_2\text{-}1,2\}]$,[30] which displays reciprocal (η^6-C_6H_4)—Sn intermolecular interactions (Sn·····C_6(centroid) = 3.23 Å). It is unusual that the Pb·····C_6(centroid) distance in **23** is less than the Sn·····C_6(centroid) distance in $[:Sn\{C_6H_4(Bu^tCH_2N)_2\text{-}1,2\}]$, when the larger ionic radius of Pb(II) (1.32 Å) over Sn(II) (0.93 Å) is considered.[6] The tin homologue does not exhibit a perpendicular Sn·····arene interaction.

In order to shed light on the nature of the weak Ga—E bonds in **17** and **18**, DFT calculations were carried out on the model anions, $[\{(Me_3Si)_2HC\}_2E\text{-}Ga\{[N(Ph)C(H)]_2\}]^-$, E = Ge or Sn by S. P. Green. These complexes converged with similar geometries to those of **17** and **18**, though the bonds about the heavier group 14 and gallium centres were overestimated by 3 – 5%, as has been previously observed in DFT studies on metal complexes of the heterocycle, $[Ga\{[N(Ph)C(H)]_2\}]^-$.[2,7,9-12,14,17,28] In addition, the angles between the planes of the phenyl substituents and the plane of the

gallium heterocycle are significantly more acute than in the experimental complexes. This is probably a result of the lack of phenyl substitution in the model anions. Despite this, and the fact that coordination to counter-cations has not been taken into account in the model systems, the angles about the E centres of the theoretical anions are close to those for **17** and **18**. Most importantly, the fold angles, θ, (E = Ge 72.4°, Sn 74.8°) are in good agreement with the experimental complexes.

An NBO analysis of the Ga—E bonds (Wiberg bond indices: E = Ge 0.997, Sn 0.745) in $[\{(Me_3Si)_2HC\}_2EGa\{[N(Ph)C(H)]_2\}]^-$ revealed that the orbital contributions from the E centres are of very high *p*-character (E = Ge *s* 4.4%, *p* 95.4%; Sn *s* 4.7%, *p* 95.1%), whilst the orbital contributions from the donating Ga centres have s- to *sp*-character (E = Ge *s* 77.6%, *p* 22.3%; Sn *s* 64.4%, *p* 35.5%). This is consistent with the apparently weak Ga—E bonds and the minimal "rehybridisation" of the E centres upon heterocycle coordination. As might be expected, the lone pairs at the E centres of the anions have significant *s*-character (E = Ge 78.6%, Sn 80.9%). The orbitals that have the greatest contribution to the Ga—E bonds and the E lone pairs are the HOMO – 3 and HOMO – 1, which differ in energy by 32.3 and 31.4 kcal mol^{-1} for the germanium and tin model complexes respectively. Illustrations of these orbitals for the germanium system are depicted in Figure 8. The HOMO and HOMO – 2 are largely ligand based orbitals.

(a)

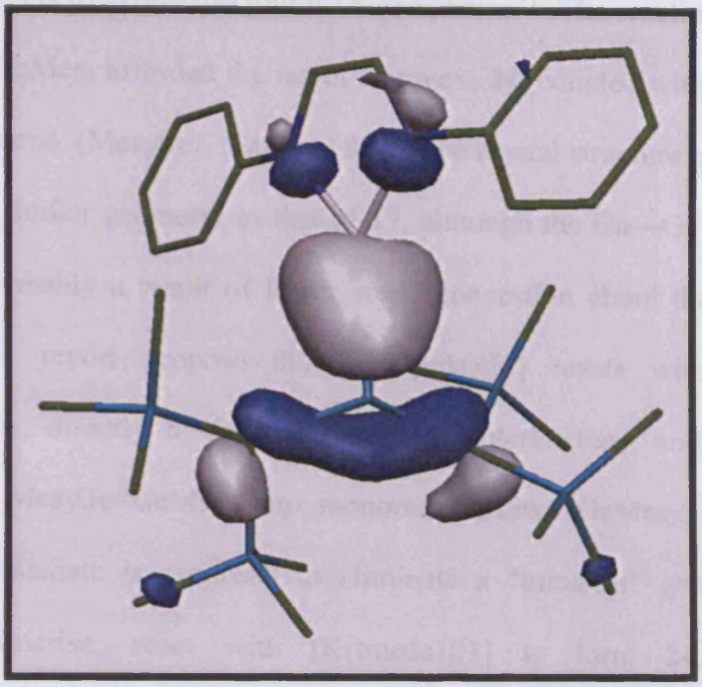

(b)

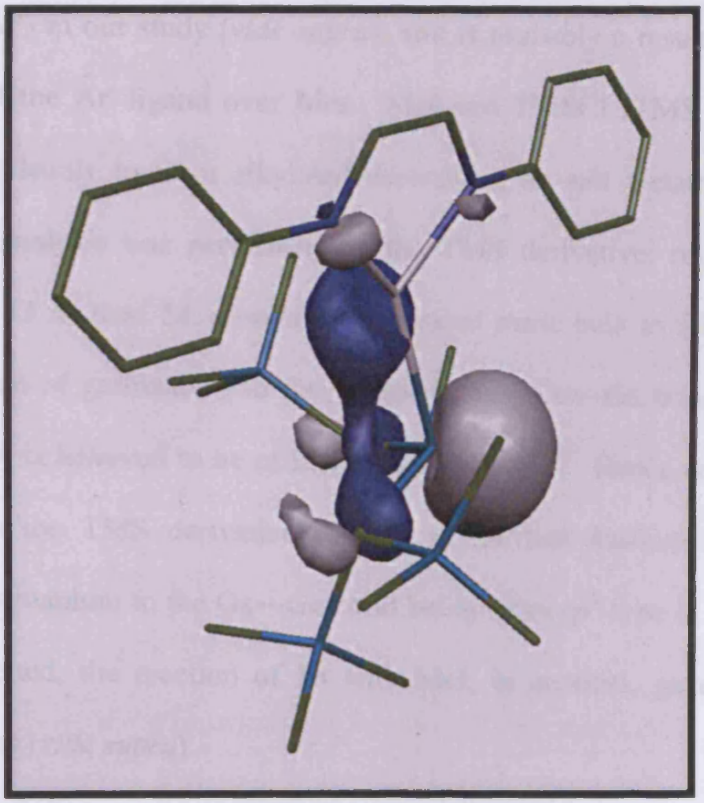

Figure 8 – Representations of (a) the HOMO – 3 and (b) the HOMO – 1 of the model anionic system, $[\{(Me_3Si)_2HC\}_2GeGa\{[N(Ph)C(H)]_2\}]^-$.

Since the publication of this work,[28f] the gallium(I) heterocycle, **1**, has been employed by others to synthesise group 14 complexes.[11] The reaction of [K(tmeda)][**1**] with $Mes_2Ge{=}GeMes_2$ afforded the novel complex, **24**, coupled with a trace amount of the cyclotrigermene, $(Mes_2Ge)_3$ (Scheme 8).[11] The crystal structure of **24** was obtained, and revealed a similar geometry to that of **17**, although the Ga—Ge bond is shorter in **24** (2.46 Å), probably a result of lower steric congestion about the Ge centre. The authors of this report propose that [K(tmeda)][**1**] reacts with the digermene, $Mes_2Ge{=}GeMes_2$, directly to form a trimetallic intermediate, and that there is no dissociation of $Mes_2Ge{=}GeMes_2$ into monomeric units, $:GeMes_2$, in solution. The trimetallic intermediate is proposed to eliminate a "transient" germylene fragment, which may dimerise, react with [K(tmeda)][**1**] to form **24**, or react with $Mes_2Ge{=}GeMes_2$ to form $(Mes_2Ge)_3$. The reactivity of [K(tmeda)][**1**] towards $Mes_2Ge{=}GeMes_2$ is in contrast to the lack of reactivity observed between [K(tmeda)][**1**] and $Ar'_2Ge{=}GeAr'_2$ in our study (*vide supra*), and is probably a result of the increased steric demand of the Ar' ligand over Mes. MeI and TMSCl (TMS = trimethylsilyl) reacted with **24** cleanly to form alkylated derivatives by salt metathesis. An X-ray crystallographic analysis was performed on the TMS derivative, revealing a shorter Ga—Ge bond (2.43 Å) than **24**, despite the increased steric bulk in this complex. The orbital contribution of germanium to the relatively long Ga—Ge bonds in complexes such as **17** and **24** is believed to be of mainly *p*-character.[28f] Hence contraction of the Ga—Ge bond in the TMS derivative relative to **24** was attributed to the orbital contribution of germanium to the Ga—Ge bond being more sp^3-type in character.[11] As previously mentioned, the reaction of **18** with MeI, in contrast, gave an intractable mixture of products (*vide supra*).

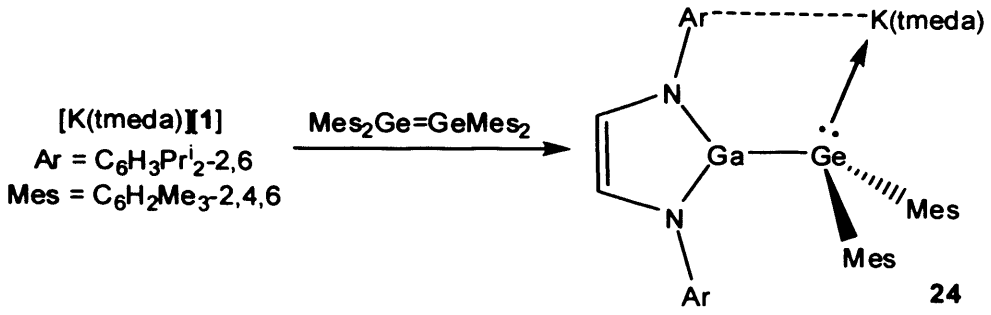

Scheme 8 – The synthesis of **24**

2.3.2 Preparation of Covalent Complexes

Complexes **17** and **18** can be considered as weakly bound "adducts" of an anionic gallium(I) heterocycle with germylene or stannylene fragments. It was thought logical to attempt the preparation of germanium(II) and tin(II) complexes of the heterocycle that contain more normal covalent bonds for purposes of comparison. Obviously, this should be achievable by salt elimination reactions between [K(tmeda)][**1**] and compounds of the type REX, E = Ge or Sn, X = halide. However, all previous attempts to utilise [K(tmeda)][**1**] in metathesis reactions with metal halide complexes have been unsuccessful, leading to paramagnetic gallium(II) dimers, $[XGa\{[N(Ar)C(H)]_2^{\cdot}\}]_2$,[31] presumably *via* insertion of the Ga(I) centre into the M—X bond of the precursor, followed by decomposition. Recently, we have discovered that if the metal halide precursor incorporates a bulky neutral or anionic chelating ligand, then the formation of $[XGa\{[N(Ar)C(H)]_2^{\cdot}\}]_2$ can be circumvented. We have developed synthetic routes to monomeric germanium(II), tin(II) and lead(II) halide complexes, e.g. [(Piso)GeCl][32] ($Piso^-$ = $[\{N(Ar)\}_2CBu^t]^-$) and [(Priso)ECl] (E = Ge,[32] Sn[33] or Pb,[33] $Priso^-$ = $[\{N(Ar)]_2\}CNPr^i_2]^-$), stabilised by very bulky amidinate and guanidinate ligands and saw these as ideal starting materials for this study.

In collaboration with K. –A. Lippert and Dr. A. Stasch, the 1 : 1 reactions of [K(tmeda)][**1**] with [(Piso)GeCl] and [(Priso)ECl], E = Ge or Sn, in toluene led to good yields of the monomeric germanium or tin-gallyl complexes, **25** – **27** (Scheme 8). Compounds **25** – **27** were found to be unreactive towards excess [K(tmeda)][**1**]. The ^{1}H and $^{13}C\{^{1}H\}$ NMR spectra of all complexes are similar and consistent with the retention of their solid state structures in solution. The presence of only two methyl doublet resonances for the isopropyl groups of the gallium heterocycle in the spectra of all compounds suggests that the rotation of that heterocycle about the Ga—E bond is not restricted. This has been noted previously for complexes of the heterocycle.[2,7,9-12,14,17,28] Despite this, resonances for four chemically inequivalent sets of methyl groups from the group 14 heterocycle aryl substituents were observed in the spectra of the complexes. The $^{119}Sn\{^{1}H\}$ NMR spectra of **27** exhibits a broad singlet (δ 454.8 ppm) in the normal region for neutral complexes containing a 3-coordinate tin centre (*cf.* **15**, δ 710 ppm). The reaction of [(Priso)PbCl] with [K(tmeda)][**1**] yielded only the digallane(4), $[Ga\{[N(Ar)C(H)]_2\}]_2$,[5] with lead metal deposition. No reaction was observed in the reaction of [K(tmeda)][**1**] with the germanium(II) heterocycle, $[:Ge\{[N(Bu^t)C(H)]_2\}]$.

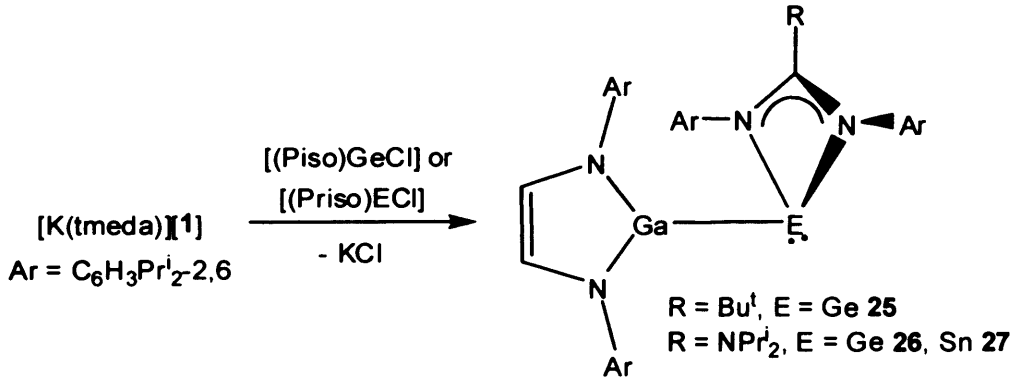

Scheme 9 – The synthesis of **25** – **27**

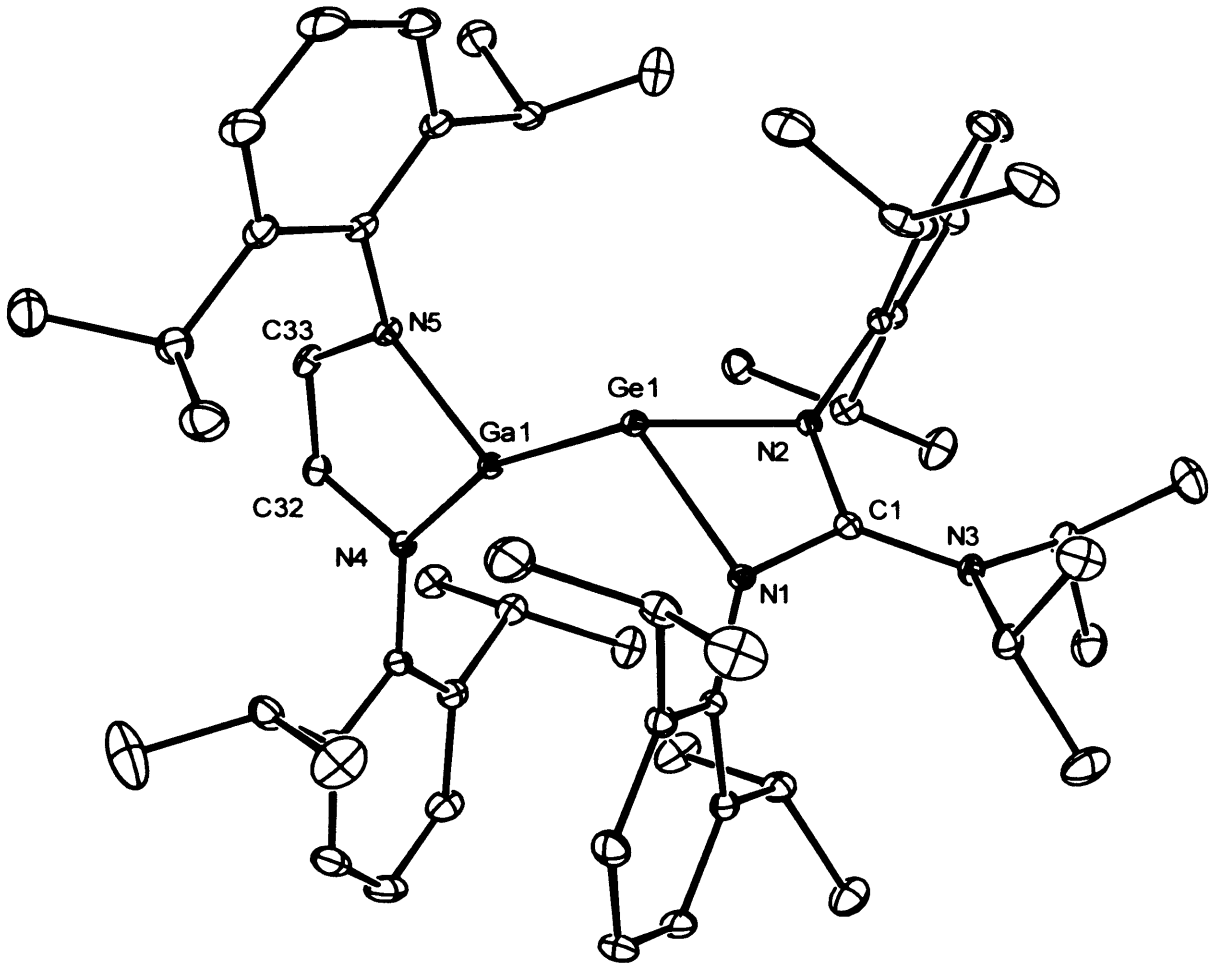

Figure 9 – Thermal ellipsoid plot (25 % probability surface) of the molecular structure of [(Priso)Ge{Ga{[N(Ar)C(H)]$_2$}}] **26**; hydrogen atoms omitted for clarity. Selected bond lengths (Å) and angles (°): Ge(1)—N(1) 1.9971(15), Ge(1)—N(2) 2.0148(16), Ge(1)—Ga(1) 2.5157(7), Ga(1)—N(4) 1.8825(16), Ga(1)—N(5) 1.8898(16), N(1)—C(1) 1.353(2), N(2)—C(1) 1.346(2), N(3)—C(1) 1.369(2), N(4)—C(32) 1.396(2), N(5)—C(33) 1.389(3), C(32)—C(33) 1.344(3), N(1)—Ge(1)—N(2) 65.03(6), N(1)—Ge(1)—Ga(1) 108.98(5), N(2)—Ge(1)—Ga(1) 105.07(4), N(4)—Ga(1)—N(5) 87.10(7), N(4)—Ga(1)—Ge(1) 161.38(5), N(5)—Ga(1)—Ge(1) 110.50(5), C(1)—N(1)—Ge(1) 93.53(11), C(1)—N(2)—Ge(1) 92.95(11), N(2)—C(1)—N(1) 106.08(16).

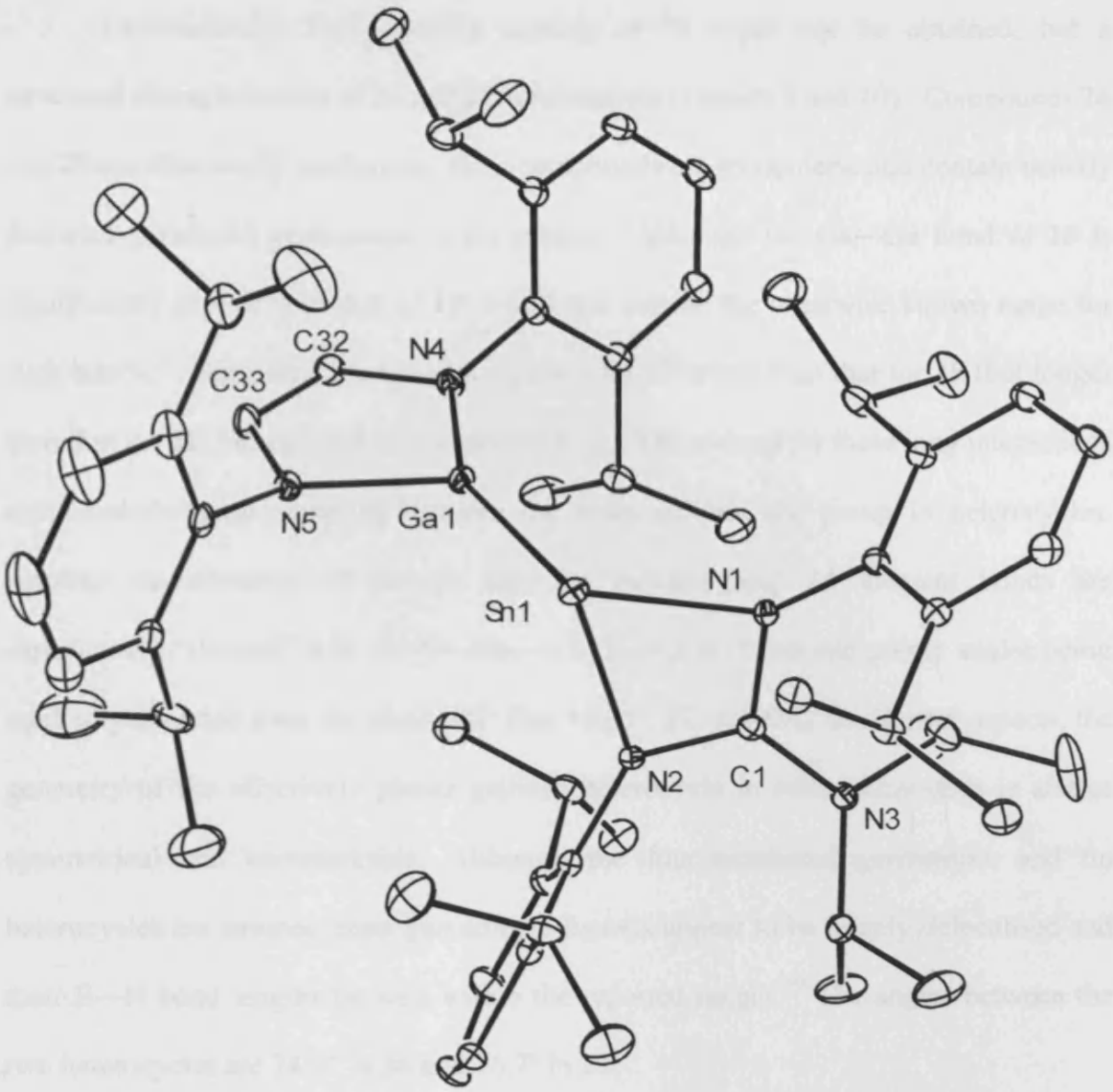

Figure 10 – Thermal ellipsoid plot (25 % probability surface) of the molecular structure of [(Priso)Sn{Ga{[N(Ar)C(H)]$_2$}}] **27**; hydrogen atoms omitted for clarity. Selected bond lengths (Å) and angles (°): Sn(1)—N(1) 2.188(3), Sn(1)—N(2) 2.215(3), Sn(1)—Ga(1) 2.6888(6), Ga(1)—N(4) 1.882(3), Ga(1)—N(5) 1.890(3), N(1)—C(1) 1.365(4), N(2)—C(1) 1.345(4), N(3)—C(1) 1.371(4), N(4)—C(32) 1.401(4), N(5)—C(33) 1.388(5), C(32)—C(33) 1.349(5), N(1)—Sn(1)—N(2) 60.18(10), N(1)—Sn(1)—Ga(1) 104.39(8), N(2)—Sn(1)—Ga(1) 99.70(7), N(4)—Ga(1)—N(5) 87.56(13), N(4)—Ga(1)—Sn(1) 157.14(9), N(5)—Ga(1)—Sn(1) 114.63(10), C(1)—N(1)—Sn(1) 95.3(2), C(1)—N(2)—Sn(1) 94.7(2), N(2)—C(1)—N(1) 109.1(3).

Unfortunately, X-ray quality crystals of **25** could not be obtained, but a structural characterisation of **26** and **27** was possible (Figures 9 and 10). Compounds **26** and **27** are structurally analogous. Both compounds are monomeric and contain heavily distorted pyramidal germanium or tin centres. Although the Ga—Ge bond of **26** is significantly shorter than that of **17**, it still lies outside the otherwise known range for such bonds.[29] Similarly, the Ga—Sn distance for **27** is less than that for **18** (but longer than that for **21**) but can still be considered long. The reasons for these long interactions must include steric crowding between the bulky gallium and group 14 heterocycles. Another manifestation of this is that the gallium-group 14 element bonds are significantly "skewed" with the E—Ga—{C(32)—C(33) bond mid point} angles being markedly distorted from the ideal 180° (**26**: 153.5°, **27**: 157.9°). In all other aspects, the geometry of the effectively planar gallium heterocycle in both compounds is almost symmetrical and unremarkable. Although the four-membered germanium and tin heterocycles are strained, their guanidinate ligands appear to be largely delocalised and their E—N bond lengths lie well within the reported ranges.[29] The angles between the two heterocycles are 74.9° in **26** and 76.7° in **27**.

2.4 Conclusion

In summary, the reactions of an anionic gallium(I) heterocyclic complex, [K(tmeda)][:Ga{[N(Ar)C(H)]$_2$}], with a variety of heavier group 14 element(II) precursors have been carried out. In the case of the reactions with $R_2E{=}ER_2$, E = Ge or Sn, the ionic complexes, [K(tmeda)][R_2E{Ga{[N(Ar)C(H)]$_2$}}], which exhibit weak Ga—E bonds, are formed. The tin complex exhibits the first structurally characterised example of such a bond in a molecular compound. The nature of the Ga—E bonds has been probed by DFT calculations and the complexes shown to be closely related to

neutral NHC adducts of group 14 dialkyls. It is of interest that the tin complex reacts with a further equivalent of the gallium heterocycle to give [K(tmeda)] [RSn{Ga{[N(Ar)C(H)]$_2$}}$_2$], whereas its germanium counterpart is unreactive. Moreover, the complexes, Ar'$_2$E=EAr'$_2$, E = Ge, Sn or Pb, were found to be, in general, less reactive than $R_2E=ER_2$ towards the gallium heterocycle. The study has also highlighted the utility of the anionic gallium(I) heterocycle in potassium halide elimination reactions for the first time. Its reactions with bulky monomeric amidinato and guanidinato group 14 halide complexes have given neutral complexes, [(Piso)Ge{Ga{[N(Ar)C(H)]$_2$}}] and [(Priso)E{Ga{[N(Ar)C(H)]$_2$}}], E = Ge or Sn, with covalent Ga—E bonds that are shorter than the weak Ga—E interactions seen in the aforementioned anionic complexes. Despite this, these bonds are still long, presumably due to considerable steric crowding within the complexes. This study also resulted in the first structural characterisation of a lead NHC analogue, [:Pb{C_6H_4(Bu^{t}CH$_2$N)$_2$-1,2}]. Most of the work discussed in this chapter has been summarised in a recent publication.[28f]

2.5 Experimental

General experimental procedures are compiled in Appendix 1 and crystallographic data are compiled in Appendix 3. ^{29}Si{^{1}H} NMR spectra were recorded on a Jeol Eclipse 300 spectrometer operating at 59.7 MHz and were referenced to $SiMe_4$. ^{119}Sn{^{1}H} NMR spectra were recorded on a Bruker AMX 500 spectrometer operating at 186.4 MHz and were referenced to $SnMe_4$. Where reproducible microanalyses could not be obtained due to solvent of crystallisation or the highly air sensitive nature of the compound, the NMR spectra of the samples suggested protic impurities < 5 %. [K(tmeda)][:Ga{[N(Ar)C(H)]$_2$}],[1] [Ge{CH(SiMe$_3$)$_2$}$_2$]$_2$,[23]

$[Sn\{CH(SiMe_3)_2\}_2]_2$,[23] $[Sn(Ar')_2]_3$,[34] $[Pb(Ar')_2]_2$,[35] and $[:Pb\{C_6H_4(Bu^tCH_2N)_2\text{-}1,2\}]$[22a] were synthesised by literature procedures. [(Piso)GeCl][32] and [(Priso)GeCl],[32] and were synthesised by K. –A. Lippert and A. Stasch by literature procedures. [(Priso)SnCl][33] was synthesised by K. –A. Lippert and Dr. A. Stasch by an unpublished procedure which involved the 1 : 1 reaction of [Li(Priso)] with $SnCl_2$ in diethyl ether. All other reagents were used as received.

Geometries of the model anions $[\{(Me_3Si)_2HC\}_2EGa\{[N(Ph)C(H)]_2\}]^-$, E = Ge or Sn were optimised using the Gaussian '98 package[36] by S. P. Green employing the methods recommended by Boehme and Frenking.[37] That is the BP86 density functional method,[38] with a 6-31G* basis set on C, N and H,[39] Stuttgart-Dresden ECP/basis sets for Si, Ga and Sn,[40] augmented by a *d*-type polarisation function with exponent 0.207 on Ga, 0.183 on Sn and 0.246 on Ge.[41] Atomic charges, orbital populations and bonding analyses were obtained from the NBO scheme[42] of the optimised structure. To comply with the maximum basis functions allowed by the NBO program, 6-31G basis sets were applied to C and H atoms outside the gallium heterocycle and those not directly bound to the group 14 centres.

Preparation of [K(tmeda)][Ge{CH(SiMe$_3$)$_2$}$_2${Ga{[N(Ar)C(H)]$_2$}}] 17: A solution of [K(tmeda)][:Ga{[N(Ar)C(H)]$_2$}] (0.31 g, 0.51 mmol) in diethyl ether (20 cm^3) was added to a solution of $[Ge\{CH(SiMe_3)_2\}_2]_2$ (0.20 g, 0.26 mmol) in diethyl ether (20 cm^3) at -78 °C. The orange reaction mixture was warmed to 20 °C and stirred overnight. Volatiles were then removed *in vacuo*, and the residue extracted into hexane (40 cm^3) and filtered. The filtrate was concentrated to *ca.* 20 cm^3 and stored at -30 °C overnight to give yellow crystals of **17** (0.28 g, 56 %). Mp 110-112 °C (decomp.); ^{1}H NMR (400 MHz, C_6D_6, 298 K): δ 0.16 (s, 18H, $(CH_3)_3Si$), 0.18 (s, 2H, $\{(CH_3)_3Si\}_2CH$)

0.22 (s, 18H, $(CH_3)_3Si$), 1.29 (d, $^3J_{HH}$ = 6.8 Hz, 12H, $(CH_3)_2CH$), 1.32 (d, $^3J_{HH}$ = 6.8 Hz, 12H, $(CH_3)_2CH$), 1.68 (s, 4H, NCH_2), 1.70 (s, 12 H, $(CH_3)_2N$), 3.84 (sept, $^3J_{HH}$ = 6.8 Hz, 4H, $(CH_3)_2CH$), 6.27 (s, 2H, NC*H*), 6.88 (t, $^3J_{HH}$ = 7.6 Hz, 2H, *p*-Ar-*H*), 7.03 (d, $^3J_{HH}$ = 7.6 Hz, 4H, *m*-Ar-*H*); $^{13}C\{^1H\}$ NMR (75.6 MHz, C_6D_6, 298 K): δ 3.1 ($\{(CH_3)_3Si\}_2CH$), 3.8 ($(CH_3)_3Si$), 4.5 ($(CH_3)_3Si$), 23.4 ($(CH_3)_2CH$), 26.6 ($(CH_3)_2CH$), 28.5 ($(CH_3)_2CH$), 45.5 ($(CH_3)_2N$), 57.0 (NCH_2), 121.9 (*C*N), 123.1 (*m*-Ar-*C*), 123.7 (*p*-Ar-*C*), 146.8 (*o*-Ar-*C*), 150.3 (*ipso*-Ar-*C*); $^{29}Si\{^1H\}$ NMR (59.7 MHz, C_6D_6, 298 K): δ -0.95, -0.20 ($Si(CH_3)_3$); MS (EI 70eV) *m/z* (%): 446 ($Ga\{[N(Ar)C(H)]_2\}H^+$, 100), 377 ($\{N(Ar)C(H)\}_2H^+$, 46); IR ν/cm^{-1} (Nujol): 1583 s, 1564 s, 1250 s, 1101 s, 1014 s, 844 s.

Preparation of [K(tmeda)][Sn{CH(SiMe$_3$)$_2$}$_2${Ga{[N(Ar)C(H)]$_2$}}] 18: A solution of [K(tmeda)][:Ga{[N(Ar)C(H)]$_2$}] (0.27 g, 0.45 mmol) in diethyl ether (60 cm^3) was added over 1 hr to a solution of [Sn{CH(SiMe$_3$)$_2$}$_2$]$_2$ (0.19 g, 0.23 mmol) in diethyl ether (40 cm^3) at -50 °C. The red reaction mixture was stirred for 2 hrs, warmed to 20 °C and stirred overnight. Volatiles were then removed *in vacuo* and the residue extracted into hexane (40 cm^3) and filtered. The filtrate was concentrated to *ca.* 20 cm^3 and stored at -30 °C overnight to give large red crystals of **18** (0.16 g, 35 %). Mp 130-132 °C (decomp.); ^1H NMR (400 MHz, C_6D_6): δ 0.17 (s, 2H, $\{(CH_3)_3Si\}_2CH$), 0.20 (s, 18H, $(CH_3)_3Si$), 0.28 (s, 18H, $(CH_3)_3Si$), 1.29 (d, $^3J_{HH}$ = 6.8 Hz, 12H, $(CH_3)_2CH$), 1.32 (d, $^3J_{HH}$ = 6.8 Hz 12H, $(CH_3)_2CH$), 1.67 (s, 4H, NCH_2), 1.72 (s, 12H, $(CH_3)_2N$), 3.87 (sept, $^3J_{HH}$ = 6.8 Hz, 4H, $(CH_3)_2CH$), 6.30 (s, 2H, NC*H*), 6.88 (t, $^3J_{HH}$ = 7.6 Hz, 2H, *p*-Ar-*H*), 7.04 (d, $^3J_{HH}$ = 7.6 Hz, 4H, *m*-Ar-*H*); $^{13}C\{^1H\}$ NMR (75.6 MHz, C_6D_6, 298 K): δ 3.8 ($\{(CH_3)_3Si\}_2CH$), 4.4 ($(CH_3)_3Si$), 4.7 ($(CH_3)_3Si$), 24.2 ($(CH_3)_2CH$), 26.4 ($(CH_3)_2CH$), 28.5 ($(CH_3)_2CH$), 45.2 ($(CH_3)_2N$), 56.7 (NCH_2), 122.2 (*C*N), 123.0 (*m*-Ar-*C*), 123.8 (*p*-Ar-*C*), 146.9 (*o*-Ar-*C*), 150.2 (*ipso*-Ar-*C*); $^{29}Si\{^1H\}$ NMR (59.7 MHz, C_6D_6, 298 K): δ -0.04, 0.31 ($Si(CH_3)_3$); $^{119}Sn\{^1H\}$ NMR (186.4 MHz, C_6D_6, 298 K): δ -

97.9 (pw 233 Hz at 1/2 peak height); MS (EI 70eV) *m/z* (%): 446 ($Ga\{N(Ar)C(H)\}_2H^+$, 67), 377 ($\{N(Ar)C(H)\}_2H^+$, 100); IR ν/cm^{-1} (Nujol): 1588 s, 1565 m, 1248 s, 1113 s, 1020 s; $C_{46}H_{90}N_4Si_4KGaSn$ requires C 53.17, H 8.73, N 5.39 %; found: C 52.42, H 8.60, N 5.38 %.

Preparation of [K(tmeda)][Sn{CH(SiMe$_3$)$_2$}{Ga{[N(Ar)C(H)]$_2$}}$_2$] 19: A solution of [K(tmeda)][:Ga{[N(Ar)C(H)]$_2$}] (0.56 g, 0.92 mmol) in diethyl ether (20 cm^3) was added to a solution of [Sn{CH(SiMe$_3$)$_2$}$_2$]$_2$ (0.20 g, 0.23 mmol) in diethyl ether (20 cm^3) at -78 °C. The red reaction mixture was warmed to 20 °C and stirred overnight. Volatiles were then removed *in vacuo* and the residue extracted into hexane (40 cm^3) and filtered. The filtrate was concentrated to *ca.* 15 cm^3 and stored at -30 °C overnight to give orange crystals of **19** (0.10 g, 16 %). Mp 188-190 °C (decomp.); ^{1}H NMR (400 MHz, C_6D_6, 298 K): δ 0.28 (s, 1H, $\{(CH_3)_3Si\}_2CH$), 0.35 (s, 18H, $(CH_3)_3Si$), 1.40 (br. overlapping m, 48H, $(CH_3)_2CH$), 1.87 (s, 12H, $(CH_3)_2N$), 1.96 (s, 4H, NCH_2), 3.84 (br. overlapping m, 8H, $(CH_3)_2CH$), 6.35 (br. s, 4H, NC*H*), 7.11-7.15 (m., 12H, Ar-*H*); $^{13}C\{^1H\}$ NMR (75.6 MHz, C_6D_6, 298 K): δ 1.2 ($\{(CH_3)_3Si\}_2CH$), 3.3 ($(CH_3)_3Si$), 23.9, 24.9, 26.0, 26.3 ($(CH_3)_2CH$), 28.1, 28.2 ($(CH_3)_2CH$), 45.3 ($(CH_3)_2N$), 57.0 (NCH_2), 123.0 (br., *C*N), 123.7 (br., *m*-Ar-*C*), 124.4 (br., *p*-Ar-*C*), 146.4 (br., *o*-Ar-*C*), 152.6 (br., *ipso*-Ar-*C*); $^{29}Si\{^1H\}$ NMR (59.7 MHz, C_6D_6, 298 K): δ 0.30 ($Si(CH_3)_3$); MS (EI 70eV) *m/z* (%): 446 ($Ga\{[N(Ar)C(H)]_2\}H^+$, 18), 377 ($\{N(Ar)C(H)\}_2H^+$, 41 %); IR ν/cm^{-1} (Nujol): 1652 m, 1625 m, 1594 m, 1249 s, 1106 s, 1021 s.

Preparation of [K(tmeda)][Sn(Ar')$_2${Ga{[N(Ar)C(H)]$_2$}}] 21: A solution of [Sn(Ar')$_2$]$_3$ (0.40 g, 0.25 mmol) in diethyl ether (60 cm^3) at -55 °C was irradiated at 256 nm for 3 hrs, yielding a red solution. This was cooled to -78 °C and a solution of [K(tmeda)] [:Ga{[N(Ar)C(H)]$_2$}] (0.46 g, 0.76 mmol) in diethyl ether (30 cm^3) was

added. The red reaction mixture was allowed to warm to 20 °C overnight. The volatiles were removed *in vacuo* and the residue was extracted with hexane (120 cm^3) and filtered. Concentration of the filtrate to *ca.* 80 cm^3 and storage at -30 °C overnight yielded orange crystals of **21** (0.79 g, 92 %). Mp 141-145 °C (decomp.); ^{1}H NMR (400 MHz, C_6D_6, 298 K): δ 0.75 (d, $^3J_{HH}$ = 6.9 Hz, 12H, *p*-(CH_3)$_2$CH, Ar'), 0.91 (v. t, $^3J_{HH}$ = 6.8 Hz, 24H, *o*-(CH_3)$_2$CH, Ar'), 0.99 (d, $^3J_{HH}$ = 6.8 Hz, 12H, (CH_3)$_2$CH, Ar), 1.08 (d, $^3J_{HH}$ = 6.8 Hz, 12H, (CH_3)$_2$CH, Ar), 1.45 (s, 12H, (CH_3)$_2$N), 1.50 (s, 4 H, NCH_2), 2.53 (sept, $^3J_{HH}$ = 6.9 Hz, 2 H, *p*-(CH_3)$_2$C*H*, Ar'), 3.46, 3.59 (2 x sept, $^3J_{HH}$ = 6.8 Hz, 2 x 4H, (CH_3)$_2$C*H*, Ar' and Ar), 6.09 (s, 2 H, NC*H*), 6.65 (t, $^3J_{HH}$ = 7.4 Hz, 2H, *p*-Ar-*H*, Ar), 6.76 (s, 4H, *m*-Ar-*H*, Ar'), 6.78 (d, $^3J_{HH}$ = 7.4 Hz, 4H, *m*-Ar-*H*, Ar); ^{13}C{^{1}H} NMR (75.6 MHz, C_6D_6, 298 K): δ 24.0, 24.4, 24.8, 25.1, 25.7 ((CH_3)$_2$CH), 28.5, 34.5, 39.6 ((CH_3)$_2$*C*H), 45.0 ((CH_3)$_2$N), 56.8 (NCH_2), 120.3 (*C*N), 122.5, 122.9, 123.9, 146.3, 146.9, 150.2, 153.9, 155.0 (Ar-*C*); ^{119}Sn{^{1}H} NMR (186.4 MHz, C_6D_6, 298 K): δ -306.7 (pw 251 Hz at 1/2 peak height); MS (EI 70eV) *m/z* (%): 1126 (MH^+, 3), 648 (Ar'Ga{[N(Ar)C(H)]$_2$H$^+$, 100), 446 (Ga{[N(Ar)C(H)]$_2$}H$^+$, 13), 377 ({N(Ar)C(H)}$_2$H$^+$, 14); IR ν/cm^{-1} (Nujol): 1842 m, 1666 m, 1594 s, 1556 s, 1260 s, 1099 s.

Preparation of [Ar'Ga{[N(Ar)C(H)]$_2$}] 22: A solution of [K(tmeda)] [:Ga{[N(Ar)C(H)]$_2$}] (0.28 g, 0.46 mmol) in diethyl ether (30 cm^3) was added to a solution of [Pb(Ar')$_2$]$_2$ (0.28 g, 0.23 mmol) in diethyl ether (20 cm^3) at -78 °C. The deep red reaction mixture was warmed to room temperature over 2 hrs, during which time a lead mirror formed on the side of the vessel. Volatiles were then removed *in vacuo* and the residue was extracted into hexane (40 cm^3) and filtered. The filtrate was concentrated to *ca.* 5 cm^3 and stored at -30 °C overnight to give yellow crystals of **22** (0.04 g, 13 %). Mp 112-114 °C; ^{1}H NMR (400 MHz, C_6D_6, 298 K): δ 0.77 (d, $^3J_{HH}$ = 6.7 Hz, 12H, *o*-(CH_3)$_2$CH, Ar'), 0.80 (d, $^3J_{HH}$ = 6.9 Hz, 6H, *p*-(CH_3)$_2$CH, Ar'), 0.87 (d,

$^3J_{HH}$ = 6.8 Hz, 12H, (CH_3)$_2$CH, Ar), 0.98 (d, $^3J_{HH}$ = 6.8 Hz, 12H, (CH_3)$_2$CH, Ar), 2.36 (sept, $^3J_{HH}$ = 6.9 Hz, 1H, *p*-(CH$_3$)$_2$C*H*, Ar'), 2.48 (sept, $^3J_{HH}$ = 6.7 Hz, 2H, *o*-(CH$_3$)$_2$C*H*, Ar'), 3.45 (sept, $^3J_{HH}$ = 6.8 Hz, 4H, (CH$_3$)$_2$C*H*, Ar), 6.14 (s, 2H, NC*H*), 6.58 (s, 2H, *m*-Ar-*H*, Ar'), 6.71-6.89 (m, 6H, Ar-*H*, Ar); ^{13}C{^{1}H} NMR (75.6 MHz, C_6D_6, 298 K): δ 23.7, 23.9, 24.6, 25.7 ((*C*H$_3$)$_2$CH), 28.5, 34.4, 40.9 ((CH$_3$)$_2$*C*H), 120.2 (*C*N), 121.42, 123.8, 125.3, 133.3, 144.5, 144.7, 151.9, 155.3 (Ar-*C*); MS (EI 70eV) *m/z* (%): 648 (MH^+, 80), 446 (Ga{[N(Ar)C(H)]$_2$}H$^+$, 5), 377 ({N(Ar)C(H)}$_2$H$^+$, 83); IR ν/cm^{-1} (Nujol): 1659 m, 1593 s, 1557 m, 1260 s, 1203 s, 1118 s, 1101 s, 1058 s, 934 s; EI acc. mass on M^+: calc. for $C_{41}H_{59}N_2Ga$: 648.3929, found 648.3926; $C_{41}H_{59}N_2Ga$ requires C 75.80, H 9.15, N 4.31; found: C 74.97, H 9.20, N 4.40.

Preparation of [(Piso)Ge{Ga{[N(Ar)C(H)]$_2$}}] 25: A solution of [K(tmeda)][:Ga{[N(Ar)C(H)]$_2$}] (0.06 g, 0.10 mmol) in toluene (5 cm^3) was added to a solution of [(Piso)GeCl] (0.05 g, 0.10 mmol) in toluene (5 cm^3) at -78 °C. The deep red reaction mixture was warmed to 20 °C and stirred overnight. Volatiles were then removed *in vacuo* and the residue was extracted into hexane (5 cm^3) and filtered. The filtrate was concentrated to *ca.* 0.5 cm^3 and stored at -30 °C overnight to give light red crystals of **25** (0.04 g, 44 %). Mp 151-152 °C (decomp.); ^{1}H NMR (400 MHz, C_6D_6, 298 K): δ 0.92 (s, 9 H, (CH_3)$_3$C), 1.09 (d, $^3J_{HH}$ = 6.7 Hz, 6 H, (CH_3)$_2$CH, Ge ring), 1.14 (d, $^3J_{HH}$ = 6.7 Hz, 6 H, (CH_3)$_2$CH, Ge ring), 1.23 (d, $^3J_{HH}$ = 6.9 Hz, 12 H, (CH_3)$_2$CH, Ga ring), 1.29 (d, $^3J_{HH}$ = 6.8 Hz, 6 H, (CH_3)$_2$CH, Ge ring), 1.39 (dd, $^3J_{HH}$ = 6.9 Hz, $^3J_{HH}$ = 6.8 Hz, 18 H, (CH_3)$_2$CH, Ga ring + Ge ring), 3.58 (sept, $^3J_{HH}$ = 6.8 Hz, 2 H, (CH$_3$)$_2$C*H*, Ge ring), 3.64 (sept, $^3J_{HH}$ = 6.7 Hz, 2 H, (CH$_3$)$_2$C*H*, Ge ring), 3.75 (sept, $^3J_{HH}$ = 6.9 Hz, 4 H, (CH$_3$)$_2$C*H*, Ga ring), 6.47 (s, 2 H, C*H*N) 7.08-7.29 (m, 12 H, *m*-Ar-*H*, Ga ring + Ge ring); ^{13}C{^{1}H} NMR (100.6 MHz, C_6D_6, 298 K): δ 22.3 ((*C*H$_3$)$_3$C), 24.2, 25.6 ((*C*H$_3$)$_2$CH, Ga ring), 26.7, 27.8 ((*C*H$_3$)$_2$CH, Ge ring), 28.2, 28.5 ((CH$_3$)$_2$*C*H, Ga ring),

28.8, 29.2 ($(CH_3)_2CH$, Ge ring), 42.2 ($(CH_3)_3C$), 122.7 (*C*N), 123.0, 123.7, 125.1, 126.9, 138.6, 143.9, 145.3, 146.7 (Ar-*C*), 167.2 (CN_2C); MS (EI 70eV) *m/z* (%): 420 ($\{[N(Ar)]_2CBu^t\}H^+$, 100), 378 ($\{N(Ar)C(H)\}_2H^+$, 8); IR ν/cm^{-1} (Nujol): 1612 w, 1586 w, 1406 s, 1256 s, 1210 w, 1118 s.

Preparation of [(Priso)Ge{Ga{[N(Ar)C(H)]$_2$}}] 26: A solution of [K(tmeda)][:Ga{[N(Ar)C(H)]$_2$}] (0.25 g, 0.41 mmol) in toluene (20 cm^3) was added to [(Priso)GeCl] (0.24 g, 0.41 mmol) in toluene (10 cm^3) at -78 °C. The red reaction mixture was warmed to 20 °C and stirred overnight. Volatiles were then removed *in vacuo* and the residue was extracted into hexane (20 cm^3) and filtered. The filtrate was concentrated to *ca.* 5 cm^3 and stored at -30 °C overnight to give light red crystals of **26** (0.26 g, 64 %). Mp 149-152 °C (decomp.); ^{1}H NMR (400 MHz, C_6D_6, 298 K): δ 0.77 (d, $^3J_{HH}$ = 7.0 Hz, 12H, (CH_3)$_2$CHN), 1.10 (2 x coincidental d, $^3J_{HH}$ = 6.7 Hz, 12H, (CH_3)$_2$CH, Ge ring), 1.21 (d, $^3J_{HH}$ = 6.9 Hz, 12H, (CH_3)$_2$CH, Ga ring), 1.28 (d, $^3J_{HH}$ = 6.8 Hz, 6H, (CH_3)$_2$CH, Ge ring), 1.34 (d, $^3J_{HH}$ = 6.8 Hz, 6H, (CH_3)$_2$CH, Ge ring), 1.40 (d, $^3J_{HH}$ = 6.9 Hz, 12H, (CH_3)$_2$CH, Ga ring), 3.57 (sept, $^3J_{HH}$ = 6.7 Hz, 2H, (CH_3)$_2$C*H*, Ge ring), 3.68 (sept, $^3J_{HH}$ = 6.8 Hz, 2H, (CH_3)$_2$C*H*, Ge ring), 3.74 (sept, $^3J_{HH}$ = 6.9 Hz, 4H, (CH_3)$_2$C*H*, Ga ring), 3.87 (sept, $^3J_{HH}$ = 7.0 Hz, 2H, (CH_3)$_2$C*H*N), 6.40 (s, 2H, C*H*N) 7.03-7.29 (m, 12H, Ar-*H*); ^{13}C{^{1}H} NMR (100.6 MHz, C_6D_6, 298 K): δ 22.9 ((CH_3)$_2$CH, Ge ring), 23.0 ((CH_3)$_2$CH, Ge ring), 23.2 ((CH_3)$_2$CHN), 24.3 ((CH_3)$_2$CH, Ga ring), 25.6 ((CH_3)$_2$CH, Ga ring), 26.1 ((CH_3)$_2$CH, Ge ring), 27.8 ((CH_3)$_2$CH, Ge ring), 28.2 ((CH_3)$_2$CH, Ga ring), 28.4 ((CH_3)$_2$CH, Ge ring), 28.7 ((CH_3)$_2$CH, Ge ring), 49.0 ((CH_3)$_2$CHN), 122.5 (*C*N), 122.9, 124.1, 124.1, 124.8, 126.6, 138.5, 144.8, 145.3, 145.8, 147.5 (Ar-*C*), 154.9 (CN_3); MS (EI 70eV) *m/z* (%): 981 (MH^+, 5), 377 ($\{N(Ar)C(H)\}_2H^+$, 8); IR ν/cm^{-1} (Nujol): 1612 w, 1586 w, 1408 s, 1256 s, 1211 w, 1120 s, 1055 m, 937 w; EI acc. mass on M^+: calc. for $C_{57}H_{84}N_5GaGe$: 981.5189, found:

981.5182; $C_{57}H_{84}N_5GaGe$ requires C 69.74, H 8.62, N 7.13; found: C 69.61, H 8.76, N 7.32.

Preparation of [(Priso)Sn{Ga{[N(Ar)C(H)]$_2$}}] 27: A solution of [K(tmeda)][:Ga{[N(Ar)C(H)]$_2$}] (0.29 g, 0.48 mmol) in toluene (20 cm^3) was added to [(Priso)SnCl] (0.30 g, 0.48 mmol) in toluene (10 cm^3) at -78 °C. The deep red reaction mixture was warmed to 20 °C and allowed to stir overnight. Volatiles were then removed *in vacuo* and the residue was extracted into hexane (20 cm^3) and filtered. The filtrate was concentrated to *ca.* 5 cm^3 and stored at -30 °C overnight to give deep red crystals of **27** (0.26 g, 52 %). Mp 205-206 °C; ^{1}H NMR (400 MHz, C_6D_6, 298 K): δ 0.81 (d, $^3J_{HH}$ = 6.9 Hz, 12H, (C*H*$_3$)$_2$CHN), 1.12 (2 x coincidental d, $^3J_{HH}$ = 6.8 Hz, 12H, (C*H*$_3$)$_2$CH, Sn ring), 1.23 (d, $^3J_{HH}$ = 6.9 Hz, 12H, (C*H*$_3$)$_2$CH, Ga ring), 1.30 (d, $^3J_{HH}$ = 6.8 Hz, 6H, (C*H*$_3$)$_2$CH, Sn ring), 1.37 (d, $^3J_{HH}$ = 6.8 Hz, 6H, (C*H*$_3$)$_2$CH, Sn ring), 1.40 (d, $^3J_{HH}$ = 6.9 Hz, 12H, (C*H*$_3$)$_2$CH, Ga ring), 3.61 (sept, $^3J_{HH}$ = 6.8 Hz, 2H, (CH$_3$)$_2$C*H*, Sn ring), 3.76 (overlapping m., 6H, (CH$_3$)$_2$C*H*, Ga (4H) and Sn (2H) rings), 3.92 (sept, $^3J_{HH}$ = 6.9 Hz, 2H, (CH$_3$)$_2$C*H*N), 6.51 (s, 2H, C*H*N) 7.10-7.28 (m, 12H, Ar-*H*); ^{13}C{^{1}H} NMR (100.6 MHz, C_6D_6, 298 K): δ 22.9 ((*C*H$_3$)$_2$CH, Sn ring), 23.2 ((*C*H$_3$)$_2$CH, Sn ring), 23.4 ((*C*H$_3$)$_2$CHN), 24.6 ((*C*H$_3$)$_2$CH, Ga ring), 25.6 ((*C*H$_3$)$_2$CH, Ga ring), 26.0 ((*C*H$_3$)$_2$CH, Sn ring), 27.6 ((*C*H$_3$)$_2$CH, Sn ring), 28.1 ((CH$_3$)$_2$*C*H, Ga ring), 28.5 ((CH$_3$)$_2$*C*H, Sn ring), 28.6 ((CH$_3$)$_2$*C*H, Sn ring), 49.1 ((CH$_3$)$_2$*C*HN), 122.9 (*C*N), 123.1, 123.9, 124.1, 125.0, 125.8, 139.9, 143.9, 145.2, 145.4, 147.0 (Ar-*C*), 159.8 (*C*N$_3$); ^{119}Sn{^{1}H} NMR (186.4 MHz, C_6D_6, 298 K): δ 454.8 (pw 420 Hz at 1/2 peak height); MS (EI 70eV) *m/z* (%): 1027 (MH$^+$, 15), 377 ({N(Ar)C(H)}$_2$H$^+$, 7); IR ν/cm^{-1} (Nujol): 1613 m, 1584 m, 1256 s, 1212 m, 1116 s, 1056 m, 934 w; EI acc. mass on M$^+$: calc. for $C_{57}H_{84}N_5GaSn$: 1027.4999, found: 1027.5002; $C_{57}H_{84}N_5GaSn$ requires C 66.62, H 8.24, N 6.81; found: C 66.20, H 8.30, N 6.90.

2.6 References

1. R. J. Baker, R. D. Farley, C. Jones, M. Kloth, D. M. Murphy, *Dalton Trans.*, 2002, 3844.
2. C. Jones, D. P. Mills, J. A. Platts, R. P. Rose, *Inorg. Chem.*, 2006, **45**, 3146.
3. T. Pott, P. Jutzi, W. Kaim, W. W. Schoeller, B. Neumann, A. Stammler, H. –G. Stammler, M. Wanner, *Organometallics*, 2002, **21**, 3169.
4. R. J. Baker, R. D. Farley, C. Jones, D. P. Mills, M. Kloth, D. M. Murphy, *Chem. Eur. J.*, 2005, **11**, 2972.
5. T. Pott, P. Jutzi, W. W. Schoeller, A. Stammler, H. –G. Stammler, *Organometallics*, 2001, **20**, 5492.
6. J. Emsley, *The Elements*, 3rd Edition, New York, Oxford University Press, 1998.
7. R. J. Baker, C. Jones, M. Kloth, J. A. Platts, *Angew. Chem. Int. Ed.*, 2003, **42**, 2660.
8. C. Jones, *Chem. Commun.*, 2001, 2293, and references therein.
9. R. J. Baker, C. Jones, M. Kloth, J. A. Platts, *Organometallics*, 2004, **23**, 4811.
10. C. Jones, D. P. Mills, R. P. Rose, *J. Organomet. Chem.*, 2006, **691**, 3060.
11. P. A. Rupar, M. C. Jennings, K. M. Baines, *Can. J. Chem.*, 2007, **85**, 141.
12. C. Jones, M. Waugh, *Dalton Trans.*, 2004, 1971.
13. F. G. N. Cloke, P. B. Hitchcock, J. F. Nixon, D. J. Wilson, *Organometallics*, 2000, **19**, 219.
14. R. J. Baker, C. Jones, D. P. Mills, D. M. Murphy, E. Hey-Hawkins, R. Wolf, *Dalton Trans.*, 2006, 64.
15. (a) A. J. Arduengo, J. C. Calabrese, A. H. Cowley, H. V. R. Dias, J. R. Goerlich, W. J. Marshall, B. Riegel, *Inorg. Chem.*, 1997, **36**, 2151; (b) A. J. Arduengo, C.

J. Carmalt, J. A. C. Clyburne, A. H. Cowley, R. Pyati, *Chem. Commun.*, 1997, 981.

16. (a) W. Uhl, M. Benter, *Dalton Trans.*, 2000, 3133; (b) Y. Peng, H. Fan, H. Zhu, H. W. Roesky, J. Magull, C. E. Hughes, *Angew. Chem. Int. Ed.*, 2004, **43**, 3443.
17. R. J. Baker, C. Jones, M. Kloth, *Dalton Trans.*, 2005, 2106.
18. A. Schäfer, M. Weidenbruch, W. Saak, S. Pohl, *Chem. Commun.* 1995, 1157.
19. F. Stabenow, W. Saak, M. Weidenbruch, *Chem. Commun.*, 1999, 1131.
20. A. J. Arduengo, H. V. Rasika Dias, J. C. Calabrese, F. Davidson, *Inorg. Chem.*, 1993, **32**, 1541.
21. N. Kuhn, T. Kratz, R. Boese, *Chem. Ber.*, 1995, **128**, 245.
22. (a) B. Gehrhus, P. B. Hitchcock, M. F. Lappert, *Dalton Trans.*, 2000, 3094; (b) F. E. Hahn, L. Wittenbecher, M. Kühn, T. Lügger, R. Frölich, *J. Organomet. Chem.*, 2001, **617 – 618**, 629.
23. T. Fjeldberg, A. Haaland, B. E. R. Schilling, M. F. Lappert, A. J. Thorne, *Dalton Trans.* 1986, 1551, and references cited therein.
24. R. J. Baker, C. Jones, J. A. Platts, *J. Am. Chem. Soc.* 2003, **125**, 10534.
25. H. Schäfer, W. Saak, M. Weidenbruch, *Organometallics*, 1999, **18**, 3159.
26. W. Uhl, S. Melle, M. Prött, *Z. Anorg. Allg. Chem.*, 2005, **631**, 1377.
27. W. Reimann, H. G. Kulvila, D. Farah, T. Apoussidis, *Organometallics*, 1987, **6**, 557.
28. (a) R. J. Baker, C. Jones, J. A. Platts, *J. Am. Chem. Soc.*, 2003, **125**, 10534; (b) R. J. Baker, C. Jones, D. M. Murphy, *Chem. Commun.*, 2005, 1339; (c) S. Aldridge, R. J. Baker, N. D. Coombs, C. Jones, R. P. Rose, A. Rossin, D. J. Willock, *Dalton Trans.*, 2006, 3313; (d) R. J. Baker, C. Jones, J. A. Platts, *Dalton Trans.*, 2003, 3673; (e) P. L. Arnold, S. T. Liddle, J. McMaster, C. Jones, D. P. Mills, *J. Am. Chem. Soc.*, 2007, **129**, 5360; (f) S. P. Green, C. Jones, K. –

A. Lippert, D. P. Mills, A. Stasch, *Inorg. Chem.*, 2006, **45**, 7242; (g) S. P. Green, C. Jones, D. P. Mills, A. Stasch, *Organometallics*, 2007, **26**, 3424.

29. CSD version 5.28, November 2006, update 2 (May 2007); F. H. Allen, *Acta Cryst.*, 2002, **B58**, 380.

30. H. Braunschweig, B. Gehrhus, P. B. Hitchcock, M. F. Lappert, *Z. Anorg. Allg. Chem.*, 1995, **621**, 1922.

31. R. J. Baker, C. Jones, *Coord. Chem. Rev.*, 2005, **249**, 1857.

32. S. P. Green, C. Jones, P. C. Junk, K. –A. Lippert, A. Stasch, *Chem. Commun.*, 2006, 3978.

33. C. Jones, P. C. Junk, K. –A. Lippert, A. Stasch, *unpublished results.*

34. M. Weidenbruch, A. Schäfer, H. Kilian, S. Pohl, W. Saak, H. Marsmann, *Chem. Ber.*, 1992, **125**, 563.

35. M. Stürmann, W. Saak, H. Marsmann, M. Weidenbruch, *Angew. Chem. Int. Ed.*, 1999, **38**, 187.

36. M. J. Frisch, G. W. Trucks, H. B. Schlegel, G. E. Scuseria, M. A. Robb, J. R. Cheeseman, J. A. Montgomery Jr., T. Vreven, K. N. Kudin, J. C. Burant, J. M. Millam, S. S. Iyengar, J. Tomasi, V. Barone, B. Mennucci, M. Cossi, G. Scalmani, N. Rega, G. A. Petersson, H. Nakatsuji, M. Hada, M. Ehara, K. Toyota, R. Fukuda, J. Hasegawa, M. Ishida, T. Nakajima, Y. Honda, O. Kitao, H. Nakai, M. Klene, X. Li, J. E. Knox, H. P. Hratchian, J. B. Cross, C. Adamo, J. Jaramillo, R. Gomperts, R. E. Stratmann, O. Yazyev, A. J. Austin, R. Cammi, C. Pomelli, J. W. Ochterski, P. Y. Ayala, K. Morokuma, G. A. Voth, P. Salvador, J. J. Dannenberg, V. G. Zakrzewski, S. Dapprich, A. D. Daniels, M. C. Strain, O. Farkas, D. K. Malick, A. D. Rabuck, K. Raghavachari, J. B. Foresman, J. V. Ortiz, Q. Cui, A. G. Baboul, S. Clifford, J. Cioslowski, B. B. Stefanov, G. Liu, A. Liashenko, P. Piskorz, I. Komaromi, R. L. Martin, D. J.

Fox, T. Keith, M. A. Al-Laham, C. Y. Peng, A. Nanayakkara, M. Challacombe, P. M. W. Gill, B. Johnson, W. Chen, M. W. Wong, C. Gonzalez, J. A. Pople, *Gaussian '98, Revision A.10*, Pittsburgh PA, Gaussian, Inc., 2001.

37. C. Boehme, G. Frenking, *Chem. Eur. J.*, 1999, **5**, 7.

38. (a) A. D. Becke, *Phys. Rev. A*, 1988, **38**, 3098; (b) J. P. Perdew, *Phys. Rev. A*, 1986, **33**, 8822.

39. (a) R. Ditchfield, W. J. Hehre, J. A. Pople, *J. Chem. Phys.*, 1971, **54**, 724; (b) W. J. Hehre, R. Ditchfield, J. A. Pople, *J. Chem. Phys.*, 1972, **56**, 2257; (c) M. S. Gordon, *Chem. Phys. Lett.*, 1980, **76**, 163; (d) P. C. Hariharan, J. A. Pople, *Theor. Chim. Acta*, 1973, **28**, 213.

40. (a) M. Dolg, U. Wedig, H. Stoll, H. Preuss, *J. Chem. Phys.*, 1987, **86**, 866; (b) A. Bergner, M. Dolg, W. Kuehle, H. Stoll, H. Preuss, *Mol. Phys.*, 1993, **80**, 1431.

41. J. Andzelm, S. Huzinaga, M. Klobukowski, E. Radzio, Y. Sakai, H. Tatekawi, *Gaussian Basis Sets for Molecular Calculations*, Amsterdam, Elsevier, 1984.

42. A. E. Reed, L. A. Curtiss, F. Weinhold, *Chem. Rev.*, 1988, **88**, 899.

Chapter 3

The Synthesis and Reactivity of Transition Metal Gallyl Complexes Stabilised by *N*-Heterocyclic Carbene Coordination

3.1 Introduction

3.1.1 Transition Metal Gallyl Complexes Incorporating the Heterocycle, $[:Ga\{[N(Ar)C(H)]_2\}]^-$

There have been several investigations into the reactivity of the anionic gallium(I) *N*-heterocyclic carbene (NHC) analogue, $[:Ga\{[N(Ar)C(H)]_2\}]^-$ **1**,[1] (Ar = $C_6H_3Pr^i_2$-2,6) with transition metal and lanthanide complexes in the last several years. However, compared with the extensive study of main group complexes of **1**,[2] transition metal complexes of **1** are fewer in number. To date, most success has been achieved in the reactions of [K(tmeda)][**1**] with metallocene and piano stool complexes.[3-6] Treatment of nickelocene or cobaltocene with [K(tmeda)][**1**] in any stoichiometry gave the bis(gallyl) metal(II) salts, **2** and **3**, after elimination of KCp (Scheme 1).[3,4] The displacement of Cp^- from the metallocenes mirrors the reactivity of the NHC, $[:C\{[N(Me)C(Me)]_2\}]$ **4**, towards nickelocene, which forms the salt $[CpNi\{C\{[N(Me)C(Me)]_2\}\}][Cp]$ **5**.[7] A density functional theory (DFT) study on a model of **2** attempted to explain the short Ga—Ni bond lengths in this complex, and revealed a value of 28 % for the π-component of these bonds.[4] Considering that the metal-metal interactions are largely ionic in nature, this value is not significant. In this study, a ligand competition study attempted to define the comparative σ-donor abilities of **1** and **4**.[3] This was not entirely successful, as complex **2** did not react with an excess of [K(tmeda)][**1**], and the reaction of **2** with **4** surprisingly induced elimination of a

further equivalent of KCp and yielded the neutral complex, **6**.[3] The cobalt analogue, **3**, was not reported to react with **4**.[4] The nickel(II) centre in **6** displays a distorted square planar geometry with a *trans*-arrangement of ligands.[3]

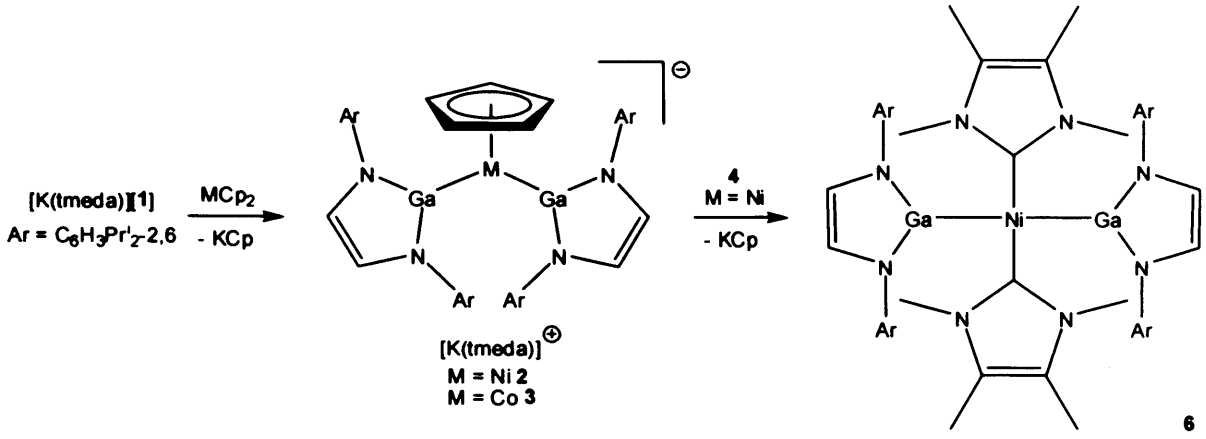

Scheme 1 – The synthesis of **2**, **3** and **6**

The treatment of a range of other first row metallocenes with [K(tmeda)][**1**] either led to no reaction, in the case of $FeCp_2$, or to intractable mixtures of products, for MCp_2 (M = V, Cr, Mn).[6] As such a different synthetic strategy was required to prepare other metallocene complexes of **1**. It was found that the digallane(4), $[Ga\{[N(Ar)C(H)]_2\}]_2$ **7**, could be prepared in high yield by the oxidative coupling of **1** with the ferrocenium ion, $[FeCp_2][PF_6]$, or $Co_2(CO)_8$.[4,6] This compound had previously been synthesised from a different synthetic route.[8] It was believed that metallocenes could potentially oxidatively insert into the Ga—Ga bond of the digallane, **7**, in a similar manner to the oxidative insertion of "WCp_2" into the B—B bond of the diborane, $B_2Cat'_2$ (Cat' = 4-Bu^{t}C$_6$H$_3$O$_2$-1,2 or 3,5-Bu$^t_2$C$_6$H$_2$O$_2$-1,2).[9] Hence the reaction of "$ZrCp_2$", generated in situ from Bu^{n}Li and $[Cp_2ZrCl_2]$, reacted with **7** and an excess of Bu^{n}Li to give the unusual Zr^{III} salt, **8** (Scheme 2).[5] The desired neutral Zr(IV) complex, $[Cp_2Zr\{Ga\{[N(Ar)C(H)]_2\}\}_2]$, could not be isolated, though it is proposed that this Zr(IV) intermediate is initially generated and subsequently reduced by the alkyllithium reagent. Interestingly, the Zr(III) or Zr(IV) gallyl complexes could not be

synthesised by the direct treatment of [K(tmeda)][**1**] with [Cp_2ZrCl_2]. A combination of EPR and X-ray crystallographic studies showed that the Ga—Zr bonds in **8** are quite weak, with negligible back-bonding from the d^1-Zr centre into the empty *p*-orbital on the gallium centres.

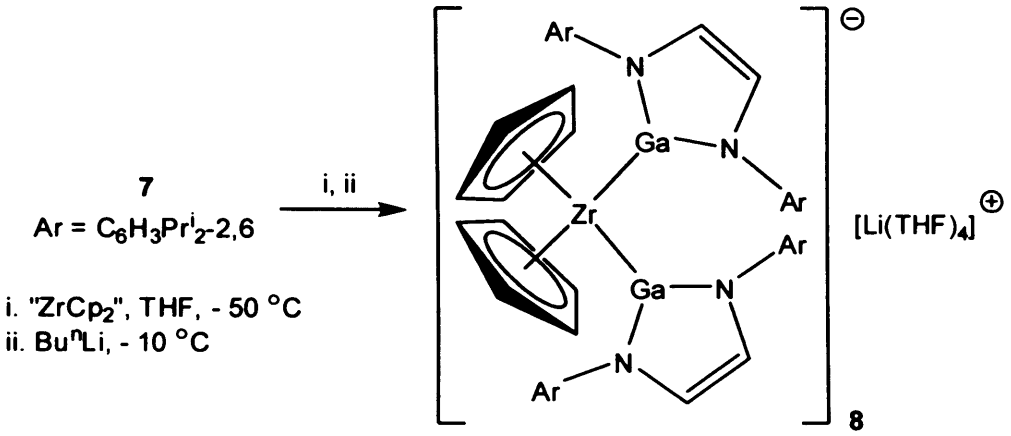

Scheme 2 – The synthesis of **8**

Following the successful synthesis of **8** by the oxidative insertion of the metallocene into the Ga—Ga bond of the digallane, **7**, other metallocene systems were investigated.[4,6] The metallocenes, $M(C_5H_4Me)_2$ (M = V, Cr), reacted with **7** to give the neutral mono-gallyl complexes, **9** and **10** (Scheme 3). It is assumed that initial oxidative insertion takes place to afford a bis-gallyl M(IV) intermediate, **11**, which comproportionates with $M(C_5H_4Me)_2$ to yield the observed product. Treatment of **9** and **10** with the NHC, **4**, did not result in a reaction. In contrast, [K(tmeda)][**1**] reacted with **9**, but not with **10**, to yield the bis-gallyl salt, **12**. The difference in reactivity of **9** and **10** towards [K(tmeda)][**1**] was attributed to the larger, more accessible vanadium centre relative to chromium and the instability that the nineteen-electron chromium analogue of **12** would display.

A number of half-sandwich anionic complexes of **1** (**13** – **15**) have been synthesised from the cyclopentadienyl-metal carbonyl complexes, [Cp'M(CO)$_n$] (M =

V, Cp' = Cp, n = 4; M = Mn, Cp' = MeCp, n = 3; M = Co, Cp' = Cp, n = 2) (Scheme 4).[4,6] These compounds were synthesised because analogous neutral NHC complexes of this type have proved useful in catalysis.[10] Only one carbonyl group was substituted by **1**, regardless of the reaction stoichiometry. The short Ga—M bonds in **13** – **15** warranted a DFT study of the bonding in related model complexes.[6] As would be expected, the π : σ ratio of the Ga—M bonds increased for the more electron rich M centres, which had a decreased number of competing π-acidic CO ligands. However, as these π : σ ratios calculated were found to be similar in analogous boryl and NHC model complexes, there was deemed to be little π-character in the Ga—M bonds in **13** – **15**.

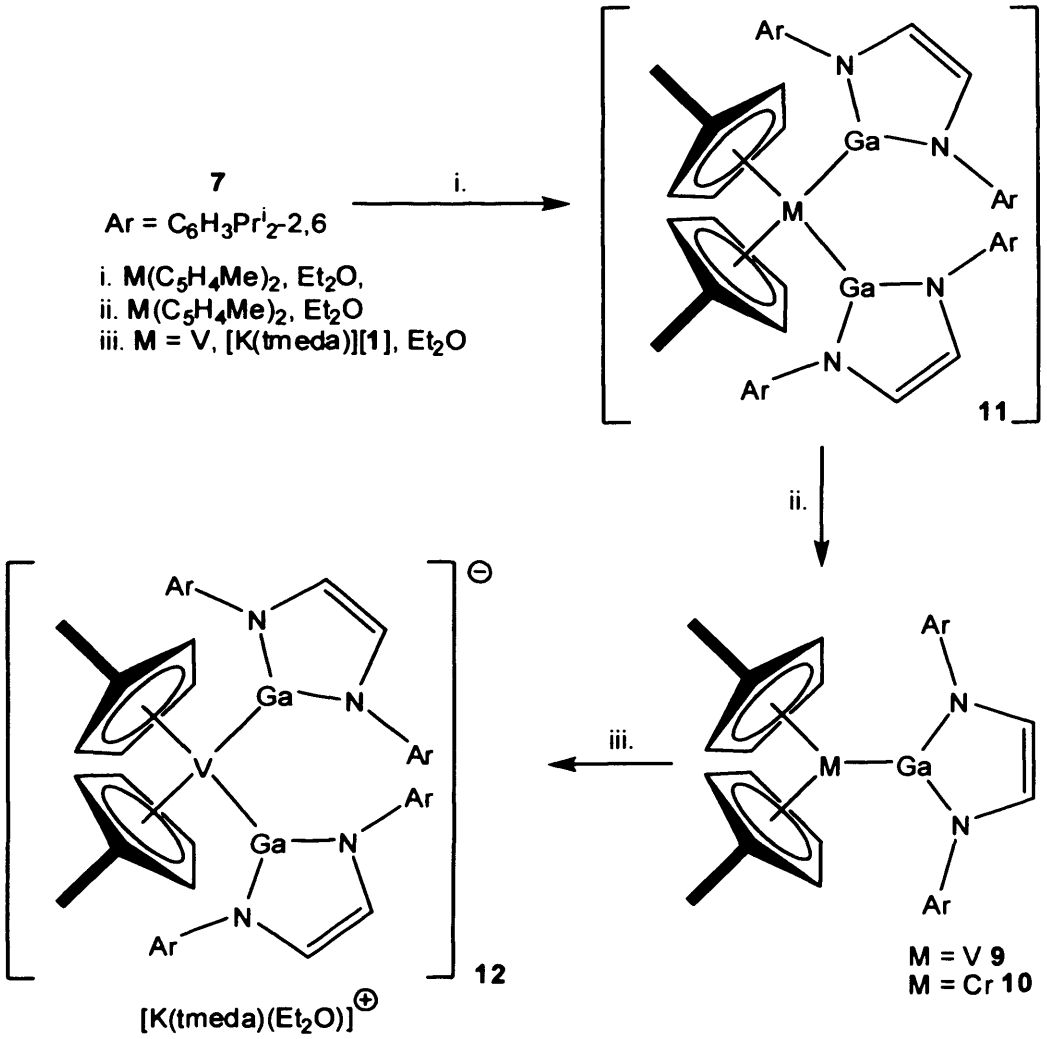

Scheme 3 – The synthesis of **9**, **10** and **12**

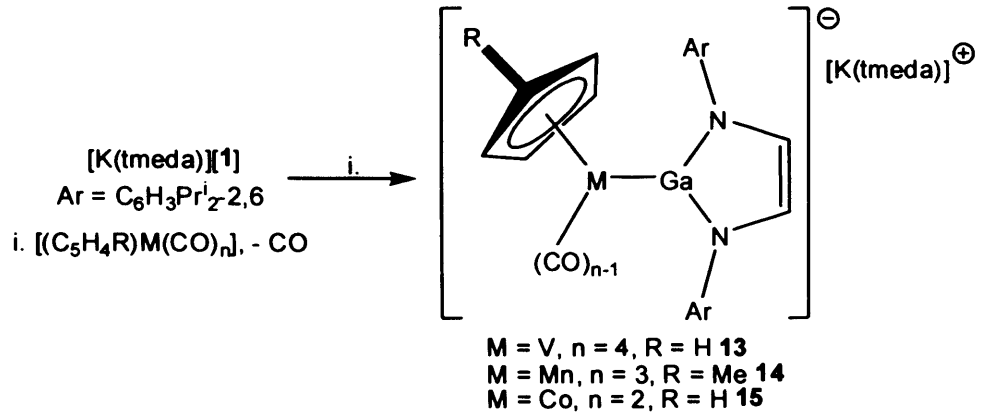

Scheme 4 – The synthesis of **13 – 15**

The ability of **1** to displace CO on a metal centre was also demonstrated in the synthesis of the salt, **16**, from iron pentacarbonyl (Scheme 5).[11] The reaction of [K(tmeda)][**1**] with several other homoleptic metal carbonyls proved unsuccessful. The facile displacement of CO is testament to the strong σ-donor capability of **1**, and an IR analysis and DFT studies concurred that there is negligible π-back-bonding in **16**. In another study, a manganese(II) dialkyl, $[Mn\{CH(SiMe_3)_2\}_2]$, reacted with [K(tmeda)][**1**] to form the salt, **17**. The Ga—Mn bond length in **17** is comparatively weak, being much longer (> 0.3 Å) than in the half-sandwich manganese complex, **14**. It is of note that addition of a further equivalent of [K(tmeda)][**1**] did not lead to $K[CH(SiMe_3)_2]$ elimination, in contrast to the reactivity of the previously discussed tin complex, $[\{(SiMe_3)_2HC\}_2Sn\{Ga\{[N(Ar)C(H)]_2\}\}]$.[2e]

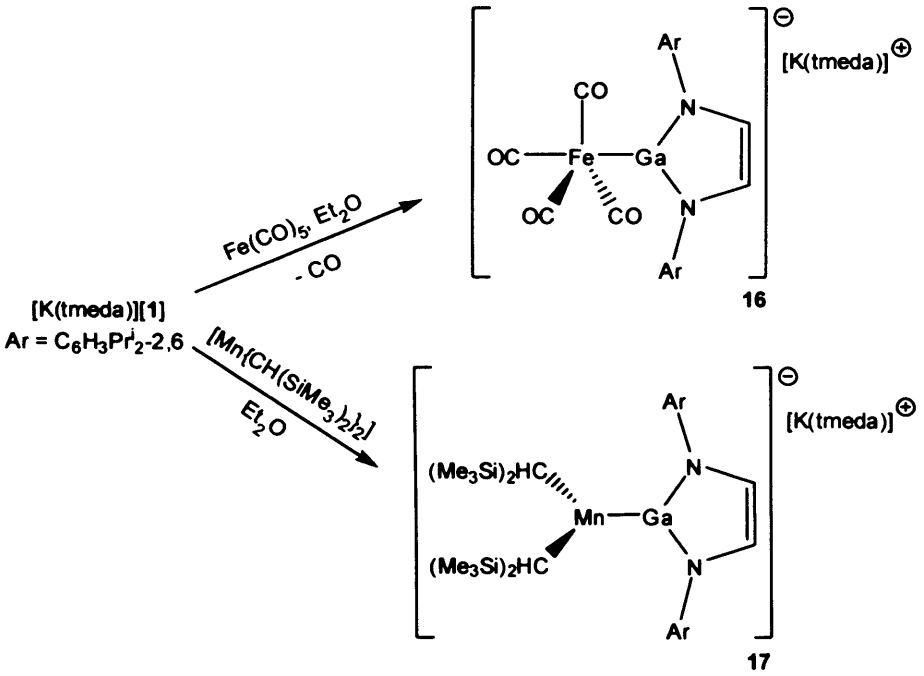

Scheme 5 – The synthesis of **16** and **17**

One area where [K(tmeda)][**1**] has not proved as useful as first thought is in salt metathesis reactions with metal halides (MX_n) and their complexes. Until recently these invariably led to paramagnetic gallium(II) dimers, $[XGa\{[N(Ar)C(H)]_2'\}]_2$, X = Cl, Br or I, presumably *via* an initial oxidative insertion of the Ga(I) centre of **1** into the M—X bond of the metal halide, followed by reductive elimination of the gallium(II) dimer.[12] Of late, the problems associated with reactions of [K(tmeda)][**1**] with metal halides have been overcome by coordination of the metal halide with bulky and electron rich amidinates and guanidinates. This finding allowed the Jones group to access neutral group 14 metal-gallyl complexes containing the first structurally characterised Ga—Sn bonds.[2a] In an extension to this work, the neutral zinc-gallyl complex, **18**, was synthesised by the salt metathesis of [K(tmeda)][**1**] and [(Priso)ZnCl] ($Priso^-$ = $[\{N(Ar)\}_2CNPr^i_2]^-$) (Scheme 6).[13] Interestingly, the tetrahedral bis-gallyl complex, **19**, was synthesised in a similar manner from the 2 : 1 reaction of [K(tmeda)][**1**] and $[(tmeda)ZnCl_2]$. The corresponding 1 : 1 reaction gave an intractable mixture of products. The tmeda ligand is not bulky, so the stabilising factors preventing reductive

eliminations of Ga(II) dimers in the formation of **19** are thought to derive from the strong σ-donor and chelating abilities of this ligand. The zinc-gallyl complexes, **18** and **19**, represent the first structurally characterised examples of Ga—Zn bonds. Unfortunately, the reducing nature of **1** prevented the formation of a stable cadmium analogue of **19** from its reaction with $[(tmeda)CdCl_2]$. Instead this reaction led to the deposition of cadmium metal.

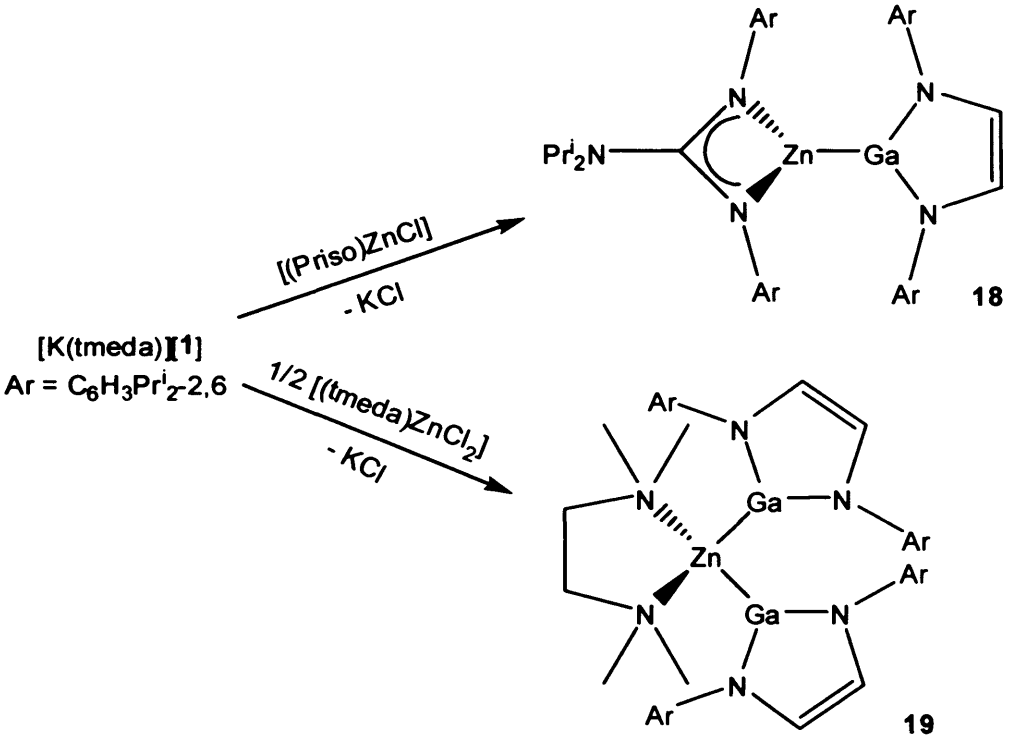

Scheme 6 – The synthesis of **18** and **19**

Following on from these successes, the 2 : 1 reactions of [K(tmeda)][**1**] and the metal(II) complexes, $[(tmeda)_nMX_2]$ (M = Mn, Fe, Co, Ni, Cu; X = Cl, Br; n = 1 or 2), were carried out.[14] Although the 2 : 1 reaction of [K(tmeda)][**1**] with $[(tmeda)CuCl_2]$ gave only the known digallane(4), $[Ga\{[N(Ar)C(H)]_2\}]_2$,[8] and deposition of metallic copper, the other reactions successfully yielded the desired neutral transition metal bis-gallyl complexes, $[(tmeda)M\{Ga\{[N(Ar)C(H)]_2\}\}_2]$ (M = Mn, Fe, Co, Ni) **20 – 23** (Scheme 7). The manganese and iron derivatives are tetrahedral, whilst the cobalt and nickel analogues are of a square planar geometry. Only the nickel complex is

diamagnetic. The attempted preparations of [(dppe)M{Ga{[N(Ar)C(H)]$_2$}}$_2$] complexes, by reacting two equivalents of [K(tmeda)][**1**] with [(dppe)MX$_2$] (M = Mn, Fe, Co, Ni, Cu, Zn; X = Cl, Br, I) were unsuccessful.[14] The zinc, managanese, iron, and cobalt reactions yielded trace amounts of **19 – 22** respectively and free dppe. The nickel and copper reactions gave intractable mixtures of products, with metal deposition. Interestingly, the 1 : 2 reaction of the copper(I) dimer, [(dppe)CuI]$_2$, with [K(tmeda)][**1**] afforded the copper-gallyl complex, **24** (Scheme 7).[14] Complex **24** displays the first structurally characterised example of a Ga—Cu bond.

It was concluded from these studies that the synthesis of transition metal complexes of **1** by salt metathesis is possible if the metal centre in a generalised complex, [(L)$_n$MX$_m$] (L = ligand; M = metal; X = halide; n, m = integer), is bound by a sufficiently strong σ-donating and/or chelating ligand, L. Provided that the metal centre M is electronically satisfied, it is then much less prone to reduction by **1**, and the formation of the undesired gallium(II) dimers, [Ga{[N(Ar)C(H)]$_2$}]$_2$[8] and [XGa{[N(Ar)C(H)]$_2$˙}]$_2$,[12] is restricted. An extension of this methodology to *f*-block chemistry has recently allowed the preparation of the first reported gallium-lanthanide complex, **25** (Scheme 8).[15] A highly nucleophilic NHC ligand was employed in this study, which incorporates a chelating amide function on one *N*-substituent, making the neodymium centre resistant to reduction by **1**.[16] Compound **25** displays the first structurally authenticated Ga—Nd bond, which was probed by DFT analysis to show that the covalent contribution to the bond is 87.2 % Ga and 12.8 % Nd in character, and is remarkably stable in solution. It is noteworthy that the only other group 13 element-lanthanide complexes, [Cp*$_2$Ln(AlCp*)] (Ln = Eu, Yb), were recently prepared in solvent-free conditions, and decompose in the presence of solvent to [LnCp*$_2$] and

AlCp*.[17] The Ga—Nd bond length in **25** is long, being > 0.3 Å longer than the sum of the covalent radii of gallium and neodymium.[18]

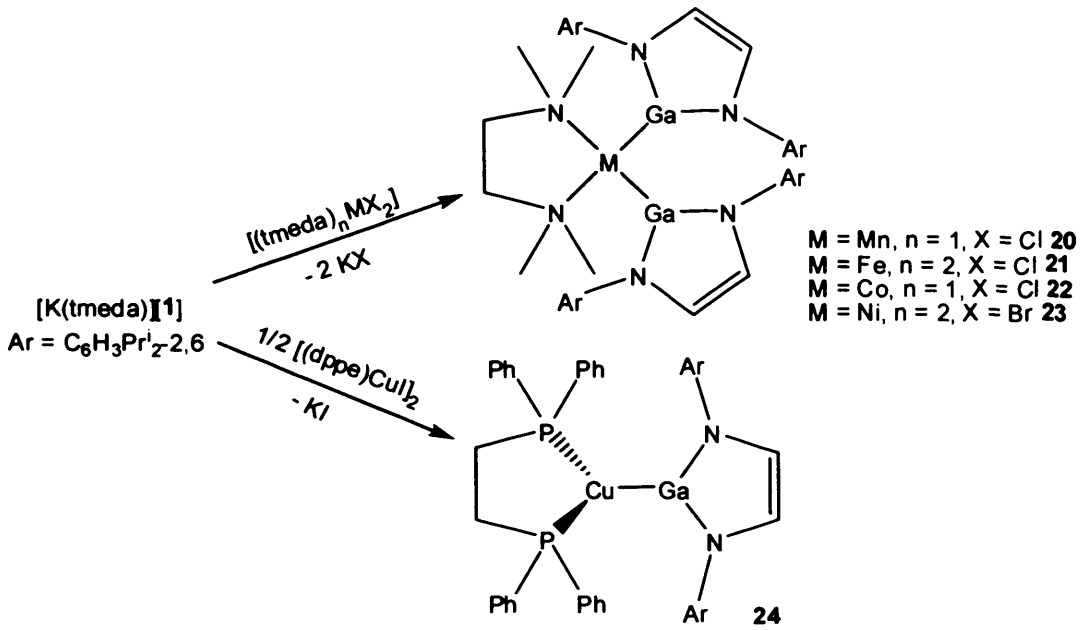

Scheme 7 – The synthesis of **20 – 24**

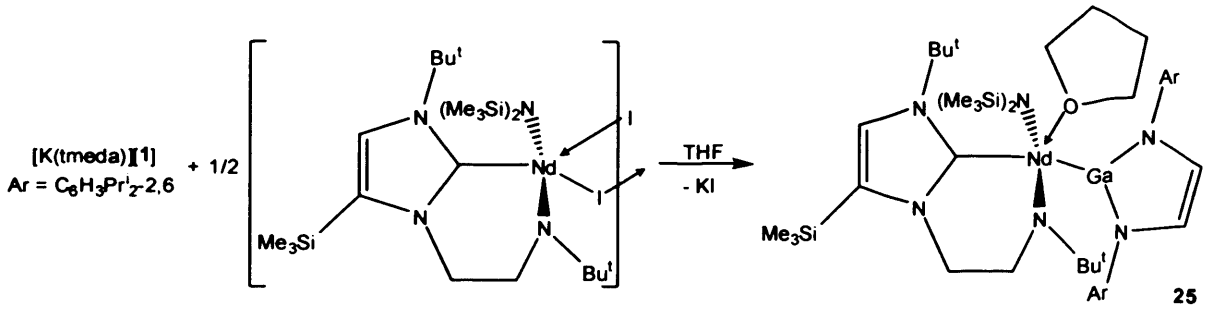

Scheme 8 – The synthesis of **25**

3.1.2 Transition Metal Boryl Complexes

A wide variety of transition metal-cyclic boryl complexes have proved useful as catalysts for a number of synthetic transformations.[19] They have been utilised for, or suggested as intermediates in, the catalytic borylation or hydroboration of unsaturated compounds, and the C—H activation of alkanes, arenes and heteroarenes. A transition metal boryl complex of particular relevance to this study is the copper(I) complex, [(IPr)Cu{B(pin)}] **26** (IPr = [:C{[N(Ar)C(H)]$_2$}], B(pin) = [B{[OCMe$_2$]}$_2$]$^-$) (Figure

1).[20] This complex is stabilised by NHC coordination and has been reported by Sadighi and co-workers to borylate alkenes and to catalytically diborylate aldehydes.[21] In addition, it has been shown to be an effective catalyst in the reduction of CO_2 to CO.[20] Boryl complexes of the group 9 metals are, however, more prevalent and a number of catecholato- and pinacolato-boryl complexes of Co, Rh and Ir have been described.[19] Despite this, no structurally characterised NHC coordinated group 9 metal boryl complexes have yet been reported. Recently, several linear group 11 transition metal boryl complexes (**27 – 29**) have been prepared by the salt metathesis reaction of [(IMes)MCl] (M = Cu, Ag, Au, IMes = [:C{[N(Mes)C(H)]$_2$}]) with the boryl NHC analogue, [LiB{[N(Ar)C(H)]$_2$}], **30**, which is a lighter homologue of [K(tmeda)][**1**] (Figure 2).[22] The silver, **28**, and gold, **29**, complexes are the first structurally characterised boryl silver and boryl gold molecular complexes. An investigation into the reactivity of **27 – 29** is currently in progress. In the context of this study it is of note that there are no structurally characterised examples of cyclic boryl complexes of the group 6 metal chromium.

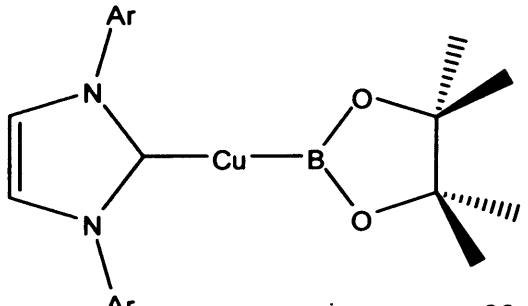

Figure 1 – The NHC-stabilised copper(I) boryl complex, **26**

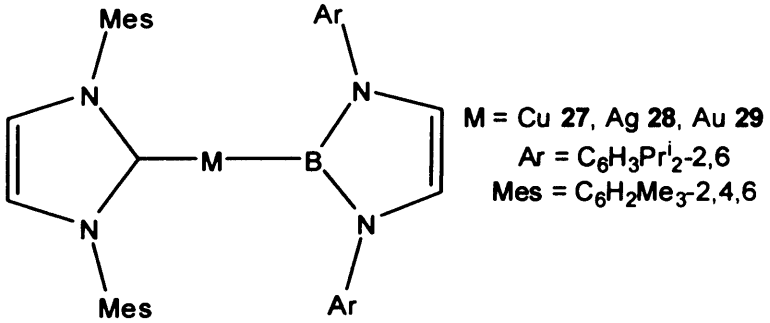

Figure 2 – The NHC-stabilised group 11 metal(I) boryl complexes, **27 – 29**

3.2 Research Proposal

The successful application of salt metathesis reactions towards the synthesis of transition metal gallyl complexes has been demonstrated.[13,15] It has also been shown that the employment of a stabilising NHC ligand may facilitate the synthesis of lanthanide metal-gallyl complexes.[17] Neutral transition metal gallyl complexes, $[L_nM\{Ga\{[N(Ar)C(H)]_2\}\}_m]$, should have parallels with the wide variety of catalytically active transition metal-cyclic boryl complexes.[19] It was therefore proposed that a variety of NHC-coordinated metal-gallyl complexes be prepared and their catalytic potential investigated. The preparation of a gallyl complex analogous to the catalytically proficient copper(I) boryl complex, **26**,[20,21] was seen as a worthy objective as this complex could also exhibit catalytic behaviour. The preparation of heavier homologues of **27 – 29** would also allow a direct comparison of the σ-donor strengths and therefore the *trans*-influences of the group 13 NHC analogues [K(tmeda)][**1**] and **30** for the first time. It was also hoped that this study would provide structurally characterised examples of novel Ga—M bonds.

3.3 Results and Discussion

3.3.1 The Preparation of a Group 6 Metal Gallyl Complex

Our previous work with **1** has shown that it can readily reduce transition metal fragments to lower accessible oxidation states.[4] As a result, for this study suitable NHC-coordinated transition metal halide precursors were selected with the metal displaying a stable low oxidation state. It was thought that the fourteen-electron chromium(II) complex, $[(\eta^5\text{-Cp})Cr(IMes)Cl]$,[23] would be a suitable candidate for a

successful salt metathesis reaction with [K(tmeda)][**1**]. This proved to be the case, with the 1 : 1 reaction in THF affording the expected product, **31**, in excellent yield (Scheme 9). Earlier studies into the reactions of [K(tmeda)][**1**] with metallocenes showed that the gallium(I) heterocycle is capable of displacing Cp^- from metal complexes, eliminating KCp.[3,4] However, the addition of a second equivalent of [K(tmeda)][**1**] to **31** did not lead to further substitution at the Cr(II) centre. In contrast, the related chromium(III) complex, $[(\eta^5\text{-Cp})Cr(IMes)Cl_2]$,[23] reacted with two equivalents of [K(tmeda)][**1**] to yield the paramagnetic gallium(II) dimer, $[ClGa\{[N(Ar)C(H)]_2^{\cdot}\}]_2$,[12] as expected. **31** was treated separately with carbon disulphide (CS_2), silver tetraphenylborate and *tert*-butylphosphaalkyne (Bu^tCP), in all cases giving an intractable mixture of products.

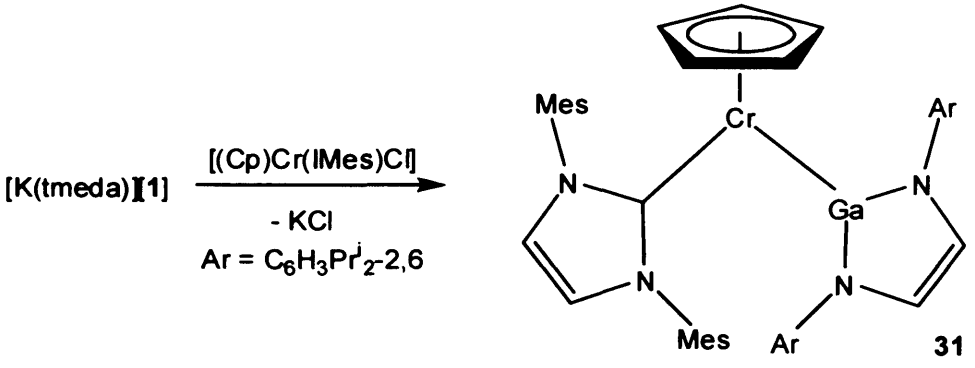

Scheme 9 – The synthesis of **31**

The data on **31** are incomplete. A reproducible microanalysis could not be obtained and no molecular ion was observed in the mass spectrum. However, a fragment corresponding to $IMesH^+$ was detected. Due to the paramagnetic nature of the compound, no meaningful ^1H NMR spectroscopic assignments could be made. However, the magnetic susceptibility of the compound in solution (Evan's method,[24] 298 K, μ_{eff} = 1.65 μB) was measured, employing an 0.1 M tetramethylsilane (TMS) in C_6D_6 insert as a standard. Although this value is lower than expected, the complex can be viewed as low-spin with two unpaired electrons. The halide starting material, $[(\eta^5$-

Cp)Cr(IMes)Cl], was found to be high-spin with four unpaired electrons by this method (μ_{eff} = 4.62 μB).[23] This difference in spin multiplicity of the two chromium(II) centres can be easily explained by the strong σ-donating ability of **1** in comparison to chloride. Most CpCr(II) derivatives in the literature are low-spin with two unpaired electrons,[25] though it must be noted that in most of these examples the chromium(II) centre is six-coordinate. No EPR measurement of **31** was attempted as it was assumed that the compound is likely to be EPR silent, as is [(η^5-Cp)Cr(IMes)Cl] and other paramagnetic chromium(II) complexes.[25a]

An X-ray structural determination of **31** was performed and its molecular structure is depicted in Figure 3. The Ga—Cr bond length of 2.5800(5) Å is remarkably long in comparison to the known range of such interactions (2.390 – 2.479 Å).[26] Perhaps the best comparison is with the chromium(III) gallyl complex, **10**, which displays a Ga—Cr bond length of 2.4231 Å.[4,6] This difference can be attributed to the larger ionic radii and smaller electrostatic attraction of chromium(II) (*r* = 0.84 Å) over chromium(III) (*r* = 0.64 Å),[18] as well as the possibility of increased steric crowding around the metal centre. Although no crystallographic determination of the halide starting material, [(η^5-Cp)Cr(IMes)Cl], has been performed to date, a related phenyl complex, [(η^5-Cp)Cr(IMes)Ph], has been prepared and structurally characterised.[23] Both [(η^5-Cp)Cr(IMes)Ph] and **31** display a "piano stool" arrangement of ligands around the nearly trigonal planar chromium centre (Σ angles Ga/C—Cr—C(carbene), Cp(centroid)—Cr—C(carbene) and Ga/C—Cr—Cp(centroid) is 359.85° for **31** and 359.8° for [(η^5-Cp)Cr(IMes)Ph]). However, the Ga—Cr—C(carbene) angle of **31** (110.52°) is far more obtuse than the C(phenyl)—Cr—C(carbene) angle in [(η^5-Cp)Cr(IMes)Ph] (97.98°), probably as a result of the increased steric demands of **1** over

the phenyl ligand. As well as this, the C=C backbones of the gallyl and IMes ligands in **31** are skewed with respect to each other (torsion angle C(6)C(7)—C(33)C(34) 52.4°).

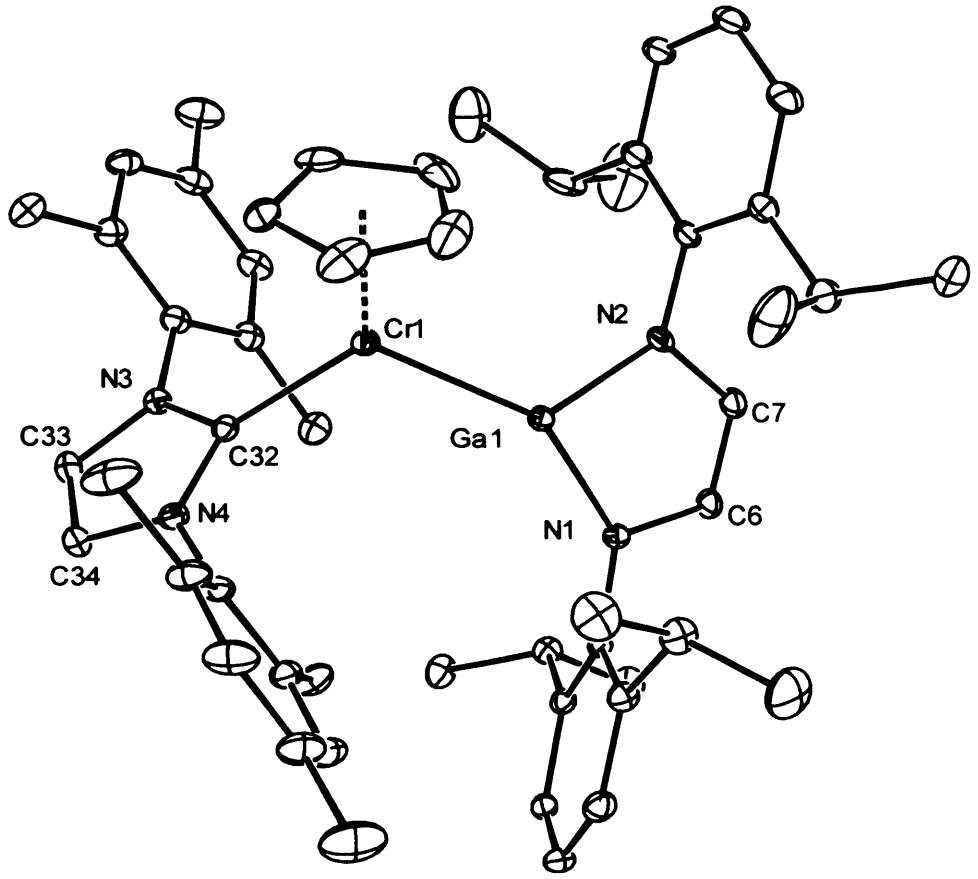

Figure 3 – Thermal ellipsoid plot (25% probability surface) of the molecular structure of $[(\eta^5\text{-Cp})Cr(IMes)\{Ga\{[N(Ar)C(H)]_2\}\}]$ **31**; hydrogen atoms are omitted for clarity. Selected bond lengths (Å) and angles (°): Ga(1)—N(1) 1.9209(19), Ga(1)—N(2) 1.923(2), Ga(1)—Cr(1) 2.5800(5), Cr(1)—C(32) 2.115(2), Cr(1)—centroid (C(1)-C(5)) 1.985, N(1)—C(6) 1.393(3), N(2)—C(7) 1.396(3), N(3)—C(32) 1.373(3), N(3)—C(33) 1.390(3), N(4)—C(32) 1.356(3), N(4)—C(34) 1.390(3), C(1)—C(2) 1.348(7), C(1)—C(5) 1.395(5), C(2)—C(3) 1.409(7), C(3)—C(4) 1.421(5), C(4)—C(5) 1.388(4), C(6)—C(7) 1.348(3), C(33)—C(34) 1.349(4), N(1)—Ga(1)—N(2) 84.67(8), C(32)—Cr(1)—Ga(1) 110.52(6), C(6)—N(1)—Ga(1) 110.95(14), C(7)—N(2)—Ga(1) 111.55(15), C(32)—N(3)—C(33) 111.6(2), C(32)—N(4)—C(34) 111.9(2), C(7)—C(6)—N(1) 117.2(2), C(6)—C(7)—N(2) 115.6(2), N(4)—C(32)—N(3) 103.4(2), C(34)—C(33)—N(3) 106.4(2), C(33)—C(34)—N(4) 106.7(2).

3.3.2 The Preparation of a Group 9 Metal Gallyl Complex

In this study, all attempts to form group 9 metal gallyl complexes involved the use of metal(I) halide precursors. In earlier work, Dr. R. J. Baker reacted [K(tmeda)][**1**] with either $[(\eta^4\text{-COD})MCl]_2$ (M = Rh or Ir, COD = 1,5-cyclooctadiene), $[(PPh_3)_3CoCl]$, $[(PPh_3)_2RhCl]_2$, or $[(PPh_3)_2Ir(CO)Cl]$. In all cases, the gallium(II) dimer, $[ClGa\{[N(Ar)C(H)]_2\cdot\}]_2$,[12] was the only identifiable product. As previously mentioned, it is believed that this occurs *via* an initial oxidative insertion of the Ga(I) centre of **1** into the M—Cl bond of the transition metal precursor, followed by reductive elimination of the dimer. In this respect, it is worthy of mention that the related neutral 6-membered heterocycle, $[:Ga\{[N(Ar)C(Me)]_2CH\}]$ ($Ar = C_6H_3Pr^i_2$), has been shown to insert into Rh—Cl bonds.[27]

Treatment of $[(\eta^4\text{-COD})Ir(IMes)Cl]$ with one equivalent of [K(tmeda)][**1**] yielded the novel complex, $[(\eta^4\text{-COD})Ir(IMes)\{Ga\{N(Ar)C(H)\}_2\}]$ **32**, in moderate yield (Scheme 10). The rhodium(I) analogue, **33**, was synthesised by S. P. Green, and will not be commented on further here. Addition of a further equivalent of [K(tmeda)][**1**] to **32** gave no reaction. Complexes **31** and **32** are air sensitive but indefinitely stable at ambient temperature under argon. It, therefore, seems that IMes coordination of the group 6 or 9 metal halide precursor effectively protects the metal centre from reduction by **1**, presumably because of the donor strength and steric bulk of the NHC ligand.

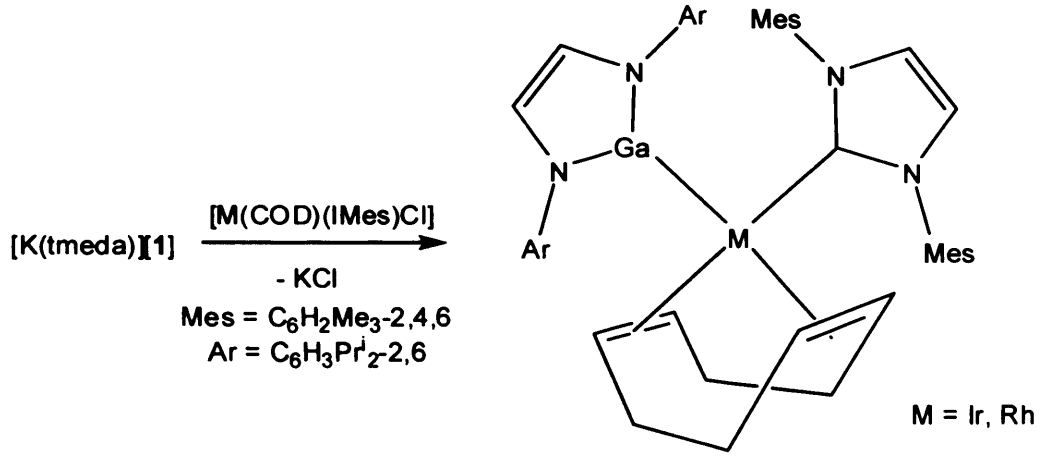

Scheme 10 – The synthesis of **32** and **33**

The ^{1}H and $^{13}C\{^{1}H\}$ NMR spectroscopic data for **32** are consistent with its proposed formulation. Compounds **32** and **33** are structurally analagous, but only the molecular structure of **32** is depicted in Figure 4. The iridium(I) compound, **32**, is monomeric and possesses a distorted square planar group 9 metal centre. The geometry of the gallyl ligand is similar to those of previously reported transition metal complexes of **1**.[3-6,11,13,15] There has only been one previously structurally characterised Ga—Ir bond in [Ir{Ga(Me)$_2$N(SiMe$_2$CH$_2$PPh$_2$)$_2$} {C(=CH$_2$)(Me)}], which at 2.4480 Å[28] is considerably shorter than that observed in **32**. The more or less identical cyclooctadiene C=C distances in **32** (both 1.394(4) Å) point toward the *trans*-influences for the gallyl and NHC ligands being similar. Comparisons between **32** and [(η^4-COD)Ir(IMes)Cl] cannot be carried out as the latter has not been structurally characterised.

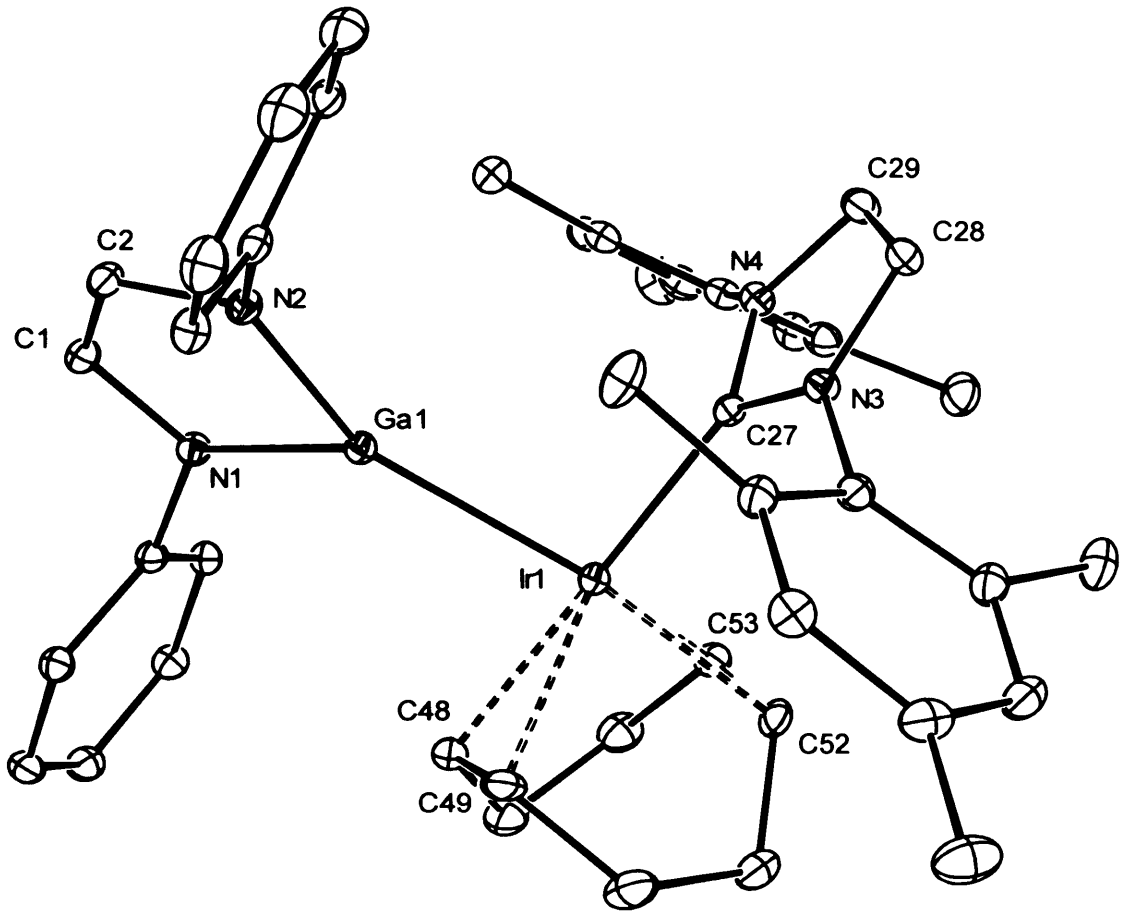

Figure 4 – Thermal ellipsoid plot (25% probability surface) of the molecular structure of [(η^4-COD)Ir(IMes){Ga{[N(Ar)C(H)]$_2$}}] **32**; hydrogen atoms and isopropyl groups are omitted for clarity. Selected bond lengths (Å) and angles (°): Ir(1)—C(27) 2.039(2), Ir(1)—C(53) 2.155(2), Ir(1)—C(49) 2.164(2), Ir(1)—C(52) 2.204(2), Ir(1)—C(48) 2.232(2), Ir(1)—Ga(1) 2.4689(5), Ga(1)—N(2) 1.9198(19), Ga(1)—N(1) 1.9274(19), N(1)—C(1) 1.399(3), N(2)—C(2) 1.399(3), C(1)—C(2) 1.340(3), C(48)—C(49) 1.394(4), C(52)—C(53) 1.394(4), C(27)—Ir(1)—Ga(1) 96.23(6), N(2)—Ga(1)—N(1) 85.69(8), N(4)—C(27)—N(3) 103.24(18).

3.3.3 The Preparation of Group 11 Metal Gallyl Complexes

In earlier work, Dr. R. J. Baker reacted [K(tmeda)][**1**] with [(PPh_3)AuCl], giving the gallium(II) dimer, [ClGa{[N(Ar)C(H)]$_2$·}]$_2$,[12] as the only identifiable product. In consideration of the stability of **31** – **33**, the 1 : 1 reactions of [K(tmeda)][**1**] with a

series of NHC complexes of group 11 metal(I) halides, [(NHC)MCl] (M = Cu, Ag or Au; NHC = IMes or IPr), were carried out. In each case, the salt metathesis product, [(NHC)M{Ga{[N(Ar)C(H)]$_2$}}] (**34 – 39**), was obtained in moderate to high yield (NHC = IPr), or low to moderate yield (NHC = IMes) (Scheme 11). During the course of all reactions, deposition of some elemental group 11 metal was observed upon warming the mixtures from -78 °C to 25 °C. More metal deposition was observed in reactions involving [(IMes)MCl], which suggests that the greater steric bulk of IPr over IMes contributes to the greater yields of **37 – 39** compared to **34 – 36**. However, the yields of **34 – 39** were much greater than in the preparation of the homologous boryl complexes, **27 – 29**.[22] This is perhaps evidence that the gallium centre in [K(tmeda)][**1**] is not as reducing as the boron centre in **30**. The importance of the steric bulk of the NHC in these syntheses was further tested in the reaction of [K(tmeda)][**1**] with [(ICy_{Me})CuCl] (ICy_{Me} = [:C{[N(C_6H_{11})C(Me)]$_2$}]), which incorporates a less bulky NHC. Despite this, a moderate yield of **40** resulted (Scheme 11). In addition, the complex has a thermal stability in the solid state similar to that of **34**. The higher than expected yield and stability of **40** can perhaps be explained by the greater donor strength of ICy_{Me} over IMes,[29] which gives the smaller ligand a similar ability to stabilise copper gallyl fragments as the larger NHC.

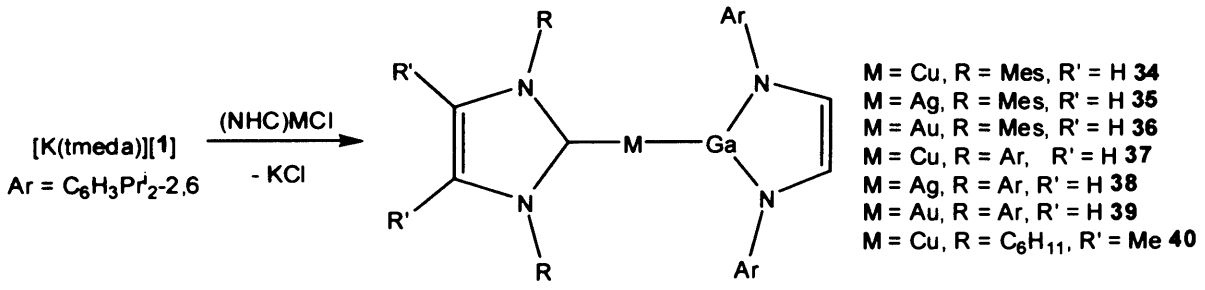

Scheme 11 – The synthesis of **34 – 40**

The ^{1}H and ^{13}C{^{1}H} NMR spectroscopic data for **34 – 40** reflect their proposed monomeric structures. Unfortunately, the carbene resonances in the ^{13}C{^{1}H} NMR

spectra of the silver gallyl complexes were not observed and no signals were seen in the $^{109}Ag\{^{1}H\}$ NMR spectra of **35** and **38**. This is most likely due to the quadrupolar gallium centres broadening the signal and the spin-active ^{107}Ag and ^{109}Ag centres splitting the signal until it becomes indistinguishable from the baseline noise. This means that a comparison of the $^{1}J_{AgC}$ coupling constants of **28** (81 and 88 Hz) with those of **35** and **38** was not possible. The carbene resonances of **34** (δ 181.2 ppm) and **36** (δ 205.2 ppm) are shifted downfield from those of the starting materials, [(IMes)CuCl] (δ 178.7 ppm),[30] and [(IMes)AuCl] (δ 173.4 ppm),[31] but not as far shifted as that of **27** (δ 185.3 ppm) or **29** (δ 217.0 ppm).[22] These values suggest that **1** has a stronger *trans*-influence than chloride, but is weaker than the boryl anion of **30**. Signals due to molecular ions exhibiting the expected isotopic distribution patterns are present in the EI mass spectra of all complexes.

The X-ray crystal structures of **34** – **38** were obtained, and all display similar distorted linear group 11 metal geometries, the Ga—M—C angle deviating the most from linearity in **35** (165.85°) (Figures 5 – 9). It is noteworthy that the copper(I) centre in the boryl complex **27** is much closer to linearity (179.43°)[22] than the gallyl complex **34** (170.72°). The geometries of the heterocyclic ligands in the complexes are similar to each other and to the majority of previously reported complexes incorporating them.[2-6,11,13,15,16,32] In no complex do the gallyl and NHC heterocycles approach co-planarity as the angles between their least squares planes vary from 25.3° to 44.9° in the series. The Ga—Cu bonds in **34** and **37** are similar to the only other reported Ga—Cu bond in **24** (2.3054(9) Å).[15] There have been no previously reported examples of structurally characterised Ga—Ag bonds in molecular compounds, so comparisons cannot be made with the Ga—Ag distances in **35** and **38**. The Ga—Au distance in **36** (2.3782(6) Å) is,

however, at the low end of the known range (2.377 - 2.620 Å) for the four previously reported complexes exhibiting a Ga—Au bond.[26]

The Ga—M bonds in **34 – 36** were compared. Not surprisingly, the Ga—Cu interaction in **34** is the shortest, but interestingly, the Ga—Ag distance in **35** is significantly larger (by *ca.* 0.04 Å) than the Ga—Au separation in **36**. In addition, the Ag—C bond in **35** is longer than the Au—C bond in **36** by *ca.* 0.08 Å. In this respect, the relative sizes of gold and silver have been the subject of a study by Schmidbaur *et al.* using a pair of isomorphic complexes, $[M(PMes_3)_2][BF_4]$ (M = Ag, Au; Mes = mesityl).[33] In contrast to the values usually quoted for the ionic or covalent radii of Ag(I) and Au(I), where silver is smaller or equal in size to gold,[14] the data from the structures of this pair indicated that the M—P distance is smaller for M = Au by 0.09 Å. The M—C bond lengths observed in **27 – 29** (M = Cu 1.918, M = Ag 2.1207, M = Au 2.078 Å) are very similar to those observed in **34 – 36** (M = Cu 1.924, M = Ag 2.125, M = Au 2.053 Å). In addition, the Ag—C distance in [(IMes)AgCl] (2.056 Å)[34] is shorter than those observed in **28** and **35** and the Au—C distance in [(IMes)AuCl] (1.998 Å)[31] is shorter than those observed in **29** and **36**. These observations concur with the interpretation of the carbene resonances in the $^{13}C\{^1H\}$ NMR spectra of these complexes, so we propose that **1** has a stronger *trans*-influence than chloride. However, the similarity of the M—C bond lengths for **27 – 29** and **34 – 36** are not consistent with the large chemical shift differences observed between the carbene resonances in the $^{13}C\{^1H\}$ NMR spectra of the gallium and boron complexes, for reasons unknown.

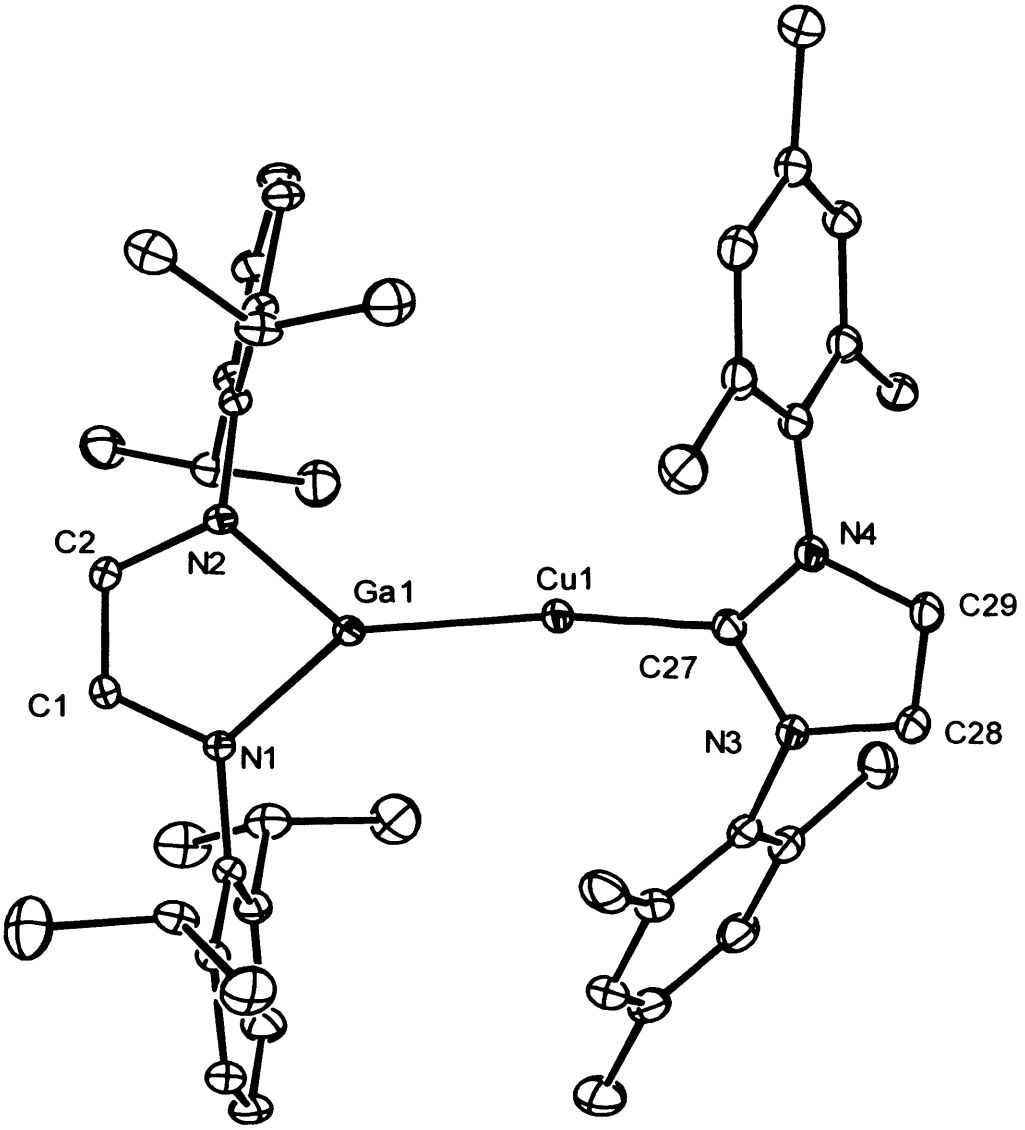

Figure 5 – Thermal ellipsoid plot (25% probability surface) of the molecular structure of [(IMes)Cu{Ga{[N(Ar)C(H)]$_2$}}] **34**; hydrogen atoms are omitted for clarity. Selected bond lengths (Å) and angles (°): Ga(1)—N(2) 1.897(2), Ga(1)—N(1) 1.904(2), Ga(1)—Cu(1) 2.3066(6), Cu(1)—C(27) 1.924(3), N(1)—C(1) 1.390(3), C(1)—C(2) 1.347(4), N(2)—C(2) 1.392(4), N(3)—C(27) 1.363(4), N(3)—C(28) 1.385(4), N(4)—C(27) 1.359(4), N(4)—C(29) 1.389(4), C(28)—C(29) 1.336(5), N(2)—Ga(1)—N(1) 85.36(9), C(27)—Cu(1)—Ga(1) 170.72(8), C(1)—N(1)—Ga(1) 110.79(17), C(2)—C(1)—N(1) 116.7(2), C(2)—N(2)—Ga(1) 111.40(17), C(1)—C(2)—N(2) 115.8(2), C(27)—N(3)—C(28) 111.2(3), C(27)—N(4)—C(29) 111.5(3), N(4)—C(27)—N(3) 103.6(2), C(29)—C(28)—N(3) 107.2(3), C(28)—C(29)—N(4) 106.5(3).

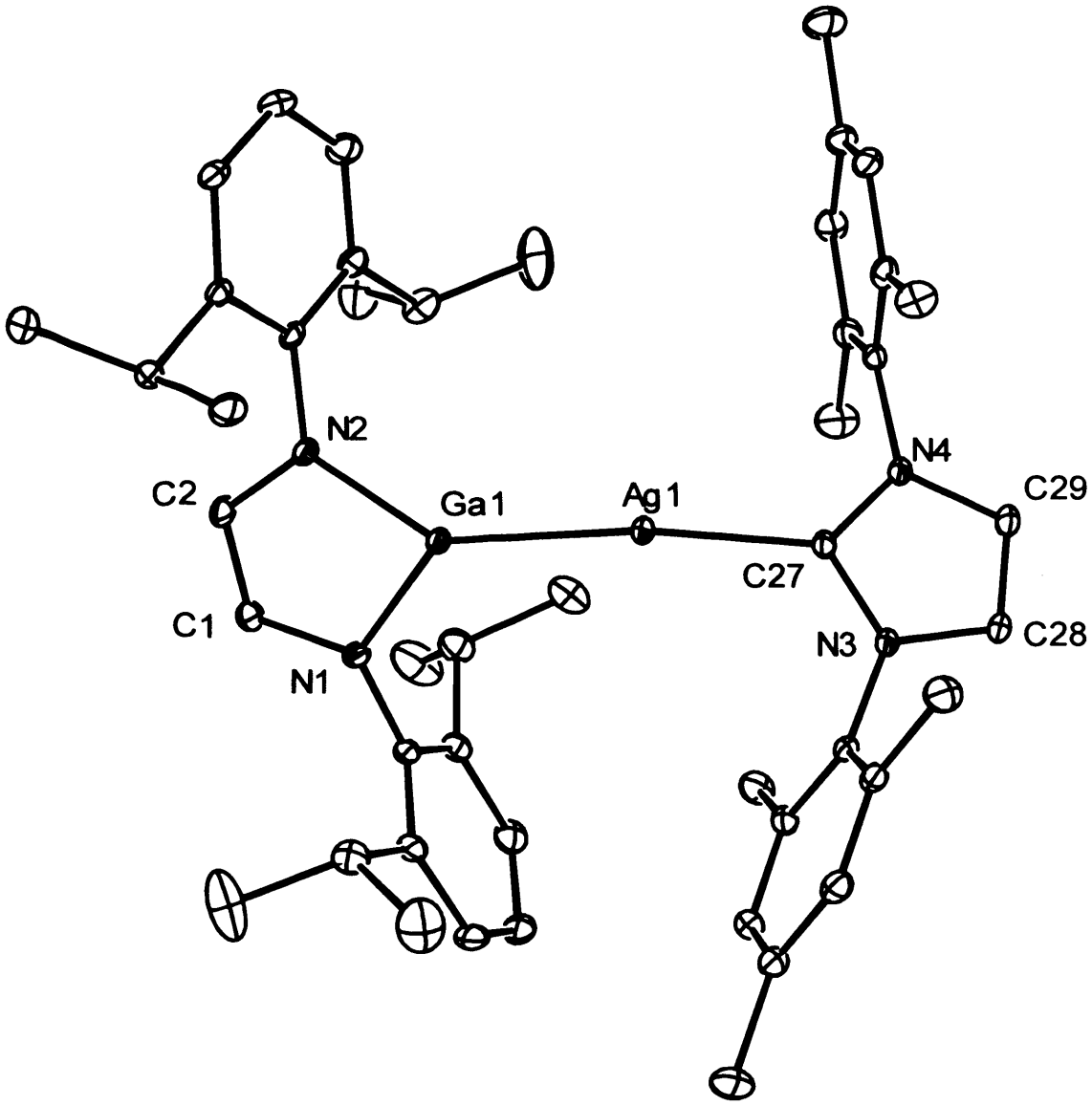

Figure 6 – Thermal ellipsoid plot (25% probability surface) of the molecular structure of [(IMes)Ag{Ga{[N(Ar)C(H)]$_2$}}] **35**; hydrogen atoms are omitted for clarity. Selected bond lengths (Å) and angles (°): Ag(1)—C(27) 2.125(2), Ag(1)—Ga(1) 2.4161(5), Ga(1)—N(2) 1.8897(17), Ga(1)—N(1) 1.8916(18), N(1)—C(1) 1.396(3), C(1)—C(2) 1.345(3), N(2)—C(2) 1.391(3), N(3)—C(27) 1.359(3), N(3)—C(28) 1.387(3), N(4)—C(27) 1.351(3) N(4)—C(29) 1.391(3), C(28)—C(29) 1.337(3), C(27)—Ag(1) —Ga(1) 165.85(6), N(2)—Ga(1)—N(1) 85.41(7), C(1)—N(1)—Ga(1) 111.34(14), C(2)—C(1)—N(1) 115.7(2), C(2)—N(2)—Ga(1) 111.31(13), C(1)—C(2)—N(2) 116.22(19), C(27)—N(3)—C(28) 111.07(18), C(27)—N(4)—C(29) 111.41(18), N(4)—C(27)—N(3) 104.07(17), C(29)—C(28)—N(3) 106.94(19), C(28)—C(29) —N(4) 106.50(19).

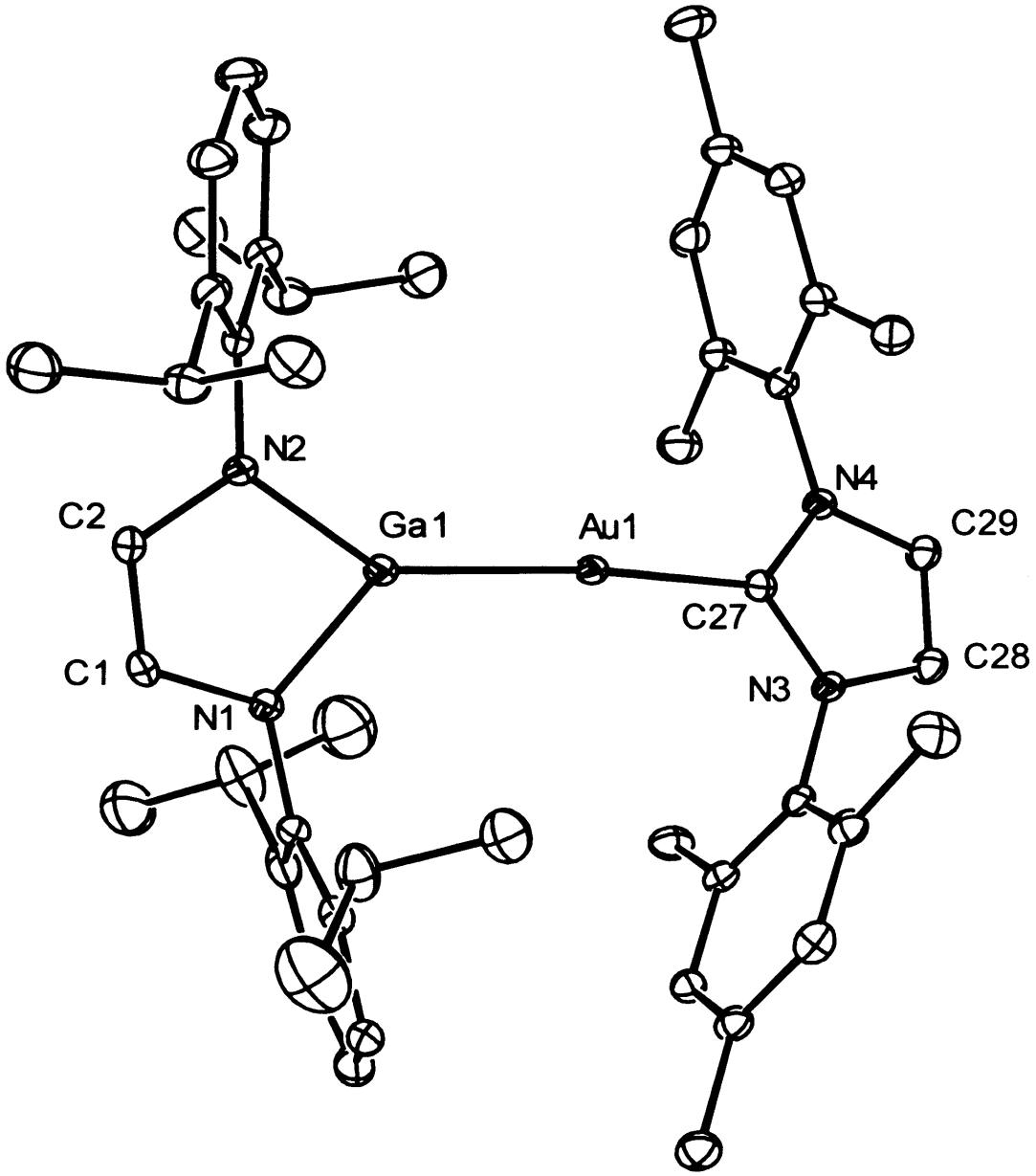

Figure 7 – Thermal ellipsoid plot (25% probability surface) of the molecular structure of [(IMes)Au{Ga{[N(Ar)C(H)]$_2$}}] **36**; hydrogen atoms are omitted for clarity. Selected bond lengths (Å) and angles (°): Au(1)—C(27) 2.053(4), Au(1)—Ga(1) 2.3782(6), Ga(1)—N(1) 1.881(3), Ga(1)—N(2) 1.887(3), N(1)—C(1) 1.390(5), N(2)—C(2) 1.389(5), N(3)—C(27) 1.360(5), N(3)—C(28) 1.388(5), N(4)—C(27) 1.341(5), N(4)—C(29) 1.384(5), C(1)—C(2) 1.345(6), C(28)—C(29) 1.338(6), C(27)—Au(1) —Ga(1) 174.06(11), N(1)—Ga(1)—N(2) 86.27(14), C(1)—N(1)—Ga(1) 110.8(3), C(2)—N(2)—Ga(1) 110.3(3), C(27)—N(3)—C(28) 110.7(3), C(27)—N(4)—C(29) 110.9(3), C(2)—C(1)—N(1) 116.0(4), C(1)—C(2)—N(2) 116.7(4), N(4)—C(27) —N(3) 104.8(3), C(29)—C(28)—N(3) 106.3(4), C(28)—C(29)—N(4) 107.3(4).

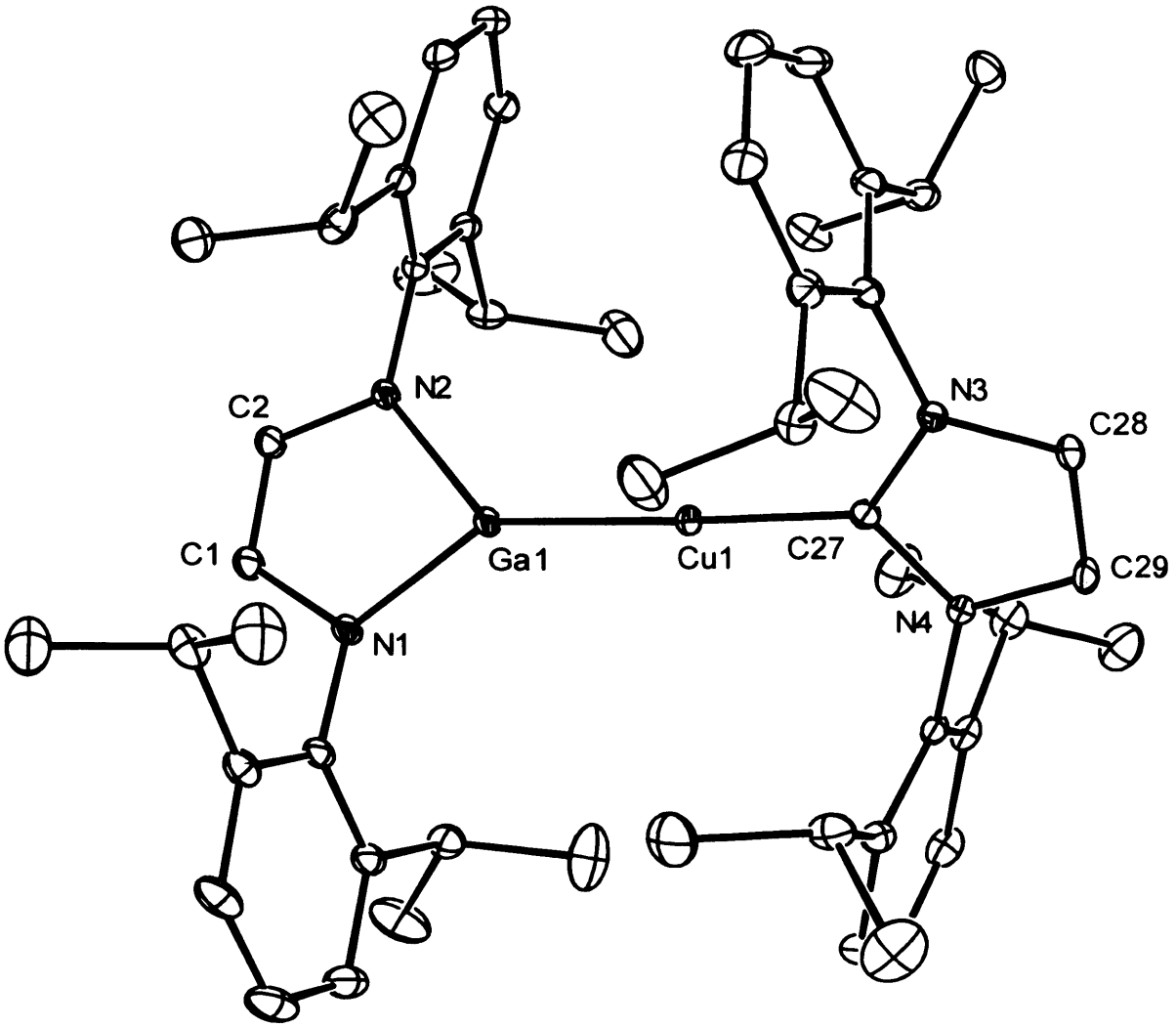

Figure 8 – Thermal ellipsoid plot (25% probability surface) of the molecular structure of [(IPr)Cu{Ga{[N(Ar)C(H)]$_2$}}] **37**; hydrogen atoms are omitted for clarity. Selected bond lengths (Å) and angles (°): Ga(1)—N(2) 1.891(2), Ga(1)—N(1) 1.891(2), Ga(1)—Cu(1) 2.2807(5), Cu(1)—C(27) 1.911(2), N(1)—C(1) 1.389(3), C(1)—C(2) 1.342(4), N(2)—C(2) 1.398(3), N(3)—C(27) 1.354(3), N(3)—C(28) 1.381(3), N(4)—C(27) 1.358(3), N(4)—C(29) 1.380(3), C(28)—C(29) 1.345(4), N(2)—Ga(1)—N(1) 85.59(9), C(27)—Cu(1)—Ga(1) 177.14(7), C(1)—N(1)—C(3) 119.6(2), C(1)—N(1)—Ga(1) 110.97(16), C(2)—C(1)—N(1) 116.6(2), C(2)—N(2)—Ga(1) 111.13(16), C(1)—C(2)—N(2) 115.7(2), C(27)—N(3)—C(28) 111.4(2), C(27)—N(4)—C(29) 111.2(2), N(3)—C(27)—N(4) 104.1(2), C(29)—C(28)—N(3) 106.5(2), C(28)—C(29)—N(4) 106.9(2).

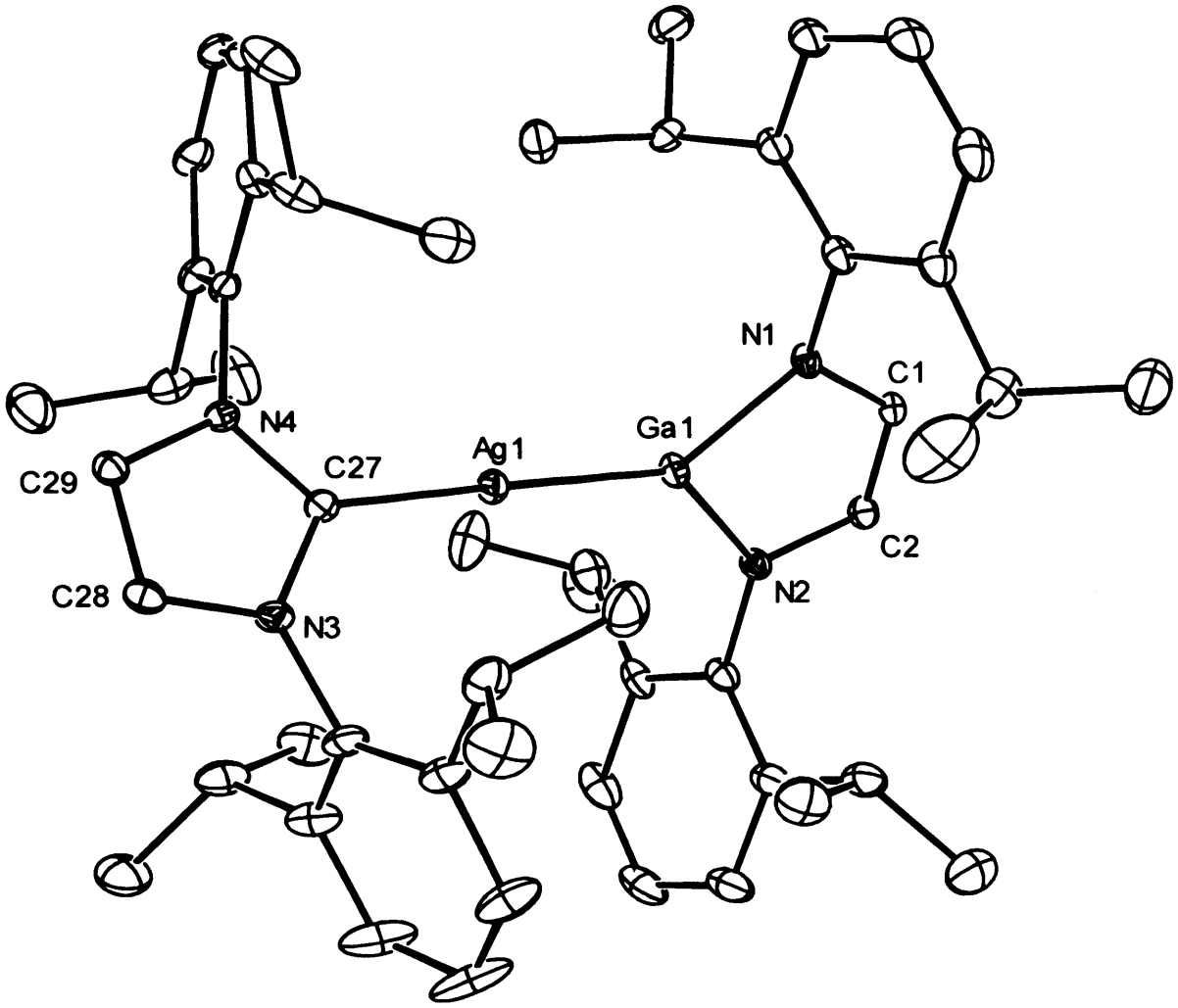

Figure 9 – Thermal ellipsoid plot (25% probability surface) of the molecular structure of [(IPr)Ag{Ga{[N(Ar)C(H)]$_2$}}] **38**; hydrogen atoms are omitted for clarity. Selected bond lengths (Å) and angles (°): Ag(1)—C(27) 2.120(4), Ag(1)—Ga(1) 2.4108(7), Ga(1)—N(1) 1.898(3), Ga(1)—N(2) 1.900(3), N(1)—C(1) 1.392(5), C(1)—C(2) 1.353(6), N(2)—C(2) 1.395(5), N(3)—C(27) 1.357(5), N(3)—C(28) 1.380(6), N(4)—C(27) 1.359(5), N(4)—C(29) 1.390(5), C(28)—C(29) 1.340(6), C(27)—Ag(1)—Ga(1) 178.73(11), N(1)—Ga(1)—N(2) 85.89(15), C(1)—N(1)—Ga(1) 110.8(3), C(2)—C(1)—N(1) 116.1(4), C(2)—N(2)—Ga(1) 110.4(2), C(1)—C(2)—N(2) 116.5(3), C(27)—N(3)—C(28) 111.0(3), C(27)—N(4)—C(29) 111.5(3), N(3)—C(27)—N(4) 103.9(3), C(29)—C(28)—N(3) 107.7(4), C(28)—C(29)—N(4) 105.8(3).

The presence of trace amounts of moisture in the reaction mixture that gave **36** led to the formation of a small amount of the crystalline hydride, $[O\{HGa\{[N(Ar)C(H)]_2\}\}_2][K_2(OEt_2)_2]$, **41**. The assignment of the structure of **41** was based on a partial X-ray structure, which is not included as the diffraction data were weak. The ^1H and $^{13}C\{^1H\}$ NMR spectra of **41** are as expected, and the mass spectrum displays a number of characteristic fragmentation patterns. Most importantly, its IR spectrum confirms the presence of a Ga—H bond, with a stretch occurring at 1855 cm^{-1}, which compares well with that for the related complex, $[(IMes)_2H][HO\{HGa\{[N(Ar)C(H)]_2\}\}_2]$ (1902 cm^{-1}).[2d]

Once formed, the products **34** – **40** were found to be stable in solution at ambient temperature under an inert atmosphere for days. On one occasion, prolonged storage (*ca.* 2 weeks) of a hexane solution of **39** led to deposition of several yellow crystals of the salt, $[Au(IPr)_2][Ga\{[N(Ar)C(H)]_2\}_2]$ **42**. This has presumably formed *via* the partial decomposition of **39**. No data on the compound was obtained due to its low yield, though details of its crystal structure are included (Figure 10). Salts containing the cation, $[Au(IPr)_2]^+$, have not been prepared previously, although the copper[35] and silver[36] homologues have. These previous studies have seen the copper homologue as an effective catalyst in the hydrosilylation of carbonyl compounds[35] and the silver homologue is an NHC transfer reagent.[36] Other salts containing $[(NHC)_2Au]^+$ cations are known, such as $[(ICy)_2Au][PF_6]$ (ICy = $[:C\{[N(C_6H_{11})C(H)]_2\}]$),[37] although the cation in this complex does not deviate from linearity (C—Au—C = 180°), unlike the cation in **42** (C—Au—C = 178.70°). The mean Au—C bond length in **42** (2.024 Å) is slightly greater than in $[(ICy)_2Au]^+$ (1.995 Å), most likely a result of the greater donor strength of ICy over IMes.[29] A complex containing the anion of **42** was previously

synthesised as a byproduct in the reaction of [K(tmeda)][**1**] with $[AlH_3(NMe_3)]$, and as such will not be further discussed here.[2b]

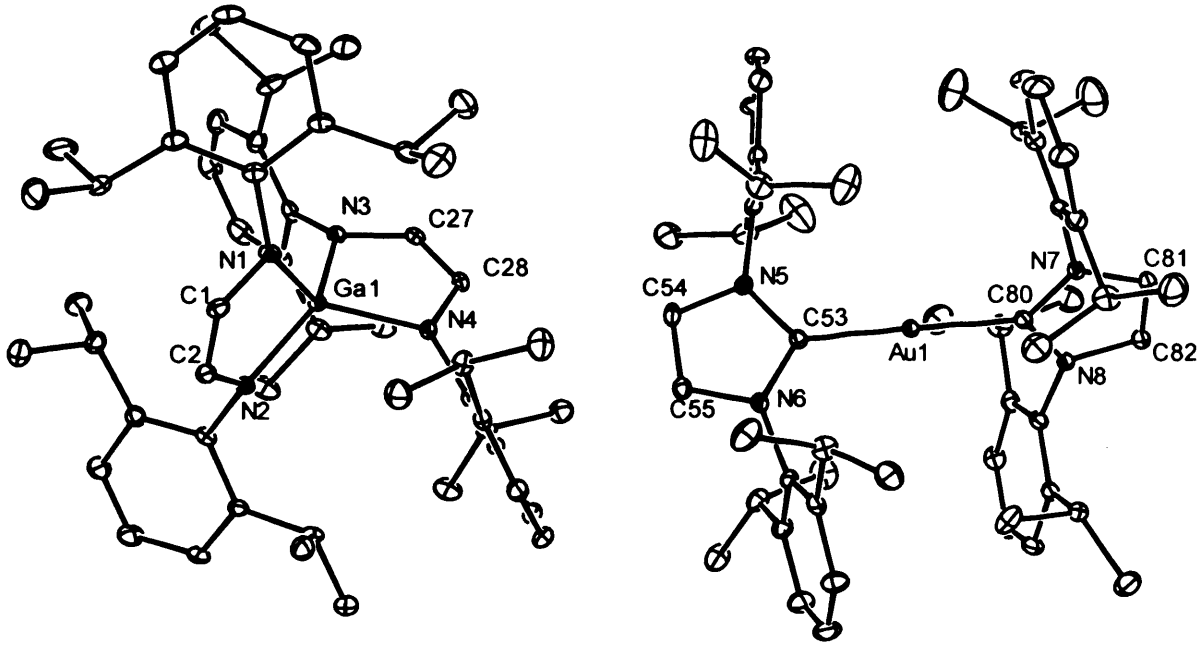

Figure 10 – Thermal ellipsoid plot (25% probability surface) of the structure of $[Au(IPr)_2][Ga\{[N(Ar)C(H)]_2\}_2]$ **42**; hydrogen atoms are omitted for clarity. Selected bond lengths (Å) and angles (°): Au(1)—C(80) 2.022(4), Au(1)—C(53) 2.025(4), Ga(1)—N(3) 1.919(3), Ga(1)—N(2) 1.929(3), Ga(1)—N(1) 1.944(3), Ga(1)—N(4) 1.956(3), N(1)—C(1) 1.405(5), N(2)—C(2) 1.414(5), N(3)—C(27) 1.412(5), N(4)—C(28) 1.403(5), C(1)—C(2) 1.322(5), C(27)—C(28) 1.329(5), C(54)—C(55) 1.339(6), C(81)—C(82) 1.338(5), C(80)—Au(1)—C(53) 178.70(16), N(3)—Ga(1)—N(2) 134.60(13), N(3)—Ga(1)—N(1) 112.64(13), N(2)—Ga(1)—N(1) 88.62(13), N(3)—Ga(1)—N(4) 88.19(13), N(2)—Ga(1)—N(4) 115.70(13), N(1)—Ga(1)—N(4) 120.66(13).

Exposing a solution of **39** to air briefly, followed by overnight storage at -25 °C, afforded a small amount of colourless crystals of the amido complex, $[(IPr)Au\{\eta^1\text{-}N(Ar)COCH_2NH(Ar)\}]$ **43**. Compound **43** was crystallographically characterised

(Figure 11), and forms *via* oxidation of the DAB backbone of **39**, with one equivalent of OH formally adding to it.

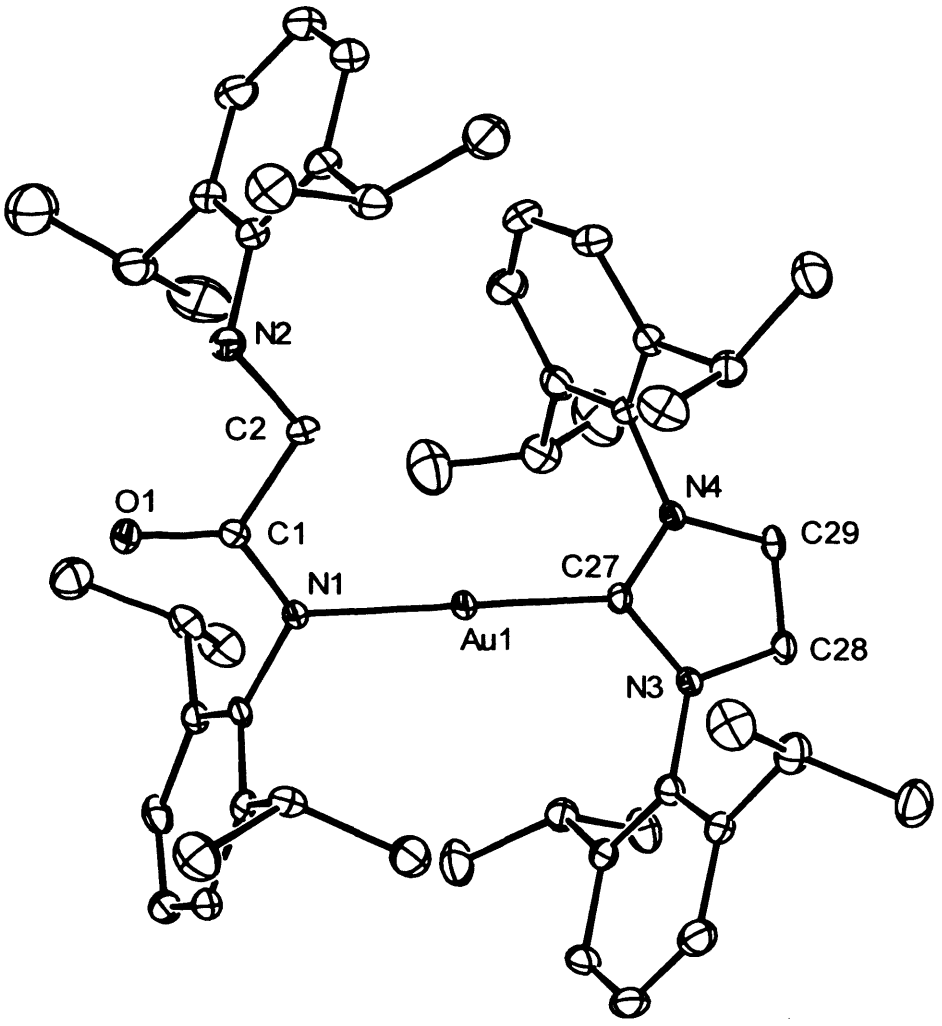

Figure 11 – Thermal ellipsoid plot (25% probability surface) of the molecular structure of [(IPr)Au{η^1-N(Ar)COCH$_2$NH(Ar)}] **43**; hydrogen atoms are omitted for clarity. Selected bond lengths (Å) and angles (°): Au(1)—C(27) 1.980(5), Au(1)—N(1) 2.036(4), O(1)—C(1) 1.251(6), N(1)—C(1) 1.345(7), C(1)—C(2) 1.525(8), N(2)—C(2) 1.467(7), N(3)—C(27) 1.372(7), N(3)—C(28) 1.387(7), N(4)—C(27) 1.334(7), N(4)—C(29) 1.388(6), C(28)—C(29) 1.353(8), C(1)—N(1)—Au(1) 123.8(4), O(1)—C(1)—N(1) 124.6(5), O(1)—C(1)—C(2) 119.7(5), N(1)—C(1)—C(2) 115.7(5), N(2)—C(2)—C(1) 110.9(5), C(27)—N(3)—C(28) 110.4(5), C(27)—N(4)—C(29) 112.5(5), N(4)—C(27)—N(3) 104.3(4), C(29)—C(28)—N(3) 107.1(5), C(28)—C(29)—N(4) 105.7(5).

The crystal structure of **43** is included (Figure 11). A recently reported gold(I) complex, [(IPr)Au(NCMe)],[38] displays a similar Au—N bond distance (2.022 Å) to that observed in **43** (2.036 Å). In contrast, a shorter Au—C bond length is observed in [(IPr)Au(NCMe)] (1.952 Å) than that seen in **43** (1.980 Å). A molecular ion observed in the mass spectrum of **43** and its ^{1}H and $^{13}C\{^{1}H\}$ NMR spectroscopic data correspond well with the molecular structure obtained. This result suggests that the unsaturated C=C DAB backbone of transition metal complexes of **1** is reactive, a result confirmed by later studies (*vide infra*).

3.3.4 The Reactivity of Group 11 Metal(I) Gallyls with Unsaturated Substrates

Considering the wide synthetic use of group 9 and 11 metal boryl complexes,[19] there is much potential in this area for gallyl complexes of these metals. Complexes of the type [(NHC)Cu{Ga{[N(Ar)C(H)]$_2$}}] (NHC = IMes, IPr, ICy_{Me}) are closely related to the copper boryl, [(IPr)Cu{B(pin)}] **26**, that has been used to great effect as a borylating reagent by Sadighi's group in recent years.[20-21] The high yielding synthesis of **37**, the direct analogue of **26**, ensured that this reagent would be the most studied by us. The treatment of **26** with a range of alkenes affords copper(I) β-boroalkyls via insertion of the C=C bond into the Cu—B bond.[21a] The copper(I) β-boroalkyls formed are unusually stable towards β-hydride elimination processes that are typical for this type of compound.[39] However, the treatment of **34**, **37**, **38** and **40** with the alkene, styrene, and the internal alkyne, but-2-yne, led to no reaction. Similarly, when ethylene was bubbled through a toluene solution of **37**, no reaction occurred. In contrast, the terminal alkyne, phenylacetylene, reacted with **37** to yield **44** as the only isolable product in poor yield (Scheme 12). Complex **44** has previously been synthesised in quantitative yield from [(IPr)Cu(Me)] and phenylacetylene by cleavage of the weakly

acidic alkynic C—H bond of phenylacetylene.[42] Only the resonances for the two acetylide carbons in the $^{13}C\{^1H\}$ NMR spectrum of **44** were given in this report, so it was decided to perform a full characterisation, including a single crystal X-ray crystallographic analysis here (Figure 12).

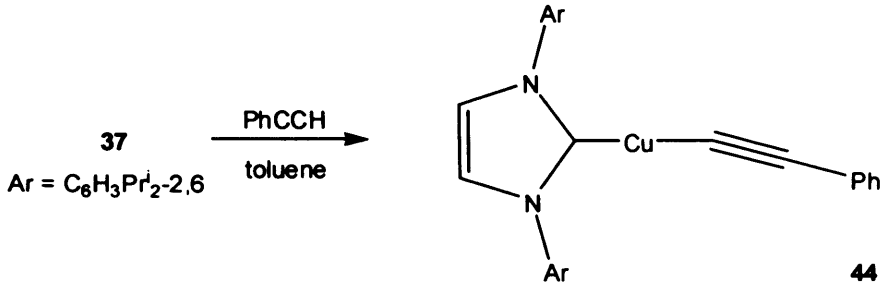

Scheme 12 – The synthesis of **44**

It is believed that the acidic acetylide proton of phenylacetylene reacts with the gallium heterocycle of **37**, which decomposes to a mixture of products, one of which was identified as Ar-DAB ($\{N(Ar)C(H)\}_2$, ^1H NMR spectrum). The ^1H and $^{13}C\{^1H\}$ NMR spectroscopic data for **44** agree with its proposed structure and a molecular ion was observed in the mass spectrum. The original report on the synthesis of **44** states that one of the acetylide carbons of the compound resonates at a chemical shift of δ 101.0 ppm in the $^{13}C\{^1H\}$ NMR spectrum.[40] No signal was observed at this field in our analysis of **44**. Instead, a signal at δ 129.1 ppm was assigned to the terminal acetylide carbon. This value is very close to that observed in the $^{13}C\{^1H\}$ NMR spectrum of the closely related compound, [(SIPr)Cu(η^1-C≡CPh)] (SIPr = [:C{[N(Ar)C(H)$_2$]$_2$}) (δ 129.3 ppm).[41] Calculations were performed on the model complex, [PhC≡CCu-C{[N(Me)C(H)$_2$]$_2$}],[41] and the values obtained for its calculated $^{13}C\{^1H\}$ NMR spectrum agree with the experimental values, so the assignment of the terminal acetylide carbon signal for **44** is logical. The C≡C stretch in the IR spectrum of **44** (2090 cm^{-1}) is very similar to that of [(SIPr)Cu(η^1-C≡CPh)] (2085 cm^{-1}), but the carbene

resonance in the $^{13}C\{^1H\}$ NMR spectrum of **44** at δ 183.7 ppm is, however, much more shielded than that observed in [(SIPr)Cu(η^1-C≡CPh)] (δ 205.9 ppm).[41]

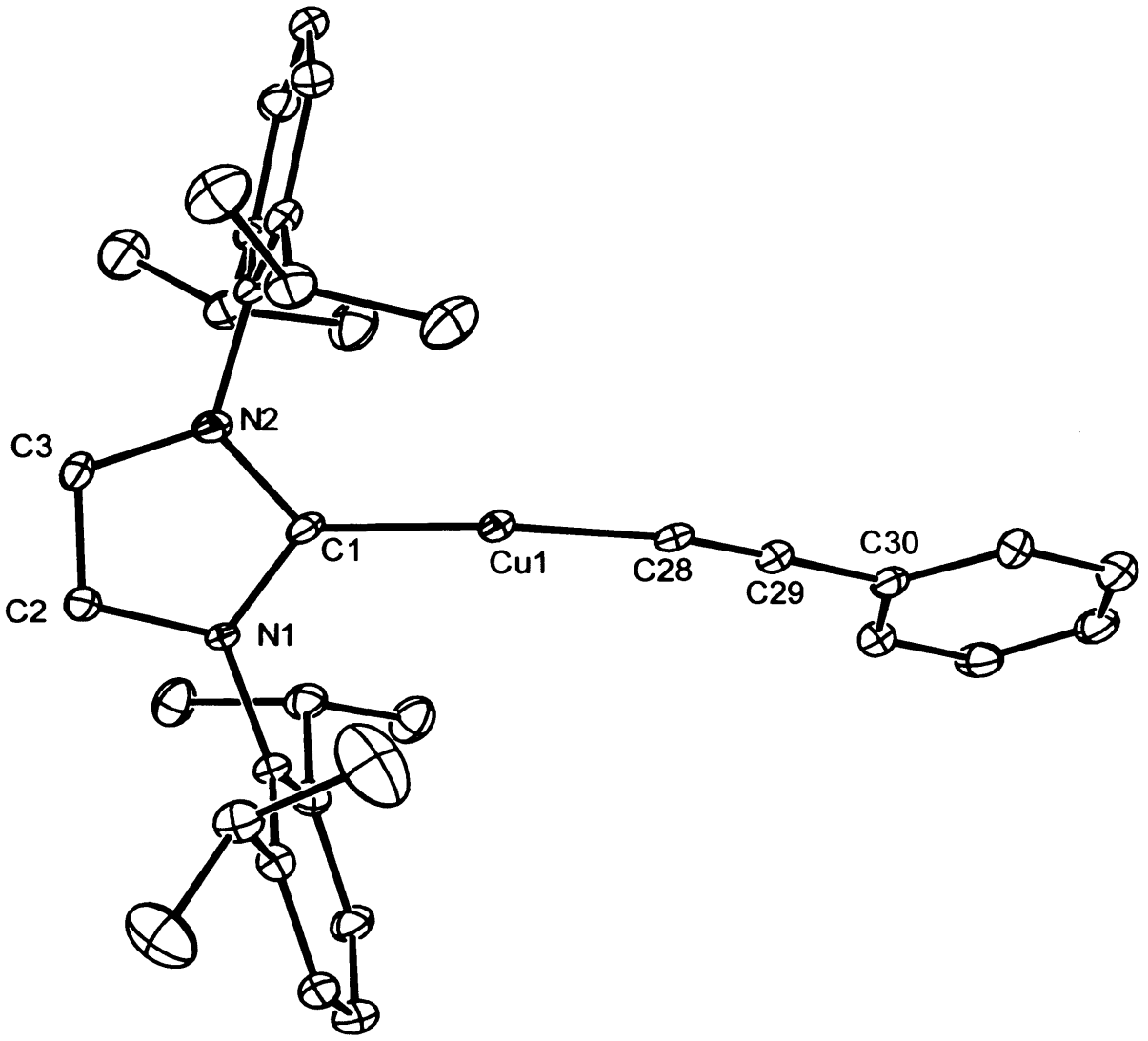

Figure 12 – Thermal ellipsoid plot (25% probability surface) of the molecular structure of [(IPr)Cu(η^1-C≡CPh)] **44**; hydrogen atoms are omitted for clarity. Selected bond lengths (Å) and angles (°): Cu(1)—C(28) 1.861(4), Cu(1)—C(1) 1.890(4), N(1)—C(1) 1.365(5), N(1)—C(2) 1.401(4), C(1)—N(2) 1.358(4), N(2)—C(3) 1.378(5), C(2)—C(3) 1.345(5), C(28)—C(29) 1.209(5), C(29)—C(30) 1.455(6), C(28)—Cu(1)—C(1) 172.74(16), C(1)—N(1)—C(2) 111.2(3), N(2)—C(1)—N(1) 103.5(3), C(1)—N(2) —C(3) 112.2(3), C(3)—C(2)—N(1) 106.2(3), C(2)—C(3)—N(2) 106.9(3), C(29) —C(28)—Cu(1) 168.4(3), C(28)—C(29)—C(30) 177.4(4).

The geometry around the copper(I) centre in **44** is non-linear (C—Cu—C 172.74(16)°) and the Cu—$C_{carbene}$ bond is 0.02 Å shorter than that observed in **37** (Figure 12). This suggests that phenylacetylide is a weaker donor than **1**. The phenylacetylide ligand does not approach the copper(I) centre in a linear fashion, the C—C—Cu angle being 168.4(3)°. To the best of our knowledge, there are no structurally characterised examples of terminal, non-bridging acetylide copper(I) complexes for comparison with **44**, but the C≡C bond length is typical when compared with terminal acetylide complexes of gold(I).[26]

The reaction of mesitaldehyde with **26** yields the novel complex, [(IPr)Cu(Mes)(H)O{B(pin)}], via insertion of the aldehyde into the Cu—B bond.[21b] In the presence of an excess of $B_2(pin)_2$ and aldehyde, complexes of this type react to form 1,2-diborated products of the general formula, [RC{OB(pin)}{B(pin)}], in a catalytic manner. In contrast, no reaction occurred when benzaldehyde was added to **34**, **37** or **38**. These complexes were subsequently treated with a wide range of other unsaturated organic substrates. No reaction occurred when **34**, **37** or **38** were treated with azobenzene, *tert*-butylisocyanate, *tert*-butylisothiocyanate or *tert*-butylphosphaalkyne. Reactions occurred when **34**, **37** or **38** were treated with *N,N'*-diisopropylcarbodiimide, *N,N'*-dicyclohexylcarbodiimide, 3-buten-2-one, dimethylacetylene dicarboxylate or xylylisonitrile but no products could be isolated or identified. In contrast, the treatment of **37** with an excess of *tert*-butylisonitrile, Bu^tNC, gave the three-coordinate copper(I) complex, **45** (Scheme 13). It is thought that the reaction proceeds almost quantitatively, but the isonitrile ligand is weakly coordinated and **45** is in equilibrium with **37** and free isonitrile in solution. As such, **45** co-crystallised with **37** directly from the reaction mixture, and could not be isolated in greater purity in the solid state, even when a large

excess of Bu^{t}NC was used. These findings are in common with those by Goj *et al.* in the treatment of [(IPr)CuNHPh] with Bu^{t}NC.[42]

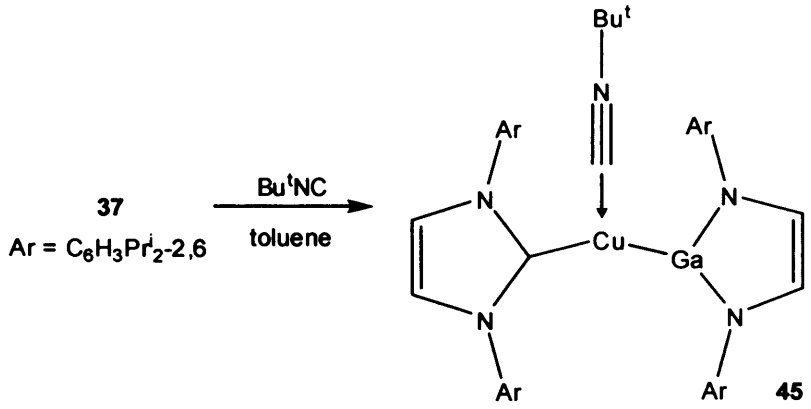

Scheme 13 – The synthesis of **45**

The crystal structure of **45** is included (Figure 13). ^{1}H and ^{13}C{^{1}H} NMR spectroscopic analyses of **45** were possible by the subtraction of signals due to **37** and free Bu^{t}NC from the spectra of the reaction mixture. A signal at δ 54.8 ppm in the ^{13}C{^{1}H} NMR spectrum of **45** was assigned as the terminal carbon of the isonitrile, and is suggestive of a weaker Cu—C bond than in the three coordinate copper(I) isonitrile complex, [{R$_3$C(OMe)}Cu(Bu^{t}NC)][PF$_6$] (R = C{N(Me)C(Ph)C(Ph)N}) (δ 66.2 ppm).[43] As would be expected, the carbene signal in the ^{13}C{^{1}H} NMR spectrum (δ 188.7 ppm) is considerably deshielded (6 ppm) compared to that of **37**, a result of the increased electron density at the copper centre in the three-coordinate complex. A molecular ion was observed in the mass spectrum. The C≡N stretch in the IR spectrum of **45** (2148 cm^{-1}) suggests that the C≡N bond is much weaker than that observed in the complex, [{R$_3$C(OMe)}Cu(Bu^{t}NC)][PF$_6$] (2189 cm^{-1}).[43] This in turn suggests that there is a considerable amount of π-backbonding from the electron-rich copper(I) centre of **45** to the coordinated isonitrile ligand.

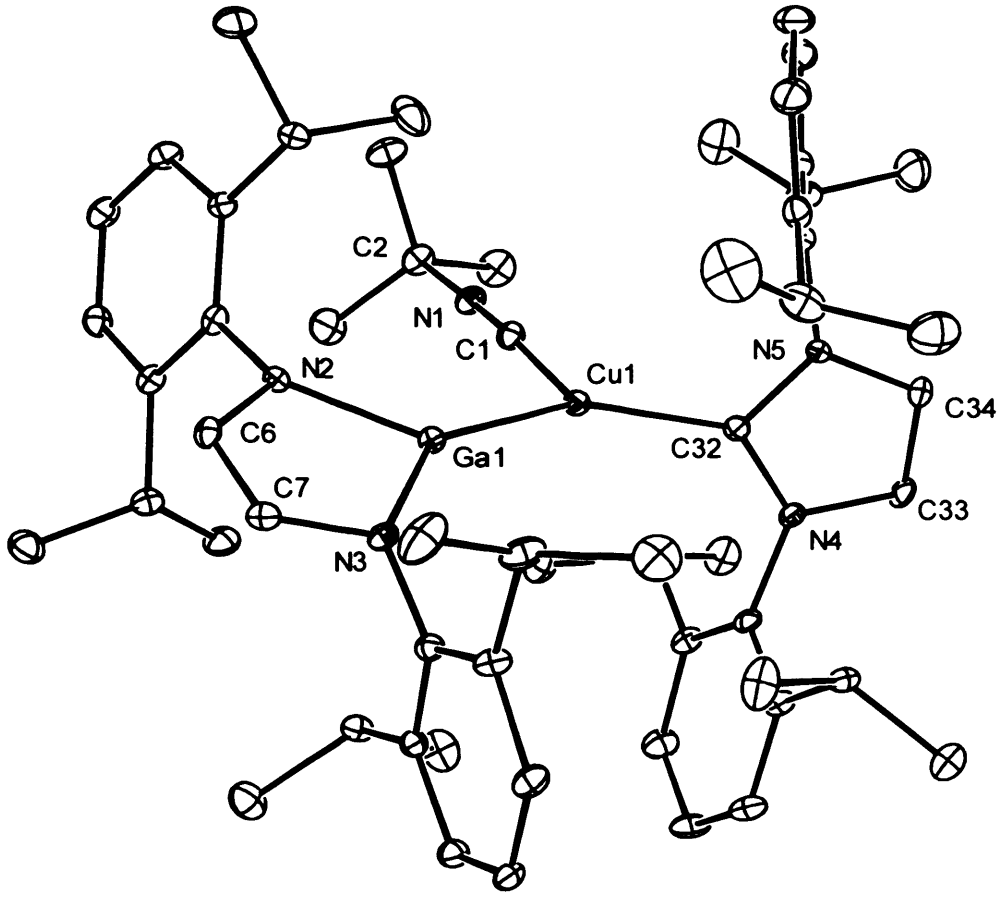

Figure 13 – Thermal ellipsoid plot (25% probability surface) of the molecular structure of [(IPr)(Bu^{t}NC)Cu{Ga{[N(Ar)C(H)]$_2$}}] **45**; hydrogen atoms are omitted for clarity. Selected bond lengths (Å) and angles (°): Ga(1)—N(3) 1.926(4), Ga(1)—N(2) 1.940(4), Ga(1)—Cu(1) 2.3707(11), Cu(1)—C(1) 1.935(6), Cu(1)—C(32) 1.968(5), N(1)—C(1) 1.162(6), N(1)—C(2) 1.476(6), N(2)—C(6) 1.389(6), C(2)—C(3) 1.535(7), N(3)—C(7) 1.379(6), N(4)—C(32) 1.363(6), N(4)—C(33) 1.384(6), N(5)—C(32) 1.364(6), N(5)—C(34) 1.387(6), C(6)—C(7) 1.346(6), C(33)—C(34) 1.331(7), N(3)—Ga(1) —N(2) 84.74(16), C(1)—Cu(1)—C(32) 115.9(2), C(1)—Cu(1)—Ga(1) 108.95(16), C(32)—Cu(1)—Ga(1) 135.15(13), C(1)—N(1)—C(2) 177.8(5), N(1)—C(1)—Cu(1) 177.6(5), C(6)—N(2)—Ga(1) 110.3(3), N(1)—C(2)—C(4) 108.0(4), N(1)—C(2)—C(3) 106.3(4), C(7)—N(3)—Ga(1) 110.8(3), C(32)—N(4)—C(33) 111.6(4), C(32)—N(5) —C(34) 111.7(4), C(7)—C(6)—N(2) 116.7(5), C(6)—C(7)—N(3) 117.4(4), N(4)—C(32)—N(5) 103.0(4), N(4)—C(32)—Cu(1) 130.2(4), N(5)—C(32)—Cu(1) 125.9(4), C(34)—C(33)—N(4) 107.0(5), C(33)—C(34)—N(5) 106.7(5).

The copper(I) centre in **45** is trigonal planar (Σ E—Cu—C (E = Ga, C) angles 360°), with the largest angle about copper being 135.15° between the two sterically demanding heterocycles (Figure 13). The Cu—$C_{isonitrile}$ bond length seen in **45** is over 0.1 Å longer than that observed in [{$R_3C(OMe)$}Cu(Bu^tNC)][PF_6],[43] which is line with the facile dissociation of the Bu^tNC ligand from this complex in solution. In addition, the C≡N bond length of **45** is longer than that observed in [{$R_3C(OMe)$}Cu(Bu^tNC)][PF_6] (1.131 Å),[43] supporting the inferences made from the IR study. The Ga—Cu bond in **45** is 0.09 Å longer than in **37** and there is a similar lengthening of the Cu—$C_{carbene}$ bond (0.056 Å) upon isonitrile coordination. These observations can be explained by the increased electron density around the three coordinate copper(I) centre, supporting the conclusions drawn from the $^{13}C\{^1H\}$ NMR spectroscopic study. As with complex **31**, the C=C backbones of the gallyl and IMes ligands in **45** are skewed with respect to each other (torsion angle C(6)C(7)—C(33)C(34) 62.8°).

The copper(I) boryl complex, **26**, has proved effective in the abstraction of oxygen from CO_2, forming [(IPr)Cu{OB(pin)}] and CO.[20a] This system has been exploited as an efficient homogeneous catalyst in the reduction of CO_2. Theoretical studies suggest that the reaction proceeds *via* an initial insertion of CO_2 into the Cu—B bond.[20b] When **37** was treated with CO_2, a small amount of **46** was isolated from the reaction mixture (Scheme 14). A possible mechanism for the formation of **46** could involve an initial attack of the activated DAB backbone of the gallyl ligand at the carbon of CO_2, followed by the formation of a Cu—O bond. The fate of the gallium atom is unknown. A proton has also added to the DAB fragment, either abstracted from the solvent or due to a trace of water in the reaction mixture. X-ray quality crystals were grown from hexane and the structure determined (Figure 14). The ^1H NMR

spectrum of the complex complements the proposed structure but analysis of the $^{13}C\{^1H\}$ NMR spectrum of the complex was inconclusive due to the weakness of the sample used. No reaction occurred when **37** was treated with CO, but the addition of a stoichiometric amount of CS_2 to **37** gave a deep red solution. A small amount of a red complex was isolated, which was thought to be **47** from a partial X-ray structure determination (Scheme 14). This complex is poorly characterised and will not be discussed in detail here as its formulation is uncertain. However, it appears that a C—C bond has formed in a similar manner to the formation of **46**, and that the CS_2 prefers to adopt a chelating rather than terminal coordination mode to the copper centre. In an attempt to synthesise a more characterisable product, CS_2 was reacted with **40**, but only an intractable mixture of products resulted.

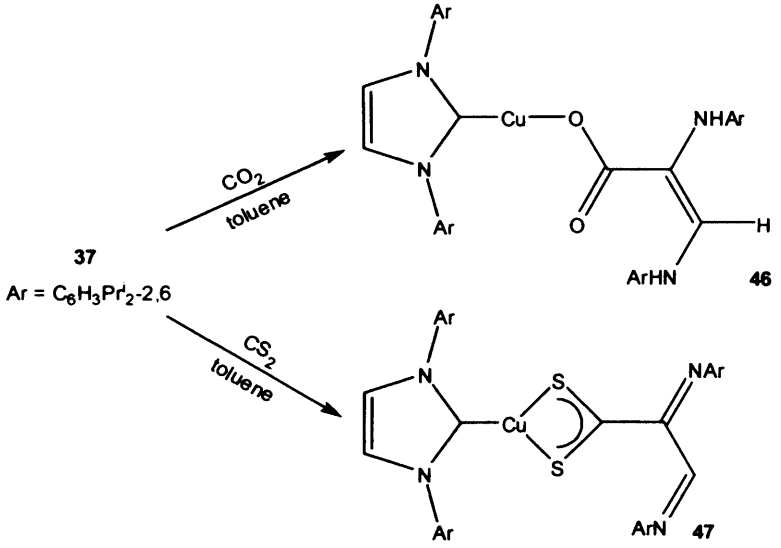

Scheme 14 – The synthesis of **46** and **47**

The crystal structure of **46** (Figure 14) shows a non-linear geometry about the copper(I) centre. An analysis of the bond lengths and angles suggests that there is an sp^2-type hybridisation of the orbitals on C(2), complimenting the formal assignment of C=C double bonds and C—N single bonds in this complex. Although the CO_2 fragment is bound to the copper(I) centre in an η^1-fashion, the two C=O bond lengths in **46** are similar. This finding is in agreement with the Cu—O bond being relatively weak, in

comparison with that observed for [(IPr)Cu(OAc)] (Ac = acetyl) (1.836 Å).[41] In addition, the Cu—C bond length in [(IPr)Cu(OAc)] ((1.864 Å))[41] is similar to that observed for **46**.

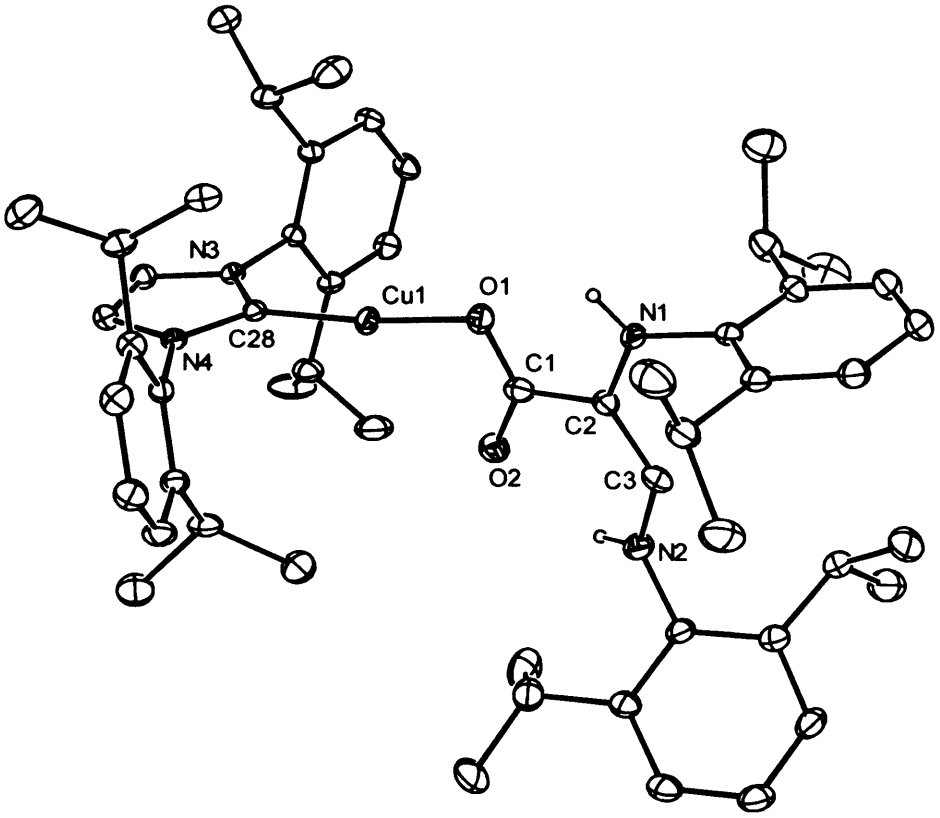

Figure 14 – Thermal ellipsoid plot (25% probability surface) of the molecular structure of [(IPr)Cu(η^1-$CO_2C_2N_2Ar_2$)] **46**; hydrogen atoms are omitted for clarity. Selected bond lengths (Å) and angles (°): Cu(1)—C(28) 1.873(4), Cu(1)—O(1) 1.915(3), O(1)—C(1) 1.244(6), N(1)—C(2) 1.396(6), C(1)—O(2) 1.252(6), C(1)—C(2) 1.491(7), N(2)—C(3) 1.372(7), C(2)—C(3) 1.376(7), N(3)—C(28) 1.360(5), N(3)—C(29) 1.377(5), N(4)—C(28) 1.360(5), N(4)—C(30) 1.373(6), C(29)—C(30) 1.332(6), C(28)—Cu(1)—O(1) 172.61(18), C(1)—O(1)—Cu(1) 109.3(3), O(1)—C(1)—O(2) 126.2(5), O(1)—C(1)—C(2) 114.4(5), O(2)—C(1)—C(2) 119.3(5), C(3)—C(2)—N(1) 120.5(4), C(3)—C(2)—C(1) 121.4(5), N(1)—C(2)—C(1) 118.0(4), C(28)—N(3)—C(29) 111.0(4), N(2)—C(3)—C(2) 126.9(5), C(28)—N(4)—C(30) 110.7(4), N(3)—C(28)—N(4) 103.9(4), N(3)—C(28)—Cu(1) 128.5(3), N(4)—C(28)—Cu(1) 127.5(3), C(30)—C(29)—N(3) 106.7(4), C(29)—C(30)—N(4) 107.5(4).

3.4 Conclusion

In summary, the ability of the gallyl anion, $[:Ga\{[N(Ar)C(H)]_2\}]^-$ **1**, to participate in salt metathesis reactions with a range of NHC coordinated group 6, 9 and 11 metal chloride complexes has been demonstrated. The NHC ligands appear to play a vital role in the stabilisation of the formed complexes and/or reaction intermediates towards reductive elimination processes. This has allowed access to a variety of group 6, 9 and 11 metal gallyl complexes, examples of which exhibit the first structurally characterised Ga—Cu or Ga—Ag bonds in molecular complexes. Some of these complexes are direct homologues of recently reported group 11 metal(I) boryl complexes. Analogies have also been drawn between **1** and other cyclic boryl ligands, complexes of which are widely used in organic transformations. The reactivity of the copper(I) gallyl complexes towards unsaturated substrates appears to be very different to related boryl systems that have been studied. Furthermore, a scale of *trans*-influences has been tentatively established for the series, $B(OR)_2 > \mathbf{1} > Cl^-$. Most of the work discussed in this chapter has been summarised in a recent publication.[44]

3.5 Experimental

General experimental procedures are compiled in Appendix 1 and crystallographic data are compiled in Appendix 3. A reproducible microanalysis of **36** was not obtained, but the ^1H NMR spectrum of the compound shows it to have protic impurities of < 5 %. The compounds [K(tmeda)][**1**],[1] [Cp*CrCl],[23] [(η^4-COD)Ir(IMes)Cl][45], [(IMes)MCl] (M = Cu,[30] Ag[34] or Au[31]) and [(IPr)MCl] (M = Cu,[46] Ag[47] or Au[31]) were synthesised by literature procedures. [(ICy)CuCl] was prepared by

a variation of a literature procedure.[47] CS_2 was freshly distilled prior to use. All other reagents were used as received.

Preparation of [(η^5-Cp)Cr(IMes){Ga{[N(Ar)C(H)]$_2$}}] 31: A solution of [K(tmeda)][:Ga{[N(Ar)C(H)]$_2$}] (0.32 g, 0.53 mmol) in THF (10 cm^3) was added to a suspension of [(η^5-Cp)Cr(IMes)Cl] (0.24 g, 0.53 mmol) in THF (10 cm^3) at -78 °C to give a deep purple solution. The reaction mixture was warmed to 20 °C and stirred overnight. All volatiles were then removed *in vacuo*, and the residue was washed with hexane (20 cm^3) and extracted into diethyl ether (40 cm^3) and filtered. The filtrate was concentrated to *ca.* 15 cm^3 and stored at -30 °C to give deep purple blocks of **31**. Further concentration of the supernatant solution gave another crop of **31** (0.33 g, 94 %). Mp 110 °C (decomp.); μ_{eff} = 1.65 μ_B (Evan's method); EI acc. mass: on M^+: calc. for: 305 (C{N(Mes)C(H)}$_2H^+$, 100); IR ν/cm^{-1} (Nujol): 1671 m, 1609 m, 1585 m, 1557 m, 1324 m, 1258 s, 1110 m, 929 m, 895 m, 854 s, 803 s, 765 s.

Preparation of [(η^4-COD)Ir(IMes){Ga{[N(Ar)C(H)]$_2$}}] 32: A solution of [K(tmeda)][:Ga{[N(Ar)C(H)]$_2$}] (0.19 g, 0.31 mmol) in Et_2O (20 cm^3) was added to a solution of [(η^4-COD)Ir(IMes)Cl] (0.20 g, 0.31 mmol) in Et_2O (10 cm^3) at -78 °C to give a deep purple solution. The reaction mixture was warmed to 20 °C and stirred for 3 hours. Volatiles were then removed *in vacuo* and the residue was extracted into hexane (60 cm^3) and filtered. The filtrate was concentrated to *ca.* 15 cm^3 and stored at -30 °C overnight to give deep purple blocks of **32** (0.19 g, 51 %). Mp 157-159 °C (decomp.); ^{1}H NMR (400 MHz, C_6D_6, 298 K): δ 1.35-2.20 (m, 8 H, CH_2), 1.43 (d, $^3J_{HH}$ = 6.9 Hz, 6 H, (CH_3)$_2$CH), 1.45 (d, $^3J_{HH}$ = 6.9 Hz, 6 H, (CH_3)$_2$CH), 1.58 (d, $^3J_{HH}$ = 6.9 Hz, 6 H, (CH_3)$_2$CH), 1.61 (d, $^3J_{HH}$ = 6.9 Hz, 6 H, (CH_3)$_2$CH), 2.10 (s, 6 H, *p*-CH_3), 2.22 (br. s, 12 H, *o*-CH_3), 3.78 (br. m, 2 H, CH_2C*H*), 4.08 (sept, $^3J_{HH}$ = 6.9 Hz, 2 H, (CH_3)$_2$C*H*), 4.12,

(sept, $^3J_{HH}$ = 6.9 Hz, 2 H, $(CH_3)_2CH$), 4.72 (br. m, 2 H, CH_2CH), 6.10 (br. s, 2 H, NC*H*), 6.55 (br. s, 2 H, NC*H*), 6.71-7.39 (m, 10 H, Ar-*H*); $^{13}C\{^1H\}$ NMR (75.6 MHz, C_6D_6, 298 K): δ 17.8, 19.5 (*o*-CH_3), 20.7 (*p*-CH_3) 23.2, 23.4, 26.7, 26.8 ($(CH_3)_2CH$), 27.9, 28.4 ($(CH_3)_2CH$), 31.7, 32.9 (CH_2), 67.8, 68.5 (CH_2CH), 122.4, 124.5 (br, *C*N), 122.8, 123.0, 124.0, 128.6, 129.7, 134.4, 134.7, 136.7, 138.5, 146.1, 146.2, 149.7 (Ar-*C*), 185.8 (br., CN_2); MS (EI 70eV), *m/z* (%): 602 ((COD)IrC{N(Mes)C(H)}$_2H^+$, 42), 496 (IrC{N(Mes)C(H)}$_2H^+$, 72), 305 (C{N(Mes)C(H)}$_2H^+$, 55); IR ν/cm^{-1} (Nujol): 1658 m, 1608 m, 1588 m, 1316 m, 1254 m, 851 m; EI acc. mass: on M^+: calc. for $C_{55}H_{72}N_4GaIr$: 1048.4613, found: 1048.4609; $C_{55}H_{72}N_4GaIr$ requires C 62.85, H 6.90, N 5.33; found C 62.71, H 7.05, N 5.22.

Preparation of [(IMes)Cu{Ga{[N(Ar)C(H)]$_2$}}] 34: A solution of [K(tmeda)] [:Ga{[N(Ar)C(H)]$_2$}] (0.24 g, 0.40 mmol) in THF (10 cm^3) was added to a suspension of [(IMes)CuCl] (0.16 g, 0.40 mmol) in THF (10 cm^3) at -78 °C to give a yellow solution. The reaction mixture was warmed to 20 °C and stirred overnight. Volatiles were then removed *in vacuo* and the residue was extracted into hexane (40 cm^3) and filtered. The filtrate was concentrated to *ca.* 15 cm^3 and stored at -30 °C overnight to give yellow blocks of **34** (0.12 g, 37 %). Mp 149-152 °C (decomp.); ^1H NMR (400 MHz, C_6D_6, 298 K): δ 1.26 (d, $^3J_{HH}$ = 6.9 Hz, 12 H, $(CH_3)_2CH$), 1.47 (d, $^3J_{HH}$ = 6.9 Hz, 12 H, $(CH_3)_2CH$), 1.87 (s, 12 H, *o*-CH_3), 2.20 (s, 6 H, *p*-CH_3), 3.90 (sept, $^3J_{HH}$ = 6.9 Hz, 4 H, $(CH_3)_2CH$), 5.94 (s, 2 H, NC*H*), 6.57 (s, 2 H, NC*H*), 6.76 (s, 4 H, Ar-*H*, *IMes*), 7.05-7.35 (m, 6 H, Ar-*H*); $^{13}C\{^1H\}$ NMR (75.6 MHz, C_6D_6, 298 K): δ 17.3 (*o*-CH_3), 20.9 (*p*-CH_3) 24.6, 26.0 ($(CH_3)_2CH$), 27.7 ($(CH_3)_2CH$), 121.1, 123.7 (*C*N), 121.6, 122.4, 129.3, 134.2, 134.9, 138.8, 145.7, 147.8 (Ar-*C*), 181.2 (br., CN_2); MS (EI 70eV), *m/z* (%): 814 (MH^+, 3), 378 ({N(Ar)C(H)}$_2H^+$, 100); IR ν/cm^{-1} (Nujol): 1656 m, 1586 m, 1549 m, 1321 m, 1259 m, 1113 m, 851 m, 806 m; EI acc. mass: on M^+: calc. for

$C_{47}H_{60}N_4CuGa$: 812.3364, found 812.3372; $C_{47}H_{60}N_4CuGa$ requires C 69.33, H 7.43, N 6.88; found C 69.25, H 7.53, N 7.01.

Preparation of [(IMes)Ag{Ga{[N(Ar)C(H)]$_2$}}] 35: A solution of [K(tmeda)][:Ga{[N(Ar)C(H)]$_2$}] (0.27 g, 0.45 mmol) in THF (15 cm^3) was added to a suspension of [(IMes)AgCl] (0.20 g, 0.45 mmol) in THF (15 cm^3) at -78 °C to give a deep yellow solution. The reaction mixture was warmed to 20 °C and stirred overnight. Volatiles were then removed *in vacuo* and the residue was extracted into hexane (40 cm^3) and filtered. The filtrate was concentrated to *ca.* 15 cm^3 and stored at -30 °C overnight to give yellow blocks of **35** (0.05 g, 13 %). Mp 105-109 °C (decomp); ^{1}H NMR (400 MHz, C_6D_6, 298 K): δ 1.30 (d, $^3J_{HH}$ = 6.9 Hz, 12 H, (C*H*$_3$)$_2$CH), 1.48 (d, $^3J_{HH}$ = 6.9 Hz, 12 H, (C*H*$_3$)$_2$CH), 1.86 (s, 12 H, *o*-C*H*$_3$), 2.27 (s, 6 H, *p*-C*H*$_3$), 3.95 (sept, $^3J_{HH}$ = 6.9 Hz, 4 H, (CH$_3$)$_2$C*H*), 6.07 (s, 2 H, NC*H*), 6.60 (s, 2 H, NC*H*), 6.76 (s, 4 H, Ar-*H*, *IMes*), 7.17-7.37 (m, 6 H, Ar-*H*); ^{13}C{^{1}H} NMR (75.6 MHz, C_6D_6, 298 K): δ 17.2 (*o*-*C*H$_3$), 20.8 (*p*-*C*H$_3$) 24.5, 26.0 ((*C*H$_3$)$_2$CH), 27.7 ((CH$_3$)$_2$*C*H), 121.4, 123.8 (*C*N), 121.7, 122.4, 129.3, 134.3, 135.4, 138.8, 145.8, 147.5 (Ar-*C*), *C*N$_2$ not observed; MS (EI 70eV), *m/z* (%): 858 (MH$^+$, 1), 378 ({N(Ar)C(H)}$_2$H$^+$, 28); IR ν/cm^{-1} (Nujol): 1607 m, 1587 m, 1578 m, 1546 m, 1264 m, 1115 m, 852 m; EI acc. mass: on M$^+$: calc. for $C_{47}H_{60}N_4AgGa$: 856.3119, found 856.3123; $C_{47}H_{60}N_4AgGa$ requires C 65.75, H 7.04, N 6.52; found C 65.75, H 7.43, N 6.29.

Preparation of [(IMes)Au{Ga{[N(Ar)C(H)]$_2$}}] 36: A solution of [K(tmeda)][:Ga{[N(Ar)C(H)]$_2$}] (0.21 g, 0.35 mmol) in THF (10 cm^3) was added to a suspension of [(IMes)AuCl] (0.19 g, 0.35 mmol) in THF (10 cm^3) at -78 °C to give a yellow solution. The reaction mixture was warmed to 20 °C and stirred overnight. Volatiles were then removed *in vacuo* and the residue was extracted into hexane (30 cm^3) and

filtered. The filtrate was concentrated to *ca.* 15 cm^3 and stored at -30 °C for 48 hrs to give yellow blocks of **36** (0.04 g, 12 %). Mp 104-108 °C (decomp.); ^1H NMR (400 MHz, C_6D_6, 298 K): δ 1.46 (d, $^3J_{HH}$ = 6.9 Hz, 12 H, $(CH_3)_2CH$), 1.63 (d, $^3J_{HH}$ = 6.9 Hz, 12 H, $(CH_3)_2CH$), 2.04 (s, 12 H, *o*-CH_3), 2.46 (s, 6 H, *p*-CH_3), 4.05 (sept, $^3J_{HH}$ = 6.9 Hz, 4 H, $(CH_3)_2CH$), 6.15 (s, 2 H, NC*H*), 6.73 (s, 2 H, NC*H*), 6.91 (s, 4 H, Ar-*H*, *IMes*), 7.39-7.51 (m, 6 H, Ar-*H*); $^{13}C\{^1H\}$ NMR (75.6 MHz, C_6D_6, 298 K): δ 17.2 (*o*-CH_3), 20.9 (*p*-CH_3) 24.4, 26.0 ($(CH_3)_2CH$), 27.7 ($(CH_3)_2CH$), 121.2, 124.1 (*C*N), 121.3, 122.5, 129.2, 134.3, 134.7, 138.9, 145.9, 146.9 (Ar-*C*), 205.2 (CN_2); MS (EI 70eV), *m/z* (%): 946 (MH^+, 10), 378 ($\{N(Ar)C(H)\}_2H^+$, 43); IR ν/cm^{-1} (Nujol): 1661 m, 1610 m, 1260 m, 1098 m, 1020 m, 800 m; EI acc. mass: on M^+: calc. for $C_{47}H_{60}N_4AuGa$: 946.3734, found 946.3740.

Preparation of [(IPr)Cu{Ga{[N(Ar)C(H)]$_2$}}] 37: A solution of [K(tmeda)] [:Ga{[N(Ar)C(H)]$_2$}] (0.22 g, 0.37 mmol) in THF (10 cm^3) was added to a suspension of [(IPr)CuCl] (0.18 g, 0.37 mmol) in THF (10 cm^3) at -78 °C to give a yellow solution. The reaction mixture was warmed to 20 °C and stirred overnight. Volatiles were then removed *in vacuo* and the residue was extracted into diethyl ether (50 cm^3) and filtered. The filtrate was concentrated to *ca.* 10 cm^3 and stored at -30 °C overnight to give yellow blocks of **37** (0.24 g, 73 %). Mp 160-164 °C (decomp.); ^1H NMR (400 MHz, C_6D_6, 298 K): δ 1.13 (d, $^3J_{HH}$ = 6.9 Hz, 12 H, $(CH_3)_2CH$), 1.16 (d, $^3J_{HH}$ = 6.9 Hz, 12 H, $(CH_3)_2CH$), 1.21 (d, $^3J_{HH}$ = 6.9 Hz, 12 H, $(CH_3)_2CH$), 1.50 (d, $^3J_{HH}$ = 6.9 Hz, 12 H, $(CH_3)_2CH$), 2.46 (sept, $^3J_{HH}$ = 6.9 Hz, 4 H, $(CH_3)_2CH$), 3.82 (sept, $^3J_{HH}$ = 6.9 Hz, 4 H, $(CH_3)_2CH$), 6.16 (s, 2 H, NC*H*), 6.58 (s, 2 H, NC*H*), 7.10-7.32 (m, 12 H, Ar-*H*); $^{13}C\{^1H\}$ NMR (75.6 MHz, C_6D_6, 298 K): δ 23.1, 24.4, 25.0, 26.3 ($(CH_3)_2CH$), 27.7, 28.6 ($(CH_3)_2CH$), 121.3, 123.8 (*C*N), 121.9, 122.1, 123.9, 130.4, 134.1, 145.4, 145.9, 147.7 (Ar-*C*), 182.7 (br., CN_2); MS (EI 70eV), *m/z* (%): 898 (MH^+, 36), 451

(Ga{N(Ar)C(H)}$_2$H$^+$, 50), 390 (C{N(Ar)C(H)}$_2$H$^+$, 100), 378 ({N(Ar)C(H)}$_2$H$^+$, 27); IR ν/cm^{-1} (Nujol): 1662 m, 1574 m, 1405 m, 1322 m, 1262 m, 1060 m, 934 m, 802 m; EI acc. mass: on M$^+$: calc. for $C_{53}H_{72}N_4CuGa$: 896.4303, found 896.4323; $C_{53}H_{72}N_4CuGa$ requires C 70.85, H 8.08, N 6.23; found C 70.46, H 8.20, N 6.16.

Preparation of [(IPr)Ag{Ga{[N(Ar)C(H)]$_2$}}] 38: A solution of [K(tmeda)][:Ga{[N(Ar)C(H)]$_2$}] (0.25 g, 0.41 mmol) in THF (10 cm^3) was added to a suspension of [(IPr)AgCl] (0.22 g, 0.41 mmol) in THF (10 cm^3) at -78 °C to give a yellow solution. The reaction mixture was warmed to 20 °C and stirred overnight. Volatiles were then removed *in vacuo* and the residue was extracted into hexane (60 cm^3) and filtered. The filtrate was concentrated to *ca.* 20 cm^3 and stored at -30 °C overnight to give yellow blocks of **38** (0.27 g, 69 %). Mp 83-86 °C (decomp.); ^{1}H NMR (400 MHz, C_6D_6, 298 K): δ 1.24 (d, $^3J_{HH}$ = 6.9 Hz, 12 H, (C*H*$_3$)$_2$CH), 1.28 (d, $^3J_{HH}$ = 6.9 Hz, 12 H, (C*H*$_3$)$_2$CH), 1.37 (d, $^3J_{HH}$ = 6.9 Hz, 12 H, (C*H*$_3$)$_2$CH), 1.58 (d, $^3J_{HH}$ = 6.9 Hz, 12 H, (C*H*$_3$)$_2$CH), 2.52 (sept, $^3J_{HH}$ = 6.9 Hz, 4 H, (CH$_3$)$_2$C*H*), 3.96 (sept, $^3J_{HH}$ = 6.9 Hz, 4 H, (CH$_3$)$_2$C*H*), 6.37 (s, 2 H, NC*H*), 6.70 (s, 2 H, NC*H*), 7.18-7.47 (m, 12 H, Ar-*H*); ^{13}C{^{1}H} NMR (75.6 MHz, C_6D_6, 298 K): δ 23.4, 24.4, 24.7, 26.4 ((*C*H$_3$)$_2$CH), 27.6, 28.5 ((CH$_3$)$_2$*C*H), 121.5, 123.8 (*C*N), 122.2, 123.5, 123.9, 130.4, 134.4, 145.4, 145.8, 147.3 (Ar-*C*), *C*N$_2$ not observed; MS (EI 70eV), *m/z* (%): 941 (MH$^+$, 3), 390 (C{N(Ar)C(H)}$_2$H$^+$, 73); IR ν/cm^{-1} (Nujol): 1662 m, 1590 m, 1551 m, 1407 m, 1257 m, 1113 m, 801 m; EI acc. mass: on M$^+$: calc. for $C_{53}H_{72}N_4AgGa$: 940.4058, found 940.4061; $C_{53}H_{72}N_4AgGa$ requires C 67.52, H 7.70, N 5.94; found C 67.32, H 7.68, N 5.90.

Preparation of [(IPr)Au{Ga{[N(Ar)C(H)]$_2$}}] 39: A solution of [K(tmeda)][:Ga{[N(Ar)C(H)]$_2$}] (0.22 g, 0.37 mmol) in THF (10 cm^3) was added to a suspension

of [(IPr)AuCl] (0.23 g, 0.37 mmol) in THF (10 cm^3) at -78 °C to give a yellow solution. The reaction mixture was warmed to 20 °C and stirred overnight. Volatiles were then removed *in vacuo* and the residue was extracted into hexane (35 cm^3) and filtered. The filtrate was concentrated to *ca.* 10 cm^3 and stored at -30 °C overnight to give yellow blocks of **39** (0.22 g, 58 %). Mp 80-83 °C (decomp.); ^{1}H NMR (400 MHz, C_6D_6, 298 K): δ 0.98 (d, $^3J_{HH}$ = 6.9 Hz, 12 H, $(CH_3)_2CH$), 1.09 (d, $^3J_{HH}$ = 6.9 Hz, 12 H, $(CH_3)_2CH$), 1.12 (d, $^3J_{HH}$ = 6.9 Hz, 12 H, $(CH_3)_2CH$), 1.33 (d, $^3J_{HH}$ = 6.9 Hz, 12 H, $(CH_3)_2CH$), 2.32 (sept, $^3J_{HH}$ = 6.9 Hz, 4 H, $(CH_3)_2CH$), 3.66 (sept, $^3J_{HH}$ = 6.9 Hz, 4 H, $(CH_3)_2CH$), 6.09 (s, 2 H, NC*H*), 6.42 (s, 2 H, NC*H*), 6.95-7.18 (m, 12 H, Ar-*H*); $^{13}C\{^1H\}$ NMR (75.6 MHz, C_6D_6, 298 K): δ23.4, 24.2 24.5, 26.3 ($(CH_3)_2CH$), 27.7, 28.6 ($(CH_3)_2CH$), 120.8, 123.8 (*C*N), 122.2, 123.8, 124.1, 130.4, 133.9, 145.4, 146.0, 146.7 (Ar-*C*), 206.4 (CN_2); MS (EI 70eV), *m/z* (%): 1030 (MH^+, 8), 390 ($C\{N(Ar)C(H)\}_2H^+$, 78); IR ν/cm^{-1} (Nujol): 1670 m, 1589 m, 1572 m, 1413 m, 1261 m, 865 m; EI acc. mass: on M^+: calc. for $C_{53}H_{72}N_4AuGa$: 1030.4673, found 1030.4677; $C_{53}H_{72}N_4AuGa$ requires C 61.69, H 7.03, N 5.43; found C 61.37, H 7.05, N 5.49.

Preparation of $[(ICy_{Me})Cu\{Ga\{[N(Ar)C(H)]_2\}\}]$ 40: A solution of [K(tmeda)] $[:Ga\{[N(Ar)C(H)]_2\}]$ (0.25 g, 0.41 mmol) in THF (10 cm^3) was added to a suspension of $[(ICy_{Me})CuCl]$ (0.15 g, 0.41 mmol) in THF (10 cm^3) at -78 °C to give a yellow solution. The reaction mixture was warmed to 20 °C and stirred for 3 hours. Volatiles were then removed *in vacuo* and the residue was extracted into hexane (40 cm^3) and filtered. The filtrate was concentrated to *ca.* 15 cm^3 and stored at -30 °C overnight to give yellow blocks of **40** (0.13 g, 44 %). Mp 155-160 °C (decomp.); ^{1}H NMR (400 MHz, C_6D_6, 298 K): δ 1.11-2.36 (m, 20 H, CH_2), 1.48 (s, 6 H, Me), 1.56 (d, $^3J_{HH}$ = 6.9 Hz, 12 H, $(CH_3)_2CH$), 1.62 (d, $^3J_{HH}$ = 6.9 Hz, 12 H, $(CH_3)_2CH$), 3.39 (m, 2 H, CH_2CH), 4.08 (sept, $^3J_{HH}$ = 6.9 Hz, 4 H, $(CH_3)_2CH$), 6.71 (s, 2 H, NC*H*), 7.36 (t, $^3J_{HH}$ =

7.2 Hz, 2 H, *p*-Ar-*H*), 7.42 (d, $^3J_{HH}$ = 7.2 Hz, 4 H, *m*-Ar-*H*); $^{13}C\{^1H\}$ NMR (75.6 MHz, C_6D_6, 298 K): δ 8.1 (Me), 24.6, 28.0 (($CH_3)_2CH$), 26.2, 28.6, 36.7 (CH_2), 57.0 ((CH_2CH), 121.8, 124.1 (*C*N), 122.2 (*m*-Ar-*C*), 122.6 (*p*-Ar-*C*), 146.0 (*o*-Ar-*C*), 148.3 (*ipso*-Ar-*C*), 173.7 (br., CN_2); MS (EI 70eV), *m/z* (%): 768 (MH^+, 65), 445 ($Ga\{N(Ar)C(H)\}_2H^+$, 24), 378 ($\{N(Ar)C(H)\}_2H^+$, 100); IR ν/cm^{-1} (Nujol): 1643 m, 1585 m, 1548 m, 1260 m, 1098 m, 1057 m; EI acc. mass: on M^+: calc. for $C_{43}H_{64}N_4CuGa$: 768.3677, found 768.3682; $C_{43}H_{64}N_4CuGa$ requires C 67.05, H 8.37, N 7.27 %; found C 67.21, H 8.65, N 7.48.

Preparation of $[O\{HGa\{[N(Ar)C(H)]_2\}\}_2]^{2-}[K_2(OEt_2)_2]^{2+}$ 41: A solution of [K(tmeda)][:Ga{[N(Ar)C(H)]$_2$}] (0.21 g, 0.30 mmol) in THF (10 cm^3) was added to a suspension of [(IMes)AuCl] (0.19 g, 0.35 mmol) at -78 °C. The reaction mixture was warmed to 20 °C and stirred for 3 hours. Volatiles were then removed *in vacuo*, and the residue was extracted into hexane (30 cm^3) and diethyl ether (20 cm^3) and filtered. The diethyl ether filtrate was concentrated to *ca.* 5 cm^3 and stored at -30 °C overnight to give colourless blocks of **41** (0.02 g, 6 %). Mp 71 °C (decomp.); ^1H NMR (400 MHz, C_6D_6, 298 K): δ 1.05 (d, $^3J_{HH}$ = 6.9 Hz, 12 H, ($CH_3)_2CH$), 1.12, (t, $^3J_{HH}$ = 7.0 Hz, 12 H, CH_3CH_2), 1.21 (d, $^3J_{HH}$ = 6.9 Hz, 12 H, ($CH_3)_2CH$), 1.47 (d, $^3J_{HH}$ = 6.9 Hz, 12 H, ($CH_3)_2CH$), 1.53 (d, $^3J_{HH}$ = 6.9 Hz, 12 H, ($CH_3)_2CH$), 2.20 (s, 2 H, Ga*H*), 2.80 (sept, $^3J_{HH}$ = 6.9 Hz, 4 H, ($CH_3)_2CH$), 3.25 (q, $^3J_{HH}$ = 7.0 Hz, 8 H, CH_2), 3.86 (sept, $^3J_{HH}$ = 6.9 Hz, 4 H, ($CH_3)_2CH$), 5.45 (s, 4 H, NC*H*), 7.09 (d, $^3J_{HH}$ = 7.5 Hz, 8 H, *m*-Ar-*H*), 7.20 (t, $^3J_{HH}$ = 7.5 Hz, 4 H, *p*-Ar-*H*); $^{13}C\{^1H\}$ NMR (75.6 MHz, C_6D_6, 298 K): δ 15.3 (CH_3CH_2), 22.3, 23.9, 24.2, 24.6, 26.0 (($CH_3)_2CH$), 27.6, 28.0, 28.7 (($CH_3)_2CH$), 65.6 (CH_2), 122.2 (*C*N), 123.6 (*m*-Ar-*C*), 123.7 (*p*-Ar-*C*), 124.3 (*o*-Ar-*C*), 149.2 (*ipso*-Ar-*C*); MS (EI 70eV), *m/z* (%): 378 ($\{N(Ar)C(H)\}_2H^+$, 13), 333 ($\{N(Ar)C(H)\}_2H^+$ -Pr^i,

100); IR ν/cm^{-1} (Nujol): 1855 m (GaH), 1608 s, 1586 s, 1323 s, 1259 s, 1206 m, 1102 s, 931 m, 851 s, 802 s.

Preparation of [Au(IPr)$_2$][Ga{[N(Ar)C(H)]$_2$}$_2$] 42: A solution of [(IPr)Au-{Ga{[N(Ar)C(H)]$_2$}}] (0.05 g, 0.06 mmol) in hexane (5 cm^3) was stored at room temperature for two weeks. Concentration to *ca.* 2 cm^3 and overnight storage at -25 °C gave colourless blocks of **42** (*ca.* 0.01 g). Following an X-ray crystallographic analysis, no other data could be obtained.

Preparation of [(IPr)Au{η^1-N(Ar)COCH$_2$NH(Ar)}] 43: A solution of [(IPr)Au{Ga{[N(Ar)C(H)]$_2$}}] (0.18 g, 0.17 mmol) in toluene (10 cm^3) was exposed to air briefly. The solution was concentrated to *ca.* 2 cm^3 and stored at -30 °C overnight to give colourless blocks of **43** (0.01 g, 6 %). Mp 171 °C; ^{1}H NMR (400 MHz, C_6D_6, 298 K): δ 0.90 (d, $^3J_{HH}$ = 6.9 Hz, 12 H, (C*H*$_3$)$_2$CH), 1.02 (d, $^3J_{HH}$ = 6.9 Hz, 6 H, (C*H*$_3$)$_2$CH), 1.06 (d, $^3J_{HH}$ = 6.9 Hz, 12 H, (C*H*$_3$)$_2$CH), 1.13 (d, $^3J_{HH}$ = 6.9 Hz, 6 H, (C*H*$_3$)$_2$CH), 1.19 (d, $^3J_{HH}$ = 6.9 Hz, 6 H, (C*H*$_3$)$_2$CH), 1.43 (d, $^3J_{HH}$ = 6.9 Hz, 6 H, (C*H*$_3$)$_2$CH), 2.05 (s, 2 H, C*H*$_2$), 2.38 (sept, $^3J_{HH}$ = 6.9 Hz, 2 H, (CH$_3$)$_2$C*H*), 2.53 (sept, $^3J_{HH}$ = 6.9 Hz, 2 H, (CH$_3$)$_2$C*H*), 2.55 (sept, $^3J_{HH}$ = 6.9 Hz, 4 H, (CH$_3$)$_2$C*H*), 6.15 (s, 2 H, NC*H*), 6.83-7.21 (m, 12 H, Ar-*H*), 8.11 (s, 1 H, N*H*); MS (EI 70eV), *m/z* (%): 978 (MH$^+$, 4), 585 (AuC{N(Ar)C(H)}$_2$H$^+$, 49), 390 (C{N(Ar)C(H)}$_2$H$^+$, 26); IR ν/cm^{-1} (Nujol): 3067 m (NH), 1605 s (C=O), 1580 m, 1551 m, 1256 m, 1117 m, 801 m; EI acc. mass: on M$^+$: calc. for $C_{53}H_{73}N_4OAu$: 978.5444, found 978.5446.

Preparation of [(IPr)Cu(η^1-C≡CPh)] 44: Phenylacetylene (13 µl, 0.12 mmol) was added to a solution of [(IPr)Cu{Ga{[N(Ar)C(H)]$_2$}}] (0.10 g, 0.11 mmol) in toluene (10 cm^3) *via* a microsyringe at -78 °C to give a yellow solution. The reaction mixture was

warmed to 20 °C and stirred overnight. All volatiles were then removed *in vacuo*, and the residue was washed with hexane (20 cm^3) and extracted into toluene (20 cm^3) and filtered. The filtrate was concentrated to *ca.* 5 cm^3 and stored at -30 °C overnight to give colourless blocks of **44** (0.01 g, 17 %). Mp 181-182 °C; ^{1}H NMR (400 MHz, C_6D_6, 298 K): δ 0.95 (d, $^3J_{HH}$ = 6.9 Hz, 12 H, $(CH_3)_2CH$), 1.29 (d, $^3J_{HH}$ = 6.9 Hz, 12 H, $(CH_3)_2CH$), 2.44 (sept, $^3J_{HH}$ = 6.9 Hz, 4 H, $(CH_3)_2CH$), 6.07 (s, 2 H, NC*H*), 6.69-7.32 (m, 11H, Ar-*H*); ^{13}C{^{1}H} NMR (75.6 MHz, C_6D_6, 298 K): δ 23.4, 25.0 ($(CH_3)_2CH$), 28.7 ($(CH_3)_2CH$), 104.8 (C≡*C*Ph) 122.3 (*C*N), 124.0, 124.6, 125.0, 128.1 (Ar-*C*), 129.1 (*C*≡CPh), 130.4, 132.0, 134.6, 145.4 (Ar-*C*), 183.7 (CN_2); MS (EI 70eV), *m/z* (%): 552 (MH^+, 6), 390 ($C\{N(Ar)C(H)\}_2H^+$, 100); IR ν/cm^{-1} (Nujol): 2090 s (C≡C), 1650 m, 1595 m, 1329 m, 1260 m, 1102 m, 1026 m, 804 m; EI acc. mass: on M^+: calc. for $C_{35}H_{41}N_2Cu$: 552.2560, found 552.2550.

Preparation of [(IPr)(Bu^{t}NC)Cu{Ga{[N(Ar)C(H)]$_2$}}] 45: *tert*-butylisocyanide (100 µl, 0.88 mmol) was added to a solution of [(IPr)Cu{Ga{[N(Ar)C(H)]$_2$}}] (0.15 g, 0.17 mmol) in hexane (20 cm^3) *via* a microsyringe at -78 °C to give an orange solution. The reaction mixture was warmed to 20 °C, stirred for 3 hours and filtered. The filtrate was then concentrated to *ca.* 15 cm^3 and stored at -30 °C overnight to give orange blocks of **45** (0.02 g, 13 %). Mp 45 °C (decomp.); ^{1}H NMR (400 MHz, C_6D_6, 298 K): δ 0.76 (s, 9 H, $(CH_3)_3C$), 1.04 (d, $^3J_{HH}$ = 6.9 Hz, 12 H, $(CH_3)_2CH$), 1.18 (d, $^3J_{HH}$ = 6.9 Hz, 12 H, $(CH_3)_2CH$), 1.40 (d, $^3J_{HH}$ = 6.9 Hz, 12 H, $(CH_3)_2CH$), 1.46 (d, $^3J_{HH}$ = 6.9 Hz, 12 H, $(CH_3)_2CH$), 2.83 (sept, $^3J_{HH}$ = 6.9 Hz, 4 H, $(CH_3)_2CH$), 4.15 (sept, $^3J_{HH}$ = 6.9 Hz, 4 H, $(CH_3)_2CH$), 6.48 (s, 2 H, NC*H*), 6.52 (s, 2 H, NC*H*), 6.90-7.18 (m, 10 H, Ar-*H*); ^{13}C{^{1}H} NMR (75.6 MHz, C_6D_6, 298 K): δ 14.0 ($(CH_3)_3C$), 24.0, 24.5, 24.7, 26.5 ($(CH_3)_2CH$), 27.9, 28.5 ($(CH_3)_2CH$), 31.7 ($(CH_3)_3C$), 54.8 (*C*NBu^t), 121.3 (*C*N), 122.3, 122.6 (Ar-*C*), 123.4 (*C*N), 124.2, 134.0, 138.7, 145.5, 145.8, 150.2 (Ar-*C*), 188.7 (CN_2);

MS (EI 70eV), *m/z* (%): 981 (MH^+, 3), 450 ($Ga\{N(Ar)C(H)\}_2H^+$, 4), 390 ($C\{N(Ar)C(H)\}_2H^+$, 100), 378 ($\{N(Ar)C(H)\}_2H^+$, 6), 333 ($\{N(Ar)C(H)\}_2H^+$ -Pr^i, 23); IR ν/cm^{-1} (Nujol): 2148 s (C≡N), 1661 m, 1587 m, 1560 m, 1257 m, 935 m, 872 m, 802 m.

Preparation of [(IPr)Cu(η^1-$CO_2C_2N_2Ar_2$)] 46: A solution of [(IPr)Cu-{Ga{[N(Ar)C(H)]$_2$}}] (0.13 g, 0.15 mmol) in toluene (10 cm^3) was bubbled with CO_2 (g) for 5 minutes and the flask sealed and stirred overnight. All volatiles were removed *in vacuo*, and the residue was extracted into hexane (20 cm^3) and filtered. The filtrate was concentrated to *ca.* 10 cm^3 and stored at -30 °C overnight to give colourless blocks of **46** (0.02 g, 16 %). Mp 187 °C (decomp.); ^{1}H NMR (400 MHz, C_6D_6, 298 K): δ 0.80-1.25 (overlapping d, 48 H, $(CH_3)_2CH$), 2.33 (sept, $^3J_{HH}$ = 6.9 Hz, 4 H, $(CH_3)_2CH$), 3.34 (sept, $^3J_{HH}$ = 6.9 Hz, 2 H, $(CH_3)_2CH$), 3.52 (sept, $^3J_{HH}$ = 6.9 Hz, 2 H, $(CH_3)_2CH$), 6.10 (s, 2 H, NC*H*), 6.35 (s, 1 H, NC*H*), 6.81-7.12 (m, 12 H, Ar-*H*), 9.10 (br., 2H, NH); MS (EI 70eV), *m/z* (%): 874 (MH^+, 7), 378 ($\{N(Ar)C(H)\}_2H^+$, 68), 333 ($\{N(Ar)C(H)\}_2H^+$ -Pr^i, 77); IR ν/cm^{-1} (Nujol): NH, CO not observed, 1260 m, 1093 m, 1019 m, 801 m.

Preparation of [(IPr)Cu(η^2-$CS_2C_2N_2Ar_2$)] 47: Carbon disulphide (111 μl, 0.18 mmol, 1.66 M in toluene) was added to a solution of [(IPr)Cu{Ga{[N(Ar)C(H)]$_2$}}] (0.15 g, 0.17 mmol) in toluene (10 cm^3) at -78 °C *via* a microsyringe to give a deep red reaction mixture. The reaction mixture was warmed to 20 °C and allowed to stir for 3 hours. All volatiles were then removed *in vacuo*, and the residue was extracted into hexane (20 cm^3) and filtered. The filtrate was concentrated to *ca.* 5 cm^3 and stored at -30 °C overnight to give red blocks of **47** (0.01 g, 7 %). Mp 101 °C (decomp.); ^{1}H NMR (400 MHz, C_6D_6, 298 K): δ 1.12 (d, $^3J_{HH}$ = 6.7 Hz, 24 H, $(CH_3)_2CH$), 1.23 (d, $^3J_{HH}$ = 6.9 Hz, 12 H, $(CH_3)_2CH$), 1.62 (d, $^3J_{HH}$ = 6.9 Hz, 12 H, $(CH_3)_2CH$), 2.89 (sept, $^3J_{HH}$ = 6.9 Hz, 4

H, $(CH_3)_2CH$), 3.33 (sept, $^3J_{HH}$ = 6.7 Hz, 2 H, $(CH_3)_2CH$), 3.38 (sept, $^3J_{HH}$ = 6.7 Hz, 2 H, $(CH_3)_2CH$), 6.38 (s, 1 H, NC*H*), 6.35 (s, 2 H, NC*H*), 7.03-7.46 (m, 12 H, Ar-*H*); MS (EI 70eV), *m/z* (%): 421 ($\{N(Ar)C(H)\}_2CSH^+$, 32), 390 ($C\{N(Ar)C(H)\}_2H^+$, 85), 378 ($\{N(Ar)C(H)\}_2H^+$, 68); IR ν/cm^{-1} (Nujol): 1607 m (CS), 1413 m, 1261 m, 1099 s, 1020 s, 801 s.

3.6 References

1. R. J. Baker, R. D. Farley, C. Jones, M. Kloth and D. M. Murphy, *Dalton Trans.*, 2002, 3844.
2. (a) C. Jones, D. P. Mills, J. A. Platts, R. P. Rose, *Inorg. Chem.*, 2006, **45**, 3146; (b) R. J. Baker, C. Jones, M. Kloth, J. A. Platts, *Angew. Chem. Int. Ed.*, 2003, **42**, 2660; (c) R. J. Baker, C. Jones, M. Kloth, J. A. Platts, *Organometallics*, 2004, **23**, 4811; (d) C. Jones, D. P. Mills, R. P. Rose, *J. Organomet. Chem.*, 2006, **691**, 3060; (e) S. P. Green, C. Jones, K. –A. Lippert, D. P. Mills, A. Stasch, *Inorg. Chem.*, 2006, **45**, 7242; (f) R. J. Baker, C. Jones, D. P. Mills, D. M. Murphy, E. Hey-Hawkins, R. Wolf, *Dalton Trans.*, 2006, 64; (g) R. J. Baker, C. Jones, M. Kloth, *Dalton Trans.*, 2005, 2106.
3. R. J. Baker, C. Jones, J. A. Platts, *J. Am. Chem. Soc.*, 2003, **125**, 10534.
4. R. J. Baker, C. Jones, *Coord. Chem. Rev.*, 2005, **249**, 1857, and references therein.
5. R. J. Baker, C. Jones, D. M. Murphy, *Chem. Commun.*, 2005, 1339.
6. S. Aldridge, R. J. Baker, N. D. Coombs, C. Jones, R. P. Rose, A. Rossin, D. J. Willock, *Dalton Trans.*, 2006, 3313.

7. (a) C. D. Abernethy, A. H. Cowley, R. A. Jones, C. L. B. McDonald, P. Shulka, L. K. Thompson, *Organometallics*, 2001, **20**, 3629; (b) C. D. Abernethy, J. A. C. Clyburne, A. H. Cowley, R. A. Jones, *J. Am. Chem. Soc.*, 1999, **121**, 2329.

8. T. Pott, P. Jutzi, W. W. Schoeller, A. Stammler, H. –G. Stammler, *Organometallics*, 2001, **20**, 5492.

9. J. F. Hartwig, X. He, *Organometallics*, 1996, **15**, 5350.

10. For examples, see: (a) E. Fooladi, B. Dalhus, M. Tilset, *Dalton Trans.*, 2004, 3909; (b) P. Buchgraber, L. Toupet, V. Guerchais, *Organometallics*, 2003, **22**, 5144; (c) V. K. Dioumaev, D. J. Szalda, J. Hanson, J. A. Franz, R. M. Bullock, *Chem. Commun.*, 2003, 1670; (d) R. W. Simms, M. J. Drewitt, M. C. Baird, *Organometallics*, 2002, **21**, 2958.

11. R. J. Baker, C. Jones, J. A. Platts, *Dalton Trans.*, 2003, 3673.

12. R. J. Baker, R. D. Farley, C. Jones, M. Kloth, D. P. Mills, D. M. Murphy, *Chem. Eur. J.*, 2005, **11**, 2972.

13. C. Jones, R. P. Rose, A. Stasch, *Dalton Trans.*, 2007, 2997.

14. R. P. Rose, *PhD Thesis*, University of Wales, Cardiff, 2006.

15. P. L. Arnold, S. T. Liddle, J. McMaster, C. Jones, D. P. Mills, *J. Am. Chem. Soc.*, 2007, **129**, 5360.

16. P. L. Arnold, S. T. Liddle, *Chem. Commun.*, 2005, 5638.

17. M. T. Gamer, P. W. Roesky, S. N. Konchenko, P. Nava, R. Aldrichs, *Angew. Chem. Int. Ed.*, 2006, **45**, 4447.

18. J. Emsley, *The Elements*, 3rd Edition, New York, Oxford University Press, 1998.

19. (a) H. Braunschweig, C. Kollann, D. Rais, *Angew. Chem. Int. Ed.*, 2006, **45**, 5254; (b) S. Aldridge, D. L. Coombs, *Coord. Chem. Rev.*, 2004, **248**, 535; (c) H. Braunschweig, M. Colling, *Coord. Chem. Rev.*, 2001, **223**, 1; (d) T. Ishiyama, N. Miyaura, *J. Organomet. Chem.*, 2000, **611**, 392; (e) T. B. Marder, N. C.

Norman, *Top. Catal.*, 1998, **5**, 63; (f) G. J. Irvine, M. J. G. Lesley, T. B. Marder, N. C. Norman, C. R. Rice, E. G. Robins, W. R. Roper, G. R. Whittell, L. J. Wright, *Chem. Rev.*, 1998, **98**, 2685; (g) H. Braunschweig, *Angew. Chem. Int. Ed.*, 1998, **37**, 1786, and references therein.

20. (a) D. S. Laitar, P. Müller, J. P. Sadighi, *J. Am. Chem. Soc.*, 2005, **127**, 17196; (b) See also: H. Zhao, Z. Lin, T. B. Marder, *J. Am. Chem. Soc.*, 2006, **128**, 15637.

21. (a) D. S. Laitar, E. Y. Tsui, J. P. Sadighi, *Organometallics*, 2006, **25**, 2405; (b) D. S. Laitar, E. Y. Tsui, J. P. Sadighi, *J. Am. Chem. Soc.*, 2006, **128**, 11036; (c) See also: L. Dang, H. Zhao, Z. Lin, T. B. Marder, *Organometallics*, 2007, **26**, 2824.

22. Y. Segawa, M. Yamashita, K. Nozaki, *Angew. Chem. Int. Ed.*, 2007, **46**, 6710.

23. M. H. Voges, C. Rømming, M. Tilset, *Organometallics*, 1999, **18**, 529.

24. (a) D. F. Evans, *J. Chem. Soc.*, 1959, 2003; (b) S. K. Sur, *J. Magn. Reson.*, 1989, 169; (c) D. H. Grant, *J. Chem. Educ.*, 1995, 39.

25. (a) For examples, see: (a) M. D. Fryzuk, D. B. Leznoff, S. J. Rettig, *Organometallics*, 1995, **14**, 5193; (b) G. Bhandari, Y. Kim, J. M. MacFarland, A. L. Rheingold, K. H. Theopold, *Organometallics*, 1995, **14**, 738; (c) R. A. Heintz, R. L. Ostrander, A. L. Rheingold, K. H. Theopold, *J. Am. Chem. Soc.*, 1994, **116**, 11387; (d) B. J. Thomas, S. K. Noh, G. K. Schulte, S. C. Sendlinger, K. H. Theopold, *J. Am. Chem. Soc.*, 1991, **113**, 893; (e) M. H. Chisholm, F. A. Cotton, M. W. Extine, D. C. Rideout, *Inorg. Chem.*, 1979, **18**, 120.

26. CSD version 5.28, November 2006, update 2 (May 2007); F. H. Allen, *Acta Cryst.*, 2002, **B58**, 380.

27. A. Kempter, C. Gemel, N. J. Hardman, R. A. Fischer, *Inorg. Chem.*, 2006, **45**, 3133.

28. M. D. Fryzuk, L. Huang, N. T. McManus, P. Paglia, S. J. Rettig, G. S. White, *Organometallics*, 1992, **11**, 2979.

29. S. Diez-González, S. P. Nolan, *Coord. Chem. Rev.*, 2007, **251**, 874.

30. S. Okamoto, S. Tominaga, N. Saino, K. Kase, K. Shimoda, *J. Organomet. Chem.*, 2005, **690**, 6001.

31. P. De Frémont, N. M. Scott, E. D. Stevens, S. P. Nolan, *Organometallics*, 2005, **24**, 2411.

32. (a) D. Bourissou, O. Guerret, F. P. Gabbai, G. Bertrand, *Chem. Rev.*, 2000, **100**, 39; (b) W. Kirmse, *Eur. J. Org. Chem.*, 2005, 237; (c) W. A. Herrmann, *Angew. Chem. Int. Ed.*, 2002, **41**, 1290; (d) C. M. Crudden, D. P. Allen, *Coord. Chem. Rev.*, 2004, **248**, 2247; (e) N. Kuhn, A. Al-Sheikh, *Coord. Chem. Rev.*, 2005, **249**, 829; (f) C. J. Carmalt, A. H. Cowley, *Adv. Inorg. Chem.*, 2000, **50**, 1, and references therein.

33. A. Bayler, A. Schier, G. A. Bowmaker, H. Schmidbaur, *J. Am. Chem. Soc.*, 1996, **118**, 7006.

34. T. Ramnial, C. D. Abernethy, M. D. Spicer, I. D. McKenzie, I. D. Gay, J. A. C. Clyburne, *Inorg. Chem.*, 2003, **42**, 1391.

35. S. Diez-González, N. M. Scott, S. P. Nolan, *Organometallics*, 2006, **25**, 2355.

36. X. –Y. Yu, B. O. Patrick, B. R. James, *Organometallics*, 2006, **25**, 2359.

37. M. V. Baker, P. J. Barnard, S. J. Berners-Price, S. K. Brayshaw, J. L. Hickey, B. W. Skelton, A. H. White, *Dalton Trans.*, 2006, 3708.

38. P. de Frémont, E. D. Stevens, M. R. Fructos, M. M. Díaz-Requejo, P. J. Pérez, S. P. Nolan, *Chem. Commun.*, 2006, 2045.

39. R. T. Baker, J. C. Calabrese, S. A. Westcott, P. Nguyen, T. B. Marder, *J. Am. Chem. Soc.*, 1993, **115**, 4367.

40. L. A. Goj, E. D. Blue, C. Munro-Leighton, T. B. Gunnoe, J. L. Petersen, *Inorg. Chem.*, 2005, **44**, 8647.

41. C. Nolte, P. Mayer, B. F. Straub, *Angew. Chem. Int. Ed.*, 2007, **46**, 2101.

42. L. A. Goj, E. D. Blue, S. A. Delp, T. B. Gunnoe, T. R. Cundari, A. W. Pierpont, J. L. Petersen, P. D. Boyle, *Inorg. Chem.*, 2006, **45**, 9032.

43. L. Zhou, D. Powell, K. M. Nicholas, *Inorg. Chem.*, 2007, **46**, 2316.

44. S. P. Green, C. Jones, D. P. Mills, A. Stasch, *Organometallics*, 2007, **26**, 3424.

45. L. D. Vasquez-Serrano, B. T. Owens, J. M. Buriak, *Chem. Commun.*, 2002, 2518.

46. (a) N. P. Mankad, T. G. Gray, D. S. Laitar, J. P. Sadighi, *Organometallics*, 2004, **23**, 1191; (b) H. Kaur, F. K. Zinn, E. D. Stevens, S. P. Nolan, *ibid.*, 1157.

47. P. de Frémont, N. M. Scott, E. D. Stevens, T. Ramnial, O. C. Lightbody, C. L. B. Macdonald, J. A. C. Clyburne, C. D. Abernethy, S. P. Nolan, *Organometallics*, 2005, **24**, 6301.

Chapter 4

The Preparation of Novel Group 10 Metal Gallyl Complexes

4.1 Introduction

Investigations into the *s*-, *p*-, *d*- and *f*-block chemistry of the anionic gallium(I) *N*-heterocyclic carbene (NHC) analogue, $[:Ga\{[N(Ar)C(H)]_2\}]^-$ **1** (Ar = $C_6H_3Pr^i_2$-2,6), have been frequent[1] since the synthesis of this heterocycle was first reported.[2] It is thought that transition metal complexes of **1** could exhibit similar properties to the extensively studied transition metal complexes of cyclic boryls.[3] Investigations into these complexes has been driven by their use as catalysts for a number of synthetic transformations. Transition metal complexes of cyclic boryls have been utilised for, or suggested as intermediates in, the catalytic borylation or hydroboration of unsaturated compounds, and the C—H activation of alkanes, arenes and heteroarenes. Of relevance to this study, the platinum complexes, *cis*-$[(PPh_3)_2Pt\{B(cat)\}_2]$ (cat = $C_6H_4O_2$-1,2) **2a**[4] and *cis*-$[(PPh_3)_2Pt\{B(pin)\}_2]$ (pin = $Me_4C_2O_2$) **2b**[5] (Figure 1), have proved to be effective in the catalytic diboration of alkynes and 1,3-diynes.

A catalytic cycle was proposed for the diboration of alkynes in an attempt to explain the effectiveness of **2a-b** in mediating these reactions (Scheme 1).[4b] The initial step of the cycle involves the dissociation of phosphine, hence **2a-b** are effective catalyst systems as they contain relatively weak σ-donating, monodentate phosphines. The vacant coordination site may then be occupied by the alkyne substrate, followed by insertion of the alkyne into the Pt—B bond. This is made possible by the strong *trans*-influence and *cis*-configuration of the boryl ligands. However, this system does not mediate the diboration of alkenes. The diboration of alkenes is realised by the

replacement of phosphines with diolefin ligands, such as in the complex [(η^4-COD)Pt{B(cat)}$_2$] **3** (COD = 1,5-cyclooctadiene),[6] removing the requirement for phosphine dissociation in the catalytic cycle.

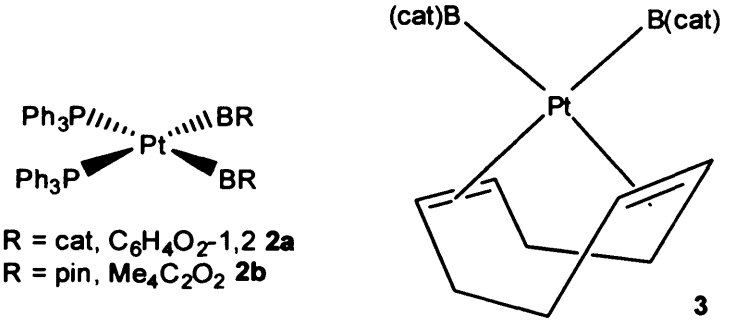

Figure 1 – The platinum diboryl complexes, **2a-b** and **3**

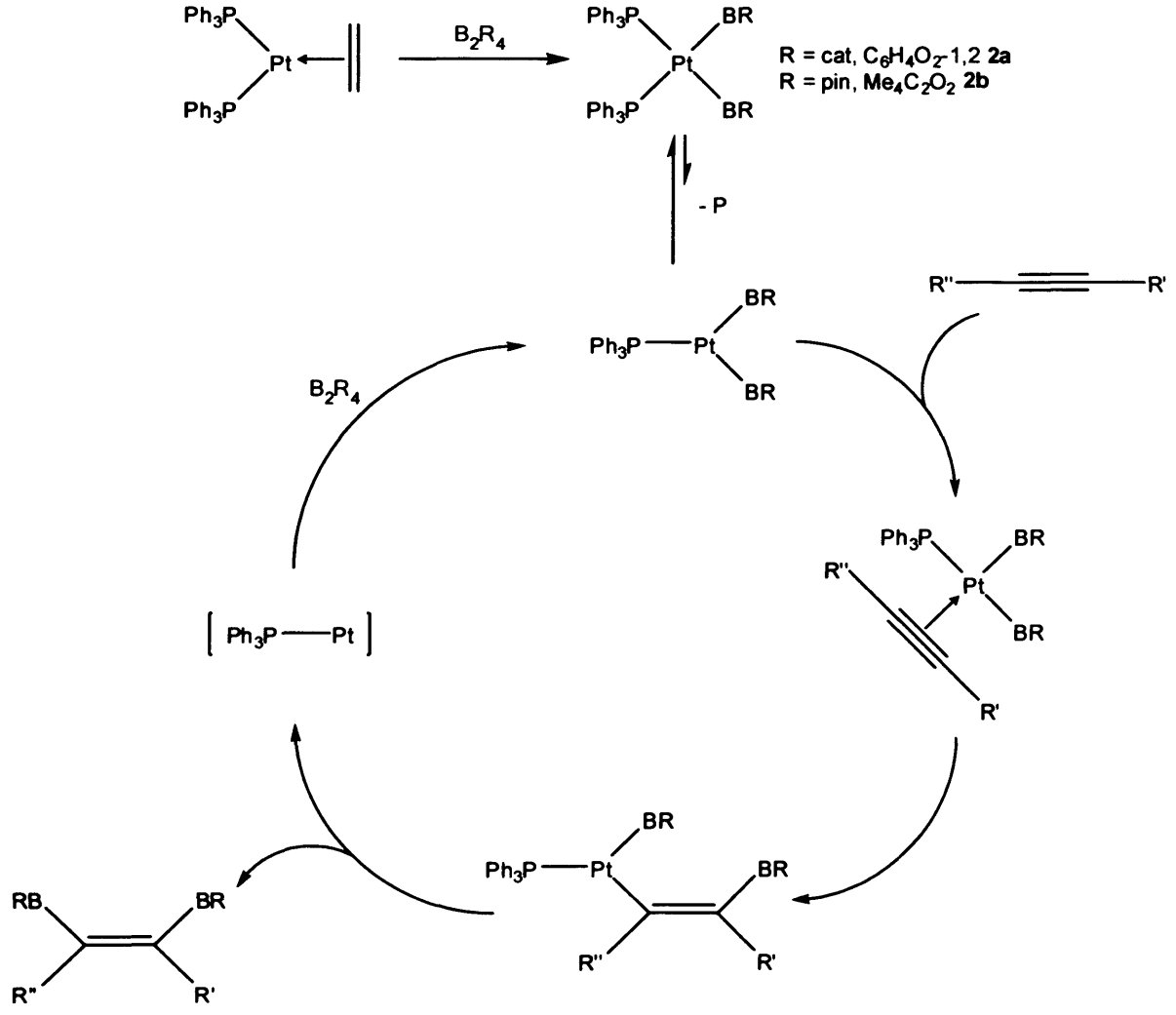

Scheme 1 – A proposed catalytic cycle for the diboration of alkynes mediated by **2a-b**

4.2 Research Proposal

The transition metal chemistry of the anionic gallium(I) heterocycle, **1**, is not as well developed as the main group chemistry of this heterocycle. Previous studies have suggested that neutral transition metal gallyl complexes, $[L_nM\{Ga\{[N(Ar)C(H)]_2\}\}_m]$, may have parallels with the wide variety of known catalytically active transition metal-cyclic boryl complexes.[7] These studies revealed that coordination of an NHC to metal halides allowed salt metathesis reactions with [K(tmeda)][**1**] to proceed without undesired redox processes. It was decided that other potentially stabilising ligands should be investigated for their ability to prevent redox activity between the metal centre and **1**, such as phosphines and chelating ligands. The preparation of complexes of **1** analogous to the catalytic cyclic boryl platinum complexes, **2a-b** and **3**, were deemed desirable synthetic targets. A study was proposed to prepare a series of group 10 metal complexes of **1**, incorporating phosphine and olefin ligands, and to investigate the reactivity of these complexes towards unsaturated organic substrates. This work is a continuation of the initial studies described in Chapter 3.

4.3 Results and Discussion

4.3.1 The Preparation of Metal Gallyl Complexes with Monodentate Phosphines

The 2 : 1 reaction of [K(tmeda)][**1**] with *cis*-$[(PPh_3)_2Pt(\eta^2\text{-}C_2H_4)]$ and the 1 : 1 reaction of [K(tmeda)][**1**] with $[Pd(PPh_3)_4]$ gave only intractable mixtures of products. Following the success of salt metathesis methods in the synthesis of NHC-coordinated transition metal complexes of **1**,[7] the 2 : 1 reactions of [K(tmeda)][**1**] with *cis*-$[(PPh_3)_2MCl_2]$ (M = Pd, Pt) were alternatively performed. Only one signal was

observed in the $^{31}P\{^{1}H\}$ NMR spectra of each reaction mixture after 1 hour. These signals correspond to the homoleptic metal(0) phosphine complexes, $[M(PPh_3)_3]$ (M = Pd,[8] Pt[9]) (Scheme 2). Subsequent work-up afforded the known paramagnetic gallium(II) dimer, $[ClGa\{[N(Ar)C(H)]_2^{\cdot}\}]_2$ **4**.[10] It is evident that triphenylphosphine (PPh_3) is not a strong enough σ-donor to stabilise the group 10 metal centre and circumvent the undesired reduction of the metal centre by the gallium(I) heterocycle. The strongly reducing ligand, **1**, most likely inserts into the M—Cl bond and subsequent reductive elimination occurs to yield **4**.

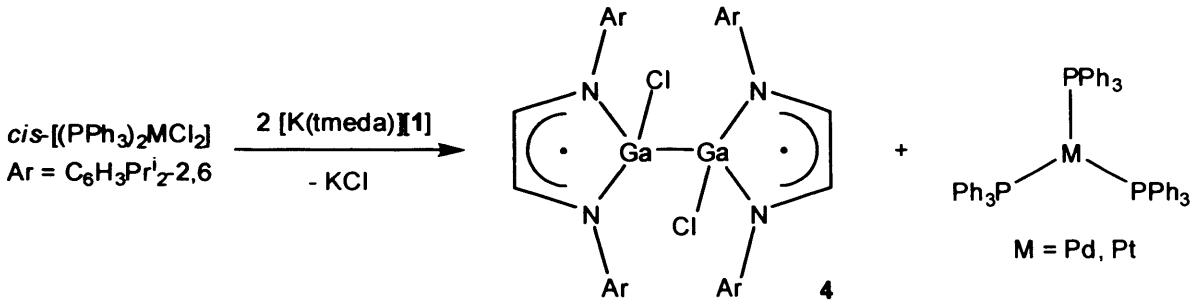

Scheme 2 – The 2 : 1 reactions of [K(tmeda)][**1**] with *cis*-$[(PPh_3)_2MCl_2]$

To test this theory, the 2 : 1 reactions of [K(tmeda)][**1**] with *trans*-$[(PEt_3)_2MCl_2]$ (M = Ni, Pd) and *cis*-$[(PEt_3)_2PtCl_2]$ were carried out, employing the more strongly σ-donating ligand, triethylphosphine (PEt_3) (Scheme 3). The reactions were followed by $^{31}P\{^{1}H\}$ NMR spectroscopy and at completion the resulting square planar bis-gallyl complexes, **5** – **7** (M = Ni, Pd, Pt), were isolated, by the elimination of two equivalents of KCl. Work-up of the reaction mixture of **7** afforded a few crystals of **8**, which exhibits a *cis*-configuration of ligands. The 1 : 1 reactions of [K(tmeda)][**1**] with *trans*-$[(PEt_3)_2MCl_2]$ (M = Ni, Pd) and *cis*-$[(PEt_3)_2PtCl_2]$ were then performed, yielding the monosubstituted products, **9** (M = Ni), and **10** (M = Pd) (Scheme 3). Only a few crystals of **10** could be isolated, which is not surprising as the reaction mixture $^{31}P\{^{1}H\}$ NMR spectra showed that the 2 : 1 product, **6**, predominates in it. The corresponding platinum analogue could not be isolated. Complex **7** can also be synthesised in poor

yield (29 %) by refluxing the gallium(II) dimer, $[Ga\{[N(Ar)C(H)]_2\}]_2$ **11**, formed from the oxidative coupling of **1**,[1,11] with $[(PEt_3)_2Pt(\eta^2\text{-}C_2H_4)]$ (Scheme 4). This reaction is proposed to proceed by the initial dissociation of ethylene and the oxidative insertion of Pt(0) into the Ga—Ga bond. The preparation of **7** by this method is similar to the synthesis of the bis-boryl complex, **2a**, which was prepared by the formal oxidative addition of $[B_2(cat)_2]$ to the olefin platinum(0) complex, *cis*-$[(PPh_3)_2Pt(\eta^2\text{-}C_2H_4)]$, with the loss of ethylene.[4] In contrast, **2b** was synthesised by the reaction of a large excess of $[B_2(pin)_2]$ with $[Pt(PPh_3)_4]$ at elevated temperature.[5]

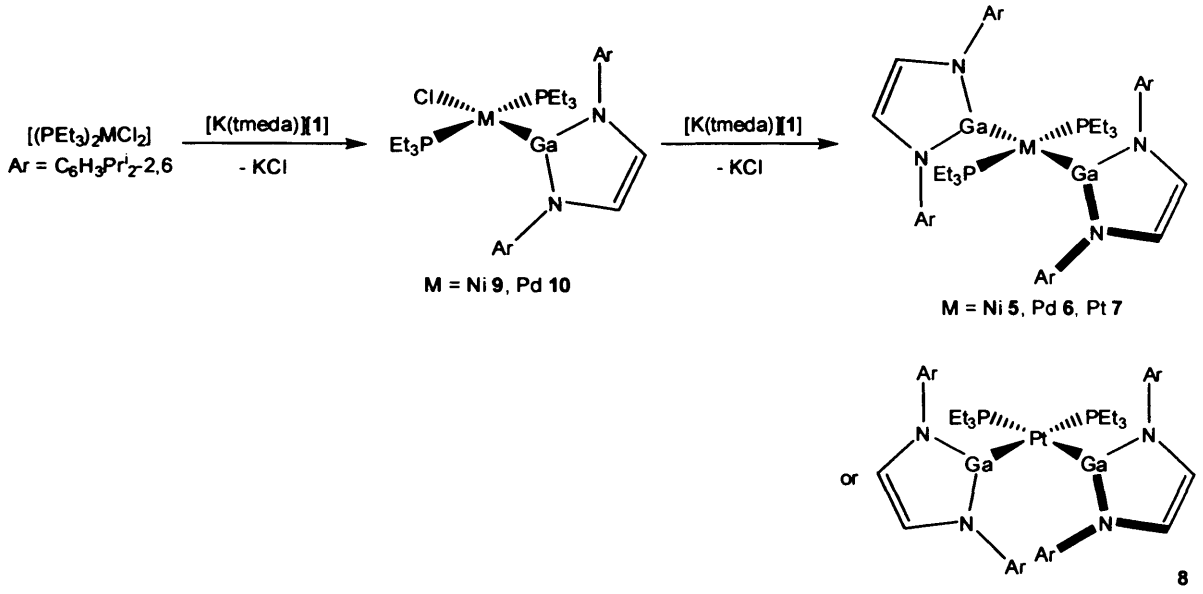

Scheme 3 – The synthesis of **5 – 10**

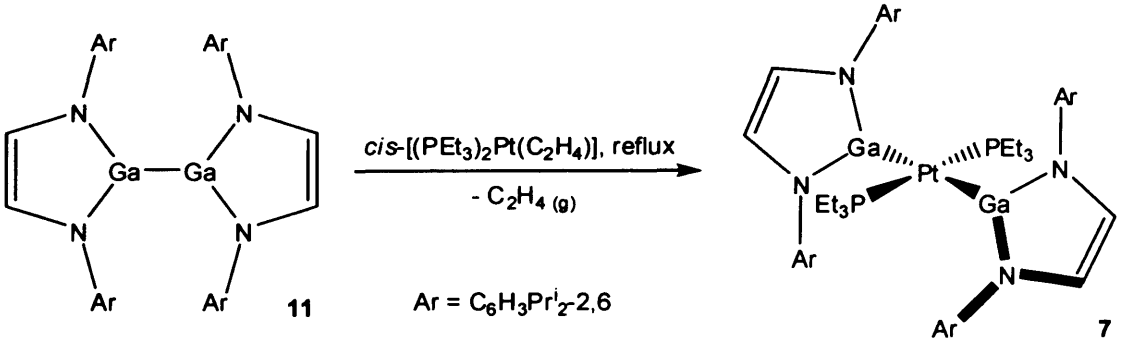

Scheme 4 – An alternative synthesis of **7**

Complexes **5** – **7** and **9** were fully characterised and all were found to be thermally robust. It was not possible to obtain more than a trace amount of the *cis*-

(bis)gallyl complex, **8**, and the monosubstituted complex, **10**, so these products were not fully characterised. The ^{1}H and $^{13}C\{^{1}H\}$ NMR spectra of **5** – **7** and **9** matched the proposed structures and will not be further commented on here, except to point out that their $^{13}C\{^{1}H\}$ NMR spectra were complicated by coupling to ^{31}P and ^{195}Pt nuclei, which made their full assignment difficult. No signals were observed in the $^{195}Pt\{^{1}H\}$ NMR spectra of **7** and **8**, probably due to the quadrupolar gallium nuclei broadening the signals until they are indistinguishable from the baseline noise. All mass spectra displayed characteristic fragmentation patterns, but a molecular ion was only observed in the mass spectrum of **7**. The preference for *trans*-isomerism in **5** – **7** is likely a result of the bulky gallium heterocycle causing steric strain in the *cis*-isomers.

A $^{31}P\{^{1}H\}$ NMR spectroscopic analysis of the reaction mixture that gave **7** shows that after 1 hour at room temperature, all of the starting material, *cis*-$[(PEt_3)_2PtCl_2]$, had been consumed. In this $^{31}P\{^{1}H\}$ NMR spectrum, the signal corresponding to the *cis*-isomer, **8**, is much weaker than that corresponding to the *trans*-isomer, **7**. The reaction mixture was allowed to stir overnight, and no changes were observed in the $^{31}P\{^{1}H\}$ NMR spectrum. This suggests that the isomerism of the platinum complex is not dictated after, but during the substitution reaction. The $^{1}J_{PtP}$ coupling constant is larger for the *cis*-isomer, **8** (2549 Hz), than the *trans*-isomer, **7** (2250 Hz). A more strongly σ-donating ligand weakens the Pt—P bond *trans*- to it to a greater extent, in turn reducing the $^{1}J_{PtP}$ coupling constant observed. This suggests that the gallyl ligand, **1**, does not have as strong a *trans*-influence as PEt_3, but is probably comparable to other phosphines, PR_3, that are poorer σ-donors than PEt_3. However, the $^{1}J_{PtP}$ coupling constant of **8** is much smaller than that for the starting material, *cis*-$[(PEt_3)_2PtCl_2]$ (3520 Hz).[12] These observations confirm earlier studies that the *trans*-influence of the gallyl ligand **1** is greater than chloride.[7] The related compound, *cis*-

$[(PEt_3)_2Pt\{B(cat)\}_2]$, has been characterised by $^{31}P\{^1H\}$ NMR spectroscopy and has a $^1J_{PtP}$ coupling constant of 1564 Hz.[13] Hence the tentative assignment of the boryl ligand, B(cat), being a stronger σ-donor than **1** has now been established. In addition, the $^1J_{PtP}$ coupling constant for **8** is greater than that observed for *cis*-$[(PEt_3)_2Pt(H)_2]$ (1984 Hz),[14] suggesting that **1** does not have as strong a *trans*-influence as the hydride ligand. A more definitive *trans*-directing series: $B(OR)_2 > H^- > PR_3 \sim \mathbf{1} > Cl^-$ can now be constructed with some certainty.

As PEt_3 is a stronger σ-donor than PPh_3,[15] **1** may have a similar *trans*-influence to the latter. This may explain the stability of the metal centre in *cis*-$[(PEt_3)_2PtCl_2]$ towards reduction in comparison to *cis*-$[(PPh_3)PtCl_2]$, and why complex **7** is a viable synthetic target. The intermediate in the formation of the PPh_3 derivative has more labile phosphine ligands, which upon dissociation facilitates the reduction of the metal centre by **1** and reductive elimination of species such as **4** and **11**. The PEt_3 ligand, being a stronger σ-donor of electron density than **1**, does not dissociate to such an extent. The $^1J_{PtP}$ coupling constant for **7** compares well with *trans*-$[(PEt_3)_2PtCl_2]$ (δ -12.3 ppm, 2400 Hz).[12] As well as this, the signal observed in the $^{31}P\{^1H\}$ NMR spectrum of **7** (δ 14.6 ppm) is more deshielded than that observed in the $^{31}P\{^1H\}$ NMR spectrum of **8** (δ 9.2 ppm). The chemical shift in the $^{31}P\{^1H\}$ NMR spectrum of **8** is, as expected from conclusions drawn from the study of $^1J_{PtP}$ coupling constants, between that of *cis*-$[(PEt_3)_2PtCl_2]$ (δ -9.3 ppm)[12] and *cis*-$[(PEt_3)_2Pt\{B(cat)\}_2]$ (δ 18.0 ppm).[13] The nickel, **5**, and palladium, **6**, complexes display one signal in their $^{31}P\{^1H\}$ NMR spectra at around the same chemical shift as **7**. The signal observed in the $^{31}P\{^1H\}$ NMR spectrum of the reaction mixture of **10** (δ 21.5) is upfield from that of **6** (δ 23.1) and the chemical shift of the monosubstituted complex, **9**, is upfield to a similar extent (by 3.8 ppm) from that of **5**, as would be predicted.

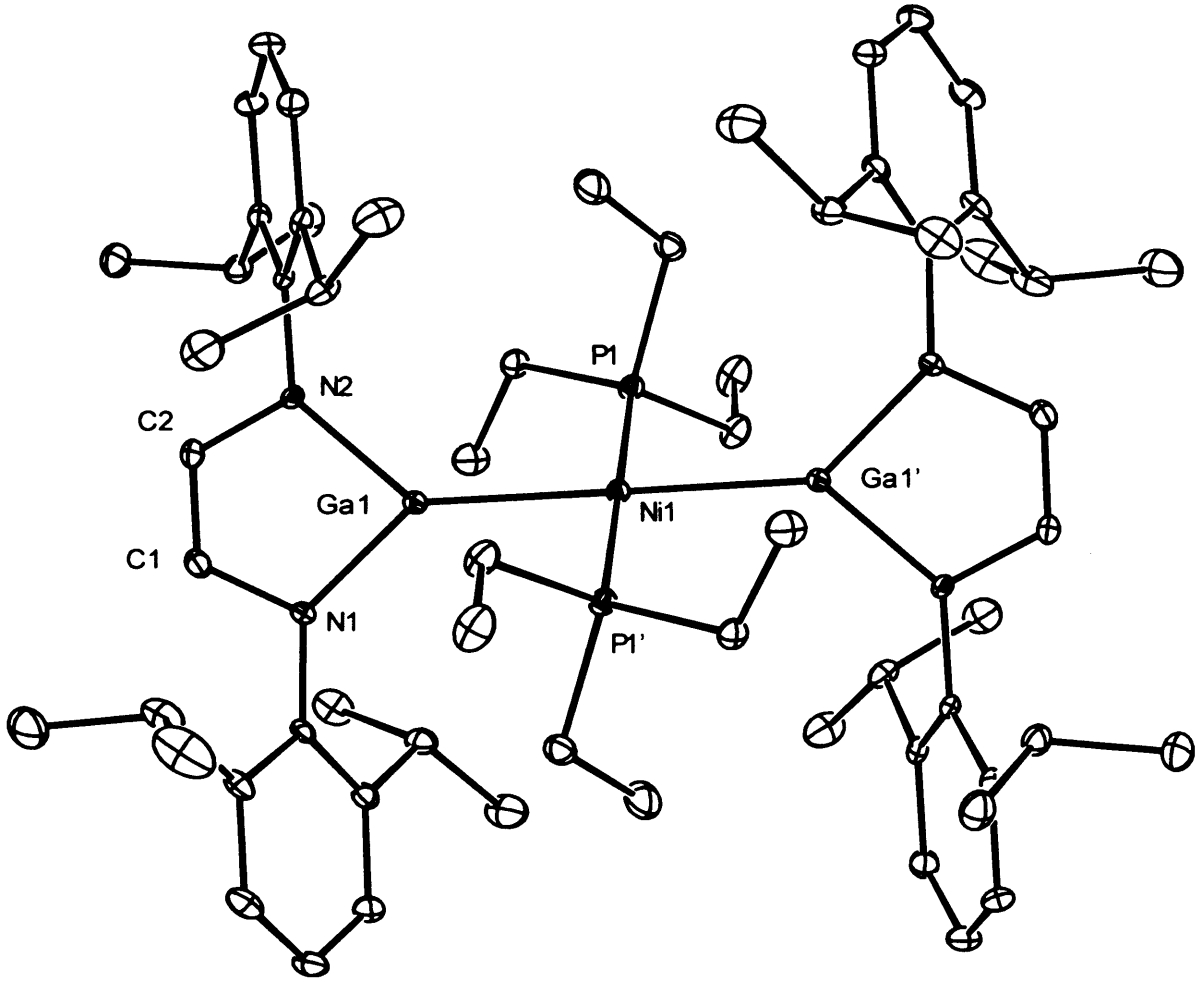

Figure 2 – Thermal ellipsoid plot (25 % probability surface) of the molecular structure of *trans*-[$(PEt_3)_2Ni\{Ga\{[N(Ar)C(H)]_2\}\}_2$] **5**; hydrogen atoms are omitted for clarity. Selected bond lengths (Å) and angles (°): Ga(1)—N(1) 1.909(2), Ga(1)—N(2) 1.912(2), Ga(1)—Ni(1) 2.3614(7), Ni(1)—P(1) 2.1908(8), N(1)—C(1) 1.398(4), N(2)—C(2) 1.399(3), C(1)—C(2) 1.337(4), N(1)—Ga(1)—N(2) 86.47(9), P(1')—Ni(1)—P(1) 180.0, P(1')—Ni(1)—Ga(1) 89.41(3), P(1)—Ni(1)—Ga(1) 90.59(3), C(1)—N(1)—Ga(1) 109.56(16), C(2)—N(2)—Ga(1) 109.50(16), C(2)—C(1)—N(1) 117.3(2), C(1)—C(2)—N(2) 117.1(3), symmetry operation ': $-x + 1, -y + 1, -z + 1$.

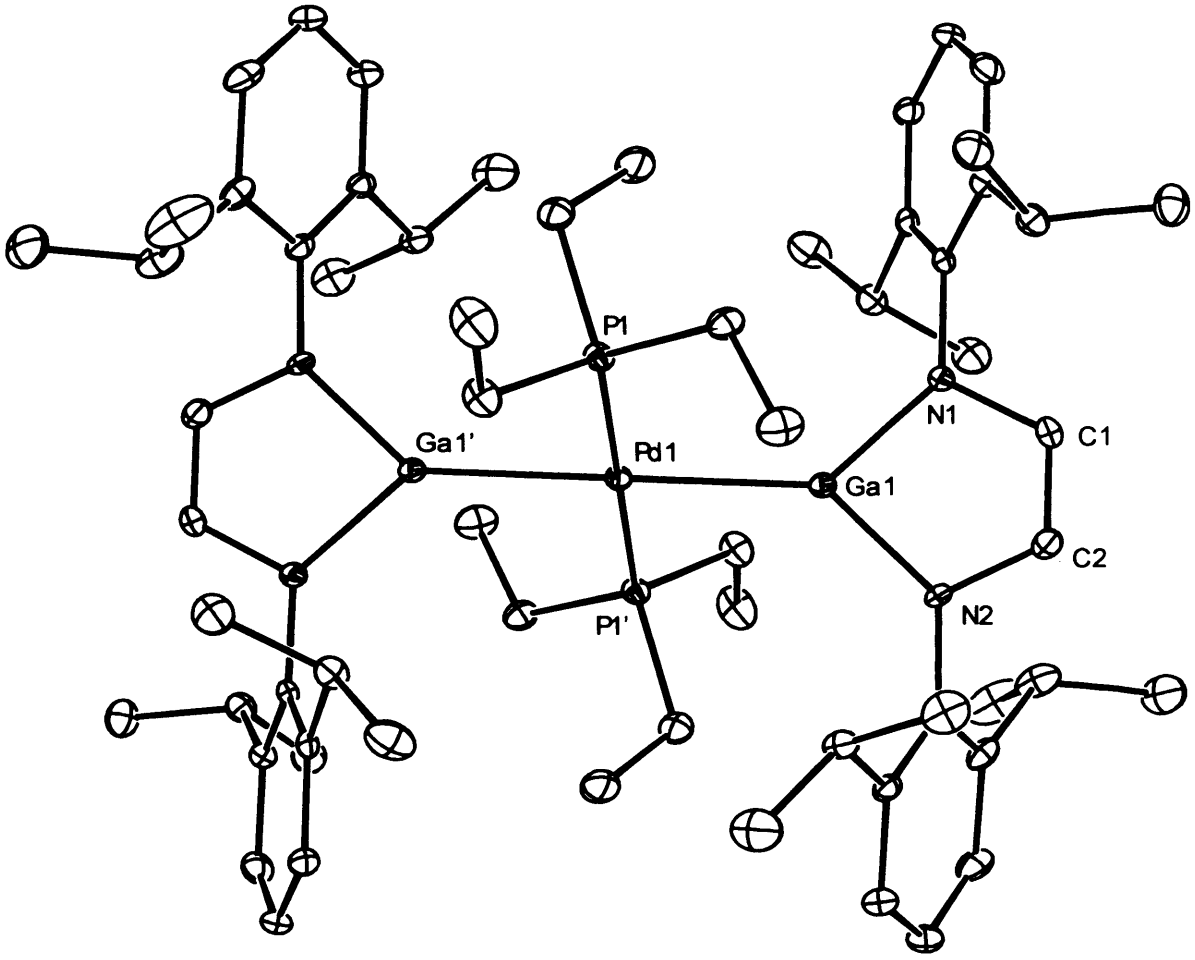

Figure 3 – Thermal ellipsoid plot (25 % probability surface) of the molecular structure of *trans*-$[(PEt_3)_2Pd\{Ga\{[N(Ar)C(H)]_2\}\}_2]$ **6**; hydrogen atoms are omitted for clarity. Selected bond lengths (Å) and angles (°): Pd(1)—P(1) 2.3038(12), Pd(1)—Ga(1) 2.4514(8), Ga(1)—N(1) 1.903(3), Ga(1)—N(2) 1.905(3), N(1)—C(1) 1.406(5), N(2)—C(2) 1.401(5), C(1)—C(2) 1.332(6), P(1')—Pd(1)—P(1) 180.000(1), P(1')—Pd(1)—Ga(1) 89.17(4), P(1)—Pd(1)—Ga(1) 90.83(4), N(1)—Ga(1)—N(2) 86.57(14), C(1)—N(1)—Ga(1) 109.6(3), C(2)—N(2)—Ga(1) 109.7(3), C(2)—C(1)—N(1) 117.0(4), C(1)—C(2)—N(2) 117.1(4), symmetry operation ': $-x + 1, -y + 1, -z + 1$.

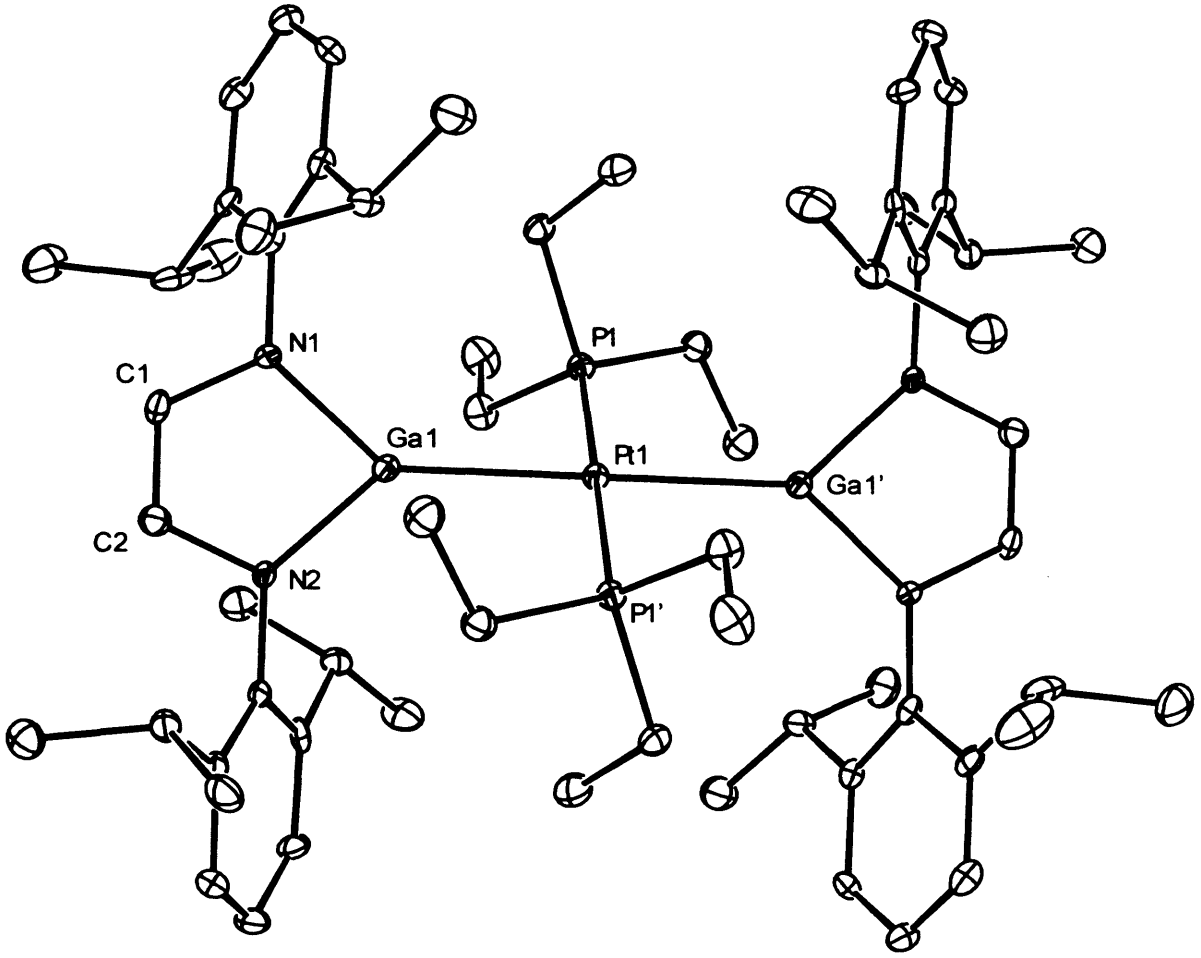

Figure 4 – Thermal ellipsoid plot (25 % probability surface) of the molecular structure of *trans*-$[(PEt_3)_2Pt\{Ga\{[N(Ar)C(H)]_2\}\}_2]$ **7**; hydrogen atoms are omitted for clarity. Selected bond lengths (Å) and angles (°): Pt(1)—P(1) 2.295(2), Pt(1)—Ga(1) 2.4477(10), Ga(1)—N(2) 1.895(6), Ga(1)—N(1) 1.899(5), N(1)—C(1) 1.400(9), N(2)—C(2) 1.398(9), C(1)—C(2) 1.346(10), P(1)—Pt(1)—P(1') 180.000(1), P(1)—Pt(1)—Ga(1') 90.61(6), P(1)—Pt(1)—Ga(1) 89.39(6), N(2)—Ga(1)—N(1) 86.8(2), C(1)—N(1)—Ga(1) 109.4(5), C(2)—N(2)—Ga(1) 110.3(5), C(2)—C(1)—N(1) 117.4(6), C(1)—C(2)—N(2) 116.1(7), symmetry operation ': $-x + 1, -y + 1, -z + 1$.

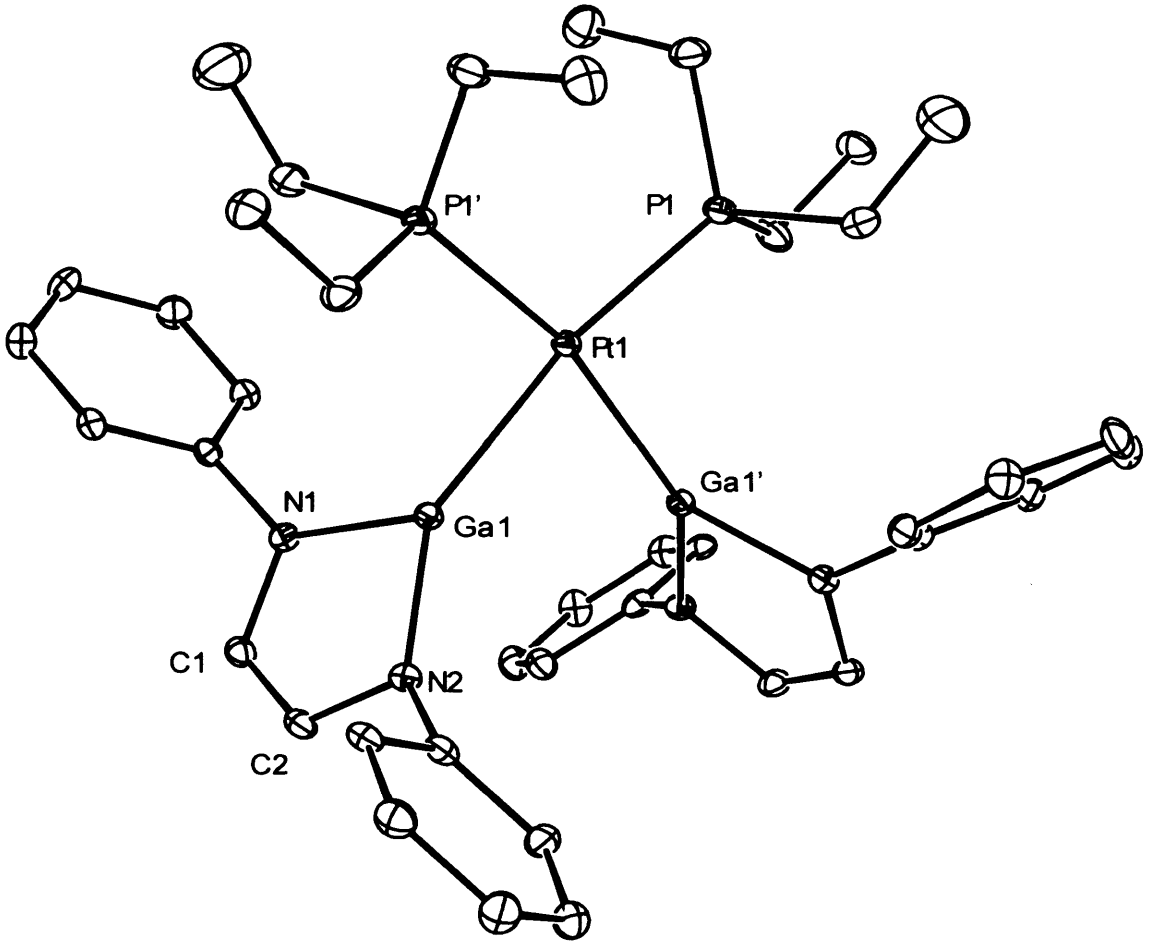

Figure 5 – Thermal ellipsoid plot (25 % probability surface) of the molecular structure of *cis*-$[(PEt_3)_2Pt\{Ga\{[N(Ar)C(H)]_2\}\}_2]$ **8**; hydrogen atoms and isopropyl groups are omitted for clarity. Selected bond lengths (Å) and angles (°): Pt(1)—P(1) 2.3173(15), Pt(1)—Ga(1) 2.4313(7), Ga(1)—N(2) 1.903(4), Ga(1)—N(1) 1.906(4), N(1)—C(1) 1.402(7), N(2)—C(2) 1.406(7), C(1)—C(2) 1.333(8), P(1)—Pt(1)—P(1') 102.71(8), P(1)—Pt(1)—Ga(1) 166.10(4), P(1')—Pt(1)—Ga(1) 91.04(4), Ga(1)—Pt(1)—Ga(1') 75.31(3), N(2)—Ga(1)—N(1) 88.03(19), C(1)—N(1)—Ga(1) 108.6(4), C(2)—N(2)—Ga(1) 107.6(3), C(2)—C(1)—N(1) 116.9(5), C(1)—C(2)—N(2) 118.8(5), symmetry operation ': $-x + 1, y, -z + 3/2$.

The crystal structures of **5 – 8** were obtained (Figures 2 – 5). Compounds **5 – 7** are structurally analagous and all display a nearly undistorted square planar geometry of

ligands around the metal centre and a crystallographic centre of inversion. The C=C backbones of the DAB fragments form angles of 57.5° (Ni) and 55.5° (Pd, Pt) with the square plane. The Ni—P bond lengths seen in **5** are slightly shorter than those observed in *trans*-$[(PEt_3)_2NiCl_2]$ (2.2329 Å mean),[16] whilst the Pt—P bond lengths in **7** are almost identical to those found in *trans*-$[(PEt_3)_2PtCl_2]$ (2.298 Å mean).[17] The structure of **8**, however, displays much longer Pt—P bond lengths than those in *cis*-$[(PEt_3)_2PtCl_2]$ (2.263 Å mean),[18] in agreement with the $^{31}P\{^1H\}$ NMR spectroscopic study. The C=C backbones of the DAB ligand in **8** form an angle to the square plane of 72.7°, which was obtuse to those in **5** – **7**. The unusually obtuse P—Pt—P and acute Ga—Pt—Ga angles in **8** bring the two gallium centres in the formally anionic heterocycles quite close to each other (Ga·····Ga 2.971 Å). This distance is much longer than typical Ga—Ga single bonds, such as in $[(tmp)_2Ga—Ga(tmp)_2]$ (tmp = tetramethylpiperidine) (2.541 Å),[19] but is similar to the Ga·····Ga interaction observed in dimeric [K(tmeda)][**1**] (2.8746 Å).[2]

It is worthy of note that acute B—Pt—B angles and relatively close B·····B interactions were observed in the related platinum(II) complexes, **2a-b**, although these were originally largely ignored[4] or attributed to steric constraints.[5] A subsequent theoretical study on the model complexes, *cis*-$[(PH_3)_2Pt\{B(OH)_2\}_2]$, reproduced the same geometries, suggesting that the acute B—Pt—B angles are not a consequence of sterics.[20] Recent reviews have commented on the possibility of $d\pi$-$p\pi$ back-bonding between the platinum and boron centres to explain the observed strong Pt—B bonds, acute B—Pt—B angles and the nearly perpendicular angles of the boryl ligands to the square plane.[3] The interplanar angles between the boron trigonal plane and the mean square plane around the platinum centres in several derivatives of **2a** range from 71.3° to 88.8°.[4b] The interplanar angle between the C=C backbones of the DAB ligand and

the square plane around the platinum centre of **8** is 72.7°. It is therefore conceivable that $d\pi$-$p\pi$ back-donation between the platinum and gallium centres of **8** could be occurring, although a theoretical study would be required to confirm this.

The crystal structures of **9** and **10** display nearly undistorted square planar geometries about the metal centre (Figures 6 and 7). The Ni—Cl bond length in **9** is, as would be expected, elongated with respect to *trans*-$[(PEt_3)_2NiCl_2]$ (2.1628 Å).[16] The Pd—Cl bond length in **10** is shorter than those observed in the two crystallographically independent molecules of *trans*-$[(PMe_3)_2PdCl\{B\{[N(Me)C(H)_2]_2\}\}_2]$ (2.484 Å mean),[21] which is in agreement with previous conclusions drawn upon the *trans*-influence of **1**. The Ga—Ni and Ga—Pd bond lengths of **9** and **10** are much shorter than those observed in **5** and **6**, by *ca.* 0.07 and 0.10 Å respectively. These observations are easily explained by the chloride ligand in **9** and **10** not donating σ-electron density to the metal centre to as great an extent as **1**. The increased steric demands of the heterocycle, **1**, should not have a great effect on the M—Cl bond lengths in **9** and **10**, as these interactions are *trans*- to the Ga—M bond. The Ga—Ni bond lengths observed in **5** and **9** are within the known range for such interactions (2.1700 – 2.4556 Å),[22] and are best compared with the only other example of a square planar nickel(II) gallyl complex, $[Ni\{C\{[N(Me)C(Me)]_2\}\}_2\{Ga\{[N(Ar)C(H)]_2\}\}_2]$ (Ga—Ni = 2.3242 Å mean).[23] The Ga—Pd bond observed in **10** is among the shortest recorded (2.336 – 2.657 Å),[22] the only shorter interaction being observed in $[Pd_2(GaCp^{*Ph})_2(\mu^2\text{-}GaCp^{*Ph})_3]$ ($GaCp^{*Ph}$ = C_5Me_4Ph).[24] To the best of our knowledge, compounds **6** and **10** represent the first structurally characterised examples of square planar palladium(II) gallyl complexes. The Ga—Pt bond lengths in **7** and **8** are within the known ranges (2.3040 – 2.5207 Å).[22] The comparable square planar bis-gallyl platinum(II) complexes, *trans*-

$[(H)_2Pt\{Ga[N(Ar)C(Me)]_2CH\}_2]$ and *cis*-$[(H)(SiEt_3)Pt\{Ga[N(Ar)C(Me)]_2CH\}_2]$,[25] both display shorter Ga—Pt bond lengths than those observed in **7** and **8**.

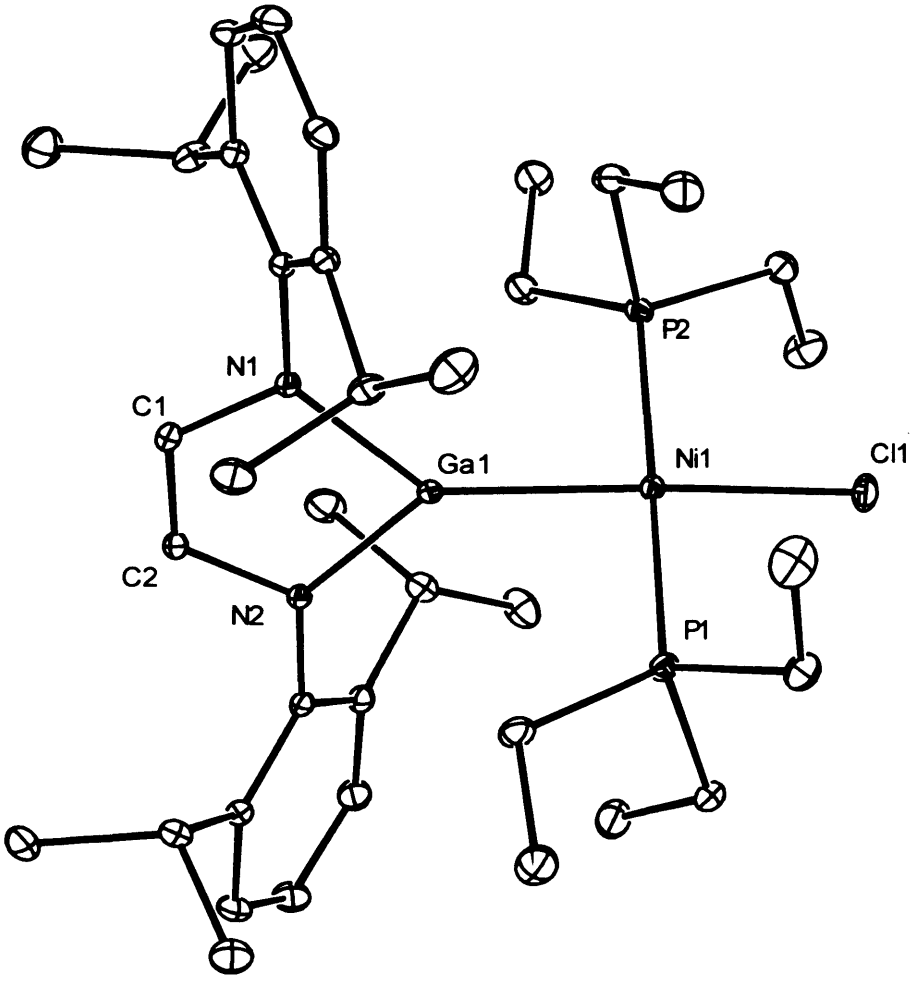

Figure 6 – Thermal ellipsoid plot (25 % probability surface) of the molecular structure of *trans*-$[(PEt_3)_2Ni\{Ga\{[N(Ar)C(H)]_2\}\}Cl]$ **9**; hydrogen atoms are omitted for clarity. Selected bond lengths (Å) and angles (°): Ga(1)—N(1) 1.8999(17), Ga(1)—N(2) 1.9029(17), Ga(1)—Ni(1) 2.2878(5), Ni(1)—P(1) 2.2115(8), Ni(1)—P(2) 2.2118(8), Ni(1)—Cl(1) 2.2138(7), N(1)—C(1) 1.396(3), C(1)—C(2) 1.336(3), N(2)—C(2) 1.400(3), N(1)—Ga(1)—N(2) 87.58(8), P(1)—Ni(1)—P(2) 175.74(2), P(1)—Ni(1)—Cl(1) 87.99(3), P(2)—Ni(1)—Cl(1) 92.64(3), P(1)—Ni(1)—Ga(1) 91.37(3), P(2)—Ni(1)—Ga(1) 88.23(3), Cl(1)—Ni(1)—Ga(1) 176.71(2), C(1)—N(1)—Ga(1) 108.65(14), C(2)—C(1)—N(1) 117.8(2), C(2)—N(2)—Ga(1) 108.57(13), C(1)—C(2)—N(2) 117.4(2).

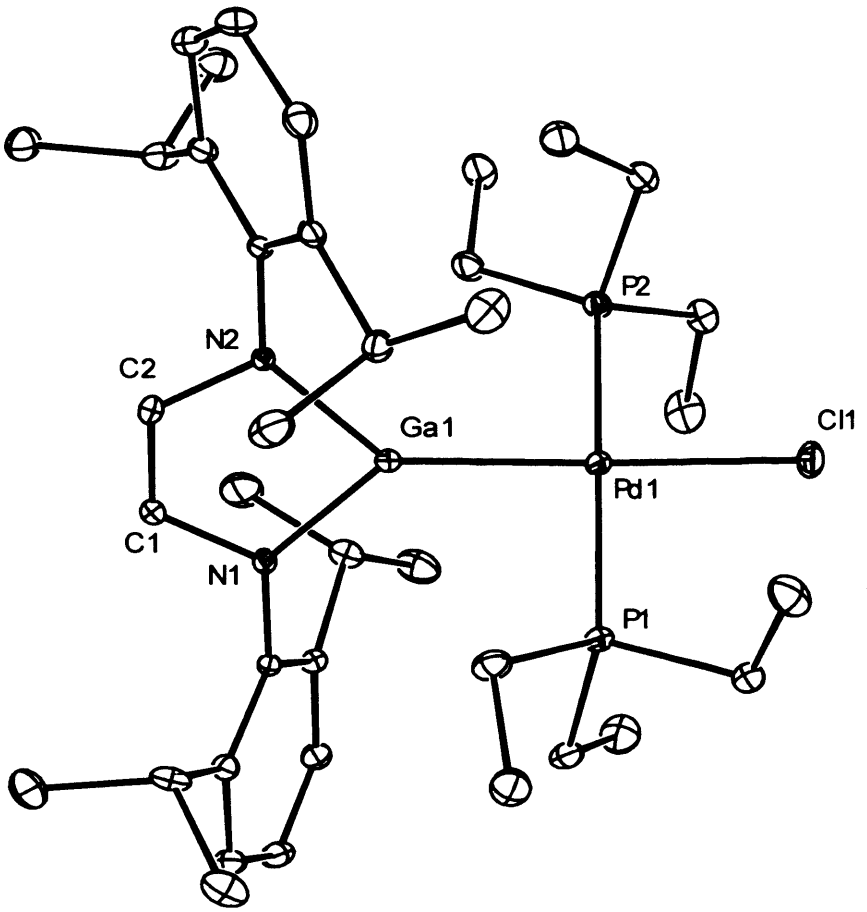

Figure 7 – Thermal ellipsoid plot (25 % probability surface) of the molecular structure of *trans*-[$(PEt_3)_2Pd\{Ga\{[N(Ar)C(H)]_2\}\}Cl$] **10**; hydrogen atoms are omitted for clarity. Selected bond lengths (Å) and angles (°): Pd(1)—P(1) 2.3160(11), Pd(1)—P(2) 2.3171(11), Pd(1)—Ga(1) 2.3551(6), Pd(1)—Cl(1) 2.3996(11), Ga(1)—N(1) 1.892(3), Ga(1)—N(2) 1.898(3), N(1)—C(1) 1.391(4), N(2)—C(2) 1.400(5), C(1)—C(2) 1.328(5), P(1)—Pd(1)—P(2) 176.35(4), P(1)—Pd(1)—Ga(1) 88.19(3), P(2)—Pd(1)—Ga(1) 92.01(3), P(1)—Pd(1)—Cl(1) 92.35(4), P(2)—Pd(1)—Cl(1) 87.61(4), Ga(1)—Pd(1)—Cl(1) 177.52(4), N(1)—Ga(1)—N(2) 88.28(13), C(1)—N(1)—Ga(1) 108.4(3), C(2)—N(2)—Ga(1) 107.2(2) C(2)—C(1)—N(1) 117.4(4), C(1)—C(2)—N(2) 118.7(4).

The reactivity of **5** towards unsaturated substrates was investigated. Treatment of a THF solution of **5** with xylylisonitrile, trimethylsilylazide and *tert*-butylphosphaalkyne (Bu^tCP) gave no reaction, as determined by the $^{31}P\{^1H\}$ NMR

spectra of the reaction mixtures. For comparison, the palladium analogue, **6**, was treated with Bu^{t}CP and no reaction was observed by $^{31}P\{^1H\}$ NMR spectroscopy. The inertness of **5** compared with the reactive boryl complexes, **2a-b**, can be explained by the *trans*-arrangement of ligands in **5**, compared with the *cis*-arrangement of the boryl complexes, **2a-b**. The strong *trans*-influence of boryl ligands, leading to facile phosphine dissociation in **2a-b**, is known to be a vital factor in the reactivity of these complexes.[4,5] In addition, the increased donor strength of triethylphosphine over triphenylphosphine gives rise to stronger phosphine coordination in **5 – 7**.

4.3.2 The Preparation of Metal Gallyl Complexes with Chelating Ligands

It was decided to investigate if chelated group 10 metal gallyl complexes could be synthesised by salt metathesis reactions. The employment of sufficiently stabilising ligands is known to prevent the formation of the gallium(II) dimers, **4** and **11**, in such reactions. This reasoning was verified by the 1 : 1 reaction of [K(tmeda)][**1**] with [(dcpe)$PtCl_2$] (dcpe = $Cy_2PCH_2CH_2PCy_2$) and [(dppe)$PtCl_2$] (dppe = Ph_2PCH_2-CH_2PPh_2), yielding the monosubstituted complexes, **12** and **13**, in poor yield (Scheme 5). Addition of a further equivalent of [K(tmeda)][**1**] to **12** did not result in a reaction, but [K(tmeda)][**1**] reacted with **13** to yield the disubstituted complex, **14**. In contrast, the 2 : 1 reaction of [K(tmeda)][**1**] with [(dppe)Pt(η^2-C_2H_4)] gave an intractable mixture of products. The difference in reactivity between **12** and **13** can probably be attributed to the increased steric congestion around the platinum centre in **12** compared to **13**, by a comparison of the cone angles of the chelating phosphines (dcpe θ = 142°, dppe θ = 125°).[15] Complex **14** could not be synthesised by refluxing the gallium(II) dimer, **11**, with [(dppe)Pt(η^2-C_2H_4)].

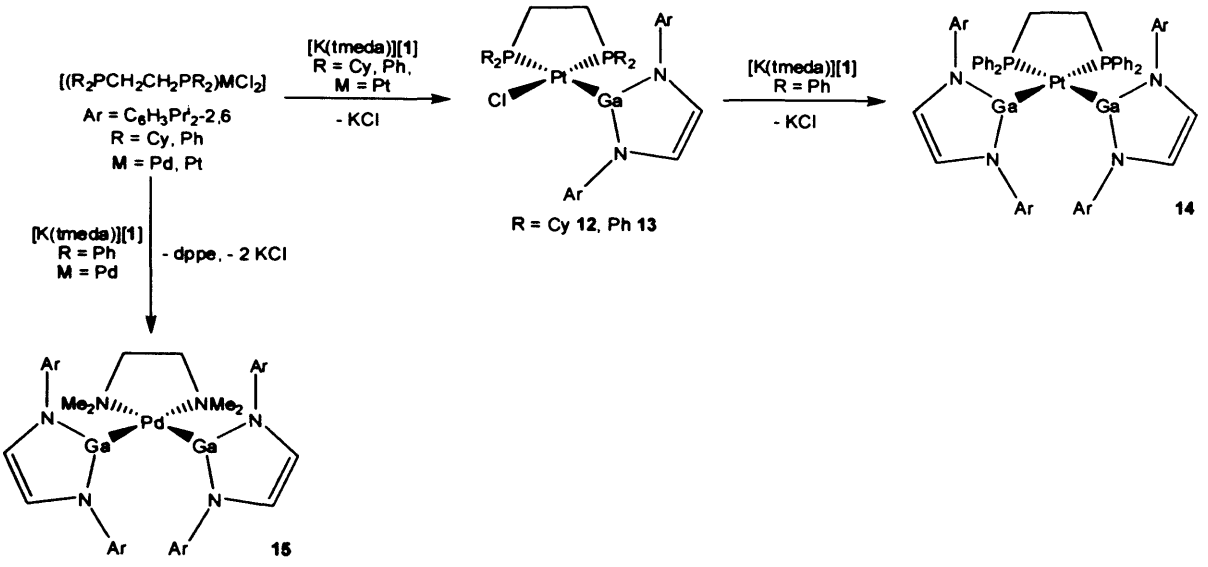

Scheme 5 – The synthesis of **12 – 15**

The 2 : 1 reaction of [K(tmeda)][**1**] with [(dppe)$PdCl_2$] resulted in the loss of dppe ($^{31}P\{^1H\}$ NMR spectroscopy) and substantial palladium metal deposition, yielding a trace amount of the tmeda-coordinated complex, **15** (Scheme 5), the tmeda ligand originating from the potassium cation of **1**. This complex was later synthesised intentionally in low yield from the 2 : 1 reaction of [K(tmeda)][**1**] with [(tmeda)$PdCl_2$] (Scheme 6). No product was isolable from the reaction of [(dppe)$NiCl_2$] with two equivalents of [K(tmeda)][**1**]. A stoichiometric amount of $Na[BAr^F{}_4]$ (Ar^F = $C_6H_3(CF_3)_2$-3,5) was added to a solution of **13** in an attempt to synthesise a highly reactive three-coordinate platinum complex with a weakly coordinating anion by a salt metathesis reaction. However, no reaction occurred.

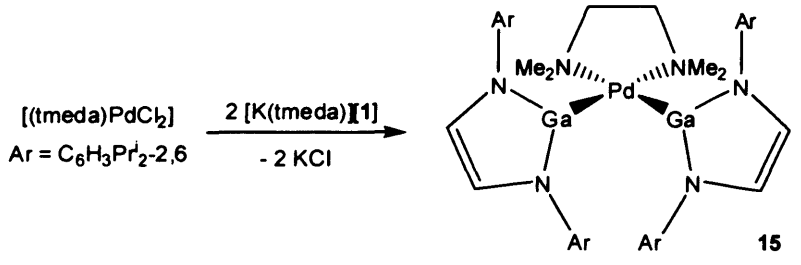

Scheme 6 – An alternative synthesis of **15**

It was thought that the employment of the less sterically demanding diphosphine ligand dppm (dppm = $Ph_2PCH_2PPh_2$, θ = 121°),[15] could circumvent the phosphine dissociation and palladium deposition seen in the 2 : 1 reaction of [K(tmeda)][**1**] with [(dppe)$PtCl_2$]. This proved to be the case, with the 2 : 1 reactions of [K(tmeda)][**1**] with [(dppm)MCl_2] (M = Pd, Pt) affording the bis-gallyl complexes, **16** and **17**, in low yield (Scheme 7). Similarly, the reaction of two equivalents of [K(tmeda)][**1**] with [(η^4-COD)$PtCl_2$] afforded the desired bis-gallyl complex, **18**. The 1 : 1 reactions of [K(tmeda)][**1**] with [(tmeda)$PdCl_2$] and [(η^4-COD)$PtCl_2$] gave intractable mixtures of products, as did the 2 : 1 reaction of [K(tmeda)][**1**] with [(η^4-COD)$PdCl_2$].

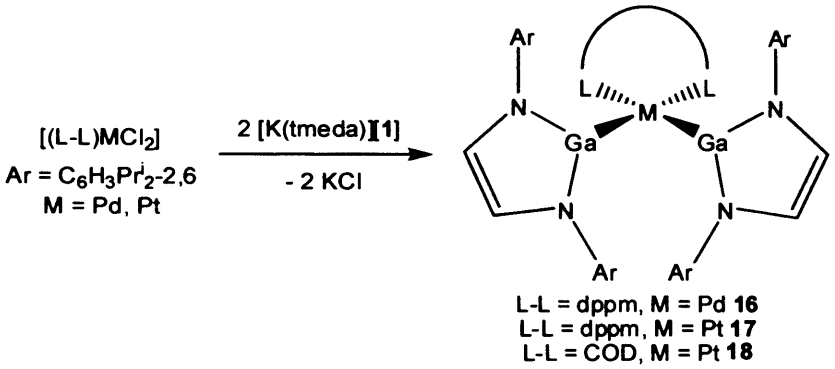

Scheme 7 – The synthesis of **16 – 18**

Complexes **12 – 18** were fully characterised. The ^{1}H NMR spectra of **12 – 18** match their proposed structures. All compounds were thermally robust, with **12** and **14** being the most stable. Complexes **15** and **18** display non-typical ^{1}H NMR spectra, with the backbone protons on the DAB ligand being chemically inequivalent and coupling with each other in an AB pattern. This is most likely due to steric crowding around the metal centre restricting the rotation of the gallium(I) heterocycles. This phenomenon has been observed in the related complex, [(tmeda)Ni{Ga{[N(Ar)C(H)]$_2$}}$_2$].[26] The ^{1}H NMR spectrum of **18** warrants further comment, as $^2J_{PtH}$ couplings were observable to the signals due to the diene protons. These couplings are much smaller than those

observed in [(η^4-COD)$PtCl_2$] ($^2J_{PtH}$ = 65 Hz)[27] and are comparable with those observed in [(η^4-COD)$PtMe_2$] ($^2J_{PtH}$ = 40 Hz),[28] as expected.

The $^{13}C\{^1H\}$ NMR spectra of **12 – 17** were too complicated to assign due to many overlapping signals and the low solubility of the complexes. The $^{13}C\{^1H\}$ NMR spectrum of **18**, however, was well resolved and $^1J_{PtC}$ couplings were observable to the signals due to the unsaturated COD carbons. These couplings ($^1J_{PtC}$ = 41.5 Hz mean) are lower than in both [(η^4-COD)$PtCl_2$] ($^1J_{PtC}$ = 154 Hz)[28] and [(η^4-COD)$PtMe_2$] ($^1J_{PtC}$ = 54 Hz),[28] suggesting that **1** has a comparable *trans*-influence to Me^-, although this is a tentative assignment. The $^{31}P\{^1H\}$ NMR spectra of **12 – 14** and **17** display smaller $^1J_{PtP}$ couplings in the signals originating from phosphorus centres *trans*- to the gallyl ligands ($^1J_{PtP}$ = 2088 Hz **12**, 2023 Hz **13**, 2316 Hz **14**, 1933 Hz **17**) than in the dihalide starting materials (e.g. [(dppe)$PtCl_2$] $^{31}P\{^1H\}$ NMR: δ 45.3 ppm, $^1J_{PtP}$ = 3618 Hz; [(dppm)$PtCl_2$] $^{31}P\{^1H\}$ NMR: δ -64.3 ppm, $^1J_{PtP}$ = 3078 Hz)[29] as expected from the study of **7** and **8**. It is noteworthy that complex **14** displays a much larger $^1J_{PtP}$ coupling constant than the analogous bis-boryl complex, [(dppe)Pt{B(cat)}$_2$] ($^1J_{PtP}$ = 1454 Hz).[4b] The high field chemical shift observed in the $^{31}P\{^1H\}$ NMR spectrum of **17** (δ -23.8 ppm) is unremarkable when comparisons are made with that of [(dppm)$PtCl_2$] (δ - 64.3 ppm).[29]

The crystal structures of **12 – 18** were obtained (Figures 8 – 14). Complex **15** is structurally analagous to the nickel homologue, [(tmeda)Ni{Ga{[N(Ar)C(H)]$_2$}}$_2$].[26] The Ga·····Ga separations of **14 – 18** vary greatly (2.990 – 3.536 Å), as do the Ga—M—Ga angles (79.02 – 94.05°). These separations may, in some cases, constitute minor interactions between the gallium nuclei. Complementary to the $^1J_{PtP}$ coupling constants in the $^{31}P\{^1H\}$ NMR spectra of **12** and **13**, the Pt—P separation of the phosphorus centres in the complexes *trans*- to the gallyl ligands, are much greater than

those *trans*- to the chloride ligands. The M—P bond lengths in **12 – 18** are, in all cases, elongated with respect to the dihalide starting materials, [(dcpe)$PtCl_2$],[30] [(dppe)$PtCl_2$],[31] [(tmeda)$PdCl_2$],[32] [(dppm)$PdCl_2$],[33] [(dppm)$PtCl_2$][34] and [(η^4-COD)$PtCl_2$].[35] It is noteworthy that the C=C bond lengths in the olefin ligand of **18** are not considerably elongated with respect to [(η^4-COD)$PtCl_2$], in contrast to an earlier study on the related complexes, [(η^4-COD)M(IMes){Ga{[N(Ar)C(H)]$_2$}}] (M = Rh, Ir),[7] where differences were observed with the halide precursors. Other structural data for **14** are best compared to those of the bis-boryl complex, [(dppe)Pt{B(cat)}$_2$],[4b] and similar conclusions can be drawn, as from the study on the monodentate phosphine complexes (*vide supra*).

Compounds **12 – 18** display a distorted square planar array of ligands about their metal centres, with the backbone of the gallyl ligands nearly orthogonal to the plane. This distortion is greatest in the sterically crowded complex, **14**. The P—Pt—P angle is less than 90° for all chelated phosphine complexes, and the P—M—P bite angles of **16** (71.91(5)°) and **17** (71.85(5)°) are far more acute than in their dppe counterparts, as would be expected. The Ga—Pd bond lengths in **15** and **16** are within the known ranges (2.336 – 2.657 Å), as are the Ga—Pt bond lengths in **12 – 14** and **17 – 18** (2.3040 – 2.5207 Å).[22] The Ga—Pt bond lengths in complexes **12** and **13** can be compared to those observed in the square planar compounds, [(dcpe)Pt(R)(GaR_2)] (R = *neo*-pentyl (Ga—Pt = 2.438 Å),[36a] CH_2SiMe_3 (Ga—Pt = 2.376 Å),[36b] whilst those in **14** and **17 – 18** are best compared with those seen in [(dppe)Pt{Ga{[N(Ar)]$_2$CNCy$_2$}}$_2$] (Ga—Pt = 2.357 Å mean).[37]

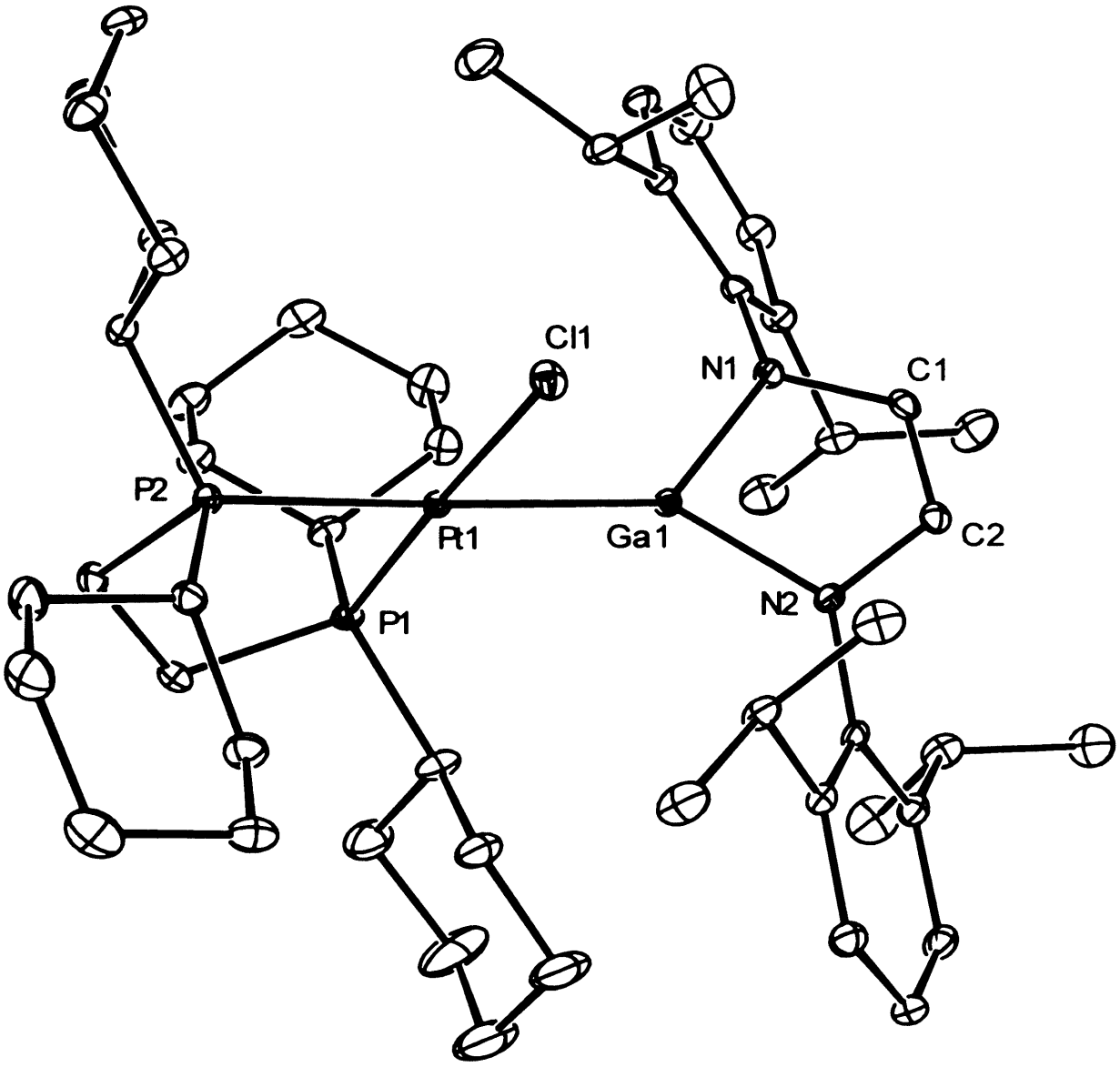

Figure 8 – Thermal ellipsoid plot (25 % probability surface) of the molecular structure of [(dcpe)Pt{Ga{[N(Ar)C(H)]$_2$}}Cl] **12**; hydrogen atoms are omitted for clarity. Selected bond lengths (Å) and angles (°): Pt(1)—P(1) 2.2031(10), Pt(1)—P(2) 2.3112(10), Pt(1)—Cl(1) 2.3723(10), Pt(1)—Ga(1) 2.4151(7), Ga(1)—N(1) 1.897(3), Ga(1)—N(2) 1.898(3), N(1)—C(1) 1.408(4), N(2)—C(2) 1.393(4), C(1)—C(2) 1.340(5), P(1)—Pt(1)—P(2) 88.17(4), P(1)—Pt(1)—Cl(1) 177.36(3), P(2)—Pt(1)—Cl(1) 93.92(4), P(1)—Pt(1)—Ga(1) 95.62(3), P(2)—Pt(1)—Ga(1) 176.13(2), Cl(1)—Pt(1)—Ga(1) 82.27(3), N(1)—Ga(1)—N(2) 88.09(12), C(1)—N(1)—Ga(1) 108.0(2), C(2)—N(2)—Ga(1) 107.9(2), C(2)—C(1)—N(1) 117.1(3), C(1)—C(2)—N(2) 118.2(3).

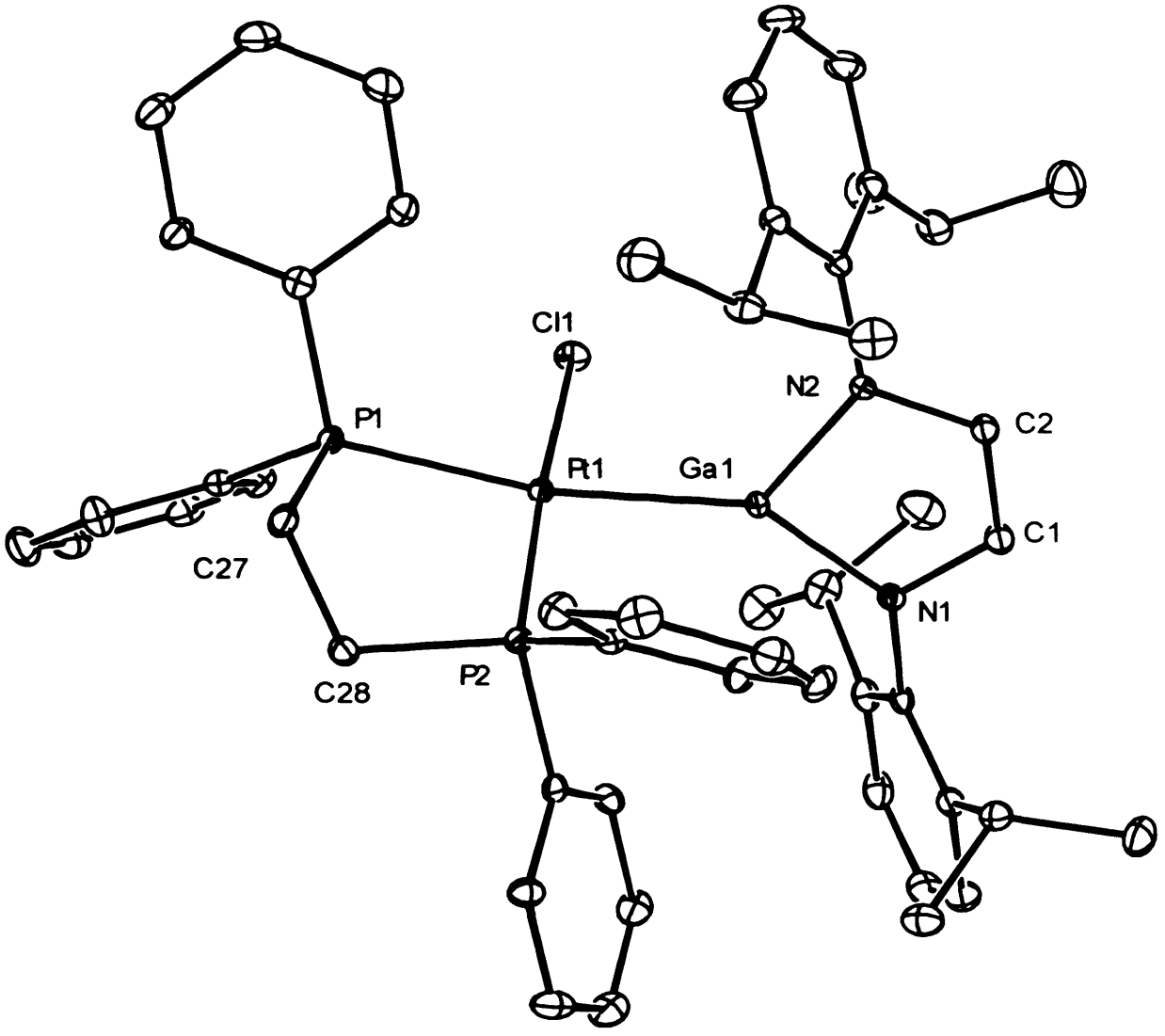

Figure 9 – Thermal ellipsoid plot (25 % probability surface) of the molecular structure of [(dppe)Pt{Ga{[N(Ar)C(H)]$_2$}}Cl] **13**; hydrogen atoms are omitted for clarity. Selected bond lengths (Å) and angles (°): Pt(1)—P(2) 2.2067(13), Pt(1)—P(1) 2.3239(14), Pt(1)—Cl(1) 2.3629(14), Pt(1)—Ga(1) 2.3929(7), Ga(1)—N(1) 1.877(4), Ga(1)—N(2) 1.885(4), P(1)—C(27) 1.837(5), N(1)—C(1) 1.410(7), C(1)—C(2) 1.349(7), P(2)—C(28) 1.849(5), N(2)—C(2) 1.389(7), C(27)—C(28) 1.515(7), P(2)—Pt(1)—P(1) 87.34(5), P(2)—Pt(1)—Cl(1) 173.81(6), P(1)—Pt(1)—Cl(1) 96.91(5), P(2)—Pt(1)—Ga(1) 93.32(4), P(1)—Pt(1)—Ga(1) 165.19(4), Cl(1)—Pt(1)—Ga(1) 83.72(4), N(1)—Ga(1)—N(2) 88.31(18), C(1)—N(1)—Ga(1) 108.6(3), C(2)—C(1)—N(1) 116.9(5), C(2)—N(2)—Ga(1) 109.0(3), C(1)—C(2)—N(2) 117.2(5), C(28)—C(27)—P(1) 109.6(4), C(27)—C(28)—P(2) 110.1(4).

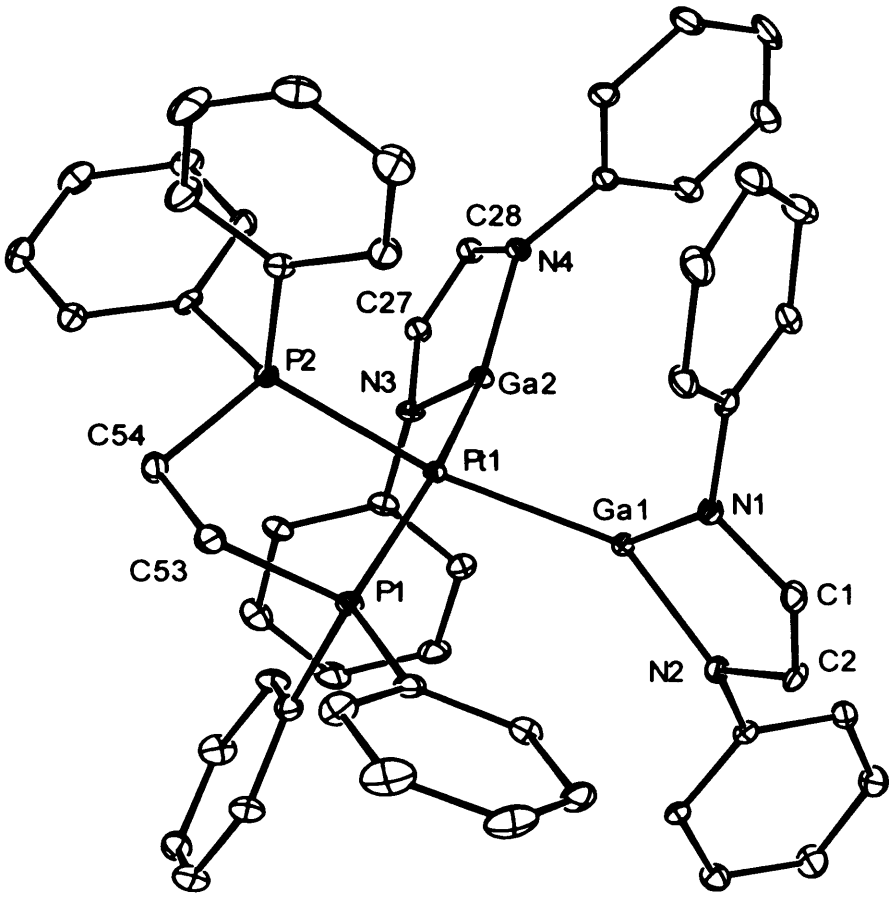

Figure 10 – Thermal ellipsoid plot (25 % probability surface) of the molecular structure of [(dppe)Pt{Ga{[N(Ar)C(H)]$_2$}}$_2$] **14**; hydrogen atoms and isopropyl groups are omitted for clarity. Selected bond lengths (Å) and angles (°): Pt(1)—P(2) 2.3016(10), Pt(1)—P(1) 2.3138(11), Pt(1)—Ga(1) 2.4157(6), Pt(1)—Ga(2) 2.4167(7), Ga(1)—N(1) 1.902(3), Ga(1)—N(2) 1.911(3), Ga(2)—N(3) 1.911(3), Ga(2)—N(4) 1.913(3), P(1)—C(53) 1.843(4), P(2)—C(54) 1.829(4), N(1)—C(1) 1.397(5), N(2)—C(2) 1.409(5), N(3)—C(27) 1.384(5), N(4)—C(28) 1.402(5), C(1)—C(2) 1.339(5), C(27)—C(28) 1.335(5), P(2)—Pt(1)—P(1) 85.18(4), P(2)—Pt(1)—Ga(1) 162.49(3), P(1)—Pt(1)—Ga(1) 93.30(3), P(2)—Pt(1)—Ga(2) 93.01(3), P(1)—Pt(1)—Ga(2) 160.61(3), Ga(1)—Pt(1)—Ga(2) 94.05(3), N(1)—Ga(1)—N(2) 87.91(13), N(3)—Ga(2)—N(4) 88.17(13), C(1)—N(1)—Ga(1) 108.9(2), C(2)—N(2)—Ga(1) 107.5(2), C(27)—N(3)—Ga(2) 108.1(2), C(28)—N(4)—Ga(2) 106.7(2), C(2)—C(1)—N(1) 117.0(4), C(1)—C(2)—N(2) 118.5(3), C(28)—C(27)—N(3) 117.8(4), C(27)—C(28)—N(4) 119.1(4).

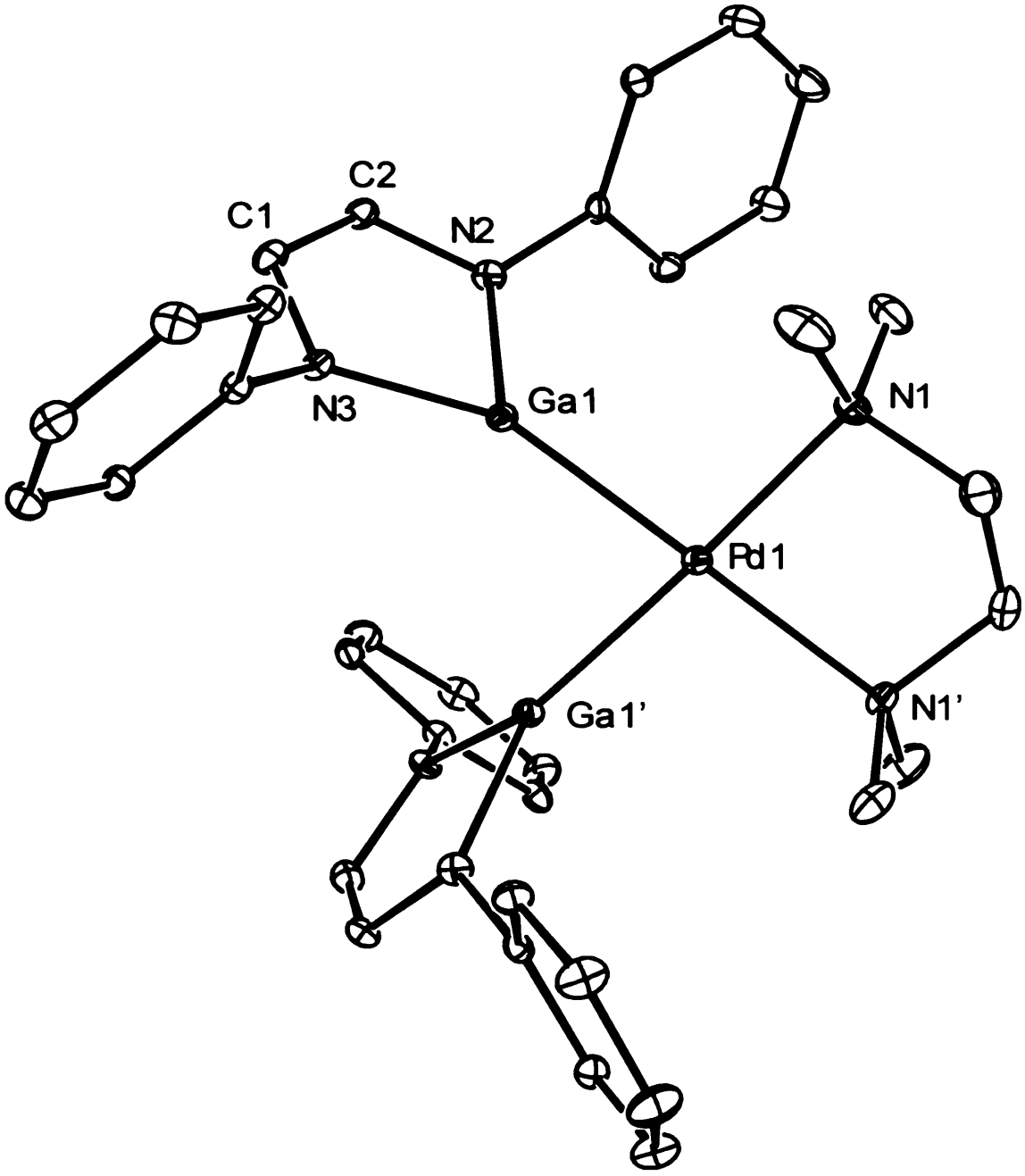

Figure 11 – Thermal ellipsoid plot (25 % probability surface) of the molecular structure of [(tmeda)Pd{Ga{[N(Ar)C(H)]$_2$}}$_2$] **15**; hydrogen atoms and isopropyl groups are omitted for clarity. Selected bond lengths (Å) and angles (°): Pd(1)—N(1) 2.231(4), Pd(1)—Ga(1) 2.3503(8), Ga(1)—N(3) 1.893(4), Ga(1)—N(2) 1.907(4), N(3)—C(1) 1.420(6), N(2)—C(2) 1.381(6), C(1)—C(2) 1.343(7), N(1)—Pd(1)—N(1') 82.1(2), Ga(1)—Pd(1) —Ga(1') 79.02(4), N(3)—Ga(1)—N(2) 87.81(17), C(1)—N(3)—Ga(1) 108.1(3), C(2)—N(2)—Ga(1) 109.0(3), C(2)—C(1)—N(3) 117.3(5), C(1)—C(2)—N(2) 117.6(5), symmetry operation ': $-x + 1, y, -z + 1/2$.

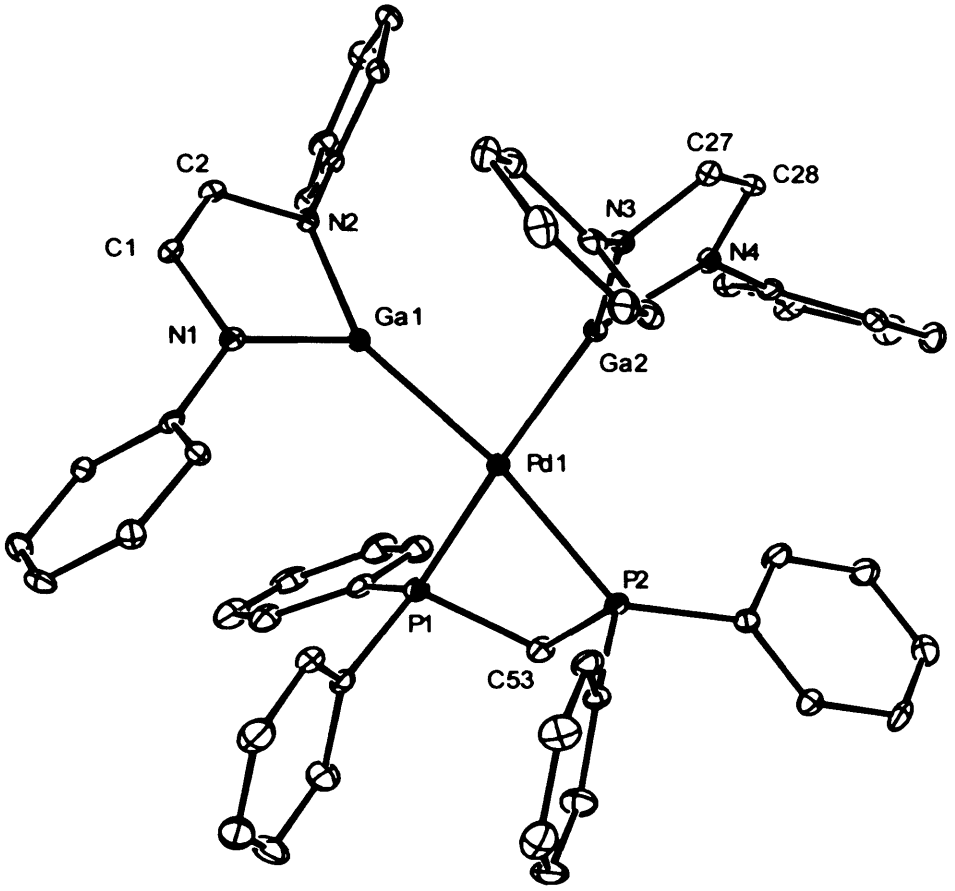

Figure 12 – Thermal ellipsoid plot (25 % probability surface) of the molecular structure of [(dppm)Pd{Ga{[N(Ar)C(H)]$_2$}}$_2$] **16**; hydrogen atoms and isopropyl groups are omitted for clarity. Selected bond lengths (Å) and angles (°): Pd(1)—P(1) 2.3871(16), Pd(1)—P(2) 2.3934(15), Pd(1)—Ga(1) 2.3959(9), Pd(1)—Ga(2) 2.4032(8), Ga(1)—N(2) 1.888(4), Ga(1)—N(1) 1.905(4), P(1)—C(53) 1.843(5), N(1)—C(1) 1.394(6), C(1)—C(2) 1.335(7), Ga(2)—N(3) 1.901(4), Ga(2)—N(4) 1.911(4), P(2)—C(53) 1.835(5), N(2)—C(2) 1.394(6), N(3)—C(27) 1.408(6), N(4)—C(28) 1.398(7), C(27)—C(28) 1.335(8), P(1)—Pd(1)—P(2) 71.91(5), P(1)—Pd(1)—Ga(1) 103.12(4), P(2)—Pd(1)—Ga(1) 170.80(4), P(1)—Pd(1)—Ga(2) 174.79(4), P(2)—Pd(1)—Ga(2) 105.96(4), Ga(1)—Pd(1)—Ga(2) 79.63(3), N(2)—Ga(1)—N(1) 87.72(17), C(1)—N(1)—Ga(1) 108.6(3), C(2)—C(1)—N(1) 117.0(5), N(3)—Ga(2)—N(4) 87.79(19), C(2)—N(2)—Ga(1) 108.4(3), C(1)—C(2)—N(2) 118.2(4), C(27)—N(3)—Ga(2) 108.1(4), C(28)—N(4)—Ga(2) 108.5(4), C(28)—C(27)—N(3) 118.2(5), C(27)—C(28)—N(4) 117.4(5), P(2)—C(53)—P(1) 99.5(3).

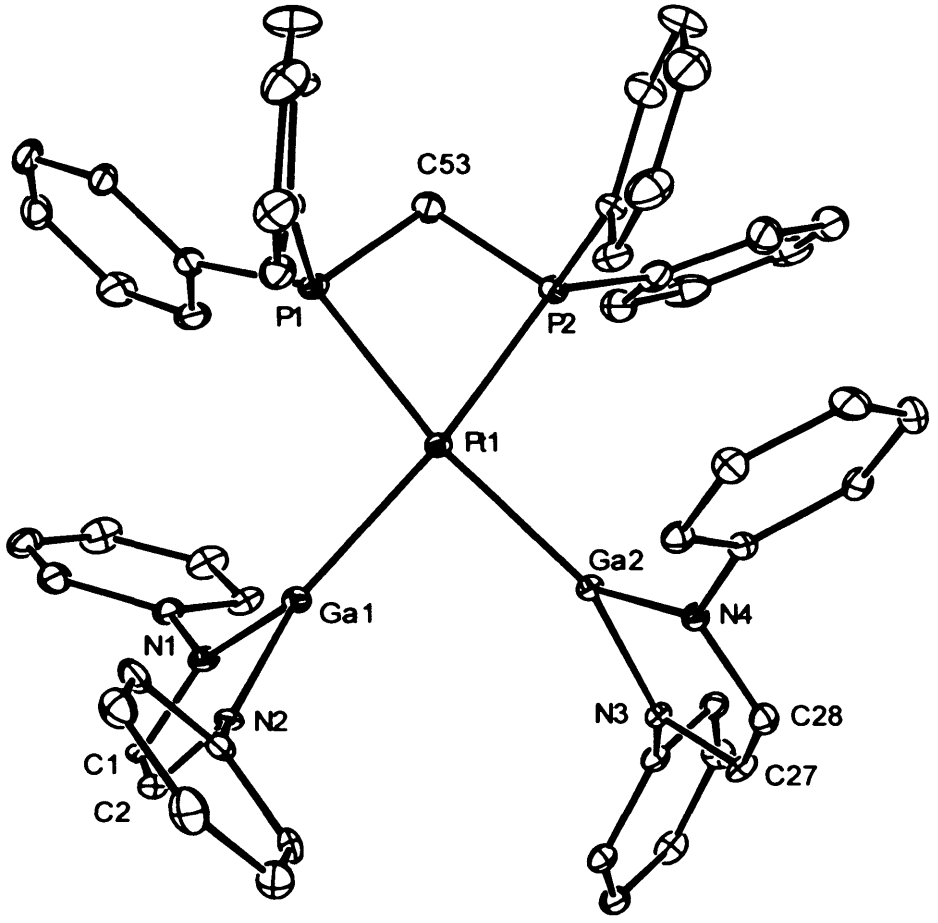

Figure 13 – Thermal ellipsoid plot (25 % probability surface) of the molecular structure of [(dppm)Pt{Ga{[N(Ar)C(H)]$_2$}}$_2$] **17**; hydrogen atoms and isopropyl groups are omitted for clarity. Selected bond lengths (Å) and angles (°): Pt(1)—P(2) 2.3291(13), Pt(1)—P(1) 2.3356(13), Pt(1)—Ga(2) 2.4170(8), Pt(1)—Ga(1) 2.4218(7), Ga(1)—N(2) 1.899(4), Ga(1)—N(1) 1.905(4), P(1)—C(53) 1.846(5), N(1)—C(1) 1.397(6), C(1)—C(2) 1.349(7), Ga(2)—N(3) 1.896(4), Ga(2)—N(4) 1.906(4), P(2)—C(53) 1.845(5), N(2)—C(2) 1.395(6), N(3)—C(27) 1.395(6), N(4)—C(28) 1.407(6), C(27)—C(28) 1.329(7), P(2)—Pt(1)—P(1) 71.85(5), P(2)—Pt(1)—Ga(2) 100.34(4), P(1)—Pt(1)—Ga(2) 168.93(4), P(2)—Pt(1)—Ga(1) 172.80(3), P(1)—Pt(1)—Ga(1) 102.96(4), Ga(2)—Pt(1)—Ga(1) 85.46(2), N(2)—Ga(1)—N(1) 87.15(17), C(1)—N(1)—Ga(1) 109.7(3), C(2)—C(1)—N(1) 116.1(4), N(3)—Ga(2)—N(4) 88.01(16), C(2)—N(2)—Ga(1) 108.9(3), C(1)—C(2)—N(2) 118.2(4), C(27)—N(3)—Ga(2) 108.7(3), C(28)—N(4)—Ga(2) 107.4(3), C(28)—C(27)—N(3) 117.3(4), C(27)—C(28)—N(4) 118.5(4), P(2)—C(53)—P(1) 95.7(2).

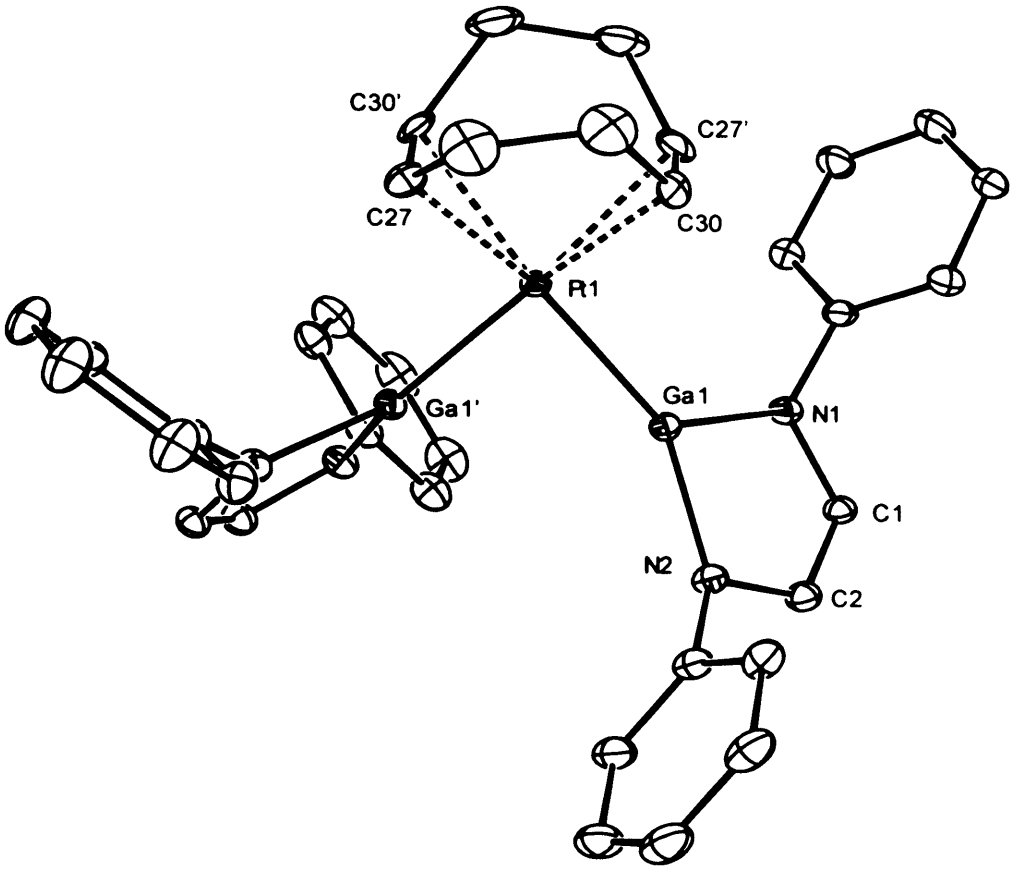

Figure 14 – Thermal ellipsoid plot (25 % probability surface) of the molecular structure of $[(\eta^4\text{-COD})Pt\{Ga\{[N(Ar)C(H)]_2\}\}_2]$ **18**; hydrogen atoms and isopropyl groups are omitted for clarity. Selected bond lengths (Å) and angles (°): Pt(1)—C(27) 2.268(6), Pt(1)—C(30) 2.273(6), Pt(1)—Ga(1) 2.3838(7), Ga(1)—N(1) 1.871(5), Ga(1)—N(2) 1.885(5), N(1)—C(1) 1.383(7), N(2)—C(2) 1.398(7), C(1)—C(2) 1.336(8), C(27)—C(30') 1.336(10), Ga(1')—Pt(1)—Ga(1) 83.84(3), N(1)—Ga(1)—N(2) 87.7(2), C(1)—N(1)—Ga(1) 109.5(4), C(2)—N(2)—Ga(1) 108.6(4), C(2)—C(1)—N(1) 117.2(5), C(1)—C(2)—N(2) 117.0(5), symmetry operation ': x, $-y + 1/2$, $-z + 3/2$.

4.3.3 The Reactivity of Chelated Metal Gallyl Complexes with Unsaturated Substrates

Compound **18** is analogous to the bis-boryl complex, **3**, and as such its reactivity towards unsaturated substrates was investigated. However, no reaction occurred when hex-3-yne or styrene were added separately to a toluene solution of **18**. Compound **14**

is analogous to [(dppe)Pt{B(cat)}$_2$], which displays poor catalytic activity due to the presence of a chelating phosphine ligand. However, it was decided to investigate the reactivity of **14** towards a variety of unsaturated substrates, as this compound could be synthesised in good yield. No reaction occurred when **14** was treated with but-2-yne, ethylene, carbon monoxide, benzonitrile or acetonitrile, and only intractable mixtures of products resulted when **14** was treated with 3-buten-2-one, carbon dioxide and carbon disulphide. The reaction of **14** with xylylisonitrile led to the displacement of dppe and the eventual formation of [Pt(dppe)$_2$],[38] as followed by $^{31}P\{^1H\}$ NMR spectroscopy, with no other isolable products. Presumably, reductive elimination of the digallane(4), [Ga{[N(Ar)C(H)]$_2$}]$_2$, occurs. However, the reaction of **14** with *tert*-butylisonitrile (Bu^{t}NC) led to the loss of dppe and the formation of compound **19**, with no [Pt(dppe)$_2$] formed in the reaction mixture (Scheme 8). The strong σ-donor Bu^{t}NC prevents dppe from coordinating to **19** in the reaction mixture. The isomer *tert*-butylnitrile (Bu^{t}CN) was found to not react with **14**.

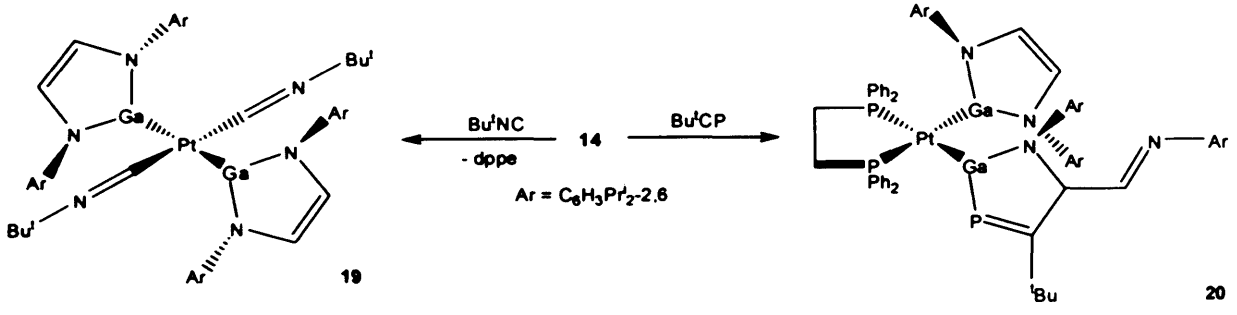

Scheme 8 – The synthesis of **19** and **20**

When compound **14** was treated with the heavier homologue, Bu^{t}CP, an unusual insertion product, **20**, formed quickly and quantitatively, as determined by $^{31}P\{^1H\}$ NMR spectroscopy, under any stoichiometry (Scheme 8). This insertion complex contains the first example of an anionic mixed *P,N*-heterocyclic gallyl ligand and contains a stereogenic centre. In contrast, the reaction of Bu^{t}CP with **17** gave an intractable mixture of products, and no reaction occurred when Bu^{t}CP was added to

[K(tmeda)][1], suggesting that the gallium heterocycle in **14** has been "activated." For comparison, Bu^{t}CP was added to a solution of **13** to observe if the same type of insertion product formed in the absence of a second bulky gallyl ligand. However, in this case the known zerovalent platinum complex, [(dppe)Pt(η_2-PCBu^t)] **21**,[39] formed (observed by $^{31}P\{^1H\}$ NMR spectroscopy), presumably via loss of the paramagnetic gallium(II) dimer, [ClGa{[N(Ar)C(H)]$_2$·}]$_2$ **4** (Scheme 9). Treatment of complex **20** with Bu^{t}NC afforded complex **19**. In contrast, the reaction of **20** with xylylisonitrile gave [Pt(dppe)$_2$], with the clean loss of Bu^{t}CP and dppe, as determined by $^{31}P\{^1H\}$ NMR spectroscopy, suggesting that the insertion of Bu^{t}CP is reversible. Compound **20** did not react with Bu^{t}CN, and gave an intractable mixture of products when treated with CS_2.

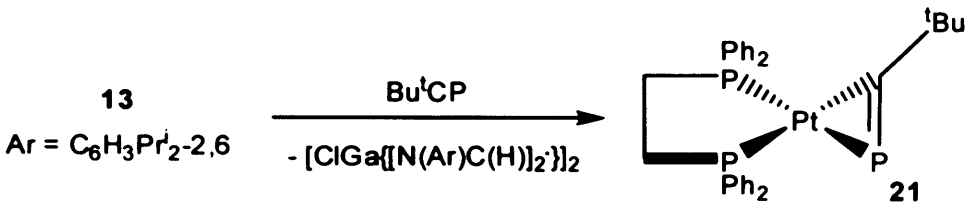

Scheme 9 – The synthesis of **21**

As square planar platinum(II) complexes typically undergo substitution through an associative mechanism with square based pyramidal intermediates,[40] it is a reasonable assumption that the initial step in the mechanism of formation of **20** is the transient coordination of Bu^{t}CP at a vacant "apical" site of **14**. The coordinated phosphaalkyne could then accept nucleophilic attack at its alkynic carbon, followed by rearrangement to give **20** (Figure 15). Theoretical studies into the polarity of the P≡C triple bond of uncoordinated phosphaalkynes have suggested that their alkynic carbons are slightly negative, with the exception of those containing π-donor substituents, such as in Pr$^i_2$NCP.[41] Experimental observations are consistent, with nucleophilic attack normally taking place at the P-terminus of Bu^{t}CP.[42] Phosphaalkynes may coordinate to

a metal in an η^1-fashion, by σ-donation of a lone pair of electrons at the P-terminus, or η^2-fashion, by donation of the HOMO π-type orbital. Though the former coordination mode is very rare, it can occur at restricted coordination sites, such as in the octahedral molecule, $[(dppe)_2W(\eta^1\text{-}PCBu^t)_2]$, and can not be discounted here.[43] However, it is far more probable that the phosphaalkyne donates in an η^2- fashion in the formation of **20**. When Bu^{t}CP is η^2-coordinated to a transition metal centre, there is an increased basicity of the phosphorus lone pair electrons and therefore the alkynic carbon may be open to nucleophilic attack.[42b,44]

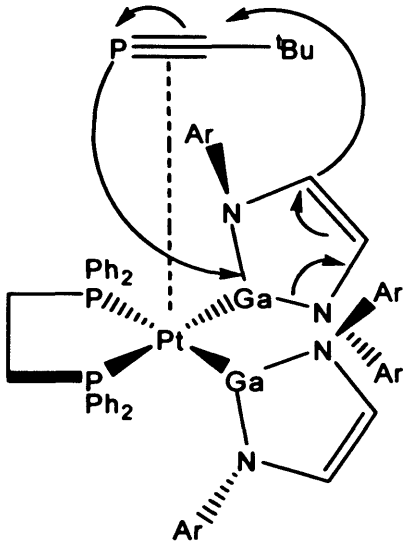

Figure 15 – A proposed intermediate in the formation of **20**

Further investigations into the formation of **20** showed that addition of two equivalents of PEt_3 to the reaction mixture before addition of Bu^{t}CP slowed the rate of formation of the insertion complex considerably, from 10 minutes to about 3 hours. The rate is not reduced when the weaker σ-donor, PPh_3, is added instead of PEt_3. It is assumed that, although there is no change in the $^{31}P\{^1H\}$ NMR spectrum of **14** following addition of PEt_3, the phosphine donates to the platinum centre at the "apical" position in transient square based pyramidal intermediates. This competition for the "apical" site fortifies the argument that pre-coordination of phosphaalkyne at platinum is required for the reaction to take place. It is proposed that, in the concerted

mechanism, the coordinated phosphaalkyne undergoes formal nucleophilic attack by the imine-type carbon backbone of the gallium heterocycle. Donation of the phosphorus lone pair of electrons to the gallium centre and simultaneous rearrangement leads to the dissociation of an N-donor and formation of a C=N double bond. Hence the original gallium heterocycle has been opened and the novel heterocyclic ring closed.

Following on from the discovery that the addition of two equivalents of PEt_3 to the reaction mixture slows the rate of reaction markedly, it was decided to study the kinetics of the reaction by $^{31}P\{^1H\}$ NMR spectroscopy. As no PEt_3 is consumed during the course of the reaction, the integration of its signal can be employed as the standard as the reaction proceeds. To perform the experiments, a nearly saturated THF solution of **14** (0.02 g in 0.6 cm^3) was made up in a Young's NMR tube with either two or ten equivalents of PEt_3 and a D_2O insert, and the spectrum obtained. Bu^tCP was added, a $^{31}P\{^1H\}$ NMR spectrum taken twelve minutes later and then in eight minute intervals for the three hour duration of the experiment. Integration of the spectra allowed the rate of reaction to be measured. As the starting concentration of **14** and the ratio of the integration of the signal at δ 47.4 ppm to the integration of the PEt_3 signal in the $^{31}P\{^1H\}$ NMR spectrum is known, all ratios obtained could then be converted to units of $moldm^{-3}$. It was latterly found to be easier to follow the rate of formation of the product, **20**, as one of its resonances at δ 301.0 ppm does not overlap with signals due to the starting material.

It was found that increasing the number of equivalents of PEt_3 from two to ten did not slow down the reaction more than when two equivalents were used. This suggests that although competition for the vacant apical site at platinum is the likely cause of slowing down the rate of reaction, the transient binding of PEt_3 to **14** is not

dependent on concentration. This observation is indicative of the weak interactions postulated. In addition, increasing the number of equivalents of Bu^{t}CP from two to ten also does not lead to a change in the rate of reaction. The reaction is therefore zero order with respect to the phosphaalkyne under these conditions. Hence it seems intuitive that the rate determining step is the formation of the proposed square based pyramidal intermediate, which in the presence of PEt_3 is formed at a rate dependent only on the concentration of **14**. Unfortunately, the concentration of **14** could not be increased to test this hypothesis due to the low solubility in THF. The concentration could also not be decreased as the reaction was already being followed on a very small scale, and halving the concentration would have led to the attempted measurement of very weak signals and would yield inaccurate results. Attempted adjustment of the solvent system to more polar solvents such as DCM to increase the concentration of **14** led only to decomposition of the starting material. The reaction was assumed to be first order under these conditions, the rate equation being: Rate = k[**14**]. As such a graph was constructed of ln[**14**] against time (Graph 1). Straight lines were obtained to give the rate constant of the reaction, $k = 3.6 \times 10^{-4}$ s^{-1}, with either two or ten equivalents of Bu^{t}CP. The high R^2 values of 0.7488 and 0.7991 suggest that there is a good correlation of both data series to the straight lines and that the reaction under these conditions is *pseudo*-first order with respect to the concentration of **14**.

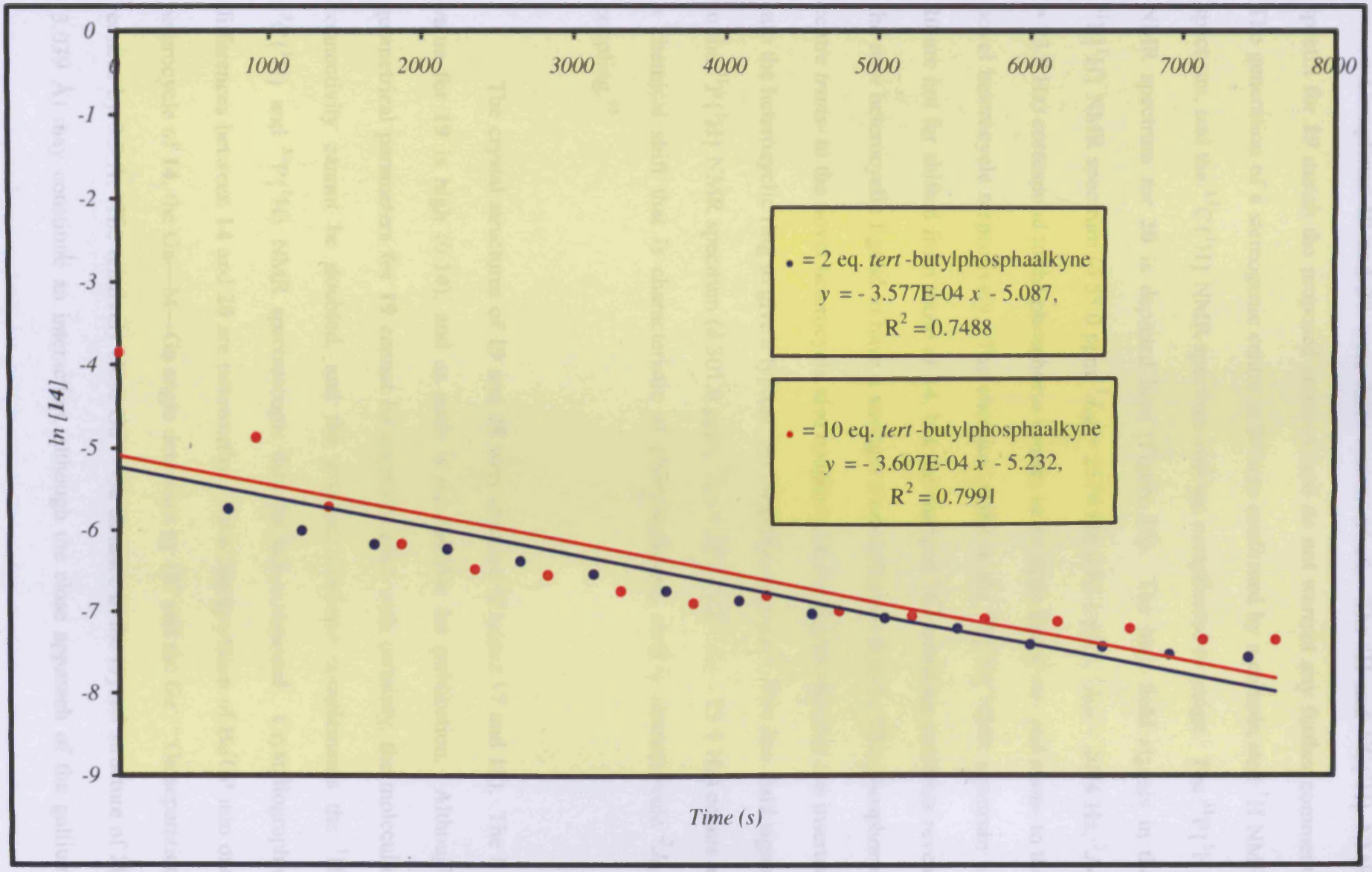

Graph 1 – First order rate equation plot of the formation of **20**

Complexes **19** and **20** were fully characterised. The ^{1}H and $^{13}C\{^{1}H\}$ NMR spectra for **19** match the proposed structure and do not warrant any further comment. The generation of a stereogenic centre in **20** was confirmed by a complicated ^{1}H NMR spectrum, and the $^{13}C\{^{1}H\}$ NMR spectrum was too complicated to assign. The $^{31}P\{^{1}H\}$ NMR spectrum for **20** is depicted here (Figure 16). The high field signals in the $^{31}P\{^{1}H\}$ NMR spectrum (δ 55.0 ppm, $^{1}J_{PtP}$ = 2579 Hz; δ 62.1 ppm, $^{1}J_{PtP}$ = 2094 Hz, $^{3}J_{PP}$ = 23.9 Hz) correspond to the phosphorus centres in the dppe ligand *cis*- and *trans*- to the novel heterocycle respectively. The chemical shifts in the $^{31}P\{^{1}H\}$ NMR spectrum of **20** are not far shifted from those of **14**, but the changed $^{1}J_{PtP}$ coupling constants reveal the new heterocyclic ligand to have a stronger *trans*-influence than **1**. The phosphorus centre *trans*- to the novel heterocycle also couples with the phosphorus that has inserted into the heterocyclic ring to give a typical $^{3}J_{PP}$ coupling constant.[45] The low field signal in the $^{31}P\{^{1}H\}$ NMR spectrum (δ 301.0 ppm, $^{2}J_{PtP}$ = 287.2 Hz, $^{3}J_{PP}$ = 23.9 Hz) occurs at a chemical shift that is characteristic of phosphaalkenes, with a characteristic $^{2}J_{PtP}$ coupling.[45]

The crystal structures of **19** and **20** were obtained (Figures 17 and 18). The R^{1} value for **19** is high (0.14), and as such is not suitable for publication. Although geometrical parameters for **19** cannot be commented on with certainty, the molecular connectivity cannot be doubted, and the structure obtained complements the ^{1}H, $^{13}C\{^{1}H\}$ and $^{31}P\{^{1}H\}$ NMR spectroscopic data for this compound. Crystallographic differences between **14** and **20** are noteworthy. Upon incorporation of Bu^{t}CP into one heterocycle of **14**, the Ga—M—Ga angle decreases by 16° and the Ga·····Ga separation reduces by 0.5 Å. The relatively close Ga·····Ga distance in the crystal structure of **20** (3.039 Å) may constitute an interaction, although the close approach of the gallium

nuclei could be attributed to reduced steric crowding around the platinum centre of **20** compared with that of **14**.

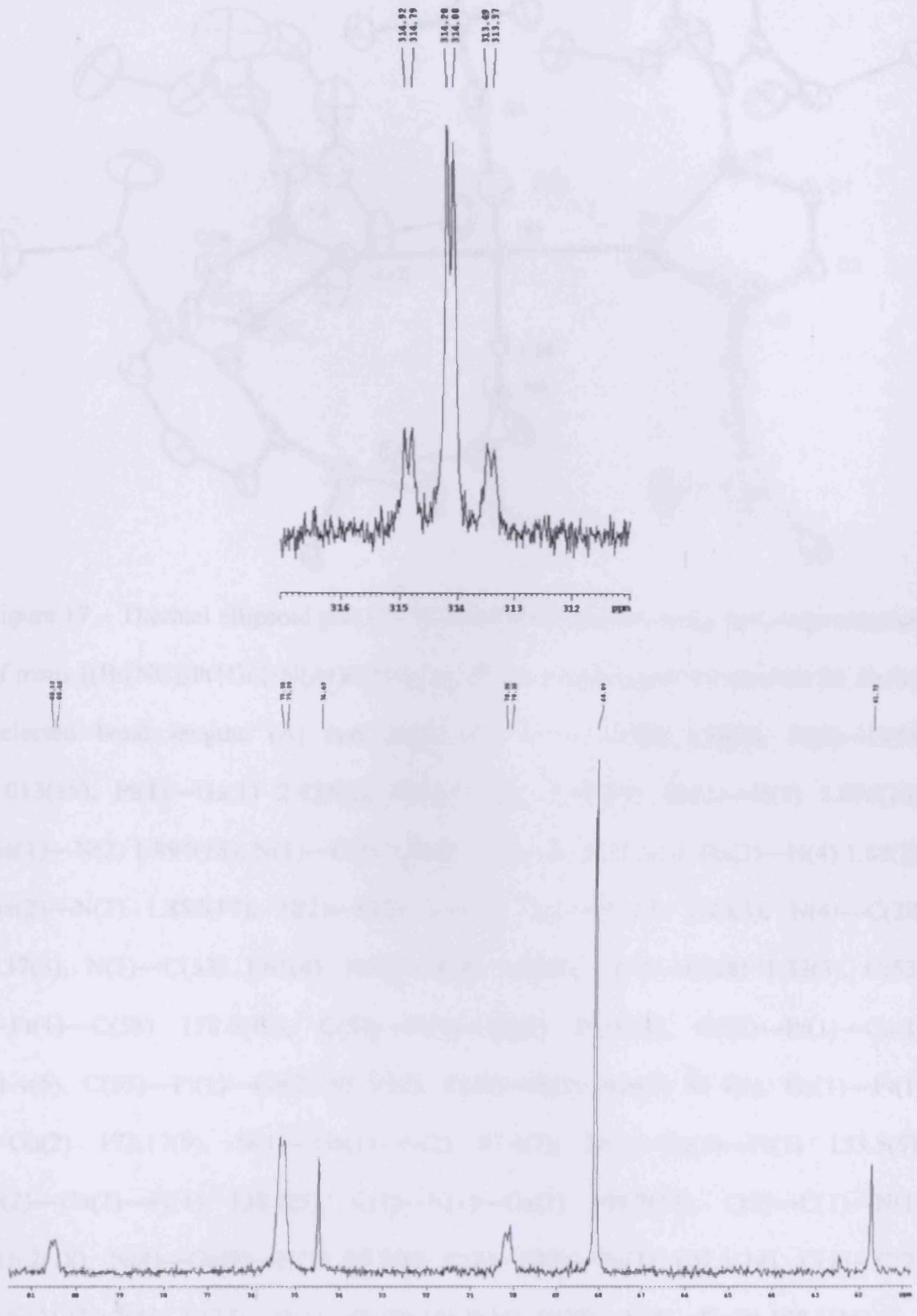

Figure 16 – The $^{31}P\{^{1}H\}$ NMR spectrum of **20**

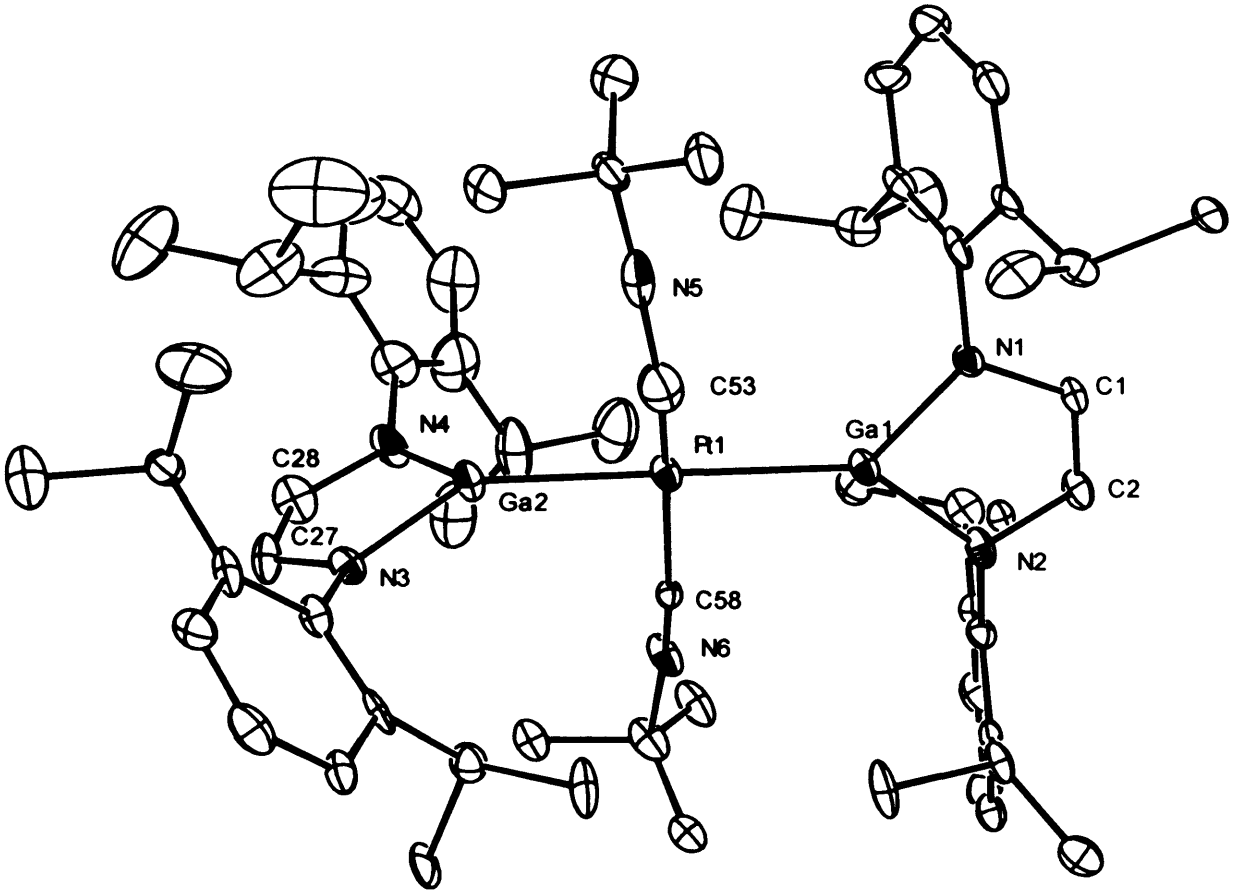

Figure 17 – Thermal ellipsoid plot (25 % probability surface) of the molecular structure of *trans*-[(Bu^tNC)$_2$Pt{Ga{[N(Ar)C(H)]$_2$}}$_2$] **19**; hydrogen atoms are omitted for clarity. Selected bond lengths (Å) and angles (°): Pt(1)—C(53) 1.38(3), Pt(1)—C(58) 2.013(19), Pt(1)—Ga(1) 2.435(2), Pt(1)—Ga(2) 2.441(3), Ga(1)—N(1) 1.876(16), Ga(1)—N(2) 1.894(18), N(1)—C(1) 1.40(2), C(1)—C(2) 1.30(3), Ga(2)—N(4) 1.88(2), Ga(2)—N(3) 1.888(17), N(2)—C(2) 1.40(3), N(3)—C(27) 1.40(3), N(4)—C(28) 1.37(3), N(5)—C(53) 1.61(4), N(6)—C(58) 1.09(2), C(27)—C(28) 1.33(3), C(53)—Pt(1)—C(58) 178.6(13), C(53)—Pt(1)—Ga(1) 89.9(12), C(58)—Pt(1)—Ga(1) 91.4(5), C(53)—Pt(1)—Ga(2) 95.5(12), C(58)—Pt(1)—Ga(2) 83.4(5), Ga(1)—Pt(1)—Ga(2) 172.17(9), N(1)—Ga(1)—N(2) 87.4(7), N(1)—Ga(1)—Pt(1) 133.5(5), N(2)—Ga(1)—Pt(1) 138.1(5), C(1)—N(1)—Ga(1) 109.7(13), C(2)—C(1)—N(1) 116.2(18), N(4)—Ga(2)—N(3) 87.7(8), C(2)—N(2)—Ga(1) 107.5(14), C(1)—C(2)—N(2) 119.3(19), C(27)—N(3)—Ga(2) 108.9(15), C(28)—N(4)—Ga(2) 108.1(16).

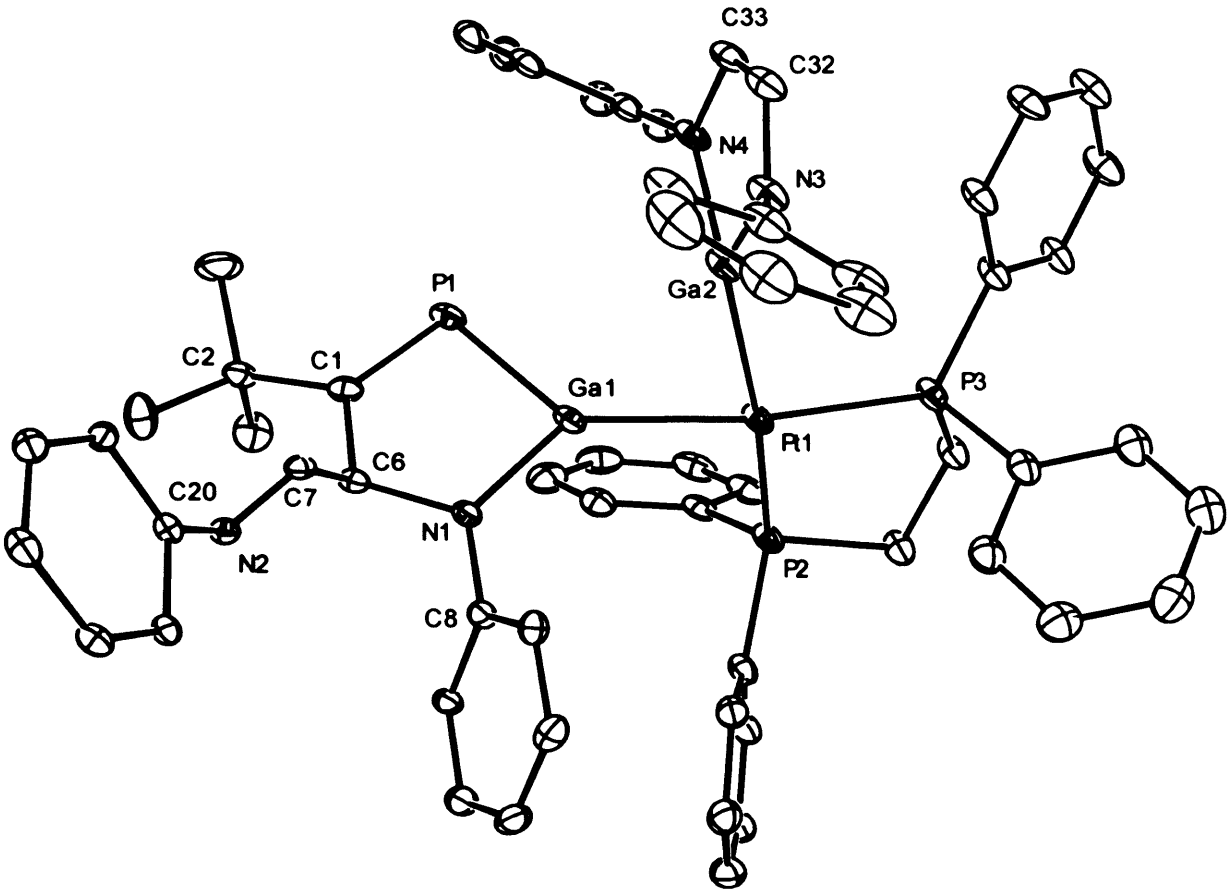

Figure 18 – Thermal ellipsoid plot (25 % probability surface) of the molecular structure of [(dppe)Pt{Ga{[N(Ar)C(H)]$_2$}}{Ga{[PC(Bu^t)C(H)(NAr)C(H)N(Ar)]}}] **20**; hydrogen atoms and isopropyl groups are omitted for clarity. Selected bond lengths (Å) and angles (°): Pt(1)—P(2) 2.2806(17), Pt(1)—P(3) 2.3169(17), Pt(1)—Ga(1) 2.4064(10), Pt(1)—Ga(2) 2.4258(10), Ga(1)—N(1) 1.873(4), Ga(1)—P(1) 2.319(2), P(1)—C(1) 1.701(6), N(1)—C(8) 1.426(7), N(1)—C(6) 1.481(7), N(2)—C(7) 1.261(6), C(1)—C(6) 1.525(8), C(1)—C(2) 1.544(8), C(6)—C(7) 1.516(7), P(2)—Pt(1)—P(3) 86.76(6), P(2)—Pt(1)—Ga(1) 96.19(5), P(3)—Pt(1)—Ga(1) 171.30(5) P(2)—Pt(1)—Ga(2) 167.83(5), P(3)—Pt(1)—Ga(2) 97.58(5), Ga(1)—Pt(1)—Ga(2) 77.95(3), N(1)—Ga(1)—P(1) 93.65(15), N(1)—Ga(1)—Pt(1) 134.76(15), P(1)—Ga(1)—Pt(1) 130.47(5), C(1)—P(1)—Ga(1) 92.3(2), C(6)—N(1)—Ga(1) 115.4(3), C(6)—C(1)—C(2) 116.9(5), C(6)—C(1)—P(1) 123.6(5), C(2)—C(1)—P(1) 119.0(4), N(1)—C(6)—C(7) 105.6(4), N(1)—C(6)—C(1) 113.4(4), C(7)—C(6)—C(1) 114.5(4), N(2)—C(7)—C(6) 120.2(5).

Some interesting bonding can be observed in the altered heterocycle of **20**. As previously mentioned, the novel heterocycle has a shorter Ga—Pt bond length than the other heterocycle, in agreement with the $^{1}J_{PtP}$ coupling constant observed in the $^{31}P\{^{1}H\}$ NMR spectrum. In addition, the P—Ga—N bond angle is more obtuse than the N—Ga—N angle of the other heterocycle, possibly suggesting stronger σ-donor properties. The Ga—N bond length has not changed considerably, and the Ga—P bond length of 2.319 Å and P=C bond length of 1.701 Å are typical.[22] The C—C backbone, originally a double bond in **14**, has undoubtedly become a single bond in the novel heterocycle of **20**, a stereogenic centre.

4.4 Conclusion

To conclude, the synthesis and structural characterisation of square planar nickel, palladium and platinum complexes of a gallium(I) *N*-heterocyclic carbene analogue have been reported. These complexes have had their reactivity studied and compared with *cis*-(bis)boryl complexes of platinum. The *trans*-gallyl complexes synthesised were shown to be relatively unreactive, whilst the *cis*-(bis)gallyl complexes were shown to be unreactive towards non-polar, but reactive towards polar unsaturated organic substrates. Most noteworthy, the addition of Bu^{t}CP to one *cis*-(bis)gallyl complex led to insertion into the gallium(I) heterocycle to form a compound that contains a novel mixed *P*,*N*-heterocyclic gallium(I) ligand. The insertion of Bu^{t}CP has been the subject of a kinetic study, and a mechanism for this process has been proposed. In addition, a *trans*-directing series has been established during the course of these studies, based on $^{1}J_{PtP}$ coupling constants in the $^{31}P\{^{1}H\}$ NMR spectra and bond length observations in crystal structures of the complexes: $B(OR)_2 > H^- > PR_3 \sim [:Ga\{[N(Ar)C(H)]_2\}]^- > Cl^-$.

4.5 Experimental

General experimental procedures are compiled in Appendix 1 and crystallographic data are compiled in Appendix 3. Reproducible microanalyses could not be obtained for most compounds due to their highly air sensitive nature, but the NMR spectra suggested protic impurities of < 5 %. [K(tmeda)][**1**],[2] *cis*-[$(PEt_3)_2PtCl_2$],[46] *cis*-[$(PEt_3)_2Pt(\eta^2\text{-}C_2H_4)$],[47] [(dcpe)$PtCl_2$],[38] [(dppe)$PtCl_2$],[29] [(tmeda)$PdCl_2$],[48] [(dppm)$PdCl_2$],[42] [(dppm)$PtCl_2$],[29] and [$(\eta^4\text{-COD})PtCl_2$][27] were synthesised by literature procedures. All other reagents were used as received.

Preparation of *trans*-[$(PEt_3)_2Ni\{Ga\{[N(Ar)C(H)]_2\}\}_2$] 5: A solution of [K(tmeda)][:Ga{[N(Ar)C(H)]$_2$}] (0.35 g, 0.58 mmol) in THF (10 cm^3) was added to a suspension of *trans*-[$(PEt_3)_2NiCl_2$] (0.09 g, 0.29 mmol) in THF (10 cm^3) at -78 °C to give a deep red solution. The reaction mixture was warmed to 20 °C and stirred overnight. All volatiles were then removed *in vacuo*, the residue washed with hexane (20 cm^3) and extracted into toluene (60 cm^3) and filtered. The filtrate was concentrated to *ca.* 15 cm^3 and stored at -30 °C to give deep red blocks of **5**. Further concentration of the supernatant solution gave another crop of **5** (0.16 g, 47 %). Mp 143-144 °C; ^{1}H NMR (400 MHz, C_6D_6, 298 K): δ 0.76 (t, $^3J_{HH}$ = 7.7 Hz, 18 H, CH_3CH_2), 1.36 (d, $^3J_{HH}$ = 6.5 Hz, 24 H, $(CH_3)_2CH$), 1.42 (d, $^3J_{HH}$ = 6.5 Hz, 24 H, $(CH_3)_2CH$), 1.67 (m, $^3J_{HH}$ = 7.7 Hz, 12 H, CH_2), 3.78 (sept, $^3J_{HH}$ = 6.5 Hz, 8 H, $(CH_3)_2CH$), 6.53 (s, 4 H, NC*H*), 7.22 (m, 4 H, *p*-Ar-*H*) 7.28 (m, 8 H, *m*-Ar-*H*); $^{13}C\{^1H\}$ NMR (75.6 MHz, C_6D_6, 298 K): δ 9.6 (CH_3CH_2), 23.7 (CH_2), 26.1, 28.0 ($(CH_3)_2CH$), 29.0 ($(CH_3)_2CH$), 122.4 (*C*N), 123.7 (*m*-Ar-*C*), 124.2 (*p*-Ar-*C*), 144.2 (*o*-Ar-*C*) 149.1 (*ipso*-Ar-*C*); $^{31}P\{^1H\}$ NMR (121.7 MHz, C_6D_6, 298 K): δ 17.7; MS (EI 70eV), *m/z* (%): 1067 (MH^+ -PEt_3, 6), 892 ([Ga{N(Ar)C(H)}$_2$]$_2H^+$, 3), 445 (Ga{N(Ar)C(H)}$_2H^+$, 41), 378 ({N(Ar)C(H)}$_2H^+$, 23),

333 ({N(Ar)C(H)}$_2$H$^+$ -Pr^i, 100); IR ν/cm^{-1} (Nujol): 1591 s, 1363 m, 1259 m, 1101 m, 1052 m, 1030 m, 892 m; $C_{64}H_{102}N_4P_2NiGa_2$ requires C 64.73, H 8.66, N 4.72; found C 66.37, H 8.80, N 4.55.

Preparation of *trans*-[(PEt$_3$)$_2$Pd{Ga{[N(Ar)C(H)]$_2$}}$_2$] 6: A solution of [K(tmeda)] [:Ga{[N(Ar)C(H)]$_2$}] (0.30 g, 0.50 mmol) in THF (10 cm^3) was added to a suspension of *trans*-[(PEt$_3$)$_2$PdCl$_2$] (0.10 g, 0.25 mmol) in THF (10 cm^3) at -78 °C to give a deep red solution. The reaction mixture was warmed to 20 °C and stirred overnight. All volatiles were then removed *in vacuo*, the residue washed with hexane (20 cm^3) and extracted into toluene (60 cm^3) and filtered. The filtrate was concentrated to *ca.* 15 cm^3 and stored at -30 °C to give deep red blocks of **6**. Further concentration of the supernatant solution gave another crop of **6** (0.20 g, 66 %). Mp 230 °C (decomp.); ^{1}H NMR (400 MHz, C_6D_6, 298 K): δ 0.52 (t, $^3J_{HH}$ = 8.4 Hz, 18 H, C*H*$_3$CH$_2$), 1.14 (d, $^3J_{HH}$ = 6.7 Hz, 24 H, (C*H*$_3$)$_2$CH), 1.22 (d, $^3J_{HH}$ = 6.7 Hz, 24 H, (C*H*$_3$)$_2$CH), 1.46 (m, $^3J_{HH}$ = 8.4 Hz, 12 H, C*H*$_2$), 3.64 (sept, $^3J_{HH}$ = 6.7 Hz, 8 H, (CH$_3$)$_2$ C*H*), 6.38 (s, 4 H, NC*H*) 6.95 (t, $^3J_{HH}$ = 7.5 Hz, 4 H, *p*-Ar-*H*) 7.06 (d, $^3J_{HH}$ = 7.5 Hz, 8 H, *m*-Ar-*H*); ^{13}C{^{1}H} NMR (75.6 MHz, C_6D_6, 298 K): δ 9.2 (*C*H$_3$CH$_2$), 21.1 (*C*H$_2$), 23.5, 26.0 ((*C*H$_3$)$_2$CH), 29.0 ((CH$_3$)$_2$*C*H), 121.9 (*C*N), 123.6, 124.0, 125.4 (*m*-Ar-*C*), 129.0 (*p*-Ar-*C*), 144.1 (*o*-Ar-*C*) 148.8 (*ipso*-Ar-*C*); ^{31}P{^{1}H} NMR (121.7 MHz, C_6D_6, 298 K): δ 22.7; MS (EI 70eV), *m/z* (%): 892 ([Ga{N(Ar)C(H)}$_2$]$_2$H$^+$, 8), 445 (Ga{N(Ar)C(H)}$_2$H$^+$, 100), 378 ({N(Ar)C(H)}$_2$H$^+$, 4), 333 ({N(Ar)C(H)}$_2$H$^+$ -Pr^i, 56); IR ν/cm^{-1} (Nujol): 1591 s, 1363 m, 1319 m, 1258 m, 1101 m, 1055 m, 894 m; $C_{64}H_{102}N_4P_2PdGa_2$ requires C 62.22, H 8.32, N 4.54; found C 63.46, H 8.24, N 4.34.

Preparation of *trans*-[(PEt$_3$)$_2$Pd{Ga{[N(Ar)C(H)]$_2$}}Cl] 10 : This compound appeared in the reaction mixture of **6** as a minor product. A small amount of **10** was isolated and the crystal structure obtained. $^{31}P\{^1H\}$ NMR (121.7 MHz, D_2O, 298 K): δ 21.5.

Preparation of *trans*-[(PEt$_3$)$_2$Pt{Ga{[N(Ar)C(H)]$_2$}}$_2$] 7: A solution of [K(tmeda)][:Ga{[N(Ar)C(H)]$_2$}] (0.31 g, 0.51 mmol) in THF (10 cm^3) was added to a suspension of *cis*-[(PEt$_3$)$_2$PtCl$_2$] (0.13 g, 0.26 mmol) in THF (10 cm^3) at -78 °C to give a deep red solution. The reaction mixture was warmed to 20 °C and stirred overnight. All volatiles were then removed *in vacuo*, the residue washed with hexane (20 cm^3) and extracted into toluene (60 cm^3) and filtered. The filtrate was concentrated to *ca.* 15 cm^3 and stored at -30 °C to give deep red blocks of **7**. Further concentration of the supernatant solution gave another crop of **7** (0.15 g, 44 %). Mp 275 °C (decomp.); ^1H NMR (400 MHz, C_6D_6, 298 K): δ 0.69 (t, $^3J_{HH}$ = 8.4 Hz, 18 H, C*H*$_3$CH$_2$), 1.39 (d, $^3J_{HH}$ = 6.7 Hz, 24 H, (C*H*$_3$)$_2$CH), 1.43 (d, $^3J_{HH}$ = 6.7 Hz, 24 H, (C*H*$_3$)$_2$CH), 1.81 (m, $^3J_{HH}$ = 8.4 Hz, 12 H, C*H*$_2$), 3.74 (sept, $^3J_{HH}$ = 6.7 Hz, 8 H, (CH$_3$)$_2$ C*H*), 6.62 (s, 4 H, NC*H*) 7.20 (t, $^3J_{HH}$ = 6.2 Hz, 4 H, *p*-Ar-*H*) 7.27 (d, $^3J_{HH}$ = 6.2 Hz, 8 H, *m*-Ar-*H*); $^{13}C\{^1H\}$ NMR (75.6 MHz, C_6D_6, 298 K): δ 9.3 (*C*H$_3$CH$_2$), 23.5 (*C*H$_2$), 25.9, 26.0 ((*C*H$_3$)$_2$CH), 28.9 ((CH$_3$)$_2$*C*H), 121.8 (*C*N), 123.6 (*m*-Ar-*C*), 124.3 (*p*-Ar-*C*), 144.1 (*o*-Ar-*C*) 148.8 (*ipso*-Ar-*C*); $^{31}P\{^1H\}$ NMR (121.7 MHz, C_6D_6, 298 K): δ 14.2 ($^1J_{PtP}$ = 2256 Hz); MS (EI 70eV), *m/z* (%):1324 (MH$^+$, 1), 333 ({N(Ar)C(H)}$_2$H$^+$ -Pr^i, 100); IR ν/cm^{-1} (Nujol): 1592 s, 1318 m, 1250 m, 1101 m, 1055 m, 1032 m, 894 m; $C_{71}H_{110}N_4P_2PtGa_2$ (1 toluene in lattice) requires C 58.06, H 7.76, N 4.23; found C 59.42, H 7.72, N 4.21.

Preparation of *cis*-[(PEt$_3$)$_2$Pt{Ga{[N(Ar)C(H)]$_2$}}$_2$] 8 : This compound appeared in the reaction mixture of **7** as a minor product. A small amount of **8** was isolated and the

crystal structure obtained. $^{31}P\{^{1}H\}$ NMR (121.7 MHz, D_2O, 298 K): δ 9.3 ($^{1}J_{PtP}$ = 2549 Hz).

Preparation of *trans*-[$(PEt_3)_2Ni\{Ga\{[N(Ar)C(H)]_2\}\}Cl$] 9: A solution of [K(tmeda)][:Ga{[N(Ar)C(H)]$_2$}] (0.30 g, 0.50 mmol) in THF (10 cm^3) was added to a suspension of *trans*-[$(PEt_3)_2NiCl_2$] (0.15 g, 0.50 mmol) in THF (10 cm^3) at -78 °C to give a deep red solution. The reaction mixture was warmed to 20 °C and stirred overnight. All volatiles were then removed *in vacuo*, the residue washed with hexane (20 cm^3) and extracted into toluene (60 cm^3) and filtered. The filtrate was concentrated to *ca.* 15 cm^3 and stored at -30 °C to give deep red blocks of **9**. Further concentration of the supernatant solution gave another crop of **9** (0.17 g, 44 %). Mp 105-106 °C (decomp.); ^{1}H NMR (400 MHz, C_6D_6, 298 K): δ 1.03 (t, $^{3}J_{HH}$ = 7.8 Hz, 18 H, CH_3CH_2), 1.42 (d, $^{3}J_{HH}$ = 6.7 Hz, 12 H, $(CH_3)_2CH$), 1.48 (d, $^{3}J_{HH}$ = 6.7 Hz, 12 H, $(CH_3)_2CH$), 1.68 (m, $^{3}J_{HH}$ = 7.8 Hz, 12 H, CH_2), 4.06 (sept, $^{3}J_{HH}$ = 6.7 Hz, 4 H, $(CH_3)_2$ CH), 6.59 (s, 2 H, NC*H*), 7.27 (t, $^{3}J_{HH}$ = 7.5 Hz, 2 H, *p*-Ar-*H*) 7.33 (d, $^{3}J_{HH}$ = 7.5 Hz, 4 H, *m*-Ar-*H*); $^{13}C\{^{1}H\}$ NMR (75.6 MHz, C_6D_6, 298 K): δ 8.8 (CH_3CH_2), 17.8 (CH_2), 23.5, 26.1 ($(CH_3)_2CH$), 29.0 ($(CH_3)_2CH$), 121.3 (*C*N), 123.8 (*m*-Ar-*C*), 128.1 (*p*-Ar-*C*), 143.5 (*o*-Ar-*C*) 147.6 (*ipso*-Ar-*C*); $^{31}P\{^{1}H\}$ NMR (121.7 MHz, C_6D_6, 298 K): δ 13.9 ; MS (EI 70eV), *m/z* (%): 892 ($[Ga\{N(Ar)C(H)\}_2]_2H^+$, 1), 445 ($Ga\{N(Ar)C(H)\}_2H^+$, 3), 378 ($\{N(Ar)C(H)\}_2H^+$, 37), 333 ($\{N(Ar)C(H)\}_2H^+$ -Pr^i, 100); IR ν/cm^{-1} (Nujol): 1594 s, 1363 m, 1318 m, 1258 m, 1202 m, 1112 m, 1057 m, 1032 m, 931 m, 896 m; $C_{38}H_{66}N_2P_2ClNiGa_2$ requires C 58.76, H 8.56, N 3.60; found C 58.39, H 8.71, N 3.70.

Preparation of [(dcpe)Pt{Ga{[N(Ar)C(H)]$_2$}}Cl] 12: A solution of [K(tmeda)][:Ga{[N(Ar)C(H)]$_2$}] (0.13 g, 0.22 mmol) in THF (10 cm^3) was added to a suspension of [(dcpe)$PtCl_2$] (0.15 g, 0.22 mmol) in THF (10 cm^3) at -78 °C to give a deep yellow

reaction mixture. The reaction mixture was warmed to 20 °C and stirred overnight, becoming orange in colour. All volatiles were then removed *in vacuo*, the residue washed with hexane (30 cm^3) and extracted into diethyl ether (70 cm^3) and filtered. The filtrate was concentrated to *ca.* 15 cm^3 and stored at -30 °C to give yellow blocks of **12**. Further concentration of the supernatant solution gave another crop of **12** (0.09 g, 38 %). Mp 278-280 °C (decomp.); ^1H NMR (400 MHz, C_6D_6, 298 K): δ 0.77-2.08 (m, 48H, Cy-*H* and PCH_2), 1.37 (d, $^3J_{HH}$ = 6.6 Hz, 12 H, $(CH_3)_2CH$), 1.40 (d, $^3J_{HH}$ = 6.6 Hz, 12 H, $(CH_3)_2CH$), 4.08 (br. m, 4 H, $(CH_3)_2CH$), 6.37 (s, 2 H, NC*H*), 7.08 (t, $^3J_{HH}$ = 7.6 Hz, 2 H, *p*-Ar-H) 7.17 (d, $^3J_{HH}$ = 7.6 Hz, 4 H, *m*-Ar-H); $^{13}C\{^1H\}$ NMR (75.6 MHz, C_6D_6, 298 K): too complicated to assign due to overlapping signals and couplings; $^{31}P\{^1H\}$ NMR (121.7 MHz, C_6D_6, 298 K) δ 69.4 ($^1J_{PtP}$ = 3620 Hz, *trans*-Cl), 72.2 ($^1J_{PtP}$ = 2088 Hz, *trans*-gallyl); MS (EI 70eV), *m/z* (%): 1098 (MH^+, 100), 1063 (MH^+ -Cl, 11), 616 ((dcpe)PtH^+, 30), 333 ($\{N(Ar)C(H)\}_2H^+$ -Pr^i, 19); IR ν/cm^{-1} (Nujol): 1590 m, 1352 m, 1326 m, 1259 m, 1111 m, 798 m; EI acc. mass on M^+: calc. for $C_{52}H_{84}N_2P_2ClPtGa$: 1097.4646, found 1097.4697; $C_{52}H_{84}N_2P_2ClPtGa$ requires C 56.81, H 7.70, N 2.55; found C 55.97, H 8.05, N 2.58.

Preparation of [(dppe)Pt{Ga{[N(Ar)C(H)]$_2$}}Cl] 13: A solution of [K(tmeda)] [:Ga{[N(Ar)C(H)]$_2$}] (0.20 g, 0.33 mmol) in THF (10 cm^3) was added to a suspension of [(dppe)$PtCl_2$] (0.22 g, 0.33 mmol) in THF (10 cm^3) at -78 °C to give an orange reaction mixture. The reaction mixture was warmed to 20 °C and stirred overnight, becoming red in colour. All volatiles were then removed *in vacuo*, the residue washed with hexane (20 cm^3) and extracted into diethyl ether (40 cm^3) and filtered. The filtrate was concentrated to *ca.* 15 cm^3 and stored at -30 °C to give red blocks of **13**. Further concentration of the supernatant solution gave another crop of **13** (0.07 g, 20 %). Mp 153-154 °C; ^1H NMR (400 MHz, C_6D_6, 298 K): δ 0.99 (d, $^3J_{HH}$ = 6.9 Hz, 12 H,

(CH_3)$_2$CH), 1.20 (d, $^3J_{HH}$ = 6.9 Hz, 12 H, (CH_3)$_2$CH), 1.53 (m, 4 H, CH_2P), 3.73 (br. m, 4 H, (CH_3)$_2$C*H*), 6.12 (s, 2 H, NC*H*), 6.60-7.46 (m, 26 H, Ar-*H*); ^{13}C{^{1}H} NMR (75.6 MHz, C_6D_6, 298 K): too complicated to assign due to overlapping signals and couplings; ^{31}P{^{1}H} NMR (121.7 MHz, C_6D_6, 298 K) δ 44.0 ($^1J_{PtP}$ = 3788 Hz, *trans*-Cl), 51.4 ($^1J_{PtP}$ = 2023 Hz, *trans*-gallyl); MS (EI 70eV), *m/z* (%): 1074 (MH^+, 2), 333 ({N(Ar)C(H)}$_2H^+$ -Pr^i, 100); IR ν/cm^{-1} (Nujol): 1591 m, 1564 m, 1435 m, 1351 m, 1262 m, 1106 m; EI acc. mass on M^+: calc. for $C_{52}H_{60}N_2P_2ClPtGa$: 1073.2818, found 1073.2812.

Preparation of [(dppe)Pt{Ga{[N(Ar)C(H)]$_2$}}$_2$] 14: A solution of [K(tmeda)][:Ga{[N(Ar)C(H)]$_2$}] (0.61 g, 1 mmol) in THF (20 cm^3) was added to a suspension of [(dppe)PtCl$_2$] (0.34 g, 0.5 mmol) in THF (20 cm^3) at -78 °C to give a deep yellow reaction mixture. The reaction mixture was warmed to 20 °C and stirred overnight, becoming deep red in colour. All volatiles were then removed *in vacuo*, the residue washed with hexane (20 cm^3) and extracted into diethyl ether (60 cm^3) and filtered. The filtrate was concentrated to *ca.* 15 cm^3 and stored at -30 °C to give dark red blocks of **14**. Further concentration of the supernatant solution gave another crop of **14** (0.48 g, 62 %). Mp 263-264 °C (decomp.); ^{1}H NMR (400 MHz, C_6D_6, 298 K): δ 1.23 (overlapping d, 48 H, (CH_3)$_2$CH), 1.58 (m, 4 H, CH_2P), 3.56 (br. m, 4 H, (CH_3)$_2$C*H*), 3.67 (br. m, 4 H, (CH_3)$_2$C*H*), 6.38 (br. s, 4 H, NC*H*), 7.07-7.50 (m, 32 H, Ar-*H*); ^{13}C{^{1}H} NMR (75.6 MHz, C_6D_6, 298 K): too complicated to assign due to overlapping signals and couplings; ^{31}P{^{1}H} NMR (121.7 MHz, C_6D_6, 298 K) δ 47.4 ($^1J_{PtP}$ = 2316 Hz); MS (EI 70eV), *m/z* (%): 445 (Ga{N(Ar)C(H)}$_2H^+$, 4), 378 ({N(Ar)C(H)}$_2H^+$, 10), 333 ({N(Ar)C(H)}$_2H^+$ -Pr^i, 100); IR ν/cm^{-1} (Nujol): 1592 m, 1357 m, 1315 m, 1254 m, 1202 m, 1108 m; $C_{78}H_{96}Ga_2N_4P_2Pt$ requires C 63.04, H 6.51, N 3.77; found C 60.68, H 6.87, N 3.55.

Preparation of [(tmeda)Pd{Ga{[N(Ar)C(H)]$_2$}}$_2$] 15: A solution of [K(tmeda)][:Ga{[N(Ar)C(H)]$_2$}] (0.35 g, 0.58 mmol) in THF (10 cm^3) was added to a suspension of [(tmeda)PdCl$_2$] (0.09 g, 0.29 mmol) in THF (10 cm^3) at -78 °C to give a deep orange reaction mixture. The reaction mixture was warmed to 20 °C and stirred overnight. All volatiles were then removed *in vacuo* and the residue washed with hexane (20 cm^3). The product was extracted into toluene (40 cm^3) and filtered. The filtrate was concentrated to *ca.* 15 cm^3 and stored at -30 °C to give red blocks of **15**. Further concentration of the supernatant solution gave another crop of **15** (0.04 g, 13 %). Mp 145-146 °C; ^{1}H NMR (400 MHz, C_6D_6, 298 K): δ 1.08 (d, $^3J_{HH}$ = 6.8 Hz, 6 H, (C*H*$_3$)$_2$CH), 1.27 (v. t, $^3J_{HH}$ = 6.8 Hz, 12 H, (C*H*$_3$)$_2$CH), 1.36 (d, $^3J_{HH}$ = 6.8 Hz, 6 H, (C*H*$_3$)$_2$CH), 1.37 (m, 12 H, (C*H*$_3$)$_2$N), 1.38 (m, 4 H, C*H*$_2$N), 1.51 (v. t, $^3J_{HH}$ = 6.8 Hz, 12 H, (C*H*$_3$)$_2$CH), 1.62 (v. t, $^3J_{HH}$ = 6.8 Hz, 12 H, (C*H*$_3$)$_2$CH), 3.28 (2 overlapping sept, $^3J_{HH}$ = 6.8 Hz, 4 H, (CH$_3$)$_2$C*H*), 3.86 (sept, $^3J_{HH}$ = 6.8 Hz, 2 H, (CH$_3$)$_2$C*H*), 4.24 (sept, $^3J_{HH}$ = 6.8 Hz, 2 H, (CH$_3$)$_2$C*H*), 6.17 (d, $^3J_{HH}$ = 3.7 Hz, 2 H, NC*H*), 6.44 (d, $^3J_{HH}$ = 3.7 Hz, 2 H, NC*H*), 7.13-7.48 (m, 12 H, *p*-Ar-*H*); MS (EI 70eV), *m/z* (%): 445 (Ga{N(Ar)C(H)}$_2$H$^+$, 62), 378 ({N(Ar)C(H)}$_2$H$^+$, 8), 333 ({N(Ar)C(H)}$_2$H$^+$ -Pr^i, 100); IR ν/cm^{-1} (Nujol): 1584 m, 1260 m, 1091 m, 1025 m, 872 m, 739 m, 691 m.

Preparation of [(dppm)Pd{Ga{[N(Ar)C(H)]$_2$}}$_2$] 16: A solution of [K(tmeda)][:Ga{[N(Ar)C(H)]$_2$}] (0.30 g, 0.50 mmol) in THF (10 cm^3) was added to a suspension of [(dppm)PdCl$_2$] (0.14 g, 0.25 mmol) in THF (10 cm^3) at -78 °C to give a yellow reaction mixture. The reaction mixture was warmed to 20 °C and stirred overnight, becoming darker. All volatiles were then removed *in vacuo*, the residue washed with hexane (20 cm^3) and extracted into diethyl ether (80 cm^3) and filtered. The filtrate was concentrated to *ca.* 15 cm^3 and stored at -30 °C to give red blocks of **16**. Further concentration of the supernatant solution gave another crop of **16** (0.11 g, 32 %). Mp

108 °C (decomp.); ^{1}H NMR (400 MHz, C_6D_6, 298 K): δ 1.10 (overlapping d's, 48H, $(CH_3)_2CH$), 3.14 (sept, $^{3}J_{HH}$ = 6.9 Hz, 4 H, $(CH_3)_2CH$), 3.30 (sept, $^{3}J_{HH}$ = 6.9 Hz, 4 H, $(CH_3)_2CH$), 4.10 (br. m, 2H, PCH_2), 6.10 (s, 4 H, NCH), 6.31-7.32 (m, 32 H, Ar-H); ^{13}C{^{1}H} NMR (75.6 MHz, C_6D_6, 298 K): too complicated to assign due to overlapping signals and couplings; ^{31}P{^{1}H} NMR (121.7 MHz, C_6D_6, 298 K) δ 22.6; MS (EI 70eV), *m/z* (%): 445 ($Ga\{N(Ar)C(H)\}_2H^+$, 24), 378 ($\{N(Ar)C(H)\}_2H^+$, 11), 333 ($\{N(Ar)C(H)\}_2H^+$-Pr^{i}, 100); IR ν/cm^{-1} (Nujol): 1659 m, 1625 m, 1592 m, 1314 m, 1254 m, 1101 m, 1056 m.

Preparation of [(dppm)Pt{Ga{[N(Ar)C(H)]$_2$}}$_2$] 17: A solution of [K(tmeda)] [:Ga{[N(Ar)C(H)]$_2$}] (0.60 g, 1.00 mmol) in THF (20 cm^3) was added to a suspension of [(dppm)PtCl$_2$] (0.32 g, 0.50 mmol) in THF (20 cm^3) at -78 °C to give a yellow reaction mixture. The reaction mixture was warmed to 20 °C and stirred overnight, becoming deep red in colour. All volatiles were then removed *in vacuo*, the residue washed with hexane (20 cm^3) and extracted into toluene (80 cm^3) and filtered. The filtrate was concentrated to *ca.* 15 cm^3 and stored at -30 °C to give red blocks of **17**. Further concentration of the supernatant solution gave another crop of **17** (0.20 g, 28 %). Mp 105 °C (decomp.); ^{1}H NMR (400 MHz, C_6D_6, 298 K): δ 1.04 (overlapping d's, 48H, $(CH_3)_2CH$), 3.00 (sept, $^{3}J_{HH}$ = 6.9 Hz, 4 H, $(CH_3)_2CH$), 3.29 (sept, $^{3}J_{HH}$ = 6.9 Hz, 4 H, $(CH_3)_2CH$), 3.99 (br. m, 2H, PCH_2), 6.10 (s, 4 H, NCH), 6.55-7.22 (m, 32 H, Ar-H); ^{13}C{^{1}H} NMR (75.6 MHz, C_6D_6, 298 K): too complicated to assign due to overlapping signals and couplings; ^{31}P{^{1}H} NMR (121.7 MHz, C_6D_6, 298 K) δ -23.8 ($^{1}J_{PtP}$ = 1933 Hz); MS (EI 70eV), *m/z* (%): 378 ($\{N(Ar)C(H)\}_2H^+$, 4), 333 ($\{N(Ar)C(H)\}_2H^+$-Pr^{i}, 100); IR ν/cm^{-1} (Nujol): 1619 m, 1588 m, 1314 m, 1249 m, 1202 m, 1108 m.

Preparation of [(η^4-COD)Pt{Ga{[N(Ar)C(H)]$_2$}}$_2$] 18: A solution of [K(tmeda)][:Ga{[N(Ar)C(H)]$_2$}] (0.32 g, 0.54 mmol) in THF (10 cm^3) was added to a suspension of [(η^4-COD)PtCl$_2$] (0.10 g, 0.27 mmol) in THF (10 cm^3) at -78 °C to give a deep yellow reaction mixture. The reaction mixture was warmed to 20 °C and stirred overnight. All volatiles were then removed *in vacuo* and the residue extracted into hexane (40 cm^3) and filtered. The filtrate was concentrated to *ca.* 15 cm^3 and stored at -30 °C to give deep turquoise blocks of **18**. Further concentration of the supernatant solution gave another crop of **18** (0.14 g, 44 %). Mp 108 °C (decomp.); ^{1}H NMR (400 MHz, C_6D_6, 298 K): δ 0.59 (d, $^3J_{HH}$ = 6.7 Hz, 6 H, (C*H*$_3$)$_2$CH), 1.24 (d, $^3J_{HH}$ = 6.7 Hz, 6 H, (C*H*$_3$)$_2$CH), 1.34 (d, $^3J_{HH}$ = 6.7 Hz, 12 H, (C*H*$_3$)$_2$CH), 1.35 (m, 4 H, C*H*$_2$), 1.46 (d, $^3J_{HH}$ = 6.7 Hz, 6 H, (C*H*$_3$)$_2$CH), 1.52 (d, $^3J_{HH}$ = 6.7 Hz, 6 H, (C*H*$_3$)$_2$CH), 1.60 (d, $^3J_{HH}$ = 6.7 Hz, 6 H, (C*H*$_3$)$_2$CH), 1.66 (d, $^3J_{HH}$ = 6.7 Hz, 6 H, (C*H*$_3$)$_2$CH), 3.25 (sept, $^3J_{HH}$ = 6.7 Hz, 2 H, (CH$_3$)$_2$C*H*), 3.44 (sept, $^3J_{HH}$ = 6.7 Hz, 2 H, (CH$_3$)$_2$C*H*), 3.68 (sept, $^3J_{HH}$ = 6.7 Hz, 2 H, (CH$_3$)$_2$C*H*), 4.43 (sept, $^3J_{HH}$ = 6.7 Hz, 2 H, (CH$_3$)$_2$C*H*), 4.96 (br. m, $^2J_{PtH}$ = 53 Hz, 2 H, CH$_2$C*H*), 5.68 (br. m, $^2J_{PtH}$ = 43 Hz, 2 H, CH$_2$C*H*), 6.37 (d, $^3J_{HH}$ = 3.5 Hz, 2 H, NC*H*), 6.50 (d, $^3J_{HH}$ = 3.5 Hz, 2 H, NC*H*), 7.18 - 7.40 (m, 12 H, Ar-*H*); ^{13}C{^{1}H} NMR (75.6 MHz, C_6D_6, 298 K): δ 23.1, 24.6, 24.7, 24.8, 25.2, 26.1, 26.4, 27.2 ((*C*H$_3$)$_2$CH), 27.4, 27.5, 28.2, 28.3 ((CH$_3$)$_2$*C*H), 28.8, 30.5 (*C*H$_2$), 100.2 ($^1J_{PtC}$ = 43 Hz, CH$_2$*C*H), 103.3 ($^1J_{PtC}$ = 40 Hz, *C*H$_2$CH), 122.9, 123.0 (*C*N), 123.1, 123.3 (*p*-Ar-*C*), 123.9, 124.0, 124.4, 125.7 (*m*-Ar-*C*), 144.6, 145.3, 145.8, 145.9 (*o*-Ar-*C*), 146.2, 146.4 (*ipso*-Ar-*C*); MS (EI 70eV), *m/z* (%): 1196 (MH$^+$, 4), 378 ({N(Ar)C(H)}$_2$H$^+$, 5), 333 ({N(Ar)C(H)}$_2$H$^+$ -Pr^i, 100); IR ν/cm^{-1} (Nujol): 1590 m, 1352 s, 1326 s, 1259 m, 1111 m, 798 m; EI acc. mass on M$^+$: calc. for $C_{60}H_{84}N_4PtGa_2$: 1193.4850, found 1193.4848; $C_{60}H_{84}N_4PtGa_2$ requires C 60.26, H 7.08, N 4.68; found C 58.05, H 6.90, N 4.68.

Preparation of *trans*-[(Bu^{t}NC)$_2$Pt{Ga{[N(Ar)C(H)]$_2$}}$_2$] 19: CNBu^t (70 μl, 0.62 mmol) was added to a solution of [(dppe)Pt{Ga{[N(Ar)C(H)]$_2$}}$_2$] (0.10 g, 0.06 mmol) in THF (10 cm^3) at -78 °C via a microsyringe. The purple reaction mixture was warmed to 20 °C and stirred for. All volatiles were removed *in vacuo* and the residue exracted into hexane (20 cm^3) and filtered. The filtrate was concentrated to *ca.* 15 cm^3 and stored at -30 °C to give purple needles of **19** (0.04 g, 50 %). Mp 91-92 °C; ^{1}H NMR (400 MHz, C_6D_6, 298 K): δ 0.70 (s, 18 H, (C*H*$_3$)$_3$C), 1.14 (d, $^3J_{HH}$ = 6.7 Hz, 24 H, (C*H*$_3$)$_2$CH), 1.29 (d, $^3J_{HH}$ = 6.7 Hz, 24 H, (C*H*$_3$)$_2$CH), 3.73 (sept, $^3J_{HH}$ = 6.7 Hz, 8 H, (CH$_3$)$_2$C*H*), 6.34 (s, 4 H, NC*H*) 6.95-7.12 (m, 12H, Ar-*H*); ^{13}C{^{1}H} NMR (75.6 MHz, C_6D_6, 298 K): δ 24.9, 25.3 ((*C*H$_3$)$_2$CH), 28.1 ((CH$_3$)$_2$*C*H), 33.9 ((*C*H$_3$)$_3$C), 55.8 ((CH$_3$)$_3$*C*), 122.7 (*C*N), 123.7 (*m*-Ar-*C*), 124.7 (*p*-Ar-*C*), 144.9 (*o*-Ar-*C*) 147.0 (*ipso*-Ar-*C*), 149.2 (*C*≡N); MS (EI 70eV), *m/z* (%): 378 ({N(Ar)C(H)}$_2$H$^+$, 36), 333 ({N(Ar)C(H)}$_2$H$^+$ -Pr^i, 100); IR ν/cm^{-1} (Nujol): 2150 s (C≡N), 1588 m, 1260 m, 1204 m, 1100 m.

Preparation of [(dppe)Pt{Ga{[N(Ar)C(H)]$_2$}}{Ga{PC(Bu^t)C(H)(NAr)C(H)N(Ar)}}] 20: PCBu^t (100 μl, 0.63 mmol) was added to a solution of [(dppe)Pt{Ga{[N(Ar)C(H)]$_2$}}$_2$] (0.10 g, 0.07 mmol) in THF (10 cm^3) at -78 °C to give a deep red reaction mixture. The reaction mixture was warmed to 20 °C and stirred overnight. All volatiles were removed *in vacuo*, and the residue extracted into hexane (20 cm^3) and filtered. The filtrate was concentrated to *ca.* 20 cm^3 and stored at -30 °C to give deep red rods of **20**. Further concentration of the supernatant solution gave another crop of **20** (0.06 g, 54 %). Mp 225 °C (decomp.); ^{1}H NMR (500 MHz, C_6D_6, 298 K): δ 1.34 (centred overlapping d's, 48H, (C*H*$_3$)$_2$CH), 1.72 (s, 9H, (C*H*$_3$)$_3$C), 3.63 (overlapping m, 8H, (CH$_3$)$_2$C*H*), 3.94 (m, 1 H, C*H* chiral), 5.80 (s, 2 H, NC*H*), 6.67-7.49 (m, 32H, Ar-*H*), 8.02 (m, 1H, NC*H*); ^{13}C{^{1}H} NMR (75.6 MHz, C_6D_6, 298 K): too

complicated to assign due to overlapping signals and couplings; $^{31}P\{^{1}H\}$ NMR (121.7 MHz, C_6D_6, 298 K): δ 55.0 ($^{1}J_{PtP}$ = 2579 Hz, *trans*-gallyl), 62.1 ($^{1}J_{PtP}$ = 2094 Hz, $^{3}J_{PP}$ = 23.9 Hz, *trans*-PNgallyl), 301.0 ($^{2}J_{PtP}$ = 287.2 Hz, $^{3}J_{PP}$ = 23.9 Hz, P=C); MS (EI 70eV), *m/z* (%): 1040 [MH^+-Ga{N(Ar)C(H)}$_2$Bu^{t}CP, 32], 445 (Ga{N(Ar)C(H)}$_2H^+$, 52), 378 ({N(Ar)C(H)}$_2H^+$, 44); IR ν/cm^{-1} (Nujol): 1592 m, 1561 m, 1261 m, 1102 m.

4.6 References

1. R. J. Baker, C. Jones, *Coord. Chem. Rev.*, 2005, **249**, 1857, and references therein.
2. R. J. Baker, R. D. Farley, C. Jones, M. Kloth and D. M. Murphy, *Dalton Trans.*, 2002, 3844.
3. (a) H. Braunschweig, C. Kollann, D. Rais, *Angew. Chem. Int. Ed.*, 2006, **45**, 5254; (b) S. Aldridge, D. L. Coombs, *Coord. Chem. Rev.*, 2004, **248**, 535; (c) H. Braunschweig, M. Colling, *Coord. Chem. Rev.*, 2001, **223**, 1; (d) T. Ishiyama, N. Miyaura, *J. Organomet. Chem.*, 2000, **611**, 392; (e) T. B. Marder, N. C. Norman, *Top. Catal.*, 1998, **5**, 63; (f) G. J. Irvine, M. J. G. Lesley, T. B. Marder, N. C. Norman, C. R. Rice, E. G. Robins, W. R. Roper, G. R. Whittell, L. J. Wright, *Chem. Rev.*, 1998, **98**, 2685; (g) H. Braunschweig, *Angew. Chem. Int. Ed.*, 1998, **37**, 1786, and references therein.
4. (a) C. N. Iverson, M. R. Smith III, *J. Am. Chem. Soc.*, 1995, **117**, 4403; (b) G. Lesley, P. Nguyen, N. J. Taylor, T. B. Marder, A. J. Scott, W. Clegg, N. C. Norman, *Organometallics*, 1996, **15**, 5137.
5. T. Ishiyama, N. Matsuda, M. Murata, F. Ozawa, A. Suzuki, N. Miyaura, *Organometallics*, 1996, **15**, 713.
6. C. N. Iverson, M. R. Smith III, *Organometallics*, 1997, **16**, 2757.

7. S. P. Green, C. Jones, D. P. Mills, A. Stasch, *Organometallics*, 2007, **26**, 3424.

8. B. E. Mann, A. Musco, *Dalton Trans.*, 1975, 1673.

9. C. A. Tolman, W. C. Seidel, D. H. Gerlach, *J. Am. Chem. Soc.*, 1972, **94**, 2689.

10. R. J. Baker, R. D. Farley, C. Jones, M. Kloth, D. P. Mills, D. M. Murphy, *Chem. Eur. J.*, 2005, **11**, 2972.

11. This compound was previously prepared *via* a different synthetic route: T. Pott, P. Jutzi, W. W. Schoeller, A. Stammler, H. –G. Stammler, *Organometallics*, 2001, **20**, 5492.

12. S. O. Grim, R. L. Keiter, W. McFarlane, *Inorg. Chem.*, 1967, **6**, 1133.

13. D. Curtis, M. J. G. Lesley, N. C. Norman, A. G. Orpen, J. Starbuck, *Dalton Trans.*, 1999, 1687.

14. R. S. Paonessa, W. C. Trogler, *J. Am. Chem. Soc.*, 1982, **104**, 1138.

15. C. A. Tolman, *Chem. Rev.*, 1977, **77**, 313, and references therein.

16. I. Schranz, G. R. Lief, C. J. Carrow, D. C. Haagenson, L. Grocholl, L. Stahl, R. J. Staples, R. Boomishankar, A. Steiner, *Dalton Trans.*, 2005, 3307.

17. G. G. Messmer, E. L. Amma, *Inorg. Chem.*, 1966, **5**, 1775.

18. S. Otto, A. J. Muller, *Acta Cryst.*, 2001, **C57**, 1405.

19. G. Linti, R. Frey, M. Schmidt, *Z. Naturforsch., B*, 1994, **49**, 958.

20. S. Sakaki, T. Kikuno, *Inorg. Chem.*, 1997, **36**, 226.

21. S. Onozawa, M. Tanaka, *Organometallics*, 2001, **20**, 2956.

22. CSD version 5.28, November 2006, update 2 (May 2007); F. H. Allen, *Acta Cryst.*, 2002, **B58**, 380.

23. R. J. Baker, C. Jones, J. A. Platts, *J. Am. Chem. Soc.*, 2003, **125**, 10534.

24. B. Buchin, C. Gemel, T. Cadenbach, R. A. Fischer, *Inorg. Chem.*, 2006, **45**, 1789.

25. A. Kempter, C. Gemel, R. A. Fischer, *Chem. Eur. J.*, 2007, **13**, 2990.

26. R. P. Rose, *PhD Thesis*, University of Wales, Cardiff, 2006.

27. D. Drew, J. R. Doyle, *Inorg. Synth.*, 1972, **13**, 48.

28. G. K. Anderson, H. C. Clark, J. A. Davies, *Inorg. Chem.*, 1981, **20**, 1636.

29. T. G. Appleton, M. A. Bennett, I. B. Tomkins, *Dalton Trans.*, 1976, 439.

30. J. T. Mague, M. J. Fink, C. A. Recatto, *Acta Cryst.*, 1993, **C49**, 1176.

31. L. M. Engelhardt, J. M. Patrick, C. L. Raston, P. Twiss, A. H. White, *Aust. J. Chem.*, 1984, **37**, 2193.

32. (a) R. C. Boyle, J. T. Mague, M. J. Fink, *Acta Cryst.*, 2004, **E60**, m40; (b) A. C. Moro, F. W. Wanatabe, S. R. Ananias, A. E. Mauro, A. V. G. Netto, A. P. R. Lima, J. G. Ferreira, R. H. A. Santos, *Inorg. Chem. Commun.*, 2006, **9**, 493.

33. W. L. Steffen, G. J. Palenik, *Inorg. Chem.*, 1976, **15**, 2432.

34. A. Babai, G. B. Deacon, A. P. Erven, G. Meyer, *Z. Anorg. Allg. Chem.*, 2006, **632**, 639.

35. A. B. Goel, S. Goel, D. Van der Veer, *Inorg. Chim. Acta*, 1982, **65**, L205.

36. (a) R. A. Fischer, D. Weiss, M. Winter, I. Müller, H. D. Kaesz, N. Frölich, G. Frenking, *J. Organomet. Chem.*, 2004, **689**, 4611; (b) R. A. Fischer, H. D. Kaesz, S. I. Khan, H. –J. Müller, *Inorg. Chem.*, 1990, **29**, 1601.

37. S. P. Green, C. Jones, A. Stasch, *Inorg. Chem.*, 2007, **46**, 11.

38. H. C. Clark, P. N. Kapoor, I. J. McMahon, *J. Organomet. Chem.*, 1984, **265**, 107.

39. S. I. Al-Resayes, P. B. Hitchcock, M. F. Meidine, J. F. Nixon, *J. Organomet. Chem.*, 1988, **341**, 457.

40. R. Romeo, L. M. Scolaro, *Royal Society of Chemistry: Perspectives in Organometallic Chemistry*, 2003, **287**, 208.

41. (a) P. M. Esteves, K. K. Laali, *Organometallics*, 2004, **23**, 3701; (b) J. –B. Robert, H. Marsmann, I. Absar, J. R. Van Wazer, *J. Am. Chem. Soc.*, 1971, **93**, 3320.

42. (a) K. K. Laali, B. Geissler, M. Regitz, J. J. Hauser, *J. Org. Chem.*, 1995, **60**, 6362; (b) J. F. Nixon, *Coord. Chem. Rev.*, 1995, **145**, 201, and references therein.

43. A. J. L. Pombeiro, *J. Organomet. Chem.*, 2001, **632**, 215, and references therein.

44. L. N. Markovski, V. D. Romanenko, *Tetrahedron*, 1989, **45**, 6019, and references therein.

45. K. B. Dillon, F. Mathey, J. F. Nixon, *Phosphorus: The Carbon Copy, from Organophosphorus to Phosphaorganic Chemistry*, New York, John Wiley and sons, 1998.

46. G. W. Parshall, *Inorg. Synth.*, 1970, **12**, 26.

47. R. A. Head, *Inorg. Synth.*, 1990, **28**, 132.

48. D. W. Meek, *Inorg. Chem.*, 1965, **4**, 250.

Chapter 5

The Preparation of Novel Gallium(I), (II) and (III) Heterocycles

5.1 Introduction

5.1.1 The Reactivity of "GaI"

The properties and formulation of "GaI" have been briefly summarised in Chapter 1. Since the facile synthesis of "GaI" was first reported,[1] this useful reagent has been studied extensively and its wide-ranging synthetic applications have been recently reviewed.[2] Treatment of "GaI" with Lewis bases leads to disproportionation, with gallium metal deposition and the formation of gallium(II), (III) or mixed-valence species.[2] The tendency of "GaI" to disproportionate has been exploited in the synthesis of gallium cluster compounds by the salt metathesis reactions of bulky alkyl, silyl or germyl anions with the Ga(I) source.[2] "GaI" has been shown to react with some transition metal complexes by the oxidative insertion of "GaI" into M—X and M—M bonds.[2] There have been relatively few investigations into the use of "GaI" as a reducing agent in organic synthesis.[2] Considering that the application of InI in Barbier allylations and Reformatsky reactions has been extensively investigated,[3] the paucity of research into the application of "GaI" in C—C bond forming reactions is quite unusual. A recent report has revealed that "GaI" is effective in mediating aldol reactions and is a stronger reducing agent than InI.[4]

"GaI" has mainly been utilised in the preparation of organogallium compounds.[2] Oxidative insertion of "GaI" with alkyl iodides yields alkyl gallium diiodides, $RGaI_2$, and salt metathesis reactions have been employed in high-yielding syntheses of

gallium(I) alkyls.[2] Of most relevance to this discussion, "GaI" is a useful reagent in the synthesis of gallium(I), (II) and (III) heterocycles. For example, the paramagnetic gallium(III) heterocycle, $[I_2Ga\{[N(Ar)C(H)]_2^{\cdot}\}]$ (Ar = $C_6H_3Pr^i_2$-2,6), is synthesised by the reaction of "GaI" with Ar-DAB ($\{N(Ar)C(H)\}_2$).[5,6] Reduction of this heterocycle with potassium yields the anionic gallium(I) *N*-heterocyclic carbene (NHC) analogue, $[:Ga\{[N(Ar)C(H)]_2\}]^-$ **1**,[6] as discussed in Chapter 1. In previous work, the gallium(III) heterocycle, $[I_2Ga(Ar\text{-}BIAN)^{\cdot}]$ **2** (Ar-BIAN = bis(2,6-diisopropylphenyl)acenapthene), was prepared from the reaction of "GaI" with Ar-BIAN (Scheme 1).[7] The attempted reduction of **2** over a potassium mirror to form a gallium(I) NHC analogue gave an intractable mixture of products.

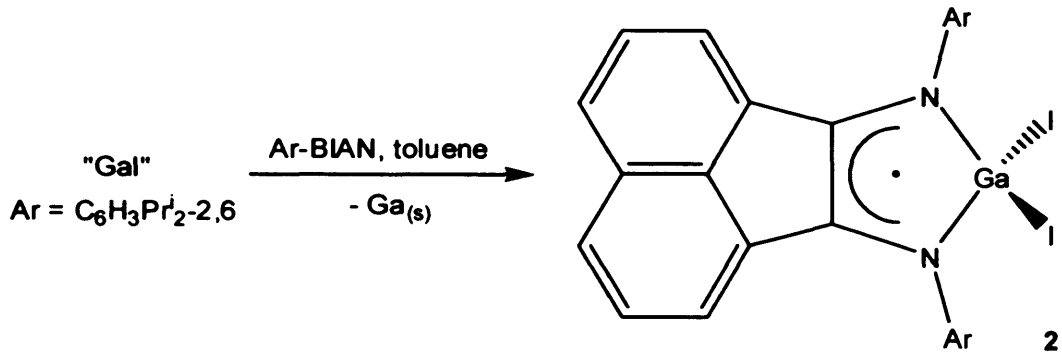

Scheme 1 – The synthesis of **2**

5.1.2 The Oxidation Chemistry of the Heterocycle, $[:Ga\{[N(Ar)C(H)]_2\}]^-$

Previous investigations into the reactivity of **1** have emphasised the facile oxidation of this compound,[8] and these reactions have been summarised in Chapters 2, 3 and 4. Attempted salt metathesis reactions of [K(tmeda)][**1**] with *s*-, *p*- and *d*-block halides, for example, often lead to the formation of the paramagnetic gallium(II) dimers, $[XGa\{[N(Ar)C(H)]_2^{\cdot}\}]_2$ (X = Cl **3a**, Br **3b**, I **3c**).[7b] These reactions are postulated to occur by the initial oxidative insertion of **1** into the M—X bond, followed by the reductive elimination of **3a-c**.[7] It is of note that the oxidative coupling of **1**, mediated

by one-electron oxidising agents such as $[Co_2(CO)_8]$, $[FeCp_2][PF_6]$ and Tl_2SO_4, affords the digallane(4), $[Ga\{[N(Ar)C(H)]_2\}]_2$ **4**.[9] Compound **4** was previously synthesised by another method.[10] Of relevance to this study, the oxidative insertion of **1** into the C—H bond of $[HC\{[N(Mes)C(H)]_2\}][Cl]$ (IMes.HCl, Mes = $C_6H_2Me_3$-2,4,6) yields the gallium hydride complex, $[(IMes)(H)Ga\{[N(Ar)C(H)]_2\}]$.[11] An understanding of the oxidation chemistry of **1** is integral to a study of its coordination chemistry.

5.1.3 The Reactivity of the Digallane(4), $[Ga\{[N(Ar)C(H)]_2\}]_2$

The reactivity of **4** towards *d*-block precursors has been summarised in Chapters 3 and 4. It is noteworthy that the oxidative insertion of metallocenes into the Ga—Ga bond of **4** has allowed the synthesis of several novel metal gallyl complexes.[7,12] The tendency for the digallane(4), **4**, to undergo oxidative insertion reactions with electron deficient metal centres is comparable to the oxidative insertion of "WCp_2" into the B—B bond of the diborane, $B_2Cat'_2$ (Cat' = 4-$Bu^tC_6H_3O_2$-1,2 or 3,5-$Bu^t_2C_6H_2O_2$-1,2).[13] The Jones group is interested in the continued investigation of the reactivity of **4** towards transition metal and main group precursors.

5.2 Research Proposal

A continued investigation of the oxidative insertion chemistry of "GaI" and its reactivity towards Lewis bases would further establish the reactivity of the gallium(I) source. In an effort to synthesise novel organogallium complexes, the reactivity of "GaI" towards a variety of main group precursors was proposed. The reactivity of **1** towards metal halides was proposed to be investigated, in an attempt to synthesise metal-gallyl complexes by salt metathesis. The reactivity of the digallane(4), **4**, has not

been extensively studied, so it was decided to address this paucity. The treatment of "GaI" with a variety of diazabutadienes was proposed, in an attempt to synthesise novel gallium(III) heterocycles, of the general formula $[I_2Ga\{[N(R)C(R)]_2^{\cdot}\}]$. Reduction of these gallium(III) heterocycles could provide synthetic routes to novel compounds analogous to the gallium(I) NHC analogue, **1**, and the digallane(4), **4**.

5.3 Results and Discussion

5.3.1 The Reactivity of "GaI"

A toluene suspension of "GaI" was treated with the diindane(4), $[In\{CH(SiMe_3)_2\}_2]_2$, but no reaction occurred. Amines and phosphines are known to react with "GaI" *via* disproportionation to give dimeric gallium(II) complexes of the type, $[L\rightarrow GaI_2]_2$,[2] so the reactivity of "GaI" with several group 14 Lewis bases were investigated. Treatment of "GaI" separately with the germanium(II) NHC analogue, $[:Ge\{[N(Bu^t)C(H)]_2\}]$, and the plumbylene sources, $[Pb(Ar')_2]_2$ and $[:Pb\{C_6H_3(NMe_2)_2\text{-}2,6\}_2]$, gave intractable mixtures of products, with lead deposition in the case of the latter. In contrast, the reaction of $[:Sn\{CH(SiMe_3)_2\}_2]$ with "GaI" yielded the known tin(IV) complex, $[SnI_2\{CH(SiMe_3)_2\}_2]$ **5** (Scheme 2), whilst no reaction occurred with the trimeric species, $[Sn(Ar')_2]_3$ (Ar' = $C_6H_2Pr^i_3$-2,4,6). Complex **5** has been previously prepared by a different route.[14] It was thought that the tin diphosphacyclobutadienyl complex, $[:Sn(\eta^4\text{-}P_2C_2Bu^t_2)]$, might effect a similar outcome. Instead, its reaction with "GaI" led to the deposition of tin metal and the formation of the novel diphosphacyclobutenyl gallium complex, $[GaI_2\{C(Bu^t)P(H)C(Bu^t)=P\}]_2$, **6**, in low yield, presumably *via* disproportionation and solvent proton abstraction processes (Scheme 2).

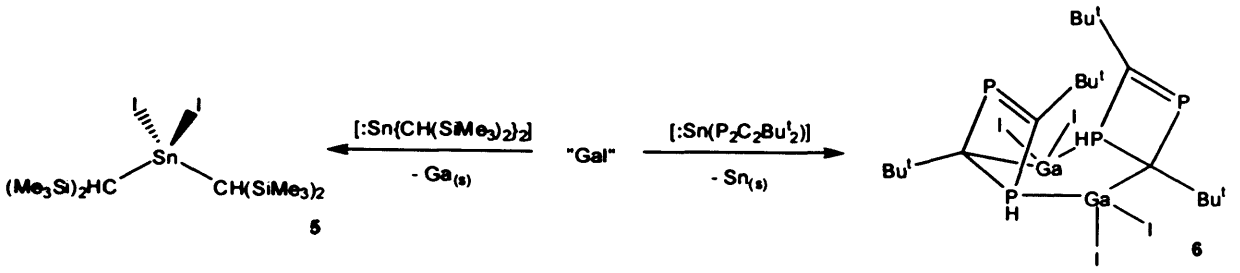

Scheme 2 – The synthesis of **5** and **6**

Complex **6** was fully characterised. The ^{1}H NMR spectrum of **6** exhibits a signal at δ 6.54 ppm, corresponding to the protons at the P-centres. This signal displays two coupling constants ($^{1}J_{PH}$ = 170.0 Hz, $^{3}J_{PH}$ = 20.4 Hz) that are of a typical magnitude.[15] Most signals in the $^{13}C\{^{1}H\}$ NMR spectrum of **6** are complicated multiplets, due to extensive couplings to the ^{31}P nuclei. No resonance was observed that corresponded to the carbon centre bonded to gallium, possibly a result of the quadrupolar gallium centre broadening this signal and making it indistinguishable from the baseline noise. The low field signal in the $^{13}C\{^{1}H\}$ NMR spectrum (δ 266.5 ppm, apparent t, $^{1}J_{PC}$ = $^{1}J_{PC}$ = 22 Hz, *C*=P) occurs at a chemical shift that is characteristic of phosphaalkenes, with characteristic $^{1}J_{PC}$ couplings.[15] The low field signal observed in the ^{31}P NMR spectrum of **6** (δ 366.6 ppm, dd, $^{2}J_{PP}$ = 41.9 Hz, $^{3}J_{PH}$ = 20.4 Hz, *P*=C) is also characteristic of phosphaalkenes.[15] The other signal observed in the ^{31}P NMR spectrum is at high field (δ -11.0 ppm, d, $^{2}J_{PP}$ = 41.9 Hz, $^{1}J_{PH}$ = 170.0 Hz, *P*H), as would be expected for four-coordinate phosphorus.[15]

The molecular structure of **6** (Figure 1) shows it to contain the first examples of diphosphacyclobutenyl rings containing secondary P-centres (P(1) and P(3)). The hydrogens attached to these centres were located from difference maps and were refined isotropically without restraints. The secondary phosphine centres coordinate gallium centres intermolecularly giving rise to a dimeric unit containing a $P_2C_2Ga_2$ ring. The

P=C double bond distances within the heterocycles (P(2)—C(2) and P(4)—C(12)) are in the normal range for localised interactions.[16]

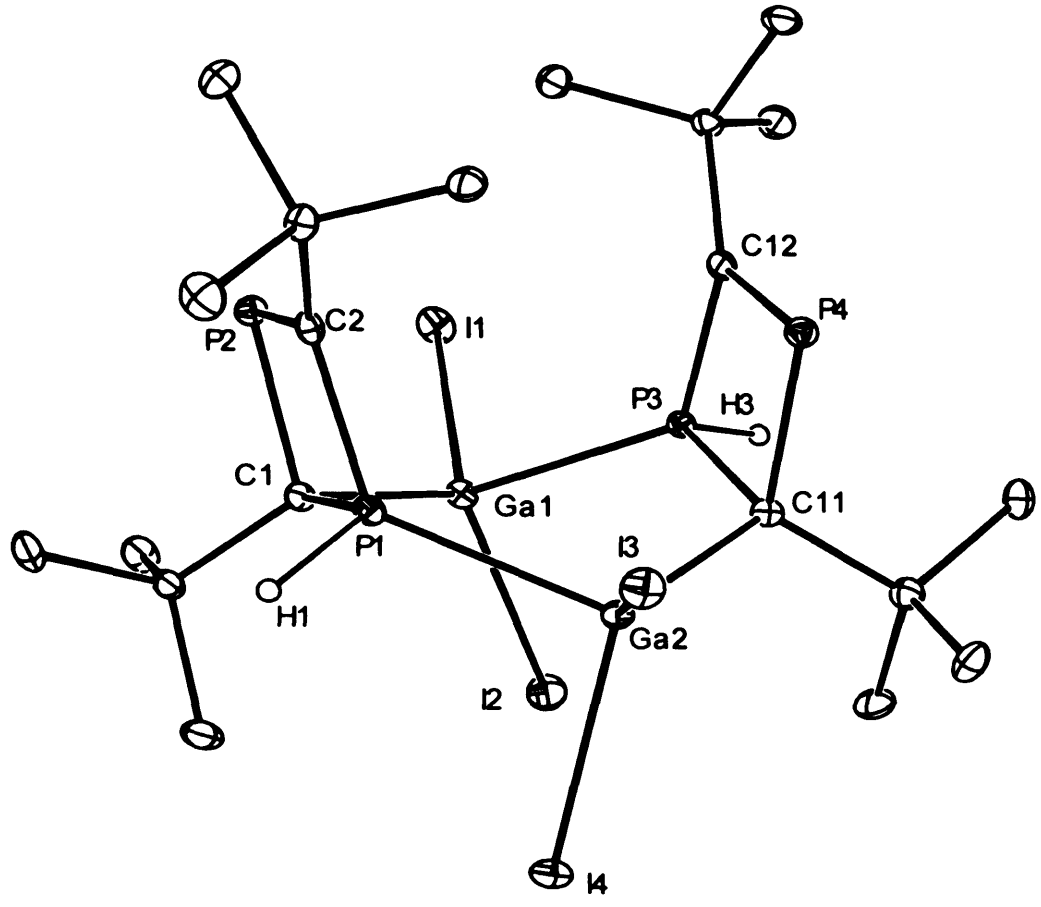

Figure 1 – Thermal ellipsoid plot (20 % probability surface) of the molecular structure of $[GaI_2\{C(Bu^t)P(H)C(Bu^t)=P\}]_2$ **6**; hydrogen atoms (except H(1) and H(3)) omitted for clarity. Selected bond lengths (Å) and angles (°): P(1)—C(2) 1.801(7), P(1)—C(1) 1.839(7), P(2)—C(2) 1.703(7), P(2)—C(1) 1.899(7), P(3)—C(12) 1.799(8), P(3)—C(11) 1.849(8), P(4)—C(12) 1.695(8), P(4)—C(11) 1.899(7), Ga(1)—C(1) 2.026(7), Ga(1)—P(3) 2.440(2), Ga(2)—C(11) 2.012(7), Ga(2)—P(1) 2.443(2), Ga(1)—I(1) 2.5567(11), I(2)—Ga(1) 2.5461(11), I(3)—Ga(2) 2.5607(16), I(4)—Ga(2) 2.5496(11); C(1)—Ga(1)—P(3) 111.9(2), P(1)—Ga(2)—C(11) 110.7(2), I(1)—Ga(1)—I(2) 107.42(5), I(3)—Ga(2)—I(4) 105.76(4), C(2)—P(1)—C(1) 87.1(3), C(1)—P(2)—C(2) 88.1(3), P(1)—C(1)—P(2) 88.5(3), P(1)—C(2)—P(2) 96.2(4), C(11)—P(3)—C(12) 87.0(3), C(11)—P(4)—C(12) 88.5(3), P(3)—C(11)—P(4) 88.1(3), P(3)—C(12)—P(4) 96.4(4).

5.3.2 Investigations into the Oxidation of the Heterocycle, $[:Ga\{[N(Ar)C(H)]_2\}]^-$

Previous studies into the reactions of the gallium(I) heterocycle, **1**, with gases such as $N_2O_{(g)}$, have shown that the heterocycle may be oxidised under appropriate conditions.[8] In contrast, treatment of a toluene solution of [K(tmeda)][**1**] with acetylene (generated *in situ* from distilled, degassed water and calcium carbide, and passed through an NaOH drying column) afforded the diazabutadiene, Ar-DAB. It is not known if the formation of Ar-DAB was caused by traces of moisture in the reaction mixture, and the fate of the gallium in this reaction is unknown. Treatment of a toluene solution of [K(tmeda)][**1**] with $H_{2(g)}$ led to no reaction.

The gallium(I) heterocycle, **1**, has previously been shown to oxidatively insert into C—H bonds.[11] A study was undertaken to expand this mode of reactivity. The treatment of the bis(imidazolium) salt, $[C_6H_4\{HC[N(Bu^t)C(H)C(H)NCH_2]\}_2\text{-}1,2]^{2+}$ $[Br]^-_2$, with two equivalents of [K(tmeda)][**1**] gave an intractable mixture of products. Similarly, no products could be isolated from the 1 : 1 reactions of [K(tmeda)][**1**] with quinuclidene.HCl, or the treatment of [K(tmeda)][**1**] with one equivalent of ethanol. The reaction of $[Ca(THF)_4][\mathbf{1}]_2$ with two equivalents of the phenol, $C_3H_3Bu^t\text{-}2,6\text{-}OH\text{-}4$, also gave an intractable mixture of products. Ar-DAB was the only isolable product when [K(tmeda)][**1**] was treated with the salt, $[HNEt_3][BPh_4]$.

The oxidation of **1** was observed in its treatment with several main group and transition metal halides, as has been previously reported.[2] The calcium salt of **1**, $[Ca(THF)_4][\mathbf{1}]_2$, reduced $[Cp'Fe(CO)_2Br]$ (Cp' = C_5H_5 or C_5Me_5) to give the dimer, $[Cp'Fe(CO)_2]_2$, and the paramagnetic gallium(II) dimer, **3b**. In contrast, when $[Ca(THF)_4][\mathbf{1}]_2$ was reacted with $[FeCl_2(THF)_{1.44}]$ in a 2 : 1 stoichiometry, the

digallane(4), **4**, formed. The reaction of three equivalents of $[Ca(THF)_4][\mathbf{1}]_2$ with $TiCl_3$ gave an intractable mixture of products, as did the 2 : 1 reaction of [K(tmeda)][**1**] with $Fe(BAr^F{}_4)_2$ ($Ar^F = C_6H_3(CF_3)_2$-3,5). In an attempt to circumvent the oxidation of **1**, The 2 : 1 reactions of [K(tmeda)][**1**] with $MnCl_2$, $[FeCl_2(THF)_{1.44}]$ and $CoCl_2$ were performed at -78 °C and work-up was carried out at -20 °C. However, the only product obtained from these reactions was the known gallium(III) compound, $[Ga\{[N(Ar)C(H)]_2\}\{[N(Ar)C(H)]_2^{\cdot}\}]$.[7b] The reactions of [K(tmeda)][**1**] with Hg_2Cl_2 or TlBr, both in the presence of one equivalent of IMes, gave intractable mixtures of products, as did the reaction of [K(tmeda)][**1**] with RbCl. The reaction of one equivalent of PPh_4Cl with [K(tmeda)][**1**] afforded PPh_3. Here, the fate of the gallium is unknown. Similarly, PCy_3 was identified in the reaction mixture of $[Ca(THF)_4][\mathbf{1}]_2$ and $[(PCy_3)_2Cl_2Ru{=}C(H)Ph]$, as measured by $^{31}P\{^1H\}$ NMR spectroscopy. The 1 : 1 reactions of [K(tmeda)][**1**] with [(Piso)FeBr] ($Piso^- = [\{N(Ar)\}_2CBu^t]^-$, $Ar = C_6H_3Pr^i{}_2$-2,6) and [(Priso)CoBr] ($Priso^- = [\{N(Ar)\}_2CNPr^i{}_2]^-$) gave intractable mixtures of products.

The gallium(I) heterocycle, **1**, was reacted with main group and transition metal precursors that do not contain halides. The main group reactions will be discussed first. The reaction of [K(tmeda)][**1**] with the digallane(4), **4**, gave an intractable mixture of products. In contrast, [K(tmeda)][**1**] showed no reactivity towards the ylides, $PPh_3P{=}CH_2$ and $PPh_3P{=}Cp$ (monitored by $^{31}P\{^1H\}$ NMR spectroscopy), even when the solution was irradiated with UV light.

No reaction occurred when the molybdenum(IV) complex, $[Cp_2MoH_2]$, was treated with two equivalents of [K(tmeda)][**1**]. This result would appear to be unusual, given the high oxidation state of the molybdenum centre and the reducing nature of the

heterocycle, **1**. Similarly, no reaction was observed in the 1 : 1 reaction of [K(tmeda)][**1**] with [Cp'Mn(CO)(dppe)] (Cp' = C_5H_4Me, dppe = $Ph_2PCH_2CH_2PPh_2$), due to the CO ligand in this complex being tightly bound to the metal centre. In contrast, the reaction of the salt, [Cp'Mn(CO)(dppe)][BPh_4], with [K(tmeda)][**1**] yielded [Cp'Mn(CO)(dppe)]. The fate of the gallium in this reaction is unknown. The treatment of [$Fe(CO)_x(CNxylyl)_{5-x}$] (xylyl = $C_6H_3Me_2$-2,6, x = 1 or 4) with [K(tmeda)][**1**] gave no reaction, whilst the treatment of the rhodium complexes, [Cp*$RhMe_2$(pyridine)] or [(η^6-toluene)$Rh(PPh_3)_2$][$BAr^F{}_4$], with [K(tmeda)][**1**] gave intractable mixtures of products. The treatment of [$Hg(C{\equiv}CPh)_2$] with one equivalent of [K(tmeda)][**1**] led to mercury deposition and an intractable mixture of products.

The successful synthesis of the first *f*-block complex of **1**, [(L){$N(SiMe_3)_2$}Nd-Ga{[N(Ar)C(H)]$_2$}] (L = [$Bu^tNCH_2CH_2${:C{[$NCSiMe_3CHNBu^t$]}]), was recently reported.[17] There have been several attempts to synthesise other *f*-block complexes of **1**. No reaction was observed when [$SmI_2(THF)_2$], [Er{$N(SiMe_3)_2$}$_3$] or [Er{$CH(SiMe_3)_2$}$_3$] were treated separately with [$Ca(THF)_4$][**1**]$_2$ or [K(tmeda)][**1**]. The 2 : 1 reaction of [K(tmeda)][**1**] with [(Piso)SmI]$_2$THF and the 1 : 1 reaction of [K(tmeda)][**1**] with [Yb($C{\equiv}CPh)_2$] gave intractable mixtures of products. In contrast, the 1 : 1 reaction of [K(tmeda)][**1**] with [$(Fiso)_2SmCl(THF)_{0.33}$] ($Fiso^-$ = [{N(Ar)}$_2$CH]$^-$) afforded the gallium(III) hydride, **7**, in 21 % yield (Scheme 3). The same product appeared to form in the 1 : 1 reaction of [K(tmeda)][**1**] with [$(Fiso)_2LaF(DME)$], DME = 1,2-dimethoxyethane (as determined by IR spectroscopy). The fate of the lanthanide metal in these reactions is unknown. The formamidine, FisoH, was also detected in the reaction mixture by ^{1}H NMR spectroscopy, presumably generated by a proton abstraction process. It was thought that the heterocycle, **1**, oxidatively inserts into the N—H bond of FisoH to form **7**. To test this hypothesis, the

direct reaction of [K(tmeda)][**1**] with FisoH was performed (Scheme 3). A similar yield of **7** (26 %) was achieved employing this synthetic route. To the best of our knowledge, this reaction is the first example of the oxidative insertion of a group 13 heterocycle into an N—H bond, and there is also no precedent for this mode of reactivity in diyl chemistry. In contrast, there have been several reports of NHCs inserting into the N—H bond of secondary amines.[18]

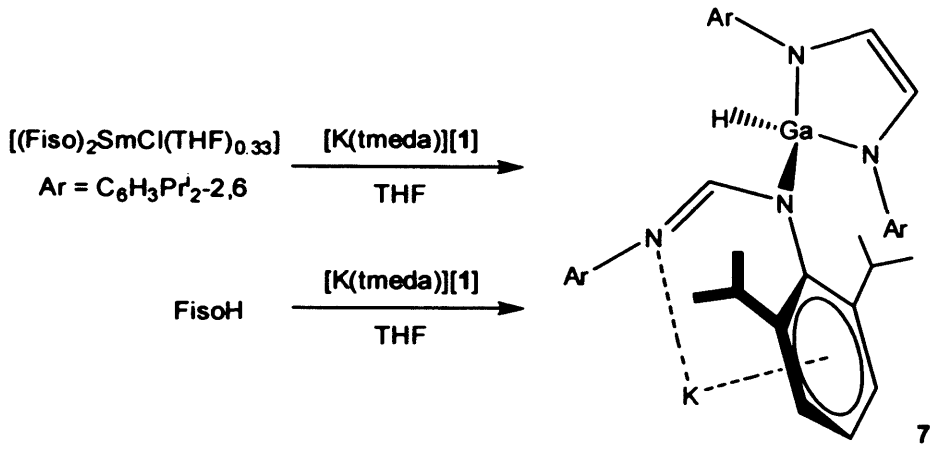

Scheme 3 – The original and alternative synthesis of **7**

The ^{1}H NMR spectrum of **7** is in agreement with its proposed structure, although no signal was observed that corresponded to the hydride ligand. This is not unusual in the ^{1}H NMR spectra of gallium hydrides, as the quadrupolar nature of gallium can cause broadening of the hydride signal until it is indistinguishable from the baseline noise.[19] The ^{13}C{^{1}H} NMR spectrum was too weak to assign. A characteristic strong, broad Ga—H stretching absorption was observed in the IR spectrum of **7** at 1878 cm^{-1}. This value corresponds well with the value observed in the related compound, [(IMes)(H)Ga{[N(Ar)C(H)]$_2$}] (1854 cm^{-1}).[11]

The structure of **7** was determined by X-ray crystallography (Figure 2). The gallium centre of **7** has a distorted tetrahedral geometry, with the geometry of the GaN_2C_2 ring suggesting the presence of a localised C=C double bond. The related

gallium hydride complex, [(IMes)(H)Ga{[N(Ar)C(H)]$_2$}], displays one Ar substituent of the heterocyclic ring being bent away from the least squares plane of the heterocycle (34.8°), and a similar distortion is observed in **7** (32.8°). Similar distortions have previously been attributed to steric buttressing with other aryl groups,[11] and this explanation adequately explains the situation in **7**.

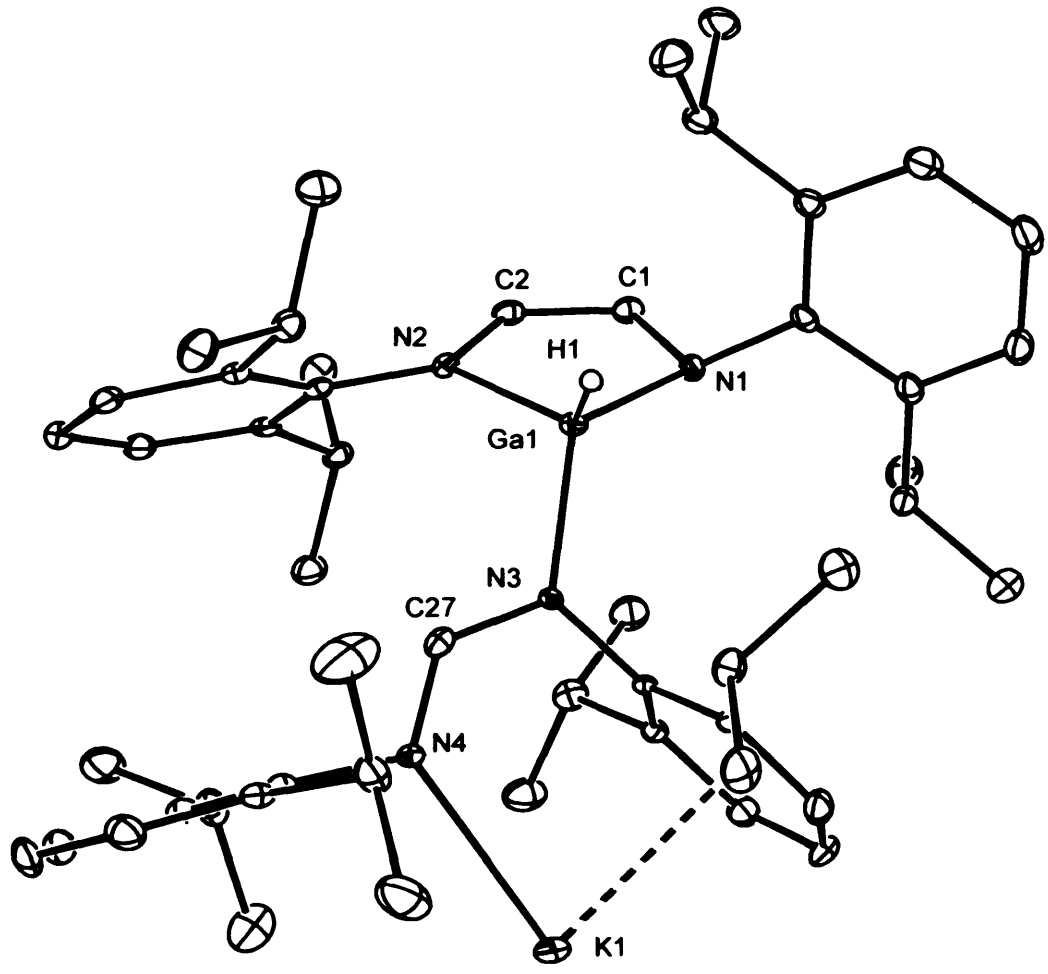

Figure 2 – Thermal ellipsoid plot (25 % probability surface) of the molecular structure of [{N(Ar)C(H)N(Ar)K}(H)Ga{[N(Ar)C(H)]$_2$}] **7**; hydrogen atoms (except H(1)) omitted for clarity. Selected bond lengths (Å) and angles (°): Ga(1)—N(1) 1.904(3), Ga(1)—N(2) 1.943(3), Ga(1)—N(3) 1.966(3), Ga(1)—H(1A) 1.48(2), N(1)—C(1) 1.411(4), N(2)—C(2) 1.404(4), N(3)—C(27) 1.341(4), N(4)—C(27) 1.296(4), C(1)—C(2) 1.342(5), N(1)—Ga(1)—N(2) 89.23(12), C(1)—N(1)—Ga(1) 106.5(2), C(2)—N(2)—Ga(1) 106.3(2), C(27)—N(3)—Ga(1) 117.6(2), C(2)—C(1)—N(1) 119.4(3), C(1)—C(2)—N(2) 118.2(3), N(4)—C(27)—N(3) 126.1(3).

5.3.3 The Reactivity of the Digallane(4), $[Ga\{[N(Ar)C(H)]_2\}]_2$

In consideration of the reactivity of the neutral Al(I) and Ga(I) heterocycles, $[:E\{[N(Ar)C(Me)]_2CH\}]$, towards organic azides (reviewed in Chapter 1), the reactions of [K(tmeda)][**1**] with azides of varying steric bulk, N_3-R, R = $SiMe_3$, 9-triptycenyl, Mes* (Mes* = $C_6H_2Bu^t_3$-2,4,6) or Ar* (Ar* = $C_6H_3(C_6H_2Pr^i_3$-2,4,6$)_2$-2,6), were investigated by Dr. R. J. Baker. In all cases intractable mixtures were obtained. We considered that reaction of these azides with the digallane(4), **4**, could lead to the oxidative insertion of imide fragments into the Ga—Ga bond of **4**. In collaboration with Dr. R. J. Baker, the reaction of **4** with two equivalents of N_3-$SiMe_3$ yielded the blue-green paramagnetic complex, **8**, in good yield (79 %) after stirring for 48 hours (Scheme 4). Repeating the reaction with a large excess of N_3-$SiMe_3$ led to the same complex and did not appreciably increase the rate of reaction. Although the formation of **8** is relatively slow (as judged by the colour change of the reaction mixture), no intermediates in its formation could be isolated. It is clear, however, that the mechanism involves single electron oxidations of the gallium heterocycles of **4**. Compound **8** can be considered as a dimer of the gallium-terminal imide complex, $[(SiMe_3)N{=}Ga\{[N(Ar)C(H)]_2^{\cdot}\}]$, and can be compared to the related dimeric, diamagnetic imidogallane, $[\{(\eta^1$-Cp*$)GaN(xylyl)\}_2]$, which arises from the reaction of N_3-xylyl and $[:Ga(\eta^5$-Cp*$)]$.[20] There are also parallels between the formation of **8** and the singlet biradicaloid germanium imide complex, $[\{Ar''GeN(SiMe_3)\}_2]$ (Ar'' = $C_6H_3(C_6H_3Pr^i_2$-2,6$)_2$-2,6), which results from the reaction of the digermyne, Ar''GeGeAr'', with N_3-$SiMe_3$.[21] It is worthy of note that the reactions of **4** with either N_3-(9-triptycenyl), N_3-Mes or N_3-Ar* were carried out by Dr. R. J. Baker, but all led to intractable mixtures of products.

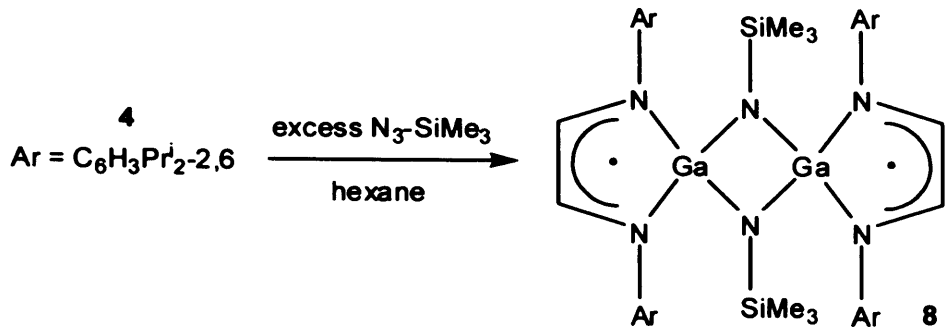

Scheme 4 – The synthesis of **8**

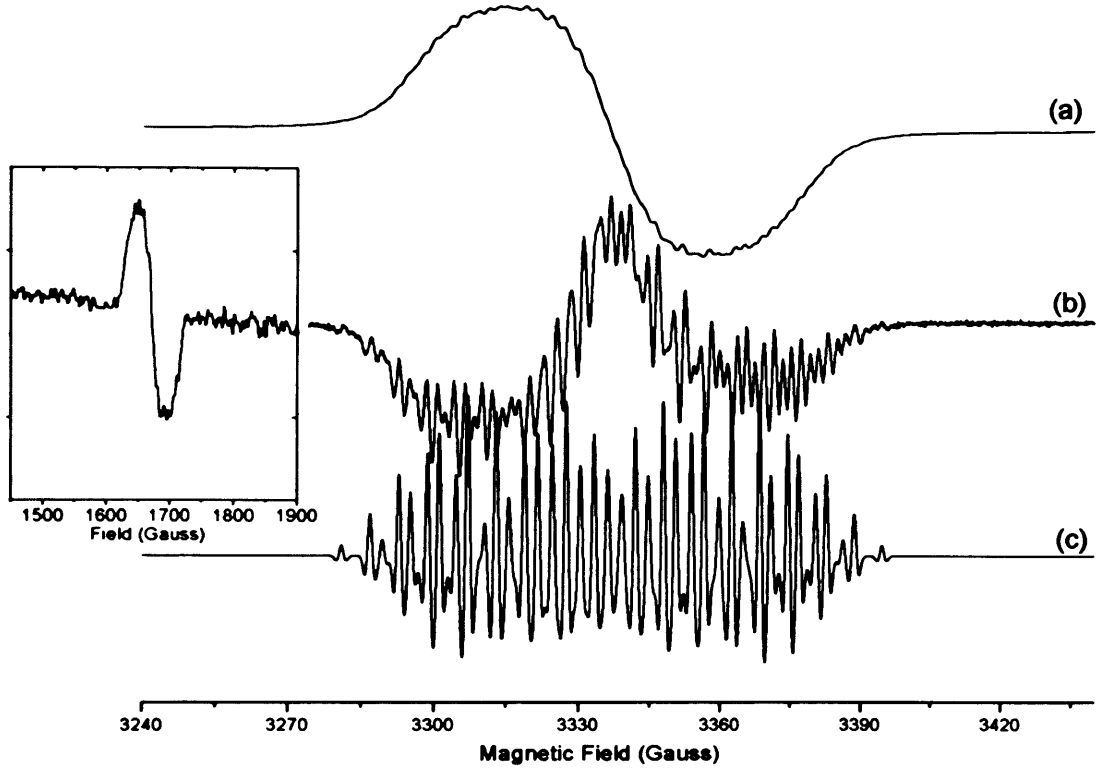

Figure 3 – X-band (9.360 GHz) EPR spectrum of **8** recorded at 298 K in toluene: (a) first harmonic signal, (b) second harmonic signal, and (c) simulated spectrum. Inset figure shows the $\Delta M_S = 2$ transition due to the weakly interacting S = 1 triplet at half field.

As **8** is paramagnetic, no meaningful data could be obtained from its ^1H and $^{13}C\{^1H\}$ NMR spectra. However, X-band continuous wave EPR spectra for this compound were recorded at room temperature and 77 K by Dr. D. M. Murphy (Cardiff University). Only the spectra acquired at 298 K are shown (Figure 3), as the anisotropic

frozen solution spectrum did not yield any additional information. Owing to the poor resolution of the first derivative spectrum (Figure 3a), the second derivative spectrum (Figure 3b) was recorded. The resulting isotropic spectrum was simulated (Figure 3c) based on the following spin Hamiltonian parameters; g_{iso} = 2.0035, a_H = 5.8 G, a_N = 6.0 G, $a_{^{69}Ga}$ = 20.4 G and $a_{^{71}Ga}$ = 26.0 G. Therefore, the strong EPR signal for **8** is centred close to that of free spin. In addition, the EPR spectrum of **8** is typical for paramagnetic diazabutadiene-gallium complexes previously reported by us,[7,22] in that it is dominated by isotropic hyperfine couplings (HFC) to two equivalent ^{1}H nuclei, two equivalent ^{14}N nuclei and a $^{69,71}Ga$ nucleus. The relatively large HFCs to the gallium nucleus originate from the large theoretical isotropic hyperfine couplings for gallium (^{69}Ga; I = 3/2, a_o = 4356 G, 60.1 % natural abundance; ^{71}Ga: I = 3/2, a_o = 5535 G, 39.9 % natural abundance). This means that even the small electron spin density (0.47 %) at the gallium nucleus of **8** produces easily observable HFCs to both gallium isotopes.

Evidence for the diradical nature of **8** can also be obtained from its EPR spectra. For two interacting unpaired electrons (S = ½), an S = 1 triplet ground state can be observed in the spectrum, provided the coupling between the two spin systems is sufficiently strong. In that case the zero field splitting term for the randomly oriented triplet should produce a characteristic pattern in the ΔMs = 1 region (centre field). Unfortunately, due to the intense nature of the signals arising from the individual S = ½ spins in **8**, the zero field splitting parameter (D) could not be observed. However, the ΔMs = 2 transition at half field was seen at 1670 G (see inset in Figure 3). While this half field transition is extremely weak, indicating that the two S = ½ spins are only weakly coupled, it nevertheless confirms the diradical nature of **8**. The weak interaction between the two S = ½ spins is due to the fact that the unpaired electrons are primarily

localised on the diazabutadiene backbone, and the tetrahedral bonding arrangement around the gallium centres prevents efficient spin-spin coupling.

The molecular structure of **8** is depicted in Figure 4 and shows it to be dimeric with bridging imido ligands. Its gallium centres have heavily distorted tetrahedral geometries and are slightly displaced from the least squares planes defined by the chelating diazabutadiene ligands (0.375 Å mean). In contrast, the Ga_2N_2 heterocycle is effectively planar and its Ga—N bonds (1.885 Å mean) are significantly shorter than those to the diazabutadiene ligand (2.014 Å mean), but longer than those seen in [{(η^1-Cp*)GaN(xylyl)}$_2$] (1.860 Å mean),[20] which possesses 3-coordinate gallium centres. The N-centres of the Ga_2N_2 heterocycle in **8** have distorted trigonal planar geometries (Σ angles = 358.3° mean). An examination of the C—C and N—C bond lengths within the diazabutadiene ligands of **8** suggests a significant degree of delocalisation, as has previously been seen in related paramagnetic complexes employing this ligand, e.g. [I_2Ga{[N(Ar)C(H)]$_2$·}].[5] Although the Ga·····Ga separation in **8** (2.654(3) Å) is well within the sum of the van der Waals radii (3.8 Å),[23] there is no evidence for a Ga—Ga bond in the compound, as has been previously discussed for similar compounds, e.g. [{(η^1-Cp*)GaN(xylyl)}$_2$] (Ga·····Ga separation = 2.6495 Å).[7]

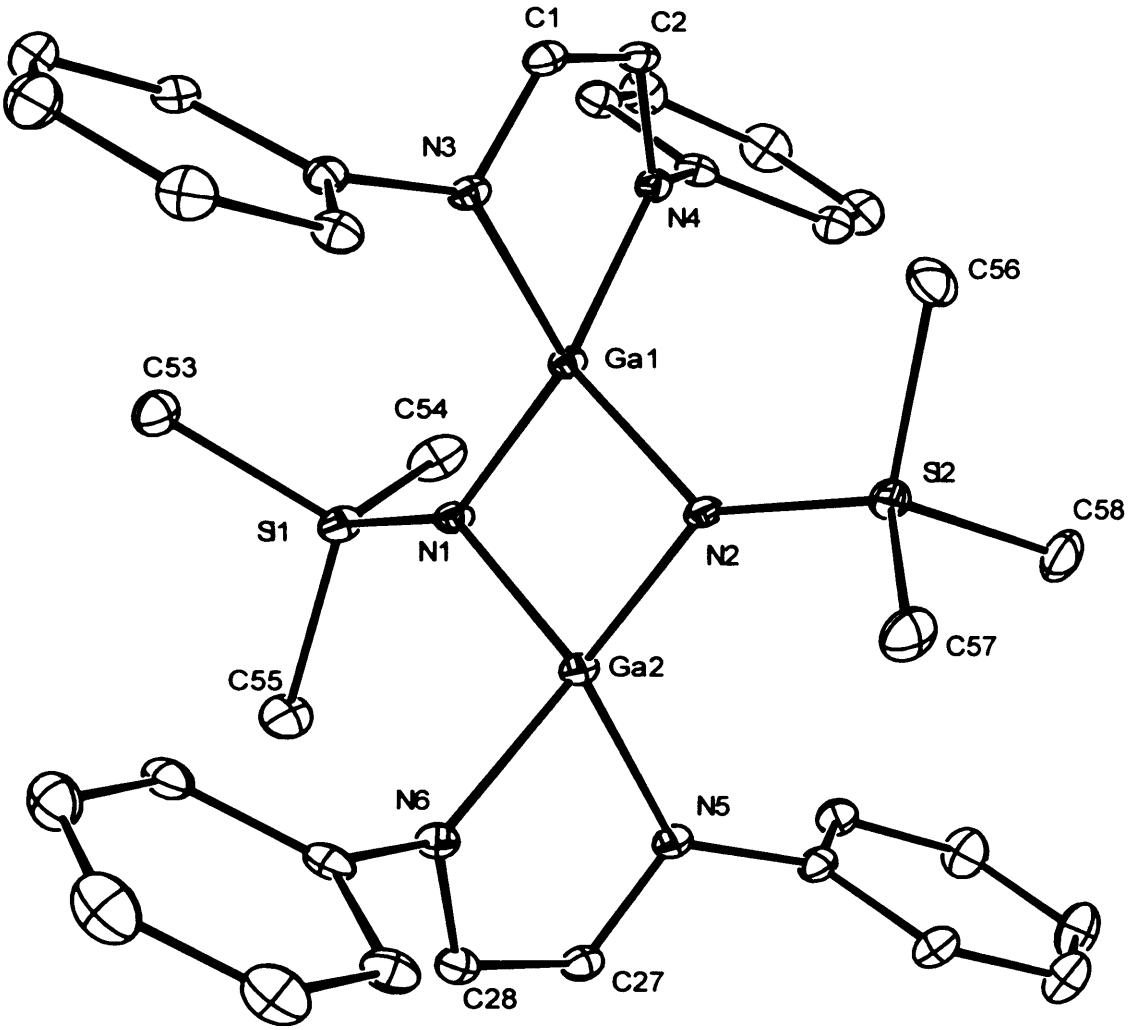

Figure 4 – Thermal ellipsoid plot (25 % probability surface) of the molecular structure of $[\{\mu\text{-N(SiMe}_3)\}\text{Ga}\{[\text{N(Ar)C(H)}]_2^{\cdot}\}]_2$ **8**; hydrogen atoms and isopropyl groups omitted for clarity. Selected bond lengths (Å) and angles (°): Ga(1)—N(1) 1.871(3), Ga(1)—N(2) 1.900(2), Ga(1)—N(3) 2.017(2), Ga(1)—N(4) 2.012(3), Ga(2)—N(1) 1.895(2), Ga(2)—N(2) 1.876(3), Ga(2)—N(5) 2.005(3), Ga(2)—N(6) 2.030(3), C(1)—C(2) 1.392(4), C(27)—C(28) 1.407(5), Si(1)—N(1) 1.706(3), Si(2)—N(2) 1.706(3), N(1)—Ga(1)—N(2) 90.50(11), N(1)—Ga(1)—N(3) 126.11(11), N(1)—Ga(1)—N(4) 123.45(11), N(2)—Ga(1)—N(3) 113.58(10), N(2)—Ga(1)—N(4) 123.45(11), N(3)—Ga(1)—N(4) 83.62(11), N(1)—Ga(2)—N(2) 90.50(11), N(1)—Ga(2)—N(5) 121.91(10), N(1)—Ga(2)—N(6) 112.90(11), N(2)—Ga(2)—N(5) 123.95(11), N(2)—Ga(2)—N(6) 127.50(11), N(5)—Ga(2)—N(6) 83.50(11), Ga(1)—N(1)—Ga(2) 89.61(11), Ga(1)—N(2)—Ga(2) 89.30(11).

Other investigations into the reactivity of the digallane(4), **4**, met with limited success. The digallane(4), **4**, did not react with Bu^tCP, Bu^tOOBu^t or Bu^tNC. In contrast, the addition of MeCP to a diethyl ether solution of **4** gave an intractable mixture of products. No products could be isolated from the reactions of **4** with rubidium metal, propylene sulphide, $N_2CH(SiMe_3)$ or $[Yb(C{\equiv}CPh)_2]$. Addition of **4** to hexane solutions of $[CpCo(\eta^2\text{-}C_2H_4)_2]$, $[Cp^*Rh(\eta^2\text{-}C_2H_4)_2]$ or $[Pt(norbornene)_3]$ did not result in reactions, and the treatment of $[Cp_2MoH_2]$ or $[(\eta^6\text{-toluene})Rh(PPh_3)_2][BAr^F{}_4]$ with **4** gave intractable mixtures of products. Passing $N_2O_{(g)}$ through a hexane solution of **4** for 30 minutes resulted in the formation of the gallium(III) diradical product, **9**, in poor yield (Scheme 5). This outcome has parallels with the reaction of the digermyne, Ar"GeGeAr", with $N_2O_{(g)}$, which yielded a peroxide-bridged product, $[Ar"(OH)Ge(\mu^2\text{-}O)(\mu^2{:}\eta^2\text{-}O_2)Ge(OH)Ar"]$ **10**.[21] Although the exact mechanism of the formation of the **10** is unknown, the authors proposed that the reaction could go through a radical mechanism to form a [Ar"GeOOGeAr"] intermediate, which reacts further with $N_2O_{(g)}$, and subsequently abstracts a proton from the solvent to form the terminal hydroxy groups.[21] It is feasible that a similar process occurred in the formation of **9**, although in this case the most likely intermediates would be $[(\mu^2\text{-}O)_nGa\{[N(Ar)C(H)]_2^{\cdot}\}]_2$ (n = 1 or 2), following single electron oxidation of the heterocyclic ligands. These intermediates could react further with $N_2O_{(g)}$ and abstract two protons from the solvent to form the terminal hydroxyl groups.

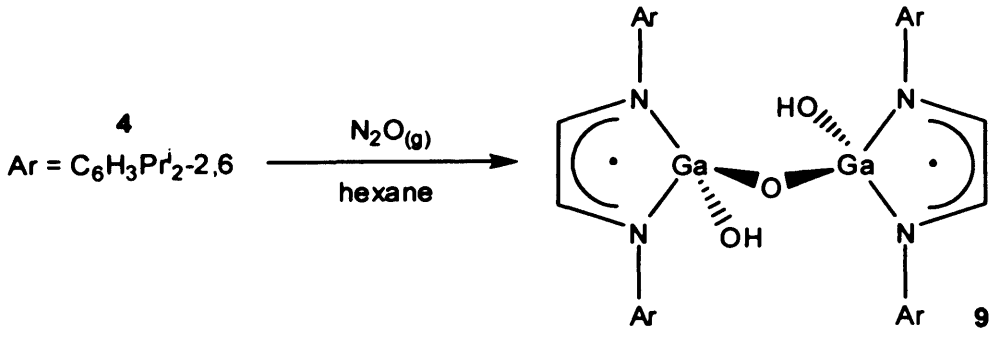

Scheme 5 – The synthesis of **9**

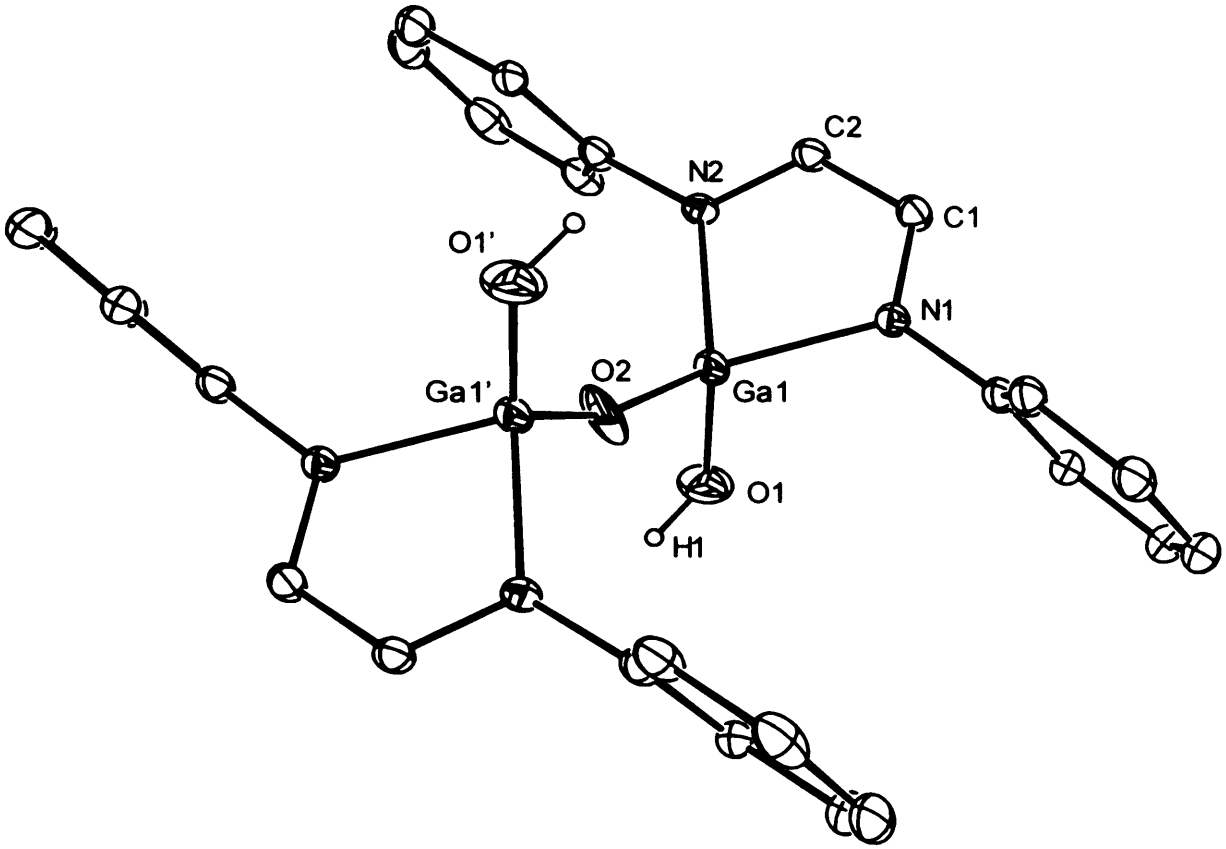

Figure 5 – Thermal ellipsoid plot (25 % probability surface) of the molecular structure of $[(\mu^2\text{-O})\{(HO)Ga\{[N(Ar)C(H)]_2^{\cdot}\}\}_2]$ **9**; hydrogen atoms and isopropyl groups (except H(1) and H(1')) omitted for clarity. Selected bond lengths (Å) and angles (°): Ga(1)—O(2) 1.706(16), Ga(1)—O(1) 1.812(4), Ga(1)—N(2) 1.964(3), Ga(1)—N(1) 1.965(3), N(1)—C(1) 1.325(5), N(2)—C(2) 1.327(5), C(1)—C(2) 1.395(6), N(2)—Ga(1)—N(1) 83.51(13), Ga(1)—O(2)—Ga(1') 157.5(8), C(1)—N(1)—Ga(1) 110.8(3), C(2)—N(2)—Ga(1) 110.7(3), N(1)—C(1)—C(2) 117.4(4), N(2)—C(2)—C(1) 117.5(4), symmetry operation ': $-x + 1, -y + 2, -z + 1$.

Useful ^1H and $^{13}C\{^1H\}$ NMR spectroscopic data could not be obtained for **9** due to the paramagnetic nature of this complex. An EPR spectrum of **9** was not recorded. A broad resonance was observed at 3601 cm^{-1} in its IR spectrum, corresponding to an O—H stretching absorption. This absorption is similar to that observed in the IR spectrum of the related complex, **10** (3621 cm^{-1}).[21] The crystal structure of **9** was obtained (Figure 5). The gallium centres display a distorted tetrahedral geometry. The

backbone C—C distance of **9** (1.395 Å mean) is elongated with respect to that observed in **4** (1.346 Å),[10] and is similar to that observed in **8** (1.400 Å mean). This provides evidence for the one electron oxidation of the heterocycle. The Ga—O distances in **9** (1.759 Å mean) are short but are within the known ranges (1.571 – 2.885 Å),[16] and are shorter than those observed in the related diamagnetic compounds, $[(IMes)_2H][(\mu^2\text{-}OH)\{HGa\{[N(Ar)C(H)]_2\}\}_2]$ (1.942 Å mean)[11] and $[K(tmeda)]_2[\{(\mu^2\text{-}O)Ga\text{-}\{[N(Ar)C(H)]_2\}\}_2]$ (1.860 Å mean).[24]

5.3.4 Investigations into the Preparation of Novel Gallium(I) Heterocyclic Compounds

Sterically bulky N-substituents are essential for the stabilisation of anionic group 13 metal(I) heterocycles such as **1**. Extra steric bulk could be incorporated in these heterocycles by adding substituents to the backbone carbon atoms. It was, therefore, our intention to prepare backbone substituted gallium(I) heterocycles with the bulky N-substituent, Ar ($C_6H_3Pr^i_2$-2,6) or the terphenyl, Ar''' (Ar''' = $C_6H_3(C_6H_4Bu^t\text{-}4)_2$-2,6). A similar synthetic route to that used in the preparation of **1** was chosen. In collaboration with G. A. Pierce, the appropriate diazabutadiene (DAB) was reacted with "GaI," which led to a one-electron reduction of the DAB ligand, which in concert with disproportion reactions, gave the paramagnetic gallium(III) complexes, **11** and **12**, in moderate yields (Scheme 6). It is of note that the terphenyl substituted DAB ligand has previously been used to prepare chiral C_2-symmetric transition metal complexes.[25] The reduction of **11** with an excess of potassium metal in THF led to the new anionic gallium(I) heterocyclic complex, **13**, in good yield (Scheme 6). Unfortunately, a similar reduction of **12** led only to an intractable mixture of products for unknown reasons. It is worthy of note that

the reduction of **11** with calcium metal has previously been reported to give the first calcium-gallyl complex, $[Ca(THF)_4\{Ga\{[N(Ar)C(Me)]_2\}\}_2]$.[26]

We have previously shown that **1** can be readily oxidatively coupled in its reaction with the ferrocenium cation to give the digallane(4), **4**.[9] Considering this, and the scarcity of related digallane(4) compounds, the oxidative coupling of the anionic heterocycle of [K(tmeda)][**13**] by its treatment with Tl_2SO_4 was carried out and led to the new digallane(4), **14**, in moderate yield (NB: Treatment of [K(tmeda)][**13**] with the ferrocenium ion also gives **14**) (Scheme 6). This route is favourable to that employing the ferrocenium cation as both by-products, thallium metal and K_2SO_4, are insoluble in hexane and are easily filtered off from the reaction mixture.

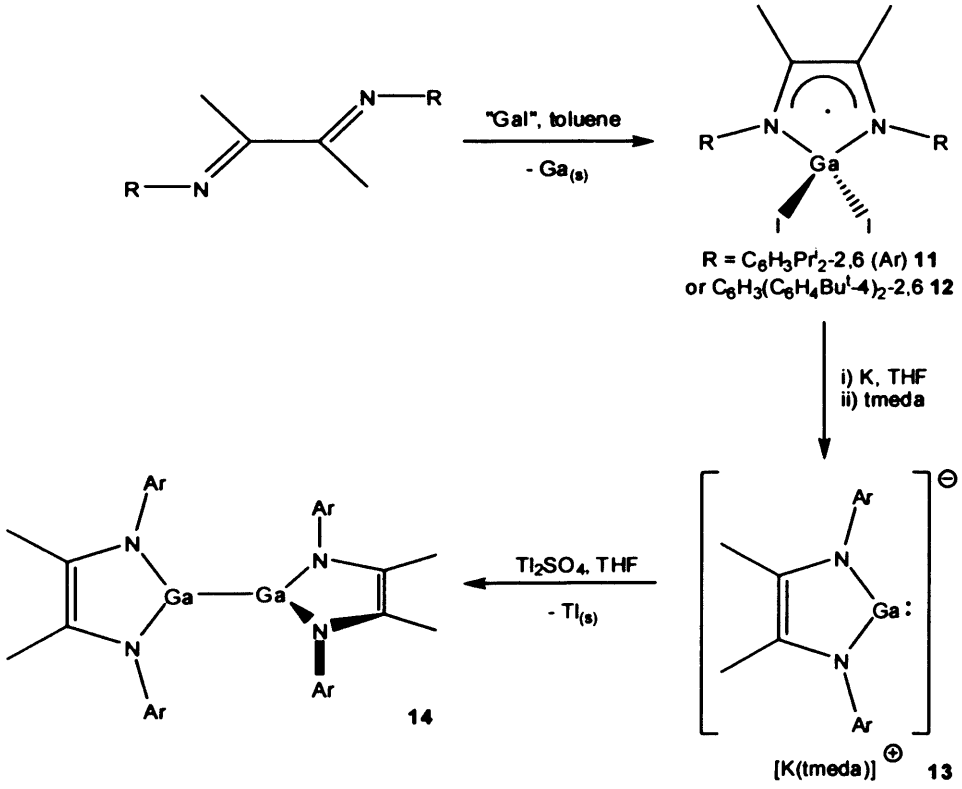

Scheme 6 – The synthesis of **11** – **14**

As **11** and **12** are paramagnetic, no meaningful ^1H and $^{13}C\{^1H\}$ NMR spectroscopic data could be obtained for these complexes. They were, however, examined by solution state EPR spectroscopy at 120 K and 300 K by Dr. D. M.

Murphy, but all resultant spectra revealed broad, unresolved signals, as has been seen before for similar complexes.[5,6] The g-values determined for both complexes (**11** 2.0025, **12** 2.0015) are close to free spin (g = 2.0023), which indicates the essentially organic nature of both radicals. As the ^{1}H and $^{13}C\{^{1}H\}$ NMR spectra of [K(tmeda)][**13**] and **14** are consistent with their solid state structures and are similar to those of the equivalent potassium salt of **1**[6] and the digallane(4), **4**,[10] respectively, no comment will be made here.

The X-ray crystal structures of **11**, **12** and **14** were obtained and are depicted in Figures 7 – 9 respectively. That for **11** is effectively structurally analagous with its backbone H-substituted counterpart, $[I_2Ga\{[N(Ar)C(H)]_2\}]$,[5] and as in that compound the bond lengths within the N_2C_2 fragment are suggestive of significant delocalisation. The structure of **12** shows it to have a similarly delocalised DAB ligand with Ga—I and Ga—N bond lengths close to those observed in **11**. The complex is, however, chiral (existing as both enantiomers in the crystal) in that it has a C_2 symmetric coordination geometry due to the repulsive interactions between the sterically demanding terphenyl substituents. A similar situation exists for the $PdCl_2$ complex of this DAB ligand.[25] The structure of **14** is very similar to that of **4**,[10] and as in that compound the bond lengths within the DAB fragment are indicative of localised C—C double and N—C single bonds, *cf.* the DAB delocalisation in **11**. As the Ga—N bonds in **14** are covalent, they are significantly shorter than the formally dative Ga—N bonds in **11**, despite the higher oxidation state metal centre in the latter. The Ga—Ga distance is in the normal range[16] and close to that observed in **4** (2.3482 Å),[10] whilst the two heterocycle least squares planes bisect each other with an angle of 43.4°.

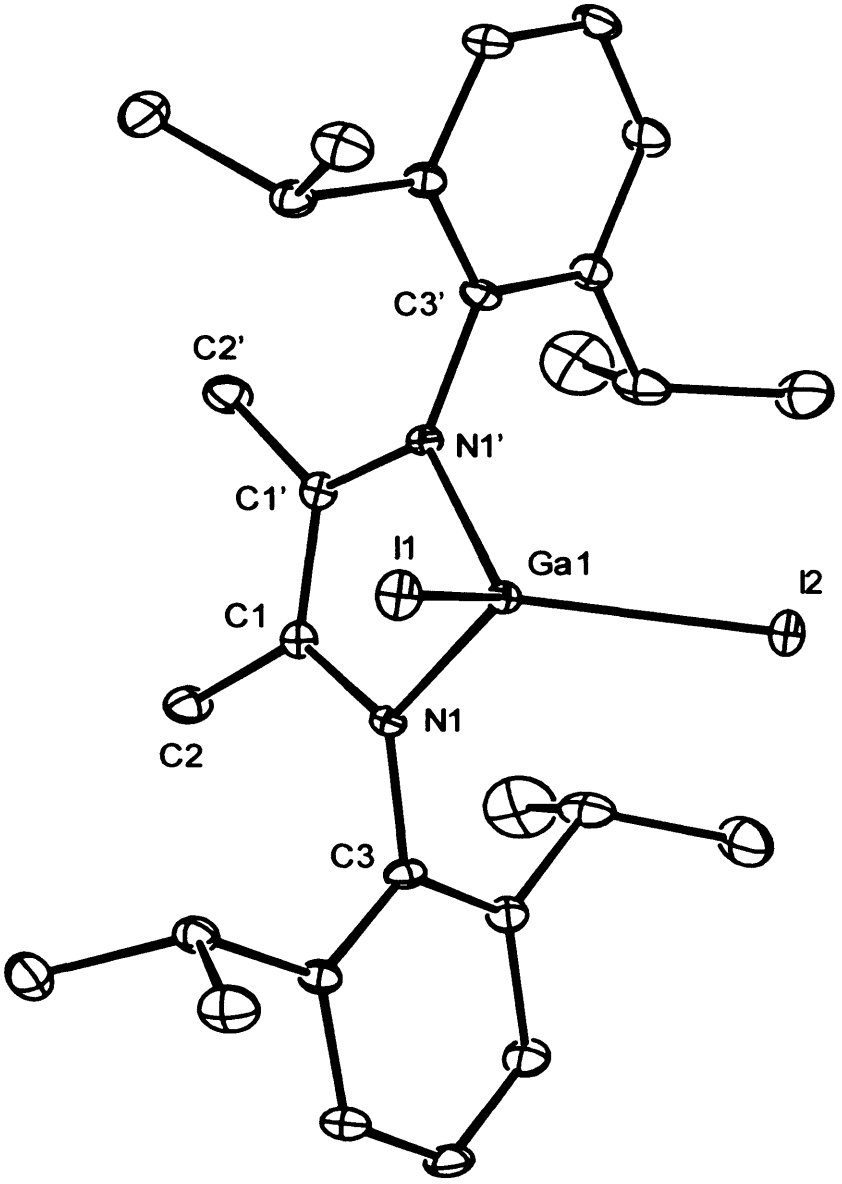

Figure 7 – Thermal ellipsoid plot (25 % probability surface) of the molecular structure of $[I_2Ga\{[N(Ar)C(Me)]_2\}]$ **11**; hydrogen atoms omitted for clarity. Selected bond lengths (Å) and angles (°): I(1)—Ga(1) 2.5343(8), I(2)—Ga(1) 2.4949(8), Ga(1)—N(1) 1.929(3), N(1)—C(1) 1.353(4), C(1)—C(1') 1.410(7), N(1')—Ga(1)—N(1) 85.72(17), N(1)—Ga(1)—I(2) 117.05(9), N(1)—Ga(1)—I(1) 113.04(9), I(2)—Ga(1)—I(1) 109.37(2), symmetry operation ': x, $-y + 3/2$, z.

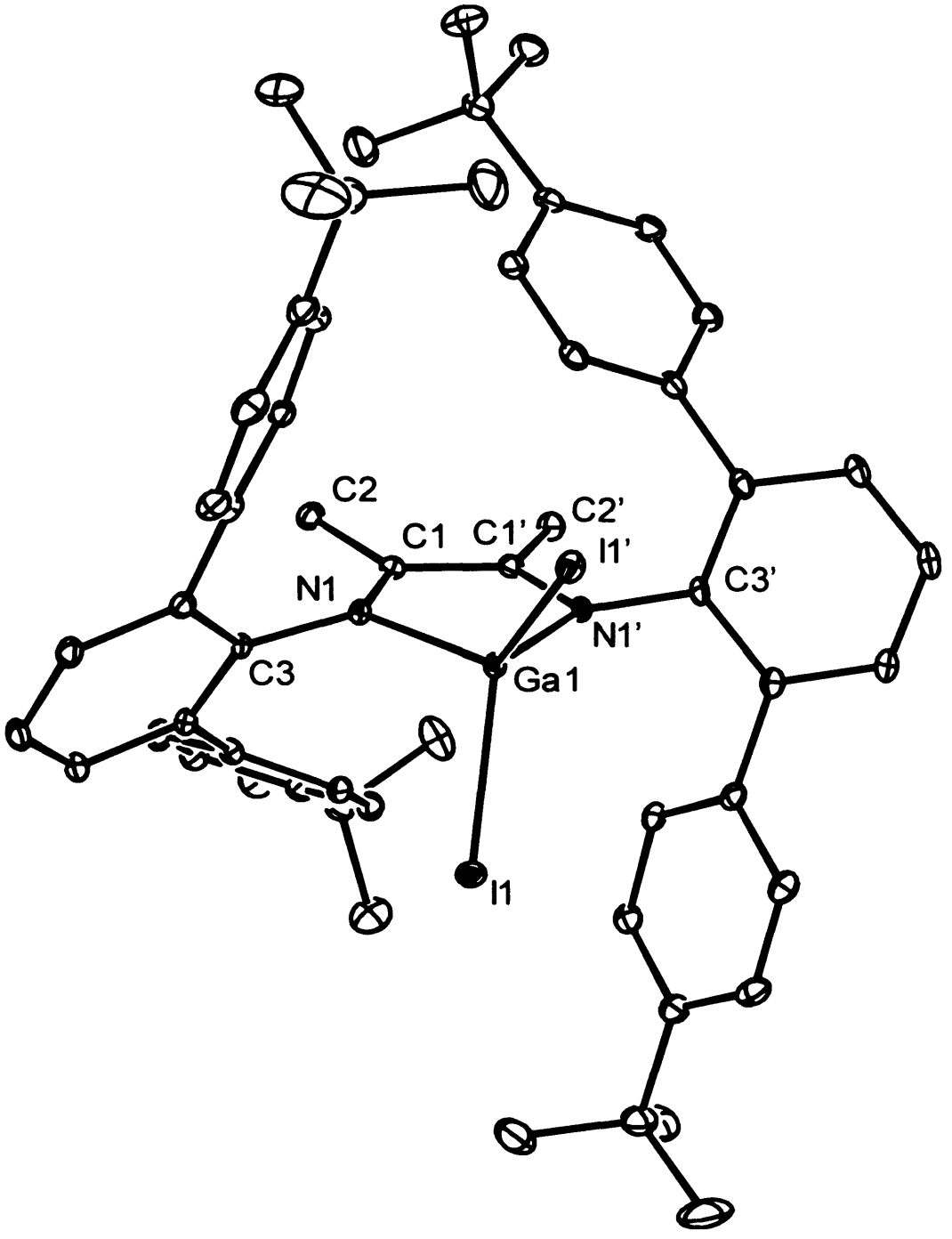

Figure 8 – Thermal ellipsoid plot (25 % probability surface) of the molecular structure of $[I_2Ga\{[N(Ar''')C(Me)]_2\}]$ **12**; hydrogen atoms omitted for clarity. Selected bond lengths (Å) and angles (°): I(1)—Ga(1) 2.5205(6), Ga(1)—N(1) 1.939(3), N(1)—C(1) 1.341(5), N(1)—C(3) 1.437(4), C(1)—C(1') 1.422(7), N(1')—Ga(1)—N(1) 84.79(18), N(1)—Ga(1)—I(1') 122.12(9), N(1)—Ga(1)—I(1) 108.61(9), I(1')—Ga(1)—I(1) 109.66(3) symmetry operation ': $-x + 1, y, -z + 3/2$.

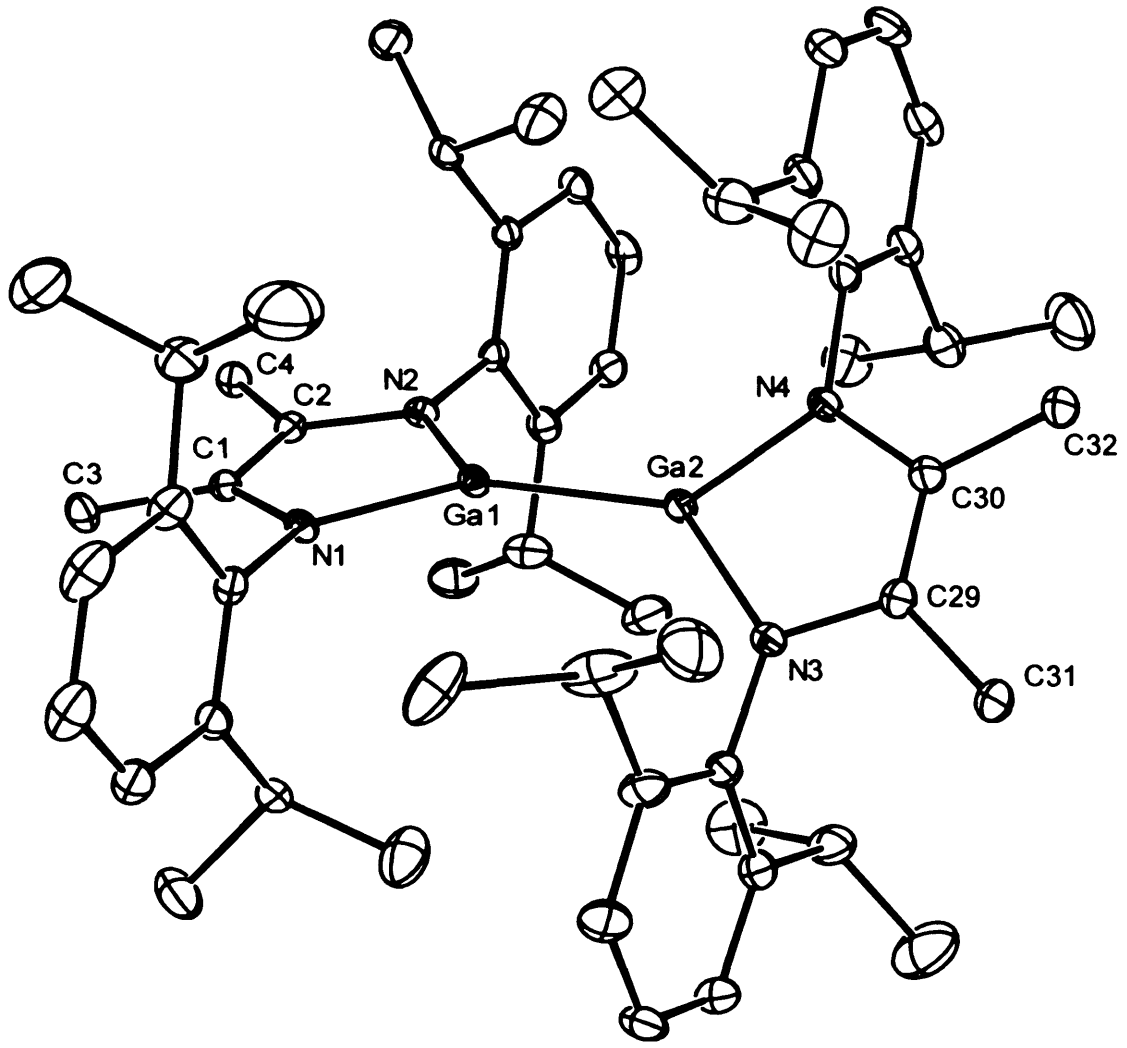

Figure 9 – Thermal ellipsoid plot (25 % probability surface) of the molecular structure of $[Ga\{[N(Ar)C(Me)]_2\}]_2$ **14**; hydrogen atoms omitted for clarity. Selected bond lengths (Å) and angles (°): Ga(1)—N(1) 1.847(4), Ga(1)—N(2) 1.854(4), Ga(1)—Ga(2) 2.3634(9), Ga(2)—N(3) 1.842(5), Ga(2)—N(4) 1.847(5), N(1)—C(1) 1.404(7), N(2)—C(2) 1.408(7), N(3)—C(29) 1.420(8), N(4)—C(30) 1.403(8), N(1)—Ga(1)—N(2) 88.3(2), N(1)—Ga(1)—Ga(2) 136.94(14), N(2)—Ga(1)—Ga(2) 134.70(14), N(3)—Ga(2)—N(4) 88.5(2).

The 1,2-phenylenediamide ligand, $[C_6H_4\{N(CH_2Bu^t)\}_2\text{-}1,2]^{2-}$, has been employed by Lappert and co-workers in the stabilisation of the heavier group 14 NHC analogues, $[:E\{C_6H_4\{N(CH_2Bu^t)\}_2\text{-}1,2\}]$ (E = Si **15**,[27] Ge **16**,[28] Sn **17**,[29] or Pb[28] **18**). The germanium(II) compound, **16**, was synthesised by the salt metathesis reaction of

$[GeCl_2(dioxane)]$ with the dilithiated precursor, $[C_6H_4\{NLi(CH_2Bu^t)\}_2\text{-}1,2]$.[28] As the digallane(4), $[Ga\{[N(Bu^t)C(H)]_2\}]_2$, has been synthesised from a similar salt metathesis reaction of $[Ga_2Cl_4(dioxane)_2]$ with two equivalents of $[\{LiN(Bu^t)CH\}_2]$,[30] it was envisaged that the treatment of $[C_6H_4\{NLi(CH_2Bu^t)\}_2\text{-}1,2]$ with 0.5 equivalents of $[Ga_2Cl_4(dioxane)_2]$ could yield the digallane(4), $[Ga\{C_6H_4[N(CH_2Bu^t)]_2\text{-}1,2\}]_2$, but the salt, **19**, formed in poor yield (Scheme 7). The mechanism of this reaction is unknown, but presumably it proceeds by salt metathesis and a disproportionation process at the gallium centre.

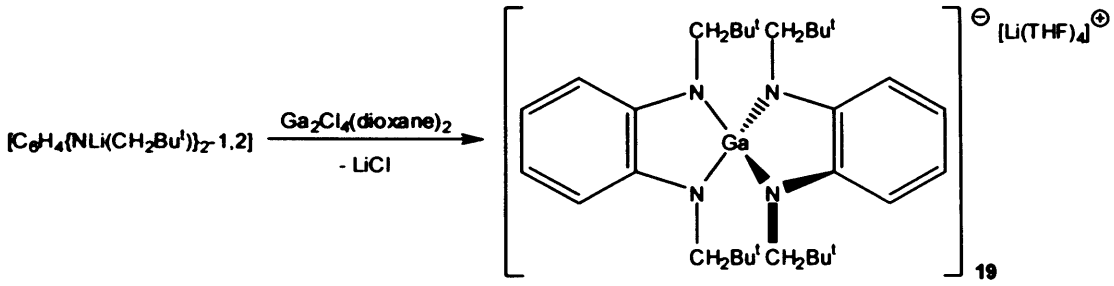

Scheme 7 – The synthesis of **19**

In the first step of the preparation of the gallium(I) NHC analogue, $[Ga\{[N(Bu^t)C(H)]_2\}]^-$, Schmidbaur and co-workers reacted $GaCl_3$ with $[\{LiN(Bu^t)CH\}_2]$ to give a (chloro)galla-imidazole.[31] In contrast, the reaction of $GaCl_3$ with $[C_6H_4\{NLi(CH_2Bu^t)\}_2\text{-}1,2]$ gave an intractable mixture of products. Monolithiation of $[C_6H_4\{NH(CH_2Bu^t)\}_2\text{-}1,2]$ with Bu^nLi, followed by treatment with two equivalents of $GaCl_3$, yielded the novel gallium(III) complex, **20** (Scheme 8). A related product, $[Cl_2Ga\{[N(Bu^t)CH_2CH_2NH(Bu^t)]\}]$, **21**, was previously obtained in the reaction of $[NaN(Bu^t)CH_2CH_2NH(Bu^t)]$ with $GaCl_3$.[32] In an attempt to form the desired gallium(II) product, **20** was treated with DBU (1,8-diazabicyclo[5.4.0]undec-7-ene), but only an intractable mixture of products resulted.

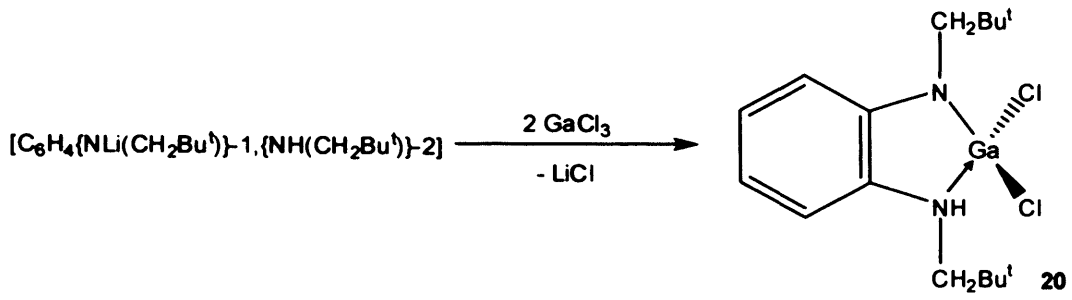

Scheme 8 – The synthesis of **20**

The ^{1}H and $^{13}C\{^{1}H\}$ NMR spectra of **19** and **20** are consistent with their solid state structures and are comparable to those of the related group 14 complexes, **15** – **18**.[27-29] As would be predicted, the ^{1}H and $^{13}C\{^{1}H\}$ NMR spectra for **20** are unsymmetrical. A characteristic broad and strong absorption at 3229 cm^{-1} was observed in the IR spectrum of **20**, corresponding to an N—H stretch.

The X-ray crystal structures of **19** and **20** were obtained (Figures 10 and 11). Both complexes display a distorted tetrahedral geometry about their gallium centres. The structural parameters of the anion of **19** are comparable with the related complex, $[K(DME)_4][Ga\{[N(Ar)C(H)]_2\}_2]$ **22**.[33] In the solid state structure of **19**, the two heterocycle least squares planes bisect each other with an angle of 66.1°, which is much less than the corresponding value observed in **22** (77.2°).[33] This is most likely due to increased steric buttressing in the latter. The Ga—Cl distances in **20** (2.160 Å mean) are similar to those observed in **21** (2.193 Å mean).[32] The protonated N-centre in **20** displays a much greater Ga—N distance than the other N-centre in the heterocyclic ring, as would be expected (Ga—N = 1.875 and 2.000 Å). Similar differences between the Ga—N distances were observed in the molecular structure of **21** (Ga—N = 1.842 and 2.020 Å).[32] The backbone C—C distances in **19** (1.437 Å mean) and **20** (1.410 Å) are much longer than the C=C distance observed in **22** (1.334 Å mean),[33] but are comparable with those in **15** – **18**.[27-29]

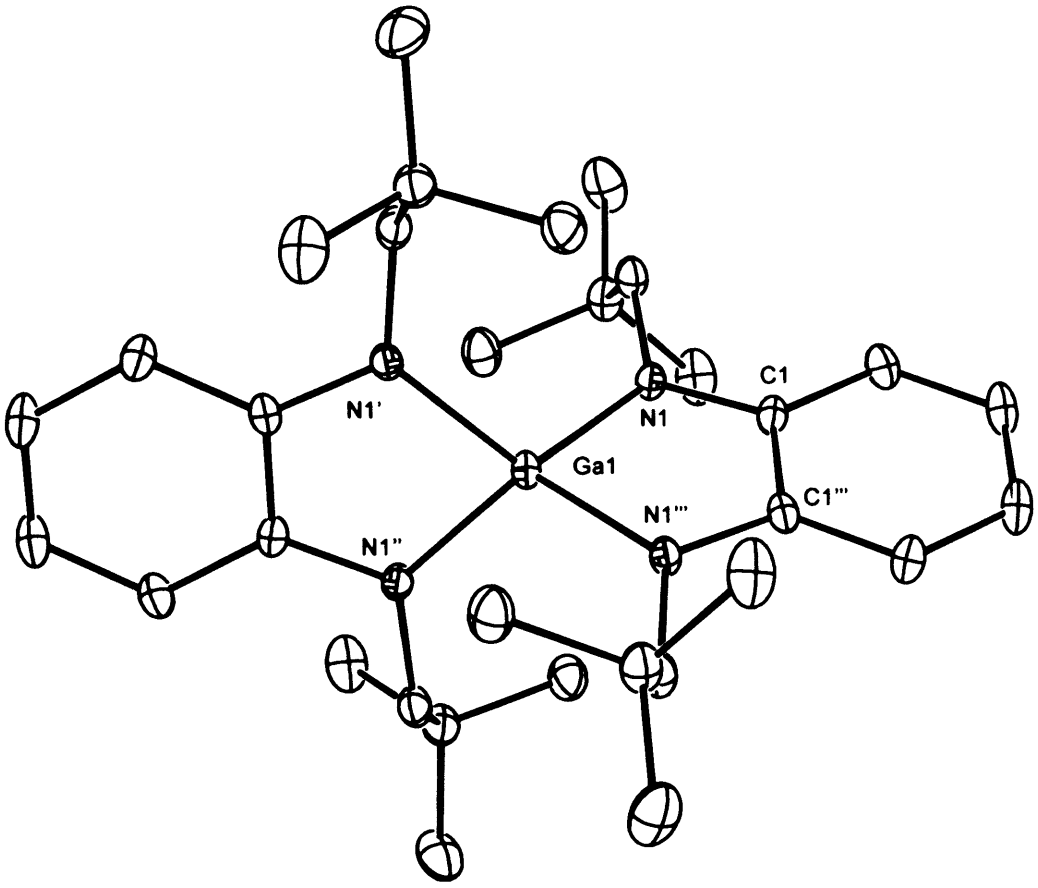

Figure 10 – Thermal ellipsoid plot (25 % probability surface) of the structure of the anionic component of $[Li(THF)_4][Ga\{C_6H_4[N(CH_2Bu^t)]_2\text{-}1,2\}_2]$ **19**; hydrogen atoms omitted for clarity. Selected bond lengths (Å) and angles (°): Ga(1)—N(1) 1.898(3), Ga(1)—N(1') 1.898(3), Ga(1)—N(1") 1.898(3), Ga(1)—N(1'") 1.898(3), N(1)—C(1) 1.391(4), C(1)—C(1'") 1.437(7), N(1)—Ga(1)—N(1') 111.06(17), N(1)—Ga(1)—N(1") 133.22(15), N(1')—Ga(1)—N(1") 87.47(16), N(1)—Ga(1)—N(1'") 87.47(16), N(1')—Ga(1)—N(1'") 133.22(15), N(1")—Ga(1)—N(1'") 111.06(17), C(1)—N(1)—Ga(1) 111.0(2), N(1)—C(1)—C(2) 126.6(3), symmetry operation ': $-x + 1/2, -y + 3/2, z$, symmetry operation ": $x, -y + 3/2, -z + 3/2$, symmetry operation '": $-x + 1/2, y, -z + 3/2$.

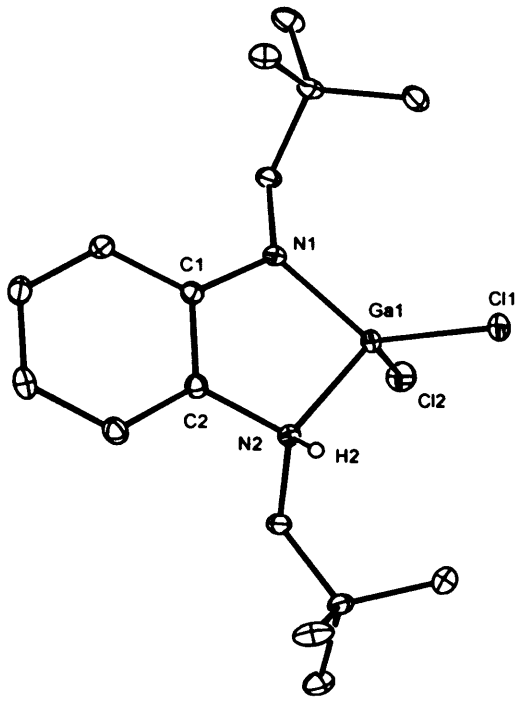

Figure 11 – Thermal ellipsoid plot (25 % probability surface) of the molecular structure of $[Cl_2Ga\{C_6H_4[N(CH_2Bu^t)]$-1-$[NH(CH_2Bu^t)]-2\}]$ **20**; hydrogen atoms (except H(2)) omitted for clarity. Selected bond lengths (Å) and angles (°): Ga(1)—N(1) 1.8748(16), Ga(1)—N(2) 2.0002(16), Ga(1)—Cl(2) 2.1570(9), Ga(1)—Cl(1) 2.1632(7), N(1)—C(1) 1.391(2), C(1)—C(2) 1.410(3), N(2)—C(2) 1.471(2), N(1)—Ga(1)—N(2) 89.75(7), Cl(2)—Ga(1)—Cl(1) 110.79(3), C(1)—N(1)—Ga(1) 110.62(12), N(1)—C(1)—C(2) 118.09(16), C(2)—N(2)—Ga(1) 104.44(11), C(1)—C(2)—N(2) 117.07(16).

5.4 Conclusion

The reactivity of "GaI" has been investigated and the novel heterocycle, $[GaI_2\{C(Bu^t)P(H)C(Bu^t)=P\}]_2$, has been synthesised in this study. The oxidation chemistry of the heterocycle, $[:Ga\{[N(Ar)C(H)]_2\}]^-$, has been investigated and the novel gallium hydride complex, $[\{N(Ar)C(H)N(Ar)K\}(H)Ga\{[N(Ar)C(H)]_2\}]$, has been fully characterised. The reactivity of the Ga—Ga bond of the digallane(4), $[Ga\{[N(Ar)C(H)]_2\}]_2$, has been exploited in the synthesis of the dimeric imido-gallane complex, $[\{\mu\text{-}N(SiMe_3)\}Ga\{[N(Ar)C(H)]_2\cdot\}]_2$, which can be considered to be a dimer of

the gallium-terminal imide, $[(SiMe_3)N{=}Ga\{[N(Ar)C(H)]_2^{\cdot}\}]$. The syntheses of several novel gallium (I), (II) and (III) heterocycles have also been reported. EPR spectroscopy has shown that the unpaired electron of all paramagnetic complexes investigated is primarily based on their diazabutadiene ligands. Some of the work discussed in this chapter has been summarised in recent publications.[34-36]

5.5 Experimental

General experimental procedures are compiled in Appendix 1 and crystallographic data are compiled in Appendix 3. The continuous wave (cw) EPR spectra were recorded by Dr. D. M. Murphy on an X-Band Bruker ESP 300E series spectrometer, operating at 12.5 kHz field modulation in a Bruker EN 801 cavity. Computer simulations were carried out by Dr. D. M. Murphy using Bruker's Simfonia program.[37] "GaI",[1] [K(tmeda)][**1**],[6] $[Ga\{[N(Ar)C(H)]_2\}]_2$,[10] FisoH,[38] $[Ga_2Cl_4(dioxane)_2]$[39] and $[C_6H_4\{NLi(CH_2Bu^t)_2\}_2\text{-}1,2]$[40] were prepared by literature procedures. $[C_6H_4\{NLi(CH_2Bu^t)\}\text{-}1\text{-}\{NH(CH_2Bu^t)\}\text{-}2]$ was synthesised by a modification of the literature procedure.[40] $[Sn(\eta^4\text{-}P_2C_2Bu^t_2)]$[41] was donated by Dr. M. D. Francis, $[(Fiso)_2SmCl(THF)_{0.33}]$ was donated by Dr. J. Wang (Monash University), and $\{N(Ar)C(Me)\}_2$[42] and $\{N(Ar''')C(Me)\}_2$[25] were prepared by G. A. Pierce. All other reagents were used as received.

Preparation of $[GaI_2\{C(Bu^t)P(H)C(Bu^t){=}P\}]_2$ 6: A solution of $[:Sn(\eta^4\text{-}P_2C_2Bu^t_2)]$ (0.20 g, 0.63 mmol) in toluene (20 cm^3) was added over 10 minutes to a suspension of "GaI" (0.50 g, 2.50 mmol) in toluene (25 cm^3) at -78 °C. The reaction mixture was warmed to 20 °C overnight, with tin metal being deposited. Volatiles were then removed *in vacuo* and the residue was washed with hexane (40 cm^3) and extracted into

toluene (20 cm^3) and filtered. The filtrate was concentrated to *ca.* 10 cm^3 and stored at -30 °C overnight to give pale yellow crystals of **6** (0.03 g, 8 %). Mp 208 °C (decomp.); ^{1}H NMR (400 MHz, d_8-THF, 298 K): δ 1.13 (s, 18 H, $(CH_3)_3C$), 1.31 (s, 18 H, $(CH_3)_3C$), 6.54 (dd, $^1J_{PH}$ = 170.0 Hz, $^3J_{PH}$ = 20.4 Hz, 2 H, P*H*); $^{13}C\{^1H\}$ NMR (75.6 MHz, d_8-THF, 298 K): δ 29.6 (m, $(CH_3)_3C$), 36.3 (m, $(CH_3)_3C$), 39.8 (overlapping m, $(CH_3)_3C$), 266.5 (apparent t, $^1J_{PC}$ = $^1J_{PC}$ = 22 Hz, *C*=P), *C*Ga not observed; ^{31}P NMR (121.66 MHz, d_8-THF, 298 K): δ -11.0 (d, $^2J_{PP}$ = 41.9 Hz, $^1J_{PH}$ = 170.0 Hz, *P*H), 366.6 (dd, $^2J_{PP}$ = 41.9 Hz, $^3J_{PH}$ = 20.4 Hz, *P*=C); MS (EI 70 eV), *m/z* (%): 101 ($PCBu^tH^+$, 41), 70 (CBu^tH^+, 62); IR ν/cm^{-1} (Nujol): 1633 m, 1110 m, 940 m, 809 s.

Preparation of [{N(Ar)C(H)N(Ar)K}(H)Ga{[N(Ar)C(H)]$_2$}] 7: A solution of [K(tmeda)][:Ga{[N(Ar)C(H)]$_2$}] (0.30 g, 0.49 mmol) in THF (10 cm^3) was added to a solution of FisoH (0.18 g, 0.49 mmol) in THF (10 cm^3) at -78 °C. The orange reaction mixture was warmed to 20 °C and stirred for 1 hr. Volatiles were then removed *in vacuo* and the residue was extracted into toluene (50 cm^3) and filtered. The filtrate was concentrated to *ca.* 5 cm^3 and stored at -30 °C overnight to give pale yellow crystals of **7**. A second crop was obtained (0.11 g, 26 %). Mp 171-173 °C (decomp.); ^{1}H NMR (200 MHz, C_6D_6, 298 K): δ 1.02-1.67 (m, 48 H, $(CH_3)_2CH$), 3.21 (sept., $^3J_{HH}$ = 6.8 Hz, 2 H, $(CH_3)_2CH$ Fiso), 3.51 (sept., $^3J_{HH}$ = 6.5 Hz, 6 H, $(CH_3)_2CH$), 7.02-7.25 (m, 14 H, NC*H* and Ar-*H*), Ga-*H* not observed; MS (APCI), *m/z* (%): 445 ($Ga\{N(Ar)C(H)\}_2H^+$, 100), 377 ($\{N(Ar)C(H)\}_2H^+$, 75) 363 ($\{[N(Ar)]_2CH\}H^+$, 63); IR ν/cm^{-1} (Nujol): 1878 br., s (Ga—H), 1665 s, 1595 s, 1563 s, 1354 s, 1316 m, 1256 m, 1210 m, 1100 m, 757 m.

Preparation of [{μ-N(SiMe$_3$)}Ga{[N(Ar)C(H)]$_2$}]$_2$ 8: Excess N_3-$SiMe_3$ (0.40 cm^3) was added to a solution of [Ga{[N(Ar)C(H)]$_2$}]$_2$ (0.32 g, 0.34 mmol) in hexane (30 cm^3)

at -78 °C. The reaction mixture was warmed to 20 °C and stirred for 48 hrs, during which time the colour changed from red to deep purple. This solution was then concentrated to *ca.*10 cm^3, filtered and stored at -30 °C overnight to give blue-green crystals of **8** (0.29 g, 79 %). Mp 182-186 °C (decomp.); MS (APCI), *m/z* (%): 377 ($\{N(Ar)C(H)\}_2H^+$, 100); IR ν/cm^{-1} (Nujol): 1455 s, 1376 s, 1260 m, 1223 w, 1096 s, 964 s, 799 m, 754 m.

Preparation of $[(\mu^2\text{-}O)\{(HO)Ga\{[N(Ar)C(H)]_2\}\}_2]$ 9: $N_2O_{(g)}$ was bubbled through a solution of $[Ga\{[N(Ar)C(H)]_2\}]_2$ (0.25 g, 0.28 mmol) in hexane (20 cm^3) for 30 minutes to give a deep red reaction mixture. Volatiles were then removed *in vacuo* and the residue was extracted into hexane (20 cm^3) and filtered. The filtrate was concentrated to *ca.* 5 cm^3 and stored at -30 °C overnight to give pale yellow blocks of **9** (0.03 g, 12 %). Mp 88-90 °C; MS (EI 70eV) *m/z* (%): 377 ($\{N(Ar)C(H)\}_2H^+$, 18), 333 ($\{N(Ar)C(H)\}_2H^+$ -Pr^i, 100); IR ν/cm^{-1} (Nujol): 3601 (br., OH), 1626 m, 1591 m, 1363 m, 1327 m, 1261 m, 1100 m, 800 m, 758 m.

Preparation of $[I_2Ga\{[N(Ar)C(Me)]_2\}]$ 11: A solution of $\{N(Ar)C(Me)\}_2$ (2.90g, 7.2 mmol) in toluene (20 cm^3) was added to a suspension of "GaI" (2.86 g, 14.3 mmol) in toluene (80 cm^3) at -78 °C. The reaction mixture was warmed to 20 °C and stirred for 48 hrs to yield a dark brown solution. Volatiles were then removed *in vacuo* and the residue was extracted into THF (50 cm^3) and filtered. The filtrate was stored at -30 °C overnight to give orange-brown crystals of **11** (2.25 g, 43 %). Mp 195-197 °C; MS (APCI), *m/z* (%): 727 (MH^+, 11), 599 (MH^+ -I, 100), 472 (MH^+ -2I, 10); IR (Nujol) ν/cm^{-1}: 1627 m, 1464 m, 1377 s, 1358 s; APCI acc. mass on M^+: calc. for $C_{28}H_{40}N_2I_2Ga$: 727.0531, found 727.0529.

Preparation of $[I_2Ga\{[N(Ar''')C(Me)]_2\}]$ ($Ar''' = C_6H_3(C_6H_4Bu^t\text{-}4)_2\text{-}2,6$) 12: A solution of $\{N(Ar''')C(Me)\}_2$ (0.22 g, 0.28 mmol) in toluene (20 cm^3) was added to a suspension of "GaI" (0.57 g, 2.85 mmol) in toluene (80 cm^3) at -78 °C. The reaction mixture was warmed to 20 °C and stirred for 48 hrs to yield a dark brown solution. Volatiles were then removed *in vacuo* and the residue was extracted into diethyl ether (10 cm^3) and filtered. The filtrate was stored at -30 °C overnight to give red crystals of **12** (0.11 g, 36 %). Mp 215-218 °C; MS (EI 70 eV), *m/z* (%): 1088 (MH^+, 4), 961 (MH^+ - I, 100); IR (Nujol) ν/cm^{-1}: 1624 m, 1465 m, 1377 s, 1361 s; $C_{56}H_{64}N_2GaI_2$ requires C 61.78, H 5.93, N 2.57; found C 61.08, H 5.78, N 2.49.

Preparation of $[K(tmeda)][:Ga\{[N(Ar)C(Me)]_2\}]$ 13: A solution of $[I_2Ga\{[N(Ar)C(Me)]_2\}]$ (1.65g, 2.27 mmol) in THF (110 cm^3) was added to a potassium mirror at -78 °C. The reaction mixture was stirred for 120 hours and filtered. Volatiles were then removed *in vacuo*. Diethyl ether (10 cm^3) and tmeda (5 cm^3) were added to the residue and the mixture was stirred for 1 hour. Volatiles were then removed *in vacuo* and the residue was extracted into hexane (40 cm^3) and filtered. The filtrate was stored at -30 °C overnight to give **13** as an orange solid (0.76 g, 54 %); Mp 144-150°C; ^1H NMR (400 MHz, C_6D_6, 298 K): δ 1.33 (d, $^3J_{HH}$ = 6.8 Hz, 12H, $(CH_3)_2CH$), 1.38 (d, $^3J_{HH}$ = 6.8 Hz, 12H, $(CH_3)_2CH$), 1.98 (s, 12H, NCH_3), 2.11 (s, 6H, CH_3), 2.15 (s, 4H, NCH_2), 3.87 (sept, $^3J_{HH}$ = 6.8 Hz, 4H, $(CH_3)_2CH$), 7.15 (t, $^3J_{HH}$ = 6.8 Hz, 2H, *p*-Ar-*H*), 7.24 (d, $^3J_{HH}$ = 6.8 Hz, 4H, *m*-Ar-*H*); $^{13}C\{^1H\}$ NMR (75.6 MHz, C_6D_6, 298 K): δ 15.7 (CH_3), 23.4 ($(CH_3)_2CH$) , 26.8 ($CH_3)_2CH$), 27.3 ($(CH_3)_2CH$), 45.3 (NCH_3), 57.4 (NCH_2), 121.1 (*C*N), 122.5 (*m*-Ar-*C*), 123.0 (*p*-Ar-*C*)), 146.4 (*o*-Ar-*C*), 148.8 (*ipso*-Ar-*C*); MS (EI 70 eV), *m/z* (%): 405 ($\{N(Ar)C(Me)\}_2H^+$, 100); IR (Nujol) ν/cm^{-1}: 1586 s, 1558 m, 1260 s, 1096 s, 933 m.

Preparation of [Ga{[N(Ar)C(Me)]$_2$}]$_2$ 14: Tl_2SO_4 (0.28 g, 0.55mmol) was added to a solution of [K(tmeda)][:Ga{[N(Ar)C(Me)]$_2$}] (0.34 g, 0.56 mmol) in THF (20 cm^3) at 20 °C. The reaction mixture was stirred for 120 hours to yield a purple/red solution. Volatiles were then removed *in vacuo* and the residue was extracted into diethyl ether (40 cm^3) and filtered. The filtrate was concentrated to *ca.* 20 cm^3 and stored at -30 °C overnight to yield deep red crystals of **14** (0.09 g, 34 %); Mp 123-126°C; ^{1}H NMR (400 MHz, C_6D_6, 298 K): δ 1.19 (d, $^3J_{HH}$ = 6.8 Hz, 24H, (C*H*$_3$)$_2$CH), 1.30 (d, $^3J_{HH}$ = 6.8 Hz, 24H, (C*H*$_3$)$_2$CH), 1.75 (s, 12H, C*H*$_3$), 3.27 (sept, $^3J_{HH}$ = 6.8 Hz, 8H, (CH$_3$)$_2$C*H*), 7.18-7.26 (m, 12H, Ar-*H*); ^{13}C{^{1}H} NMR (75.6 MHz, C_6D_6, 298 K): δ 14.4 (*C*H$_3$), 23.0 ((*C*H$_3$)$_2$CH), 25.4 ((*C*H$_3$)$_2$CH), 28.0 ((CH$_3$)$_2$*C*H), 123.1 (*C*N), 126.2 (*m*-Ar-*C*), 135.0 (*p*-Ar-*C*), 142.6 (*o*-Ar-*C*), 145.4 (*ipso*-Ar-*C*); MS (EI 70 eV), *m/z* (%): 405 ({N(Ar)C(Me)}$_2$H$^+$, 100); IR (Nujol) ν/cm^{-1}: 1652 m, 1459 m, 1376 s; $C_{112}H_{128}N_4Ga_2$ requires C 80.57, H 7.73, N 3.36; found C 79.92, H 7.64, N 3.28.

Preparation of [Li(THF)$_4$][Ga{C$_6$H$_4$[N(CH$_2$Bu^t)]$_2$-1,2}$_2$] 19: A solution of [Ga$_2$Cl$_4$(dioxane)$_2$] (0.51 g, 1.16 mmol) in THF (10 cm^3) was added to a solution of [C$_6$H$_4${NLi(CH$_2$Bu^t)$_2$}$_2$-1,2] (0.60 g, 2.32 mmol) in THF (30 cm^3) at -78 °C. The reaction mixture was warmed to 20 °C and stirred for 1 hr to yield a red solution. Volatiles were then removed *in vacuo* and the residue was washed with hexane (20 cm^3) and extracted into diethyl ether (60 cm^3) and filtered. The filtrate was concentrated to *ca.* 5 cm^3 and stored at -30 °C overnight to give colourless crystals of **19** (0.07 g, 7 %). Mp > 300 °C; ^{1}H NMR (200 MHz, C_6D_6, 298 K): δ 0.89 (s, 36 H, (C*H*$_3$)$_3$C), 1.41 (br. m, 16 H, C*H*$_2$), 2.67 (s, 4 H, (CH$_3$)$_2$CC*H*$_2$), 2.70 (s, 4 H, (CH$_3$)$_2$CC*H*$_2$), 3.69 (br. m, 16 H, C*H*$_2$O), 6.74 (dd, $^3J_{HH}$ = 5.8 Hz, $^4J_{HH}$ = 3.5 Hz, 4 H, 3,6-Ar-*H*), 6.99 (m, 4 H, 4,5-Ar-*H*); ^{13}C{^{1}H} NMR (75.6 MHz, C_6D_6, 298 K): δ 25.8 (*C*H$_2$), 28.4 ((*C*H$_3$)$_3$C), 31.4 ((CH$_3$)$_3$*C*), 56.7 ((CH$_3$)$_3$*C*CH$_2$), 67.8 (*C*H$_2$O), 113.2 (3,6-Ar-*C*), 120.0 (4,5-Ar-*C*), 139.0

(1,2-Ar-*C*); MS (APCI), *m/z* (%): 562 (MH^+, 1), 248 ({$C_6H_4[N(CH_2Bu^t)]_2$-1,2}H^+, 6); IR (Nujol) ν/cm^{-1}: 1564 s, 1257 m, 1200 w, 1134 w, 1040 m, 880 m; APCI acc. mass on M^+: calc. for $C_{32}H_{52}N_4Ga$: 561.3453, found 561.3455; $C_{48}H_{84}N_4O_4LiGa$ requires C 67.20, H 9.87, N 6.53; found C 65.97, H 9.91, N 6.52.

Preparation of [$Cl_2Ga\{C_6H_4[N(CH_2Bu^t)]$-1-$[NH(CH_2Bu^t)]$-2}] 20: A solution of $GaCl_3$ (0.64 g, 1.82 mmol) in hexane (15 cm^3) was added to a suspension of [$C_6H_4\{NLi(CH_2Bu^t)\}$-1,$\{NH(CH_2Bu^t)\}$-2] (0.47 g, 1.82 mmol) in toluene (20 cm^3) at -78 °C to give an orange suspension. The reaction mixture was warmed to 20 °C and stirred for 1 hr to yield a deep blue suspension. Volatiles were then removed *in vacuo* and the residue was extracted into hexane (50 cm^3) and filtered. The filtrate was concentrated to *ca.* 10 cm^3 and stored at -30 °C overnight to give deep purple blocks of **20** (0.14 g, 20 %). Mp 112-114 °C; ^{1}H NMR (300 MHz, C_6D_6, 298 K): δ 0.78 (s, 9 H, $(CH_3)_3CCH_2N$), 1.54 (s, 9 H, $(CH_3)_3CCH_2NH$), 2.26 (d, $^3J_{HH}$ = 12.3 Hz, 1 H, CH_2NH), 3.38 (d, $^2J_{HH}$ = 2.5 Hz, 2 H, CH_2N), 3.46 (m, 1 H, CH_2NH), 3.57 (br. s, 1 H, N*H*), 6.53 (t, $^3J_{HH}$ = 7.6 Hz, 1 H, 5-Ar-*H*), 6.64 (d, $^3J_{HH}$ = 7.8 Hz, 1 H, 6-Ar-*H*), 6.86 (d, $^3J_{HH}$ = 8.4 Hz, 1 H, 3-Ar-*H*), 7.16 (t, $^3J_{HH}$ = 7.8 Hz, 1 H, 4-Ar-*H*); $^{13}C\{^1H\}$ NMR (50.3 MHz, C_6D_6, 298 K): δ 27.1 ($(CH_3)_3CCH_2N$), 28.5 ($(CH_3)_3CCH_2NH$), 30.8 ($(CH_3)_3CCH_2N$), 34.1 ($(CH_3)_3CCH_2NH$), 58.9 (CH_2N), 66.1 (CH_2NH), 112.5 (6-Ar-*C*), 114.6 (3-Ar-*C*), 124.2 (5-Ar-*C*), 129.2 (1-Ar-*C*), 129.9 (4-Ar-*C*), 151.1 (2-Ar-*C*); MS (EI 70 eV), *m/z* (%): 386 (MH^+, 1), 329 (MH^+ - Bu^t, 4), 248 ({$C_6H_4[N(CH_2Bu^t)]_2$-1,2}H^+, 93), 191 ({$C_6H_4[N(CH_2Bu^t)]_2$-1,2}H^+ - Bu^t, 100); IR (Nujol) ν/cm^{-1}: 3229 s (N—H), 1598 s, 1338 s, 1297 s, 1268 m, 1209 m, 1162 m, 1130 m, 1084 w, 1023 w, 974 m, 834 w, 794 m; EI acc. mass on M^+: calc. for $C_{16}H_{27}N_2Cl_2Ga$: 386.0802, found 386.0800.

5.6 References

1. M. L. H. Green, P. Mountford, G. J. Smout, S. R. Speel, *Polyhedron*, 1990, **9**, 2763.
2. R. J. Baker, C. Jones, *Dalton Trans.*, 2005, 1341.
3. V. Nair, S. Ros, C. N. Jayan, B. S. Pillai, *Tetrahedron*, 2004, **60**, 1959, and references therein.
4. S. Green, C. Jones, A. Stasch, R. P. Rose, *New J. Chem.*, 2007, **31**, 127.
5. T. Pott, P. Jutzi, W. Kaim, W. W. Schoeller, B. Neumann, A. Stammler, H. –G. Stammler, M. Wanner, *Organometallics*, 2002, **21**, 3169.
6. R. J. Baker, R. D. Farley, C. Jones, M. Kloth, D. M. Murphy, *Dalton Trans.*, 2002, 3844.
7. (a) R. J. Baker, M. Kloth, C. Jones, D. P. Mills, *New J. Chem.*, 2004, **28**, 207; (b) R. J. Baker, R. D. Farley, C. Jones, M. Kloth, D. P. Mills, D. M. Murphy, *Chem. Eur. J.*, 2005, **11**, 2972.
8. R. J. Baker, C. Jones, *Coord. Chem. Rev.*, 2005, **249**, 1857, and references therein.
9. R. J. Baker, C. Jones, M. Kloth, J. A. Platts, *Organometallics*, 2004, **23**, 4811.
10. T. Pott, P. Jutzi, W. W. Schoeller, A. Stammler, H. –G. Stammler, *Organometallics*, 2001, **20**, 5492.
11. C. Jones, D. P. Mills, R. P. Rose, *J. Organomet. Chem.*, 2006, **691**, 3060.
12. (a) R. J. Baker, C. Jones, D. M. Murphy, *Chem. Commun.*, 2005, 1339, (b) S. Aldridge, R. J. Baker, N. D. Coombs, C. Jones, R. P. Rose, A. Rossin, D. J. Willock, *Dalton Trans.*, 2006, 3313.
13. J. F. Hartwig, X. He, *Organometallics*, 1996, **15**, 5350.

14. P. B. Hitchcock, M. F. Lappert, L. J. –M. Pierssens, *Organometallics*, 1998, **17**, 2686.

15. K. B. Dillon, F. Mathey, J. F. Nixon, *Phosphorus: The Carbon Copy, from Organophosphorus to Phosphaorganic Chemistry*, New York, John Wiley and sons, 1998.

16. CSD version 5.28, November 2006, update 2 (May 2007); F. H. Allen, *Acta Cryst.*, 2002, **B58**, 380.

17. P. A. Arnold, S. T. Liddle, J. McMaster, C. Jones, D. P. Mills, *J. Am. Chem. Soc.*, 2007, **129**, 5360.

18. D. Enders, T. Balensiefer, *Acc. Chem. Res.*, 2004, **37**, 534, and references therein.

19. (a) S. Aldridge, A. J. Downs, *Chem. Rev.*, 2001, **101**, 3305; (b) C. Jones, G. A. Koutsantonis, C. L. Raston, *Polyhedron*, 1993, **12**, 1829, and references therein.

20. P. Jutzi, B. Neumann, G. Reumann, H. –G. Stammler, *Organometallics*, 1999, **18**, 2037.

21. C. Cui, M. Brynda, M. M. Olmstead, P. P. Power, *J. Am. Chem. Soc.*, 2004, **126**, 6510.

22. K. L. Antcliff, R. J. Baker, C. Jones, D. M. Murphy, R. P. Rose, *Inorg. Chem.*, 2005, **44**, 2098.

23. J. Emsley, *The Elements*, 3rd Edition, New York, Oxford University Press, 1998.

24. R. J. Baker, C. Jones, M. Kloth, *Dalton Trans.*, 2005, 2106.

25. M. Schmid, R. Eberhardt, M. Klinga, M. Leskelä, B. Rieger, *Organometallics*, 2001, **20**, 2321.

26. C. Jones, D. P. Mills, R. P. Rose, *Inorg. Chem.*, 2006, **45**, 3416.

27. B. Gehrhus, P. B. Hitchcock, M. F. Lappert, J. Heinicke, R. Boese, D. Bläser, *J. Organomet. Chem.*, 1996, **521**, 211.

28. B. Gehrhus, P. B. Hitchcock, M. F. Lappert, *Dalton Trans.*, 2000, 3094.

29. H. Braunschweig, B. Gehrhus, P. B. Hitchcock, M. F. Lappert, *Z. Anorg. Allg. Chem.*, 1995, **621**, 1922.

30. D. S. Brown, A. Decken, A. H. Cowley, *J. Am. Chem. Soc.*, 1995, **117**, 5421.

31. (a) E. S. Schmidt, A. Jockisch, H. Schmidbaur, *J. Am. Chem. Soc.*, 1999, **121**, 9758; (b) E. S. Schmidt, A. Schier, H. Schmidbaur, *Dalton Trans.*, 2001, 505.

32. E. S. Schmidt, A. Schier, N. W. Mitzel, H. Schmidbaur, *Z. Naturforsch., Teil B*, 2001, **56**, 458.

33. R. J. Baker, C. Jones, M. Kloth, J. A. Platts, *Angew. Chem. Int. Ed.*, 2003, **42**, 2660.

34. R. J. Baker, C. Jones, D. P. Mills, D. M. Murphy, E. Hey-Hawkins, R. Wolf, *J. Chem. Soc., Dalton Trans.*, 2006, 64.

35. M. D. Francis, C. Jones, D. P. Mills, *Main Group Metal Chem.*, 2006, **29**, 147.

36. C. Jones, D. P. Mills, G. A. Pierce, M. Waugh, *Inorg. Chim. Acta*, 2008, **361**, 427.

37. *WINEPR SIMFONIA* version 1.25, Brüker Analytische, Messtechnick, 1996.

38. M. L. Cole, P. C. Junk, *J. Organomet. Chem.*, 2003, **666**, 55.

39. J. C. Beamish, R. W. H. Small, I. J. Worrall, *Inorg. Chem.*, **18**, 220.

40. S. Danièle, C. Drost, B. Gehrhus, S. M. Hawkins, P. B. Hitchcock, M. F. Lappert, P. G. Merle, S. G. Bott, *Dalton Trans.*, 2001, 3179.

41. M. D. Francis, P. B. Hitchcock, *Organometallics*, 2003, **22**, 2891.

42. D. J. Tempel, L. K. Johnson, R. L. Huff, P. S. White, M. Brookhart, *J. Am. Chem. Soc.*, 2000, **122**, 6686.

Chapter 6

The Preparation and Reactivity of Novel Amidinate and Guanidinate Complexes

6.1 Introduction

Following the relocation of our research group to Monash University, it was decided to investigate the ligand properties of negatively charged amidinate, $[\{N(R)\}_2CR]^-$, and guanidinate, $[\{N(R)\}_2CNR_2]^-$, ions, which have been the subject of much interest.[1] This is unsurprising, given the facile and varied synthetic routes to these ligands. Variation of the R-groups at the backbone carbon and N-substituents allows easy modification of their steric and electronic properties. These ligands display a variety of coordination modes to a wide range of metals in low and high oxidation states.[1] The four most common binding modes of amidinates, **1a-d**, are depicted below (Figure 1), although there are several other rarer binding modes that these ligands exhibit, such as cluster-capping and *ortho*-metallation.[1] In the monodentate binding mode, **1a**, the amidinate binds through σ-donation of a lone pair of electrons at nitrogen, with the second nitrogen centre not bonding with the metal and forming a double bond with the central carbon atom. Amidinate ligands may chelate a metal centre in a symmetrical or unsymmetrical fashion. The nature of the chelating binding mode is commonly determined by X-ray crystallographic studies. The σ,σ-symmetrical chelating binding mode, **1b**, displays delocalised bonding around the NCN ligand backbone, and as such exhibits two similar N—C distances in the ligand backbone. Contrastingly, in the σ,σ-unsymmetrical chelating binding mode, **1c**, the bonding is localised and one nitrogen centre formally binds with the imine lone pair of electrons. As such, the two N—C distances in the NCN ligand backbone in the σ,σ-unsymmetrical

chelating mode vary considerably. Recently, a novel η^3-symmetrical chelating binding mode was reported, where the amidinate ligand is bound to the metal centre by the donation of π-electron density from the conjugated system of the amidinate ligand backbone.[3] In the bridging binding mode, **1d**, the amidinate ligand may bind identical (M, M) or different (M, M') metal centres. This binding mode commonly induces metal-metal bonding.

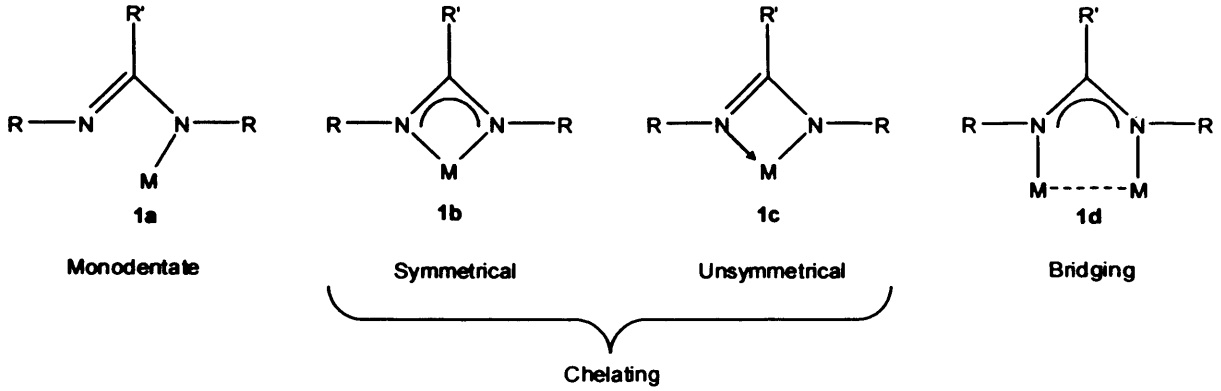

Figure 1 – Four common binding modes of the amidinate class of ligand, **1a-d**

Guanidinate ligands, although less studied than their amidinate counterparts, have been shown to exhibit similar binding properties.[1d] However, the electronic tuneability of these systems is greater than in their amidinate counterparts, due to the coordinated guanidinate ligand displaying three resonance forms, **2a-c** (Figure 2). Resonance forms similar to **2a-b** are solely adopted by amidinates, but guanidinates may also adopt the imidium/diamide resonance form, **2c**. The contribution of resonance form **2c** to the overall bonding in guanidinates gives these ligands additional π-donor capabilities over amidinates.[1d] These π-donor properties facilitate the stabilisation of electron-deficient metal centres coordinated by guanidinate ligands, as they increase the electron density at the metal centre and therefore reduce the tendency for oxidation in these systems. As a result of this important advantage over amidinates, there has been a surge of interest in the coordination chemistry of guanidinate ligands in the last fifteen years.[1d]

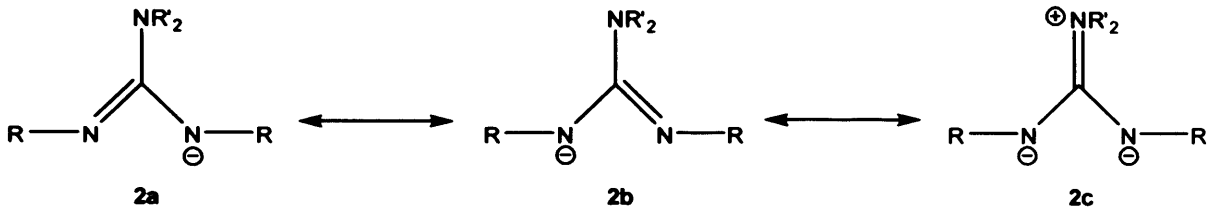

Figure 2 – Resonance forms of guanidinate ligands, **2a-c**

We in the Jones group have recently become interested in the coordination chemistry of amidinates and guanidinates, following the development of synthetic routes to the bulky ligands, $[\{N(Ar)\}_2CBu^t]^-$ ($Piso^-$),[3] $[\{N(Ar)\}_2CNPr^i_2]^-$ ($Priso^-$),[4] and $[\{N(Ar)\}_2CNCy_2]^-$ ($Giso^-$)[4] (Ar = $C_6H_3Pr^i_2$-2,6). The enhanced steric bulk of these ligands was predicted to facilitate the preparation of previously unobtainable amidinate and guanidinate complexes of metal centres that are prone to oxidation, by providing kinetic protection of the metal centre. This has indeed proved to be the case, and the developing *s*-, *p*- and *f*-block coordination chemistry of these ligands is reviewed here.

Lithium and potassium salts of $Piso^-$, $Priso^-$ and $Giso^-$ are known,[4] but will not be discussed here. Only one group 2 complex of $Piso^-$ has been reported.[5] The neutral amidine ligand, PisoH, reacted with half an equivalent of $[CpMgMe(Et_2O)]_2$ to give the *N*,*N'*-chelated compound, [(Piso)MgCp] **3**, by the loss of methane (Figure 3).[5] There has been much greater interest in group 13 complexes of $Piso^-$. It was found that [Li(Piso)] reacts with one equivalent of either $AlCl_3$ or $AlMe_2Cl$ by salt metathesis to give the Al(III) complexes, $[(Piso)AlCl_2]$ **4a** and $[(Piso)AlMe_2]$ **5**, respectively (Figure 3).[5] Subsequent work by the Jones group in this area found that the treatment of PisoH with $LiAlH_4$ or $[AlH_3(NMe_3)]$ gave the dimeric hydride, $[(Piso)AlH_2]_2$ **6** (Figure 3).[6] The corresponding gallium and indium homologues could not be obtained. It is noteworthy that differences in the coordination chemistry of $Piso^-$ and the related formamidinate, $[\{N(Ar)\}_2CBu^t]^-$ ($Fiso^-$) (Ar = $C_6H_3Pr^i_2$-2,6), were highlighted in this

report. In a subsequent publication, it was found that the treatment of **5** or **6** with two equivalents of diiodine gave the monomeric halide, [(Piso)AlI_2] **4b** (Figure 3).[7] The attempted reduction of **4b** with potassium, sodium or KC_8 to a neutral, aluminium(I) heterocycle was unsuccessful.[7]

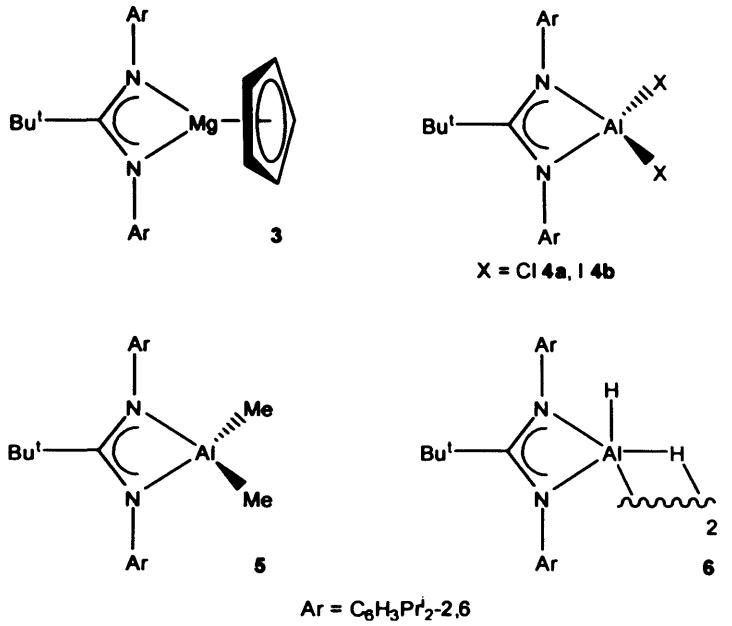

Figure 3 – Complexes **3 – 6**

Further attempts were made by the Jones group in the attempted synthesis of group 13 amidinato- and guanidinato-metal(I) heterocycles. The reaction of InCl or TlCl with [K(Piso)] gave the amidinato-metal(I) complexes, [E(Piso)] (E = In **7**, Tl **8a**) respectively, which display an unusual η^1-*N*,η^3-arene-coordination mode of the amidinate ligand (Figure 4).[8] Complexes **7** and **8a** crystallise with one equivalent of PisoH, which was proposed to arise from the partial decomposition of [E(Piso)].[8] It was found that the addition of one equivalent of PisoH to [K(Piso)] and the metal halide gave increased yields of **7** and **8a**.[8] A density functional theory (DFT) study concluded that the *N*,*N*′-chelated isomer of **7** and **8a** is thermodynamically more stable than the η^1-*N*,η^3-arene-coordination mode adopted by these complexes.[8] It was reasoned that the employment of a more electron rich guanidinate ligand with a bulkier backbone substituent, such as $Giso^-$, could favour *N*,*N*′-chelation at the metal centre. The reaction

of [Li(Giso)] with TlBr gave the η^1-*N*,η^3-arene-coordinated complex, **8b**, which, unlike **7** and **8a**, was isolable without co-crystallisation of the protonated ligand (Figure 4).[4] In contrast, the treatment of "GaI" or InCl with [Li(Giso)] gave the desired *N*,*N'*-chelated 4-membered *N*-heterocyclic carbene (NHC) analogues, **9** and **10** (Figure 4).[4] Initial studies into the coordination chemistry of **9** and **10** have been reported,[9] and a full summary of investigations into the reactivity of these heterocycles has been given in Chapter 1.

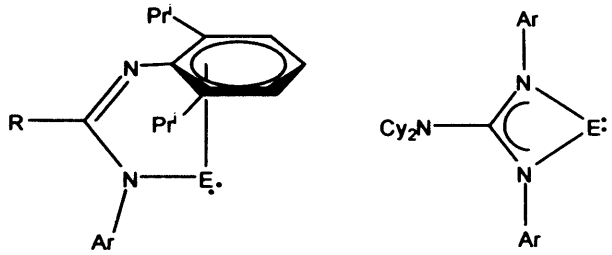

R = Bu^t, E = In **7**, Tl **8a**
R = NCy$_2$, E = Tl **8b**

E = Ga **9**, In **10**

Ar = $C_6H_3Pr^i_2$-2,6

Figure 4 – Complexes **7 – 10**

The group 14 amidinato- and guanidinato-complexes, [(Piso)GeCl] **11a** and [(Priso)ECl] (E = Ge **11b**, Sn **12**, Pb **13**), were prepared by the treatment of [$GeCl_2$(dioxane)], $SnCl_2$ or $PbCl_2$ with [Li(Piso)] or [Li(Priso)] (Figure 5).[10] Interestingly, the reduction of **11a-b** with potassium gave the neutral germanium(I) dimers, [Ge(Piso)]$_2$ **14a-b**.[10a] DFT studies on model complexes of **14a-b** suggested that these compounds have no multiple bond character, but have LUMOs that are of mainly π-bonding character.[10a] The salt metathesis reactions of **11 – 13** with a gallium(I) NHC analogue, [K(tmeda)][:Ga{[N(Ar)C(H)]$_2$}], are described in Chapter 2.[10b]

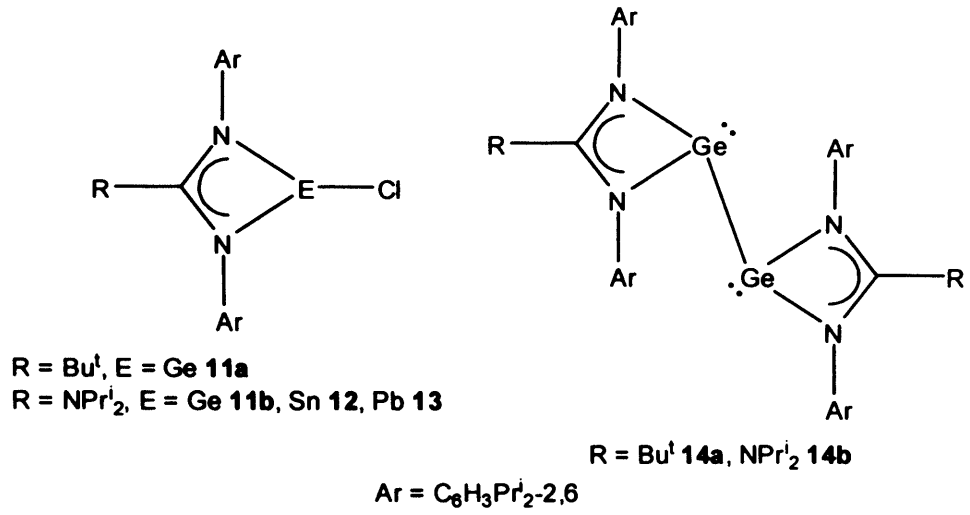

Figure 5 – Complexes **11 – 14**

Treatment of the anions, Piso$^-$, Priso$^-$ or Giso$^-$, with the group 15 element trihalides, EX_3 (E = P, As, Sb, X = Cl, I), afforded the novel complexes, $[X_2E\{[N(Ar)]_2CR\}]$ (**15**, **16a-c** and **17a-b**), by a salt metathesis reaction, with the amidinate and guanidinate ligands exhibiting a σ,σ-unsymmetrical chelating binding mode (Figure 6).[11] Complexes **15 – 17** were each treated with two equivalents of KC_8, in an attempt to synthesise the desired dipnictenes. The attempted reduction of **15** gave an intractable mixture of products, and the attempted reduction of **17a-b** resulted in the deposition of elemental antimony above 0 °C.[11] In contrast, reduction of **16a-c** afforded the base-stabilised diarsenes, **18a-c** (Figure 6).[11] The amidinate and guanidinate ligands exhibit an *N,N'*-bridging coordination mode in complexes **18a-c**, thought to be a result of the similar As=As and ligand N·····N separations that these complexes display.[11] A DFT analysis on a model complex of **18a-c** revealed that the As—N bonds are mainly ionic in nature, and that the HOMO of the As=As bond is mainly of π-character.[11]

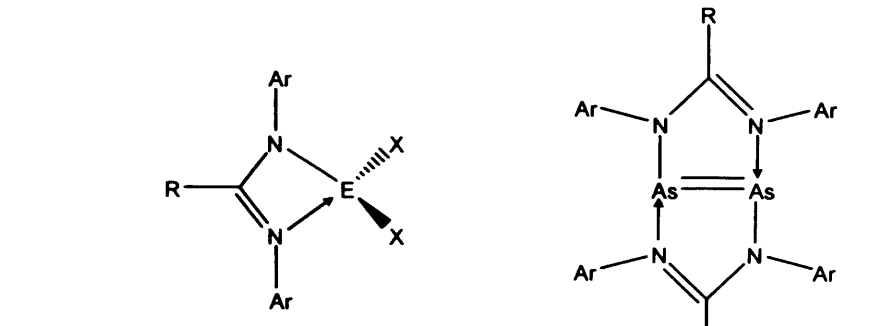

E = P, X = Cl, R = NCy_2 **15**
E = As, X = Cl, R = NCy_2 **16a**, NPr^i_2 **16b**, Bu^t **16c**
E = Sb, R = NCy_2, X = Cl **17a**, I **17b**

R = Bu^t **18a**, NPr^i_2 **18b**, NCy_2 **18c**

Ar = $C_6H_3Pr^i_2$-2,6

Figure 6 – Complexes **15 – 18**

A recent report described *f*-block complexes of $Giso^-$.[12] The reaction of two equivalents of [K(Giso)] with lanthanide diiodides, LnI_2, afforded the homoleptic complexes, $[Ln(Giso)_2]$ (Ln = Sm **19**, Eu **20**, Yb **21**) (Figure 7).[12] Whilst there is a distorted tetrahedral geometry about the ytterbium centre in **21**, the metal centres in **19** and **20** exhibit square planar ligand environments.[12] The use of SmI_2 as a one electron reducing agent in organic synthesis is well documented.[13] This reagent displays remarkable selectivity in a wide range of organic transformations.[13] Moreover, there have been numerous investigations into the reductive transformations of unsaturated substrates effected by organosamarium(II) complexes, such as $[Cp^*_2Sm(THF)_2]$ ($Cp^* = C_5Me_5$).[14] It is thought that the coordinatively unsaturated samarium(II) complex, **19**, could find application in the selective reduction of unsaturated substrates.[12] A small amount of the monosubstituted product, **22** (Figure 7), was obtained from the reaction mixture that gave **21**.[12] Placing a sample of **22** under a vacuum for several minutes afforded the rearranged η^1-*N*,η^6-arene-chelated complex, **23**, by the loss of coordinated THF (Figure 7).[12] This isomerism was found to be reversible, as samples of **23** dissolved in THF to give **22** quantitatively. The samarium and europium analogues of **22** could not be obtained. To the best of our knowledge, no *d*-block complexes of $Piso^-$, $Priso^-$ or $Giso^-$ have been reported to date.

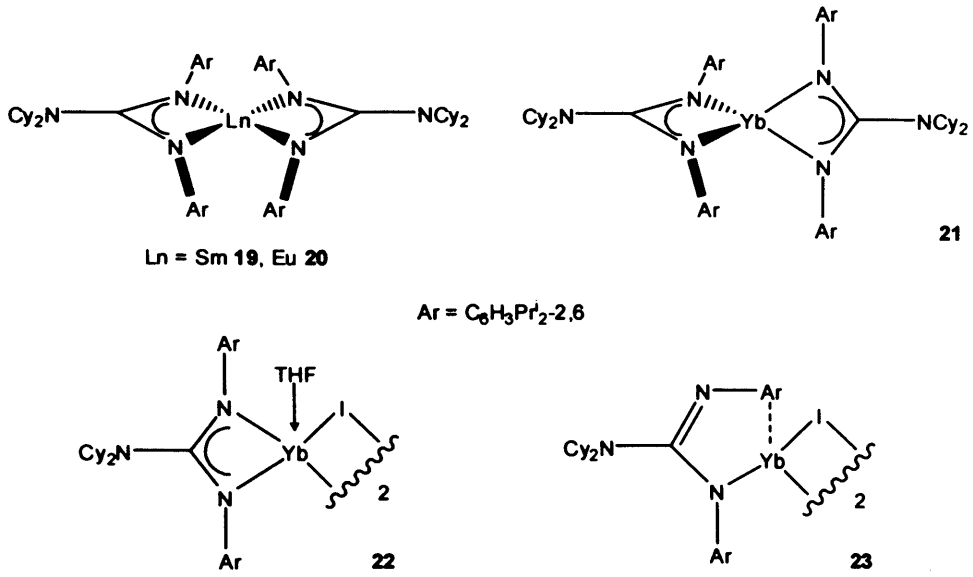

Figure 7 – Complexes **19 – 23**

6.2 Research Proposal

The coordination chemistry of the 4-membered gallium(I) NHC analogue, [:Ga{[N(Ar)]$_2$CNCy$_2$}], has been little explored. It was therefore decided to further investigate the reactivity of this heterocycle. It was also thought that the recently prepared samarium(II) complex, [Sm{[N(Ar)]$_2$CNCy$_2$}$_2$], could act as a selective one-electron reducing agent. As such, it was proposed to investigate the reactivity of this complex towards a range of unsaturated substrates. There have been no reported investigations into the transition metal coordination chemistry of the amidinate, [{N(Ar)}$_2$CBu^t]$^-$, and the bulky guanidinates, [{N(Ar)}$_2$CNPr$^i_2$]$^-$ and [{N(Ar)}$_2$CNCy$_2$]$^-$. It was envisaged that the considerable steric bulk of these ligands would dictate their adopted binding modes in metal complexes, as was observed in studies of the *p*- and *f*-block complexes of these ligands. Therefore, an investigation into the *d*-block chemistry of these ligands was proposed.

6.3 Results and Discussion

6.3.1 The Reactivity of the Heterocycle, [:Ga{[N(Ar)]$_2$CNCy$_2$}]

Initial investigations into the reactivity of the gallium(I) NHC analogue, **9**, have shown that the heterocycle is capable of displacing weakly bound olefin ligands in transition metal complexes.[9] As such, the platinum(0) complex, [(PEt$_3$)$_2$Pt(η^2-C$_2$H$_4$)], was treated with two equivalents of **9**. No reaction occurred at room temperature, even when the reaction vessel was irradiated with UV light for one hour. The reaction mixture was heated at reflux for three hours, forming an intractable mixture of products. Similarly, an intractable mixture of products resulted when the platinum(II) complex, [(η^4-COD)Pt{Ga{[N(Ar)C(H)]$_2$}}$_2$], was treated with two equivalents of **9**.

As the *p*-block chemistry of the heterocycle, **9**, is not as well developed as its *d*-block chemistry, it was decided to investigate the reactivity of **9** with main group precursors. The heterocycle was found not to react with xylylisonitrile ({(C$_6$H$_4$Me$_2$-2,6)-NC}), and the distannenes, [R$_2$Sn=SnR$_2$] (R = CH(SiMe$_3$)$_2$), or [Ar'$_2$Sn=SnAr'$_2$] (Ar' = C$_6$H$_2$Pr$^i_3$-2,4,6). The reaction of **9** with [BrB(cat)] (cat = C$_6$H$_4$O$_2$-1,2) gave GisoH.HBr. The reaction was monitored by ^{11}B{^{1}H} NMR spectroscopy, revealing the formation of [B$_2$(cat)$_3$]. A signal at δ 10.0 ppm was attributed to the formation of a Lewis acid-base adduct, such as [(Br$_3$B)Ga{[N(Ar)]$_2$CNCy$_2$}], which could not be isolated. This inference was based on earlier reports that weak donor phosphines, such as triphenylphosphine, react with [ClB(cat)] to give [B$_2$(cat)$_3$] and [(Ph$_3$P)BCl$_3$], following a redistribution of the initially formed adduct, [(Ph$_3$P)ClB(cat)], with two equivalents of [ClB(cat)].[15] It was decided to attempt the preparation of the Lewis base adduct, [(Br$_3$B)Ga{[N(Ar)]$_2$CNCy$_2$}], by the direct reaction of **9** with boron tribromide.

Unusually, boron tribromide reacts with **9** to give the salt, **24** (Scheme 1). The reaction was monitored by $^{11}B\{^1H\}$ NMR spectroscopy, revealing that several other products were produced. Although the mechanism of formation of **24** is unknown, boron has formally replaced gallium in the heterocycle, and the gallium has been oxidised to gallium(III), and exists as $GaBr_4^-$ in the counter-ion.

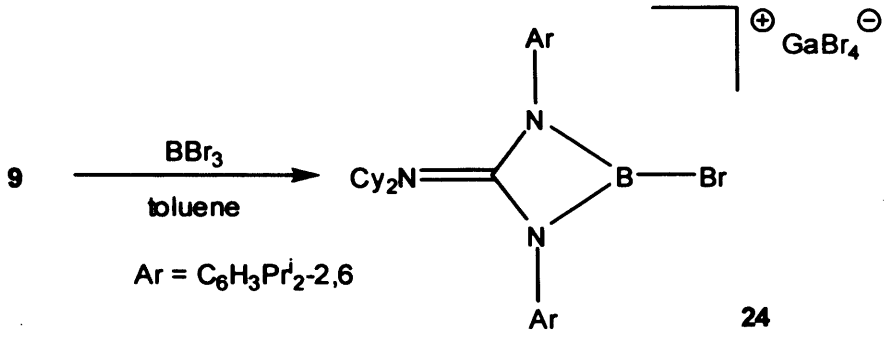

Scheme 1 – The synthesis of **24**

Compound **24** was fully characterised. The compound is sparingly soluble in THF, so only weak ^1H, $^{13}C\{^1H\}$ and $^{11}B\{^1H\}$ NMR spectral data could be obtained. The spectra are unsymmetrical, possibly due to the coordination of THF at boron. Samples of **24** reacted with DCM to give intractable mixtures of products, preventing the use of this solvent in the NMR studies. The only signal observed in the $^{11}B\{^1H\}$ NMR spectrum of **24** at δ 18.5 ppm is at a much lower field than is typical for related four coordinate neutral boron halide amidinates, which typically resonate from δ -9.2 to +9.7 ppm.[16] The resonance of a cationic boron species in the $^{11}B\{^1H\}$ NMR spectrum would, however, be expected to be at a lower field than a neutral system.

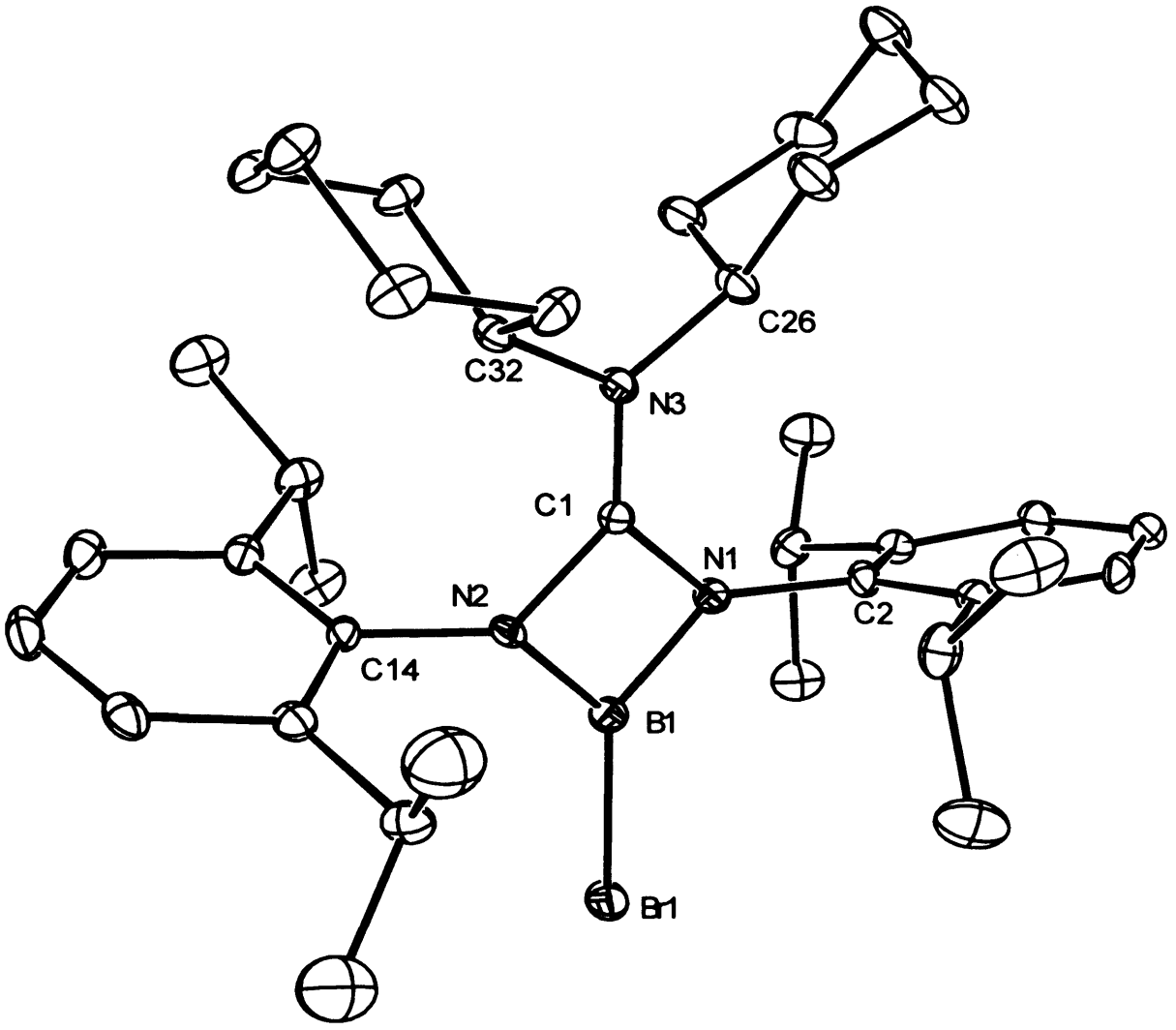

Figure 8 – Thermal ellipsoid plot (25 % probability surface) of the structure of the cationic component of [BrB(Giso)][$GaBr_4$] **24**; hydrogen atoms omitted for clarity. Selected bond lengths (Å) and angles (°): Br(1)—B(1) 1.881(8), N(1)—C(1) 1.400(9), N(1)—B(1) 1.451(11), C(1)—N(3) 1.288(9), C(1)—N(2) 1.409(9), B(1)—N(2) 1.425(11), C(1)—N(1)—B(1) 85.9(6), N(1)—C(1)—N(2) 95.2(5), N(2)—B(1)—N(1) 92.3(6), C(1)—N(2)—B(1) 86.6(6).

The structure of the cationic component of **24** is depicted in Figure 8. In contrast to **9**, there is little delocalisation of π-electron density in the NCN backbone, as evidenced by the relatively long N—C bond lengths (1.405 Å mean), in comparison to, for example, those observed in [$Br_2B\{[N(SiMe_3)]_2CPh\}$] (1.339 Å mean).[16c] The short N—C bond between the backbone carbon and the NCy_2 fragment (1.288(9) Å) is

indicative of a localised N=C double bond. Hence the imidium/diamide resonance form of the guanidinate ligand, **2c**, predominates in **24** and as such the three-coordinate boron centre is stabilised. The B—Br (1.881(8) Å) and B—N bond lengths (1.438 Å mean) observed in **24** are, as would be predicted, much shorter than those observed in the related four-coordinate compound, $[Br_2B\{[N(SiMe_3)]_2CPh\}]$ (B—Br 2.001 Å, B—N 1.559 Å mean).[16c] The boron centre of **24** exhibits a trigonal planar geometry (Σ angles = 360.0°), with the most acute angle being the N—B—N angle of 92.3(6)°, which is more obtuse than that observed in $[Br_2B\{[N(SiMe_3)]_2CPh\}]$ (85.2°).[16c]

6.3.2 The Reactivity of the Samarium(II) Complex, $[Sm(Giso)_2]$

The reactivity of **19** towards a range of organic substrates was investigated. $[Cp^*_2Sm(THF)_2]$ has been shown to react with nitriles in a variety of ways, such as adduct formation or C—C bond cleavage to form cyanides, depending on the conditions employed.[14] In contrast, **19** did not react with pivaloylnitrile (Bu^tCN) or the isomer, *tert*-butylisonitrile (Bu^tNC). The lack of reactivity of **19** towards Bu^tCN, in comparison with $[Cp^*_2Sm(THF)_2]$, can be explained by the facile displacement of two molecules of THF in the latter complex generating vacant coordination sites at the samarium centre. The samarium centre of **19** is kinetically protected by bulky guanidinate ligands, inhibiting the close approach of sterically demanding ligands. Similarly, no reaction was observed when **19** was treated separately with *tert*-butylisothiocyanate (Bu^tNCS), pyridine or *N,N'*-dicyclohexylcarbodiimide. It was thought that carbon monoxide, CO, could insert into an Sm—N bond of **19**, but no reaction was observed when **19** was exposed to an atmosphere of CO for twelve hours. The reaction of **19** with $[Hg(C{\equiv}CPh)_2]$ gave an intractable mixture of products. The only isolable product from the reaction of benzaldehyde with **19** was GisoH.

Previous studies into the reactivity of $[Cp^*_2Sm(THF)_2]$ revealed that this complex reductively couples carbon dioxide, CO_2, to form an oxalate complex, $[(Cp^*_2Sm)_2(\mu\text{-}\eta^2\text{:}\eta^2\text{-}O_2CCO_2)]$, and reacts separately with COS to form a disproportionation product, $[Cp^*_2Sm(\mu\text{-}\eta^2\text{:}\eta^1\text{-}S_2CO)SmCp^*_2(THF)]$ **26**.[17] Recently, a samarium(II) complex with a sterically demanding substituent was employed to mediate the reductive disproportionation of CO_2 to form a carbonate complex and CO.[18] In contrast, compound **19** reacted with CO_2 to give GisoH as the only isolable product, possibly *via* a proton abstraction process. The fate of the samarium in this reaction is unknown. Treatment of a toluene solution of $[Sm(Giso)_2]$ with carbon disulphide, CS_2, under any stoichiometry, led to a different outcome, namely the formation of **25**, by the reductive coupling of CS_2 and oxidation of two samarium(II) centres (Scheme 2). An S—C bond has formed in this reaction, and **25** formally exhibits two Sm(III) centres and a dianionic bridging $[SCSCS_2]^{2-}$ fragment.

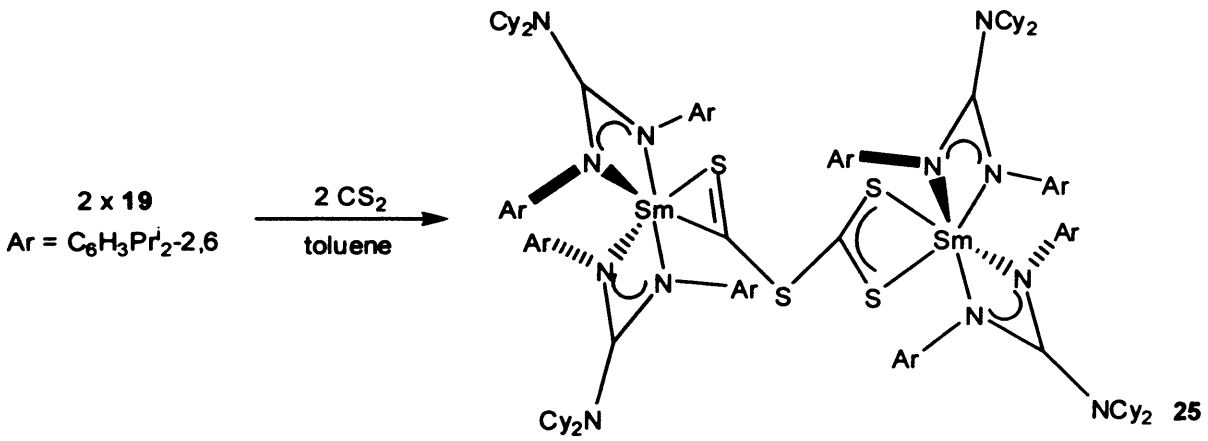

Scheme 2 – The synthesis of **25**

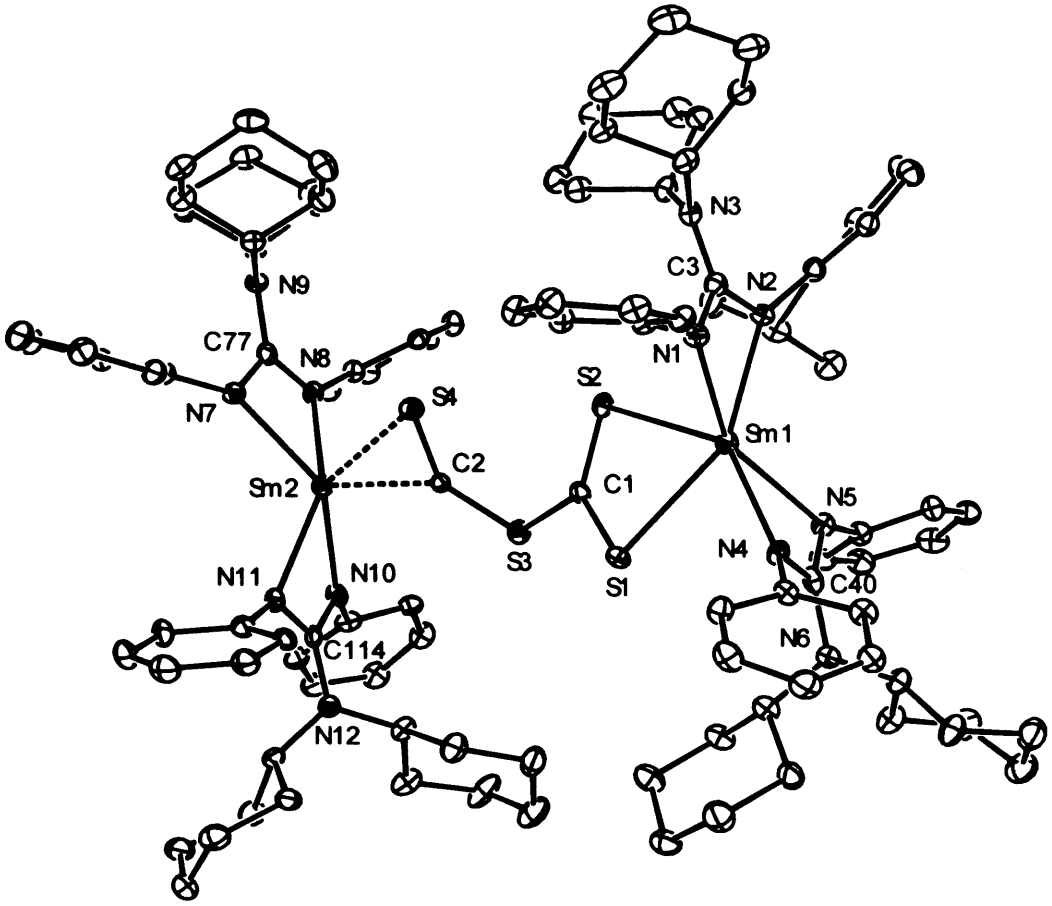

Figure 9 – Thermal ellipsoid plot (25 % probability surface) of the molecular structure of [{Sm(Giso)$_2$}$_2$(μ-η^2:η^2-SCSCS$_2$)] **25**; isopropyl groups and hydrogen atoms omitted for clarity. Selected bond lengths (Å) and angles (°): Sm(1)—N(4) 2.386(5), Sm(1)—N(2) 2.416(5), Sm(1)—N(5) 2.455(5), Sm(1)—N(1) 2.486(5), Sm(1)—C(3) 2.881(7), Sm(1)—S(1) 2.979(10), Sm(1)—S(2) 2.998(5), S(1)—C(1) 1.710(12), C(1)—S(2) 1.682(11), C(1)—S(3) 1.778(12), Sm(2)—N(7) 2.403(5), Sm(2)—N(10) 2.416(6), Sm(2)—C(2) 2.444(14), Sm(2)—N(8) 2.448(6), Sm(2)—N(11) 2.473(6), Sm(2)—S(4) 2.813(8), C(2)—S(4) 1.605(13), C(2)—S(3) 1.720(14), N(4)—Sm(1)—N(5) 55.50(19), N(2)—Sm(1)—N(1) 54.82(18), S(1)—Sm(1)—S(2) 59.85(19), C(1)—S(1)—Sm(1) 88.2(5), C(3)—N(1)—Sm(1) 92.4(4), S(2)—C(1)—S(1) 123.0(8), S(2)—C(1)—S(3) 125.0(7), S(1)—C(1)—S(3) 111.9(7), N(7)—Sm(2)—N(8) 55.11(19), N(10)—Sm(2)—N(11) 55.03(19), C(2)—Sm(2)—S(4) 34.7(3), C(1)—S(2)—Sm(1) 88.1(4), S(4)—C(2)—S(3) 130.9(9), S(4)—C(2)—Sm(2) 85.4(7), S(3)—C(2)—Sm(2) 143.2(7), C(2)—S(3)—C(1) 113.6(6), C(2)—S(4)—Sm(2) 60.0(6).

As **25** is paramagnetic, no meaningful data could be obtained from its ^{1}H and $^{13}C\{^{1}H\}$ NMR spectra. Crystals of **25** are only sparingly soluble in toluene and THF. As spectroscopic data were not structurally definitive, an X-ray diffraction study was carried out (Figure 9). The samarium(III) centres of **25** are six-coordinate and display distorted octahedral ligand environments. One samarium(III) centre is chelated by a $[CS_2]^-$ fragment and an $[SCS]^-$ fragment is bonded to the other by the formal donation of π-electron density from the S=C bond. A comparison of the S—C distances within the $[SCSCS_2]^{2-}$ fragment of **25** reveals one formal S—C single bond (C(1)—S(3) 1.778(12) Å) and one formal S=C double bond (C(2)—S(4) 1.605(13) Å). The other three S—C distances (1.704 Å mean) are indicative of the partial delocalisation of π-electron density over the $[SCSCS_2]^{2-}$ fragment and the S—C distances are between that expected for S—C single (1.82 Å) and S=C double (1.60 Å) bonds.[19] The Sm—S bond lengths of the chelating $[CS_2]^-$ fragment in **25** (2.989 Å mean) are longer than those observed in the related complex, **26** (2.797 Å mean), whereas the other Sm—S bond length in **25** (2.813(8) Å) is comparable to those observed in **26**.[17] All Sm—S distances observed in **25** are long in comparison to the related complex, $[\{Cp^*_2Sm(THF)\}_2(\mu\text{-}S)]$ (2.664 Å mean),[20] indicating that the Sm—S interactions observed in **25** are relatively weak. All Sm—S distances observed in **25** are, however, within the known range for such interactions (2.645 – 3.117 Å).[21] The bite angle of the chelating $[CS_2]^-$ fragment with the samarium(III) centre in **25** (S(1)—Sm(1)—S(2) 59.85(19)°) is considerably more acute than that seen in **26** (64.89°).[17] The Sm—N bond lengths observed in **25** (2.435 Å mean) are within the known range (2.118 – 2.976 Å),[21] but are considerably shortened with respect to the starting material, $[Sm(Giso)_2]$ (2.546 Å mean),[12] a direct result of the change in oxidation state of the samarium centres.

6.3.3 Preparation of Rhodium(I) Amidinate and Guanidinate Complexes

Tiripicchio, Oro and co-workers have previously shown that the reaction of $[(\eta^4\text{-COD})RhCl]_2$ with two equivalents of potassium *N,N'*-diphenylbenzamidinate, $K[\{N(Ph)\}_2CPh]$, affords a good yield of the rhodium(I) complex, $[(\eta^4\text{-COD})Rh\{\eta^2\text{-}[N(Ph)]_2CPh\}]$ **27**, by a salt metathesis reaction.[22] It was envisaged that rhodium(I) complexes of $Piso^-$, $Priso^-$ and $Giso^-$ could be prepared by using a similar methodology to that employed in the synthesis of **27**. The treatment of toluene solutions of $[(\eta^4\text{-COD})RhCl]_2$ with two equivalents of either [K(Piso)], [K(Priso)] or [K(Giso)], however, afforded complexes **28 – 30** respectively (Scheme 3). The amidinate or guanidinate ligand in **28 – 30** adopts a novel π-arene binding mode, which is tentatively described as an η^6-interaction of the arene ring with the rhodium centre. The same products formed when the reactions were carried out in the presence of THF. A small amount of $[\{Rh(\eta^4\text{-COD})\}_4(\mu^4\text{-}Me_2SiO_2)_2]$, **31**, formed in the reaction mixture that gave **30**, in the presence of adventitious silicone grease, $(Me_2SiO)_n$. The mechanism for this process is unknown, although the incorporation of Me_2SiO_2 units from silicone grease and subsequent inorganic ring formation has been observed previously.[23] No attempt was made to intentionally synthesise **31** in a higher yield. The treatment of $[(\eta^4\text{-COD})IrCl]_2$ with two equivalents of [K(Giso)] resulted in the deposition of iridium metal and gave an intractable mixture of products. Similarly, the treatment of $[(\eta^2\text{-COE})_2RhCl]_2$ (COE = cyclooctene) with two equivalents of [K(Priso)] resulted in the deposition of rhodium metal and gave an intractable mixture of products.

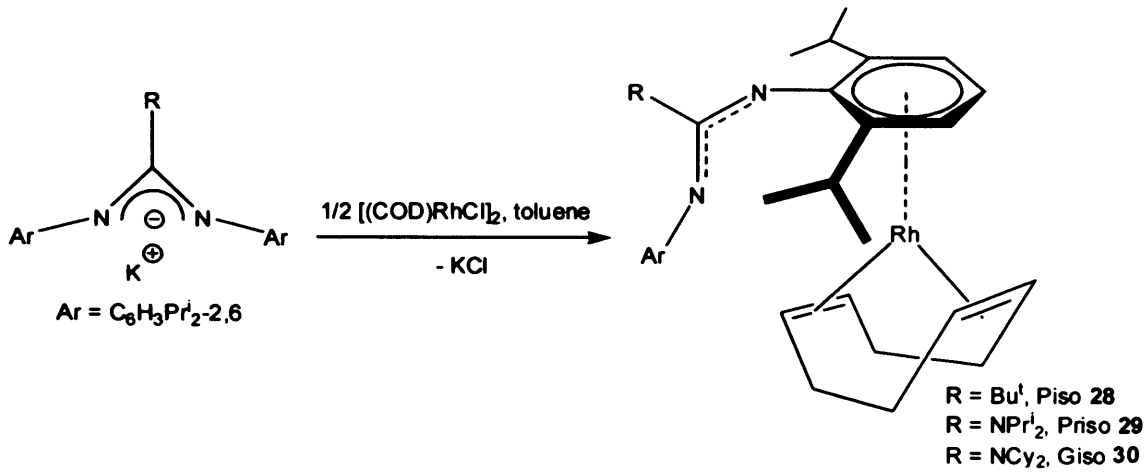

Scheme 3 – The synthesis of **28 – 30**

Complexes **28 – 30** were fully characterised and were found to be air-stable in the solid state and thermally robust. Some interesting features were noted in their ^{1}H and $^{13}C\{^{1}H\}$ NMR spectra. Firstly, these spectra are unsymmetrical, suggesting that complexes **28 – 30** retain their solid state structures (*vide infra*) in solution. Secondly, the signals in the ^{1}H NMR spectra of **28 – 30** corresponding to the *m*-Ar-*H* and *p*-Ar-*H* resonances of the η^6-bound arene ring are shifted up-field to *ca.* δ 5.7 ppm and 3.9 ppm respectively. A similar trend is observed in the $^{13}C\{^{1}H\}$ NMR spectra of these complexes, with the signals corresponding to the *o*-Ar-*C*, *m*-Ar-*C* and *p*-Ar-*C* resonances of the η^6-bound arene ring being shifted up-field to *ca.* δ 116 ppm, 101 ppm and 74 ppm respectively. For these three signals, $^{1}J_{RhC}$ couplings were observed, with the largest $^{1}J_{RhC}$ coupling constant (*ca.* 6 Hz) being to the resonance of the *p*-Ar-*C* of the η^6-bound arene ring. Hence, the signals corresponding to the η^6-bound arene ring in the ^{1}H and $^{13}C\{^{1}H\}$ NMR spectra of **28 – 30** have been shifted up-field to chemical shifts that are more typical of vinylic systems than aromatic systems. The up-field shift of resonances in the ^{1}H and $^{13}C\{^{1}H\}$ NMR spectra of η^6-aryl rhodium(I) complexes is well-documented,[24] but the extent of the up-field shifts seen for complexes **28 – 30** is much greater than is usually observed.[24] The chemical shifts and $^{1}J_{RhC(COD)}$ couplings observed in the $^{13}C\{^{1}H\}$ NMR spectra of **29** corresponding to the unsaturated carbon

centres of the COD ligand (δ 72.1 ppm, $^1J_{RhC(COD)}$ = 13.3 Hz) and **30** (δ 75.4 ppm, $^1J_{RhC(COD)}$ = 13.0 Hz) are comparable with those observed for the starting material, [(η^4-COD)RhCl]$_2$ (δ 78.5 ppm, $^1J_{RhC(COD)}$ = 13.9 Hz).[25] It is of note that L. H. Gade and co-workers have recently reported an η^6-bound arene rhodium(I) cyclooctadiene complex, [MeSi{SiMe$_2$N(Ar')}$_2$Sn{SiMe$_2$N(η^6-Ar')}Rh(η^4-COD)] **32** (Ar' = C$_6$H$_3$Me$_2$-3,5) (Figure 10),[24a] which displays comparable chemical shifts and $^1J_{RhC}$ coupling constants for the π-arene substituent resonances in its ^{1}H and ^{13}C{^{1}H} NMR spectra with those observed in **28 – 30**.

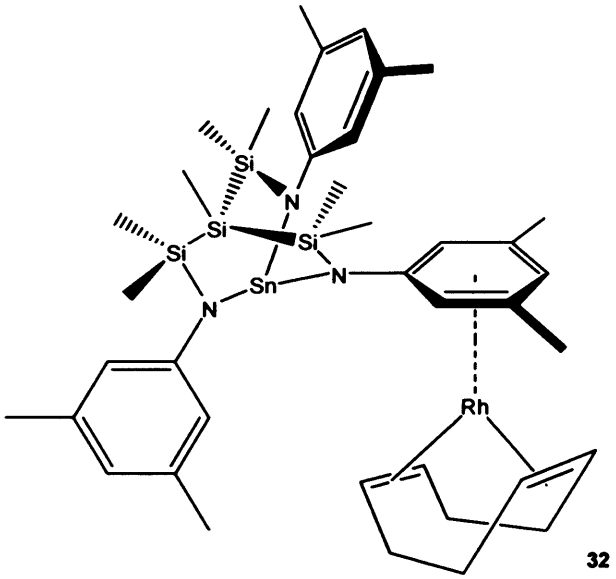

32

Figure 10 – Complex **32**

An X-ray crystallographic study was proposed to further examine the bonding in **28 – 30**, and the structures of these complexes were obtained (Figures 11 – 13). Piso$^-$ and Giso$^-$ have previously been shown to adopt bidentate η^1-*N*,η^3-Ar- and η^1-*N*,η^6-Ar-coordination modes,[4,8,12] but complexes **28 – 30** represent the first structurally characterised examples of amidinate or guanidinate ligands binding a metal centre with only an arene interaction. As complexes **28 – 30** are structurally analagous and have similar geometric parameters, only the structure of **29** shall be discussed here for brevity. All N—C distances within the CN$_3$ backbone of the guanidinate fragment of **29**

are short in comparison with a typical N—C single bond (1.47 Å),[19] which provides evidence for π-electron delocalisation over the CN_3 fragment. The extent of this π-electron delocalisation, however, is not as great as in other reported complexes of $Priso^-$,[10a,11] as the N(2)—C(1) distance observed in **29** (1.294(3) Å) is considerably shorter than the other two N—C distances in the CN_3 fragment (1.388 Å mean). The N(2)—C(1) distance observed in **29** is best described as an N=C double bond, the lengths of which are typically around 1.30 Å.[19] The N(1)—C(2) distance observed in **29** (1.300(3) Å), the bond between the CN_3 fragment and the *ipso*-C of the η^6-bound arene ring, is also best described as an N=C double bond. L. H. Gade and co-workers observed a short N—C distance (1.339 Å) at the *ipso*-C of the η^6-bound arene ring in **32**, but did not comment further on this data.[24a] The C(2)—C(3) (1.483(4) Å) and C(2)—C(7) (1.472(3) Å) distances in the coordinated η^6-bound arene ring of **29** are long in comparison to the other C—C distances in the ring (1.405 Å mean), and are only slightly shorter than typical C—C single bonds (1.54 Å).[19] Although increased C—C distances would be anticipated upon coordination of the arene ring to the metal centre, these increases would be expected to be more uniform than those observed in **29**, such as those exhibited by **32** (C—C = 1.398 – 1.452 Å).[24a] The Rh—C distances seen for **29** are within the known range (1.638 – 2.775 Å),[21] although the Rh(1)—C(2) distance (2.662 Å) is remarkably long and indicative of a weak interaction. All other interatomic distances and angles are unremarkable.

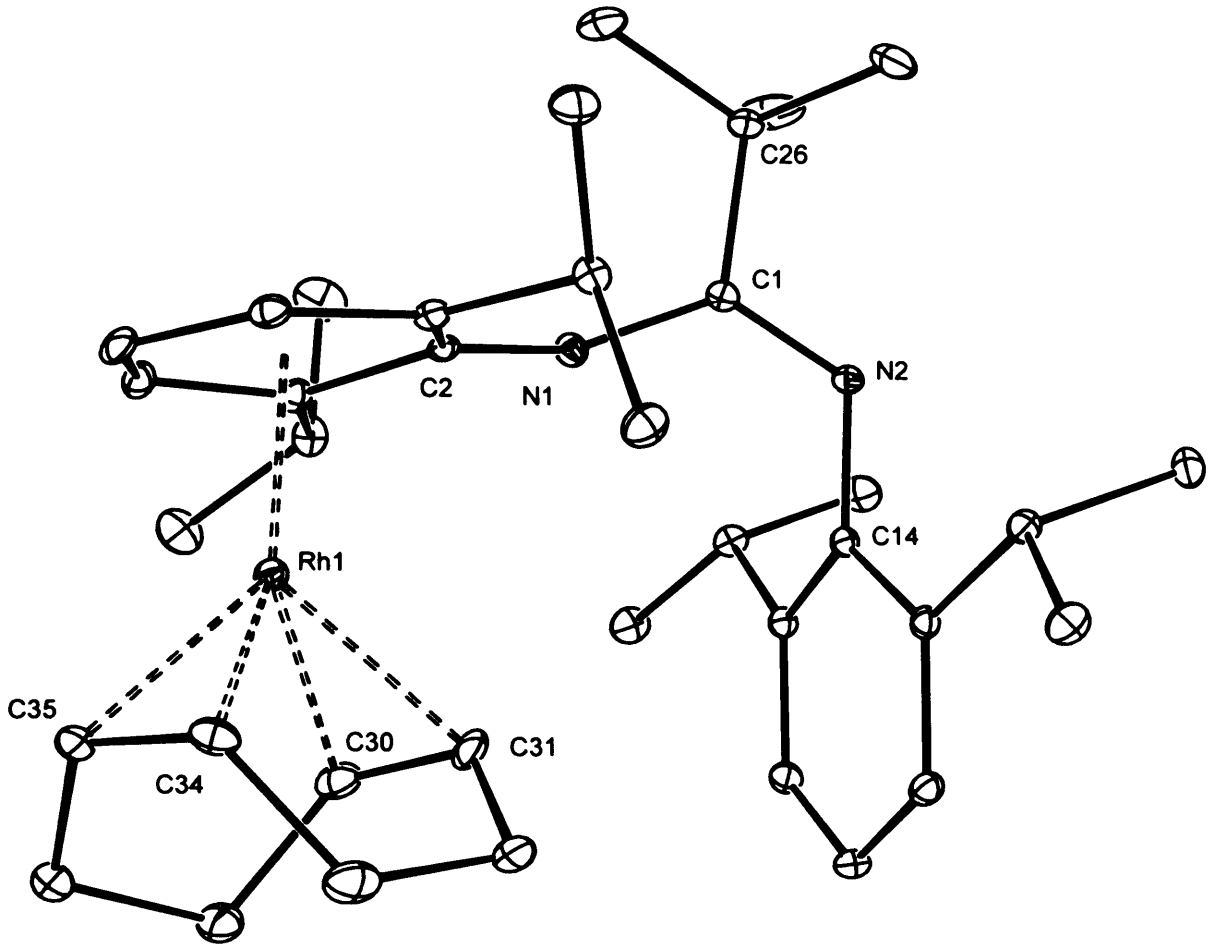

Figure 11 – Thermal ellipsoid plot (25 % probability surface) of the molecular structure of [(η^4-COD)Rh(η^6-Piso)] **28**; hydrogen atoms omitted for clarity. Selected bond lengths (Å) and angles (°): Rh(1)—C(35) 2.125(2), Rh(1)—C(34) 2.138(2), Rh(1)—C(30) 2.148(2), Rh(1)—C(31) 2.154(2), Rh(1)—C(5) 2.207(2), Rh(1)—C(6) 2.272(2), Rh(1)—C(4) 2.324(2), Rh(1)—C(7) 2.341(2), Rh(1)—C(3) 2.508(2), Rh(1)—C(2) 2.600(2), N(1)—C(2) 1.306(3), N(1)—C(1) 1.367(3), N(2)—C(1) 1.284(3), C(1)—C(26) 1.542(3), C(2)—C(3) 1.467(3), C(2)—C(7) 1.472(3), C(3)—C(4) 1.391(3), C(4)—C(5) 1.416(4), C(5)—C(6) 1.403(3), C(6)—C(7) 1.400(3), C(30)—C(31) 1.380(4), C(34)—C(35) 1.411(4), N(2)—C(1)—N(1) 125.9(2).

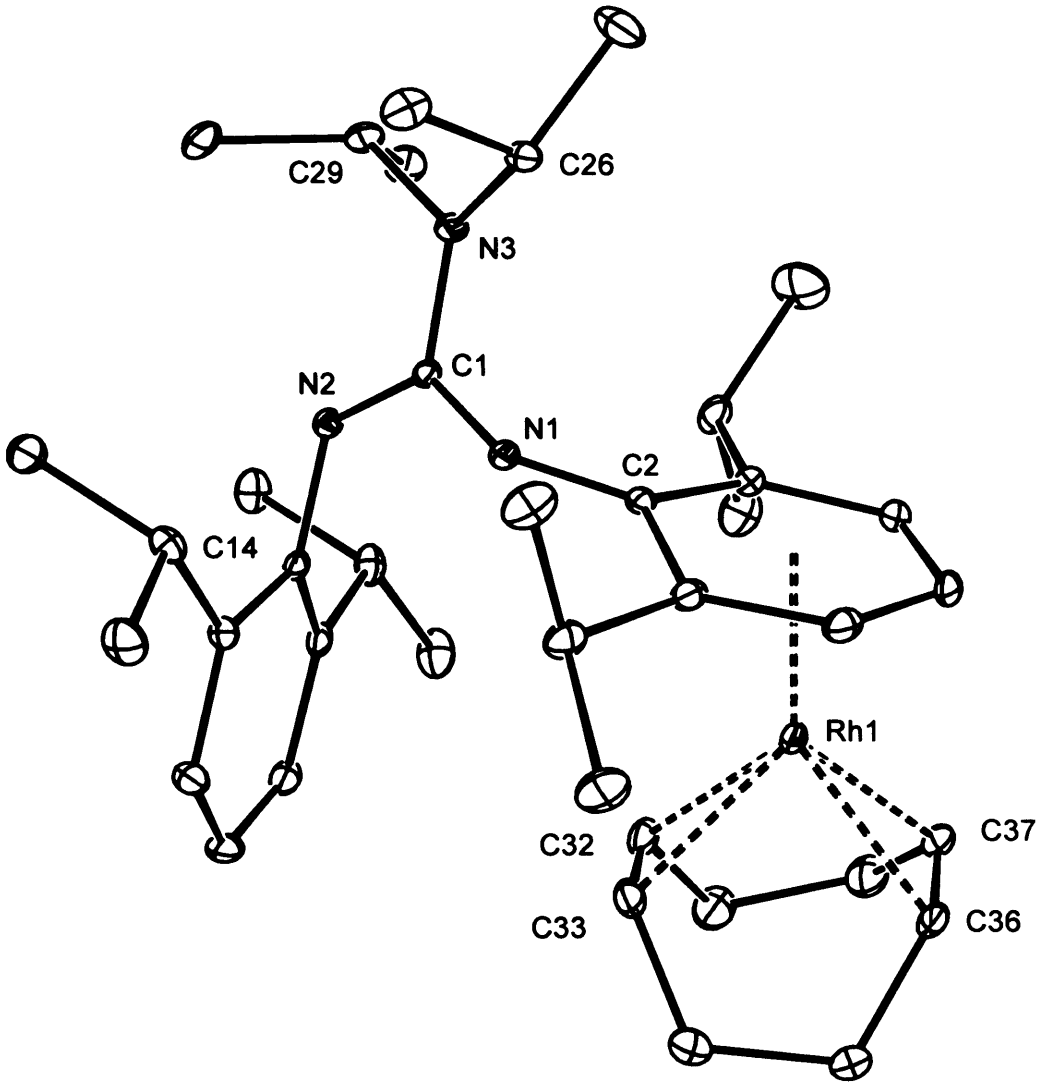

Figure 12 – Thermal ellipsoid plot (25 % probability surface) of the molecular structure of [(η^4-COD)Rh(η^6-Priso)] **29**; hydrogen atoms omitted for clarity. Selected bond lengths (Å) and angles (°): Rh(1)—C(37) 2.126(3), Rh(1)—C(36) 2.126(3), Rh(1)—C(33) 2.137(3), Rh(1)—C(32) 2.156(3), Rh(1)—C(5) 2.185(3), Rh(1)—C(4) 2.255(3), Rh(1)—C(6) 2.291(3), Rh(1)—C(3) 2.367(3), Rh(1)—C(7) 2.478(3), N(1)—C(2) 1.300(3), N(1)—C(1) 1.381(3), N(2)—C(1) 1.294(3), N(3)—C(1) 1.395(3), C(2)—C(7) 1.472(3), C(2)—C(3) 1.483(4), C(3)—C(4) 1.394(4), C(4)—C(5) 1.409(4), C(5)—C(6) 1.417(4), C(6)—C(7) 1.398(4), C(32)—C(33) 1.390(5), C(36)—C(37) 1.401(4), N(2)—C(1)—N(1) 123.6(2).

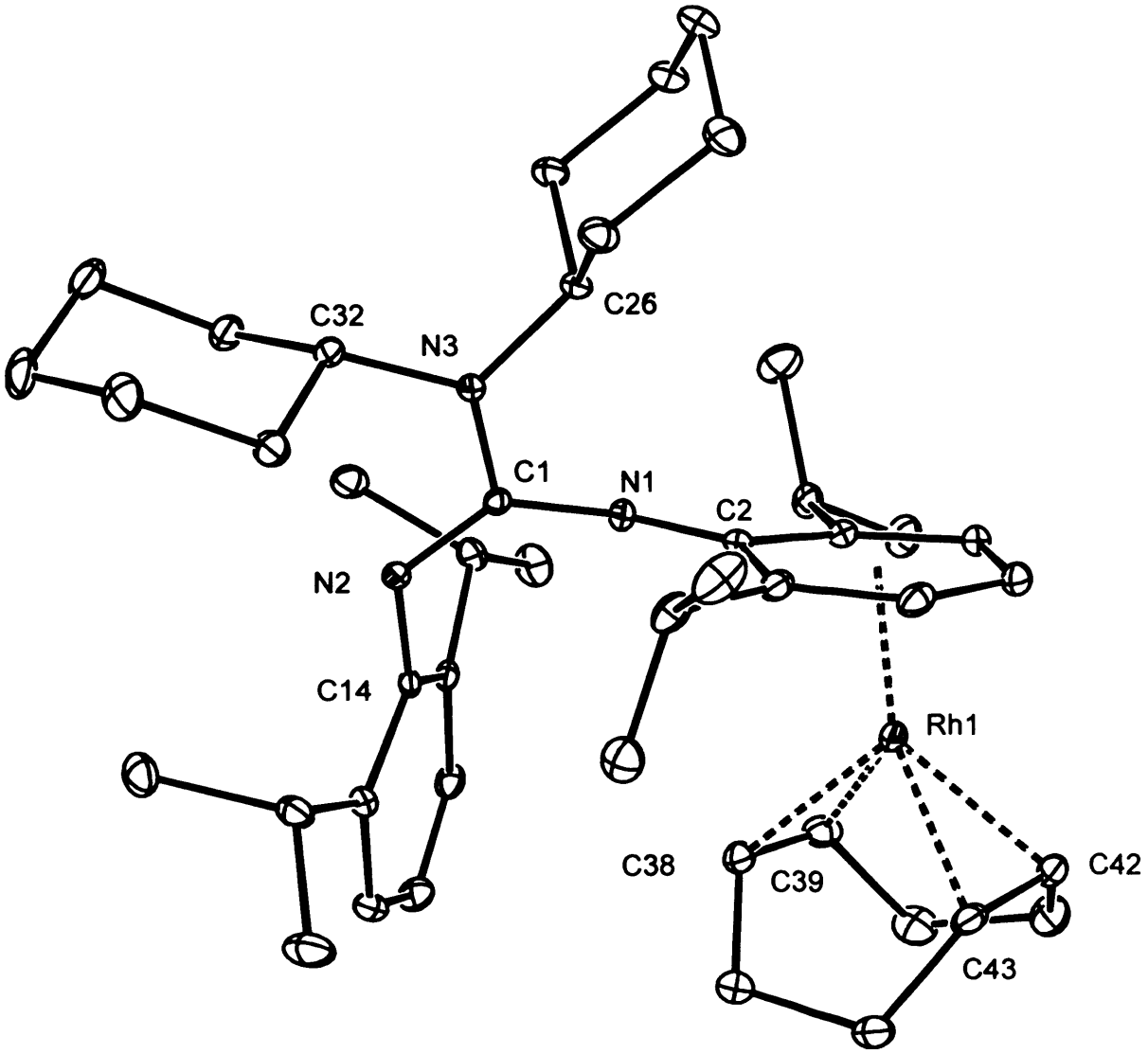

Figure 13 – Thermal ellipsoid plot (25 % probability surface) of the molecular structure of [(η^4-COD)Rh(η^6-Giso)] **30**; hydrogen atoms omitted for clarity. Selected bond lengths (Å) and angles (°): Rh(1)—C(42) 2.124(3), Rh(1)—C(43) 2.127(3), Rh(1)—C(39) 2.141(3), Rh(1)—C(38) 2.146(3), Rh(1)—C(5) 2.213(3), Rh(1)—C(4) 2.257(3), Rh(1)—C(3) 2.316(3), Rh(1)—C(6) 2.326(3), Rh(1)—C(7) 2.497(3), Rh(1)—C(2) 2.569(2), N(1)—C(2) 1.310(3), N(1)—C(1) 1.373(3), N(2)—C(1) 1.300(3), N(3)—C(1) 1.390(3), C(38)—C(39) 1.390(4), C(42)—C(43) 1.403(4), N(2)—C(1)—N(1) 124.8(2).

By coupling observations from the X-ray crystallographic studies of **28 – 30** with the observations from the ^{1}H and ^{13}C{^{1}H} NMR spectra of these complexes, it was

possible to construct resonance structures, **33a-c**, to describe the bonding in these complexes (Figure 14). The guanidinate ligands of complexes **29** and **30** additionally display an imidium/diamide resonance structure, **2c**, as depicted in Figure 2. Resonance structures **33a-b** describe classical amidinate and guanidinate π-electron delocalisation about the CN_2/CN_3 fragment. Simple electron movement about the η^6-bound arene ring affords resonance structure **33c**, which exhibits localised bonding in the CN_2/CN_3 fragment and an N=C double bond involving the *ipso*-C of the arene ring. The description of the bonding in resonance structure **33c** is in agreement with observations made in the X-ray crystallographic studies of **28 – 30**. In addition, resonance structure **33c** displays two formal C=C double bonds within the coordinated η^6-bound arene ring, with the *p*-Ar-*C* formally described as a carbanion. The loss of "aromaticity" in the η^6-bound arene ring ring of **33c** is in agreement with observations made from the ^1H and $^{13}C\{^1H\}$ NMR spectra of **28 – 30**. Finally, the bonding in the η^6-bound arene ring of **33c** explains the long Rh—C_{ipso} bonds observed in the X-ray crystallographic structures of **28 – 30**. All experimental evidence suggests that **33c** is the dominant resonance structure and that it best describes the bonding situation in **28 – 30**.

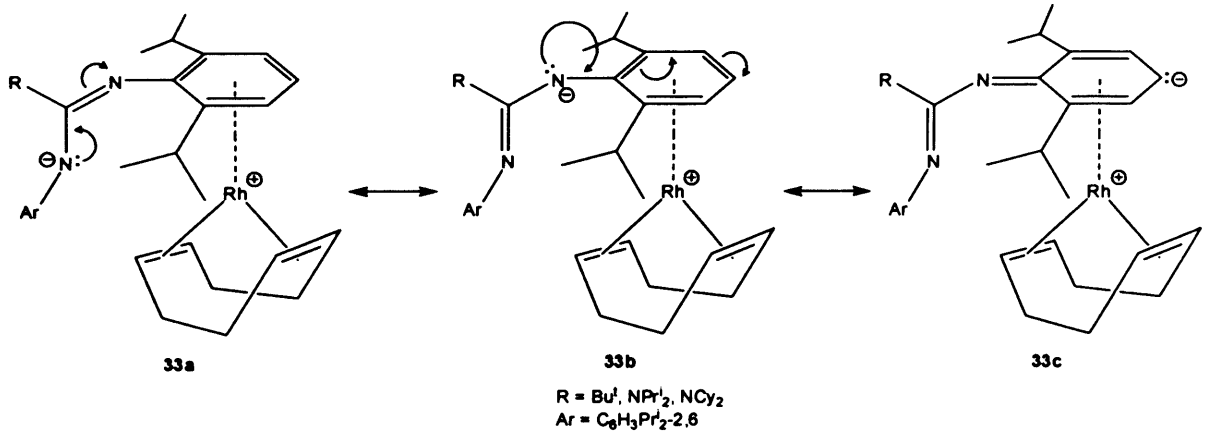

Figure 14 – The resonance structures, **33a-c**

The crystal structure of **31** was also obtained (Figure 15). As previously mentioned, there are several reported examples of inorganic rings formed through the

incorporation of Me_2SiO_2 units.[26] Six-membered rings of the general formula M_2SiO_3 (M = Ge,[26a] Sn,[26b] Nb[26c]) are often exhibited in these complexes, whereas the structure of **31** displays four fused Rh_2SiO_3 six-membered rings, all with "chair" conformations. The bonding in **31** is best described as two formally dianionic $[Me_2SiO_2]^{2-}$ units bridging four distorted square planar rhodium(I) centres.

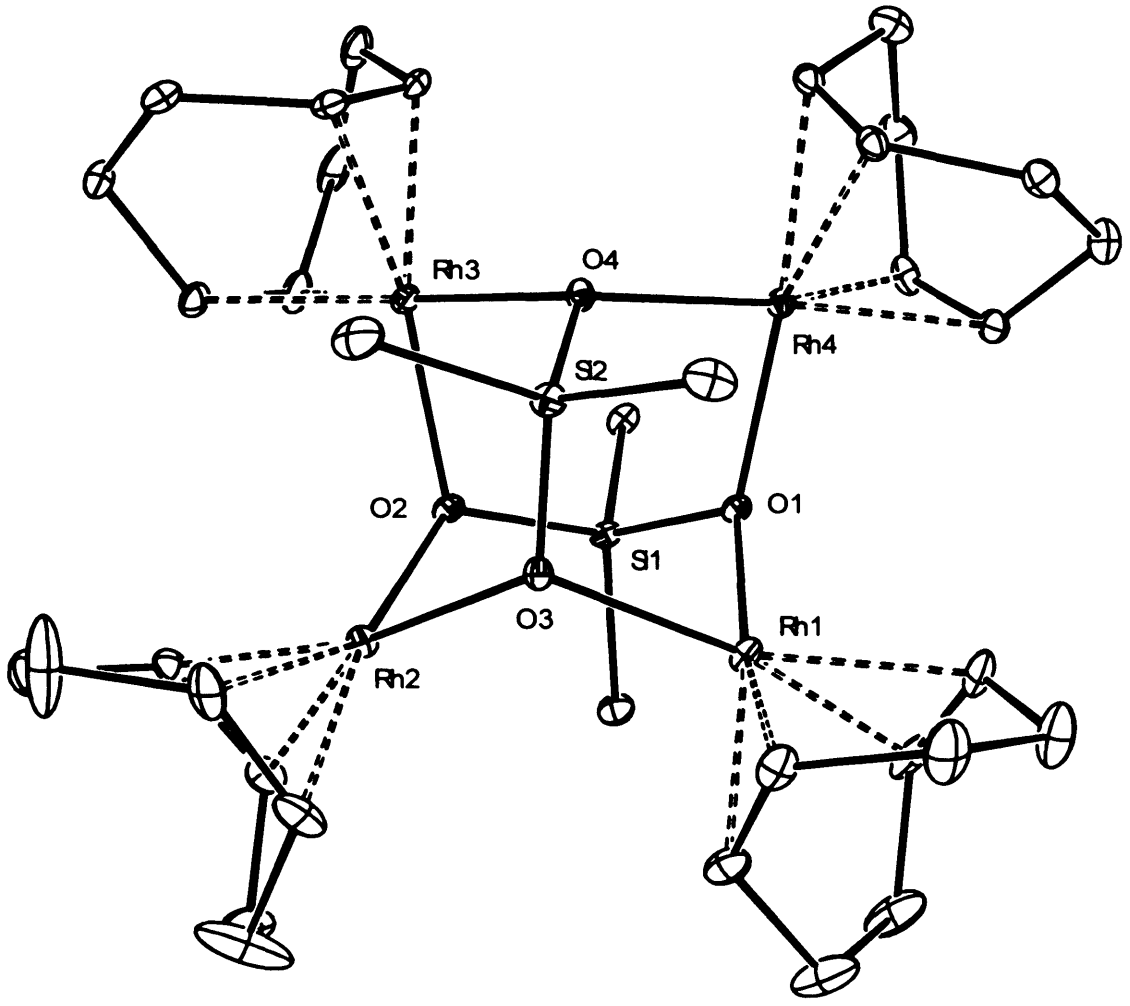

Figure 15 – Thermal ellipsoid plot (25 % probability surface) of the molecular structure of $[\{Rh(\eta^4\text{-COD})\}_4(\mu^4\text{-}Me_2SiO_2)_2]$ **31**; hydrogen atoms omitted for clarity. Selected bond lengths (Å) and angles (°): Rh(1)—O(3) 2.126(3), Rh(1)—O(1) 2.130(3), Rh(2)—O(3) 2.088(3), Rh(2)—O(2) 2.091(3), Rh(3)—O(2) 2.122(3), Rh(3)—O(4) 2.127(3), Rh(4)—O(1) 2.092(3), Rh(4)—O(4) 2.094(3), O(3)—Rh(1)—O(1) 91.24(10), O(3)—Rh(2)—O(2) 88.70(11), O(2)—Rh(3)—O(4) 91.46(10), O(1)—Rh(4)—O(4) 88.60(11), Rh(4)—O(1)—Rh(1) 110.86(12), Rh(2)—O(2)—Rh(3) 108.37(12), Rh(2)—O(3)—Rh(1) 110.98(12), Rh(4)—O(4)—Rh(3) 111.39(12).

Tiripicchio, Oro and co-workers have shown that the rhodium(I) amidinate complex, **27**, reacts with CO to afford the tetracarbonyl derivative, $[(CO)_2Rh\{\eta^2\text{-}[N(Ph)]_2CPh\}]_2$.[22] In contrast, **30** reacted with CO to give rhodium metal deposition and GisoH. Gade and co-workers have shown that the addition of Lewis bases, such as triphenylphosphine, PPh_3, to the rhodium(I) η^6-arene complex, **32**, affords square planar four-coordinate Rh(I) complexes.[24a] During these reactions, the tris(arylamido)-stannate ligand converts from a six-electron donor to a two-electron donor.[24a] In contrast, rhodium metal deposition and an intractable mixture of products resulted when **30** was treated with PPh_3. It was decided to investigate if the η^6-bound arene complexes, **28 – 30** could be converted to their *N,N'*-chelated isomers. No reaction occurred when a toluene solution of **30** was irradiated with UV light for three hours. In contrast, heating toluene solutions of **28 – 30** at 80 °C for five hours afforded the η^2-*N,N'*-chelated complexes, **34 – 36** (Scheme 4). Similarly, sublimation of crystalline **28** at 150 °C and 5 x 10^{-6} Torr afforded complex **34** exclusively. A toluene solution of **36** was irradiated with UV light for three hours, but no reaction occurred.

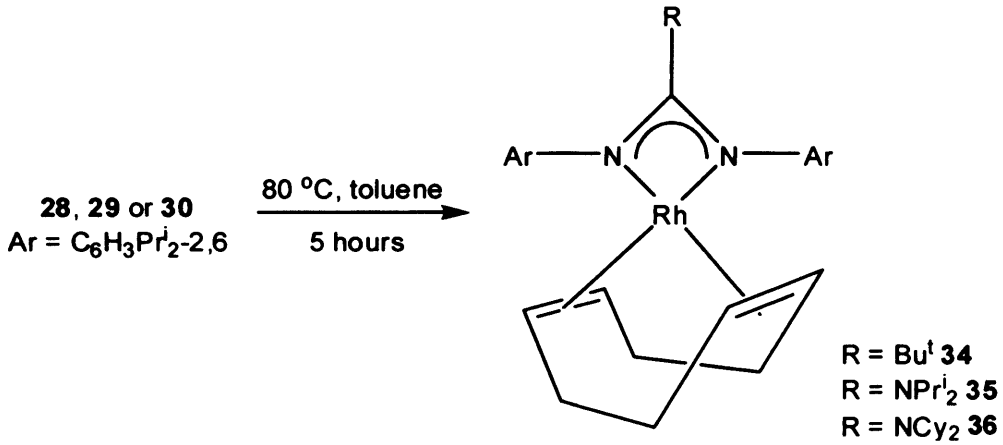

Scheme 4 – The synthesis of **34 – 36**

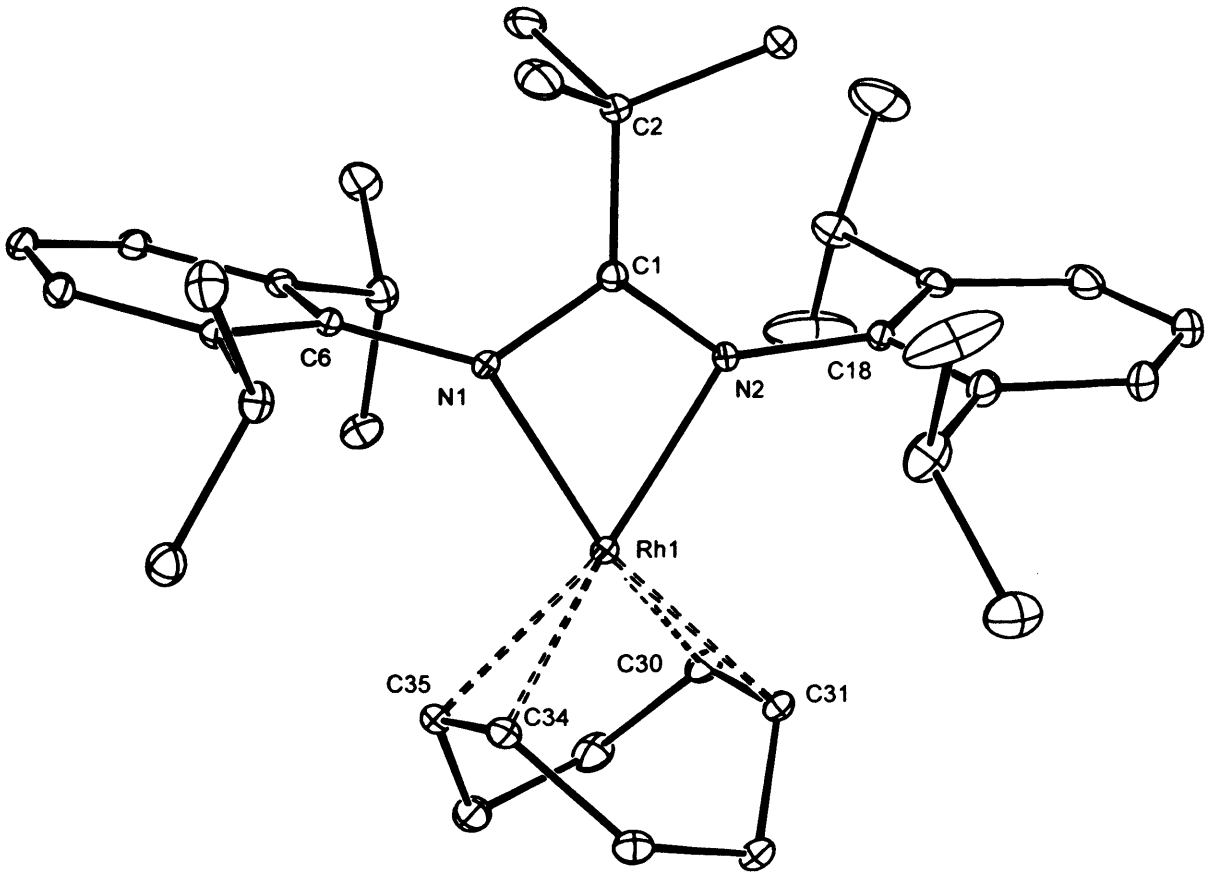

Figure 16 – Thermal ellipsoid plot (25 % probability surface) of the molecular structure of [(η^4-COD)Rh(η^2-Piso)] **34**; hydrogen atoms omitted for clarity. Selected bond lengths (Å) and angles (°): Rh(1)—N(2) 2.0836(17), Rh(1)—N(1) 2.0926(18), Rh(1)—C(34) 2.098(2), Rh(1)—C(30) 2.119(2), Rh(1)—C(31) 2.145(2), Rh(1)—C(35) 2.150(2), N(1)—C(1) 1.351(2), C(1)—N(2) 1.332(3), C(1)—C(2) 1.543(3), C(30)—C(31) 1.399(3), C(34)—C(35) 1.393(3), N(2)—Rh(1)—N(1) 62.98(7), C(1)—N(1)—Rh(1) 93.62(12), C(1)—N(2)—Rh(1) 94.59(12), N(2)—C(1)—N(1) 108.76(17).

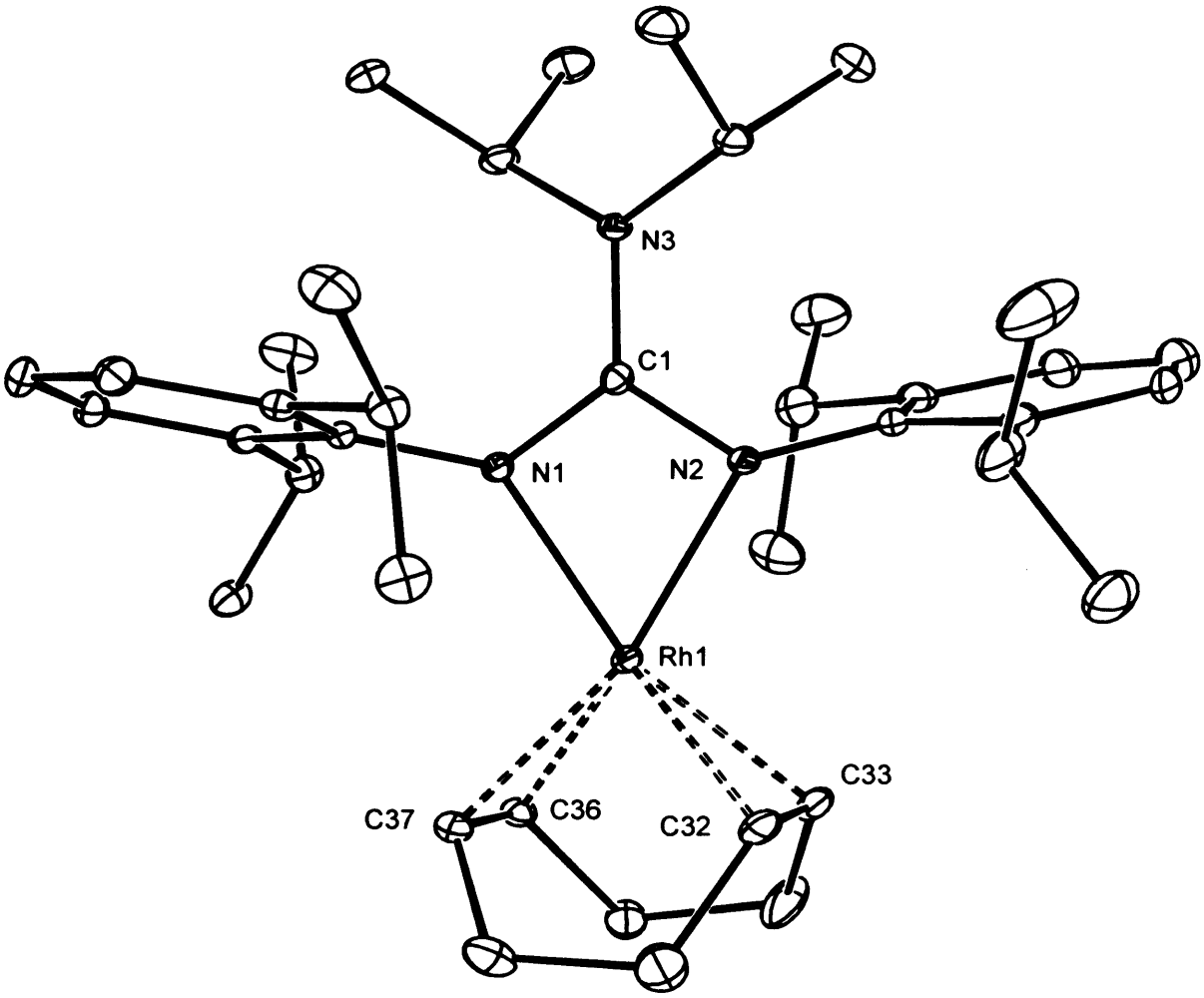

Figure 17 – Thermal ellipsoid plot (25 % probability surface) of the molecular structure of [(η^4-COD)Rh(η^2-Priso)] **35**; hydrogen atoms omitted for clarity. Selected bond lengths (Å) and angles (°): Rh(1)—N(2) 2.087(2), Rh(1)—N(1) 2.091(2), Rh(1)—C(36) 2.111(3), Rh(1)—C(33) 2.117(3), Rh(1)—C(32) 2.118(3), Rh(1)—C(37) 2.131(3), N(1)—C(1) 1.337(3), N(2)—C(1) 1.353(3), N(3)—C(1) 1.380(3), C(32)—C(33) 1.388(5), C(36)—C(37) 1.388(4), N(2)—Rh(1)—N(1) 63.54(8), C(1)—N(1)—Rh(1) 93.55(15), C(1)—N(2)—Rh(1) 93.23(16), N(1)—C(1)—N(2) 109.7(2).

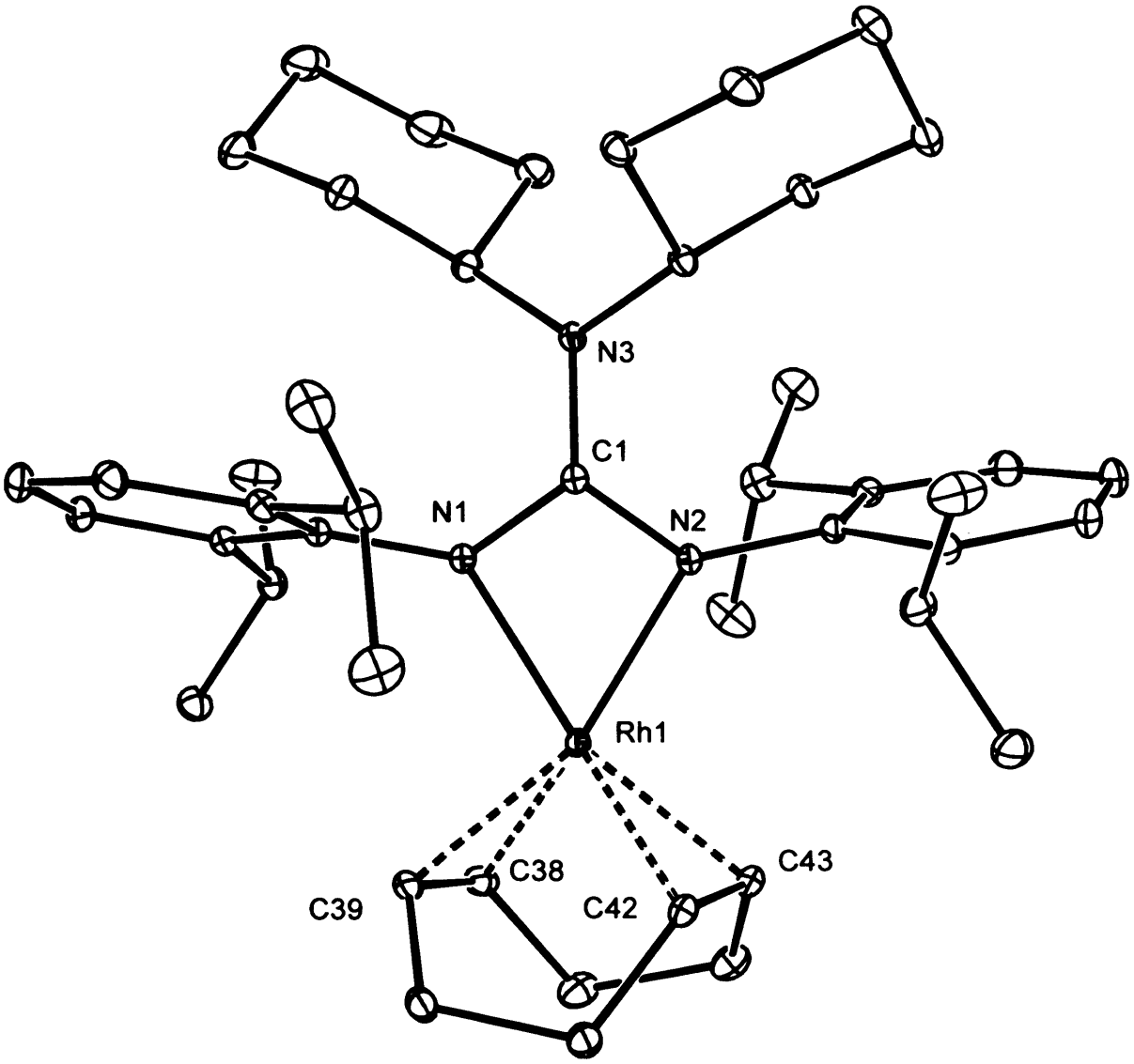

Figure 18 – Thermal ellipsoid plot (25 % probability surface) of the molecular structure of [(η^4-COD)Rh(η^2-Giso)] **36**; hydrogen atoms omitted for clarity. Selected bond lengths (Å) and angles (°): Rh(1)—N(1) 2.0889(13), Rh(1)—N(2) 2.0939(13), Rh(1)—C(39) 2.1170(16), Rh(1)—C(42) 2.1193(16), Rh(1)—C(38) 2.1201(17), Rh(1)—C(43) 2.1214(16), N(1)—C(1) 1.346(2), N(2)—C(1) 1.350(2), N(3)—C(1) 1.378(2), C(38)—C(39) 1.399(3), C(42)—C(43) 1.398(2), N(1)—Rh(1)—N(2) 63.46(5), C(1)—N(1)—Rh(1) 93.79(10), C(1)—N(2)—Rh(1) 93.45(10), N(1)—C(1)—N(2) 109.31(14).

Complexes **34 – 36** were fully characterised. The ^{1}H and ^{13}C{^{1}H} NMR spectra of these complexes are symmetrical and are consistent with their solid state structures;

as such they do not warrant further comment. X-ray crystallographic analyses of complexes **34 – 36** were carried out (Figures 16 – 18). The rhodium atoms of **34 – 36** have distorted square planar ligand environments (Σ angles m(1)—Rh(1)—m(2), N(1)—Rh(1)—m(2), N(2)—Rh(1)—m(1), N(1)—Rh(1)—N(2) = 360.65° mean; m(1) and m(2) are the mid-points of the olefinic C(30)—C(31) and C(34)—C(35) bonds). Complex **34** exhibits the greatest deviation from planarity, with the dihedral angle between the N(1)—N(2) plane and the m(1)—m(2) plane (14.0°) being far greater than that exhibited by **27** (1.8°),[22] most likely a consequence of the increased steric bulk of $Piso^-$ in comparison with the *N,N'*-diphenylbenzamidinate ligand. The N(1)—Rh(1)—N(2) bite angles exhibited by **34** (62.98°), **35** (63.54°), **36** (63.46°) are narrow, but are similar to that observed in **27** (63.2°).[22] The N(1)—C(1) and N(2)—C(1) distances observed in **34 – 36** are similar (1.332 – 1.351 Å) and the N(3)—C(1) distances exhibited by **35** (1.380(3) Å) and **36** (1.378(2) Å) are shorter than typical N—C single bonds (1.47 Å).[19] These observations point towards significant π-electron delocalisation over the CN_2 or CN_3 fragments of **34 – 36**. The Rh—N distances exhibited by **34 – 36** (2.087(2) – 2.0939(13) Å) are within the known range (1.757 – 2.893 Å)[21] and are comparable to those observed in **27** (2.101 Å mean).[22] All other interatomic distances and angles are unremarkable.

A kinetic study was proposed to investigate the rate of reaction for the thermal conversion of the kinetic products, **28 – 30**, to the thermodynamic products, **34 – 36**. This was achieved by preparing nearly saturated C_6D_6 solutions of **28 – 30** (0.02 g in 0.6 cm^3) in Young's NMR tubes with a tetramethylsilane (TMS, $SiMe_4$) standard. As TMS does not take any part in the reaction, the integration of its signal can be employed as the standard as the reaction proceeds. The ^1H NMR spectra of these samples were obtained and the tubes were heated at 80 °C. ^1H NMR spectra of these reaction

mixtures were obtained in fifteen minute intervals. Integration of these spectra allowed the rates of reaction to be measured. As the starting concentrations of **28 – 30** and the ratios of the integration of the signals at *ca.* δ 5.5 ppm to the TMS signals in the ^{1}H NMR spectra are known, all ratios obtained could then be converted to units of moldm^{-3}. The integration of the signal at *ca.* δ 5.5 ppm in the ^{1}H NMR spectra was chosen as this signal does not overlap with any signals observed in the ^{1}H NMR spectra of **34 – 36**. The thermal conversion of **28** to the thermodynamic product, **34**, was complete after heating to 80 °C for fifteen minutes. Hence the rate of conversion is greatest for the amidinate complex, **28**, which may possibly explain why only complex **27** was isolated by Tiripicchio, Oro and co-workers whilst utilising the less bulky *N,N'*-diphenylamidinate ligand. The thermal conversion of **28 – 30** to the thermodynamic complexes, **34 – 36**, is expected to be a unimolecular, first order reaction, the rate equation being: Rate = k[π-arene complex]. As such a graph was constructed of ln[π-arene complexes] against time (Graph 1). Straight lines were obtained to give the rate constants, $k = 5.41 \times 10^{-4}$ s^{-1} for the rate of conversion of **29** and $k = 2.87 \times 10^{-4}$ s^{-1} for the rate of conversion of **30**. The high R^2 values of 0.992 and 0.972 for these lines suggest an excellent correlation of this data series to the straight line graphs. This also shows that the reactions are first order with respect to the concentrations of **29** and **30**. The kinetics of the thermal conversion of **29** into **35** was not measured after 105 minutes as the signal at *ca.* δ 5.5 ppm in the ^{1}H NMR spectra were almost indistinguishable from the baseline noise after this time, making the errors of these measurements high. The thermal conversion of **29** into **35** is complete after three hours of heating at 80 °C, and the complete thermal conversion of **30** into **36** takes five hours at this temperature. Hence the rate of conversion of the kinetic products, **28 – 30**, into the thermodynamic products, **34 – 36** is: **28** > **29** > **30**.

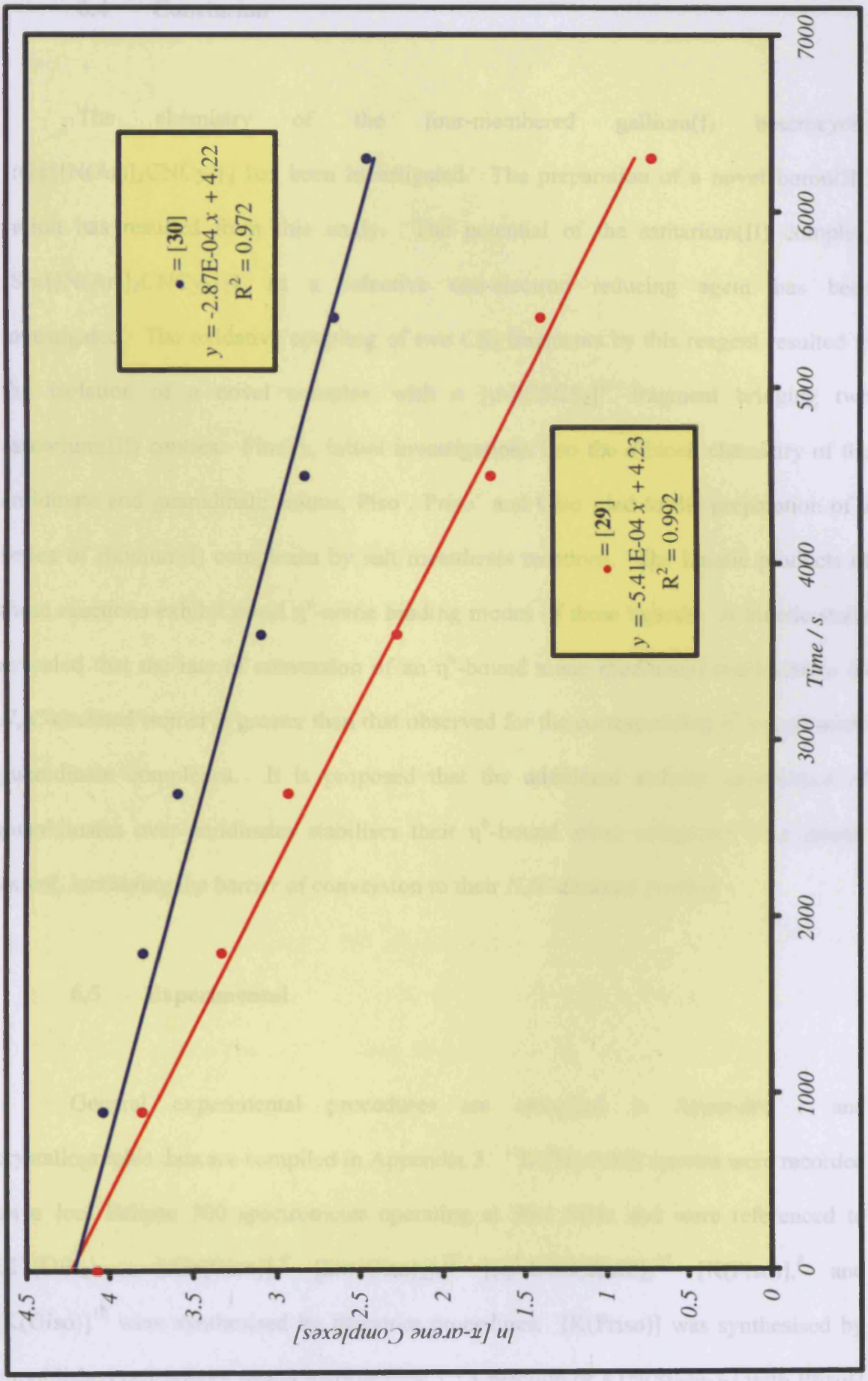

Graph 1 – First order rate equation plot for the thermal conversion of **29** and **30**

6.4 Conclusion

The chemistry of the four-membered gallium(I) heterocycle, [:Ga{[N(Ar)]$_2$CNCy$_2$}] has been investigated. The preparation of a novel boron(III) cation has resulted from this study. The potential of the samarium(II) complex, [Sm{[N(Ar)]$_2$CNCy$_2$}$_2$], as a selective one-electron reducing agent has been investigated. The oxidative coupling of two CS_2 fragments by this reagent resulted in the isolation of a novel complex with a [μ-SCSCS$_2$]$^{2-}$ fragment bridging two samarium(III) centres. Finally, initial investigations into the *d*-block chemistry of the amidinate and guanidinate anions, Piso$^-$, Priso$^-$ and Giso$^-$, led to the preparation of a series of rhodium(I) complexes by salt metathesis reactions. The kinetic products of these reactions exhibit novel η^6-arene binding modes of these ligands. A kinetic study revealed that the rate of conversion of an η^6-bound arene rhodium(I) amidinate to its *N,N'*-chelated isomer is greater than that observed for the corresponding η^6-bound arene guanidinate complexes. It is proposed that the additional π-donor capabilities of guanidinates over amidinates stabilises their η^6-bound arene complexes to a greater extent, increasing the barrier of conversion to their *N,N'*-chelated isomers.

6.5 Experimental

General experimental procedures are compiled in Appendix 1 and crystallographic data are compiled in Appendix 3. $^{11}B\{^1H\}$ NMR spectra were recorded on a Jeol Eclipse 300 spectrometer operating at 96.4 MHz and were referenced to $BF_3(OEt_2)$. [:Ga(Giso)],[4] [Sm(Giso)$_2$],[12] [(η^4-COD)RhCl]$_2$[27] [K(Piso)],[8] and [K(Giso)][12] were synthesised by literature procedures. [K(Priso)] was synthesised by unpublished procedures which involved the 1 : 1 reaction of K[N(SiMe$_3$)$_2$] with PrisoH

in toluene.[28] CS_2 was freshly distilled prior to use. All other reagents were used as received.

Preparation of [BrB(Giso)][$GaBr_4$] 24: BBr_3 (35 μl, 0.37 mmol) was added *via* a microsyringe to a solution of [:Ga(Giso)] (0.19 g, 0.31 mmol) in toluene (10 cm^3) at -78 °C to give a deep yellow solution. The reaction mixture was warmed to 20 °C, becoming colourless, and stirred for 24 hrs to yield a precipitate. Volatiles were then removed *in vacuo* and the residue was washed with hexane (20 cm^3) and extracted into THF (40 cm^3) and filtered. The filtrate was concentrated to *ca.* 10 cm^3 and stored at -30 °C overnight to give colourless crystals of **24**. A second crop was obtained (0.11 g, 34 %). Mp 206 °C (decomp.); ^{1}H NMR (400 MHz, d_8-THF, 298 K): δ 1.17-1.93 (br. m, 20H, CH_2), 1.43 (br, 24H, (CH_3)$_2$CH), 3.22 (m, 2 H, CH_2C*H*), 3.61 (m, 4 H, $(CH_3)_2$C*H*), 7.10-7.52 (m, 6 H, *m*-Ar-*H*); ^{11}B{^{1}H} NMR (96.4 MHz, d_8-THF, 298 K): δ 18.5; MS (EI 70eV), *m/z* (%): 544 ({[N(Ar)]$_2$CNCy$_2$}H$^+$, 6), 501 ({[N(Ar)]$_2$CNCy$_2$}H$^+$ - Pr^i, 43); IR ν/cm^{-1} (Nujol): 1588 m, 1568 m, 1260 m, 1096 m, 1018 m, 801 m.

Preparation of [{Sm(Giso)$_2$}$_2$(μ-η^2:η^2-$SCSCS_2$)] 25: A 1.66 M solution of CS_2 in toluene (0.5 cm^3, 0.81 mmol) was added to a suspension of [Sm(Giso)$_2$] (0.40 g, 0.32 mmol) in toluene (10 cm^3) at -78 °C to give a deep green solution. The reaction mixture was warmed to 20 °C and stirred for three hours. The solution was concentrated to *ca.* 4 cm^3, filtered and stored at -30 °C to give deep green blocks of **25** (0.24 g, 55 %). Mp 131 °C (decomp.); MS (APCI), *m/z* (%): 545 ({[N(Ar)]$_2$CNCy$_2$}H$^+$, 100); IR ν/cm^{-1} (Nujol): 1612 s, 1583 s, 1322 m, 1240 m, 1013 m, 933 m, 894 m, 794 m, 778 m.

Preparation of [(η^4-COD)Rh(η^6-Piso)] 28: A slurry of [K(Piso)] (0.50 g, 1.09 mmol) in toluene (25 cm^3) at -78 °C was added to a solution of [(η^4-COD)RhCl]$_2$ (0.27 g, 0.55 mmol) in toluene (15 cm^3) over 10 mins. The reaction mixture was warmed to 20 °C over 2 hrs and stirred for a further hour to give a yellow solution. Volatiles were then removed *in vacuo* and the residue was extracted into hexane (60 cm^3) and filtered. The filtrate was concentrated to *ca.* 20 cm^3 and stored at -30 °C overnight to give pale yellow blocks of **28**. A second crop was obtained (0.19 g, 28 %). Mp 133-135 °C (decomp.); ^{1}H NMR (200.13 MHz, C_6D_6, 298 K): δ 1.41 (d, $^3J_{HH}$ = 6.6 Hz, 12 H, (C*H*$_3$)$_2$CH), 1.60 (d, $^3J_{HH}$ = 6.7 Hz, 12 H, (C*H*$_3$)$_2$CH), 1.61 (d, $^3J_{HH}$ = 6.9 Hz, 12 H, (C*H*$_3$)$_2$CH), 1.64 (s, 9H, (C*H*$_3$)$_3$C), 1.78 (m, 4 H, C*H*$_2$CH), 2.07 (m, 4 H, C*H*$_2$CH), 3.20 (sept, $^3J_{HH}$ = 6.8 Hz, 2 H, (CH$_3$)$_2$C*H*) 3.27 (br. m, 4 H, CH$_2$C*H*), 3.65 (sept, $^3J_{HH}$ = 6.7 Hz, 2 H, (CH$_3$)$_2$C*H*), 3.85 (t, $^3J_{HH}$ = 5.8 Hz, 1 H, η^6-arene-*p*-Ar-*H*), 5.65 (d, $^3J_{HH}$ = 5.8 Hz, 2 H, η^6-arene-*m*-Ar-*H*), 7.11 (t, $^3J_{HH}$ = 6.7 Hz, 1 H, *p*-Ar-*H*), 7.30 (br. m, 2 H, *m*-Ar-*H*); ^{13}C{^{1}H} NMR (50.33 MHz, C_6D_6, 298 K): δ 21.6 ((*C*H$_3$)$_3$C), 23.9, 24.8, 25.4, 26.7 ((*C*H$_3$)$_2$CH), 29.1, 29.8 ((CH$_3$)$_2$*C*H), 31.7 (*C*H$_2$), 42.2 ((CH$_3$)$_3$*C*), 73.3 (br., CH$_2$*C*H), 74.5 (d, $^1J_{RhC}$ = 5.2 Hz, η^6-arene-*p*-Ar-*C*), 101.5 (d, $^1J_{RhC}$ = 3.6 Hz, η^6-arene-*m*-Ar-*C*), 115.5 (d, $^1J_{RhC}$ = 2.3 Hz, η^6-arene-*o*-Ar-*C*), 121.4, 121.9, 138.8, 148.6 (Ar-*C*), 164.8 (*C*N$_2$C); MS (EI 70eV), *m/z* (%): 630 (MH$^+$, 13), 573 (MH$^+$ - Bu^t, 31), 522 (MH$^+$ - COD, 29), 420 ({[N(Ar)$_2$CBu^t}H$^+$, 17); IR ν/cm^{-1} (Nujol): 1593 s, 1567 s, 1538 s, 1360 m, 1253 m, 1139 m, 910 m, 866 m 842 m, 800 m; EI acc. mass on M$^+$: calc. for $C_{37}H_{55}N_2Rh$: 630.3415, found 630.3415; $C_{37}H_{55}N_2Rh$ requires C 70.46, H 8.79, N 4.44 %; found C 70.46, H 8.53, N 4.45 %.

Preparation of [(η^4-COD)Rh(η^6-Priso)] 29: A slurry of [K(Priso)] (0.50 g, 1.11 mmol) in toluene (30 cm^3) at -78 °C was added to a solution of [(η^4-COD)RhCl]$_2$ (0.25 g, 0.56 mmol) in toluene (10 cm^3) at -78 °C over 10 mins. The reaction mixture was

warmed to 20 °C over 2 hrs and stirred for a further hour to give a yellow solution. Volatiles were then removed *in vacuo* and the product was extracted into hexane (100 cm^3) and filtered. The filtrate was concentrated to *ca.* 20 cm^3 and stored at -30 °C overnight to give pale yellow blocks of **29**. A second crop was obtained (0.28 g, 42 %). Mp 164-166 °C (decomp.); ^{1}H NMR (200.13 MHz, C_6D_6, 298 K): δ 1.50 (d, $^3J_{HH}$ = 6.7 Hz, 12 H, $(CH_3)_2CH$), 1.57 (d, $^3J_{HH}$ = 6.6 Hz, 12 H, $(CH_3)_2CH$), 1.68 (d, $^3J_{HH}$ = 6.8 Hz, 12 H, $(CH_3)_2CH$), 1.83 (m, 4 H, CH_2), 2.12 (m, 4 H, CH_2), 3.40 (br. m, 4 H, CH_2CH), 3.60 (sept, $^3J_{HH}$ = 6.9 Hz, 2 H, $(CH_3)_2CHN$), 3.83 (t, $^3J_{HH}$ = 5.8 Hz, 1 H, η^6-arene-*p*-Ar-*H*), 3.94 (sept, $^3J_{HH}$ = 6.9 Hz, 4 H, $(CH_3)_2CH$), 5.72 (d, $^3J_{HH}$ = 5.8 Hz, 2 H, η^6-arene-*m*-Ar-*H*), 7.11 (t, $^3J_{HH}$ = 7.9 Hz, 1 H, *p*-Ar-*H*), 7.22-7.36 (m, 2 H, Ar-*H*); $^{13}C\{^1H\}$ NMR (50.33 MHz, C_6D_6, 298 K): δ 21.9 ($(CH_3)_2CHN$), 24.4, 24.8, 26.0, 26.4 ($(CH_3)_2CH$), 29.1 ($(CH_3)_2CH$), 31.7 (CH_2), 47.0 ($(CH_3)_2CHN$), 72.1 (d, $^1J_{RhC}$ = 13.3 Hz, CH_2CH), 74.6 (d, $^1J_{RhC}$ = 5.4 Hz, η^6-arene-*p*-Ar-*C*), 101.1 (d, $^1J_{RhC}$ = 3.5 Hz, η^6-arene-*m*-Ar-*C*), 116.5 (d, $^1J_{RhC}$ = 2.3 Hz, η^6-arene-*o*-Ar-*C*), 120.5, 122.2, 140.0, 142.4, 147.0, 152.0 (Ar-*C*), 175.7 (CN_3); MS (EI 70eV), *m/z* (%): 673 (MH^+, 8), 630 (MH^+ - Pr^i, 16), 573 (MH^+ - NPr^i_2, 3), 565 (MH^+ - COD, 4), 520 (MH^+ - COD - Pr^i, 5), 462 ($\{[N(Ar)]_2CNPr^i_2\}H^+$, 3); IR ν/cm^{-1} (Nujol): 1555 s, 1537 s, 1366 m, 1311 m, 1279 m, 1260 m, 1218 m, 1134 m, 992 m, 848 m, 800 m; EI acc. mass on M^+: calc. for $C_{39}H_{60}N_3Rh$: 673.3837, found 673.3839; $C_{39}H_{60}N_3Rh$ requires C 69.52, H 8.98, N 6.24 %; found C 69.50, H 8.93, N 6.28 %.

Preparation of [(η^4-COD)Rh(η^6-Giso)] 30: A slurry of [K(Giso)] (0.50 g, 0.86 mmol) in toluene (30 cm^3) at -78 °C was added to a solution of $[(\eta^4\text{-COD})RhCl]_2$ (0.21 g, 0.43 mmol) in toluene (20 cm^3) at -78 °C over 10 mins. The reaction mixture was warmed to 20 °C over 2 hrs and stirred for a further hour to give a yellow solution. Volatiles were then removed *in vacuo* and the product was extracted into hexane (120 cm^3) and

filtered. The filtrate was concentrated to *ca.* 60 cm^3 and stored at -30 °C overnight to give pale yellow blocks of **30**. A second crop was obtained (0.35 g, 54 %). Mp 169-171 °C (decomp.); ^{1}H NMR (200.13 MHz, C_6D_6, 298 K): δ 1.45 (m, 12 H, cy CH_2), 1.54 (dd, $^3J_{HH}$ = 7.0 Hz, 12 H, $(CH_3)_2CH$), 1.62 (d, $^3J_{HH}$ = 6.6 Hz, 6 H, $(CH_3)_2CH$), 1.70 (d, $^3J_{HH}$ = 6.7 Hz, 6 H, $(CH_3)_2CH$), 1.84 (br. m, 8 H, cy CH_2), 2.12 (br. m, 8 H, COD CH_2), 3.46 (br. m, 4 H, COD CH_2CH), 3.57 (m, 2 H, cy CH_2CH), 3.59 (sept, $^3J_{HH}$ = 6.4 Hz, 2 H, $(CH_3)_2CH$), 3.91 (t, 1 H, $^3J_{HH}$ = 5.8 Hz, η^6-arene-*p*-Ar-*H*), 3.94 (sept, $^3J_{HH}$ = 7.0 Hz, 2 H, $(CH_3)_2CH$), 5.74 (d, $^3J_{HH}$ = 5.8 Hz, 2 H, η^6-arene-*m*-Ar-*H*), 7.13 (t, $^3J_{HH}$ = 7.5 Hz, 1 H, *p*-Ar-*H*), 7.34 (m, 2 H, *m*-Ar-*H*); $^{13}C\{^1H\}$ NMR (75.48 MHz, C_6D_6, 298 K): δ 20.8, 23.5 (cy CH_2), 25.0 ($(CH_3)_2CH$), 25.2 (cy CH_2), 26.1, (br., $(CH_3)_2CH$), 28.1 (cy CH_2), 29.5 ($(CH_3)_2CH$), 30.7 (COD CH_2), 34.6 (cy *ipso*-CH_2), 57.0, 57.4 ($(CH_3)_2CHN$), 73.5 (d, $^1J_{RhC}$ = 5.2 Hz, η^6-arene-*p*-Ar-*C*), 75.4 (d, $^1J_{RhC}$ = 13.0 Hz, COD CH_2CH), 99.8 (d, $^1J_{RhC}$ = 3.6 Hz, η^6-arene-*m*-Ar-*C*), 119.1, 121.1, 122.0, 122.6, 138.7, 141.8, 144.0, 145.6 (Ar-*C*); MS (EI 70eV), *m/z* (%): 753 (MH^+, 2), 710 (MH^+ - Pr^i, 1), 670 (MH^+ - cy, 2), 645 (MH^+ - COD, 1), 542 ($\{[N(Ar)]_2CNCy_2\}H^+$, 12); IR ν/cm^{-1} (Nujol): 1563 s, 1520 s, 1352 m, 1283 m, 1235 m, 1206 m, 1170 m, 1127 m, 1007 m, 970 m, 932 m, 891 m, 848 m, 802 m; EI acc. mass on M^+: calc. for $C_{45}H_{68}N_3Rh$: 753.4467, found 753.4463; $C_{45}H_{68}N_3Rh$ requires C 71.69, H 9.09, N 5.57 %; found C 70.21, H 9.15, N 5.31 %.

Preparation of [(η^4-COD)Rh(η^2-Piso)] 34: A solution of **28** (0.10 g, 0.16 mmol) in toluene (10 cm^3) was heated at 80 °C for 15 mins. Volatiles were then removed *in vacuo* and the product was extracted into hexane (10 cm^3) and filtered. The filtrate was concentrated to *ca.* 2 cm^3 and stored at -30 °C overnight to give pale yellow blocks of **34**. A second crop was obtained (0.06 g, 60 %). Mp 133-135 °C (decomp.); ^{1}H NMR (200.13 MHz, C_6D_6, 298 K): δ 1.10 (s, 9 H, $(CH_3)_3C$), 1.58 (d, $^3J_{HH}$ = 6.8 Hz, 12 H,

(CH_3)$_2$CH), 1.59 (br. m, 4 H, CH_2), 1.76 (d, $^3J_{HH}$ = 6.7 Hz, 12 H, (CH_3)$_2$CH), 2.43 (br. m, 4 H, CH_2), 3.83 (br. m, 4 H, CH_2CH), 4.14 (sept, $^3J_{HH}$ = 6.8 Hz, 4 H, (CH_3)$_2$$CH$), 7.15-7.29 (m, 6 H, Ar-*H*); $^{13}C\{^1H\}$ NMR (50.33 MHz, C_6D_6, 298 K): δ 24.0 ((CH_3)$_3$C), 25.9 ((CH_3)$_2$CH), 28.2 ((CH_3)$_2$$CH$), 30.2, 30.7 ($CH_2$), 44.5 (($CH_3$)$_3$$C$), 78.5 (d, $^1J_{RhC}$ = 13.7 Hz, CH_2CH), 123.8, 124.5, 143.0, 143.9 (Ar-*C*), 186.8 (d, $^2J_{RhC}$ = 5.0 Hz, CN_2C); MS (EI 70eV), *m/z* (%): 630 (MH^+, 45), 573 (MH^+ - Bu^t, 78), 522 (MH^+ - COD, 92), 420 ({[N(Ar)$_2$CBu^t}H^+, 21); IR ν/cm^{-1} (Nujol): 1315 m, 1241 m, 1170 m, 1098 m, 949 m, 800 m, 761 m; EI acc. mass on M^+: calc. for $C_{37}H_{55}N_2Rh$: 630.3415, found 630.3418; $C_{37}H_{55}N_2Rh$ requires C 70.46, H 8.79, N 4.44 %; found C 70.19, H 8.91, N 4.45 %.

Preparation of [(η^4-COD)Rh(η^2-Priso)] 35: A solution of **29** (0.16 g, 0.27 mmol) in toluene (20 cm^3) was heated at 80 °C for 3 hrs. Volatiles were then removed *in vacuo* and the product was extracted into hexane (40 cm^3) and filtered. The filtrate was concentrated to *ca.* 4 cm^3 and stored at -30 °C overnight to give pale yellow blocks of **35**. A second crop was obtained (0.10 g, 56 %). Mp 183-185 °C (decomp.); ^1H NMR (200.13 MHz, C_6D_6, 298 K): δ 0.91 (d, $^3J_{HH}$ = 7.0 Hz, 12 H, (CH_3)$_2$CHN), 1.54 (d, $^3J_{HH}$ = 6.9 Hz, 12 H, (CH_3)$_2$CH), 1.61 (m, 4 H, CH_2), 1.94 (d, $^3J_{HH}$ = 6.8 Hz, 12 H, (CH_3)$_2$CH), 2.42 (m, 4 H, CH_2), 3.94 (br. m, 4 H, CH_2CH), 4.11 (sept, $^3J_{HH}$ = 6.9 Hz, 8 H, (CH_3)$_2$$CH$), 7.18-7.34 (m, 6 H, Ar-*H*); $^{13}C\{^1H\}$ NMR (50.33 MHz, C_6D_6, 298 K): δ 23.5 ((CH_3)$_2$CHN), 26.2 ((CH_3)$_2$CH), 27.6 ((CH_3)$_2$$CH$), 30.9 ($CH_2$), 49.0 (($CH_3$)$_2$$CHN$), 76.2 (d, $^1J_{RhC}$ = 14.0 Hz, CH_2CH), 123.8, 124.0, 143.8, 144.7 (Ar-*C*), 174.5 (d, $^2J_{RhC}$ = 5.7 Hz, CN_3); MS (EI 70eV), *m/z* (%): 673 (MH^+, 50), 630 (MH^+ - Pr^i, 100), 573 (MH^+ - NPr$^i_2$, 13), 565 (MH^+ - COD, 18), 462 ({[N(Ar)]$_2$CNPr$^i_2$}H^+, 10); IR ν/cm^{-1} (Nujol): 1434 s, 1407 s, 1316 m, 1275 m, 1245 m, 1176 m, 1124 m, 1109 m, 952 m, 932 m, 871 m, 799 s, 757 s, 658 m; EI acc. mass on M^+: calc. for $C_{39}H_{60}N_3Rh$: 673.3837, found

673.3834; $C_{39}H_{60}N_3Rh$ requires C 69.52, H 8.98, N 6.24 %; found C 69.82, H 9.00, N 6.35 %.

Preparation of [(η^4-COD)Rh(η^2-Giso)] 36: A solution of **30** (0.17 g, 0.23 mmol) in toluene (20 cm^3) was heated to 80 °C for 5 hrs. Volatiles were then removed *in vacuo* and the product was extracted into hexane (20 cm^3) and filtered. The filtrate was concentrated to *ca.* 4 cm^3 and stored at -30 °C overnight to give pale yellow blocks of **36**. A second crop was obtained (0.05 g, 29 %). Mp 164-166 °C (decomp.); ^{1}H NMR (300.13 MHz, C_6D_6, 298 K): δ 0.91-1.08 (m, 8 H, cy CH_2), 1.52 (m, 12 H, cy CH_2), 1.58 (d, $^3J_{HH}$ = 6.8 Hz, 12 H, (CH_3)$_2$CH), 1.59 (m, 4 H, COD CH_2), 1.93 (d, $^3J_{HH}$ = 6.8 Hz, 12 H, (CH_3)$_2$CH), 2.32 (m, 4 H, COD CH_2), 3.72 (m, 2 H, cy CH$_2$CH), 3.91 (br. m, 4 H, COD CH$_2$CH), 3.95 (sept, $^3J_{HH}$ = 6.8 Hz, 4 H, (CH$_3$)$_2$CH), 7.17 (dd, $^3J_{HH}$ = 6.4 Hz, 2 H, *p*-Ar-*H*), 7.26 (d, $^3J_{HH}$ = 6.8 Hz, 4 H, *m*-Ar-*H*); ^{13}C{^{1}H} NMR (50.33 MHz, C_6D_6, 298 K): δ 23.6 (cy *p*-CH$_2$), 26.1, 26.4 ((*C*H$_3$)$_2$CH), 26.9 (cy *m*-CH$_2$), 27.6 ((CH$_3$)$_2$*C*H), 30.8, 31.1 (COD *C*H$_2$), 35.8 (cy o-*C*H$_2$), 58.6 (cy (CH$_2$)$_2$*C*HN), 76.7 (d, $^1J_{RhC}$ = 13.0 Hz, COD CH$_2$*C*H), 123.6, 123.8, 143.1, 145.1 (Ar-*C*), 174.1 (d, $^2J_{RhC}$ = 5.5 Hz, *C*N$_3$); MS (EI 70eV), *m/z* (%): 753 (MH$^+$, 100), 710 (MH$^+$ - Pr^i, 51), 670 (MH$^+$ - cy, 87), 645 (MH$^+$ - COD, 39), 560 (MH$^+$ - COD - cy, 29), 542 ({[N(Ar)]$_2$CNCy$_2$}H$^+$, 47); IR ν/cm^{-1} (Nujol): 1434 s, 1393 s, 1323 s, 1279 s, 1243 s, 1096 m, 1020 s, 896 m, 866 m, 825 m, 791 s, 772 m, 750 s, 660 m; EI acc. mass on M$^+$: calc. for $C_{45}H_{68}N_3Rh$: 753.4463, found 753.4463; $C_{45}H_{68}N_3Rh$ requires C 71.69, H 9.09, N 5.57 %; found C 71.88, H 9.36, N 5.67 %.

6.6 References

1. (a) J. Barker, M. Kilner, *Coord. Chem. Rev.*, 1994, **133**, 219; (b) F. T. Edelmann, *Coord. Chem. Rev.*, 1994, **137**, 403; (c) F. T. Edelmann, *Top. Curr. Chem.*, 1996, **179**, 113; (d) P. J. Bailey, S. Pace, *Coord. Chem. Rev.*, 2001, **214**, 91, and references therein.
2. (a) H. Kondo, K. Matsubara, H. Nagashima, *J. Am. Chem. Soc.*, 2002, **124**, 534; (b) H. Kondo, Y. Yamaguchi, H. Nagashima, *J. Am. Chem. Soc.*, 2001, **123**, 500.
3. M. P. Coles, D. C. Swenson, R. F. Jordan, V. G. Young Jr., *Organometallics*, 1998, **17**, 4042.
4. C. Jones, P. C. Junk, J. A. Platts, A. Stasch, *J. Am. Chem. Soc.*, 2006, **128**, 2206.
5. A. Xia, H. M. El-Kaderi, M. J. Heeg, C. H. Winter, *J. Organomet. Chem.*, 2003, **682**, 224.
6. M. L. Cole, C. Jones, P. C. Junk, M. Kloth, A. Stasch, *Chem. Eur. J.*, 2005, **11**, 4482.
7. C. Jones, P. C. Junk, M. Kloth, K. M. Proctor, A. Stasch, *Polyhedron*, 2006, **25**, 1592.
8. C. Jones, P. C. Junk, J. A. Platts, D. Rathmann, A. Stasch, *Dalton Trans.*, 2005, 2497.
9. S. P. Green, C. Jones, A. Stasch, *Inorg. Chem.*, 2007, **46**, 11.
10. (a) S. P. Green, C. Jones, P. C. Junk, K. –A. Lippert, A. Stasch, *Chem. Commun.*, 2006, 3978; (b) S. P. Green, C. Jones, K. –A. Lippert, D. P. Mills, A. Stasch, *Inorg. Chem.*, 2006, **45**, 7242.
11. S. P. Green, C. Jones, G. Jin, A. Stasch, *Inorg. Chem.*, 2007, **46**, 8.

12. D. Heitmann, C. Jones, P. C. Junk, K. –A. Lippert, A. Stasch, *Dalton Trans.*, 2007, 187.

13. G. A. Molander, C. R. Harris, *Chem. Rev.*, 1996, **96**, 307, and references therein.

14. W. J. Evans, E. Montalvo, S. E. Foster, K. A. Harada, J. W. Ziller, *Organometallics*, 2007, **26**, 2904.

15. R. B. Coapes, F. E. S. Souza, M. A. Fox, A. S. Batsanov, A. E. Goeta, D. S. Yufit, M. A. Leech, J. A. K. Howard, A. J. Scott, W. Clegg, T. B. Marder, *Dalton Trans.*, 2001, 1201.

16. (a) Z. Lu, N. J. Hill, M. Findlater, A. H. Cowley, *Inorg. Chim. Acta*, 2007, **360**, 1316; (b) M. Findlater, N. J. Hill, A. H. Cowley, *Polyhedron*, 2006, **25**, 983; (c) N. J. Hill, M. Findlater, A. H. Cowley, *Dalton Trans.*, 2005, 3229; (d) N. J. Hill, J. A. Moore, M. Findlater, A. H. Cowley, *Chem. Commun.*, 2005, 5462; (e) P. Blais, T. Chivers, A. Downard, M. Parvez, *Can. J. Chem.*, 2000, **78**, 10; (f) D. J. Brauer, S. Bucheim-Speigel, H. Burger, R. Gielen, G. Pawelke, J. Rothe, *Organometallics*, 1997, **16**, 5321; (g) M. R. Terry, L. A. Mercando, C. Kelley, G. L. Geoffroy, P. Nombel, N. Lugen, R. Mathieu, R. L. Ostrander, B. E. Owens-Waltermire, A. L. Rheingold, *Organometallics*, 1994, **13**, 843; (h) C. Ergezinger, F. Weller, K. Dehnicke, *Z. Naturforsch., Teil B*, 1988, **43**, 1621.

17. W. J. Evans, C. A. Seibel, J. W. Ziller, *Inorg. Chem.*, 1998, **37**, 770.

18. N. W. Davies, A. S. P. Frey, M. G. Gardiner, J. Wang, *Chem. Commun.*, 2006, 4853.

19. J. Emsley, *The Elements*, 3rd Edition, New York, Oxford University Press, 1998.

20. W. J. Evans, G. W. Rabe, J. W. Ziller, R. J. Doeden, *Inorg. Chem.*, 1994, **33**, 2719.

21. CSD version 5.28, November 2006, update 2 (May 2007); F. H. Allen, *Acta Cryst.*, 2002, **B58**, 380.

22. F. L. Lahoz, A. Tiripicchio, M. T. Camellini, L. A. Oro, M. T. Pinillos, *Dalton Trans.*, 1985, 1487.

23. I. Haiduc, *Organometallics*, 2004, **23**, 3, and references therein.

24. For recent examples, see: (a) M. Kilian, H. Wadepohl, L. H. Gade, *Organometallics*, 2007, **26**, 3076; (b) G. Canepa, C. D. Brandt, K. Ilg, J. Wolf, H. Werner, *Chem. Eur. J.*, 2003, **9**, 2502; (c) H. Werner, G. Canepa, K. Ilg, J. Wolf, *Organometallics*, 2000, **19**, 4757; (d) J. R. Farrell, A. H. Eisenberg, C. A. Mirkin, I. A. Guzei, L. M. Liable-Sands, C. D. Incarvito, A. L. Rheingold, C. L. Stern, *Organometallics*, 1999, **18**, 4856; (e) E. T. Singewald, X. Shi, C. A. Mirkin, S. J. Schofer, C. L. Stern, *Organometallics*, 1996, **15**, 3062.

25. D. E. Alexson, C. E. Holloway, A. J. Oliver, *Inorg. Nucl. Chem. Lett.*, 1973, **9**, 885.

26. (a) D. M. Smith, C. –W. Park, J. A. Ibers, *Inorg. Chem.*, 1997, **36**, 3798; (b) F. Cervantes-Lee, H. K. Sharma, I. Haiduc, K. H. Pannell, *Dalton Trans.*, 1998, 1; (c) F. Bottomley, S. Karslioglu, *Organometallics*, 1992, **11**, 326.

27. G. Giordano, R. H. Crabtree, *Inorg. Synth.*, 1990, **28**, 88.

28. C. Jones, A. Stasch, *unpublished results.*

Appendix 1

General Experimental Procedures

All manipulations were performed using standard Schlenk and glovebox techniques under an atmosphere of high purity argon or dinitrogen (BOC 99.9 %) in flame-dried glassware. All glassware was cleaned by overnight storage in an isopropyl alcohol solution of sodium hydroxide, followed by rinsing with dilute hydrochloric acid, distilled water and acetone, and was stored in an oven at 110 °C. Hexane, diethyl ether, toluene and tetrahydrofuran were pre-dried by storage over sodium wire and were refluxed under an atmosphere of high purity dinitrogen for twelve hours over either potassium or Na/K alloy prior to collection. ^{1}H and $^{13}C\{^{1}H\}$ NMR spectra were recorded on either a Bruker AMX 500 spectrometer (500.13 MHz, 125.76 MHz), Bruker DPX 400 spectrometer (400.13 MHz, 100.62 MHz), a Bruker DPX 300 spectrometer (300.13 MHz, 75.47 MHz), a Jeol Eclipse 300 spectrometer (300.52 MHz, 75.57 MHz), or a Bruker AV 200 spectrometer (200.13 MHz, 50.33 MHz) in C_6D_6 or d_8-THF (freeze-thaw degassed and dried over sodium) and were referenced to the residual ^{1}H or ^{13}C resonances of the solvent used. $^{31}P\{^{1}H\}$ NMR spectra were recorded on a Jeol Eclipse 300 spectrometer operating at 121.66 MHz were referenced to 85 % H_3PO_4. EI and APCI mass spectra and accurate mass EI and APCI mass spectra were obtained from the EPSRC National Mass Spectrometric Service at Swansea University. IR spectra were recorded using a Nicolet 510 FT-IR spectrometer as Nujol mulls between NaCl plates. Melting points were determined in sealed glass capillaries under argon and are uncorrected. Microanalyses were obtained from Medac Ltd. or the Campbell Microanalytical Laboratory, University of Otago. Crystals suitable for X-ray structural determination were mounted in silicone oil. Crystallographic measurements

were performed by Prof. C. Jones and Dr. A. Stasch using a Nonius Kappa CCD diffractometer using a graphite monochromator with Mo Kα radiation (λ = 0.71073 Å). The data were collected at 150 K and the structures were solved by direct methods and refined on F^2 by full matrix least squares (SHELX-97)[1] using all unique data.

1. G. M. Sheldrick, *SHELX-97*, University of Göttingen, 1997.

Appendix 2

Publications in Support of this Thesis

1. Investigations into the Preparation of Group 13-15 *N*-Heterocyclic Carbene Analogues, R. J. Baker, C. Jones, D. P. Mills, G. A. Pierce, M. Waugh, *Inorg. Chim. Acta*, 2008, **361**, 427.

2. Groups 9 and 11 Metal(I) Gallyl Complexes Stabilised by *N*-Heterocyclic Carbene Coordination: First Structural Characterisation of Ga—M (M = Cu or Ag) Bonds, S. P. Green, C. Jones, D. P. Mills, A. Stasch, *Organometallics*, 2007, **26**, 3424.

3. A Lanthanide-Gallium Complex Stabilised by the *N*-Heterocyclic Carbene Group, P. L. Arnold, S. T. Liddle, J. McMaster, C. Jones, D. P. Mills, *J. Am. Chem. Soc.*, 2007, **129**, 5360.

4. Complexes of an Anionic Gallium(I) *N*-Heterocyclic Carbene Analogue with Group 14 Element(II) Fragments: Synthetic, Structural and Theoretical Studies, S. P. Green, K. –A. Lippert, C. Jones, D. P. Mills, A. Stasch, *Inorg. Chem.*, 2006, **45**, 7242.

5. An X-ray Crystallographic Study of the Diphosphacyclobutenyl Gallium Complex, $[GaI_2\{C(Bu^t)P(H)C(Bu^t)=P\}]_2$, M. D. Francis, C. Jones, D. P. Mills, *Main Group Metal Chem.*, 2006, **29**, 147.

6. Oxidative Addition of an Imidazolium Cation to an Anionic Gallium(I) *N*-Heterocyclic Carbene Analogue: Synthesis and Characterisation of Novel Gallium Hydride Complexes, C. Jones, R. P. Rose, D. P. Mills, *J. Organomet. Chem.*, 2006, **691**, 3060.

7. Synthesis, Structural Characterisation and Theoretical Studies of Complexes of Magnesium and Calcium with Gallium Heterocycles, C. Jones, D. P. Mills, J. A. Platts, R. P. Rose, *Inorg. Chem.*, 2006, **45**, 3146.

8. The Reactivity of Gallium-(I), -(II) and -(III) Heterocycles Towards Group 15 Substrates: Attempts to Prepare Gallium-Terminal Pnictinidene Complexes, R. J. Baker, C. Jones, D. P. Mills, D. M. Murphy, E. Hey-Hawkins, R. Wolf, *J. Chem. Soc., Dalton Trans.*, 2006, 64.

Oral Presentation in Support of this Thesis

The Preparation of Novel Complexes Derived From an Anionic Gallium(I) *N*-Heterocyclic Carbene Analogue, Main Group Chemistry Group Dalton Division Meeting, University College London, 30 June 2006.